Phylogeny, divergence time estimates and systematics of African cichlids (Cichlidae: Pseudocrenilabrinae), with a focus on the rheophilic cichlids of East and Central Africa

Dissertation zur Erlangung des Doktorgrades der Naturwissenschaften der Fakultät für Biologie der Ludwig-Maximilians-Universität München

Dissertation to Obtain a Doctoral Degree in Natural Sciences from the Faculty of Biology of the Ludwig-Maximilian University of Munich

vorgelegt von
presented by

Frédéric D.B. Schedel
May 2020

Cover Art: Various cichlid species from Southern-Central Africa. Clockwise from top right: *Orthochromis uvinzae De Vos & Seegers, 1998*, *Tilapia* sp. “Upper Lufubu”, *Orthochromis polyacanthus* (Boulenger 1899a), *Orthochromis gecki* Schedel, Vreven, Katemo Manda, Abwe, Chocha Manda & Schliewen, 2018*,* Haplochromine genus *sp. 'Lubudi blue cheek', Serranochromis* cf. *angusticeps* (Boulenger 1907)*, Orthochromis* sp. cf. *torrenticola* (Thys van den Audenaerde 1963), *Orthochromis torrenticola* (Thys van den Audenaerde 1963)*, Orthochromis kalungwishiensis* (Greenwood and Kullander 1994)*, Orthochromis luongoensis* (Greenwood and Kullander 1994)*, Pseudocrenilabrus* sp. 'Mukuleshi', *Palaeoplex palimpsest* Schedel, Kupriyanov, Katongo, & Schliewen 2020*, Lufubuchromis relictus* Schedel, Kupriyanov, Katongo, & Schliewen 2020*, Hemibates koningsi* Schedel & Schliewen, 2017. All photos by F.D.B. Schedel.

Erstgutachter: Prof. Dr. Gerhard Haszprunar
Zweitgutachter: Prof. Dr. Herwig Stibor

Tag der Einreichung: 14.05.2020
Tag der mündlichen Prüfung: 11.09.2020

Eidesstattliche Erklärung

Ich versichere hiermit an Eides statt, dass die vorgelegte Dissertation von mir selbständig und ohne unerlaubte Hilfe angefertigt wurde.

München, den 14.05.2020

_____

Frederic D.B. Schedel

Erklärung

Hiermit erkläre ich, dass die Dissertation nicht ganz oder in wesentlichen Teilen einer anderen Prüfungskommission vorgelegt worden ist und dass ich mich nicht anderweitig einer Doktorprüfung ohne Erfolg unterzogen habe.

München, den 14.05.2020

_____

Frederic D.B. Schedel

Table of Contents

Declaration of contribution

The cumulative dissertation presented here includes four peer-reviewed publications and one draft manuscript and I (Frederic D.B. Schedel) hereby declare that:

All presented publications and manuscripts (Chapters 1 to 5) were designed by Frederic D.B. Schedel and the PhD supervisor Ulrich K. Schliewen. Frederic D.B. Schedel carried out much of the associated field work (e.g. specimen collection), data collection and processing (including morphological and molecular data), data analysis, manuscript preparation (including preparation of all figures and tables) and publishing related work under the guidance of Ulrich K. Schliewen and the input of the corresponding co-authors. Further, all figures and tables presented on the cover, the introduction and discussion of this thesis were designed by Frederic D.B. Schedel and all corresponding photographs were taken by Frederic D.B. Schedel, if not stated otherwise.

Notable exceptions are listed below:

Chapter 1.
Schedel, F.D.B. & U. K. Schliewen (2017): *Hemibates koningsi* spec. nov: a new deep-water cichlid (Teleostei: Cichlidae) from Lake Tanganyika. *Zootaxa* 4312(1):092–112. http://dx.doi.org/10.11646/zootaxa.4312.1.4

- Fieldwork (e.g. collection of specimens and corresponding tissue material) was done by F.D.B. Schedel.

Chapter 2.
Schedel, F.D.B., Katemo Manda B., Chocha Manda A., Abwe E., Vreven E.J.W.M.N., & U.K. Schliewen (2018): Description of five new rheophilic *Orthochromis* species (Teleostei: Cichlidae) from the Upper Congo drainage in Zambia and the Democratic Republic of the Congo. *Zootaxa* 4461:301–349.
http://dx.doi.org/10.11646/zootaxa.4464.3.1

- Fieldwork (e.g. collection of specimens and corresponding tissue material) was conducted by all coauthors

Chapter 3.

Schedel F.D.B., Kupriyanov, V.M.S., Katongo, C., & U.K. Schliewen (2020): *Palaeoplex* gen. nov. and *Lufubuchromis* gen. non, two new monotypic cichlid genera (Teleostei: Cichlidae) from northern Zambia. Zootaxa 4781(2):191–229.
http://dx.doi.org/10.11646/zootaxa.4718.2.3

- Fieldwork (e.g. collection of specimens and corresponding tissue material) was done by U.K. Schliewen and F.D.B. Schedel.

- Data collection (e.g. measuring of specimens and counting of meristic characters) was done by V.M.S. Kupriyanov and F.D.B. Schedel.

Chapter 4.

Schedel, F.D.B., Musilová, Z. & U.K. Schliewen (2019): East African cichlid lineages (Teleostei: Cichlidae) might be older than their ancient host lakes: new divergence estimates for the East African cichlid radiation. *BMC Evolutionary Biolgoy* 19:94.
https://doi.org/10.1186/s12862-019-1417-0

- Fieldwork (e.g. collection of specimens and corresponding tissue material) was conducted by all coauthors, and additional samples were obtained from many additional contributors.

- Molecular genetic laboratory work was done to large parts by myself except of the laboratory work conducted for the sequencing of the mitochondrial genomes with the following GenBank accession numbers (MK170260 – MK170265) and which was done by Z. Musilová.

Chapter 5.

Schedel, F.D.B., Weiss, J. D., Walheim, L.F., Vreven E.J.W.M.N., Esmaeili, H.R., & U.K. Schliewen (Manuscript, in prep.): The ghost of a hybrids past uncovers ancient river tectonic captures

- Fieldwork (e.g. collection of specimens and corresponding tissue material) was conducted by U.K. Schliewen & and F.D.B. Schedel, and additional samples were obtained from many additional contributors.

- Molecular genetic laboratory work for the ddRAD data set was conducted by F.D.B. Schedel, while laboratory work for the sequencing of the partial mitochondrial genomes was partially conducted by L. Walheim and E. Paulus (research internship) and by F.D.B. Schedel.

_____

Frederic D.B. Schedel

_____

Dr. Ulrich K. Schliewen

_____

Prof. Dr. Gerhard Haszprunar

Taxonomic disclaimer

This thesis is not to be considered as published in the sense of the International Code of Zoological Nomenclature, and statements made herein are not made available for nomenclatural purposes from this document.

Abbreviations

asl: above sea level
BS: Bootstrap support
cf.: *confer* (term derived from Latin and means ‘compare with’)
ddRAD: double digest restriction-site associated DNA
DRC: Democratic Republic of the Congo
EAR: East African Cichlid Radiation
HPD: Highest posterior density
ICZN: International Code of Zoological Nomenclature
ML: Maximum likelihood
MRCA: Most recent common ancestor
Mya: Million years ago
sp.: species
sp. aff.: *species affinis* (term derived from Latin and means ‘species with affinities to’)

Summary

The teleost family Cichlidae (Teleostei: Percomorphaceae), comprising almost two thousand described species, clearly ranks among the largest fish families. Their outstanding morphological, behavioral and ecological diversity and their propensity to generate adaptive radiations made cichlids prime model systems in various fields of biology. Consequently, tremendous efforts have been devoted into the reconstruction of their evolutionary history, albeit with yet partial success. The relationships between major lineages of the megadiverse East African cichlid radiation (EAR) as well as the precise reconstruction of their evolutionary time line remain still hotly debated. This apparent intractability can be partially attributed to their complex evolutionary history, which includes phases of ancient hybridization leading to massive introgression, and to the rapid origin of multiple major lineages. The reconstruction of the spatio-temporal scene that enabled the evolutionary success of African austrotilapiine cichlids is further hampered by the yet unsettled age of the origin of the family Cichlidae, which is due to the paucity of suitable calibration points.

This dissertation focuses on the evolutionary history of African austrotilapiine cichlids (Pseudocrenilabrinae), with particular attention to the riverine haplochromine lineages from Southern-Central Africa. In contrast to the famous EAR of the African Great Lakes, their riverine precursor lineages have been considerably less well studied, which applies both to their phylogenetic relationships as well as to their systematics and taxonomy.

The first section of this thesis concentrates on the classification and taxonomy of several riverine cichlid lineages endemic to the Upper Congo drainage as well as on selected taxa of neighbouring Lake Tanganyika (chapters 1 – 3). In total, eight new species and two new genera were described including one ancient member of the EAR, a *Hemibates* species from Lake Tanganyika. Further five species of the rheophilic genus *Orthochromis* are described from isolated rivers from the southeastern Democratic Republic of the Congo (DRC) and Zambia, and finally two new species belonging to two new genera *Lufubuchromis* and *Palaeoplex.* The latter are endemic to two neighbouring areas in northeastern Zambia. These descriptions represent an important contribution to the knowledge on the still underexplored cichlid diversity of the Katanga-Chambeshi region (see discussion).

The second section provides new insights into the complex phylogenetic history of African cichlids related to the EAR. They are analyzed and presented in the geomorphological context of the palaeo-drainage evolution of the East African Rift and tectonically related areas (chapters

4 – 5 & discussion). First, new divergence age estimates were obtained for the phylogeny of the family Cichlidae and particularly for austrotilapiine Pseudocrenilabrinae. These are based on an extensive mitogenomic data set with DNA sequences of ten protein coding genes from 180 cichlid species. The corresponding molecular clock analyses were conservatively constrained by carefully selected calibration points including six fossils and one geological event. The divergence of the monophyletic African Pseudocrenilabrinae and American Cichlinae was dated to the Late Cretaceous, thus tentatively supporting the "Marine Dispersal Hypothesis" and thus contradicting a strict Gondwana-break up scenario for the origin of the two continental cichlid radiations. In the same analyses the origin of the EAR was dated to as early as of Late Eocene/Early Oligocene age, and more importantly, the divergence ages of multiple endemic Lake Tanganyika cichlid tribes were firmly estimated to predate the formation of extant Lake Tanganyika basin itself. This result supports the recently suggested "Melting-pot Tanganyika hypothesis", which hypothesized Lake Tanganyika to be a comparatively young reservoir of lineages partially originating from hybridization of more ancient precursor lineages.

Finally, a refined and comprehensive phylogenetic hypothesis based on a comprehensive genomic nuclear DNA (ddRAD) dataset is provided for all major australotilapiine cichlid lineages related to the EAR. This massive dataset not only includes representatives of all major lacustrine tribes and lineages but particularly all potential riverine precursor lineages, altogether 206 specimens from 160 species. This dataset, in combination with a further increased taxon-sampling of the mitogenomic dataset, now with about 330 cichlid species, was used to infer candidate ancient hybridization events among australotilapiines lineages that may have contributed to the complex network-like evolutionary history and success of the EAR. This was done applying statistical methods previously applied to reconstruct the equally complex human phylogenetic history, i.e. the so-called D-statistics or the genomic evaluation of cyto-nuclear discordances. Apart from many previously reported candidate cases of ancient hybridization, numerous new ones were detected especially within major haplochromine lineages. The analysis of these results in the light of recent tectonic re-arrangements in the region strongly suggest that hybridization has played an even more important role in shaping the evolutionary history of African cichlids than already presumed.

An important methodological result of the comparative mitogenomic and nuclear genomic molecular clock analyses contrasts with previous assumptions, i.e. surprisingly divergence time

estimates based on mitochondrial and nuclear (ddRAD) data emerged as largely comparable across austrotilapiine cichlids and Neogene timescales.

Zusammenfassung

Die Knochenfischfamilie Cichlidae gehört mit fast zweitausend beschriebenen Arten eindeutig zu den größten Fischfamilien. Ihre außergewöhnliche morphologische, verhaltensbiologische und ökologische Vielfalt, als auch ihre Tendenz adaptive Radiation hervorzubringen, machte Buntbarsche zu erstklassigen Modelorganismen für verschiedenste biologische Forschungsfelder. Trotz der großen Bemühungen um die Rekonstruktion der evolutionären Entwicklungsgeschichte der Buntbarsche ist diese bis heute nicht vollständig verstanden. Dabei werden nicht nur die Verwandtschaftsverhältnisse zwischen den Haupt-Entwicklungslinien der sogenannten „East African cichlid radiation (EAR)“, sondern auch der genaue zeitliche Ablauf der Evolutionsgeschichte dieser hochdiversen Buntbarschgruppe kontrovers diskutiert. Die Rekonstruktion der räumlich-zeitlichen Prozesse, die den evolutionären Erfolg der afrikanischen austrotilapiinen Buntbarsche ermöglichten, wird auch durch das noch immer ungeklärte Entstehungsalter sowie durch den bisher nicht präzisierten zeitlichen Ursprung der Familie Cichlidae erschwert. Der Grund dafür ist teilweise auf den Mangel geeigneter Kalibrierungspunkte für entsprechende Rekonstruktionen zurückzuführen.

Die vorgelegte Dissertation beschäftigt sich primär mit der Evolutionsgeschichte afrikanischer austrotilapiiner Buntbarsche mit einem besonderem Fokus auf die fluviatilen haplochrominen Buntbarsch-Linien des südlichen Zentralafrikas. Im Gegensatz zu den berühmten Entwicklungslinien der EAR in den Grabenbruchseen Ostafrikas, wurden den fluviatilen Linien der EAR und ihrer Vorläuferlinien bedeutend weniger Beachtung geschenkt. Dies betrifft sowohl die Erforschung der phylogenetischen Verwandtschaftsverhältnisse, als auch ihre Systematik und Taxonomie.

Der erste Abschnitt dieser Dissertation befasst sich daher mit der systematischen Einordnung und der Taxonomie mehrerer fluviatiler Buntbarschlinien, allesamt Endemiten des oberen Einzugsgebiets des Kongo, als auch ausgewählter Taxa aus dem benachbarten Tanganjikasee (Kapitel 1 – 3). Insgesamt wurden acht neue Arten sowie zwei neue Gattungen beschrieben. Darunter eine neue *Hemibates* Art aus dem Tanganjikasee, die einer alten Linie (Tribus) der EAR angehört. Außerdem wurden fünf Arten der rheophilen Gattung *Orthochromis*

beschrieben, die in verschiedenen isolierten Flusssystemen Sambias und der südöstlichen Demokratischen Republik Kongo (DRC) vorkommen. Weiter wurden zwei neue Arten beschrieben, die jeweils ebenfalls zwei neu aufgestellten Gattungen *Lufubuchromis* und *Palaeoplex* angehören. Diese Beschreibungen stellen einen wichtigen Beitrag zur Erfassung der bis heute wenig erforschten Diversität der Buntbarsche der Katanga-Chambeshi Region dar (siehe Diskussion).

Der zweite Abschnitt liefert neue Erkenntnisse über die komplexen phylogenetischen Zusammenhänge der afrikanischen Buntbarsche aus der Verwandtschaftsgruppe der EAR. Diese wurden im Kontext der Entwicklung der Paläo-Flusssysteme des ostafrikanischen Grabenbruchs sowie tektonisch angrenzender Gebiete analysiert und präsentiert (Kapitel 4 – 5 & Diskussion). Dabei wurden zuerst neue Altersabschätzungen für die Phylogenie der Buntbarsche und insbesondere der austrotilapiiner Pseudocrenilabrinae berechnet. Diese basieren auf einem umfangreichen mito-genomischen Datensatz, der DNS Sequenzen von zehn proteincodierenden Genen von 180 Buntbarscharten umfasst. Die „Molekulare Uhr“ der korrespondierenden altersabschätzenden Analysen wurde dabei mittels vorsichtig ausgewählter Kalibrierungspunkte kalibriert, darunter sechs Fossilien sowie ein geologisches Ereignis. Dabei wurde das Divergenzereignis zwischen den jeweils monophyletischen afrikanischen Pseudocrenilabrinae sowie der amerikanischen Cichlinae als in der Oberkreide liegend datiert. Dies spricht zumindest vorläufig für die sogenannte „Marine Dispersal Hypothesis“ und widerspricht somit der Annahme, dass die Divergenz der beiden kontinentalen Buntbarschradiationen direkt auf dem Auseinanderbrechen von Gondwana basiert. In der gleichen Analyse wurde der Ursprung der EAR in das späte Eozän bis frühes Oligozän datiert. Darüber hinaus wurde das Divergenzalter mehrerer im Tanganjikasee endemischer Triben als deutlich älter als die Entstehung des rezenten Tanganjikasee-Beckens selbst abgeschätzt. Dies unterstützt die vor kurzem vorgeschlagene „Melting-pot Tanganyika“-Hypothese, die formuliert, dass der Tanganjikasee ein verhältnismäßig junges Reservoir für verschiedene evolutionär alte Linien sowie Linien, die aus Hybridisierungen ebendieser hervorgegangen sind darstellt.

Des Weiteren wurde basierend auf einem umfangreichen kerngenomischen DNS (ddRAD) Datensatz eine überarbeitete und umfassende Phylogenie der australotilapiinen Buntbarsche erstellt. Der Datensatz bestand aus 206 Individuen, die 160 Arten zugeordnet werden, und enthielt dabei nicht nur Vertreter aller lakustrischen Triben und Linien der EAR, sondern auch

Vertreter aller potentieller Vorgängerlinien aus den Flüssen. In Kombination mit einem noch weiter vergrößerten mitochondrialen Datensatz, der etwa 330 Buntbarscharten berücksichtige, wurde der kerngenomische Datensatz genutzt um potentielle alte Hybridisations-Ereignisse zwischen den australotilapiinen Linien zu detektieren. Diese könnten möglicherweise nicht nur den evolutionären Erfolg der EAR erklären, sondern auch ihre komplexen, teilweise retikulären Verwandtschaftsverhältnisse. In dieser Teilstudie wurden vor allem statistische Analysen durchgeführt, die kürzlich zur Analyse der ebenfalls hochkomplexen Evolutionsgeschichte des Menschen zum Einsatz gekommen waren, z.B. die so genannte „D-statistics“ oder die genomische Auswertung von cyto-nuklearen Diskordanzen. Neben vielen bereits schon früher dokumentierten potentiellen alten Hybridisations-Ereignissen konnten dabei auch zahlreiche neue detektiert werden, vor allem zwischen und innerhalb der Hauptlinien des Tribus Haplochromini. Die Analyse dieser Ergebnisse im Kontext der jüngeren tektonischen Umlagerungen in der Region zeigt deutlich, dass der Hybridisierung als Evolutionsfaktor eine noch wichtigere Rolle in der Evolutionsgeschichte der afrikanischen Buntbarsche zukommt als bisher angenommen.

Ein wichtiges methodisches Ergebnis resultierte aus dem Vergleich altersabschätzender Analysen, die entweder auf mitochondrialen Daten oder auf kerngenomischen Daten basierten. Entgegen früherer Annahmen, waren die korrespondierenden Altersabschätzungen der beiden Analysen für die austrotilapiinen Buntbarsche (Zeitraum: Neogen) erstaunlicherweise weitgehend miteinander vergleichbar.

Introduction

The family Cichlidae

Famous for their outstanding morphological, behavioral and ecological diversity and specializations, cichlids (family: Cichlidae) represent one of the most species-rich vertebrate families with about 1726 valid species and a total of 3000 estimated species (Fricke et al. 2020; Kocher 2004). Within the ray-finned fishes (Actinopterygii), cichlids are placed together with the marine convict blennies (family: Pholichdichthyidae) in the recently introduced order Cichliformes within the diverse percomorph clade Ovalentaria (Alfaro et al. 2018; Betancur-R et al. 2013; Wainwright et al. 2012). Currently, four cichlid subfamilies are recognized (Fricke et al. 2020; Sparks and Smith 2004): the Etroplinae (Indian subcontinent & Madagascar; 16 valid species), the Ptychochrominae (Madagascar; 16 valid species), the Cichlinae (South & Central Amerika; 568 valid species) and the diverse Pseudocrenilabrinae (Africa, Middle East, Iran; 1126 valid species).

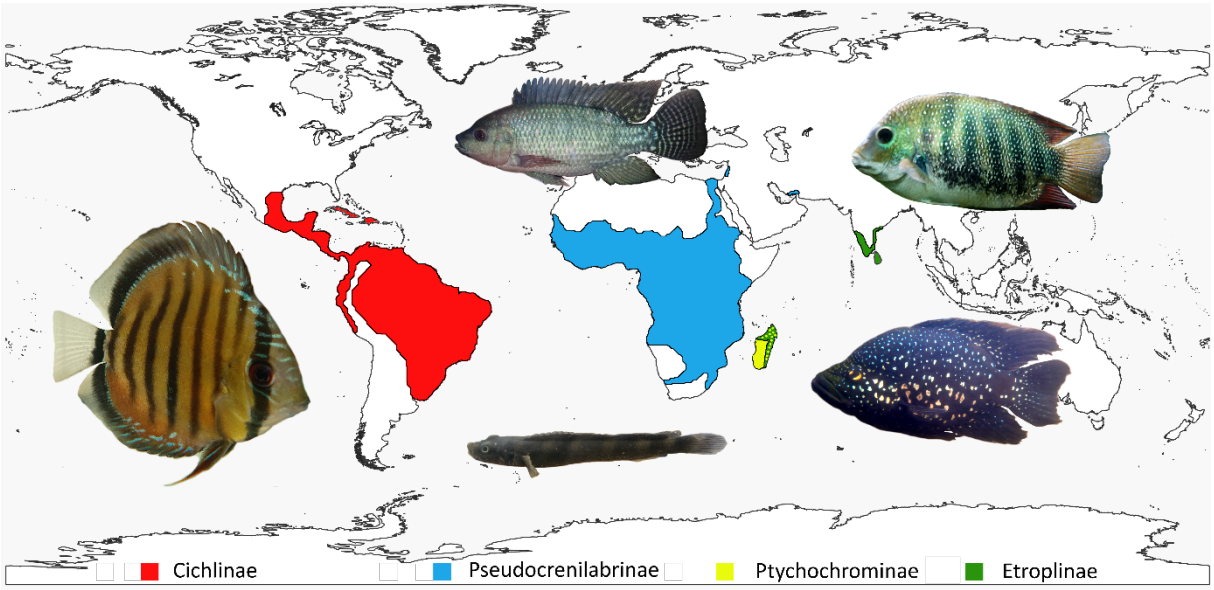

Figure 1: Map roughly showing the distribution of the four cichlid subfamilies Cichlinae, Pseudocrenilabrinae, Ptychochrominae (co-occurring with the Etroplinae in the North and East of Madagascar) and Etroplinae; based on (Matschiner 2019; Sparks and Smith 2004). Depicted cichlids are clockwise from top center: *Oreochromis niloticus* (Linnaeus 1758), photo: F.D.B. Schedel; *Etroplus suratensis* (Bloch 1790), photo: F.D.B. Schedel; *Paratilapia* cf. *polleni* Bleeker 1868, photo: A. Indermaur; *Teleogramma* cf. *depressa* Roberts & Stewart 1976, photo: SNSB-ZSM Inga 2013 expedition; and *Symphysodon aequifasciatus* Pellegrin 1904, photo: F.D.B. Schedel. Base map was obtained from Natural Earth (www.naturalearthdata.com).

Although cichlids exhibit a wide range of body shapes (from highly elongated to "typical perch like" to strongly laterally compressed, see Figure 1) and body sizes (from approximately 25 mm up to 1 meter length), cichlids are easily recognized by several external morphological features. For instance, cichlids are characterized by an interrupted lateral line (except for the genera *Gobiocichla* Kanazawa 1951 and *Teleogramma* Boulenger 1899 with uninterrupted lateral lines), a single nostril on each side on their snout (versus two nostrils in most other teleost fish families) and by the division of the dorsal and anal fins into a spiny and soft-rayed portion (Barlow 2000; Kullander 2003; Nelson et al. 2016). All cichlids display uniparental or biparental parental care, and feature various mating systems, e.g. monogamous, polygamous or agamous. Their breeding strategies range from open substrate brooders, cave brooders, ovophilic or larvophilic mouthbrooders, and even complex cooperative breeding systems have been described (Barlow 2000; Goodwin et al. 1998; Klett and Meyer 2002; Sefc 2011; Wong and Balshine 2011).

Likewise, cichlids occupied various trophic niches and evolved countless feeding specializations including, for example: detritivores, herbivores, planktivores, molluscivores, piscivores, paedophages and lepidophages (Albertson et al. 1999; Konings 2019). Their extreme plasticity and adaptability has been attributed to another cichlid key character, the cichlid pharyngeal jaw apparatus involving the fusion of lower pharyngeal jaws. This anatomical feature which was hypothesized to allow for the functional decoupling of the food acquisition by the oral jaw and food processing starting with pharyngeal jaw movements (Liem 1973). The evolutionary success of cichlids, especially those of the East African cichlids radiations, was further postulated to be the result of a combination of further lineage-specific key innovations and traits, among others diverse body coloration allowing for pronounced sexual dichromatism and increased divergent sexual selection (Maan and Sefc 2013), increased visional sensitivity with an adaptive potential to thrive under different light environments (Seehausen et al. 2008) and maternal mouthbrooding (Salzburger et al. 2005). Additional intrinsic factors of their success may be, last but not least, genomic features such as an increased gene duplication rates (Brawand et al. 2014). All these intrinsic factors unfolded their potential in conditions of novel ecological opportunities, as e.g. present in emerging tectonic or crater lakes (Salzburger et al. 2005; Wagner et al. 2012). Finally, there is increasing evidence that hybridization associated with introgression played and potentially still plays a significant role for enabling the rapid evolutionary success of cichlids through the provision of novel genetic

variation sourced from recombining ancient variation of different lineages in novel moscaic hybrid genotypes (Meier et al. 2017; Meier et al. 2019; Schwarzer et al. 2012b).

Especially the African Pseudocrenilabrinae received considerable research interest in the field of evolutionary biology due their exceptional diversity and their propensity to generate adaptive radiations exemplified by the celebrated adaptive radiations of Lake Tanganyika, Lake Malawi and Lake Victoria (Kocher 2004; Salzburger 2018; Seehausen 2015; Turner 2007). Attempts to clarify cichlid intrarelationships particularly within the Pseudocrenilabrinae and deriving a phylogenetically sound suprageneric classification based on morphological characters started already in the early 19th century, e.g. using scale and squamation, pharyngeal apophysis, lateral line foramina characters, but they failed to be completed in a comprehensive way (Greenwood 1978; Lippitsch 1990; Lippitsch 1997; Lippitsch 1998; Poll 1986; Regan 1920; Regan 1922; Stiassny 1991; Takahashi 2003a; Takahashi 2003b). With the advent of molecular phylogenetics, recognition of tribes and major lineages had been increasingly based on molecular characters. Currently, approximately 26 and 28 major lineages and tribes for the Pseudocrenilabrinae are currently recognized. The discrepancies in the counts are the result of different views about the classification of several taxa, i.e. whether *Heterochromis*, *Orthochromis* sensu stricto and the Tropheini should be treated as tribes of their own or not (Dunz and Schliewen 2013; Koblmüller et al. 2008b; Schwarzer et al. 2009; Weiss et al. 2015). For example, *Heterochromis* was found to represent the earliest splitting lineage within the Pseudocrenilabrinae based on molecular data (Farias et al. 1999; Friedman et al. 2013; Keck and Hulsey 2014; Smith et al. 2008), whereas morphological data failed to recover an unambiguous relationship of *Heterochromis* with the Pseudocrenilabrinae (Kullander 1998; Stiassny 1991).

It should be noted that although several major lineages have been assigned to the tribus level, several corresponding tribus names (ending with "-ini") are currently not available based on the rules of the ICZN due to various reasons (van der Laan et al. 2014). To facilitate the verbal communication about cichlid relationships, it was suggested to rephrase taxonomically unavailable tribus names with the ending "-ines" (see e.g. Dunz and Schliewen 2010; Schwarzer 2011). In addition to these recognized tribal assemblages, numerous clades and lineages have been informally named and are widely used in the cichlid literature as well as in the chapters of this thesis as they simplify the communication about cichlid relationships (see Table 1). However, some of the informal clades are only supported by nuclear or mitochondrial data (Meyer et al. 2015; Weiss et al. 2015).

Table 1: Overview of currently recognized major lineages and tribus names of the cichlid subfamily Pseudocrenilabrinae as well as of selected informal clade names above tribus level as used in the cichlid literature. Several major lineages informally assigned to tribus level are currently without taxonomic available tribus name (see van der Laan et al. 2014) and corresponding names are therefore placed in quotation marks and they are written with the suffix "-ines", or, if they are monotypic, they are listed with the corresponding genus name.

Tribes or major lineages previously assigned to tribal level	**Haplotilapiines (Schliewen and Stiassny 2003)**	**Austrotilapiines (Schwarzer et al. 2009)**	**East African cichlid radiation (EAR) e.g. (Schwarzer et al. 2009)**	**C-lineage (Clabaut et al. 2005)**	**MVhL-clade (Takahashi et al., 2001)**	**H-lineage (Nishida 1991)**
Heterochromis Regan 1922						
"tylochromines"						
"chromidotilapiines"						
"pelmatochromines"						
"hemichromines"						
Etia Schliewen & Stiassny 2003	*X*					
Heterotilapiini	*X*					
Coelotilapiini	*X*					
Gobiocichlini	*X*					
Coptodonini	*X*					
Pelmatolapiini	*X*					
Oreochromini	*X*					
Tilapiini	*X*	*X*				
Steatocranini	*X*	*X*				
Boulengerochromini	*X*	*X*	*X*			
Bathybatini incl. Hemibatini	*X*	*X*	*X*			
Trematocarini	*X*	*X*	*X*			
Lamprologini	*X*	*X*	*X*		*X*	
Eretmodini	*X*	*X*	*X*		*X*	*X*
Cyphotilapiini	*X*	*X*	*X*	*X*	*X*	*X*
Limnochromini	*X*	*X*	*X*	*X*	*X*	*X*
Ectodini	*X*	*X*	*X*	*X*	*X*	*X*
Perissodini	*X*	*X*	*X*	*X*	*X*	*X*
Cyprichromini	*X*	*X*	*X*	*X*	*X*	*X*
Benthochromini	*X*	*X*	*X*	*X*	*X*	*X*
Orthochromis sensu stricto	*X*	*X*	*X*	*X*	*X*	*X*
Haplochromini	*X*	*X*	*X*	*X*	*X*	*X*
Tropheini (placed within the Haplochromini)	*X*	*X*	*X*	*X*	*X*	*X*

Cichlid diversity in Southern-Central Africa

Although cichlids show an almost pan-African distribution as they are only absent in the extreme southern part of Southern Africa, their center of diversity clearly lays in East Africa and in the Great African lakes (Matschiner 2019; Skelton 2001). Understandably, the outstanding phenotypical, behavioral and genetic diversity of the adaptive cichlid radiations (EAR) of the Great African lakes, especially those of Lake Tanganyika, received a considerable amount of research interest and haven been intensively studied (Kocher 2004; Salzburger 2018). Nevertheless, the importance of including riverine lineages as, e.g., early diverging haplotilapiine cichlids and riverine haplochromine taxa for the reconstruction and understanding of the evolutionary history of EAR is increasingly recognized (Genner et al. 2015; Irisarri et al. 2018; Koblmüller et al. 2008a; Meier et al. 2017; Meier et al. 2019; Salzburger et al. 2005; Schedel et al. 2019; Schwarzer et al. 2009; Weiss et al. 2015). Therefore, one of the objectives of the thesis presented here was to elucidate the evolutionary relationships of riverine haplochromine lineages in the larger cichlid phylogenetic context, in particular those endemic the ancient upper Congo subdrainage systems, e.g. in the northern part of the Katanga-Chambeshi region (sensu Cotterill 2005) located in Southern-Central Africa.

Nowadays, the Katanga-Chambeshi region is characterized by a landscape mosaic of savannah grasslands and wetlands and is centered within the Zambezian phytochorion (White 1983). The region covers several freshwater ecoregions (sensu Abell et al. 2008; Thieme et al. 2005), among others the “Bangweulu-Mweru ecoregion”, the “Upper Lualaba ecoregion” and the southern part of the “Lake Tanganyika ecoregion”, all of which are of particular interest for the taxonomical studies presented in this thesis. The Katanga-Chambeshi region includes several biodiversity hotspots and harbors an extremely rich aquatic fauna with a high degree of endemism. This is exemplified by the Bangweulu-Mweru ecoregion where one third of the fish species have been reported to be endemic (Balon and Stewart 1983; Thieme et al. 2005; van Steenberge et al. 2014). Cichlids in particular contribute to the ichthyological diversity of the focal area and are represented by several lineages, predominantly by members of the Tilapiini and two major haplochromine lineages referred herein as the ‘extended *Pseudocrenilabrus*-group’ (sensu Schedel et al. in prep.) and the ‘extended serranochromines’ (sensu Schedel et al. in prep.). In addition, species of Oreochromini, Tylochromini and Coptodonini are documented from the focal area of this thesis (Balon and Stewart 1983; Meier et al. 2019; Schedel et al. 2018; Schedel et al. 2020; van Steenberge et al. 2014; Vreven et al. 2015).

The ‘extended *Pseudocrenilabrus*-group’ is delineated based on nuclear (ddRAD) data and follows the concept of the *Pseudocrenilabrus*-group introduced by Weiss et al. (2015), which later was widened by Schedel et al. (2019). It represents one the four major haplochromine lineages in addition to *Ctenochromis pectoralis* Pfeffer 1893, the ‘extended serranochromines’, and the ‘ocellated eggspot Haplochromini’ (including the Tropheini) as suggested in Schedel et al. (in prep.) (see Figure 1, Chapter 5). The center of diversity of this clade clearly is located within the Katanga-Chambeshi region and four of the six principal lineages appear to be endemic to the region namely: *Lufubuchromis* Schedel, Kupriyanov, Katongo, & Schliewen 2020, *Orthochromis indermauri* Schedel, Vreven, Katemo Manda, Abwe, Chocha Manda & Schliewen, 2018, *Palaeoplex* Schedel, Kupriyanov, Katongo, & Schliewen 2020 and the Northern-Zambian-*Orthochromis* (sensu Weiss et al. 2015). The two remaining lineages, the ‘LML-*Orthochromis’* (sensu Weiss et al. 2015) and the genus *Pseudocrenilabrus* Fowler 1934, are much more widespread. Particularly, the genus *Pseudocrenilabrus* is widely distributed in northern, eastern, southern and central Africa (Greenwood 1989; Katongo et al. 2017; Schedel et al. 2020). *Pseudocrenilabrus* specimens found in the Katanga-Chambeshi region have been usually and uncritically assigned to *Pseudocrenilabrus philander* (Weber, 1897). However, morphological as well as genetic evidence clearly suggest that *P. philander* as currently defined represents a species complex (Egger et al. 2015; Katongo et al. 2005; Koblmüller et al. 2012; Seegers 1996). Moreover, an adaptive radiation of *Pseudocrenilabrus*-related species has recently been recognized from Lake Mweru, which appears to be of hybrid origin originating from different lineages of the ‘*Pseudocrenilabrus philander* species complex’ (Katongo et al. 2006; Meier et al. 2019). Note that in the study of Meier et. al (2019) all representatives of the ‘extended *Pseudocrenilabrus*-group’ are referred to as ‘Orthochromines’, a usage which might possibly be misleading with regard to the undoubtedly polyphyletic status of the name bearing genus (see below).

In contrast, the ‘extended serranochromines’ are primarily distributed in Southern Africa, although several early splitting lineages of this clade are found in the upper tributaries of the Congo and Kasai as well as in the Lower Congo (Joyce et al. 2005; Musilová et al. 2013; Schwarzer et al. 2012b). Within the ‘extended serranochromines’ the comparatively diverse subclade commonly referred as ‘serranochromines sensu stricto’ (see e.g. Musilová et al. 2013). It was suggested to represent an ancient radiation that had been hypothesized to have evolved within the palaeolake Makgadikgadi located in northern Botswana in the Kalahari Desert; descendants of this ancient lacustrine radiation would then have secondarily dispersed to

adjacent drainage systems of Southern Africa such as that of the Okavango and Zambezi (Joyce et al. 2005; Katongo et al. 2007). Recently, two adaptive radiations, most likely of hybrid origin but phylogenetically nested within the 'serranochromines senus stricto', have been identified from Lake Mweru (Meier et al. 2019). Moreover, two strongly rheophilic lineages, the 'Katanga-*Orthochromis*' (sensu Schedel et al. in prep.) and the '*Orthochromis torrenticola* species complex' (sensu Schedel et al. in prep.), together with two undescribed genera representing two clearly distinct lineages within the 'extended serranochromines' from the Lubudi River appear to be endemic to the Katanga-Chambeshi region (Schedel et al. 2018).
As a separate independent but closely related lineage the Tilapiini are widely distributed over Central and Southern Africa. Of the three genera currently placed within the tribe only the genus *Tilapia* Smith, 1840 is represented in the Katanga-Chambeshi region with three out of the four described species (Dunz and Schliewen 2013). *Tilapia baloni* Trewavas & Stewart 1975 represents the only described endemic species of the genus for the region and is only known from the Luongo River (Balon and Stewart 1983). *Tilapia sparrmanii* Smith, 1840 on the other hand, represents most likely a species complex and several undescribed *Tilapia* species appear to occur in the region (Dunz 2012; Seegers 1996).

Overview of the polyphyletic genus *Orthochromis* Greenwood, 1954

As indicated above, the genus *Orthochromis* Greenwood, 1954 as currently defined is polyphyletic and includes as one part the type species *Orthochromis malagaraziensis* (David, 1937) and its congeners, which are distributed in three eastern tributaries of the Lake Tanganyika (Malagarasi, Rugufu and Luiche River). This partial group is commonly referred to as Malagarasi-*Orthochromis* (sensu Weiss et al. 2015) or as *Orthochromis* sensu stricto, but other rheophilic haplochromines currently placed in *Orthochromis* either belong to the 'extended serranochromines' or to the 'extended Pseudocrenilabrus-group' (De Vos and Seegers 1998; Koblmüller et al. 2008a; Schedel et al. 2018; Schedel et al. 2019; Schedel et al. in preparation; Schwarzer et al. 2012b; Weiss et al. 2015).
The genus *Orthochromis* was established by Greenwood (1954) for *Haplochromis malagaraziensis* David, 1937, a species previously described from the Malagarasi River. It was characterized by its elongated body shape and having no scales on the cheeks and chest (Greenwood 1954). Already at time, additional rheophilic cichlid species and genera, eco-morphologically vaguely characterized by a comparatively slender body, a reduced squamation

on chest, nape and head as well by rounded pelvic fins (Roberts and Stewart 1976), had been already described from the Upper Congo drainage. *Schwetzochromis neodon* Poll 1948 (and its synonym *Haplochromis rheophilus* Poll, 1948), for example, had been described from the karst river "Lac" Fwa. *Orthochromis polyacanthus* (Boulenger 1899) and *Orthochromis stormsi* (Boulenger 1902), had already been described from Lake Mweru and the Upper Congo, respectively, but originally assigned to the genus *Tilapia* (Boulenger 1899a; Boulenger 1902). Several years later, *Haplochromis torrenticola* Thys van den Audenaerde 1963, originally described as *Haplochromis rheophilus* Thys van den Audenaerde, 1963 was described from above the Kyubo falls (sometimes spelled Kiubo) on the Lufira River, a tributary of the Lualaba River. In the same study, *Rheohaplochromis* Thys van den Audenaerde 1963 was described as a subgenus of *Haplochromis* Hilgendorf, 1888, in which Thys van Audenaerde (1963) grouped his new taxon from the Lufira as well as *O. polyacanthus*. Later, Thys van Audenarde (1964) raised *Rheohaplochromis* to the genus level, while clearly differentiating between *Rheohaplochromis* from *Orthochromis* as defined at the time by the presence of minute scales on the nape and chest. Unfortunately however, no type species was assigned for the genus *Rheohaplochromis* by Thys van den Audenaerde (1963), which renders the genus name *Rheohaplochromis* Thys van den Audenaerde 1963 taxonomically unavailable (see Article 13.3 of the ICZN, Greenwood 1979). Over the following years Greenwood revised his genus *Orthochromis* several times (Greenwood 1979; Greenwood 1984). In doing so he synonymized *Rheohaplochromis* with *Orthochromis* as he considered the ecomorphological characters shared by the respective species taxa as putatively shared derived characters, e.g. the reduced squamation, and thus as an argument for their monophyly and congenerity. Consequently, he further included *Haplochromis machadoi* Poll, 1967 from the Cunene River in Namibia and Angola into the genus *Orthochromis.* One decade later, Roberts and Kullander (1994) revised the taxonomy of the Lac Fwa endemic cichlids and found that most of the putatively diagnostic characters of *Orthochromis* as defined by Greenwood (1979) were also present in *Schwetzochromis neodon* Poll, 1948. Thus, they synonymized *Orthochromis* with the older available name *Schwetzochromis*. Accepting the new classification, Greenwood and Kullander (1994) revalidated and re-classified *Tilapia stormsi* Boulenger, 1902, which was considered as synonym of *Tilapia polyacanthus* Boulenger 1899 since the classification of Regan (1922), as *Schwetzochromis stormsi* (Boulenger, 1902). They further described *Schwetzochromis luongoensis* Greenwood and Kullander, 1994 *Schwetzochromis kalungwishiensis* Greenwood and Kullander, 1994 from the Luongo River, a tributary of the Luapula River, and from the

Kalungwishi River, a tributary of Lake Mweru, respectively. However, a few years later De Vos and Seegers (1998) removed the genus *Orthochromis* from the synonymy with *Schwetzochromis.* They argued that the putatively synapomorphic characters uniting *S. neodon* and all other *Orthochromis* species, including seven new species they described from eastern Lake Tanganyika affluent in the same study, must have evolved convergently. To consolidate they action, they further provided new morphological and chromatic characters to better diagnose both genera. For example both genera can be distinguished by the presence of sexual dichromatism in *Schwetzochromis* vs. no or only weak sexual dichromatism in *Orthochromis*; by the presence of *Haplochromis*-like egg spots in *Schwetzochromis* vs. their absence in *Orthochromis;* and by the absence of lachrymal stripes in *Schwetzochromis* vs. their presence in *Orthochromis* (De Vos and Seegers 1998). Twenty years later, five rheophilic species from the Katanga-Chambeshi region were described in the genus *Orthochromis* (Schedel et al. 2018). Although phenotypically similar to the Malagarasi-*Orthochromis,* these new species feature characters which are not fully compatible with the latest generic diagnosis of *Orthochromis* by De Vos and Seegers (1998), yet the authors decided to place those species only provisionally in the genus *Orthochromis,* i.e. until a generic revision of all haplochromine genera becomes available as an important precondition to describe new haplochromine genera (see Chapter 2 for more details).

Currently, 19 valid species are included in the genus *Orthochromis* with only eight belong to the 'Malagarasi-*Orthochromis'* (Fricke et al. 2020; Schedel et al. 2018). Monophyly of the 'Malagarasi-*Orthochromis*' is well supported by molecular data and they were repeatedly recovered as sister group to the Haplochromini including the remaining species currently placed in *Orthochromis* (Clabaut et al. 2005; Irisarri et al. 2018; Matschiner et al. 2016; Schedel et al. 2019; Weiss et al. 2015). The eleven remaining "haplochromine *Orthochromis*" species on the other hand appear to belong to at least six different evolutionary lineages (see Figure 2 for representative members of the corresponding lineages) based on molecular data (Meier et al. 2019; Schedel et al. 2019; Schedel et al. in preparation; Weiss et al. 2015). Based on nuclear data, three of these lineages ('*Orthochromis indermauri*', 'Northern-Zambia-*Orthochromis*' and the 'LML-*Orthochromis*') can be assigned to the 'extended *Pseudocrenilabrus*-group', although extensive cyto-nuclear discordances were reported to occur for several lineages of this clade (Schedel et al. in prep.; see Chapter 5). For example, the so-called 'LML-*Orthochromis*' are regularly recovered to be closely related with serranochromine taxa based on mitochondrial data (Koblmüller et al. 2008a; Musilová et al. 2013; Salzburger et al. 2002; Schedel et al. 2019;

Schwarzer et al. 2012b; Weiss et al. 2015), but nuclear DNA based phylogenies recover a closer relationship with taxa of the '*Pseudocrenilabrus*-group' (Schedel et al. in preparation; Schwarzer et al. 2012b; Weiss et al. 2015). *Orthochromis machadoi* (Poll, 1967) represents the fourth lineage recovered within the 'extended *Pseudocrenilabrus*-group', but is was found to be a member of the *Pseudocrenilabrus philander* species complex based on mitochondrial data and nuclear (RAD data) (Egger et al. 2015; Koblmüller et al. 2008a; Meier et al. 2019). Within the 'extended serranochromines' two "haplochromine *Orthochromis*" lineages are recovered based on nuclear as well as on mitochondrial data namely the '*Orthochromis torrenticola* species complex' and the 'Katanga-*Orthochromis*' (Schedel et al. in preparation; Schwarzer et al. 2012b; Weiss et al. 2015). As for the 'extended *Pseudocrenilabrus*-group', cyto-nuclear discordance appears widespread among the lineages of the 'extended serranochromines' and the monophyly of the 'Katanga-*Orthochromis*' is supported by nuclear data only (Schedel et al. in preparation; Schwarzer et al. 2012b).

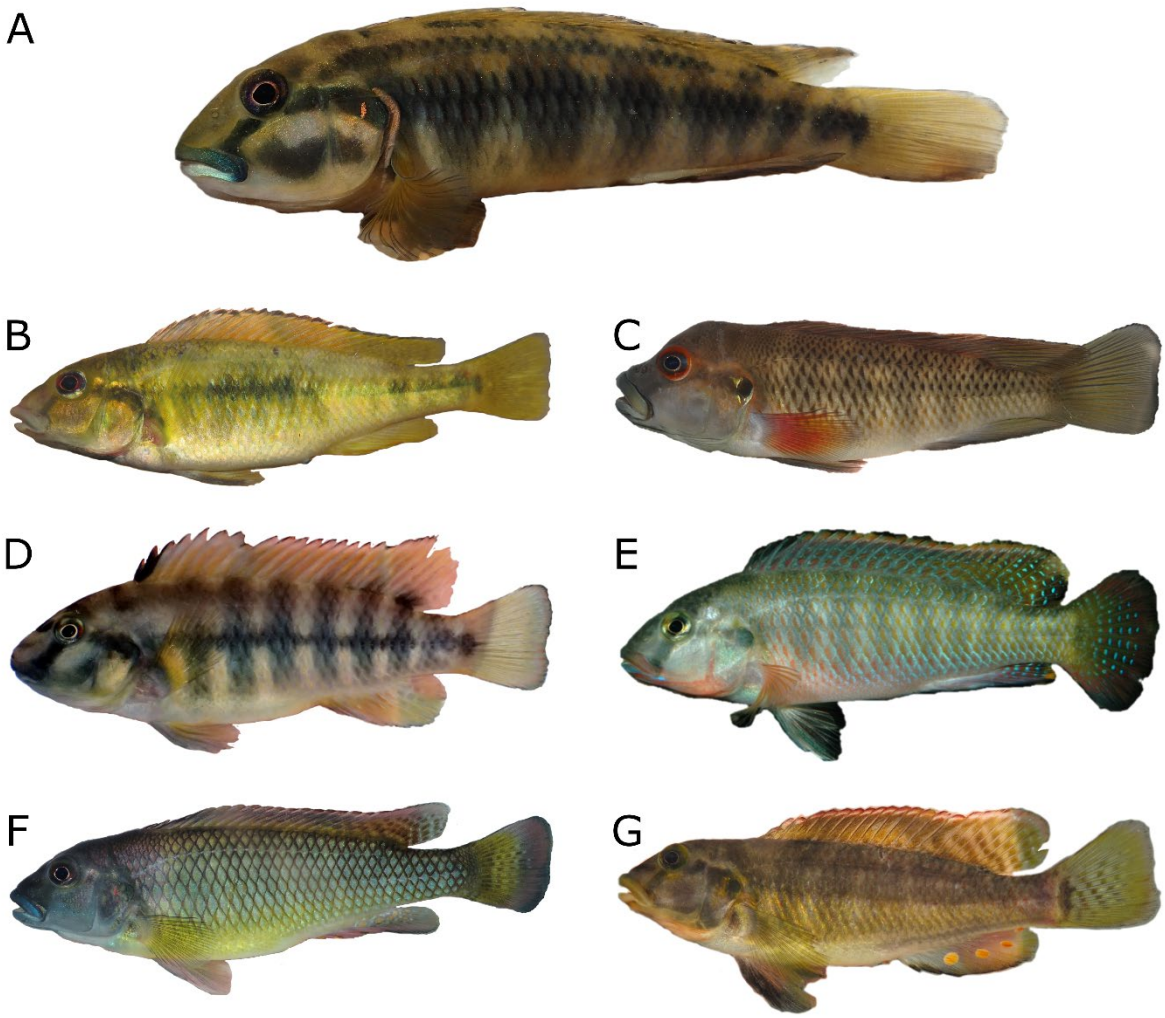

Figure 2: Overview of representative taxa currently placed in the polyphyletic genus *Orthochromis*. Preliminary working names for lineages which appear clearly distinct of the *Orthochromis* sensu stricto (Malagarasi-*Orthochromis*; sensu Weiss et al. 2015) based on molecular data and the corresponding phylogenetic relationships are indicated and follow the studies of (Schedel et al. 2020; Schedel et al. 2019; Schedel et al. in preparation; Weiss et al. 2015). A. *Orthochromis uvinzae* (Tribe/Lineage: *Orthochromis* sensu stricto; photo: F.D.B. Schedel); **B.** *Orthochromis luongoensis* (Tribe/Lineage: Haplochromini; 'extended *Pseudocrenilabrus*-group', 'Northern-Zambia-Orthochromis'; photo: F.D.B. Schedel); **C.** *Orthochromis polyacanthus* (Tribe/Lineage: Haplochromini, 'extended *Pseudocrenilabrus*-group', LML-*Orthochromis*; photo: F.D.B. Schedel); **D.** *Orthochromis indermauri* (Tribe/Lineage: Haplochromini, 'extended *Pseudocrenilabrus*-group', '*Orthochromis indermauri*'; photo: F.D.B. Schedel); **E.** *Orthochromis machadoi* (Tribe/Lineage: Haplochromini, 'extended Pseudocrenilabrus-group', most likely a member of the genus *Pseudocrenilabrus*; photo: E. Schraml); **F.** *Orthochromis torrenticola* (Tribe/Lineage: Haplochromini, 'extended serranochromines', '*Orthochromis. torrenticola* species complex'; photo: F.D.B. Schedel); **G.** *Orthochromis gecki* (Tribe/Lineage: Haplochromini, 'extended serranochromines', Katanga-*Orthochromis*; photo: Katanga 2016 Expedition).

Divergence time estimates for the family Cichlidae

Over the past decades, tremendous efforts have been made to elucidate the age and origin of the family Cichlidae and the reconstruction of their biogeographical history. Although evidence is accumulating for a Late Cretaceous to Palaeocene age for the family (reviewed in Matschiner 2019), a long-standing discussion on the evolutionary time scale of cichlids preceded those findings.

The striking Gondwana-like distribution of the family Cichlidae (see Figure 1) led to the traditional predisposition that the divergence of the four cichlid subfamilies was linked to the fragmentation of the this supercontinent, i.e. implying a Late Jurassic or Early Cretaceous origin of the family (Farias et al. 1999; Sparks and Smith 2004; Stiassny 1987; Stiassny 1991; Streelman et al. 1998). This "vicariance hypothesis" is further supported by the phylogenetic relationships of cichlid subfamilies which reflects the well-studied chronological sequence of the fragmentation of the supercontinent (Sparks and Smith 2004). For example, the divergence of the Ptychrominae from its sister group, the monophylum comprising the Old World Pseudocrenilabrinae and New World Cichlinae, matches the breakup of the Madagascar/Indian landmass from the remaining Gondwanaland, which started around 150 Mya; this, while it is assumed that Madagascar reached its current position in relation to Africa roughly 120 Mya (Ali and Aitchison 2008; Matschiner 2019; Matthews et al. 2016). The sister relationship of Pseudocrenilabrinae and Cichlinae could be linked to the tectonic separation of Africa and South America which is assumed to have been completed around 103 Mya (Heine et al. 2013; Matthews et al. 2016). Likewise, the relationships of three genera Madagascan *Paretroplus* Bleeker 1868 and *Etroplus* Cuvier 1830 and *Pseudetroplus* Bleeker 1862 [in Günther 1862] from India and Sri Lanka of the subfamily Etroplinae mirrors the separation of the Indian subcontinent and Madagascar which was dated to 90-85 Mya (Ali and Aitchison 2008; Storey 1995).

In contrast to these ancient tectonic events, the oldest cichlid fossils are much younger. They belong to the extinct genus †*Mahengechromis* Murray 2000 from palaeo-crater lake Mahenge (Singida Plateau, Tanzania), whose sediments have been dated to 45.83 ± 0.17 Mya based on U/Pb isotope analysis (Harrison et al. 2001; Murray 2000; Murray 2001b). Although the precise phylogenetic placement of †*Mahengechromis* is uncertain, the presence of a single supraneural bone suggests a placement within a subgroup of the extant Pseudocrenilabrinae, i.e. excluding

Heterochromis, *Tylochromis* Regan 1920 and *Etia* Schliewen & Stiassny 2003 which have two supraneural bones (Murray 2001b; Schliewen and Stiassny 2003). The oldest South American cichlid fossils †*Gymnogeophagus eocenicus* Malabarba, Malabarba & Del Papa 2010, †*Plesioheros chaulidus* Perez, Malabarba & Del Papa 2010 and †*Proterocara argentina* Malabarba, Zuleta & Del Papa 2006 have been described from the lacustrine "Faja Verde" deposits of the Lumbrera Formation (Argentina). The exact age of the "Faja Verde" deposits are still under discussion but it most likely ranges between 40 Mya, constrained by the age of the above lying tuffs (del Papa et al. 2010), and 45 Mya representing the maximum age of the Casamyoran South American Land Mammal Age (SALMA) to which the Lumbrera Formation was assigned to (del Papa et al. 2010; Matschiner 2019; Vucetich et al. 2007). The young age of these oldest cichlid fossils appear (~ 46 Mya) in stark contrast to the old divergence ages implied by the vicariance hypothesis, e.g. for the ~ 103 Mya split of Pseudocrenilabrinae and Cichlinae. According to this, Pseudocrenilabrinae and Cichlinae would have left not fossil trace for a time span of roughly 60 Mya, and even longer if a Late Jurassic to Early Cretaceous age of origin is assumed for the family Cichlidae (Friedman et al. 2013; Matschiner 2019; Murray 2001a). Therefore, it was proposed that the observed biogeographic patterns are the result of 'through oceanic dispersal', i.e. implying that the divergence of cichlids must have started only after the final breakup of Gondwana (Murray 2001a; Vences 2001). Although most cichlids are freshwater fishes, a few species are known to thrive in brackish and sometimes even marine conditions, and they are even capable to breed in these environments (Matschiner 2019). This has been reported, for example, for introductions of the African cichlid *Oreochromis mossambicus* (Peters 1852) into the lagoons and estuaries on the marine Fanning Atoll (Lobel 1980). This and similar findings render a trans-oceanic dispersal scenario likely, or, at least it is not improbable; this particularly, if the factor of time is taken into account, because marine dispersal potential most likely has not remained unchanged over the last ~ 100 Mya (see Matschiner (2019) for a detailed discussion).

The two competing hypotheses have led to highly divergent assumptions about the age and biogeographic history of cichlids. This, in turn, is reflected by highly conflicting divergence time estimates obtained by a growing body of molecular clock studies aiming to skrutinize the phylogenetic time line of cichlids, i.e. divergence time estimates for the family Cichlidae range from 45 Mya to 160 Mya (Matschiner 2019; Schedel et al. 2019). Likewise, divergence time estimates of more shallow nodes, e.g. for those of the radiations of the Great African lakes, are highly contradicting and hence also of limited use with regard to inferences and insights drawn

from these results for the evolutionary biology of cichlids, particularly the explanations about the rapid origin of ecologically and morphologically megadiverse species flocks (Matschiner 2019).

Bayesian molecular clock analyses have mostly been used in these studies, but it is important to note, that they are highly dependent on numerous assumptions, which may compromise their confidence in resulting estimates. Most importantly, molecular clock calibrations are commonly conducted by applying temporal constraints on at least one node of the tree, because real substitution rates are unknown. These constraints are either provided by fossil or geological evidence (Bromham et al. 2018; Ho and Duchêne 2014). In particular, calibrations applied to the root were shown to affect divergence time estimates more than those applied on shallower internal nodes. Application of multiple well-scrutinized calibration points should render divergence estimates more consistent (Duchêne et al. 2014; Ho and Duchêne 2014). Many calibration points for various cichlid clades have been proposed over the last decades, but not all have been well scrutinized. Several assume a correlated divergence of endemic clades, e.g. those of the Great African Lakes, with the onset of geological formation of the respective lakes, for instance the estimated age of the most ancient Lake Tanganyika has been used as a calibration point for the origin of the EAR (Day et al. 2008; Koblmüller et al. 2008a). Analogously, presumed desiccation and refilling events of lake basins, e.g. the re-establishment of lacustrine conditions of the Lake Malawi has been used to constrain the node age for the origin of the Lake Malawi cichlid radiation (Sturmbauer et al. 2001). Unfortunately, these approaches are problematic, not only because of the complex and not yet fully understood history of the formation of the East African rift lakes, but also because of accumulating evidence from fossils and molecules that several of the Lake Tanganyika endemic tribes might have evolved well before the formation of the lake itself (Altner et al. 2017; Schedel et al. 2019; Weiss et al. 2015).

Likewise, the incorporation of cichlid fossils into molecular clock analyses has remained a demanding task. In contrast to the incredible extant species richness, only comparatively few cichlid fossil species have been described (Murray 2001a), and this despite several new fossil taxa have been described recently from East Africa (Altner et al. 2017; Kevrekidis et al. 2019; Penk et al. 2019). Up to now, only about 37 cichlid fossil species are known from articulated fossils and additional ones have been described from disarticulated material such as bones and teeth, which are even more difficult to place phylogenetically (Kevrekidis et al. 2019; Penk et al. 2019). As an additional problem, phylogenetic assignment of cichlid fossil species into the

cichlid tree of life remains difficult due to, among others factors, the paucity of phylogenetically informative morphological characters (see Penk et al. 2019). It was further pointed by Friedman (2013) that convergent evolution of morphological characters is a widespread phenomenon, and this complicates morphology-based phylogenetic placement of cichlid fossils (Albertson and Kocher 2006; Hulsey et al. 2018; Muschick et al. 2012; Rüber and Adams 2001). Yet, after careful examination at least six cichlid fossils could established as calibration points (Matschiner et al. 2016; Schedel et al. 2019), although only a single recently described fossil (†*Tugenchromis pickfordi* Altner, Schliewen, Penk & Reichenbacher 2017) is available for the calibration of the megadiverse EAR. Notably, up to now there is no fossil calibration point available for the EAR-subclade Haplochromini, i.e. the lineage which gave rise to the megadiverse species flocks of Lake Malawi and Lake Victoria.

Despite of all these obstacles, the spatio-temporal reconstruction of cichlid phylogenetic relationships is continuously progressing and remains crucial to understand the evolutionary history of cichlids as well as the underlying processes which shaped the incredible diversity of this fish family.

The genomic record of rheophilic cichlids in the light of landscape evolution

The multidisciplinary field of "biogeomorphology", a subdiscipline of geomorphology, aims to elucidate the complex interactions between geomorphological, ecological and biological systems and processes over a broad temporal and spatial spectrum (Viles 2019). Although the underlying ideas of the concept can be traced back to the 19th century, the term biogeomorphology was coined by Viles (1988) and is based on the observation that the distribution of various organisms is often tightly linked to the underlying geomorphology (landforms), while, vice versa, organisms do influence earth surface processes impacting the evolution of landforms (Naylor 2005; Viles 2011; Viles 2019). Within the larger framework of biogeomorphology and comparative biogeography recently, the concept of geoecodynamics was introduced by Cotterill and De Wit (2011). The concept integrates landscape evolution with the evolutionary history of living biota and theoretically enables to reconstruct the tempo and mode of geomorphological processes by exploiting the genomic record. Geoecodynamical research relies on the assumption that the history of landforms and that of organism living on those are causally interlinked by ecological associations. Hence, the formative events, e.g. tectonic events altering the landscape structure, potentially leave signatures in the form of

DNA- (nucleotide sequence) changes in the genomic record of species, either due to ecological selection or due to disrupted or newly generated genetic connectivity between species inhabiting these landscapes (Cotterill and de Wit 2011). Ultimately, these temporal correlates of these signatures can be traced along phylogenetic trees, and thus, can be dated using molecular clock analysis (Cotterill and de Wit 2011). Clearly, not all taxa are equally well suited for this purpose, as species differ in their ecology ranging from ecological generalists (eurytopic species) to ecologically highly specialized species (stenotopic species). The latter are commonly more confined to certain types of landforms and habitats, which further is reflected by their generally higher vulnerability to landscape changes (Cotterill and de Wit 2011; Pickett et al. 2007). Therefore, especially stenotopic species and their corresponding phylogeographic records are supposedly ideally predisposed to preserve co-evolutionary signatures of landform and associated biota changes; this renders aquatic species of special interest for geoecodynamic questions, because they are naturally confined stringently to geographically and ecologically well defined landforms (Cotterill and de Wit 2011).

While fish in general are stenotopic because they are confined to aquatic habitats, they nevertheless have evolved countless ecological specializations, expressed by very narrow ecological niche boundaries and thus, many taxa are tightly restricted to their habitats. For example, members of the predatory genus *Hydrocynus* Cuvier 1816 (family: Alestidae, tigerfish) are restricted to large rivers and lakes of Africa due to their dependence on well-oxygenated freshwater (Otero et al. 2011; Skelton 1994); hence, their biogeographic patterns have been recently linked to Neogene tectonic events that, despite all tectonic changes, must have allowed for the persistence of large, well-oxygenatied river landscapes (Goodier et al. 2011). Other examples are the highly specialized cichlids of the Great African Lakes, particularly rock-dwelling cichlids of Lake Malawi ("mbuna"), which are specialized to a life in rocky habitats and show a tight fidelity to their habitats (Fryer and Iles 1972; Konings 2007; Konings 2019). But most nogetably the rheophilic cichlids, e.g. those fluviatile cichlids confined and specialized to live in rocky rapids, as e.g. members of the genus *Steatocranus* Boulenger 1899 and, to some extent, members of the genus *Nanochromis* Pellegrin 1904, can be regarded as highly valuably biotic indicators for studies in geoecodynamics (Cotterill and de Wit 2011). Indeed, it has been shown that the geomorphological evolution and hydrological origin of the modern Congo River with its principal knickpoints, e.g. the Inga rapids, is tightly interlinked to the evolutionary history of the species flocks of *Steatocranus* and *Nanochromis* endemic to the Lower Congo rapids (Schwarzer et al. 2011). Interestingly, the onset of

speciation of a third riverine species flock endemic to the Lower Congo rapids, i.e. 'Lower Congo *Lamprologus* clade' formed by several species of the genus *Lamprologus* Schilthuis 1891, was dated to Late Miocene to Early Pliocene age, too, which is concordant with the onset of divergence of the two other lower Congo endemic radiations of *Steatocranus* and *Nanochromis* (Schedel et al. 2019).

Another promising cichlid group for the spatio-temporal reconstruction of the landscape evolution using a geoecodynamical approach are those rheophilic haplochromine cichlids currently placed in the polyphyletic genus *Orthochromis* (see above). Notably, among the six different recognized "haplochromine *Orthochromis"* lineages, five occur in fast flowing rivers and rapids of the Katanga-Chambeshi region. Large parts of this region are located in the southwestern extension of the East African Rift system which is a tectonically highly dynamic landscape (Chorowicz 2005; Cotterill 2005; Kipata et al. 2013; Mondeguer et al. 1989). Since the late Miocene, the landscape of the region has been radically reshaped through recurrent episodes of active faulting and rifting which led to substantial changes in the course of major rivers and to reorganizations of the ancient drainage networks including river and stream captures, and furthermore, to the formation of several large lakes in the region such as Lake Bangweulu, Lake Mweru and Lake Upemba (Chorowicz 2005; Cotterill 2004; Cotterill and de Wit 2011; Moore et al. 2012; Moore et al. 2007; Olivotos et al. in review). Particularly the intense seismic activity lead to the creation of numerous knickpoints in the focal area including several major waterfalls (Flügel et al. 2015; Flügel et al. 2017; Olivotos et al. in review). It is commonly assumed that these major knickpoints, rapids and waterfalls, constrained limits of and shaped fish dispersal in south-central Africa (Bell-Cross 1968; Skelton 1994). Interestingly, some waterfalls in the Katanga-Chambeshi region appear to represent effective barriers for upstream migration of fish even leading to allopatric speciation events, which maybe best exemplified by the sister group pair of '*Orthochromis torrenticola* species complex'. It is endemic to the Lufira River with at least two species known, one yet undescribed species from below the Kyubo waterfalls and its described sister species *O. torrenticola* from above the falls (Schedel et al. 2018; Schedel et al. in preparation). In the same way, the waterfall series of three falls of the Kalungwishi River, i.e. the Lumangwe, Kabweluma and Kundabikwa appear to have given rise to a small species assemblage consisting of members of the 'Northern-Zambia-*Orthochromis'* (Schedel et al. in preparation). In particular, several unnamed species closely related to *O. kalungwishiensis* described from above the Kundabikwa falls by Greenwood and Kullander (1994), have been recorded from Kalungwishi River system; these species are

referred here to as '*Orthochromis kalungwishiensis* species complex'. However, the evolutionary history of those candidate species belonging to the '*Orthochromis kalungwishiensis* species complex' are less well understood and their taxonomic status still needs to be clarified (see discussion). Independent of that, the molecular-clock-derived divergence age estimates for the most recent comment ancestor (MRCA) of the '*Orthochromis torrenticola* species complex' as well as for the divergence of the '*Orthochromis kalungwishiensis* species complex' are of paramount interest for geo-ecomorphology, as both can be used to date the knickpoint formation of these major landforms; or, alternatively, they might be used to scrutinize node age estimates in other parts of the cichlid phylogenetic tree, which, in turn would allow for scrutinizing dates of additional geomorphological key events related to cichlid evolution. This in turn, might lead to a better overall understanding of cichlid evolution of haplochromine species complexes in East African, particularly with regard to the presumed tectonic controls on the famous explosive cichlid speciation (see discussion).

Thesis outline

The Results part of this thesis is organized in two sections. The first section includes three publications (chapters 1 – 3) which aimed to provide new insights into the biodiversity of East African cichlid radiations with focus on the taxonomy of the still understudied riverine and rheophilic cichlids of the Katanga-Chambeshi region. The second section comprises two publications (chapters 4 – 5) and focusses on the reconstruction of the evolutionary history of austrotilapiine cichlids by providing new divergence time estimates as well as additional support for widespread hybridization and introgression among the lineages of this megadiverse clade.

Section 1: Diversity and taxonomy of cichlids in southern and central Africa with a focus on rheophilic taxa

The first publication (**chapter 1**) presented in this section aimed to clarify whether there is a second species of the previously monotypic Lake Tanganyika endemic genus *Hemibates* Regan 1920. This had been was suggested by Konings (1998) who reported male *Hemibates* specimens from Chituta Bay (Zambia) with flank color patterns clearly distinctive from those known from *Hemibates stenosoma* (Boulenger 1901a). Based on the morphological and molecular evidence

as well as on differences in the mentioned male color pattern, *Hemibates koningsi* Schedel & Schliewen 2017 could be described, thereby adding a valuable contribution to the still ongoing assessment of the taxonomic diversity of the endemic cichlids of Lake Tanganyika (Ronco et al. 2019). Further, the chapter provides a critical compilation of previously (Barel et al. 1977; Dunz and Schliewen 2010; Schedel et al. 2014) and newly defined meristic characters as well as morphological measurements used in African cichlid taxonomy. This compilation proved to be helpful for the description of African cichlid species, because many taxonomic data acquisition methods have remained poorly communicated and defined. Hence it will facilitate future alpha-taxonomical studies on this family.

The second publication (**chapter 2**) represents a first step towards the systematic revision of the polyphyletic genus *Orthochromis.* In total, five new rheophilic species were described, two from the Upper Lualaba ecoregion (*Orthochromis kimpala* Schedel, Vreven, Katemo Manda, Abwe, Chocha Manda & Schliewen, 2018 and *O. gecki*), two from the Bangewlu-Mweru-ecoregion (*Orthochromis mporokoso* Schedel, Vreven, Katemo Manda, Abwe, Chocha Manda & Schliewen, 2018 and *O. katumbii* Schedel, Vreven, Katemo Manda, Abwe, Chocha Manda & Schliewen, 2018) and one from the lower reaches of the Lufubu River ,i.e. from within the drainage of the Lake Tanganyika ecoregion (*O. indermauri*). Due to their superficial phenotypical similarity with the Malagarasi-*Orthochromis,* these new species were only provisionally placed in the genus *Orthochromis,* a generic assignment that will last only until a comprehensive revision of haplochromine genera becomes available. This provisional step was further justifiable by the fact that the phylogenetic relationships of haplochromine cichlids, especially those of the rheophilic taxa currently placed in the genus *Orthochromis*, had not been fully elaborated by the time: however, at the time of the submission of the present thesis this gap of knowledge has been partly being filled by results presented in **chapter 4 & 5**. Overall, the study highlights our lack of knowledge on the ichthyological diversity of the Katanga-Chambeshi region and stipulates the urgent need of further systematic research in that region.

The third publication (**chapter 3**) introduced and formally described two new monotypic haplochromine genera, namely *Palaeoplex* endemic to the Kalungwishi and Luongo River (Bangweulu-Mweru ecoregion) and *Lufubuchromis* endemic to the upper reaches of the Lufubu River. These genus descriptions with their necessary genus-wide comparison initialized the overdue taxonomic revision of the 'extended *Pseudocrenilabrus* group'. The species of the two new genera had been included in several phylogenetic studies before their formal description. These studies had already partially revealed their complex evolutionary origin with evidence

for ancient hybridization events and the capture of mitochondrial haplotypes; this despite their phenotypical similarity with the species of the genus *Pseudocrenilabrus,* (Koblmüller et al. 2012; Koblmüller et al. 2008a; Meier et al. 2019; Schedel et al. 2019; Schedel et al. in preparation). Yet, both genera are clearly diagnosable from the genus *Pseudocrenilabrus* by several morphological characters as well as from potential ancient hybridization partners (different precursor lineages of the 'Northern-Zambian-*Orthochromis*'). Up to date, the *Pseudocrenilabrus*-group (sensu Weiss et al. 2015; Schedel et al. 2019) has only been defined by molecular evidence. Therefore, a comparison of morphological characters of the different species and genera associated with the *Pseudocrenilabrus*-group was provided as a starting point for further systematic research on this major haplochromine lineage.

Section 2: New divergence age estimates for the major cichlid lineages with focus on the African austrotilapiine cichlids.

The first publication (**chapter 4**) presented in this section represents another important contribution to the spatio-temporal reconstruction of the evolutionary history of cichlids. Based on a large mitogenomic dataset encompassing ten mitochondrial protein coding genes and including representative species of almost all major cichlid lineages and tribes, new divergence age estimates were estimated successfully for the family Cichlidae. The focus was set on the East African cichlid cichlid radiation (EAR), for which a new fossil calibration point (†*Tugenchromis pickfordi*) had become available in the course of my thesis. The systematic assignment of cichlid fossils to extant lineages and genera proved to be a difficult task (see e.g. Penk et al. 2019), and hence the suitability of all cichlid fossils as calibration points for molecular clock analysis have to be carefully scrutinized before using them as informative constraints for selected clade ages. The presented study therefore provides a critical re-evaluation of cichlid fossils as well as of geological constraints used in previous studies as calibration points for various cichlid clade ages, and this assessment will undoubtedly serve as a guideline for following molecular clock studies. Acknowledging the remaining uncertainties concerning the true age of the Cichlidae (see introduction) as well as those of the exact phylogenetic placement of certain cichlid fossils (e.g. of †*Tugenchromis*, see Penk et al. 2019), eighteen different calibration schemes were applied to thoroughly evaluate the impact of alternative calibration settings on divergence time estimates. Roughly, the resulting Bayesian divergence time estimates were in line with the 'dispersal hypothesis' (e.g. Friedman et al.

2013; Matschiner et al. 2016; Murray 2001a) and tentatively support the assumption for a Late Cretaceous to Palaeocene age for the Cichlidae as recently advocated for by Matschiner (2019). Yet, divergence time estimates for MRCA of EAR and most Lake Tanganyika endemic cichlid tribes were recovered to be substantially older than the supposed maximum age for the formation of the Lake Tanganyika basin. This result is consistent with the "Melting-pot Tanganyika" hypothesis (Weiss et al. 2015) and the "Ancient Reservoir" hypothesis (Genner et al. 2007). The "Melting-pot Tanganyika" hypothesis postulates that the precursor lineages of the various Lake Tanganyika endemic tribes had diverged already before the formation of extant Lake Tanganyika, e.g. in precursor lakes and adjacent river systems; only subsequently they would have amalgamated within the Lake Tanganyika basin (Weiss et al. 2015). In summary, the study underlines the important role that riverine cichlid taxa must have played in the evolutionary history of the EAR. This may best be exemplified by the case of *Haplochromis vanheusdeni* Schedel, Friel & Schliewen 2014. This species was described from the Great Ruaha River drainage, a coastal East African drainage. It was included here for the first time in a molecular phylogenetic study, and, interestingly, it was recovered as a sister group of the Lake Tanganyika endemic Tropheini, suggesting for the first time a past connection between the proto-Malagarasi / Lake Tanganyia and the Great Ruaha River drainage.

The last manuscript (**chapter 5**) presented in this thesis focused on the detection of ancient hybridization events among austrotilapiine cichlid lineages. Ancient hybridization and introgression are increasingly recognized to have played a key role in the evolutionary history of cichlids and might even have fueled the adaptive radiation of the Great African Lakes (Irisarri et al. 2018; Meier et al. 2017; Meier et al. 2019; Schwarzer et al. 2012a; Schwarzer et al. 2012b; Weiss et al. 2015). Using a combination of extensive molecular datasets including nuclear ddRAD data and mitochondrial genome data and applying different lines of evidence (D statistics and cyto-nuclear discordance) allowed not only to re-evaluate previously detected signals of hybridization but also led to the detection of numerous new potential hybridization events. Especially between and among the three major haplochromine lineages, the 'extended serranochromines', the 'extended *Pseudocrenilabrus*-group' and the 'ocellated eggspot Haplochromini', hybridization appears to be widespread. Particularly, lineages belonging to the polyphyletic genus *Orthochromis* appear to have been involved in different ancient hybridization events. Furthermore, several cases of ancient mitochondrial haplotype captures have been detected, e.g. for the aforementioned case of *H. vanheusdeni*, some of which, intriguingly, went without leaving an apparent nuclear genomic signature of introgression. This

important latter point highlights the importance of mitochondrial genome data for studying the evolutionary history of cichlids, even in the “age of phylogenomics”. In addition, the study aimed to clarify the comparability of divergence time estimates derived from different data, i.e. either obtained from data sets based on mitochondrial sequences or from massive nuclear (ddRAD) data sets. For a meaningful comparison, two reduced datasets have been generated, covering almost exactly the same representative taxon sampling. While one was based on 610 nuclear ddRAD loci (alignment length: 113.578 bp), the other one was based on ten mitochondrial protein coding genes (alignment length: 7884 bp). Subsequently, two molecular clock analyses were conducted based on these two data sets under fully identical calibration schemes. Resulting divergence time estimates of the two analyses were largely congruent, as reflected, e.g., by widely or totally overlapping 95 % highest posterior density (HPD) intervals of the corresponding node ages; however, 95 % HPD intervals obtained from the nuclear dataset were generally wider than those obtained from the mitochondrial data. These results are in line with previous findings which had suggest that site rates of ddRAD loci and of mitochondrial DNA might be similar (see Near et al. 2018), and that that divergence time estimates obtained from these datatypes are likely to yield comparable estimates.

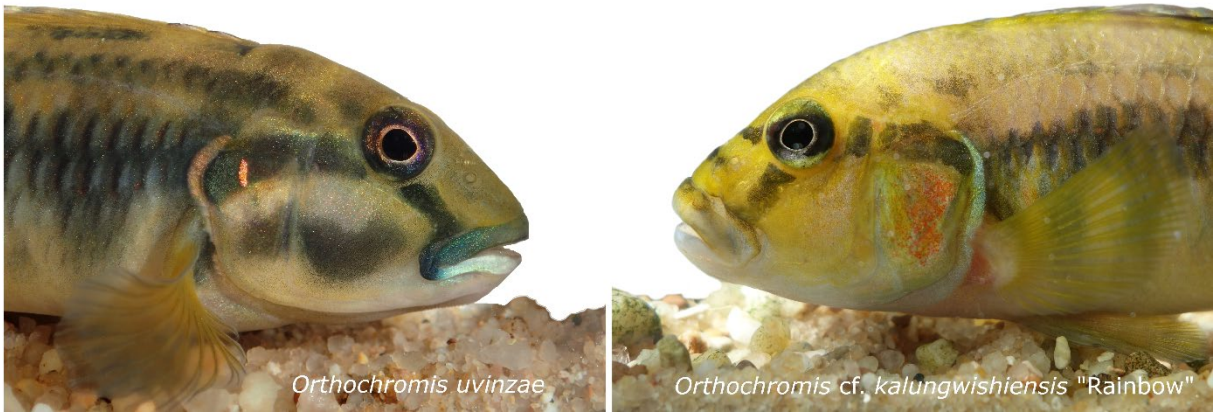

Results

Section 1: Diversity and taxonomy of cichlids in southern and central Africa with a focus on rheophilic taxa

The papers presented in this section are copyrighted and were published by Zootaxa (https://www.mapress.com/j/zt)

Orthochromis indermauri in the natural habitat (Lufubu River)

Zootaxa 4312 (1): 092–112
http://www.mapress.com/j/zt/

Article

ISSN 1175-5326 (print edition)
ZOOTAXA
ISSN 1175-5334 (online edition)

https://doi.org/10.11646/zootaxa.4312.1.4
http://zoobank.org/urn:lsid:zoobank.org:pub:D48F2C29-8553-4926-A449-9FB9D34D52CE

Hemibates koningsi spec. nov: a new deep-water cichlid (Teleostei: Cichlidae) from Lake Tanganyika

FREDERIC DIETER BENEDIKT SCHEDEL[1] & ULRICH KURT SCHLIEWEN
SNSB-Bavarian State Collection Zoology, Münchhausenstr. 21, 81247 München, Germany.
E-mail: schedelfred@hotmail.de; schliewen@zsm.mwn.de
[1]Corresponding author. E-mail: schedelfred@hotmail.de

Abstract

Hemibates koningsi, new species, is described from southern Lake Tanganyika (Republic of Zambia) as the second species of *Hemibates* Regan, 1920. Males of the new species are easily distinguished from *H. stenosoma* (Boulenger, 1901) based on their adult color pattern, i.e. black vertical bars on the anterior flanks part and posterior horizontal bands on a silvery-whitish body coloration vs. an anterior flank color pattern of black blotches of variable number, size and shape and posterior horizontal bands. Males and females of the new species are further distinguished by their longer lower pharyngeal jaw (37.6–38.2% HL vs. 27.8–32.5% HL) with a characteristically curved keel, which is straight or only slightly curved towards the tips in *H. stenosoma*. The new species has on average fewer gill rakers on the first gill arch than its only congener (33–37 vs 35–43).

Key words: Lake Tanganyika, Bathybatini, *Hemibates*, new species

Introduction

Lake Tanganyika, the deepest of the East African Great Lakes, harbors the most diverse cichlid species flock with regard to behavioral, phenotypic, and ancient genetic diversity (Muschick et al 2012). The monotypic deep-water genus *Hemibates stenosoma* Boulenger, 1901 is one of its least known and most enigmatic members of the ancient Lake Tanganyika cichlid flock. Like some of the closely related *Bathybate*s species, *H. stenosoma* is an epibenthic shrimp and fish predator, inhabits depths between around 40 and 210 m, even approaching anoxic deepwater layers. Despite its lake-wide distribution it appears abundant only at the southern part of the lake, possibly because of its preference for very deep sandy and muddy bottoms, which are only oxygenated in the southern part of Lake Tanganyika (Poll 1956, Coulter *et al.* 1991). It is a maternal mouthbrooder, and, together with *Bathybates vittatus*, *B. ferox* and *Petrochromis polyodon* it is the cichlid with largest eggs (7.0 mm diameter) known so far (Kuwamura 1986, Coulter *et al.* 1991, Duponchelle *et al.* 2008).

Species of *Bathybates* and *Hemibates* are sexually dimorphic with male species-specific flank color patterns, which have been suggested to play an important role in mate recognition and for reproductive isolation among closely related congeners (Kirchberger *et al.* 2012). The pattern of male *H. stenosoma* consists of black blotches of variable number, size and shape on the anterior flank, which are followed posteriorly by broad horizontal bands. Females are entirely silvery-whitish without any distinctive color pattern (Boulenger 1901, Coulter 1991). Interestingly, a second male color morph with black vertical bars instead of blotches on the anterior flanks followed by narrow horizontal bands had been reported from Chituta Bay (Zambia) by Konings (1998). He offered three alternative hypotheses with regard to that male phenotype: it could be (1) either an ontogenetic color phase that would develop only in large males, (2) a polychromatic species, i.e. with alternative coloration of all life history stages, as only large males with stripe pattern have been documented until then, or (3) it simply might represent a second *Hemibates* species (Konings 1998, 2015, Koblmüller et a. 2005). Koblmüller *et al.* (2005) in their mtDNA based investigation of Lake Tanganyika deepwater cichlids were unable to differentiate unambiguously between both phenotypes, but they had only one colored male and three females in their sample. Although they had detected

92 *Accepted by J. Armbruster: 11 Jul. 2017; published: 28 Aug. 2017*

in *Hemibates* strongly divergent haplotypes as compared to the species of the genus *Bathybates*, they could not refer them to one of the two color morphs.

Based on a preliminary inspection of a *Hemibates* sample from southern Lake Tanganyika (Mpulungu region) it became apparent that both phenotypes are not only distinguishable based on coloration but also exhibit differences in body shape and the lower pharyngeal jaw morphology. Morphological comparisons of this sample with the syntype series as well as genetic comparisons of a comparatively large sample support a view of species specific differences of the two phenotypes. Here, we present these data and describe the striped phenotype as a second *Hemibates* species.

Material and methods

Material. Morphometric comparisons are based on 42 specimens of *Hemibates stenosoma* specimens including all syntypes and nine specimens of the new *Hemibates* species described in this paper from the following institutions: the Royal Museum for Central Africa, Tervuren, Belgium (MRAC); the Natural History Museum, London, United Kingdom (BMNH); the Bavarian State Collection of Zoology, Munich, Germany (ZSM).

TABLE 1. Overview of meristics and their corresponding definitions based on: 1 = Barel *et al.* 1977, 2 = Dunz and Schliewen 2010, 3 = Schedel *et al.* 2014 and/or 4 = new or alternatively defined meristics.

Meristics:	Short Definition:	Recommended tool:
Dorsal-fin spines[1]	Total number of spinous rays	radiograph
Dorsal-fin rays[1]	Total number of soft (branched) rays	radiograph
Anal-fin spines[1]	Total number of spinous rays	radiograph
Anal-fin rays[1]	Total number of soft (branched) rays	radiograph
Pelvic-fin spines[4]	Total number of spinous rays	stereomicroscope
Pelvic-fin rays[4]	Total number of soft (branched) rays	stereomicroscope
Pectoral-fin rays[2]	Total number of soft (branched) rays	stereomicroscope
Upper procurrent caudal fin rays[4]	Total number of upper procurrent caudal rays; only rays not connected to upper hypurals (3,4 and 5) are counted	radiograph
Lower procurrent caudal fin rays[4]	Total lower procurrent caudal rays; only rays not connected to lower hypurals (1 and 2) and parhypural are counted	radiograph
Caudal fin rays[4]	Total caudal rays, all caudal rays are counted (including rays on hypurals)	radiograph
Scales (horizontal line)[2]	Number of scales along the horizontal line from the edge of the opercle to the base of caudal fin; including the lower lateral line scales and excluding scales on the caudal fin	stereomicroscope
Upper lateral line scale[2]	Number of scales on the upper lateral line (only pored scales are counted)	stereomicroscope
Lower lateral line scales[2]	Number of scales on the lower lateral line (only pored scales are counted)	stereomicroscope
Circumpeduncular scales[3]	Circumpeduncular scales on the level of the 4th pored scale (posterior most scales = 1st scale, excluding pored scales on caudal fin) of the lower lateral line	stereomicroscope
Series of Scales on check[1]	Number of scales ventrally of eye counted on a vertical line (representing more or less horizontal rows)	stereomicroscope
Scales (horizontal line) on operculum[3]	Scales between edge of the postero-dorsal angle of the operculum to the anterior edge of the operculum where the preoperculum begins	stereomicroscope
Scales between lateral line and dorsal-fin origin[3]	Scales between lateral line and dorsal fin origin (below insertion of the 1st dorsal fin spine); counted in a vertical alternating (zigzag) manner; excluding the pored lateral line scale	stereomicroscope

.....continued on the next page

TABLE 1. (Continued)

Meristics:	Short Definition:	Recommended tool:
Scales between upper lateral line and last dorsal-fin spine[3]	Scales below insertion of last dorsal spine and upper lateral line; counted in a vertical alternating (zigzag); excluding the lateral line pored scale	stereomicroscope
Abdominal vertebrae[1]	Total number of abdominal vertebrae; bear laterally displaced parapophyses and lack closed hemal arches and spines	radiograph
Caudal vertebrae[1]	Total number of caudal vertebrae; lack parapohyses and pleural ribs and bear well-developed hemal and neural spines; urostyle is excluded from count	radiograph
Total number of vertebrae[1]	Total number of vertebrae excluding the urostyle	radiograph
Teeth in upper outer row[1]	Total number of teeth in upper outer row	stereomicroscope
Teeth in lower outer row[4]	Total number of teeth in lower outer row	stereomicroscope
Teeth rows in upper jaw[1, 3]	Number of jaw tooth rows (one outer and one or more inner) in upper jaw; counted from behind the anterior tip of the premaxillae	stereomicroscope
Teeth rows in lower jaw[1, 3]	Number of jaw tooth rows (one outer and one or more inner) in lower jaw; counted from behind the anterior tip of lower jaw	stereomicroscope
Gill rakers (ceratobranchial)[1, 2]	Number of gill rakers on the first (most rostral) ceratobranchial (lower) gill-arch are counted; excluding gill rakers on the cartilaginous plug (angle between ceratobranchial and epibranchial gill-arch)	stereomicroscope
Gill rakers (angle + epibranchial)[2]	Number of gill rakers on the first (most rostral) epibranchial (upper) gill-arch are counted; including gill rakers on cartilaginous plug	stereomicroscope
Total gill rakers[4]	Total number of gill rakers on the first (most rostral) gill-arch; including gill rakers form the ceratobranchial, cartilaginous plug and epibranchial	stereomicroscope
Morphological features:		
State of hypurals (1 and 2)[3]	(1) hypurals fused (seamless unit); (2) hypurals separated by a clearly visible seam but never fused into a single seamless unit; (3) hypurals separated.	radiograph
State of hypurals (2 and 3)[3]	(1) hypurals fused (seamless unit); (2) hypurals separated by a clearly visible seam but never fused into a single seamless unit; (3) hypurals separated.	radiograph
Position of the pterygiophore supporting last dorsal fin spine[4]	Recorded is the vertebra number (counted from anterior to posterior) at which pterygiophore of last dorsal fin spine is attached to the neural spines (inferred by proximity to the neural spine) of corresponding vertebrae (e.g. if pterygiophore is embedded between neural spines of 18th and 19th vertebrae the 18th vertebra is recorded)	radiograph
Position of pterygiophore supporting last anal fin spine[4]	Recorded is the vertebra number (counted from anterior to posterior) at which pterygiophore of last anal fin spine is attached to the hemal spine (inferred by proximity to haemal spine) of corresponding vertebrae; (e.g. if pterygiophore is embedded between hemal spine of 14th and 15th vertebrae the 15th vertebra is recorded; in rare cases hemal spine are not fully developed or the corresponding vertebra is still an abdominal vertebra)	radiograph

Morphology and principal component analysis. Twenty-eight meristic characters were examined either based on stereomicroscope observations or on digital x-rays (Faxitron UltraFocus LLC x-ray unit), following either Barel *et al.* (1977), Dunz & Schliewen (2010) or Schedel *et al.* (2014), and some are new or are alternatively defined in this study; for a comprehensive list see Table 1. The anterior basis of flank scales of *Hemibates* might be covered with minute, cycloid to weakly ctenoid scales (Fig 4). Those minute scales were not included in squamation counts. In addition, we recorded several anatomical features concerning the caudal fin skeleton (state

of hypuralfusion), the pterygiophore insertion pattern of dorsal and anal fins see Table 1. Distance measurements followed either Barel *et al.* (1977), Dunz & Schliewen (2010) or Schedel *et al.* (2014) while one measurement (interpectoral width) is newly defined in this study; for a comprehensive list see Table 2. Measurements were taken point-to-point on the left side of specimens using digital caliper (accuracy of 0.01 mm) and were rounded to the nearest 0.1 mm. Head measurements taken are given as percentage of head length (HL), all remaining measurements are given as percentage of standard length (SL). Additionally, we took three measurements from X-ray pictures of dissected lower pharyngeal jaws and which are given in percentage of the head length (HL). Principal component analysis (PCA) using a covariance matrix was performed with the statistical program PAST 3.07 (Hammer *et al.* 2001) for 24 log transformed morphometric measurements indicated in Table 2. Scores of most informative principal components PC II and PC III are plotted against each other for visualization and variables contributing most to PC variation were identified using their loadings as tabulated.

TABLE 2. Overview of morphometric measurements and their corresponding definitions based on: 1 = Barel *et al.* 1977, 2 = Dunz and Schliewen 2010, 3 = Schedel *et al.* 2014 and/or 4 = new or alternatively defined morphometric measurements.

Measurement:	Short Definition:	Used for PCA in this study (log-transformed raw measurements):
Total length[2]	Distance between rostral tip of snout and an imaginary line drawn between the two lobe tips of caudal fin (bilobular length)	No
Standard length (SL)[1, 2]	Distance between rostral tip of snout and caudal-fin base at articulation (flexion point of hypurals at end of hypural plate)	X
Head length (HL) given in % SL[1, 2]	Distance from the rostral tip of snout to the caudal end of the membranous border of operculum; interorbital width, minimal distance between orbits (membranous)	X
Given in % HL		
Interorbital width[1, 2]	Minimal distance between orbits (membranous)	X
Preorbital width[2]	Width between the left and right preorbital process	X
Horizontal eye length[1, 2]	Distance (excluding ligamentous ring) from the rostral point of the orbit (at lateroethmoid to lacrymal bone) to the ventral point (at sphenotic-circumorbitals) of the postorbital process of the neurocranium	X
Snout length[1, 2]	Distance from the rostral tip of upper lip to the rostral point of the membranous border of the orbit (as in the horizontal eye length but including the ligamentous ring)	X
Internostril distance[2]	Minimum distance between the bases of the tubular nostrils	X
Cheek depth[1, 2]	Vertical distance from the rearmost point on the lower rim of the preopercle to the membranous margin of the orbit	X
Upper lip length[2]	Distance from anterior tip of upper lip (at symphysis of upper jaw) to posteriormost point of upper lip	X
Lower lip length[2]	Distance from anterior point of lower lip (at symphysis of lower jaw) to posteriormost point of lower lip	X
Lower lip width[2]	Horizontal distance from left to right distal corner of lower lip (taken across the width of the head)	X
Lower jaw length[1, 2]	Distance from the rostral to the caudal tip of the retroarticular process marked by the insertion of the well-developed interopercular-mandibular ligament	X
Lower pharyngeal jaw length[1, 4]	Measurements are taken from radiographs or digital pictures; measured from the rostral point of the element (seen on its dentigerous area) perpendicularly to the line connecting the caudal tips of the horns	No

.....continued on the next page

TABLE 2. (Continued)

Measurement:	Short Definition:	Used for PCA in this study (log-transformed raw measurements):
Lower pharyngeal jaw width[1, 4]	Measurements are taken from radiographs or digital pictures; distance between the caudal tips of the horns is measured	No
Width of dentigerous area of Lower pharyngeal jaw[1, 4]	Measurements are taken from radiographs or digital pictures; distance between the lateral margins of the most lateral left and right teeth (or tooth-sockets).	No
Given in % SL		
Predorsal distance[2]	Horizontal length from anterior tip of upper lip (at symphysis of the upper jaw) to the insertion of the first dorsal-fin spine	X
Dorsal fin base length[2]	Length of dorsal-fin base distance between rostral and caudal base	X
Last dorsal-fin spine length[2]	Length of last dorsal-fin spine from the insertion to its distal end	X
Anal-fin base length[2]	Length of anal-fin base distance between the rostral and caudal base	X
Third anal-fin spine length[2]	Length of third anal-fin spine, from the insertion to its distal end	X
Pelvic fin length[2]	Distance between insertion of pelvic-fin spine and distal end of longest pelvic-fin ray	No
Pectoral fin length[1, 2]	Distance from insertion of uppermost pectoral-fin ray to distal end of longest ray	X
Caudal peduncle depth[1, 3]	Measured on the level of the 4th scale (posterior most scales = 1st scale, excluding pored scales on caudal fin) of the lower lateral line	X
Caudal peduncle length[1, 2]	Horizontal distance between the vertical line through the caudal most point of the anal-fin base to the end of hypural plate	X
Body depth (pelvic fin base)[1, 2]	Body depth at the pelvic-fin base	X
Preanal length[2, 4]	Distance between the rostral tip of symphysis of lower jaws and the posterior edge of the anus	X
Anus-anal fin base distance[2]	Distance between caudal border of anus and the articulation of first anal-fin spine	X
Interpectoral width[4]	Distance between pectoral fin base to pectoral fin base	X

Molecular methods and phylogenetic analysis. Fin clips were taken from freshly caught (dead) specimens obtained from local fishermen. Each specimen was photographed and subsequently fixed in formalin roughly following suggested sample procedures of Neumann (2010). Extraction of total genomic DNA was done by using the DNeasy Blood & Tissue Kit (Qiagen) following the manufacturer´s protocol. Amplification of the mitochondrial protein coding gene ND2 (NADH dehydrogenase subunit 2) of 21 specimens was performed using the primer pair ND2Met/ND2Trp (Kocher *et al.* 1995) and the PCR protocol of Schwarzer *et al.* (2009). PCR products were purified using ExoSAP-IT (Affymetrix). Sequencing was performed using the Big Dye 3.1 sequencing chemistry (Applied Biosystems) on an ABI 3730 48 capillary sequencer (Applied Biosystems) at the Sequencing Service Unit of the Ludwig Maximilians Unversity Munich, Germany. Quality control and sequence editing based on electropherograms was done in Geneious v.7.05 (http://www.geneious.com, Kearse *et al.*, 2012) and uploaded to Genbank (see Table 3 for Genbank IDs). In addition, our data set was complemented with 30 sequences from GenBank (see Table 3 for Genbank IDs) of the genera *Bathybates* (N=20), *Hemibates* (N=4) and *Trematocara* (N=6). The 51 sequences were then aligned using the Geneious Alignment tool (implemented Geneious, default settings) and subsequently trimmed to a uniform length of 900 bp. Maximum likelihood (ML) analysis was performed on the CIPRES Science Gateway (Miller *et al.* 2010) using RAxML v8.2.6 (Stamatakis 2014). For doing so the alignment was partitioned into the first, second and third codon position and the substitution model GTR + Gamma was applied. Trematocarini and Bathybatini (including *Hemibates*) were recovered as sister groups in several phylogenetic studies bases on mitochondrial and as well on nuclear data (e.g. Salzburger *et al.* 2002, Koblmüller *et al.* 2005, Weiss *et al.* 2015, Takahashi & Sota 2016). Therefore, *Trematocara*

TABLE 3. Samples used for phylogenetic analysis are listed. Where applicable voucher information is given. GenBank accession numbers with corresponding main reference are given.

Genus	Species	Author	ZSM tissue No. / DNA Field number	ZSM collection number/or other repository number	Sampling location	Sex	Type status	Genbank accession no.	Reference study
Hemibates	*stenosoma*	(Boulenger, 1901)	DRC-2012/3106	ZSM-PIS-044564	Chituta Bay, purchased from fishermen	male	-	KY940058	This study
Hemibates	*stenosoma*	(Boulenger, 1901)	DRC-2012/3107	ZSM-PIS-044564	Chituta Bay, purchased from fishermen	male	-	KY940059	This study
Hemibates	*stenosoma*	(Boulenger, 1901)	DRC-2012/3108	ZSM-PIS-044564	Chituta Bay, purchased from fishermen	male	-	KY940060	This study
Hemibates	*stenosoma*	(Boulenger, 1901)	DRC-2012/3109	ZSM-PIS-044564	Chituta Bay, purchased from fishermen	male	-	KY940061	This study
Hemibates	*stenosoma*	(Boulenger, 1901)	DRC-2012/3120	ZSM-PIS-044679	Mpulungu, fish market	male	-	KY940062	This study
Hemibates	*stenosoma*	(Boulenger, 1901)	DRC-2012/3121	ZSM-PIS-044679	Mpulungu, fish market	male	-	KY940063	This study
Hemibates	*stenosoma*	(Boulenger, 1901)	DRC-2012/3122	ZSM-PIS-044679	Mpulungu, fish market	male	-	KY940064	This study
Hemibates	*stenosoma*	(Boulenger, 1901)	DRC-2012/3208	ZSM-PIS-044573	Mpulungu, fish market	male	-	KY940069	This study
Hemibates	*stenosoma*	(Boulenger, 1901)	DRC-2012/3123	ZSM-PIS-044567	Mpulungu, fish market	female	-	KY940065	This study
Hemibates	*stenosoma*	(Boulenger, 1901)	DRC-2012/3124	ZSM-PIS-044567	Mpulungu, fish market	female	-	KY940066	This study
Hemibates	*stenosoma*	(Boulenger, 1901)	DRC-2012/3125	ZSM-PIS-044567	Mpulungu, fish market	female	-	KY940067	This study
Hemibates	*stenosoma*	(Boulenger, 1901)	DRC-2012/3126	ZSM-PIS-044567	Mpulungu, fish market	female	-	KY940068	This study
Hemibates	*stenosoma*	(Boulenger, 1901)	-	-	Sumbu	-	-	AY663716	Koblmüller *et al.* 2005
Hemibates	*stenosoma*	(Boulenger, 1901)	-	-	Mpulungu	-	-	AY663717	Koblmüller *et al.* 2005
Hemibates	*stenosoma*	(Boulenger, 1901)	-	-	Mpulungu	-	-	AY663719	Koblmüller *et al.* 2005
Hemibates	*koningsi* sp. nov.		DRC-2012/3138	ZSM-PIS-045056	Mpulungu, fish market	male	Holotype	KY940051	This study
Hemibates	*koningsi* sp. nov..		DRC-2012/3139	ZSM-PIS-044677	Mpulungu, fish market	male	Paratype	KY940052	This study
Hemibates	*koningsi* sp. nov.		DRC-2012/3104	ZSM-PIS-044678	Mpulungu, fish market	male	Paratype	KY940050	This study
Hemibates	*koningsi* sp. nov.		DRC-2012/3179	ZSM-PIS-044571	Mpulungu, fish market	male	Paratype	KY940053	This study
Hemibates	*koningsi* sp. nov.		DRC-2012/3186	ZSM-PIS-044570	Mpulungu, fish market	male	Paratype	KY940054	This study

……*continued on the next page*

TABLE 3. (Continued)

Genus	Species	Author	ZSM tissue No. / DNA Field number	ZSM collection number/or other repository number	Sampling location	Sex	Type status	Genbank accession no.	Reference study
Hemibates	*koningsi* sp. nov.		DRC-2012/3243	ZSM-PIS-044565	Mpulungu, fish market	male	Paratype	KY940056	This study
Hemibates	*koningsi* sp. nov.		DRC-2012/3275	ZSM-PIS-044566	Mpulungu, fish market	female	Paratype	KY940057	This study
Hemibates	*koningsi* sp. nov.		DRC-2012/3342	BMNH 2016.9.1.2.	Mpulungu, fish market	male	Paratype	KY940055	This study
Hemibates	*koningsi* sp. nov.		DRC-2012/3103	MRAC 2017–005–P-0001	Mpulungu, fish market	male	Paratype	KY940049	This study
Hemibates	*sp.*		-	-	Mpulungu	-	-	AY663718	Koblmüller *et al.* 2005
Bathybates	*fasciatus*	Boulenger 1901	-	-	Lufubu estuary	-	-	AY663732	Koblmüller *et al.* 2005
Bathybates	*fasciatus*	Boulenger 1901	-	-	Lufubu estuary	-	-	AY663733	Koblmüller *et al.* 2005
Bathybates	*fasciatus*	Boulenger 1901	-	-	Lufubu estuary	-	-	AY663734	Koblmüller *et al.* 2005
Bathybates	*fasciatus*	Boulenger 1901	-	-	Near Kigoma	-	-	EF679236	Wagner *et al.* 2009
Bathybates	*ferox*	Boulenger 1898	-	-	Ulwile Island	-	-	AY663736	Koblmüller *et al.* 2005
Bathybates	*ferox*	Boulenger 1898	-	-	Mpulungu	-	-	AY663737	Koblmüller *et al.* 2005
Bathybates	*ferox*	Boulenger 1898	-	-	-	-	-	GQ167832	Schwarzer *et al.* 2009
Bathybates	*graueri*	Steindachner, 1911	-	-	Sumbu	-	-	AY663723	Koblmüller *et al.* 2005
Bathybates	*graueri*	Steindachner, 1911	-	-	Ulwile Island	-	-	AY663724	Koblmüller *et al.* 2005
Bathybates	*graueri*	Steindachner, 1911	-	-	Ulwile Island	-	-	AY663724	Koblmüller *et al.* 2005
Bathybates	*graueri*	Steindachner, 1911	-	-	Mpulungu	-	-	AY663726	Koblmüller *et al.* 2005
Bathybates	*hornii*	Steindachner 1911	-	-	Mpulungu	-	-	AY663735	Koblmüller *et al.* 2005
Bathybates	*leo*	Poll, 1956	-	-	Mpulungu	-	-	AY663729	Koblmüller *et al.* 2005

……continued on the next page

TABLE 3. (Continued)

Genus	Species	Author	ZSM tissue No. / DNA Field number	ZSM collection number/or other repository number	Sampling location	Sex	Type status	Genbank accession no.	Reference study
Bathybates	*leo*	Poll, 1956	-	-	Mpulungu	-	-	AY663730	Koblmüller *et al.* 2005
Bathybates	*leo*	Poll, 1956	-	-	Mpulungu	-	-	AY663731	Koblmüller *et al.* 2005
Bathybates	*minor*	Boulenger, 1906	-	-	Ulwile Island	-	-	AY663720	Koblmüller *et al.* 2005
Bathybates	*minor*	Boulenger, 1906	-	-	Ulwile Island	-	-	AY663721	Koblmüller *et al.* 2005
Bathybates	*minor*	Boulenger, 1906	-	-	Ulwile Island	-	-	AY663722	Koblmüller *et al.* 2005
Bathybates	*vittatus*	Boulenger, 1914	-	-	Mpulungu	-	-	AY663727	Koblmüller *et al.* 2005
Bathybates	*vittatus*	Boulenger, 1914	-	-	Mpulungu	-	-	AY663728	Koblmüller *et al.* 2005
Trematocara	*unimaculatum*	Boulenger 1901	-	-	Lake Tanganyika	-	-	AF317268	Klett & Meyer 2002
Trematocara	*marginatum*	Boulenger 1899	-	-	Lake Tanganyika	-	-	JX910898	Dunz & Schliewen 2013
Trematocara	*marginatum*	Boulenger 1899	-	-	Lake Tanganyika	-	-	JF900327	Muschick *et al.* 2012
Trematocara	*nigrifrons*	Boulenger 1906	-	-	Lake Tanganyika	-	-	JF900328	Muschick *et al.* 2012
Trematocara	*cf. variabile*	Poll 1952	-	-	Lake Tanganyika, Zambia	-	-	KJ176272	Weiss *et al.* 2015
Trematocara	*macrostoma*	Poll, 1952	-	-	Mpulungu	-	-	AY663715	Koblmüller *et al.* 2005

was chosen as outgroup for our RAxML analysis. Bootstrap analysis was automatically halted by RAxML (majority rule criterion) after 360 replications. Based on male color pattern and lower pharyngeal shape we assigned our *Hemibates* to one of the two phenotypes and subsequently compared mitochondrial haplotype clade position of corresponding specimens in our phylogenetic tree. Moreover, Kimura 2-parameter (K2P) genetic distances for *Hemibates* and *Bathybates* species were computed in MEGA7 (Kumar, Stecher, and Tamura 2015) under inclusion of all codon positions (pairwise deletion of ambiguous positions).

Results

PCA based on distance measurements (Fig. 1). In the PCA which was based on 24 morphometric measurements and included 51 *Hemibates* specimens (Fig. 1), PC I explained 92.8%, PC II explained 3.0%, and PC III explained 1.1% of the total variance. Factor loadings contributed to PC II were anus-anal fin base distance, interpectoral width and preorbital width and to PC III lower lip width, interpectoral width, and caudal peduncle length (see Table 4 for factor loadings PCI-PCIII). *Hemibates koningsi* **sp. nov.** and *Hemibates stenosoma* are mainly separated on the basis of low PC III scores for *H. koningsi* **sp. nov.** and high PC III scores for *H. stenosoma*. The separation is amongst others largely based on a combination of morphometric measurements derived from the head such as upper lip length, lower lip length, lower lip width, preorbital width, interorbital width and lower jaw length but also on the interpectoral width. In summary, the 24 morphometric measurements are able to separate the two phenotypes adding convincing support for the presence of a second *Hemibates* species.

TABLE 4. Factor loadings of PCI-III for all investigated specimens (N=51, see Fig. 1). Highest loadings for each principal component indicated in boldface.

Meristic	PC I	PC II	PC III
Standard length (SL)	0.20303	-0.011832	0.14864
Head length (HL)	0.19016	0.0056058	0.11758
Interorbital width	0.21972	0.0051824	0.26492
Preorbital width	**0.22876**	**0.11397**	-0.27411
Horizontal eye length	0.14778	-0.041001	0.15605
Snout length	0.2225	0.018887	-0.11361
Internostril distance	0.2066	0.054075	-0.027884
Cheek depth	0.2219	-0.011182	-0.0074499
Upper lip length	0.1975	0.11241	-0.16631
Lower lip length	0.18381	0.074297	-0.05131
Lower lip width	**0.24116**	0.060872	**-0.45202**
Lower jaw length	0.19037	0.068581	-0.050568
Predorsal distance	0.19676	-0.003764	0.15084
Dorsal fin base length	0.20902	0.047596	0.12104
Last dorsal fin spine length	0.17373	0.097398	0.024946
Anal fin base length	0.21745	0.00035501	0.30765
Third anal fin spine length	0.14675	0.034523	0.19993
Pectoral fin length	0.18435	0.075813	0.063969
Caudal peduncle depth	0.20252	-0.0032082	0.10919
Caudal peduncle length	0.21662	-0.027686	**0.32076**
Body depth	0.22296	0.030802	0.064003
Preanal length	0.19331	0.017534	-0.0021079
Anus-anal fin base distance	**0.22625**	**-0.92356**	-0.22612
Interpectoral width	0.22352	**0.28542**	**-0.44353**
Eigenvalue	0.246735	0.008061	0.002882
% variance	92.812	3.0322	1.0842

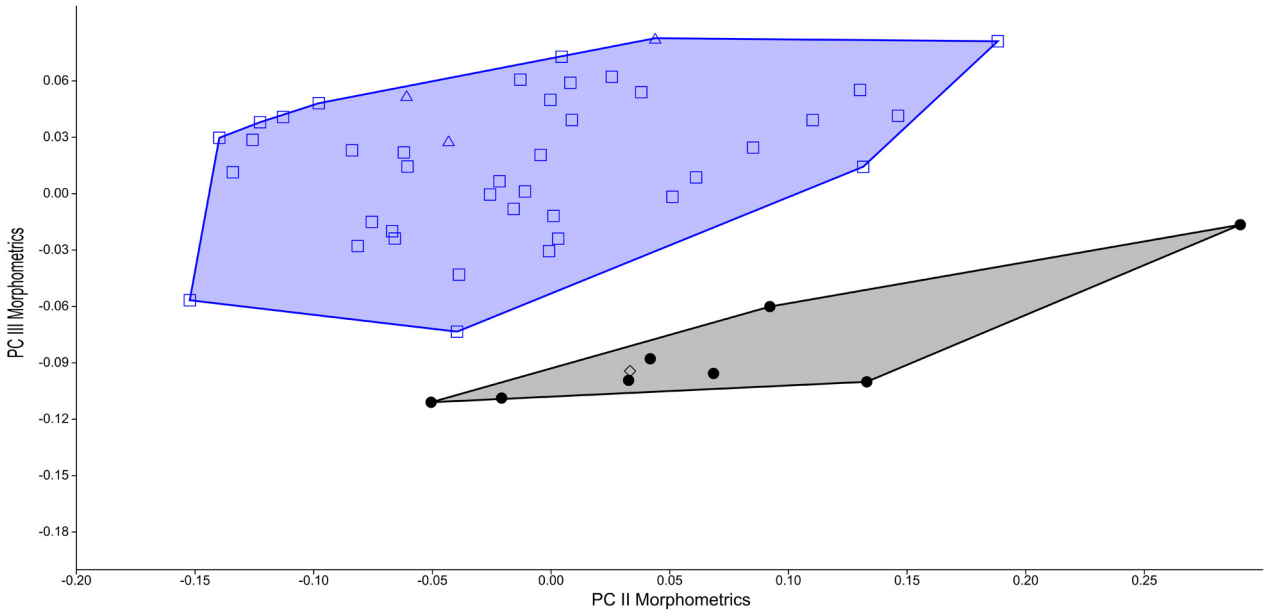

FIGURE 1. PCA scatter plot based on 24 morphometric measurements, species score limits visualized as convex hulls (N=51). PCII vs. PCIII. PC II explains 3.0% of the variance while PC II explains 1.1%. Dots = *Hemibates koningsi* **sp. nov.**, diamond = holotype of *Hemibates koningsi* **sp. nov.**, squares = *Hemibates stenosoma*, triangles = syntypes of *Hemibates stenosoma*.

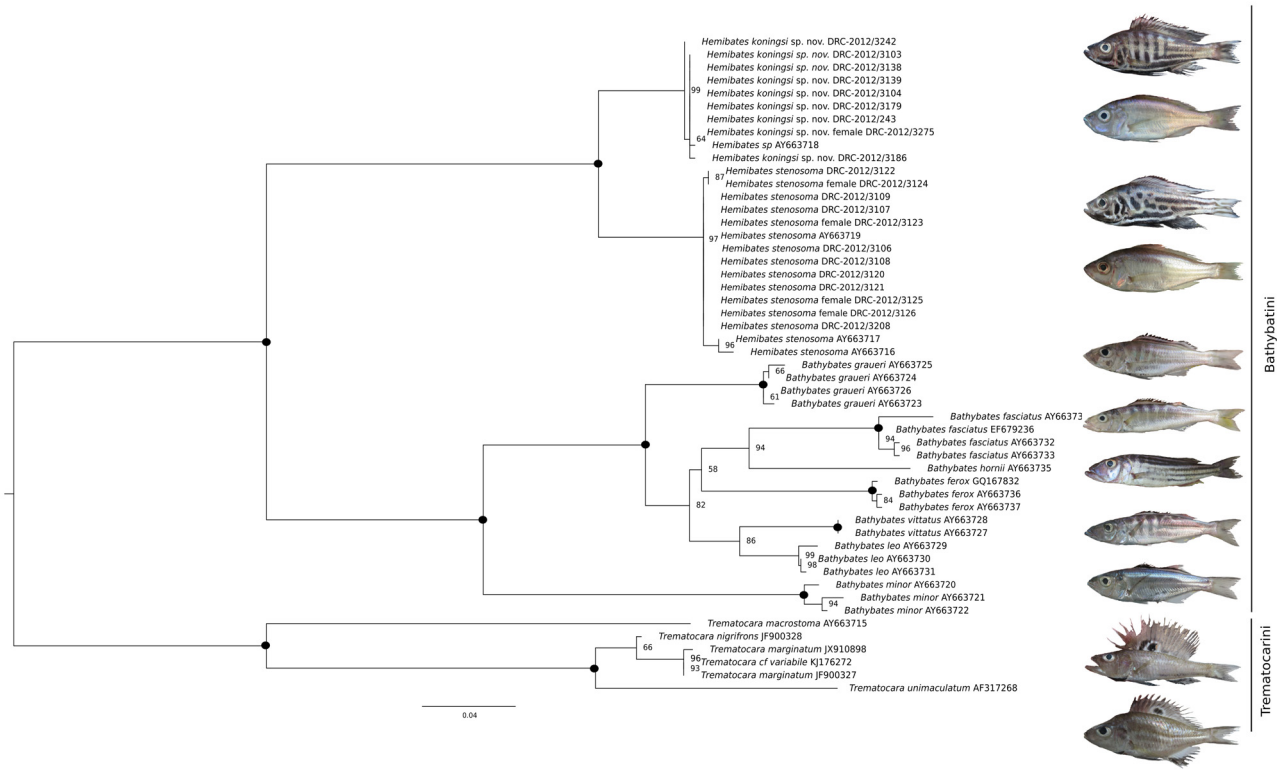

FIGURE 2. Maximum likelihood tree (RAxML; substitution model GTR + Gamma) of the Lake Tanganyika endemic cichlid genera *Hemibates* (2 species), *Bathybates* (7 species) and *Trematocara* (5 species) as outgroup based on 51 mitochondrial protein coding gene ND2 haplotypes (900 bp). Numbers at nodes represent bootstrap (BS) values based on 360 bootstrap replications. Black circles represent BS values of 100. BS values below 50 are not shown. Representative species and specimens depicted from the top to bottom: male *Hemibates koningsi* **sp. nov.** (ZSM 45056, DRC-2012/3138), female *Hemibates koningsi* **sp. nov.** (ZSM 44566, DRC-2012/3275), male *Hemibates stenosoma* (ZSM 44573, DRC-2012/3211), female *Hemibates stenosoma* (ZSM 44567, DRC-2012/3126), *Bathybates graueri*, *Bathybates fasciatus*, *Bathybates vittatus*, *Bathybates leo*, *Bathybates minor*, *Trematocara macrostoma* and *Trematocara unimaculatum*.

ML phylogenetic analysis of mtDNA haplotypes (Fig. 2). ML-analysis of ND2 data resulted in reciprocal monophyly of both genera, *Hemibates* and of *Bathybates* with high bootstrap support (100). Intrageneric relationships of *Bathybates* were largely congruent with previous mtDNA based hypotheses, i.e. with *B. minor* being the sister group of all remaining *Bathybates* species. In contrast to earlier results *B. ferox* was placed as sistergroup to a clade including *B. fasciatus* and *B. horni* instead to *B. vittatus* and *B. leo*. These relationships, however, were not well supported in our study nor in a previous study of Koblmüller *et al.* (2005). Within *Hemibates* two clades were recovered with high support. The first clade (BS 97) includes ND2-haplotypes of either males (N=8) with the blotch pattern or those of uniformly colored specimens (N=4) which had the same straight pharyngeal jaw phenotype as the blotched specimens. These are assigned to *Hemibates stenosoma*, because the syntype series is homogenous with regard to pharyngeal jaw morphology and the single male is a blotched specimen. The second clade (BS 99) included mainly males of the stripe coloration phenotype (N=8) and one female which had the curved pharyngeal jaw phenotype as our striped specimens. The four ND2-sequences generated by Koblmüller *et al.* (2005) fell into both clades, one into the stripe-clade (*H. koningsi* **sp. nov.**) and three into the blotch-clade (*H. stenosoma*), supporting the view that the two clades of Koblmüller *et al.* 2005 indeed belong to the same two phenotypes as those of our sample. The average K2P distance within *Hemibates* was 1.9% and of *Bathybates* 6.5%. The K2P distance between *Hemibates* and *Bathybates* was 13.1%, while K2P distances between *Bathybates* species varied between 3.2% (*B. leo* and *B. vittatus*) and 11.9% (*B. ferox* and *B. minor*); K2P distance between *H. stensoma* and *H. koningsi* **sp. nov.** was 3.6%, which is comparable to the range found for species pairs in the sister lineage *Bathybates*.

Hemibates koningsi sp. nov.

Hemibates sp. "stenosoma zambia" Konings 2015

Holotype. ZSM 45056 (1, 192.2 mm SL, male, DRC-2012/3138) Zambia, Northern Province, Lake Tanganyika, Mpulungu basin, no exact locality data available, purchased in Inguenyo fish market, Mpulungu (-8.73°/31.11°), F. Schedel, 28.VIII.2015

Paratypes. BMNH 2016.9.1.2. (1, 153.5 mm SL, males, DRC-2012/3242), Zambia, Northern Province, Lake Tanganyika, Mpulungu basin, no exact locality data available, purchased in Inguenyo fish market, Mpulungu (-8.73°/31.11°), F. Schedel, 05.IX.2015. MRAC 2017-005-P-0001 (1, 154.2 mm SL, males, DRC-2012/3103), Zambia, Northern Province, Lake Tanganyika, Mpulungu basin, no exact locality data available, purchased in Inguenyo fish market, Mpulungu (-8.73°/31.11°), F. Schedel, 23.VIII.2015. ZSM 44570 (1, 162.5 mm SL, male, DRC-2012/3186), Zambia, Northern Province, Lake Tanganyika, Mpulungu basin, no exact locality data available, purchased in Inguenyo fish market, Mpulungu (-8.73°/31.11°), F. Schedel, 01.IX.2015. ZSM 44565 (1, 150.8 mm SL, male, DRC-2012/3243), Zambia, Northern Province, Lake Tanganyika, Mpulungu basin, no exact locality data available, purchased in Inguenyo fish market, Mpulungu (-8.73°/31.11°), F. Schedel, 05.IX.2015. ZSM 44566 (1, 141,9 mm SL, female, DRC-2012/3275) Zambia, Northern Province, Lake Tanganyika, Mpulungu basin, no exact locality data available, purchased in Inguenyo fish market, Mpulungu (-8.73°/31.11°), F. Schedel, 07.IX.2015. ZSM 44571 (1, 99.9 mm SL, male, DRC-2012/3179) Zambia, Northern Province, Lake Tanganyika, Mpulungu basin, no exact locality data available, purchased in Inguenyo fish market, Mpulungu (-8.73°/31.11°), F. Schedel, 31.VIII.2015. ZSM 44677 (1, 106.1 mm SL, male, DRC-2012/3139) purchased with holotype. ZSM 44678 (1, 217.4 mm SL, males, DRC-2012/3104), Zambia, Northern Province, Lake Tanganyika, Mpulungu basin, no exact locality data available, purchased in Inguenyo fish market, Mpulungu (-8.73°/31.11°), F. Schedel, 23.VIII.2015.

Differential diagnosis. Adult males of the *Hemibates koningsi* can be distinguished from *H. stenosoma,* the only congener, by a flank color pattern of four to seven black vertical bars (two to three flank-scales wide) on the anterior flank region and five horizontal bands (one to two, rarely three flank-scales high) on the posterior flank region vs. black blotches of variable number, size and shape at the anterior part of the flanks and five (rarely four) horizontal bands in *H. stenosoma*. They can further be distinguished by the fourth horizontal band (counted from dorsal to ventral) starting below pectoral fin base sometimes before and extending to caudal fin base in *H. koningsi* vs. normally ending well before caudal fin base in *Hemibates stenosoma*. Moreover, both species exhibit a black band on dorsal fin membrane along the dorsal-fin base, which is however wider and more pronounced in *H. koningsi* males. Females as well as males of the new species can be unambiguously separated from *H. stenosoma*

by their longer lower pharyngeal jaw (37.6–38.2% HL, N=4 vs 27.8–32.5% HL, N=7) with a characteristically curved keel (distinctive bulge ventrally of the keel), which contrasts with the more or less straight keel of *H. stenosoma*, which is only rounded towards the tip (Fig. 4). Meristics of *H. koningsi* overlap with those of *Hemibates stenosoma,* but the new species on average has fewer gill rakers on the first gill arch (33–37 vs. 35–43). Ranges of morphometric measurements of the new species overlap with those of *H. stenosoma,* but *H. koningsi* tend to have longer lower jaws (44.0–47.1% HL vs 39.22–45.9% HL), longer upper lips (32.6–36.7% HL vs 27.6–33.6% HL) and longer lower lips (34.5–37.8% vs 30.1–36.0% HL).

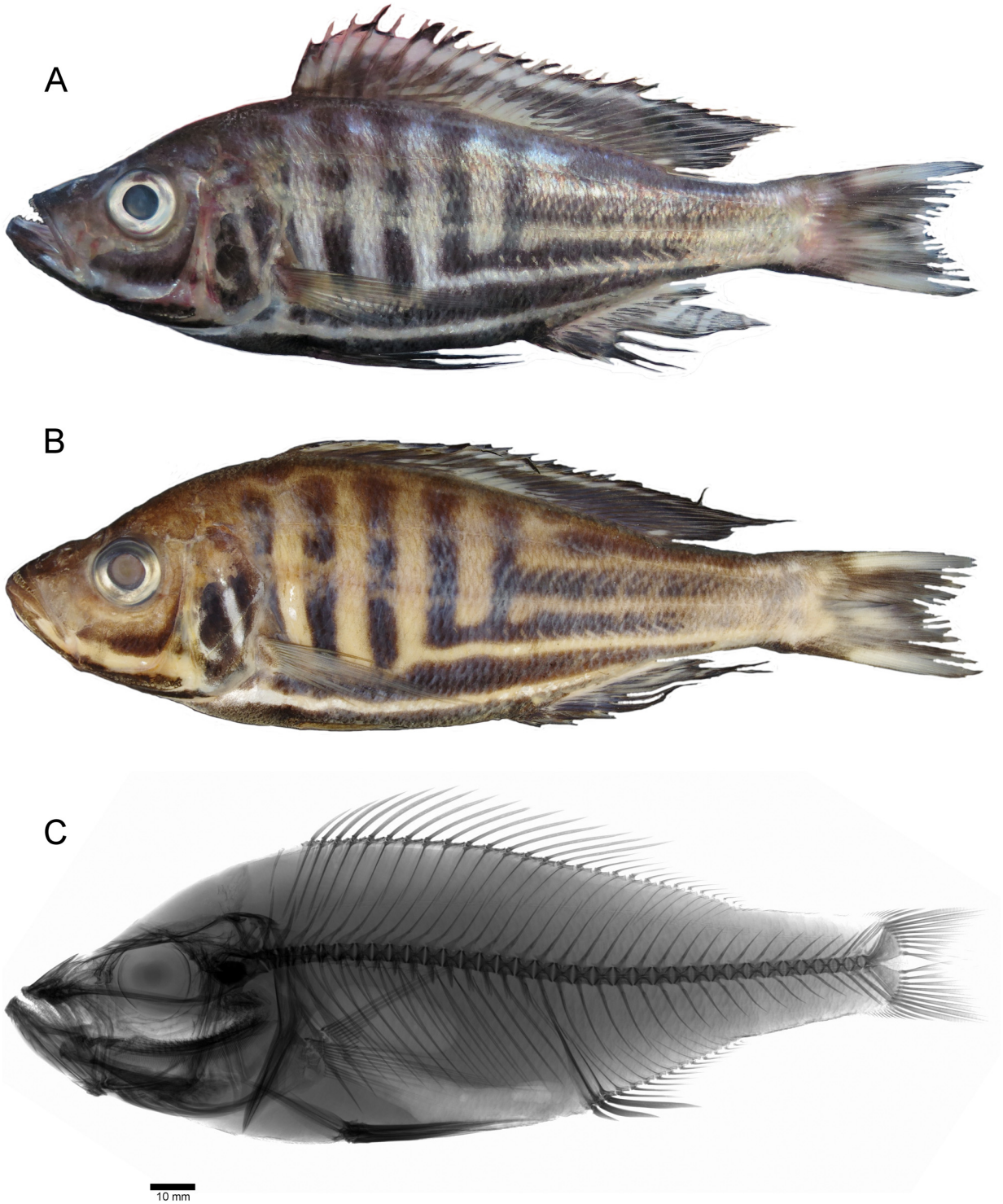

FIGURE 3. *Hemibates koningsi* **sp. nov. A.** Holotype, shortly after collection **B.** Holotype, ZSM 45056, DRC-2012/3138, 192.2 mm SL; Zambia, Northern Province, Lake Tanganyika, Mpulungu basin, no exact locality data available, purchased in Inguenyo fish market, Mpulungu **C.** radiograph of holotype.

Description. Morphometric measurements and meristic characters based on type specimens. Values and corresponding ranges presented in Table 5. For general appearance see Figs. 3 and 4. Maximum recorded total length of wild caught specimen (male) 262.2 mm with corresponding SL of 217.4 mm. Laterally compressed and relatively deep-bodied species with maximum body depth (31.6–34.8% SL) slightly behind dorsal-fin origin, decreasing towards caudal peduncle. Ratio of caudal peduncle length to depth: 1.55–1.92. Head length about one third of standard length. Dorsal head profile moderately concave with slightly visible premaxillary pedicel prominence. No nuchal gibbosity present. Eyes round, eye diameter less than one third of head length (26.2–31.1% HL) and larger than interorbital width. Jaws isognathous to slightly prognathous, lower jaw slightly protruding and comparatively narrow. Mouth strongly oblique. Posterior tip of maxilla not reaching level of eye. Lower lip anteriorly wider than upper lip. Lips not noticeably enlarged or thickened. Lachrymal with five sensory-canal pores. Two separate lateral lines.

TABLE 5. Measurements & counts for holotype and paratypes of *Hemibates koningsi* **sp. nov.**

Measurements	holotype	holotype + paratypes			
		min	Max	SD	n
Total length (mm)	235.5	124.6	262.2		9
Standard length SL (mm)	192.2	99.9	217.4		9
Head length HL (mm)	63.17	33.1	72.3		9
% HL					
Interorbital width	21.1	20.9	23.5	0.9	9
Preorbital width	29.7	27.9	31.5	1.2	9
Horizontal eye length	26.5	26.2	31.1	1.4	9
Snout length	32.6	31.5	33.3	0.6	9
Internostril distance	16.5	15.2	18.4	0.9	9
Cheek depth	26.7	22.6	26.7	1.3	9
Upper lip length	36.1	32.6	36.7	1.2	9
Lower lip length	35.8	34.5	37.8	1.1	9
Lower lip width	24.8	21.7	26.6	1.5	9
Lower jaw length	46.0	44..0	47.1	0.8	9
Lower pharyngeal jaw length	-	37.6	38.2	0.3	4
Lower pharyngeal jaw width	-	18.3	21.0	1.2	4
Width of dentigerous area of Lower pharyngeal jaw	-	12.9	14.7	0.8	4
% SL					
Predorsal distance	36.3	35.2	37.4	0.8	9
Dorsal fin base length	50.2	47.6	50.5	1.0	9
Last dorsal fin spine length	14.8	11.7	16.2	1.4	9
Anal fin base length	19.0	17.9	19.8	0.7	9
Third anal fin spine length	10.0	9.6	12.3	1.0	9
Pelvic fin length	28.4	24.4	39.1	4.3	9
Pectoral fin length	29.5	27.5	30.7	1.1	9
Caudal peduncle depth	11.2	10.7	12.0	0.4	9
Caudal peduncle length	20.0	18.4	20.9	0.9	9
Body depth (pelvic fin base)	34.2	31.6	34.8	1.1	9
Preanal length	62.5	61.8	67.0	1.7	9
Anus-anal fin base distance	3.3	1.8	3.9	0.6	9
Interpectoral width	12.0	9.7	12.4	0.9	9

.....continued on the next page

TABLE 5. (Continued)

Counts	holotype	holotype + paratypes			
		min	Max	SD	n
Dorsal fin spines	15	14(3); 15(6)			9
Dorsal fin rays	14	13(1); 14(4), 15(4)			9
Anal fin spines	3	3(9)			9
Anal fin rays	13	12(5); 13(2); 14(2)			9
Pelvic fin spines	1	1(9)			9
Pelvic fin rays	5	5(9)			9
Pectoral fin rays	13	13(6); 14 (3)			9
Upper procurrent caudal fin rays	9	8(1); 9(7); 10(1)			9
Lower procurrent caudal fin rays	10	9 (2); 10(7)			9
Caudal fin rays	34	33(1); 34(1); 35(6); 36(1)			9
Scales (horizontal line)	62	60(1); 61(3); 62(2); 63(1); 65(1)			8
Upper lateral line	65	58(1); 62(1); 63(1); 67(2); 69(2)			8
Lower lateral line	39	35(1); 36(4); 39(2); 43(1)			8
Circumpeducular	28	28(3); 30(4); 32(1)			8
Series of Scales on check	3	1(1); 2(5); 3(3)			9
Scales (horizontal line) on operculum	5	3(2); 4(2); 5(3); 6(2)			9
Scales between lateral line and dorsal fin origin	7	7(4); 8(5)			9
Scales between upper lateral line and last dorsal fin spine	5	5 (8)			8
Abdominal vertebrae	16	16(8);17(1)			9
Caudal vertebrae	18	17(2); 18(7)			9
Total number of vertebrae	34	33(1); 34(8)			9
Teeth in upper outer row	69	67(1); 69(1); 70(1); 72(1); 75(1); 77(1); 83(1); 84(2)			9
Teeth in lower outer row	58	41(1); 48(1); 51(1); 52(1); 56(1); 58(1); 59(1); 64(1); 67(1)			9
Gill rakers (ceratobranchial)	28	26(4); 27(2); 28(3)			9
Gill rakers (angle + epibranchial)	8	7(4); 8(3), 9(2)			9

Squamation. Flanks and dorsum covered with relatively large weakly ctenoid scales. Anterior base of some flank scales covered with minute, cycloid or weakly ctenoid scales (Fig. 4). Cycloid scales of ventral belly region smaller than on flanks. Cycloid chest scales, especially ventrally, smaller than flank scales; smallest scales on isthmus. Snout scaleless. Interorbital, nape and occipital region with slightly smaller scales than on flanks. Cheeks covered by one to three rows of cycloid scales about size of ventral belly scales. Operculum covered with ovoid and cycloid scales of variable size (small to about size of flank scales). Three to six scales on vertical line starting form edge of posterior-dorsal angle of operculum to anterior edge of operculum. Caudal fin scales small and becoming minute more caudally; scaled area may extend to more than half of the caudal fin.

Upper lateral line with 58–69 scales, lower lateral line with 35–43 scales and horizontal line with 60–65 scales plus one to three pored scales on caudal fin. Upper and lower lateral lines separated by three scales. Seven to eight scales between dorsal-fin origin and upper lateral line. 28–32 scales around caudal peduncle.

Jaws, dentition and gill rakers. Anterior teeth of outer row of lower and upper jaw unicuspid and widely and irregularly set. Teeth becoming smaller, less widely spaced and more regularly set towards mouth angle. Individual unicuspid teeth comparatively slender and slightly recurved with acutely pointed brownish crowns. Outer row of upper jaw with 67–84 teeth and outer row of lower jaw with 48–67 teeth in specimens between 99.9 and 217.4 mm SL. Neither number of teeth in the lower jaw nor of upper jaw is significantly correlated with SL (Pearson Correlation Coefficient: r-score for SL against number of teeth in the lower jaw -0,24593, p = 0.174533; r-score for

SL against number of teeth in upper jaw -0,32063, p= 0.399645). Unicuspid teeth of inner tooth rows smaller than those of outer rows, upper jaw with one or two inner tooth rows and lower jaw with single inner tooth row. Lower pharyngeal bone (Fig. 5) about 1.8 to 2.1 times longer than broad. Width of dentigerous area of lower pharyngeal bone 0.3 to 0.4 times length of lower pharyngeal bone length, with 26–27 teeth along posterior margin of dentigerous area. Individual teeth slender, beveled (i.e. bicuspid), with its labial side featuring several cusp protuberances, and always with a pointed major cusp. Lower pharyngeal jaw teeth largest along posterior margin of dentigerous area and becoming smaller towards the keel, anterior teeth slender and beveled sometimes unicuspid. Keel of lower pharyngeal bone characteristically curved with distinctive bulge on ventral keel. Total gill raker count 33–37, with six to eight epibranchials, one angle (cartilaginous plug) and 26–28 ceratobranchial rakers. Individual rakers long and slender. Smallest rakers anterior of ceratobranchial increasing in size towards cartilaginous plug. Gill raker of cartilaginous plug smaller than neighboring creatobranchial rakers. Epibranchial rakers decreasing in size dorsally.

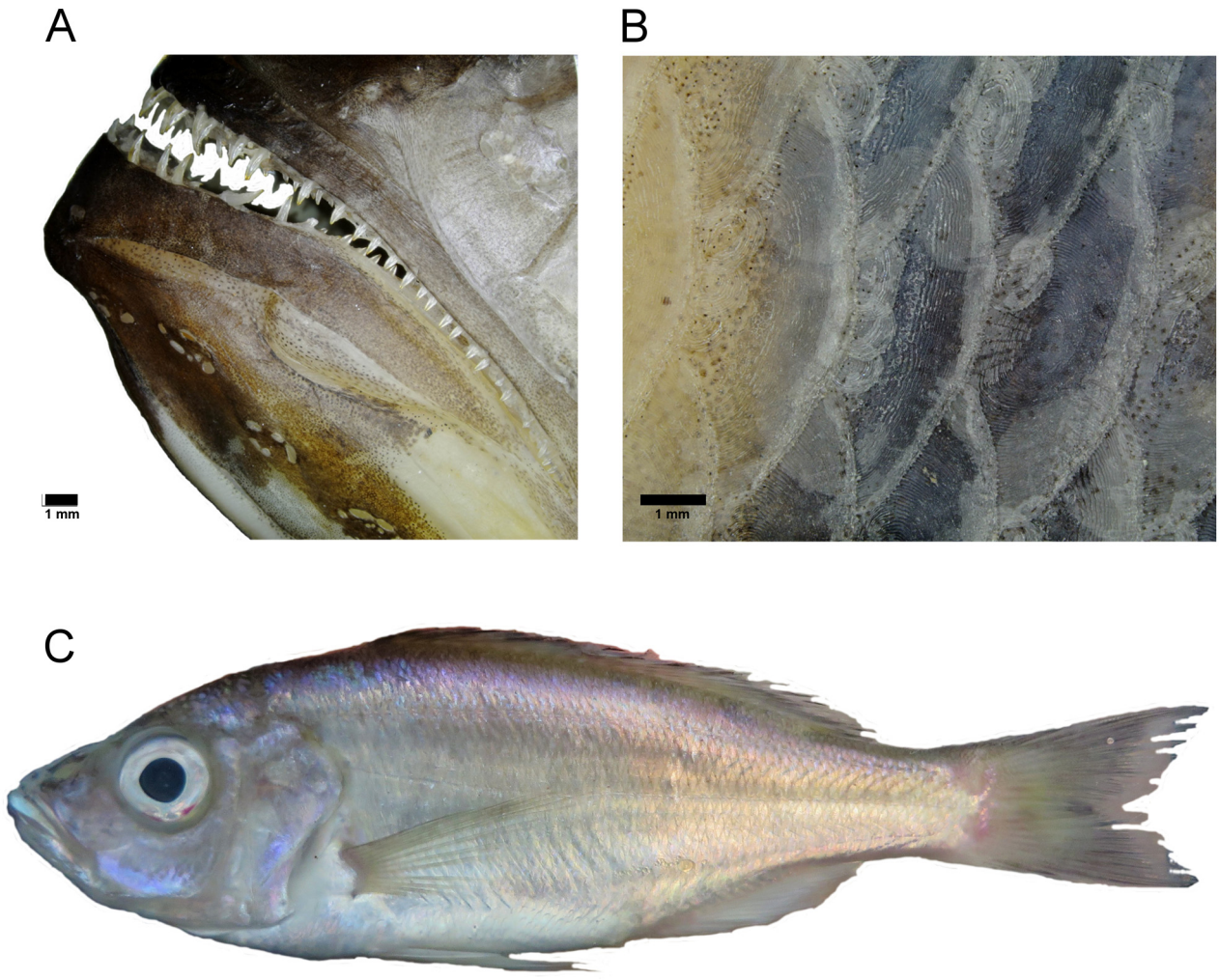

FIGURE 4. *Hemibates koningsi* **sp. nov. A.** Arrangement and morphology of oral jaw teeth (Holotype, ZSM 45056, DRC-2012/3138, 192.2 mm SL) **B.** Flank scales with minute, cycloid to weakly ctenoid scales on their anterior basis (holotype) **C.** Female *Hemibates koningsi* **sp. nov**, shortly after collection, ZSM 44566, DRC-2012/3275 141.9 mm SL; Zambia, Northern Province, Lake Tanganyika, Mpulungu basin, no exact locality data available, purchased in Inguenyo fish market, Mpulungu.

Fins. Dorsal fin XIV-XV, 13–15. First dorsal-fin spine shortest. Dorsal-fin base length 47.6–50.5% SL. Dorsal-fin rays of mature males extending to around level of caudal fin base whereas in young males (< 106 mm SL) and in females rays only extending to around the first half of caudal peduncle. Anal-fin rays not reaching caudal fin base in young males and in females, but reaching about first half of caudal peduncle. Anal fin III, 12–14; third anal-fin spine longest. Anal-fin base shorter (17.9–19.8% SL) than pectoral-fin length (27.5–30.7% SL). Pectoral fin with 13 or 14 rays; longest pectoral-fin ray (fifth ray, counted from dorsally to ventrally) more or less slightly

exceeding level of anus. Pelvic-fin base posterior to pectoral-fin base, separated by roughly three to five flank scale widths. Pelvic fin with one spine and five rays; first pelvic-fin ray longest, variably elongated in mature males, either terminating slightly before anal-fin origin or exceeding it slightly; in females and young males only slightly exceeding level of anus. Caudal-fin outline furcate and composed of 34–36 rays (16 principal caudal fin rays and 18 to 20 procurrent caudal fin rays).

Vertebrae and caudal fin skeleton (Fig. 3). Total vertebrae 33–34 (excluding the urostyle), with 16–17 abdominal and 17–18 caudal vertebrae. Pterygiophore supporting the last dorsal-fin spine located between the neural spines of the thirteenth and fourteenth vertebrae or of the fourteenth and fifteenth vertebrae. Pterygiophore supporting the last anal-fin spine located between hemal spines of seventeenth and eighteenth vertebrae, rarely between rips of the fourteenth (abdominal) vertebrae and hemal spine of the fifteenth (caudal) vertebrae. One single predorsal (supraneural) bone present. Hypurals 1 and 2 and hypurals 3 and 4 always fused into a single seamless unit.

Coloration in life (based on field photographs of freshly caught adult specimens; Fig. 3 and 4).

Pronounced sexual color dimorphism present. Males with distinct color pattern of black vertical bars (between two and three flank-scales wide) and horizontal bands (between one and two, rarely three flank-scales high). Body ground coloration silvery-whitish. Iris of eyes whitish with dusky areas. Cheeks, operculum and dorsum of freshly caught specimens sometimes in light purplish iridescent. Dorsal head surface, dorsal area of nape and area just below dorsal fin base dusky greyish-brown. Preorbital area whitish to dusky. Cheek with blackish horizontal stripe of variable shape and width below eye. Second horizontal stripe on ventral part of preoperculum, intraoperculum, and lower jaw, fused at the mental area with corresponding stripe of other side. Area between those stripes whitish including ventral area between lower jaws (area of the *musculus genio-hyoideus*) and ventral parts of branchiostegal membrane. Operculum and subopercular with two blackish vertical elements of variable shape and width. Four to seven blackish vertical bars at anterior part of flanks with first bar situated just behind gill cover; if seven vertical bars shape of most posterior bar blotchlike. Five horizontal bands present. Dorsalmost one in most specimens shortest starting on the level of first (anterior) dorsal-fin ray or behind it, extending to caudal fin base and dorsal caudal peduncle area, there fusing with the horizontal band of the other side. Second and third horizontal band (counted from dorsal to ventral) commencing anterior to dorsalmost horizontal band; third band sometimes commencing before second horizontal band and extending to caudal fin base. Fourth horizontal band commencing below pectoral-fin base, sometimes even before, and extending to caudal fin base while fusing ventrally of caudal peduncle with the corresponding band of other side. Most ventral horizontal band extending from gill cover to the anal fin base. Vertical bars in most cases ventrally fused with horizontal bands. Dorsal-fin membrane with black band along base, commencing at level of third or fourth dorsal-fin spine and extending to soft-rayed area of dorsal fin; above this black band, a smaller whitish or turquoise iridescent band; margin of dorsal-fin membrane black. Anal-fin membrane with blackish or whitish areas of variable extent; soft rayed part with one to three conspicuous markings; eggspot-like markings of ovoid shape and of greyish to whitish color and a blackish outline. Caudal-fin membrane white with black horizontal elements, which might be partially fused. Pectoral fin whitish hyaline. Pelvic fin whitish to greyish, posterior part of rays black.

Females almost entirely silvery white without any striking color pattern. Cheeks, operculum and dorsum of freshly caught specimens iridescent light purple. Chest and belly whitish. Iris of eye whitish. Dorsal head surface, dorsal area of nape and areas just below dorsal-fin base dusky (light greyish-brown to silvery) but less prominent than in males. Anal, pelvic and pectoral whitish. Caudal fin whitish to dusky. Dorsal fin membrane whitish to dusky, margin of membrane between tips of spines and rays darkish.

Coloration of juveniles unknown. Two subadult males (99.9 & 106.1 mm SL) with a less contrasting flank coloration than adults males, i.e. with vertical bars only slightly visible and horizontal bands almost invisible.

Coloration in alcohol. (Fig. 3)

Overall color pattern of vertical bars, horizontal bands, and head stripe elements comparable to fresh male specimens but dark brown. Body ground coloration in male and female beige, only ventral region might appear whitish. Dorsal head surface brownish.

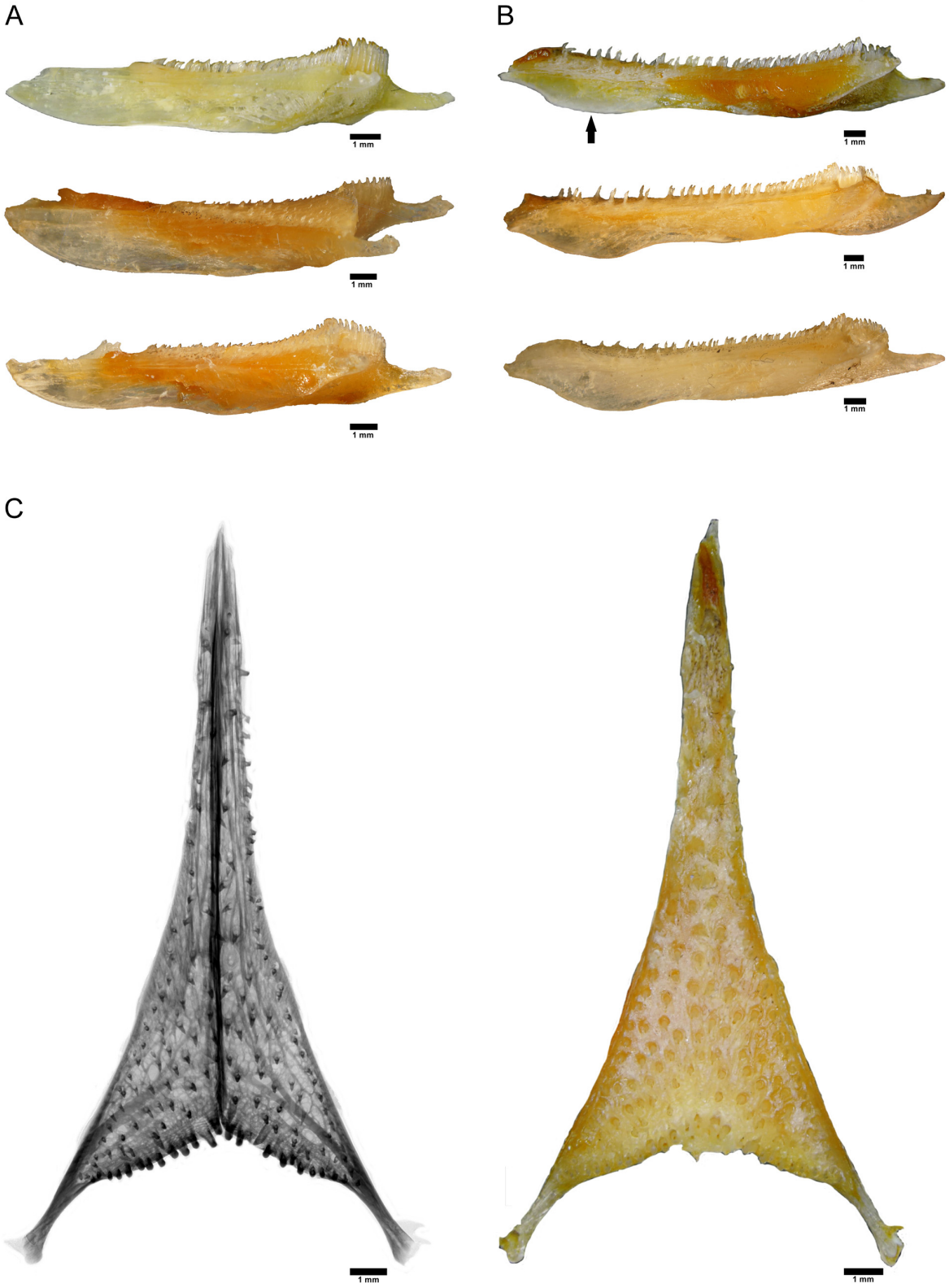

FIGURE 5. Pharyngeal jaws of the *Hemibates stenosoma* and *H. koningsi* **sp. nov.** A. Lateral view of pharyngeal jaws of *H. stenosoma* from the top to bottom: BMNH 1906–9–6–77–78 (syntype); ZSM 44567, DRC-2012/3124; ZSM 44564, DRC-2012/3116 **B.** Lateral view of pharyngeal jaws of *Hemibates koningsi* **sp. nov.** paratypes from the top to bottom: MRAC 2017–005–P-0001, DRC-2012/3103; ZSM 44570, DRC-2012/3186; ZSM 44565, DRC-2012/3243 **C.** Dorsal view of the lower pharyngeal jaw of *Hemibates koningsi* **sp. nov.** (MRAC 2017–005–P-0001, DRC-2012/3103, paratype), left: radiograph, suture of lower pharyngeal jaw straight, right: same lower pharyngeal jaw photographed through a stereomicroscope.

Distribution and biology. *Hemibates koningsi* is known only from the southern part of Lake Tanganyika from around Mpulungu and the Chituta Bay and appears to be epibenthic. It is caught with gill nets at depths between 40 and 150 meters, mainly between 40–60 meters, along with *Hemibates stenosoma* (pers. com J. Chanda, fisherman from a village near Kalambo river mouth). No stomach investigation was conducted, as they appeared to be empty in X-ray pictures, *Hemibates koningsi* appears to be rare compared to *H. stenosoma*: two and a half weeks of daily inspection of daily artisanal catches in August/September (23.08.2015–09.09.2015) yielded only a maximum of zero to two individuals per day of *H. koningsi* but hundreds of *H. stenosoma* (identification based on male color pattern). This might explain why both *Hemibates* species are named Mpande (or "Mhpandi" in Konings (2015) in Bemba language and are not differentiated by the local fishermen although both species are highly appreciated. Further, *Hemibates* catches appear to be sex-biased, with either males or females dominating single catches; this suggests sex specific schooling and homing (pers. obs., pers. comm. Joseph Chanda).

Etymology. The species is named for the first person who recognized the new *Hemibates* species as a distinct phenotype, Ad Konings, in appreciation of the inspiration to many cichlidophiles that arose from his continued popular and scientific contributions.

Discussion

Initially, the approximately 250 endemic cichlid species of Lake Tanganyika were classified into twelve tribes by Poll (1986) based on morphology. Revisions by Takahashi (2003) and Koblmüller *et al.* (2008) recognized 16 different clades based on anatomical features and molecular data, respectively. Especially the tribal assignment of the deepwater genera of *Bathybates* Boulenger, 1898, *Hemibates* Regan, 1920 and *Trematocara* Boulenger, 1899 was debated. Poll (1986) placed *Trematocara* into the tribe Trematocarini and the two genera *Bathybates* and *Hemibates* into the tribe Bathybatini whereas Takahahsi (2003) assigned all three genera into a single tribe Bathybatini. In contrast, Koblmüller *et al.* (2008) suggested placing each genus in a separate tribe. Recent studies mainly follow the classification of Poll (1986) placing *Hemibates* and *Bathybates* into Bathybatini and *Trematocara* in Trematocarini (e.g. Weiss *et al.* 2015, Takahashi & Sota 2016). Bathybatini and Trematocarini represent comparatively old lineages within the East African Radiation (e.g. Koblmüller *et al.* 2005, Weiss *et al.* 2015, Takahashi & Sota 2016). Since the genus *Hemibates* was established in 1920 by Regan with *Hemibates stenosoma* as the type species, only one additional species has been described in this genus, *Hemibates bellcrossi* Poll, 1976; however, this species was soon transferred to *Limnochromis* (Bailey & Stewart 1977) rendering *Hemibates* monotypic again. While the presence of a potential second *Hemibates* species, which is herein described as *Hemibates koningsi*, from southern Lake Tanganyika was known for some time (e.g. Konings 1998, 2015, Koblmüller *et al.* 2005) the status of this species had remained unstudied due to lack of morphological data and problems with correct assignment of molecular data to one of the two species (color morphs at that time). In addition to their distinct male color pattern, we identified several morphological and genetic characters differentiating the two. The species-specific color pattern is already exhibited by male *H. koningsi* with an SL of about 10 cm, i.e. by the smallest specimens available. Male nuptial coloration in cichlids plays an important role for species recognition and assortative mating and hence for the maintenance of reproductive isolation (Maan *et al.* 2004, Genner *et al.* 2007). The evolution of distinctive color patterns appears to be influenced by several mechanisms of sexual selection mediated through male-male competition and female mate choice (Seehausen & Schluter 2004, Knight & Turner, 2004). Interestingly, male color pattern of agamous cichlids proved to be a very useful character for differentiating *Bathybates* species despite the limited spectral light environment with only blue and green wavelengths penetrating deeper than around 20m. Apparently this limitation is compensated by increasing color pattern contrast rather than by color diversity, a tendency, which is equally present in ecologically analogous deepwater cichlids of Lake Malawi, i.e. members of the haplochromine genus *Diplotaxodon* (Genner *et al.* 2007). As both *Hemibates* species live sympatrically in the deep benthic habitats of southern Lake Tanganyika the strikingly different male color patterns of *H. stenosoma* and *H. koningsi* might have evolved to enhance reproductive isolation among those apparently ecologically different species. Both *Hemibates* species differ ecophenotypically in the morphology of their lower pharyngeal jaw bones and in mean gill raker number, which points to differences in the prey type.

Analogously in *Bathybates,* some species mainly feed on clupeids in the shallow pelagic region whereas others

rather prey on cichlids and have different depth preferences (Konings *et al.* 2015, Coulter 1991). Information concerning depth preferences of *H. koningsi* is restricted to statements of local fishermen, who report *H. stenosoma* to be caught mainly between 75–150 meters (pers. com J. Chanda), which agrees with previous studies reporting a peak of *H. stenosoma* catches at around 120 meters and deeper (Coulter 1991). In contrast, *H. koningsi* apparently prefers depths of only 40–60 meters (J. Chanda, pers. comm.). Konings (1998, 2015) stated that specimens of the stripped Hemibates (*H. koningsi*). might attain a larger size than its congener. Our results do not support this assumption, because our largest specimen had attained only 217.4 mm SL, whereas Coulter (1991) reports a maximum length of 330 mm for *Hemibates stenosoma.* Additional samples of *H. koningsi* might pinpoint the maximum size of *H. koningsi*, while examination of gut contents would help identifying alternative prey preferences of the two sympatric *Hemibates* species.

Comparative material examined

Hemibates stenosoma (Boulenger 1901): BMNH 1906.9.6.77–78 (1, 144.9–174.2 mm SL, females, syntype), Zambia, South end of Lake Tanganyika, no GPS data available, J. Moore. BMNH 1906.9.6.79 (1, 189.9 mm SL, male, syntype), Tanzania, Maswah, South of Ujiji, no GPS data available, J. Moore. BMNH 1906.9.8.150 (1, 203.0 mm SL, female), Tanzania, Kabonge, Lake Tanganyika, no GPS data available, W. Cunnington. MRAC P 43826 (1, 215.5 mm SL, female), Burundi, Usumbura, Lake Tanganyika, no GPS data available, A. Lestrade, 1935. MRAC 112103–112104 (1 out of 2, 193.5 mm SL, male), Burundi, Usumbura, (stat. 243, à 1 mille à l'ouest du pier), no GPS data available, M. Poll, 15.IV.1947. MRAC 112106–112120 (3 out of 11, 77.9–165.5 mm SL, juvenile, female and male), Burundi, (baie de Nyanza, stat. 267), no GPS data available, M. Poll, 01.V.1947. MRAC 112121–112123 (1 out of 3, 189.4 mm SL, male), Burundi, (au large de la grande Ruzizi, stat. 273), no GPS data available, M. Poll, 03.V.1947. MRAC 112124–112126 (1 out of 3, 185.0 mm SL, female), Burundi, Usumbura, (stat. 276, à l'ouest du pier jusqu' à la Ruzizi), no GPS data available, M. Poll, 05.V.1947. MRAC 112127–112131 (1 out of 6,196.5 mm SL, male), Burundi, (à 13 km au sud d'Usumbura, stat. 279, 3 à 5 km de la côte), no GPS data available, M. Poll, 06.V.1947. MRAC-P-112132 (1, 196.1 mm SL, female), Democratic Republic of the Congo, (dans le golfe de Burton, stat. 293, au large de Kazele au centre d'Ubwari), no GPS data available, M. Poll, 10.V.1947. MRAC 112134–112135 (2, 131.4–138.2 mm SL, male), United Republic of Tanazania, (au large du delta de la Malagarazi, stat. 311 (2°), à la périphérie du cône alluvionnaire), no GPS data available, M. Poll, 22.V.1947. MRAC 112136 (1, 152.8 mm SL, female), United Republic of Tanazania, (au large du delta de la Malagarazi, stat. 311 (2°), à la périphérie du cône alluvionnaire), no GPS data available, M. Poll, 22.V.1947. MRAC 94–069–P-1029–1031 (1 out of 3, 100.5 mm SL, males), Burundi, Makombe (km 37 route Bujumbura-Nyaz Lac, lac Tanganyika), no GPS data available, L. De Vos, 16.III.1994. MRAC 94–069–P-1032–1034 (3, 91.9–127.9 mm SL, males), Burundi, Magara (km 38 route Bujumbura-Nyaz Lac, lac Tanganyika), no GPS data available, L. De Vos, 11.V.1994. MRAC 95–098–P-0340–0346 (2 out of 4, 115.0–124.8 mm SL, males), Burundi, Gitaza, (km 26 route Bujumbura-Nyanaza-Lac, Lac Tanganyika), no GPS data available, L. De Vos, 20.X.1995. ZSM 44564 (7 out of 14, 112.8–206.1 mm SL, males, DRC-2012/3106–3119), Zambia, Northern Province, Lake Tanganyika, Mpulungu basin, Chituta Bay, purchased from local fishermen at lodge “Tobys place” (-8.73°/31.11°), A. Indermaur & F. Schedel, 28.VIII.2015. ZSM 44567 (4 out of 7, 165.7–178.3 mm SL, females, DRC-2012/3123–3129), Zambia, Northern Province, Lake Tanganyika, Mpulungu basin, no exact locality data available, purchased in Inguenyo fish market, Mpulungu (-8.73°/31.11°), F. Schedel, 26.VIII.2015. ZSM 44568 (1 out of 5, 117.8–146.4 mm SL, females, DRC-2012/3181–3185), Zambia, Northern Province, Lake Tanganyika, Mpulungu basin, no exact locality data available, purchased in Inguenyo fish market, Mpulungu (-8.73°/31.11°), F. Schedel, 01.IX.2015. ZSM 44572 (1 out of 4, 148.2–170.3 mm SL, females, DRC-2012/3271 & 3274), Zambia, Northern Province, Lake Tanganyika, Mpulungu basin, no exact locality data available, purchased in Inguenyo fish market, Mpulungu (-8.73°/31.11°), F. Schedel, 07.VIII.2015. ZSM 44573 (2, 180.1–186.1 mm SL, males, DRC-2012/3208 & 3211), Zambia, Northern Province, Lake Tanganyika, Mpulungu basin, no exact locality data available, purchased in Inguenyo fish market, Mpulungu (-8.73°/31.11°), F. Schedel, 03.IX.2015. ZSM 44574 (1 out of 3, 194.1–195.0 mm SL, females, DRC-2012/3130–3132), Zambia, Northern Province, Lake Tanganyika, Mpulungu basin, no exact locality data available, purchased in Inguenyo fish market, Mpulungu (-8.73°/31.11°), F. Schedel, 26.VIII.2015. ZSM 44679 (3, 171.4–180.2 mm SL, males, DRC-2012/3120–3122), Zambia, Northern

Province, Lake Tanganyika, Mpulungu basin, no exact locality data available, purchased in Inguenyo fish market, Mpulungu (-8.73°/31.11°), F. Schedel, 26.VIII.2015. ZSM 44680 (1 out of 3, 108,2–112.6 mm SL, females, DRC-2012/3133–3135), Zambia, Northern Province, Lake Tanganyika, Mpulungu basin, no exact locality data available, purchased in Inguenyo fish market, Mpulungu (-8.73°/31.11°), F. Schedel, 27.VIII.2015.

Acknowledgments

We want to thank Alex D. Chilala (Provincial Agricultural Coordinator, Western Province, Republic of Zambia) for help with collection and export permits (issued the 05.10.2015 in Kasama by the Ministry of Agriculture and Livestock; Department of Fisheries Provincial fisheries office). We thank H. Büscher (Switzerland), A. Indermaur (Univ. Basel), F. Ronco (Univ. Basel) and H. Wimmer for helpful discussions and logistic support at Chituta Bay. Chituta Bay fisherman Joseph Chanda is gratefully acknowledged for sharing his *Hemibates* knowledge. B. Ruthensteiner and D. Neumann (both ZSM) kindly helped with digital microscopy and with technical collection support, respectively. E. Vreven & M. Parrent (MRAC) for their kind reception at MRAC and the provision of specimens. J. McLaine (BMNH) kindly provided specimens on loan and the permission for dissection of the pharyngeal jaw of one of *H. stenosoma* syntypes. Last but not least the Deutsche Cichliden Gesellschaft (DCG) is acknowledged for funding this study by a grant (DCG-Förderpreis) to FS.

References

Bailey, R.M. & Stewart, D.J. (1977) Cichlid fishes from Lake Tanganyika: additions to the Zambian fauna including two new species. *Occasional Papers of the Museum of Zoology University of Michigan*, 679, 1–30.

Barel, C.D.N., van Oijen, M.J.P., Witte, F. & Witte-Maas, E.L.M. (1977) An introduction to the taxonomy and morphology of the haplochromine Cichlidae from Lake Victoria. *Netherlands Journal of Zoology*, 27 (4), 333–389.

Boulenger, G.A. (1898) Report on the fishes recently obtained by Mr. J. E. S. Moore in Lake Tanganyika. *Proceedings of the Zoological Society of London*, 3, 494–497.

Boulenger, G.A. (1899) Second contribution to the ichthyology of Lake Tanganyika. -- On the fishes obtained by the Congo Free State Expedition under Lieut. Lemaire in 1898. *Transactions of the Zoological Society of London*, 15 (4, 1), 87–96.

Boulenger, G.A. (1901) Diagnoses of new fishes discovered by Mr. J. E. S. Moore in lakes Tanganyika and Kivu. II. Cichlidae, Mastacembelidae. *Annals and Magazine of Natural History*, 7 (37), 1–6.

Boulenger, G.A. (1906) Fourth contribution to the ichthyology of Lake Tanganyika. -- Report on the collection of fishes made by Dr. W. A. Cunnington during the Third Tanganyika Expedition, 1904-1905. *Transactions of the Zoological Society of London*, 17 (6, 1), 537–601.

Boulenger, G.A. (1914) Mission Stappers au Tanganyika-Moero. Diagnoses de poissons nouveaux. I. Acanthoptérygiens, Opisthomes, Cyprinodontes. *Revue de Zoologie Africaine*, 3 (3), 442–447.

Coulter, G.W. (1991) Chapter 8: The benthic fish community. *In*: Coulter, G.W. (Ed.), *Lake Tanganyika and its life*. Oxford University Press, London, pp. 151–199.

Dunz, A. & Schliewen, U.K. (2010) Description of a new species of *"Tilapia"* Smith, 1840 (Teleostei: Cichlidae) from Ghana. *Zootaxa*, 2548, 1–21.

Dunz, A.R. & Schliewen, U.K. (2013) Molecular phylogeny and revised classification of the haplotilapiine cichlid fishes formerly referred to as "*Tilapia*". *Molecular Phylogenetics and Evolution*, 68, 64–80. https://doi.org/10.1016/j.ympev.2013.03.015

Duponchelle, F., Paradis, E., Ribbink, A.J. & Turner, G.F. (2008) Parallel life history evolution in mouthbrooding cichlids from the African Great Lakes. *Proceedings of the National Academy of Sciences*, 105 (40), 15475–15480. https://doi.org/10.1073/pnas.0802343105

Genner, M.J., Nichols, P., Carvalho, G.R., Robinson, R.L., Shaw, P.W. & Turner, G.F. (2007) Reproductive isolation among deep-water cichlid fishes of Lake Malawi differing in monochromatic male breeding dress. *Molecular Ecology*, 16, 651–662. https://doi.org/10.1111/j.1365-294X.2006.03173.x

Hammer, Ø., Harper, D.A.T. & Ryan, P.D. (2001) PAST: Paleontological statistics software package for education and data analysis. *Palaeontologia Electronica*, 4 (1), 1–9.

Kearse, M., Moir, R., Wilson, A., Stones-Havas, S., Cheung, M., Sturrock, S., Buxton, S., Cooper, A., Markowitz, S., Duran, C., Thierer, T., Ashton, B., Mentjies, P. & Drummond, A. (2012) Geneious Basic: an integrated and extendable desktop software platform for the organization and analysis of sequence data. *Bioinformatics*, 28 (12), 1647–1649. https://doi.org/10.1093/bioinformatics/bts199

Kirchberger, P.C., Sefc, K.M., Sturmbauer, C. & Koblmüller, S. (2012) Evolutionary history of lake Tangayikaka´s predatory deepwater cichlids. *International Journal of Evolutionary Biology*, 1–10. https://doi.org/10.1155/2012/716209

Klett, V. & Meyer, A. (2002) What, if anything, is a Tilapia?-mitochondrial ND2 phylogeny of tilapiines and the evolution of parental care systems in the African cichlid fishes. *Molecular Biology and Evolution*, 19 (6), 865–883. https://doi.org/10.1093/oxfordjournals.molbev.a004144

Knight, M.E. & Turner, G.F. (2004) Laboratory mating trials indicate speciation by sexual selection among populations of the cichlid

fish *Pseudotropheus zebra* from Lake Malawi. *Proceedings of the Royal Society of London*, Series B, Biological Science, 271, 675–680.
https://doi.org/10.1098/rspb.2003.2639
Koblmüller, S., Duftner, N., Katongo, C., Phiri, H. & Sturmbauer, C. (2005) Ancient divergence in bathypelagic Lake Tanganyika deepwater cichlids: Mitochondrial phylogeny of the tribe Bathybatini. *Journal of Molecular Evolution*, 60, 297–314.
https://doi.org/10.1007/s00239-004-0033-8
Koblmüller, S., Sefc, K.M. & Sturmbauer, C. (2008) The Lake Tanganyika cichlid species assemblage: recent advances in molecular phylogenetics. *Hydrobiologia*, 615, 5–20.
https://doi.org/10.1007/s10750-008-9552-4
Kocher, T.D., Conroy, J.A., McKaye, K.R., Stauffer, J.R. & Lockwood, S.F. (1995) Evolution of NADH dehydrogenase subunit 2 in East African cichlid fish. *Molecular Phylogenetics and Evolution*, 4, 420–432.
https://doi.org/10.1006/mpev.1995.1039
Konings, A. (1998) *Tanganyika cichlids in their natural habitat*. Cichlid Press, Texas, El Paso, 272 pp.
Konings, A. (2015) *Tanganyika cichlids in their natural habitat. 3rd Edition*. Cichlid Press, Texas, El Paso, 408 pp.
Maan, M.E., Seehausen, O., Söderberg, L., Johnson, L., Ripmeester, E.A.P, Mrosso, H.D.J., Taylor, M.I., van Dooren, T.J.M. & van Alphen, J.J.M. (2004) Intraspecific sexual selection on a speciation trait, male coloration, in the Lake Victoria cichlid *Pundamilia nyererei*. *Proceedings of the Royal Society of London*, Series B, Biological Science, 271, 2445–2452.
https://doi.org/10.1098/rspb.2004.2911
Neumann, D. (2010) Preservation of freshwater fishes in the field. *Abc Taxa*, 8 (2), 587–632.
Miller, M.A., Pfeiffer, W. & Schwartz, T. (2010) Creating the CIPRES Science Gateway for inference of large phylogenetic trees. *In*: Proceedings of the Gateway Computing Environments Workshop (GCE), New Orleans, LA, pp. 1–8.
https://doi.org/10.1109/GCE.2010.5676129
Muschick, M., Indermaur, A. & Salzburger, W. (2012) Convergent evolution within an adaptive radiation of cichlid fishes. *Current Biology*, 22, 2362–2368.
https://doi.org/10.1016/j.cub.2012.10.048
Poll, M. (1952) Quatrième série de Cichlidae nouveaux recueillis par la mission hydrobiologique belge au lac Tanganika (1946-1947). *Bulletin de l'Institut Royal des Sciences Naturelles de Belgique*, 28 (49), 1–20.
Poll, M. (1956) Poissons Cichlidae. *In*: *Exploration Hydrobiologique du Lac Tanganika (1946–1947)*: Résultats scientifiques. *Institut Royal des Sciences Naturelles de Belgique*, 3 (5B), 390–394.
Poll, M. (1976) *Hemibates bellcrossi* sp. n. du lac Tanganika (Pisces, Cichlidae). *Revue de Zoologie Africaine*, 90 (4), 1017–1020.
Poll, M. (1986) Classification des Cichlidae du lac Tanganika. Tribus, genres et espèces. *Classe des Sciences, Académie royale de Belgique*, 45, 1–163.
Regan, C.T. (1920) The Classification of the Fishes of the Family Cichlidae. - I. The Tanganyika Genera. *Annals & Magazine of Natural History Series*, 9 (5), 33–53.
Salzburger, W., Meyer, A., Baric, S., Verheyen, E. & Sturmbauer, C. (2002) Phylogeny of the Lake Tanganyika cichlid species flock and its relationship to the Central and East African haplochromine cichlid fish faunas. *Systematic Biology*, 51, 113–135.
https://doi.org/10.1080/106351502753475907
Schedel, F.D.B., Friel, J.P. & Schliewen, U.K. (2014) *Haplochromis vanheusdeni*, a new haplochromine cichlid species from the Great Ruaha River drainage, Rufiji basin, Tanzania (Teleostei, Perciformes, Cichlidae). *Spixiana*, 37 (1), 135–149.
Schwarzer, J., Misof, B., Tautz, D. & Schliewen, U.K. (2009) The root of the East African cichlid radiations. *BMC Evolutionary Biology*, 3, 1–11.
https://doi.org/10.1186/1471-2148-9-186
Seehausen, O. & Schluter, D. (2004) Male-male competition and nuptial color displacement as a diversifying force in Lake Victoria cichlid fish. *Proceedings of the Royal Society, Series B, Biological Science*, 271, 1345–1353.
https://doi.org/10.1098/rspb.2004.2737
Stamatakis, A. (2014) RAxML Version 8: A tool for Phylogenetic Analysis and Post- Analysis of Large Phylogenies. *Bioinformatics*, 30 (9), 1312–1313.
https://doi.org/10.1093/bioinformatics/btu033
Steindachner, F. (1911) Beiträge zur Kenntniss der Fischfauna des Tanganyikasees und des Kongogebietes. *Anzeiger der Kaiserlichen Akademie der Wissenschaften, Wien, Mathematisch-Naturwissenschaftliche Classe*, 48 (26), 528–530.
Takahashi, T. (2003) Systematics of Tanganyikan cichlid fishes (Teleostei: Perciformes). *Ichthyological Research*, 50, 367–382.
https://doi.org/10.1007/s10228-003-0181-7
Takahashi, T. & Sota, T. (2016) A robust phylogeny among major lineages of the East African cichlids. *Molecular Phylogenetics and Evolution*, 100, 234–242.
https://doi.org/10.1016/j.ympev.2016.04.012
Weiss, J.D., Cotterill, F.P.D. & Schliewen, U.K. (2015) Lake Tanganyika—A 'Melting Pot' of ancient and young cichlid lineages (Teleostei: Cichlidae)? *PLOS ONE*, 10, e0125043.
https://doi.org/10.1371/journal.pone.0125043
Wagner, C.E., McIntyre, P.B., Buels, K.S., Gilbert, D.M. & Ellinor, M. (2009) Diet predicts intestine length in Lake Tanganyika's cichlid fishes. *Functional Ecology*, 23 (6), 1122–1131.
https://doi.org/10.1111/j.1365-2435.2009.01589.x

Zootaxa 4461 (3): 301–349
http://www.mapress.com/j/zt/

Article

ISSN 1175-5326 (print edition)
ZOOTAXA
ISSN 1175-5334 (online edition)

https://doi.org/10.11646/zootaxa.4461.3.1
http://zoobank.org/urn:lsid:zoobank.org:pub:B646DF09-BADE-43F1-9CE5-39EF1E2971A8

Description of five new rheophilic *Orthochromis* species (Teleostei: Cichlidae) from the Upper Congo drainage in Zambia and the Democratic Republic of the Congo

FREDERIC DIETER BENEDIKT SCHEDEL[1], EMMANUEL J.W.M.N. VREVEN[2,3],
BAUCHET KATEMO MANDA[2,3,4], EMMANUEL ABWE[2,3,4],
AUGUSTE CHOCHA MANDA[4] & ULRICH KURT SCHLIEWEN[1,5]

[1]*SNSB-Bavarian State Collection Zoology (ZSM), Department of Ichthyology, Münchhausenstraße 21, München, Germany,*
[2]*Vertebrate Section, Royal Museum for Central Africa (RMCA), Leuvensesteenweg 13, B-3080 Tervuren, Belgium*
[3]*KU Leuven, Laboratory of Biodiversity and Evolutionary Genomics, Charles Deberiotstraat 32, B-3000 Leuven, Belgium*
[4]*Unité de Recherche en Biodiversité et Exploitation durable des Zones Humides (BEZHU), Faculté des Sciences Agronomiques, Université de Lubumbashi, Route Kasapa, Lubumbashi, R.D Congo*
[5]*Corresponding author. E-mail: schliewen@snsb.de*

Table of contents

Abstract

Five new rheophilic haplochromine cichlid species are described from the Upper Congo drainage of Zambia and the Democratic Republic of the Congo: *Orthochromis mporokoso* **sp. nov.** and *O. katumbii* **sp. nov.** from the Bangwelu-Mweru ecoregion, *O. kimpala* **sp. nov.** and *O. gecki* **sp. nov.** from the Upper Lualaba ecoregion, and *O. indermauri* **sp. nov.** from the Lufubu River of the Lake Tanganyika ecoregion. *Orthochromis kimpala* sp. nov, *O. gecki* **sp. nov.**, and *O. indermauri* **sp. nov.** are distinguished from all currently valid species of the genus *Orthochromis* Greenwood 1954*,* except for *O. torrenticola* (Thys van den Audenaerde 1963), by the presence of eggspots or eggspot-like maculae on the anal fin (vs. no eggspots). The three species can be easily distinguished from *O. torrenticola* by having three anal spines (vs. four anal spines). Moreover, all five new species can be individually distinguished from all currently known rheophilic taxa placed in the genera *Orthochromis*, *Schwetzochromis* Poll 1948 and the rheophilic species of the genus *Haplochromis* Hilgendorf 1888 (e.g. *H. bakongo* Thys van den Audenaerde 1964, *H. snoeksi* Wamuini Lunkayilako & Vreven 2010, *H. vanheusdeni* Schedel *et al.* 2014) either based on meristic values, morphometric distances and colouration patterns, or on a combination of them.

Key words: Upper Congo basin, Lualaba, Luapula, Lufubu, *Orthochromis*, *Schwetzochromis*, rheophilic cichlids

Accepted by J. Armbruster: 27 Jun. 2018; published: 22 Aug. 2018

Introduction

While literally hundreds of endemic species are described from each Lake Tanganyika, Lake Malawi and Lake Victoria, strikingly few haplochromine taxa are known to inhabit exclusively rivers (Greenwood 1979) and the number of species considered to be rheophilic is even less with currently 19 valid species. Ecomorphologically, bentho-rheophilic cichlids are vaguely characterized by morphological adaptations such as reduced squamation on head, nape, and chest, rounded pelvic fins, and a comparatively slender body presumably facilitating a bottom-oriented life in the strong, current (Roberts & Stewart 1976). Taxonomically, rheophilic haplochromine taxa are currently classified in different genera, i.e. *Orthochromis* Greenwood 1954 and the single member of the genus *Schwetzochromis* Poll 1948, *S. neodon* Poll 1948. In addition, several rheophilic taxa are placed in the catch-all genus *Haplochromis* Hilgendorf 1888, but a consensus about a phylogenetically consistent classification has not yet been reached (Schedel *et al.* 2014). Currently eight species endemic to the Malagarasi and Luiche drainages are classified as *Orthochromis* ("Malagarasi-*Orthochromis*" sensu Weiss *et al.* 2015) including the type species of the genus, *O. malagaraziensis* (David 1937), originally described as *Haplochromis malagaraziensis*. These Malagarasi-*Orthochromis* appear to form a monophyletic group (Koblmüller *et al.* 2008, Schwarzer *et al.* 2012, Dunz & Schliewen 2013, Weiss *et al.* 2015, Matschiner *et al.* 2016). An additional five *Orthochromis* have been described from the Luapula-Mweru system, i.e. *O. kalungwishiensis* (Greenwood & Kullander 1994), *O. luongoensis* (Greenwood & Kullander 1994), *O. polyacanthus* (Boulenger 1899), and *O. torrenticola* (Thys van den Audenaerde 1963) from the Lufira River and *O. stormsi* (Boulenger 1902) from the Congo-Lualaba mainstream including Lake Mweru (Greenwood & Kullander 1994). Finally, *Orthochromis machadoi* (Poll 1967) is known only from the Cunene River in Namibia and Angola. These latter six *Orthochromis* species from outside of the Malagarasi and Luiche drainage systems are not closely related to the Malagarasi-*Orthochromis* based on molecular phylogenetic results (Salzburger *et al.* 2002, Koblmüller *et al.* 2008, Schwarzer *et al.* 2012, Dunz & Schliewen 2013, Weiss *et al.* 2015, Matschiner *et al.* 2016). This is equally true for the few rheophilic haplochromines currently classified in *Haplochromis*, i.e. *H. bakongo* Thys van den Audenaerde 1964, *H. snoeksi* Wamuini Lunkayilakio & Vreven 2010 from the Lower Congo basin, and *H. vanheusdeni* Schedel, Friel & Schliewen 2014 from the Great Ruaha River drainage in Tanzania, which represent different lineages of their own (Schwarzer *et al.* 2012, unpublished data). The greater Congo drainage, i.e., including Lake Tanganyika and its affluents, is home to almost all of these taxa except for *H. vanheusdeni* and *O. machadoi* (Poll 1967).

Recently, three apparently undescribed rheophilic haplochromine cichlids have been collected in Upper Congo affluents of Zambia including the Lufubu River, a southern affluent of Lake Tanganyika (Schedel *et al.* 2014, Indermaur 2014), and two additional ones, from the Lubudi River and from Kalule North River in the Upper Lualaba (Congo) basin respectively (Fig. 1). Further, preliminary observations revealed that the new species differ in several diagnostic characters from *Orthochromis* or *Schwetzochromis* sensu De Vos & Seegers (1998). For instance, the two new species from southeastern DRC (rivers Lubudi and Kalule Nord; Upper Lualaba ecoregion) as well as the new species from the Lufubu River have eggspots or eggspot-like maculae on the anal fin, a situation that contrasts with that found in *Orthochromis,* which either have no eggspots, or, in the case of *O. torrenticola*, only eggspot-like maculae on the anterior lower margin of the anal fin (De Vos & Seegers 1998). The two species from the Luapula affluents fit with most diagnostic characteristics for the genus *Orthochromis,* but they both exhibit a well-developed cheek squamation vs. absence or extensive reduction in cheek squamation according to De Vos & Seegers (1998). Finally, genomic data suggest that all new species are not closely related to the Malagarasi-*Orthochromis* (Schedel *et al.*, unpublished). In addition, all five new species possess a lachrymal stripe which is lacking in *Schwetzochromis*. As a generic revision of haplochromine genera is still pending, all new species are described in the phenotypically overall similar genus *Orthochromis* until a phylogenetic sound generic revision of haplochromine cichlids becomes available. This approach has become common practice for haplochromine cichlids (e.g. Wamuini Lunkayilakio & Vreven 2010, De Zeeuw *et al.* 2013, Schedel *et al.* 2014) following the logic of Van Oijen *et al.* (1991) and Van Oijen (1996), with the difference, however, that the new rheophilic taxa are placed in the current catch-all genus for rheophilic haplochromine cichlids *Orthochromis* and not in *Haplochromis*. This because the genus *Haplochromis* should be rather restricted to taxa closely related to the type species of *Haplochromis* from the Lake Victoria Region superflock, i.e. *Haplochromis obliquidens* Hilgendorf, 1888.

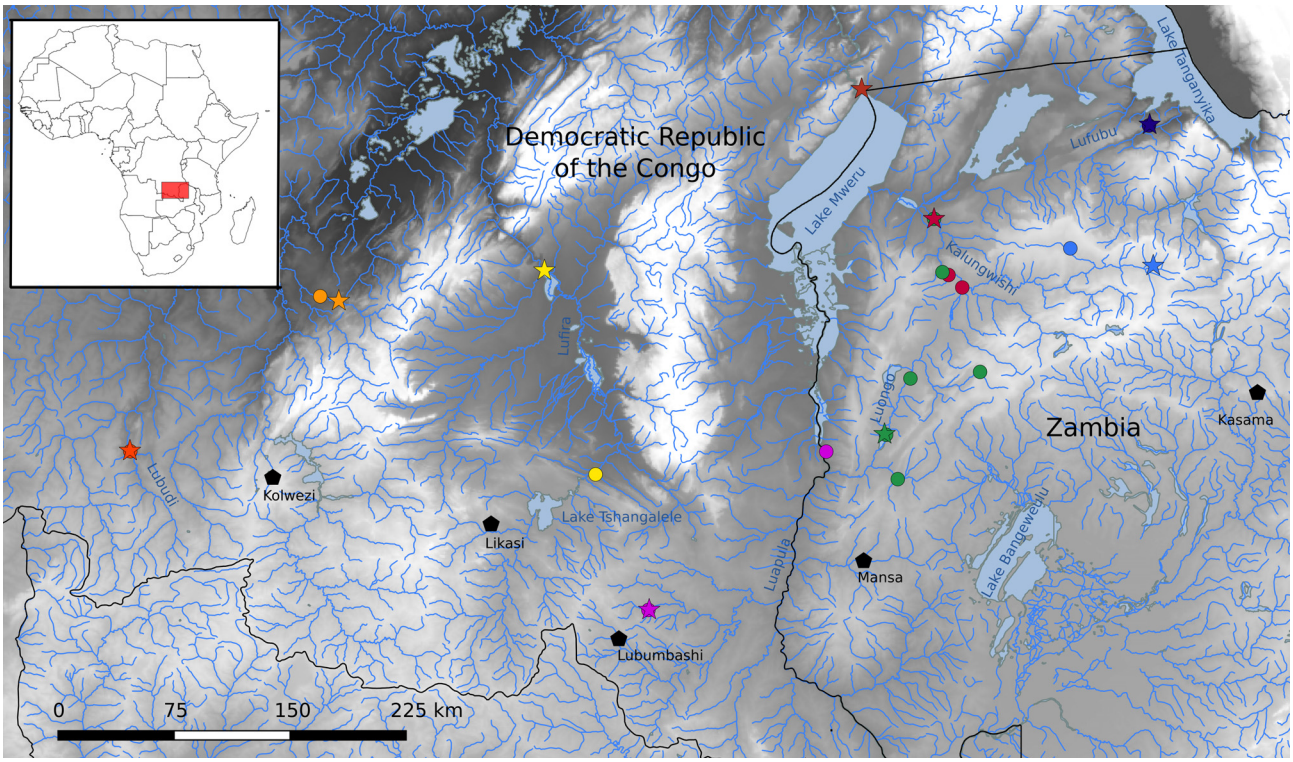

FIGURE 1. Map of south-eastern DRC and Northern Zambia, with indications of the type localities of the known *Orthochromis* species of the Upper Congo drainage system and new *Orthochromis* species. Star = type locality, circle = either paratype locality or sample locality of comparative specimens. Species indicated by colour: *O. mporokoso* **sp. nov.** (light blue); *O. katumbii* **sp. nov.** (purple); *O. kimpala* **sp. nov.** (orange); *O. gecki* **sp. nov.** (deep orange); *O. indermauri* **sp. nov.** (deep blue); *O. kalungwishiensis* (dark red); *O. luongoensis* (green). *O polyacanthus* (brown) and *O. torrenticola* (yellow). Major citys are depicted in black. Map is based on shapefiles obtained from DIVA-GIS (http://www.diva-gis.org/Data).

Materials and methods

A total of 344 specimens of rheophilic haplochromine cichlids were examined for morphological comparison (see Appendix). These are deposited in CUMV (Cornell University Museum of Vertebrates, Ithaca); NHM (Natural History Museum London); MRAC (Royal Museum for Central Africa, Tervuren); Tanganjikasee-Buntbarsch-Sammlung (collection of the University of Basel); ZSM (Bavarian State Collection of Zoology, Munich); and at the personal collection of O. Seehausen (EAWAG - Swiss Federal Institute of Aquatic Sciences and Technology, Dübendorf). All five new species described herein share morphological characters typical of rheophilic haplochromines. Therefore, the new putative species were compared with all haplochromine cichlid species currently placed in the rheophilic genera *Orthochromis* and *Schwetzochromis* as recognized in the revision of De Vos & Seegers (1998), and, in addition, with all rheophilic representatives of the genus *Haplochromis* Hilgendorf 1888 sharing *Orthochromis*-like body shape, i.e. rounded pelvic fins and a slender body. Furthermore, one yet undescribed *Orthochromis* species from the Malagarasi drainage was included in the comparisons as well.

Overall, 28 meristic characters were recorded for almost all examined specimens of the five new species, which were either based on stereomicroscope observations (18 characters) or on digital x-rays (10 characters using a Faxitron UltraFocus LLC x-ray unit) following previous publications (Barel *et al.* 1977, Dunz & Schliewen 2010, Schedel *et al.* 2014, Schedel & Schliewen 2017). In addition, four morphological character states as defined in Schedel & Schliewen 2017 were examined: (1) position of the pterygiophore supporting the last dorsal-fin spine [used for Principal Components Analyses (PCA)]; (2) position of the pterygiophore supporting the last anal-fin spine (used for PCA); (3) state of hypurals 1 and 2; and (4) state of hypurals 2 and 3. Live colour notes were based on photographs of fresh wild caught specimens (adults) as well as on live specimens kept in aquaria (if available). In addition, we took colour notes of preserved specimens with a focus on head stripes and bars (commonly referred

as “head mask”) that appear to be of diagnostic value for the different species of *Orthochromis* (De Vos & Seegers 1998). For the PCA, a subsample of 20 meristic characters (eight squamation characters and twelve skeletal characters) of most examined specimens (N=327) was used. Twenty-nine morphometric distance measurements were used for species descriptions, i.e. they were only measured in the types and additional specimens of the new species, but not in the specimens for the comparison study except for a number of selected species in which there was overlap in meristic counts with the new species, e.g. *O. machadoi*, *O. luongoensis,* and *H. vanheusdeni*. All measurements were recorded as defined in Schedel & Schliewen (2017), a compilation of distance measurement definitions largely but not completely based on previous cichlid studies (Barel *et al.* 1977, Dunz & Schliewen 2010, Schedel *et al.* 2014). Measurements were taken point-to-point on the left side of specimens using digital callipers (accuracy of the calliper 0.1 mm). Head measurements are given as percentage of the head length (HL), all remaining measurements as percentage of the standard length (SL). Measurements of the lower pharyngeal jaw were taken from digital microscope images of dissected lower pharyngeal jaws and are given in percentage of the head length (HL).

To test for morphological discreteness of putative new species and to identify diagnostic character states or combinations, a first PCA using a correlation matrix was performed for 20 meristic characters (see above) of the total data set. The monophyletic Malagarasi-*Orthochromis* were grouped together in our analysis due to their phenotypic similarity and to simplify subsequent interpretation. After identifying clearly separate clusters in the total dataset, five subsequent species-specific PCAs with reduced taxon sets were performed, each composed of one of the five new species and those described species with overlapping PC values in bivariate plots of PC I vs. PC II of the total dataset. For three of these species-specific PCAs nonvariant meristic counts were excluded. For example, in the species-specific PCA targeting the diagnostic differentiation of *O. kimpala* **sp. nov.** counts for scales between the upper lateral line and last dorsal-fin spine were nonvariant for the used data subsets while for the two species-specific PCAs targeting the diagnostic differentiation of *O. gecki* **sp. nov.** and *O. indermauri* **sp. nov.** counts for the anal-fin spines were excluded due to nonvariance. This exercise was done to reduce the total variance in each dataset to test for increased separation of each of the new species with the morphologically closest taxa. The software PAST 3.07 (Hammer *et al.* 2001) was used to calculate PCs. Scores of most informative principal components (PC I, PC II and in some cases for PC III) were visualized using bivariate plots, and variables contributing most to PC variation were identified using their loadings as tabulated. The PCA focused on meristic characters only because these characters appear to be unambiguous and are available for all included species and specimens.

Results

In the first PCA on the meristic values (all specimens included, N = 327, Fig. 2, Table 1), PC I explained 32.18 %, PC II 12.81 %, and PC III 10.16% of the total variance. Differences in the total number of vertebrae, scales in a horizontal line, and the number of scales in the upper lateral line contributed most to the factor loadings of PC I; PC II is mainly influenced by different counts for scales on the cheek and in the lower lateral line, and by the number of upper procurrent caudal-fin rays. The PC I and PC II scores of *Orthochromis mporokoso* **sp. nov.** overlap with *O. machadoi*, *Haplochromis snoeksi*, *O. katumbii* **sp. nov.**, *O. kimpala* **sp. nov.**, *O. gecki* **sp. nov.**, and *Schwetzochromis neodon*. *Orthochromis katumbii* **sp. nov.** is grouped with *O. mporokoso* **sp. nov.**, *O. gecki* **sp. nov.**, *O. kimpala* **sp. nov.**, *O. luongoensis*, *O. torrenticola, S. neodon,* and with the Malagarasi-*Orthochromis* based on the PC scores I and II. Scores of PC I and PC II of *Orthochromis kimpala* **sp. nov.** overlap with those of *H. bakongo*, *H. snoeksi*, *H. vanheusdeni*, *O. machadoi*, *O. stormsi, O. katumbii* **sp. nov.**, *O. mporokoso* **sp. nov.**, and *O. gecki* **sp. nov.** while the PC I and PC II scores of *O. gecki* **sp. nov.** overlap with those of *O. mporokoso* **sp. nov.**, *O. kimpala* **sp. nov.**, *O. katumbii* **sp. nov.**, *O. indermauri* **sp. nov.**, *O. polyacanthus, S. neodon*, and Malagarasi-*Orthochromis*. Finally, the PC I and PC II scores of *O. indermauri* **sp. nov.** overlap with those of *O. stormsi, H. vanheusdeni, O. gecki* **sp. nov.** and with the Malagarasi-*Orthochromis.*

The first species-specific PCA with a reduced taxon set (106 specimens included, Table 1; Appendix: Fig. S1) targets the diagnostic differentiation of *O. mporokoso* **sp. nov.** from the six species which overlap with their PC I and PC II scores of the total dataset (see above). In this PCA PC I explains 27.87 %, PC II 15.43 %, and PC III 10.77 % of the total variance. PC I mainly integrates the variance of the total number of vertebrae, caudal-fin rays,

and of scales in the upper lateral line, and PC II mainly the variance of the number of dorsal-fin spines, dorsal-fin rays, and position of the pterygiophore supporting the last dorsal-fin spine. PC III mainly integrates the variance of the number of caudal and abdominal vertebrae and the position of the pterygiophore supporting the last anal-fin spine. The PCA plots separate *O. mporokoso* **sp. nov.** from *H. snoeksi* based on low PC II scores and from S. *neodon* based on high PC I scores, while a combination of low PC II scores and low PC III further separates it from *O. gecki* **sp. nov.**

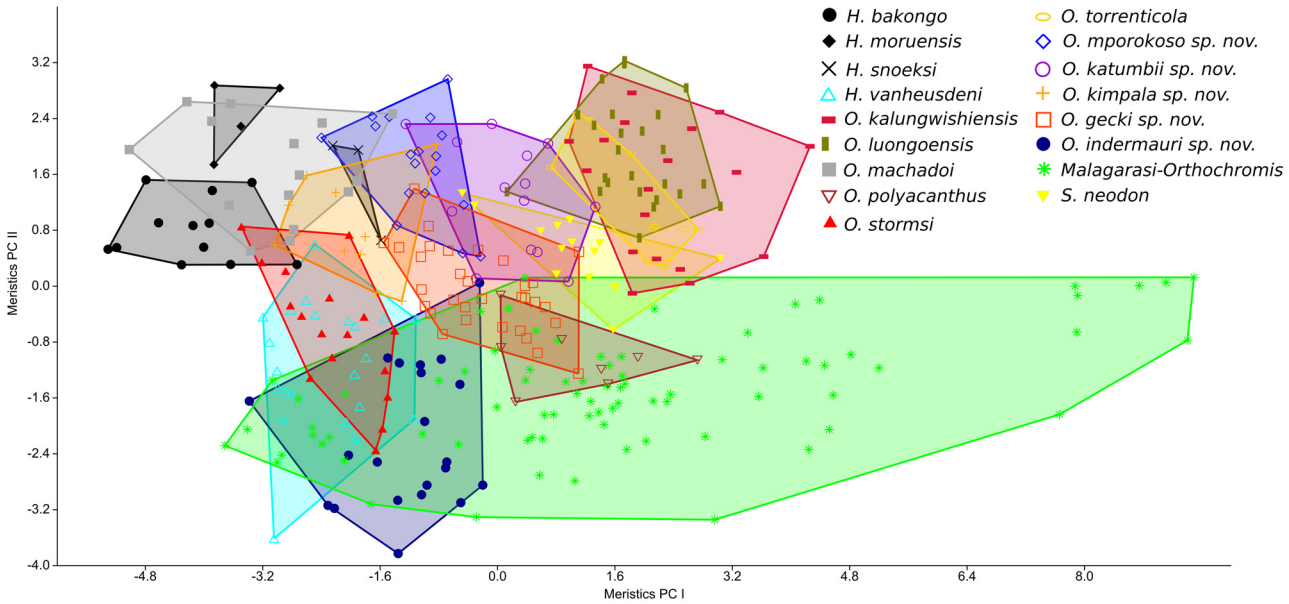

FIGURE 2. PCA scatter plots based on 20 meristic values; species score limits visualized as convex hulls. PC I vs PC II for all examined specimens (N = 327). PC I explain 32.18 % of the variance and PC II explains 12.81 %.

The second species-specific PCA (225 specimens included, Table 1; Appendix: Fig. S2) targets the diagnostic differentiation of *O. katumbii* **sp. nov.** from the six species and the Malagarasi-*Orthochromis* which overlap with their PC I and PC II scores of the total dataset (see above). In this PCA PC I explains 30.76 %, PC II 14.68 %, and PC III 9.89 % of the total variance. PC I mainly integrates the variance of the total number of vertebrae, scales in a horizontal line, and of the position of the pterygiophore supporting the last dorsal-fin spine, and PC II mainly the variance of the number of scales on cheek and in the lower lateral line, and number of anal-fin rays. The species-specific PCA separates *O. katumbii* **sp. nov.** from *O. kimpala* **sp. nov.** mainly based on low PC I scores. Values of PC II and PC III for *O. katumbii* **sp. nov.** overlapped with all remaining species.

The third species-specific PCA (143 specimens included, Table 1, Appendix: Fig. S3) targets the diagnostic differentiation of *O. kimpala* **sp. nov.** from the eight species overlapping with their PCI and PCII scores in the total dataset (see above). PC I explains 23.09 %, PC II 14.63 % and PC III 12.34 % of the total variance. The variance of the number of scales along the horizontal line, total number of vertebrae, and caudal vertebrae contributed most to PC I whereas the variance of the number of upper and lower procurrent caudal-fin rays and total number of caudal-fin rays contributed most to PC II. PC III is mainly composed of the variance of the number of abdominal vertebrae, the number of dorsal-fin spines, and the position of the pterygiophore supporting the last dorsal-fin spine. The species-specific PCA separates *O. kimpala* **sp. nov.** from *H. snoeksi* based on low PC III scores.

The fourth species-specific PCA (196 specimens included, Table 1, Appendix: Fig. S4) targets the diagnostic differentiation of *O. gecki* **sp. nov.** from the six species and the Malagarasi-*Orthochromis* which overlap with their PCI and PCII scores of the total dataset (see above). PC I explains 33.42 %, PC II 14.91 % and PC III 11.95 % of the total variance. Differences in the number of scales along the horizontal line, total number of vertebrae, and dorsal-fin spines contribute most to PC I whereas differences in the number of scales on the cheek, number of upper procurrent caudal-fin rays, and total number of caudal-fin rays mainly contribute to PC II. PC III mainly integrates variance of the number of circumpeduncular scales and in the number of dorsal- and anal-fin rays. The

TABLE 1. Factor loadings of PCI-III for all examined specimens (Fig. 2) plus for each species-specific PCA (see Fig. S1-5). Highest loadings for each principal component indicated in boldface.

	PCA with all specimens (N=327)			*Orthochromis mporokoso* **sp. nov.** (N=106)			*Orthochromis katumbii* **sp. Nov**. (N=225)		
	PC I	PC II	PC III	PC I	PC II	PC III	PC I	PC II	PC III
Series of scales on cheek	-0,0538	**0,5058**	-0,0066	-0,2745	0,0904	0,2475	-0,0504	**0,4975**	0,1096
Scales on operculum	-0,0512	0,3297	0,1617	-0,2495	0,1200	0,1003	-0,0210	0,3706	0,1952
Scales (horizontal line)	**0,3385**	0,2389	-0,0506	0,2777	0,2315	-0,1634	**0,3503**	0,1770	-0,0869
Upper lateral line scale	**0,3293**	-0,0039	-0,0612	**0,3115**	0,0203	-0,1542	0,3179	-0,0803	-0,1693
Lower lateral line scales	0,1232	**0,3751**	-0,0158	0,2074	0,1374	0,2064	0,1244	**0,3912**	0,0475
Circumpeduncular scales	-0,0487	0,0250	**0,3931**	-0,2595	0,1491	-0,3037	0,0064	0,1138	0,2233
Scales between lateral line and dorsal fin origin	0,0120	-0,1232	0,2786	0,0362	-0,2740	-0,1456	0,0791	-0,0410	-0,1569
Scales between upper lateral line and last dorsal fin spine	0,0364	0,2251	-0,1445	-0,0926	0,0188	-0,2220	0,0092	0,0580	0,0476
Abdominal vertebrae	0,2956	0,0819	0,1977	0,1889	0,1736	**0,4192**	0,3362	0,0736	-0,1027
Caudal vertebrae	0,3022	0,1597	-0,2102	0,2548	0,1006	**-0,4350**	0,2920	0,0802	0,0155
Total number of vertebrae	**0,3662**	0,1545	-0,0565	**0,3497**	0,1965	-0,1388	**0,3803**	0,0930	-0,0539
Anal-fin spines	0,0420	0,0907	0,0814	-0,0792	-0,0647	0,0934	0,0390	0,1020	0,0558
Anal-fin rays	0,1752	-0,2181	-0,2514	0,1547	-0,1911	0,1162	0,0531	**-0,4779**	-0,1426
Dorsal-fin spines	0,3166	-0,1378	**0,3135**	0,0459	**0,5130**	-0,0837	0,3416	-0,1154	-0,0114
Dorsal-fin rays	0,0864	0,1461	**-0,4678**	0,2332	**-0,3591**	0,1904	-0,0539	0,0103	-0,2847
Upper procurrent caudal-fin rays	0,1696	**-0,3438**	-0,1644	0,2835	-0,1002	-0,0781	0,0996	-0,2696	**0,4046**
Lower procurrent caudal-fin rays	0,1972	-0,0791	-0,1397	0,2361	-0,0673	0,1228	0,1546	-0,0255	**0,4757**
Caudal-fin rays	0,2162	-0,2712	-0,1874	**0,3123**	-0,1026	0,0036	0,1584	-0,1969	**0,5519**
Position of the pterygiophore supporting the last dorsal fin spine	0,3219	-0,1234	0,3043	0,0171	**0,4787**	0,0770	**0,3421**	-0,1165	-0,0314
Position of pterygiophore supporting the last anal fin spine	0,2855	0,0753	0,2581	0,1564	0,2022	**0,4429**	0,3296	0,0893	-0,1442

……continued on the next page

TABLE 1. (Continued)

	Orthochromis kimpala **sp. nov.** (N=143)			*Orthochromis gecki* **sp. nov.** (N=196)			*Orthochromis indermauri* **sp. nov.** (N=171)		
	PC I	PC II	PC III	PC I	PC II	PC III	PC I	PC II	PC III
Series of scales on cheek	0,0248	-0,3120	0,0227	-0,1689	**0,3667**	0,0915	-0,1157	0,1830	0,1384
Scales on operculum	-0,0008	-0,2372	0,0908	-0,1033	0,1429	0,2516	-0,0530	0,1433	-0,1954
Scales (horizontal line)	**0,3956**	-0,1295	-0,0580	**0,3326**	0,2514	-0,0233	**0,3421**	0,1076	0,1817
Upper lateral line scale	0,3787	0,0555	-0,1323	0,3300	0,0651	-0,0609	0,3284	0,0757	0,0975
Lower lateral line scales	0,0644	0,0383	0,1245	0,0721	0,3279	0,0232	0,0511	0,2736	0,0604
Circumpeduncular scales	0,0887	-0,1313	-0,0077	-0,0452	-0,1550	**0,3695**	-0,0584	0,1207	0,0094
Scales between lateral line and dorsal fin origin	0,0072	0,1803	0,0508	0,0559	-0,0845	0,2242	-0,0453	**0,4258**	-0,1205
Scales between upper lateral line and last dorsal fin spine	excluded from PCA			0,0683	0,2038	-0,2198	0,0563	-0,0059	**0,3406**
Abdominal vertebrae	0,0391	0,1583	**0,3919**	0,3196	0,1261	0,1910	0,2995	0,2229	-0,2027
Caudal vertebrae	**0,4111**	-0,1008	-0,1867	0,2644	0,1628	-0,2447	0,2940	-0,0699	**0,3180**
Total number of vertebrae	**0,4402**	-0,0336	-0,0346	**0,3632**	0,1820	-0,0498	**0,3627**	0,0695	0,1133
Anal-fin spines	-0,0330	-0,0565	-0,0302	excluded from PCA			excluded from PCA		
Anal-fin rays	0,2794	-0,1319	-0,1872	0,1725	-0,1549	**-0,3444**	0,2492	-0,2348	0,2526
Dorsal-fin spines	0,2593	0,1741	**0,4253**	**0,3313**	-0,1227	0,2700	0,3294	0,0784	-0,2793
Dorsal-fin rays	0,2374	-0,1346	-0,3119	0,0010	0,2911	**-0,4298**	0,0960	0,0526	**0,5315**
Upper procurrent caudal-fin rays	0,0876	**0,5017**	-0,1843	0,1337	**-0,3879**	-0,1702	0,1089	**-0,3981**	-0,1837
Lower procurrent caudal-fin rays	-0,0074	**0,3556**	-0,2083	0,1582	-0,2408	-0,1464	0,1597	-0,3228	-0,1216
Caudal-fin rays	0,0613	**0,5232**	-0,2258	0,1806	**-0,3928**	-0,1968	0,1658	**-0,4443**	-0,1880
Position of the pterygiophore supporting the last dorsal fin spine	0,2775	0,1206	**0,4299**	0,3342	-0,1101	0,2696	**0,3323**	0,0885	-0,2583
Position of pterygiophore supporting the last anal fin spine	0,1786	0,0598	0,3680	0,3092	0,1524	0,2273	0,2913	0,2581	-0,1893

species-specific PCA separates *O. gecki* **sp. nov.** from *O. indermauri* **sp. nov.** based on low PC II scores and from *H. snoeksi* based on high PC II scores and from *O. polyacanthus* by high PC III scores.

Finally, the fifth species-specific PCA (171 specimens included, Table 1, Appendix: Fig. S5) targets the diagnostic differentiation of *O. indermauri* **sp. nov.** from the three species and the Malagarasi-*Orthochromis* which overlap with their PCI and PCII scores of the total dataset (see above). PC I explains 36.45 %, PC II 13.84 % and 10.65 % of the total variance. Differences in the number of scales along the horizontal line, total number of vertebrae, and the position of the pterygiophore supporting the last dorsal-fin spine contribute most to PC I while differences in the number of scales between the upper lateral line and dorsal-fin origin, number of upper procurrent caudal-fin rays, and total number of caudal-fin rays mainly contribute to PC II. The species-specific PCA separates *O. indermauri* **sp. nov.** from *O. gecki* **sp. nov.** based on high PC II scores. Values of PC III for *O. indermauri* **sp. nov.** overlap for all remaining species.

In summary, meristic values alone allow to diagnostically separate each of the new species from almost all analysed rheophilic haplochromine species with the exception of a few taxa; these are, however, well diagnosable using morphometric measurements and colour patterns. Differential diagnoses for the new species were therefore based on a combination of meristic characters, which are supplemented by additional characters.

Orthochromis mporokoso sp. nov.

Orthochromis sp. "Kasinsha"—Schedel *et al.* 2014

Holotype. ZSM 46840 (59.04 mm SL, ex ZSM 41443), Zambia, Kasinsha stream north of Luwinga affluent to Lake Mweru (-9.4894/30.5769).

Paratypes. ZSM 41429 (9, 34.0–74.48 mm SL), Zambia, Mutoloshi stream above Kapuma Falls at Mporokoso on road Mukunsa-Luwinga (-9.3889/30.0956).—ZSM 41443 (4, 40.9–63.2 mm SL), collected with holotype.—MRAC 2018-006-P-0009-0011 (3, 48.7–51.9 mm SL) Zambia, Mutoloshi stream above Kapuma Falls at Mporokoso on road Mukunsa-Luwinga (-9.3889/30.0956).

Additional material. ZSM 46841 (1, ex 41429, 54.28 mm SL; specimen with deformed jaws), Zambia, Mutoloshi stream above Kapuma Falls at Mporokoso on road Mukunsa-Luwinga (-9.3889/30.0956).

Differential diagnosis. *Orthochromis mporokoso* can be readily distinguished from all species currently placed in *Orthochromis* species of the genus *Orthochromis* and *O*. sp. "Igamba" from the Malagarasi drainage system by having more scale rows on cheek (2–4 vs. 0–1). Furthermore, *O. mporokoso* can be distinguished from *O. kasuluensis*, *O. mosoensis,* and *O. rugufensis* by having more scales on operculum (3–4 vs. 0–2); from *O. kasuluensis* by having fewer total vertebrae (30 vs. 31–32); from *O. rugufuensis* by fewer dorsal-fin spines (16–17 vs. 19); from *O. mazimeroensis* by more horizontal line scales (29–30 vs. 26–28), more abdominal vertebrae (14 vs. 12–13) and more total vertebrae (30 vs. 28–29); from *O. rubrolabialis* and *O. uvinzae* by fewer dorsal-fin spines (16–17 vs. 18–20); it has more total gill rakers than *O. rubrolabialis* (10–12 vs. 8–9) and differs in position of pterygiophore supporting last dorsal-fin spine (vertebral count: 16 vs. 17–18). It differs from *O. uvinzae* additionally by having fewer scales between upper lateral line and dorsal-fin origin (4–5 vs. 6–8), fewer abdominal vertebrae (14 vs. 15–16), fewer total vertebrae (30 vs. 31–33), position of pterygiophore supporting last dorsal-fin spine (vertebral count: 16 vs. 18–19), position of pterygiophore supporting last anal-fin spine (vertebral count: 14-15 vs. 16–17); from *O. luongoensis* and *O. torrenticola* by having fewer caudal vertebrae (16 vs. 17–18) and total vertebrae (30 vs. 31–33); from *O. kalungwishiensis* by having fewer total vertebrae (30 vs. 31–33) and fewer horizontal line scales (29–30 vs. 31–32); from *O. torrenticola* additionally by having fewer anal-fin spines (3 vs. 4) and position of pterygiophore supporting last anal-fin spine (vertebral count: 14–15 vs. 16–17). It can be distinguished from *O. stormsi* and *O. polyacanthus* by having fewer scales between upper lateral line and dorsal-fin origin (4–5 vs. 6–9). In addition, it is distinguished from *O. stormsi* by having more horizontal line scales (29–30 vs. 26–28), more total vertebrae (30 vs. 28–29) and fewer total gill rakers (10–12 vs. 13–15); from *O. polyacanthus* by having more series of scales on cheek (2–4 vs. 0), fewer dorsal-fin spines (16–17 vs. 18–20) and in position of pterygiophore supporting last dorsal-fin spine (vertebral count: 16 vs. 17–18) as in position of pterygiophore supporting last anal-fin spine (vertebral count: 14–15 vs. 16–17). Meristic values of *O. mporokoso* overlap with those of *O. machadoi*, but it can be readily distinguished by having more vertical bars on flanks (13–15 vs. 9–10),

which moreover extend mainly ventrally; those of *O. machadoi* extend mainly dorsally. In addition, it is distinguished in head mask pattern, i.e. *V*-shape nostril stripe in *O. mporokoso* vs. straight nostril stripe in *O. machadoi*; cheek stripe present vs. absent in *O. machadoi*. It differs from *Schwetzochromis neodon* by having more circumpeduncular scales (16 vs. 12), fewer inner series of teeth (1–3 vs. 4–6) and fewer dorsal-fin rays (9–10 vs. 11–12). It differs from *H. bakongo* and *H. moeruensis* by having more horizontal line scales (29–30 vs. 26–28), more caudal vertebrae (16 vs. 12–15) and more total vertebrae (30 vs. 26–29). Additionally, it is distinguished from *H. moeruensis* by having more upper lateral line scales (21–23 vs. 19–20); from *H. bakongo* by having more dorsal-fin spines (16–17 vs. 14–15) and in position of pterygiophore supporting last dorsal-fin spine (vertebral count: 16 vs. 13–14); and from *H. snoeksi* it is distinguished by having more abdominal vertebrae (14 vs. 13), fewer caudal vertebrae (16 vs. 17), more anal-fin rays (7–9 vs. 5–6), more total gill rakers (10–12 vs. 9), and in position of pterygiophore supporting last dorsal-fin spine (vertebral count: 16 vs. 15) and position pterygiophore supporting last anal-fin spine (vertebral count: 14–15 vs. 13). Meristic values of *O. mporokoso* overlap with those of *H. vanheusdeni,* but it lacks eggspots, has a nostril stripe (vs. absent in *H. vanheusdeni*), exhibits a cheek stripe (vs. absent in *H. vanheusdeni*), and has higher number of vertical bars on flank (13–15 vs. 6–7). It differs from herein newly described species *O. kimpala* by having fewer scales between upper lateral line and dorsal-fin origin (4–5 vs. 6–7); from *O. indermauri* by having more series of scales on the cheek (2–4 vs. 0–1), more caudal vertebrae (16 vs. 14–15), and more total vertebrae (30 vs. 28–29). Meristic values of *O. mporokoso* overlap with those of *O. katumbii* but former differs by having more vertical bars on flank (13–15 vs. 7–9) and by head mask pattern (i.e.: cheek stripe present vs. absent in *O. katumbii*). Meristic values of *O. mporokoso* overlap with those of *O. gecki* but former is distinguished by having much wider interorbital (15.3–19.5 vs. 9.6–12.9 % HL) and by lacking eggspots on anal fin vs. present in *O. gecki*.

Description. Morphometric measurements and meristic characters are based on 17 type specimens and one additional deformed specimen. Values and their ranges are presented in Table 2. For general appearance see figure 3. Maximum length of wild caught specimens 74.5 mm SL. Moderately slender species with maximum body depth (24.7–29.3 % SL) at level of dorsal-fin origin, slowly decreasing towards caudal peduncle. Caudal peduncle rather elongated and moderately deep (ratio of caudal-peduncle length to depth: 1.5–2.3). Head length almost one third of standard length. Dorsal head profile slightly curved without prominent nuchal gibbosity. Eye diameter larger than interorbital width. Jaws isognathous or slightly retrognathous. Posterior tip of maxilla not reaching anterior margin of orbit but ending slightly before. Lips not noticeably enlarged or thickened. Two separate lateral lines.

Squamation. Flank above and below lateral lines covered with comparatively large ctenoid to cycloid scales, especially in large specimens only few scales of ctenoid appearance. Anterior dorsal and ventral flank area covered by cycloid scales. Belly with comparatively small cycloid scales. Chest covered with even smaller cycloid scales compared to belly squamation; chest to flank transition with larger cycloid scales. Snout scaleless up to anterior margin of orbit. Interorbital, nape, and occipital region with medium sized cycloid scales. Cheeks covered by small cycloid scales; 2–4 scale rows on cheek. Cycloid scales on operculum of variable size (small to medium sized) and shape (ovoid to circular); opercular blotch partially covered by medium sized scales, but posterior margin scaleless. 3–4 scales on horizontal line starting from edge of postero-dorsal angle of operculum to anterior edge of operculum.

Upper lateral line scales 21–23 and lower lateral line 9–11. Horizontal line scales 29–30. Caudal fin with 0–2 pored scales. Upper and lower lateral lines separated by two scales. 3–5 scales between upper lateral line and dorsal-fin origin. Anterior part of caudal fin covered with 4–5 vertical columns of small cycloid scales with median scales slightly larger; scaled area of caudal fin extended posteriorly especially at upper and lower area with minute, interradial scales (approximately up to one third of caudal fin). Sixteen scales around caudal peduncle.

Jaws and dentition. Anterior bicuspid teeth of outer row in both upper and lower jaw large and closely set; posterior teeth becoming almost subequally bicuspid; towards corner of mouth teeth smaller and less closely set, may become unicuspid or weakly bicuspid especially in upper jaw. Individual bicuspid teeth with minimally expanded brownish crown, cusps (major cusp with almost horizontal edge) uncompressed and moderately widely set, and neck moderately slender to stout. Outer row upper jaw with 31–44 teeth and outer row lower jaw with 23–33 teeth (specimens: 34.0–59.0 mm SL). Larger specimens generally with more teeth. Two to three (rarely one) inner upper and lower jaw tooth rows with small tricuspid teeth. Lower pharyngeal bone (Fig. 3) of single dissected paratype (ZSM 41429, 59.8 mm SL) about 1.3 times wider than long with short anterior keel about 0.4 times length dentigerous area. Dentigerous area of lower pharyngeal bone about 1.5 times wider than long, with 10+10 teeth

along posterior margin and 7–8 teeth along midline. Anterior pharyngeal teeth (towards keel) bevelled and slender; those of posterior row larger than anterior ones, bevelled (bicuspid; well-developed major and minor cusp). Largest teeth medially situated in posterior row. Teeth along midline slightly larger than more lateral ones.

Gill rakers. Total gill raker count 10–12, with two epibranchial, one angle, and 7–9 ceratobranchial gill rakers. Most anterior ceratobranchial gill rakers very small, increasing in size towards cartilaginous plug (angle). Gill raker in angle slightly shorter than longest ceratobranchial raker and epibranchial gill rakers further decreasing in size.

Fins. Dorsal fin with 16–17 spines and with 9–10 rays. First dorsal-fin spine always shortest. Dorsal-fin base length between 50.2–55.6 % SL. Posterior end of dorsal-fin rays ending slightly before or at caudal fin base; posterior tip of anal fin ending slightly before caudal-fin base. Caudal-fin outline subtruncate and fin composed of 26–29 rays (16 principal caudal-fin rays and 10–13 procurrent caudal-fin rays). Anal fin with three spines (third spine longest) and 7–9 rays. Anal-fin base length between 15.2–20.1 % SL. Pectoral fin with 15–16 rays. Pectoral-fin length between 21.6–25.7 % SL, longest pectoral ray not reaching level of anus. First upper and lower pectoral-fin rays very short to short. Pelvic fin with first spine thickly covered with skin and five rays. Pelvic-fin base slightly posterior of pectoral-fin base. Pelvic fin slightly longer than pectoral fin; longest pelvic-fin ray almost reaching anus (ending approximately 0.5–2 flank scale widths before).

TABLE 2. Measurements and counts of the holotype, paratypes and one additional specimen (no proportions given due to deformed jaws) of *Orthochromis mporokoso* **sp. nov.**

Measurements	holotype	holotype + paratypes				ZSM 46841
		min	Max	SD	n	
Total length (mm)	72.7	42.0	90.0		17	62.2
Standard length SL (mm)	59.0	34.0	74.5		17	54.3
Head length HL (mm)	17.5	11.3	23.0		17	17.2
% HL						
Interorbital width	18.4	29.6	34.0	1.5	17	-
Preorbital width	31.4	24.5	32.0	2.4	17	-
Horizontal eye length	23.2	21.3	28.2	1.7	17	-
Snout length	36.2	26.9	38.1	2.8	17	-
Internostril distance	15.8	13.5	18.8	1.5	17	-
Cheek depth	23.9	19.6	25.5	1.7	17	-
Upper lip length	30.6	25.4	32.1	2.1	17	-
Lower lip length	26.1	19.2	30.0	2.9	17	-
Lower lip width	29.1	19.6	34.9	3.9	17	-
Lower jaw length	29.7	22.0	34.1	3.6	17	-
Lower pharyngeal jaw length	-	28.0		-	1	-
Lower pharyngeal jaw width	-	36.2		-	1	-
Width of dentigerous area of lower pharyngeal jaw	-	25.9		-	1	-
% SL						
Predorsal distance	32.8	32.1	37.9	1.6	17	-
Dorsal-fin base length	55.5	50.2	55.6	1.5	17	-
Last dorsal-fin spine length	11.1	10.7	13.9	0.9	17	-
Anal fin-base length	16.3	15.2	20.1	1.3	17	-
Third anal-fin spine length	15.1	11.4	16.4	1.3	17	-
Pelvic fin length	22.9	22.1	27.3	1.5	17	-
Pectoral fin length	23.2	21.6	25.7	1.2	17	-
Caudal peduncle depth	10.8	7.9	11.7	1.0	17	-

.....continued on the next page

TABLE 2. (Continued)

Measurements	holotype	holotype + paratypes				ZSM 46841
		min	Max	SD	n	
Caudal peduncle length	20.7	16.5	20.7	1.2	17	-
Body depth (pelvic fin base)	15.2	24.7	29.3	1.2	17	-
Preanal length	59.7	46.1	64.5	4.1	17	-
Anus-anal fin base distance	3.8	2.0	3.8	0.5	17	-
Interpectoral width	15.1	9.0	15.8	1.6	17	-
Counts						
Dorsal-fin spines	17	16 (2); 17 (15)			17	17
Dorsal-fin rays	10	9 (4); 10 (13)			17	10
Anal-fin spines	3	3 (17)			17	3
Anal-fin rays	8	7 (4); 8 (12); 9 (1)			17	8
Pelvic-fin spines	1	1 (17)			17	1
Pelvic-fin rays	5	5 (17)			17	5
Pectoral-fin rays	16	15 (8); 16 (9)			17	16
Upper procurrent caudal-fin rays	6	5 (1); 6 (14); 7 (2)			17	7
Lower procurrent caudal-fin rays	6	5 (3); 6 (14)			17	6
Caudal-fin rays	28	26 (1); 27 (2); 28 (12); 29 (2)			17	29
Scales (horizontal line)	30	29 (9); 30 (8)			17	29
Upper lateral line	21	21 (8); 22 (8); 23 (1)			17	22
Lower lateral line	11	9 (8); 10 (2); 11 (7)			17	11
Circumpeducular	16	16 (17)			17	16
Series of scales on cheek	3	2 (3); 3 (9); 4 (5)			17	3
Scales (horizontal line) on operculum	4	3 (13); 4 (4)			17	3
Scales between lateral line and dorsal fin origin	3	3 (1); 4 (15); 5(1)			17	5
Scales between upper lateral line and last dorsal fin spine	2	2 (17)			17	2
Abdominal vertebrae	14	14 (17)			17	14
Caudal vertebrae	16	16 (17)			17	16
Total number of vertebrae	30	30 (17)			17	30
Teeth in upper outer row	44	31 (1); 33 (1); 35 (2); 39 (1); 40 (3); 41 (1); 42 (2); 43 (3); 44 (2)			17	-
Teeth in lower outer row	29	23 (1); 24 (1); 25 (1); 26 (2); 27 (2); 28 (2); 29 (2); 30 (2); 31 (1); 32 (2); 33 (1)			17	-
Gill rakers (ceratobranchial)	9	7 (3); 8 (11); 9 (2)			17	8
Gill rakers (angle + epibranchial)	3	3 (17)			17	3

Vertebrae and caudal fin skeleton. (Fig. 3)**.** A total of 30 vertebrae (excluding urostyle element), with 14 abdominal and 16 caudal vertebrae. The pterygiophore supporting last dorsal-fin spine is inserted between neural spines of 16th and 17th vertebra (counted from anterior to posterior). Pterygiophore supporting last anal-fin spine is inserted between haemal spines of 15th and 16th vertebra, rarely between ribs of 14th and haemal spine of 15th vertebra (N=2). Single predorsal bone (=supraneural bone) present. Hypurals 1 and 2 as well as hypurals 3 and 4 always fused into single seamless units.

Colouration in life (based on field photographs of adult specimens). (Fig. 3) Body ground colouration pale

brown to light grey; anterior flank with yellow to golden reticulated pattern which becomes less prominent at level of anus and stops at level of caudal peduncle. Dark grey to brownish, interrupted midlateral band from operculum to just posterior caudal fin base, ending in mostly visible blotch; intensity midlateral band varies depending on mood often hardly visible. Midlateral band crossed by 13–15 vertical bars, which extend mainly ventrally, hardly recognizable except for more distinct first 4–5 anterior bars. In some specimens dorsum with irregular dark brown areas, which sometimes connect with midlateral band. Scales on, above and below midlateral band until level of anus with blackish-blue to greyish-blue centres. Dorsum and caudal peduncle pale brown to light grey; chest and belly light beige. Dorsal head surface pale brown to light grey; snout and cheek beige, ventrally brighter. Branchiostegal membrane light beige. Operculum beige to yellowish, sometimes with metallic turquoise speckles, a black opercular spot connecting with anterior extension of midlateral band (interrupted at level of preoperculum) ending in well-pigmented blotch slightly anterior of eye. Another dark grey to brownish element of variable form on ventral corner of operculum. Cheek with small, dark grey to brownish vertical stripe of variable shape and intensity, extending to slightly below eye (not reaching eye). Dark grey to brownish lachrymal stripe ending at posterior end upper lip. Very thin, dark grey to brownish nostril stripe (sometimes interrupted) *V*-shaped, extending between nostrils. Thin, dark grey to brownish interorbital stripe present; no distinct supraorbital stripe, but area just above eye somewhat darker than remaining dorsal head region. Upper and lower lip beige to pale brown, lower margin of upper lip greyish (darker coloured), lower lip lighter than upper. Dorsal-fin membrane transparent with orange maculae, sometimes arranged in inclined rows; maculae bordered with orange and outlined with black, especially in spinous part of fin. Anal fin transparent to yellow, towards margin becoming more intensively coloured, no maculae or eggspots present. Caudal fin yellowish to greyish with two or three rows of small yellow-orange maculae near fin base. Outer caudal-fin rays with black margin. Pectoral and pelvic fins transparent but rays yellowish to greyish.

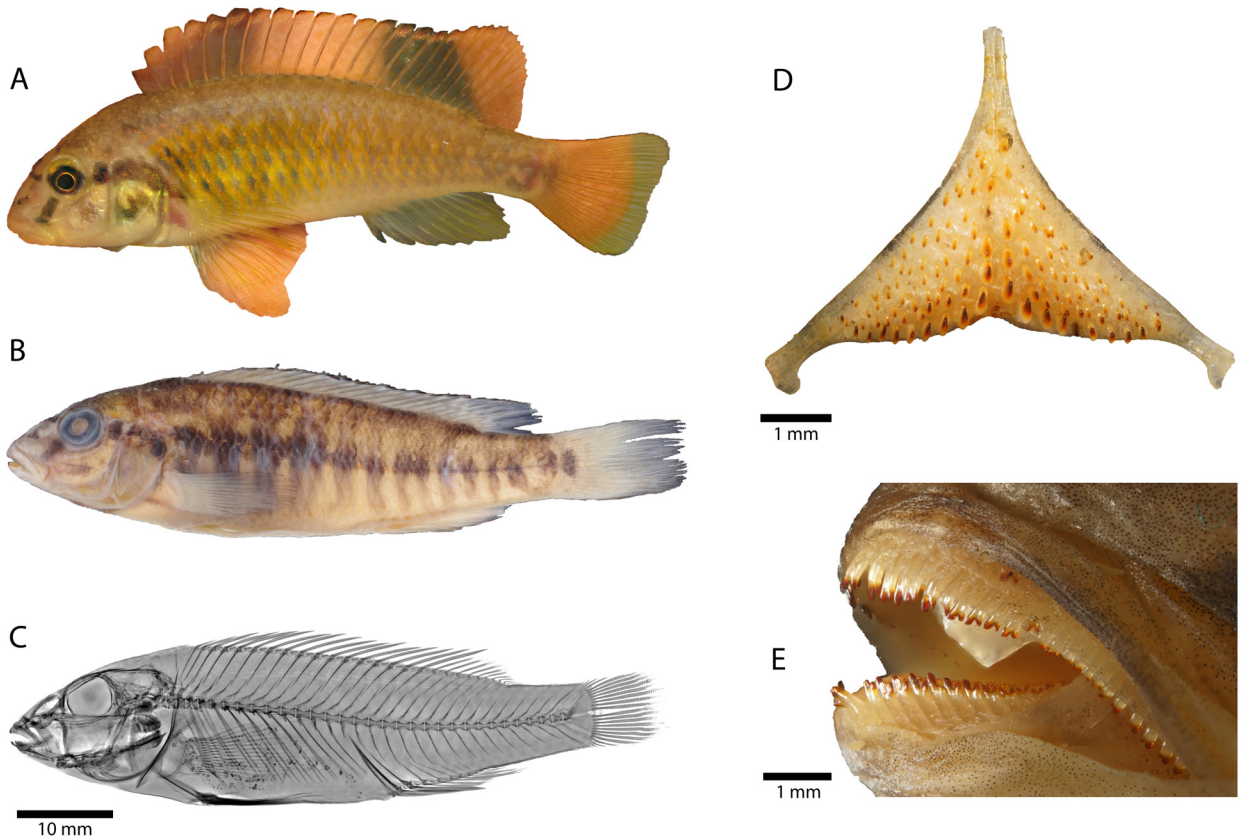

FIGURE 3. *Orthochromis mporokoso* **sp. nov. A.** probably the holotype, alive. Dorsal, anal and caudal fin background coloration is uniform semitransparent and might be lightly yellowish to greyish, i.e. not as in picture (human fingers holding the specimen in photo tank gave artificial beige color to semitransparent fins). **B.** Holotype (ZSM 46840), 59.0 mm SL; Zambia, Kasinsha stream **C.** radiograph of holotype **D.** lower pharyngeal bone (specimen with 59.8 mm SL; ZSM 41429) **E.** Overview of arrangement and morphology of oral jaw teeth (specimen with 74.5 mm SL; ZSM 41429).

Juvenile colouration in life. No information about juvenile colouration available.

Colouration in alcohol. Colouration and melanin patterns similar to live specimens, but due the preservation procedure of specimens, i.e., first formalin fixation, transfer to 75 % EtOH etc., specimens tend to lose original colouration (especially melanin patterns more intense than in live specimens). Overall body ground colouration light brownish; dorsum darker than flank below midlateral band. Chest and belly beige to yellowish-beige. Branchiostegal membrane beige, along operculum and ventrally becoming reddish brown. Dorsal head surface and dorsum brownish, ethmoidal region greyish-brown. Upper lip beige to light greyish anteriorly, lower lip beige. Cheek beige to pale brownish; vertical stripe on cheek faint. Operculum beige to pale brown greyish and with opercular spot as described above (brownish element on operculum less clearly defined than in live specimens and covering almost entire operculum). Head mask brownish. Midlateral band and vertical bars brownish and more intense (especially posterior bars). Dorsal fin whitish to light greyish and margins outlined in black; maculae visible but less intense and greyish. Anal fin whitish to beige; margins blackish outlined. Caudal fin light whitish to beige; margins blackish outlined, small greyish speckles visible on membrane. Pectoral fin and pelvic fin whitish to light grey.

Distribution and biology. *Orthochromis mporokoso* is known from two clear water streams in the vicinity of Mporokoso town. Kasinsha stream (holotype locality, Fig. 1) is about five meters wide with a rocky bottom and on average 50–100 cm deep (Fig. 8).

The water temperature at the type locality was 19.5 °C (15.07.2011, late afternoon) and had a pH of 6.7; at the second sampling locality (Mutoloshi River at Kapuma Falls) a temperature of 19.3 °C (15.07.2011) and a pH of 7.3 was recorded (pers. comm. H. van Heusden 2017). *Orthochromis mporokoso* is a benthic-rheophilic species.

Etymology. The species name *mporokoso* is derived from Mporokoso, a town in the Northern Province (Zambia) near the type locality of the species. A noun in apposition.

Orthochromis katumbii sp. nov.

Orthochromis sp. "Mambilima"—Schedel *et al.* 2014

Holotype. MRAC 2015-009-P-0006 (1, 85.9 mm SL), Democratic Republic of the Congo, Kiswishi River, near confluence with Matete stream, Luapula basin (-11.486528/ 27.650306)

Paratypes. MRAC 2015-009-P-0001 (1, 53.2 mm SL), Democratic Republic of the Congo, Kiswishi River, Futuka farm, Luapula basin (-11.488028/27.645833).—ZSM 46844 (1, ex MRAC 2015-009-P-0002, 81.8 mm SL), Democratic Republic of the Congo, Kiswishi River, Futuka farm, Luapula basin (-11.488028/ 27.645833).—MRAC 2015-009-P-0003 (1, 56.6 mm SL), Democratic Republic of the Congo, Kiswishi River, Futuka farm, Luapula basin (-11.488028/27.645833).—MRAC 2015-009-P-0007-0009 (3, 58.7–85.2 mm SL), collected with holotype.—ZSM 41450 (6, 27.2–57.4 mm SL), Zambia, Luapula River below Mambilima Falls (-10.5689/ 28.6783).

Additional material. ZSM 42322 (2, 71.3–88.9 mm SL), Zambia, Luapula River below Mambilima Falls; kept in aquarium (-10.5689/28.6783).

Differential diagnosis. *Orthochromis katumbii* is distinguished from all Malagarasi-*Orthochromis* species including *O.* sp. "Igamba" except *O. mazimeroensis* and *O. rubrolabialis* by having more scale rows on cheek (1–4 vs. 0). Further it is distinguished from *O. kasuluensis*, *O. mosoensis,* and *O. rugufuensis* by having more scales in lower lateral line (10–13 vs. 7–9) and furthermore from *O. kasuluensis* by having fewer dorsal-fin rays (7–9 vs. 10); from *O. mosoensis* by having more scales on operculum (2–3 vs. 0–1); from *O. uvinzae* by having fewer scales between upper lateral line and dorsal-fin origin (4–5 vs. 6-8), by having fewer dorsal-fin spines (16–18 vs. 19–20) and it is distinguished in position of pterygiophore supporting last dorsal-fin spine (vertebral count: 15–17 vs. 18-19). From *O. mazimeroensis* it is distinguished by having more horizontal line scales (30–31 vs. 26–28), more abdominal vertebrae (14–15 vs. 12–13) and more total vertebrae (30–31 vs. 26–28). It is distinguished from *O. rubrolabialis* by having more ceratobranchial gill rakers (7–9 vs. 5–6) and total gill raker (10–13 vs. 8-9); from *O. stormsi* by having more caudal vertebrae (16–17 vs. 14–15), more total vertebrae (30–31 vs. 28–29), more horizontal line scales (30–31 vs. 26–28) and fewer scales between upper lateral line and dorsal-fin origin (4–5 vs. 6–9); from *O. polyacanthus* by having more series of scales on cheek (1–4 vs. 0); from *O. torrenticola* by having

fewer anal-fin spines (3 vs. 4). Meristic values of *O. katumbii* overlap with those of *O. kalungwishiensis* but is distinguished by differences in colour and melanin patterns (e.g. nostril stripe in *O. katumbii* not extending to interorbital stripe vs. extending in *O. kalungwishiensis*; operculum yellowish-grey in *O. katumbii* vs. reddish-brownish in *O. kalungwishiensis*; vertical bars crossing midlateral band more pronounced in *O. kalungwishiensis*). Meristic values of *O. katumbii* overlap with those of *O. luongoensis* but is distinguished by ratio length/depth of caudal peduncle (1.6–1.9 vs. 2.0–2.4); in addition *O. katumbii* tends to have fewer vertical bars on flank (7–9 vs. 9–12). Meristic values of *O. katumbii* overlap with those of *O. machadoi* but is distinguished by smaller body depth (22.4–27.7 vs. 30.0–32.2 % SL). It is distinguished from *S. neodon* by having more circumpeduncular scales (16 vs. 12), and fewer dorsal-fin rays (9–10 vs. 11–12). It differs from *H. snoeksi* by having more scales on lower lateral line (10–13 vs. 9), more abdominal vertebrae (14–15 vs. 13), fewer caudal vertebrae (16 vs. 17), more anal-fin rays (7–9 vs. 5–6) and more total gill rakers (10–13 vs. 9), in position pterygiophore supporting last anal-fin spine (vertebral count: 15–16 vs. 13) and by having hypurals 3 and 4 fused (vs. clearly separated or fused with distinctly visible seam); differs from *H. bakongo* and *H. moeruensis* by having more horizontal line scales (30–31 vs. 26–28), more caudal vertebrae (16–17 vs. 12–15) and more total vertebrae (30–31 vs. 26–29). Additionally, *O. katumbii* differs from *H. bakongo* by having more dorsal fin spines (16–18 vs. 14–15), by having hypurals 1 and 2 and hypurals 3 and 4 fused (vs. clearly separated or fused with distinctly visible seam) and by position of pterygiophore supporting last dorsal-fin spine (vertebral count: 15–17 vs. 13–14) and from *H. moeruensis* by having more scales on upper lateral line (21–24 vs. 19–20). It differs from *H. vanheusdeni* by having more horizontal line scales (30–31 vs. 26–29). It is distinguished from herein newly described species *O. kimpala* by having more horizontal line scales (30–31 vs. 27–29), fewer scales between upper lateral line and dorsal-fin origin (4–5 vs. 6–7); from *O. indermauri* by having more horizontal line scales (30–31 vs. 25–29), caudal vertebrae (16–17 vs. 14–15), total vertebrae (30–31 vs. 28–29) and by having hypurals 1 and 2 fused vs. clearly separated or fused with distinctly visible seam). Meristic values of *O. katumbii* overlap with those of *O. mporokoso* but is distinguished by having fewer vertical bars on flank (7–9 vs. 13–15) and in head mask pattern (i.e.: no cheek stripe present vs. present in *O. mporokoso*). Meristic values of *O. katumbii* overlap with those of *O. gecki* but is distinguished by having a wider interorbital (15.5–21.7 vs. 9.6–12.9 % HL), moreover *O. katumbii* lacks eggspots on anal fin (vs. present in *O. gecki*).

Description. Morphometric measurements and meristic characters are based on 13 type specimens. Values and their ranges are presented in Table 3. For general appearance see figure 4. Maximum length of wild caught specimens 85.9 mm SL. Moderately slender species with maximum body depth (28.1 % SL) at level of first dorsal-fin spine (smaller specimens) or slightly behind dorsal-fin origin (larger specimens), decreasing towards caudal peduncle. Caudal peduncle rather elongated and moderately deep (ratio of caudal peduncle length to depth: 1.6–1.9). Head length about one third of standard length. In adult specimens dorsal head profile gently curved and without prominent nuchal gibbosity. Dorsal head profile of subadult specimens more distinctly curved (Fig. 9). Eye diameter larger than interorbital width. Jaws isognathous or slightly retrognathous. Posterior tip of maxilla reaching vertical between nostril and anterior margin orbit. Lips not noticeably enlarged or thickened. Two separate lateral lines.

Squamation. Flank above and below lateral lines covered with comparatively large ctenoid scales. Anterior dorsal and ventral flank covered by cycloid scales. Belly with comparatively small cycloid scales. Chest covered with minute, deeply embedded cycloid scales; chest to flank transition with slightly larger cycloid scales. Snout scaleless. Interorbital scales cycloid and deeply embedded. Nape and occipital region with medium sized cycloid scales. Cheeks covered by small, partly embedded cycloid scales; 2–4 scale rows on cheek. Cycloid scales on operculum of variable size (small to medium) and shape (ovoid to circular); opercular blotch only partially covered by medium sized scales, but posterior margin always scaleless. Two to three scales on horizontal line starting from edge of postero-dorsal angle of operculum to anterior edge of operculum.

Upper lateral line scales 21–24, lower lateral line 10–13. Horizontal line scales 30–31. Caudal fin with 0–2 pored scales. Upper and lower lateral lines separated by two scales; 4–5 scales between upper lateral line and dorsal-fin origin. At level of last dorsal-fin spine one dorso-ventrally compressed cycloid scale and one normal sized ctenoid scale between origin of last dorsal-fin spine and upper lateral line. Anterior part of caudal fin covered with 3–4 vertical columns of small cycloid scales; with median scales being slightly larger; scaled area of caudal fin extended posteriorly, especially at upper and lower area, with minute, interradial scales (approximately up to two fifths of caudal fin). Sixteen scales around caudal peduncle.

TABLE 3. Measurements and counts of holotype and paratypes and of additional specimens of *Orthochromis katumbii* **sp. nov.**

Measurements	holotype	holotype + paratypes				ZSM 42322	
		min	Max	SD	n	Ind. 1	Ind. 2
Total length (mm)	103.6	33.3	103.6		13	84.8	106.5
Standard length SL (mm)	85.9	27.2	85.9		13	71.3	88.9
Head length HL (mm)	25.7	8.9	25.7		13	22.2	26.6
% HL							
Interorbital width	20.6	14.5	21.7	2.1	13	17.4	19.4
Preorbital width	35.1	26.2	35.1	2.7	13	32.6	36.0
Horizontal eye length	23.7	22.5	28.9	1.6	13	23.9	21.0
Snout length	40.7	28.5	40.7	3.5	13	37.4	39.0
Internostril distance	18.6	16.4	21.7	1.4	13	19.9	21.4
Cheek depth	25.1	18.5	28.4	2.7	13	32.8	26.0
Upper lip length	31.5	24.6	34.6	2.7	13	29.6	37.6
Lower lip length	30.2	18.9	31.2	3.9	13	28.4	33.1
Lower lip width	35.4	24.6	38.3	3.3	13	34.2	41.4
Lower jaw length	33.3	26.1	36.8	2.8	13	35.1	33.7
Lower pharyngeal jaw length	-	25.7		-	1		
Lower pharyngeal jaw width	-	30.1		-	1		
Width of dentigerous area of lower pharyngeal jaw	-	21.9		-	1		
% SL							
Predorsal distance	32.0	31.6	36.1	1.4	13	32.6	31.8
Dorsal-fin base length	55.1	54.1	58.1	1.2	13	55.9	57.0
Last dorsal-fin spine length	9.5	9.5	13.8	1.2	13	12.3	11.8
Anal-fin base length	18.9	14.7	20.2	1.5	13	15.5	17.8
Third anal-fin spine length	10.5	10.5	20.2	2.5	13	11.1	12.1
Pelvic fin length	21.0	19.6	25.7	1.8	13	18.1	18.1
Pectoral fin length	22.1	19.5	23.8	1.1	13	20.1	19.4
Caudal peduncle depth	11.0	10.3	12.2	0.6	13	11.0	11.0
Caudal peduncle length	19.1	17.9	20.9	0.7	13	18.6	16.9
Body depth (pelvic fin base)	27.6	22.4	27.7	1.9	13	27.5	28.5
Preanal length	58.5	54.9	62.1	1.6	13	63.2	62.2
Anus-anal fin base distance	3.8	1.4	4.0	0.9	13	3.1	3.4
Interpectoral width	15.5	10.6	15.5	1.4	13	16.0	15.4
Counts							
Dorsal-fin spines	17	16 (2); 17 (6); 18 (4)			12	18	17
Dorsal-fin rays	9	9 (7); 10 (5)			12	9	10
Anal-fin spines	3	3 (12)			12	3	3
Anal-fin rays	7	7 (6); 8 (5); 9 (1)			12	7	8
Pelvic-fin spines	1	1 (12)			12	1	1
Pelvic-fin rays	5	5 (12)			12	5	5
Pectoral-fin rays	15	15 (10); 16 (2)			12	15	15
Upper procurrent caudal-fin rays	7	6 (6); 7 (6)			12	7	7

.....continued on the next page

TABLE 3. (Continued)

Measurements	holotype	holotype + paratypes				ZSM 42322	
		min	Max	SD	n	Ind. 1	Ind. 2
Lower procurrent caudal-fin rays	6	5 (1); 6 (11)			12	7	7
Caudal-fin rays	29	27 (1); 28 (5); 29 (6)			12	29	29
Scales (horizontal line)	30	30 (9); 31 (3)			12	30	30
Upper lateral line	21	21 (5); 22 (4); 23 (2); 24 (1)			12	24	22
Lower lateral line	13	10 (1); 11 (3); 12 (6); 13 (2)			12	11	11
Circumpeducular	16	16 (2)			12	16	16
Series of scales on cheek	2	1 (3); 2 (5); 3 (3); 4 (1)			12	3	3
Scales (horizontal line) on operculum	3	2 (6); 3 (6)			12	3	3
Scales between lateral line and dorsal fin origin	5	4 (2); 5 (10)			12	5	5
Scales between upper lateral line and last dorsal fin spine	2	2 (12)			12	2	2
Abdominal vertebrae	14	14 (10); 15 (2)			12	14	14
Caudal vertebrae	17	16 (6); 17 (6)			12	17	17
Total number of vertebrae	31	30 (4); 31 (8)			12	31	31
Teeth in upper outer row	52	29 (1); 30 (1); 32 (1); 36 (2); 38 (1); 39 (1); 41 (1); 45 (1); 48 (1); 49 (1); 52 (1)			12	46	54
Teeth in lower outer row	35	24 (1); 25 (1); 26 (2); 27 (1); 31 (1); 32 (1); 33 (2); 35 (1); 37 (1); 39 (1)			12	28	37
Gill rakers (ceratobranchial)	7	7 (8); 8 (2); 9 (2)			12	8	7
Gill rakers (angle + epibranchial)	3	3 (8); 4 (3); 5 (2)			12	4	4

Jaws and dentition. Anterior teeth of outer row of upper and lower jaw bicuspid to subequally bicuspid, large and closely set; more posterior teeth becoming subequally bicuspid, towards corner of mouth teeth smaller and less closely set and unicuspid. Individual bicuspid teeth with minimally expanded brownish crown, cusps slightly compressed and moderately widely set, neck moderately slender. Outer row of upper jaw with 29–52 teeth and outer row of lower jaw with 24–39 teeth (specimens: 37.2–85.6 mm SL). Larger specimens generally with more teeth. Two to three (rarely one or four) inner upper and lower jaw tooth rows with small tricuspid teeth. Generally larger individuals with more inner tooth rows. Lower pharyngeal bone (Fig. 4) of single dissected paratype (MRAC 2015-009-P-0007-0009, 77.2 mm SL) about 1.2 times wider than long with short anterior keel about 0.4 times length of dentigerous area. Dentigerous area of lower pharyngeal bone about 1.4 times wider than long, with 12+12 (empty tooth-sockets included) teeth along posterior margin and 6–8 (empty tooth-sockets included) teeth along midline. Anterior pharyngeal teeth (towards keel) bevelled and slender; those of posterior row larger than anterior ones, bevelled (bicuspid; well-developed major and minor cusp). Largest teeth medially situated in posterior row. Teeth along midline slightly larger than more lateral ones.

Gill rakers. Total gill raker count 10–13 with 2–4 epibranchial, one angle, and 7–9 ceratobranchial gill rakers. Most anterior ceratobranchial gill rakers smallest, increasing in size towards cartilaginous plug (angle). Anterior gill rakers on ceratobranchial unifid, towards cartilaginous plug sometimes bifid. Gill raker on cartilaginous plug shorter than longest ceratobranchial gill raker and epibranchial gill rakers further decreasing in size.

Fins. Dorsal fin with 16–18 spines and with 9–10 rays. First dorsal-fin spine always shortest. Dorsal-fin base length between 54.0–58.1 % SL. Posterior end of dorsal-fin rays almost reaching caudal-fin base; posterior tip of anal fin ending before caudal fin base. Caudal fin outline subtruncate and composed of 27–29 rays (16 principal caudal-fin rays and 11–13 procurrent caudal-fin rays). Anal fin with 3 spines (3rd spine longest) and 7–9 rays. Anal-fin base length between 14.8–20.2 % SL. Pectoral fin with 15 or 16 rays. Pectoral-fin length between 19.5–23.8 % SL; longest pectoral ray not reaching level of anus. First upper and lower pectoral-fin rays very short to short.

Pelvic fin with 1st spine thickly covered with skin, and 5 rays. Pelvic fin base slightly further posterior pectoral fin base. Longest pelvic-fin ray almost reaching (especially in smaller specimens) or ending well before anus (ending approximately 2 flank scales width before).

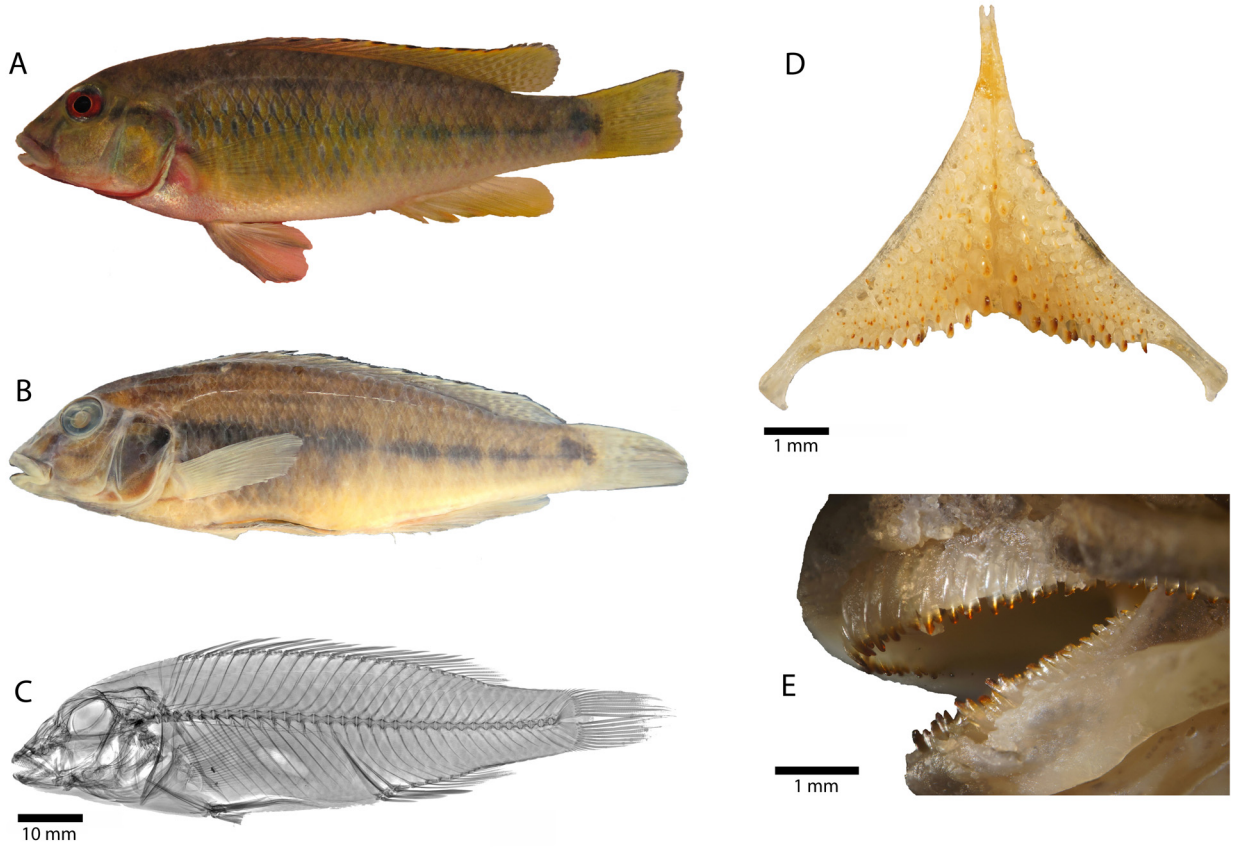

FIGURE 4. *Orthochromis katumbii* **sp. nov. A.** holotype, alive **B.** holotype (MRAC 2015-009-P-0006), 85.9 mm SL; Democratic Republic of the Congo, Kiswishi River **C.** radiograph of holotype **D.** lower pharyngeal bone (specimen: MRAC 2015-009-P-0007-0009, 77.2 mm SL) **E.** Overview of arrangement and morphology of oral jaw teeth (specimen: MRAC 2015-009-P-0007-0009, 77.2 mm SL).

Vertebrae and caudal fin skeleton. 30–31 total vertebrae (excluding urostyle element), with 14–15 abdominal and 16–17 caudal vertebrae. Pterygiophore supporting last dorsal-fin spine is inserted between neural spines of 15th and 16h, 16th and 17th, or 17th and 18th vertebra (counted from anterior to posterior). Pterygiophore supporting last anal-fin spine is inserted between haemal spines of 15th and 16 th vertebra or 16th and 17th vertebra. Single predorsal bone (=supraneural) present. Hypurals 1 and 2 as well as hypurals 3 and 4 always fused.

Colouration in life (based on field photographs of adult specimens). (Fig. 4) Body ground colouration pale brown to yellowish. Dark grey to brownish, interrupted midlateral band extending from operculum to just behind caudal fin base ending as a blotch (less distinct than in *O. luongoensis* and sometimes hardly visible at all); midlateral band intensity varies depending on mood, sometimes fainting to greyish band. Midlateral band crossed by 7–10 light brown to sooty black vertical bars; these bars are short (extending shortly above and below midlateral band) and rather faint in colouration and not always recognizable. However, it should be mentioned that intensity of body markings is strongly dependent on motivational state. Chest light beige with some reddish sparkles (especially in bigger specimens). Belly light beige. Dorsal head surface and snout pale brown to greyish; cheek beige to yellow-greyish. Iris reddish at level of interorbital stripe/anterior extension of midlateral band (red more prominent in bigger specimens). Lower jaw and mental area pale beige to reddish. Throat and branchiostegal membrane reddish (ventral side of branchiostegal membrane in *O. luongoensis* blackish). Operculum beige to yellow-greyish with a dark grey to blackish opercular spot connecting anterior extension of midlateral band that ends almost at posterior edge of eye. Another light brownish element of variable form and intensity on ventral

corner of operculum; such element also present in *O. luongoensis* but less intense in *H. katumbii*. Dark grey to brownish lachrymal stripe ending at posterior end of upper lip. Thin, dark grey to brownish nostril stripe (sometimes interrupted) in form of flattened *U* extending between nostrils. Dark grey to brownish interorbital stripe more intense than nostril stripe. No supraorbital stripe present. Upper and lower lip beige to pale brown, lower margin of upper lip greyish, lower lip lighter then upper lip. Dorsal fin membrane light orange to pale brown with columns of light reddish-orange to brownish maculae between branched rays and to some degree between last dorsal-fin spine (membrane between maculae brighter, almost hyaline); spinous dorsal fin with black marginal band and reddish-orange lappets; marginal band extending to some degree onto rayed part of dorsal fin. Anal fin light orange to pale brown, more intensively coloured towards distal margin. Spinous anal fin with faint reddish-orange margin. No maculae or eggspots present. Caudal fin light orange to pale brown becoming more intensively coloured near margin; membrane between rays with three vertical columns of small greyish maculae (membrane between maculae brighter, almost hyaline, especially in central part of caudal fin). Outer caudal-fin rays with dark orange to blackish margin. Pectoral fin light orange, especially rays of this colour. Pelvic fin compared to pectoral fin less coloured, appearing almost transparent, membrane of pelvic fin spine greyish.

Juvenile colouration in life. (based on photos of tank-raised juveniles approximately 25 mm SL; Fig. 9) Ground colouration greyish, belly beige. Patterns and stripes of head as described for adults. Greyish vertical bars on flanks more prominent than in adults. Iris greyish. Dorsal fin hyaline with some blackish spots on membrane; all other fins hyaline.

Colouration in alcohol. Colouration and melanin patterns similar to live specimens, but due the preservation procedure of specimens, i.e., first formalin fixation, transfer to 75 % EtOH etc., specimens tend to lose original colouration (especially melanin patterns more intense than in live specimens). Overall body ground colouration brownish; dorsum, flank and caudal peduncle brownish becoming beige at ventral side (band of one to two scales ventrally of flanks and caudal peduncle). Chest beige to light brownish and belly beige. Branchiostegal membrane light greyish, ventral side of branchiostegal membrane dark brown, towards anterior tip becoming brighter. Dorsal head surface brownish as dorsum, ethmoidal area becoming greyish-brown. Upper lip light greyish to beige; lower margin of upper lip greyish; lower lip beige. Cheek beige to brownish; centrally below eye a brownish blotch of variable intensity visible (as in *O. luongoensis*, which is not the case in living specimens). Operculum brown to dark brownish with opercular spot as described above; light brownish element of living specimens hardly visible or indistinguishable from operculum ground colouration in conserved specimens. Markings of head mask dark brownish to dark grey. Midlateral band dark brownish and vertical bars light brownish (less distinct than midlateral band). Dorsal fin greyish with black margin, subsequently followed by beige lappets; greyish maculae mainly on rayed part still visible but less intense. Anal fin whitish to beige. Pectoral fin beige. Pelvic fin beige; membrane of spine light greyish. Caudal fin light, at base pale brownish, caudally becoming beige; greyish maculae still present but less intense; margins blackish.

Distribution and biology. *Orthochromis katumbii* is known from Kiswishi River, a western tributary of the Luapula and from the Mambilima Falls on the Luapula (Fig. 1). At the type, locality the Kiswishi River is about ten meters wide and on average about one meter deep and the bottom substrate consists of gravel and smaller rocks (Fig. 8). Water temperature varied between 19.3 and 23.8 °C (measured in August and September), pH between 7.73–7.95, electrical conductivity 377.7 and 380.1µS. *O. katumbii* is a benthic-rheophilic maternal mouthbrooder with clutch sizes, in captivity, of between 25 and 30 eggs (pers. comm. J. Geck). Recently a monogenean gill parasite *Cichlidogyrus consobrini* Jorissen, Pariselle and Vanhove 2017 was described from specimens obtained from *O. katumbii* and *Sargochromis mellandi* (Boulenger 1905).

Etymology. The species is named after Mr. Moïse Katumbi who supported part of the 2015 ichthyological research field expedition of the Mbisa Congo project in Katanga province of the DRC, who himself is a great fish enthusiast. Some specimens of the new species were collected on his farm “Ferme de Futuka”.

Orthochromis kimpala sp. nov.

Holotype. MRAC 2012-031-P-2096 (84.58 mm SL), Democratic Republic of the Congo, Kalule Nord River, right tributary of Lualaba River, near to the bridge on road Makulakulu-Lubudi (-9.6935/25.8479).

Paratypes. ZSM 46849 (2, ex MRAC uncat., 62.7–78.8 mm SL), collected with holotype.—ZSM 46850 (1, ex

MRAC uncat., 44.0 mm SL), collected with holotype.—MRAC 2015-005-P-0032-0033 (2, 56.9–62.6 mm SL), Democratic Republic of the Congo, Kalule Nord River, bridge Lubudi-Luena (-9.693472/25.847833).—MRAC 2015-005-P-0034-0035 (2, 56.3–60.5 mm SL), Democratic Republic of Congo, Kalule Nord River, Kyabule village, bridge Mukulakulu-Kolwezi (-9.66725/25.740056).—MRAC 2015-005-P-0036-0037 (2, 57.7–61.3 mm SL), Democratic Republic of the Congo, Kalule Nord River, Kyabule village, bridge Mukulakulu-Kolwezi (-9.66725/25.740056).

Differential diagnosis. *Orthochromis kimpala* can be readily distinguished from all species currently placed in *Orthochromis* (sensu de Vos & Seegers, 1998) except *O. torrenticola,* by presence of eggspot-like maculae on anal fin. Further, it is distinguished from Malagarasi-*Orthochromis* species, including *O.* sp. "Igamba", by having more scale rows on cheek (3–4 vs. 0 or 0–1 in case of *O. mazimeroensis* and *O. rubrolabialis*). Furthermore, *O. kimpala* differs from *O. luichensis*, *O. malagaraziensis*, *O. mazimeroensis*, *O. mosoensis,* and *O. rubrolabialis* by having more scales between upper lateral line and dorsal-fin origin (6–7 vs. 4–5). Additionally, it has fewer dorsal-fin spines than *O. luichensis*, *O. malagaraziensis,* and *O. rubrolabialis* (15–16 vs. 17–19). Moreover, it differs from *O. rubrolabialis* by having more total gill rakers (11–12 vs. 8–9) and by position of pterygiophore supporting last dorsal-fin spine (vertebral count: 14-16 vs. 17-19); from *O. mazimeroensis* by having more abdominal vertebrae (14–15 vs. 12–13); from *O. mosoensis* by having more scales (horizontal line) on operculum (3 vs. 0–1). *O. kimpala* is distinguished from *O. kasuluensis*, *O. rugufuensis* and *O. uvinzae* by having fewer dorsal-fin spines (15–16 vs. 17-20); from *O. kasuluensis* and *O. rugufuensis* by having more scales (horizontal line) on operculum (3 vs. 1–2); from *O. kasuluensis* and *O. uvinzae* by having fewer scales in upper lateral line (20–22 vs. 23–25) and fewer total vertebrae (28–30 vs. 31–33). Moreover,it differs from *O. uvinzae* by having fewer horizontal line scales (27–29 vs. 30–32) and by position of pterygiophore supporting last dorsal-fin spine (vertebral count: 14–16 vs. 18–19). It can be distinguished from *O. kalungwishiensis*, *O. luongoensis, O. polyacanthus,* and *O. torrenticola* by having fewer dorsal-fin spines (15–16 vs. 17–20); further from *O. kalungwishiensis*, *O. luongoensis,* and *O. torrenticola* by fewer horizontal line scales (27–29 vs. 30–32) and fewer total vertebrae (28–30 vs. 31–33); from *O. luongoensis* and *O. torrenticola* by fewer caudal vertebrae (13–16 vs. 17–18); from *O. torrenticola* by having fewer anal-fin spines (3 vs. 4). Moreover, it is distinguished from *O. torrenticola* and *O. polyacanthus* by position of pterygiophore supporting last anal-fin spine (vertebral count: 14–15 vs. 16–17). It is distinguished from *O. stormsi* by having fewer total gill rakers (11–12 vs. 13–15). It differs from *S. neodon* by having more scale rows on cheek (3–4 vs. 1–2), fewer horizontal line scales (27–29 vs. 30–31), more circumpeduncular scales (16 vs. 12), fewer inner series of teeth (2–3 vs. 4–6). It differs from *H. snoeksi* by having fewer horizontal line scales (27–29 vs. 30–31), fewer scales on upper lateral line (20–22 vs. 23), more abdominal vertebrae (14–15 vs. 13) and fewer caudal vertebrae (13–16 vs. 17), more anal-fin rays (8–10 vs. 5–6) and more total gill rakers (11–12 vs. 9); from *H. bakongo* by having more scales between upper lateral line and dorsal-fin origin (6–7 vs. 3–5); from *H. moeruensis* by having more upper procurrent caudal-fin rays (6–7 vs. 5) and more total caudal-fin rays (26–27 vs. 28–29); from *H. vanheusdeni* by having more scale rows on cheek (3–4 vs. 0–2). It is distinguished from herein newly described species *O. mporokoso* by more scales between upper lateral line and dorsal-fin origin (6–7 vs. 4–5); from *O. katumbii* by having fewer horizontal line scales (27–29 vs. 30–31), and by more scales between upper lateral line and dorsal-fin origin (6–7 vs. 4–5); from *O. gecki* by having more series of scales on cheek (3–4 vs. 0–2); from *O. indermauri* by having more series of scales on cheek (3–4 vs. 1–2) and by fewer dorsal-fin spines (15–16 vs. 17–18).

Description. Morphometric measurements and meristic characters are based on 10 type specimens. Values and their ranges are presented in Table 4. For general appearance see figure 5. Maximum length of wild caught specimens 84.6 mm SL. Moderately slender species with maximum body depth (24.8–30.5 % SL) at level of first dorsal-fin spine, decreasing rather quickly towards caudal peduncle. Caudal peduncle rather short and deep (ratio of caudal peduncle length to depth: 1.2–1.4). Head length almost one third of standard length. Dorsal-head profile rather strongly curved and without a prominent nuchal gibbosity. Eye diameter larger than interorbital width. Jaws isognathous. Posterior tip of maxilla reaching or almost reaching to anterior margin of orbit. Lips not noticeably enlarged or thickened, but upper lip becoming thicker posteriorly. Two separate lateral lines.

Squamation. Flank above and below lateral lines covered with comparatively large, well developed ctenoid scales. Anterior dorsal and ventral flank covered by cycloid scales. Margin of belly with deeply embedded medium sized scales; central belly region scaleless. Chest covered with minute, deeply embedded cycloid scales, giving impression of a scaleless chest; chest to flank transition with larger cycloid scales, however, still deeply embedded.

Snout scaleless. Interorbital scales minute to small, cycloid and deeply embedded. Nape region covered with small, deeply embedded cycloid scales becoming slightly larger towards occipital region. Occipital region with small to medium sized cycloid scales. Cheek covered by medium sized cycloid scales; 3–4 scale rows on cheek. Cycloid scales on operculum of medium size and variable shape (ovoid to circular); opercular blotch only on anterior margins covered by medium sized scales, main area of opercular blotch scaleless. Three scales on a horizontal line starting from edge of postero-dorsal angle of operculum to anterior edge of operculum.

TABLE 4. Measurements and counts of holotype and paratypes of *Orthochromis kimpala* **sp. nov.**

Measurements	holotype	holotype + paratypes			
		min	Max	SD	n
Total length (mm)	101.7	54.4	101.7		10
Standard length SL (mm)	84.6	44.0	84.6		10
Head length HL (mm)	26.7	14.2	26.7		10
% HL					
Interorbital width	18.1	13.0	18.1	1.7	10
Preorbital width	36.1	28.2	36.1	2.8	10
Horizontal eye length	23.4	20.6	28.4	2.3	10
Snout length	38.1	29.8	40.3	3.7	10
Internostril distance	22.7	17.2	22.7	1.6	10
Cheek depth	29.9	25.3	31.8	1.9	10
Upper lip length	36.9	29.0	36.9	2.9	10
Lower lip length	35.8	26.1	35.8	3.9	10
Lower lip width	44.6	27.1	44.6	4.7	10
Lower jaw length	37.8	33.4	40.4	2.3	10
Lower pharyngeal jaw length	-	29.3		-	1
Lower pharyngeal jaw width	-	34.0		-	1
Width of dentigerous area of lower pharyngeal jaw	-	25.8		-	1
% SL					
Predorsal distance	34.9	32.9	38.1	1.6	10
Dorsal-fin base length	56.7	51.4	56.9	1.9	10
Last dorsal-fin spine length	12.9	10.4	14.0	1.2	10
Anal-fin base length	20.0	17.4	20.6	1.1	10
Third anal-fin spine length	9.9	9.7	12.7	1.0	10
Pelvic fin length	20.8	20.6	25.2	1.4	10
Pectoral fin length	20.6	20.6	24.8	1.4	10
Caudal peduncle depth	11.9	10.5	11.9	0.5	10
Caudal peduncle length	15.5	12.7	16.1	1.0	10
Body depth (pelvic fin base)	29.7	24.8	30.5	2.0	10
Preanal length	67.8	60.3	67.8	2.3	10
Anus-anal fin base distance	3.1	2.0	4.7	0.8	10
Interpectoral width	16.4	12.9	16.9	1.2	10
Counts					
Dorsal-fin spines	16	15 (4); 16 (6)			10
Dorsal-fin rays	11	10 (4); 11 (6)			10
Anal-fin spines	3	3 (10)			10

.....continued on the next page

TABLE 4. (Continued)

Measurements	holotype	holotype + paratypes			
		min	Max	SD	n
Anal-fin rays	9	8 (6); 9 (3); 10 (1)			10
Pelvic-fin spines	1	1 (10)			10
Pelvic-fin rays	5	5 (10)			10
Pectoral-fin rays	15	14 (1); 15 (6); 16 (3)			10
Upper procurrent caudal-fin rays	6	6 (5); 7 (5)			10
Lower procurrent caudal-fin rays	6	6 (10)			10
Caudal-fin rays	28	28 (5); 29 (5)			10
Scales (horizontal line)	29	27 (4); 28 (2); 29 (4)			10
Upper lateral line	22	20 (3); 21 (4); 22 (3)			10
Lower lateral line	11	8 (2); 9 (3); 10 (4); 11 (1)			10
Circumpeducular	16	16 (10)			10
Series of scales on cheek	4	3 (3); 4 (7)			10
Scales (horizontal line) on operculum	3	3 (10)			10
Scales between lateral line and dorsal fin origin	6	6 (7); 7 (3)			10
Scales between upper lateral line and last dorsal fin spine	2	2 (10)			10
Abdominal vertebrae	14	14 (9); 15 (1)			10
Caudal vertebrae	16	13 (1); 14 (1); 15 (7); 16 (1)			10
Total number of vertebrae	30	28 (2); 29 (7); 30 (1)			10
Teeth in upper outer row		30 (1); 33 (1); 37 (1); 38 (1); 43 (2); 44 (3); 47 (1)			10
Teeth in lower outer row		28 (1); 29 (2); 32 (1); 33 (2); 35 (1); 36 (1); 38 (2)			10
Gill rakers (ceratobranchial)		7 (1); 8 (8); 9 (1)			10
Gill rakers (angle + epibranchial)		3 (9); 4 (1)			10

Upper lateral line scales 20–22 and lower lateral line 8–11. Horizontal line scales 27–29. Caudal fin with 0–2 pored scales. Upper and lower lateral lines separated by two scales; 6–7 scales between upper lateral line and dorsal-fin origin. Anterior part of caudal fin covered with 2–3 vertical rows of small cycloid scales; with median scales slightly larger; scaled area of caudal fin extended posteriorly especially at upper and lower area with minute, interradial scales (approximately up to one half of caudal fin). Sixteen scales around caudal peduncle.

Jaws and dentition. Anterior teeth of outer row of upper and lower jaw bicuspid to subequal bicuspid, large and moderately closely set; towards corner of mouth, teeth smaller and more widely set and unicuspid. Individual bicuspid teeth with minimally expanded brownish crown, cusps uncompressed and moderately narrowly set, neck moderately stout. Outer row of upper jaw with 30–47 teeth and outer row of lower jaw with 28–38 teeth (specimens: 44.4–84.6 mm SL); larger specimens generally with more teeth. Two to three inner upper and lower jaw tooth rows with small tricuspid teeth (rarely bicuspid).

Lower pharyngeal bone (Fig. 5) of single dissected paratype (ZSM 46849, 62.7 mm SL) about 1.2 times wider than long with anterior keel about 0.5 times of length of dentigerous area. Dentigerous area of lower pharyngeal bone about 1.6 times wider than long, with 11+11 (empty tooth-sockets included) teeth along posterior margin and eight teeth along midline. Anterior pharyngeal teeth (towards keel) bevelled to pronounced and slender; those of posterior row larger than anterior ones, bevelled (minor cusp not well developed). Largest teeth medially situated in posterior tooth row. Teeth along midline slightly larger than more lateral ones.

Gill rakers. Total gill raker count 11, with 2–3 epibranchial, one in angle, and 7–8 ceratobranchial gill rakers. Most anterior ceratobranchial gill rakers smallest increasing quickly in size towards cartilaginous plug (angle). Gill raker in angle slightly shorter than longest ceratobranchial gill raker and epibranchial gill rakers further decreasing in size.

Fins. Dorsal fin with 15–16 spines and with 10–11 rays. First dorsal-fin spine always shortest. Dorsal-fin base length between 51.4–56.9 % SL. Posterior end of dorsal-fin rays reaching or slightly extending beyond caudal fin base; posterior tip of anal fin ending slightly before caudal fin base. Caudal fin outline subtruncate and fin composed of 28–29 rays (16 principal caudal-fin rays and 12–13 procurrent caudal-fin rays). Anal fin with 3 spines (3rd spine longest) and 8–10 rays. Anal-fin base length between 17.4–20.6 % SL. Pectoral fin with 14–16 rays. Pectoral-fin length between 20.6–24.8 % SL; longest pectoral ray not reaching level of anus. First upper and lower pectoral-fin rays very short to short. Pelvic fin with 1st spine thickly covered with skin and five rays. Pelvic-fin base slightly more posterior than pectoral fin base. Longest pelvic-fin ray not reaching anus (ending approximately 3 flank scale widths before).

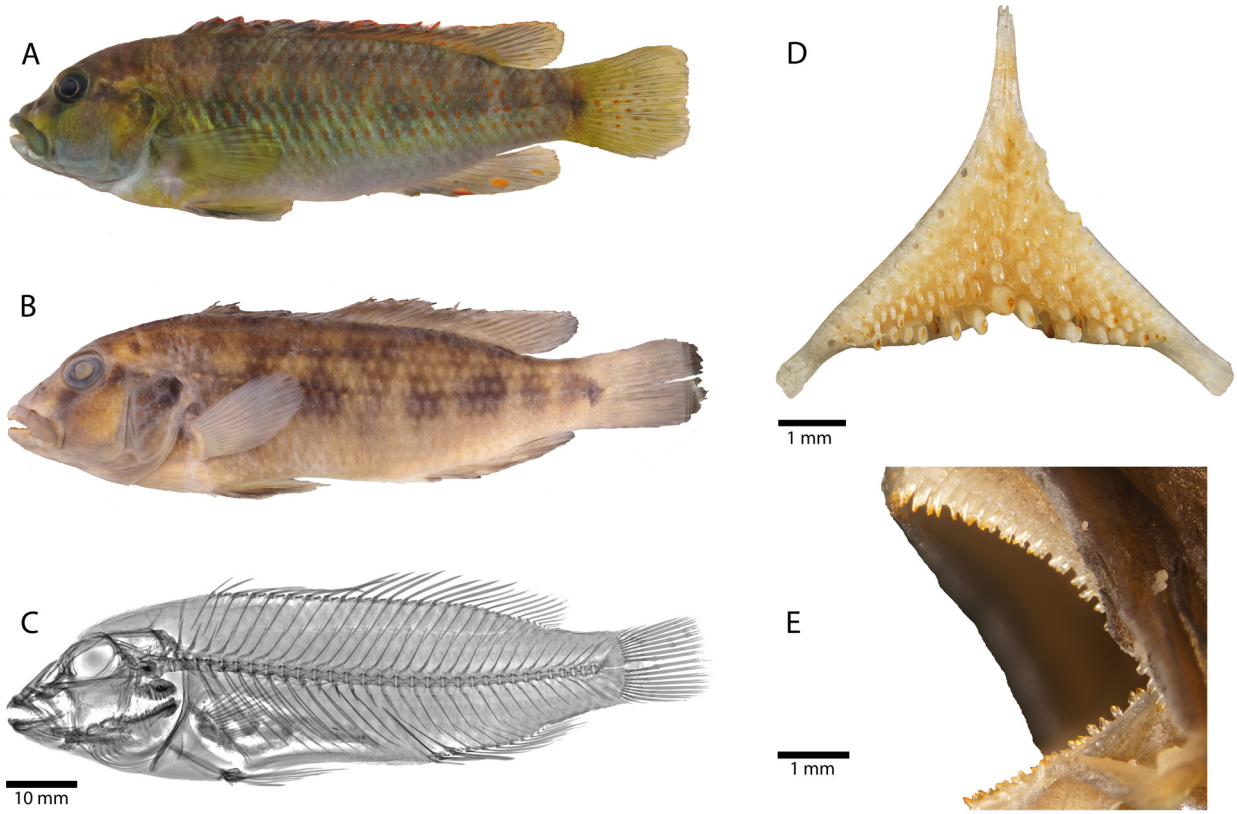

FIGURE 5. *Orthochromis kimpala* **sp. nov. A.** probably the holotype, alive **B.** Holotype, (MRAC 2012-031-P-2096), 84.6 mm SL; Democratic Republic of the Congo, Kalule Nord River stream **C.** radiograph of holotype **D.** lower pharyngeal bone (specimen: ZSM 46849, 62.7 mm SL) **E.** Overview of arrangement and morphology of oral jaw teeth (specimen: MRAC 2015-005-P-0036-0037, 61.3 mm SL).

Vertebrae and caudal fin skeleton. 28–30 total vertebrae (excluding urostyle element), with 14–15 abdominal and 13–16 caudal vertebrae. Pterygiophore supporting last dorsal-fin spine inserted between neural spines of 14th and 15th, 15th and 16th or 17th and 18th vertebra (counted from anterior to posterior). Pterygiophore supporting last anal-fin spine is inserted between rips of 14th (or 15th) and haemal spine of 15th (or 16th) vertebra or between haemal spine of 15th and 16th vertebra. Single predorsal bone (=supraneural bone) present. Hypurals 1 and 2 as well as hypurals 3 and 4 clearly separated (most common state) or fused while any other combination is possible (e.g. hypurals 1 and 2 fused and hypurals 3 and 4 separated or vice versa).

Colouration in life (based on field photographs of adult specimens). Body ground colouration pale brown to beige; dorsum, flank and caudal peduncle light brown; belly whitish; chest whitish to yellow. Dark grey to blackish, interrupted midlateral band from operculum to just behind caudal fin base, ending in dark blotch; midlateral band crossed by 7–9 light grey vertical bars (sometimes hardly visible) extending mainly dorsally; at level of upper lateral line most bars fuse forming dorso-lateral band which extends to posterior origin dorsal fin.

Scales on flank and dorsum with orange blotch on anterior surface and greenish metallic highlights, especially scales on or row above or below lower lateral line. Dorsal head surface brownish; anterior snout brownish, preorbital area and cheek yellowish to brownish; mental area and ventral parts of preoperculum and cheek light bluish. Operculum yellowish with brownish sprinkles; black opercular spot present. Greyish vertical preopercular stripe of variable intensity is always present, at least in the form of a faint blackish blotch at mid orbit level. Dark grey to brownish lachrymal stripe between orbit and posterior end upper lip. Greyish to brownish nostril stripe (less intense than lachrymal stripe) fused posteriorly with lachrymal stripe. Faint greyish interorbital stripe. Upper lip brownish to olive, beige to light bluish posteriorly and lower lip beige to light bluish. Dorsal fin membrane greyish with orange margins; soft rayed part of dorsal fin with orange maculae arranged in 2–3 rows. Anal-fin membrane greyish, margin of spinous part dark grey; 2–3 orange maculae on soft rayed part anal fin. First macula situated just posterior last anal-fin spine at outer margin of anal fin. Second macula almost in centre of rayed part anal fin. When present, third macula less prominent (smaller and less colourful). Maculae resembling eggspots but without white concentric ring. Caudal fin yellowish with grey margin and four columns of small orange maculae. Pectoral fin yellowish. Pelvic fin yellowish; skin around pelvic fin spine and adjacent membrane of first two rays blackish.

Juvenile colouration in live. No information about juvenile colouration available.

Colouration in alcohol. Colouration and melanin patterns similar to live specimens, but due the preservation procedure of specimens, i.e., first formalin fixation, transfer to 75 % EtOH etc., specimens tend to lose original colouration (especially melanin patterns more intense than in live specimens). Overall body ground colouration brownish; dorsum and flank brownish. Orange blotches on flank scales no longer visible. Chest and belly beige to light brown. Branchiostegal membrane greyish brown. Dorsal head surface brownish, ethmoidal region greyish brown. Upper lip greyish; lower lip greyish anteriorly becoming beige. Cheek light brown to brownish. Preoperculum greyish. Operculum dark brown to greyish with opercular spot as described above. Head mask dark brownish to grey. Midlateral band, vertical bars and dorso-lateral band brownish. Dorsal fin greyish, lappets with very fine black seam; maculae on soft-rayed part beige. Anal fin greyish; margin dark grey to black, eggspot-like maculae whitish. Caudal fin greyish with dark greyish margin; maculae dark grey. Pectoral fin light grey. Pelvic fin light grey, skin around pelvic fin spine and adjacent membrane of first two rays dark grey.

Distribution and biology. *Orthochromis kimpala* is known from the Kalule Nord River (Fig. 1), a right tributary of the Lualaba River in the Democratic Republic of the Congo. At the type locality the Kalule Nord River has a rocky bottom with some patches of sand and gravel, and is about 5–8 meters wide and on average about 50 cm deep (Fig. 8). Water temperature varied between 21.1 and 26.8 °C (measured over several years in August and September), pH between 7.95–8.71, electrical conductivity 333.5–359 µS. The species appears to be benthic-rheophilic.

Etymology. The species name *kimpala* refers to the local name for this species: “Kimpala” in the Sanga language. A noun in apposition.

Orthochromis gecki sp. nov.

Orthochromis sp. “Lubudi”

Holotype. MRAC 2012-031-P-2097 (73.8 mm SL), Democratic Republic of Congo, Lubudi River downstream of Kendo Rapids, near Tshifuntshi Village (-10.5635/24.6354).

Paratype. MRAC 2012-031-P-2098-2116 (19, 52.1–77.7 mm SL), collected with holotype.—ZSM 46851 (5, ex MRAC uncat., 46.3–62.9 mm SL), Democratic Republic of Congo, Lubudi River at Kendo Rapids, near Tshifuntshi Village (-10.5668/24.6373).—MRAC 2012-031-P-2117-2126 (10, 45.9–69.8 mm SL), Democratic Republic of Congo, Lubudi River at Kendo Rapids, near Tshifuntshi Village (-10.5670/24.6374). – ZSM 46852 (1, ex MRAC uncat., 67.1 mm SL), collected with holotype.

Differential diagnosis. *Orthochromis gecki* can be readily distinguished from all all species currently placed in *Orthochromis* (sensu de Vos & Seegers 1998) except *O. torrenticola* (which has eggspot-like maculae) by presence of eggspots on anal fin. It is further distinguished from *O. kasuluensis* by having fewer anal-fin rays (8–9 vs. 10); from *O. malagaraziensis* by having more scales between upper lateral line and dorsal-fin origin (5–8 vs. 3–4); from *O. mazimeroensis* by having more horizontal line scales (29–31 vs. 26–28); from *O. rubrolabialis*, *O.*

rugufuensis and *O. uvinzae* by having fewer anal-fin spines (16–17 vs. 18–20) and in position of pterygiophore supporting last dorsal-fin spine (vertebral count: 15–16 vs. 17–19). It is furthermore distinguished from *O. uvinzae* by having fewer abdominal vertebrae (13–14 vs. 15–16) and by position of pterygiophore supporting last anal-fin spine (vertebral count: 14–15 vs. 16–17). *O. gecki* is distinguished from *O. stormsi* by having more horizontal line scales (29–31 vs. 26–28) and fewer total gill rakers (9–12 vs. 13–15); from *O. polyacanthus* by having fewer dorsal-fin spines (16–17 vs. 18–20), more dorsal-fin rays (10–12 vs. 8–9) and it is distinguished by position of pterygiophore supporting last dorsal-fin spine (vertebral count: 15–16 vs. 17–18); from *O. torrenticola* by having fewer anal-fin spines (3 vs. 4). Meristic values of *O. gecki* overlap with those of *O. luongoensis*, *O. kalungwishiensis,* and *O. machadoi* but is distinguished by narrower interorbital width (9.62–12.86 vs. 13.18-21.27 % HL). It is distinguished from *S. neodon* by having more circumpeduncular scales (16 vs. 12); from *H. snoeksi* by having more anal-fin rays (8–9 vs. 5–6); from *H. bakongo* by more horizontal line scales (29–31 vs. 26–28), more dorsal-fin spines (16–17 vs. 15–15) and by position of pterygiophore supporting last dorsal-fin spine (vertebral count: 15–16 vs. 13–14); from *H. moeruensis* by having more horizontal line scales (29–31 vs. 27–28) and more scales in upper lateral line (21–25 vs. 19–20). Meristic values of *O. gecki* overlap with those of *H. vanheusdeni* but is distinguished by having a smaller interorbital width (9.62–12.86 vs. 14.20–20.30 % HL). It is distinguished from herein newly described species *O. kimpala* by having fewer series of scales on cheek (0–2 vs. 3–4). Meristic values of *O. gecki* overlap with those of *O. mporokoso*, *O. katumbii*, and *O. indermauri* but is distinguished by having smaller interorbital width (9.6–12.9 vs. 13.0–21.7 % HL).

Description. Morphometric measurements and meristic characters are based on 36 type specimens. Values and their ranges are presented in Table 5. For general appearance see figure 6. Maximum length of wild caught specimens 77.7 mm SL. Rather slender and elongated species with maximum body depth (20.2–27.4 % SL) slightly before or at level of first dorsal-fin spine, decreasing rather gradually towards caudal peduncle. Caudal peduncle moderately elongated and deep (ratio of caudal peduncle length to depth: 1.5–2.0). Head length about one third of standard length. Dorsal-head profile moderately curved, from anterior eye region to dorsal-fin origin only slightly curved. No prominent nuchal gibbosity present. Eye diameter larger than interorbital width. Jaws isognathous. Posterior tip of maxilla almost reaching to slightly beyond anterior orbit margin. Lips well developed. Two separate lateral lines.

Squamation. Flank above and below lateral lines covered with comparatively large ctenoid scales. Anterior dorsal and ventral flank covered by cycloid scales. Margin of belly with deeply embedded minute to small sized scales; central belly region scaleless. Chest completely scaleless, except for deeply embedded cycloid scales ventro-anteriorly of pectoral fin. Chest to flank transition relatively abrupt with small, embedded cycloid scales. Snout scaleless. Interorbital region scaleless or with minute, deeply embedded cycloid scales. Nape region covered with minute to small, embedded cycloid scales becoming slightly larger towards occipital region. Occipital region with small to medium sized cycloid scales. Cheek covered with small, partly deeply embedded cycloid scales sometimes almost appearing scaleless; 0-2 scale rows on cheek. Cycloid scales on operculum of variable size (small to medium) and variable shape (ovoid to circular); opercular blotch only on anterior margin covered with medium sized scales, main area of opercular blotch scaleless. 1–3 scales in column from edge of postero-dorsal angle of operculum to anterior edge of operculum.

Upper lateral line scales 21–25 and lower lateral line 8–12. Horizontal line scales 29–31. Caudal fin with 0–1 pored scale. Upper and lower lateral lines separated by two scales. 5–8 scales between upper lateral line and dorsal-fin origin. Anterior part of caudal fin covered with 2–3 columns of small cycloid scales; with median scales being slightly larger; scaled area of caudal fin extended posteriorly, especially at upper and lower end, with minute, interradial scales (approximately up to one half of caudal fin). Sixteen scales around caudal peduncle.

Jaws and dentition. Anterior teeth of outer row of upper and lower jaw bicuspid to subequally bicuspid, large and closely set; towards corner of mouth, teeth smaller and more widely set and becoming unicuspid (rarely tricuspid or subequally bicuspid teeth present in posterior upper jaw). Individual bicuspid teeth without or minimally expanded brownish crown, cusps (tips roundish) uncompressed and moderately narrowly set, neck moderately stout. Outer row of upper jaw with 33–49 teeth and outer row of lower jaw with 26–42 teeth (specimens: 46.3–77.7 mm SL); larger specimens generally with more teeth. Upper and lower jaw with 2–4 inner tooth rows with small tricuspid teeth (rarely 5 rows in upper jaw and 1 or 5 in lower jaw); larger specimens generally with more inner tooth rows. Lower pharyngeal bone (Fig. 6) of single dissected paratype (MRAC 2012-031-P-2098-2116, 69.1 mm SL) about 1.1 times wider than long with anterior keel about 0.6 times length of

dentigerous area. Dentigerous area of lower pharyngeal bone about 1.4 times wider than long, with 10+9 teeth along posterior margin and 6 teeth along midline. Anterior pharyngeal teeth (towards keel) bevelled to pronounced and slender; those of posterior row larger than anterior ones, bevelled (minor cusp not well developed). Largest teeth medially in posterior tooth row. Teeth along midline slightly larger than more lateral ones.

Gill rakers. Total gill raker count 9–12, with 1–2 epibranchial, one angle, and 7–9 ceratobranchial gill rakers. Anteriormost ceratobranchial gill rakers smallest, increasing in size towards cartilaginous plug (angle). Anterior gill rakers on ceratobranchial unifid, towards cartilaginous plug sometimes bifid or trifid. Raker on cartilaginous plug largest in size and in most cases trifid, sometimes bifid. Epibranchial gill rakers then decreasing in size.

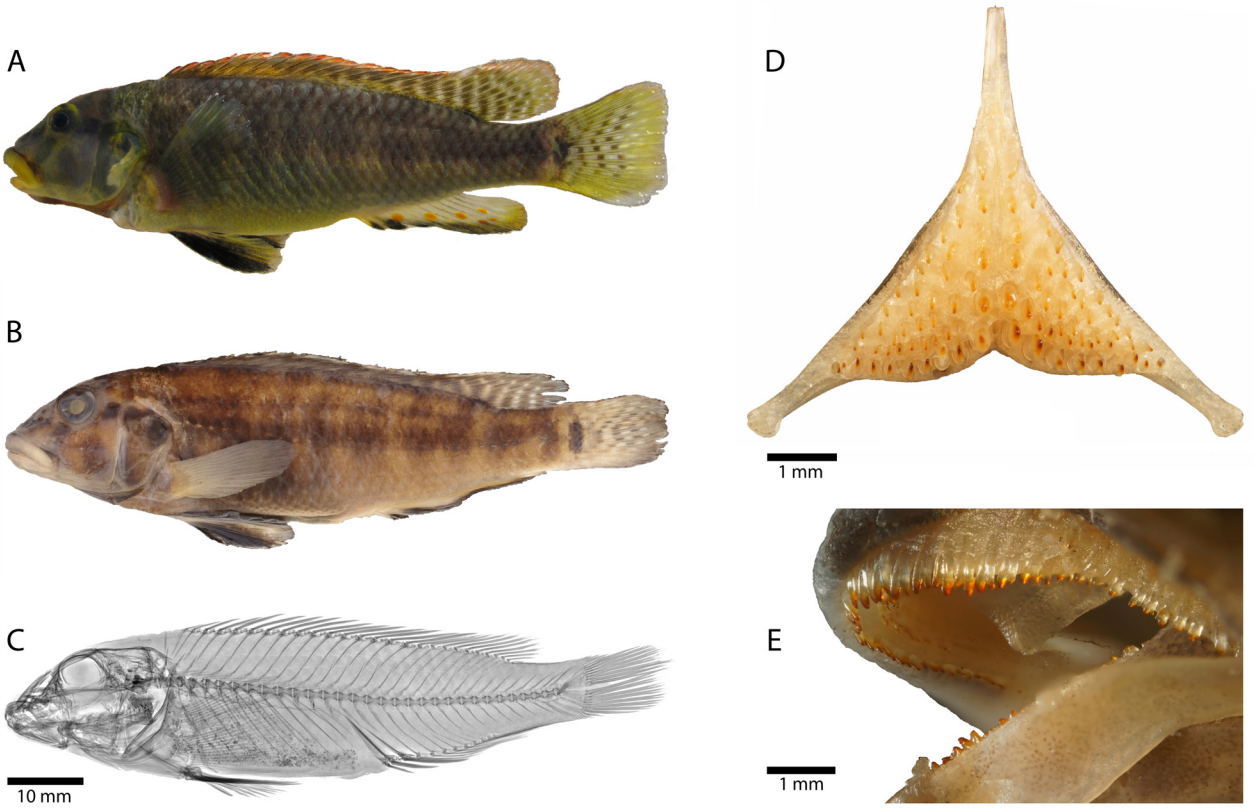

FIGURE 6. *Orthochromis gecki* **sp. nov. A.** probably the holotype, alive **B.** Holotype (MRAC 2012-031-P-2097), 73.8 mm SL; Democratic Republic of the Congo, Lubudi River **C.** radiograph of holotype **D.** lower pharyngeal bone (specimen with 69.1 mm SL; MRAC 2012-031-P-2098-2116) **E.** Overview of arrangement and morphology of oral jaw teeth (specimen with 75.0 mm SL; MRAC 2012-031-P-2098-2116).

Fins. Dorsal fin with 16–17 spines and with 10–12 rays. First dorsal-fin spine always shortest. Dorsal-fin base length between 52.1–61.0 % SL. Posterior tip of dorsal-fin rays reaching slightly beyond caudal fin base; posterior tip of anal fin reaching slightly before or at caudal-fin base. Caudal fin outline subtruncate and composed of 27–29 rays (16 principal caudal-fin rays and 11–13 procurrent caudal-fin rays). Anal fin with 3 spines (3rd spine longest) and 8–9 rays. Anal-fin base length between 15.6–20.7 % SL. Pectoral fin with 15–16 rays. Pectoral-fin length between 19.6–25.0 % SL; longest pectoral ray not reaching level of anus; first upper and lower pectoral-fin rays very short to short. Pelvic fin with 1st spine thickly covered with skin and 5 rays. Pelvic-fin base at level or slightly anterior of pectoral-fin base. Pelvic fin ending at same level as pectoral fin; longest pelvic-fin ray not reaching anus (ending approximately 2-3 flank scale widths before).

Vertebrae and caudal fin skeleton. 29–31 total vertebrae (excluding urostyle element), with 13–14 abdominal and 16–18 caudal vertebrae. Pterygiophore supporting last dorsal-fin spine inserted between neural spines of 15th and 16th or 16th and 17th vertebra (counted from anterior to posterior). Pterygiophore supporting last anal-fin spine is inserted between haemal spines of 15th and 16th vertebra or between rips of 14th and haemal spine of

15th vertebra. Single predorsal bone (=supraneural) present. Hypurals 1 and 2 in most types fused into either single, seamless unit or separated by clearly distinct seam. Hypurals 3 and 4 always fused into single seamless unit, except for one paratype which has clearly separated hypurals.

TABLE 5. Measurements and counts of holotype and paratypes of *Orthochromis gecki* **sp. nov.**

Measurements	holotype	holotype + paratypes			
		min	Max	SD	n
Total length (mm)	89.1	55.4	94.4		36
Standard length SL (mm)	73.8	46.3	77.7		36
Head length HL (mm)	22.5	14.1	25.2		36
% HL					
Interorbital width	12.9	9.6	12.9	0.7	36
Preorbital width	29.1	25.2	34.3	1.6	36
Horizontal eye length	21.2	18.1	26.8	3.0	36
Snout length	36.0	30.3	44.4	3.3	36
Internostril distance	17.9	12.7	20.2	1.6	36
Cheek depth	27.6	22.2	30.9	2.1	36
Upper lip length	34.3	27.9	36.9	2.7	36
Lower lip length	31.8	20.1	35.1	3.7	36
Lower lip width	32.6	25.0	37.0	3.4	36
Lower jaw length	32.0	28.6	38.4	2.5	36
Lower pharyngeal jaw length	-	28.1		-	1
Lower pharyngeal jaw width	-	32.3		-	1
Width of dentigerous area of lower pharyngeal jaw	-	21.8		-	1
% SL					
Predorsal distance	32.2	30.1	36.0	1.5	36
Dorsal-fin base length	57.1	52.1	61.0	2.2	36
Last dorsal-fin spine length	12.5	8.9	19.2	1.9	36
Anal-fin base length	19.2	15.6	21.7	1.4	36
Third anal-fin spine length	13.2	10.1	14.6	1.1	36
Pelvic fin length	21.4	20.4	24.7	1.1	36
Pectoral fin length	22.8	19.5	24.9	1.4	36
Caudal peduncle depth	10.3	9.3	11.5	0.6	36
Caudal peduncle length	17.4	15.9	19.8	0.9	36
Body depth (pelvic fin base)	25.3	20.2	27.4	1.6	36
Preanal length	60.3	56.8	63.8	1.5	36
Anus-anal fin base distance	3.2	2.2	5.4	0.7	36
Interpectoral width	13.6	9.0	16.0	1.4	36
Counts					
Dorsal-fin spines	16	16 (16); 17 (20)			36
Dorsal-fin rays	11	10 (17); 11 (18); 12 (1)			36
Anal-fin spines	3	3 (36)			36
Anal-fin rays	8	8 (11); 9 (25)			36
Pelvic-fin spines	1	1 (36)			36

.....continued on the next page

TABLE 5. (Continued)

Measurements	holotype	holotype + paratypes			
		min	Max	SD	n
Pelvic-fin rays	5	5 (36)			36
Pectoral-fin rays	16	15 (8); 16 (28)			36
Lower procurrent caudal-fin rays	7	6 (6); 7(24)			36
Lpper procurrent caudal-fin rays	6	5 (7); 6 (29)			36
Caudal-fin rays	29	27 (2); 28 (15); 29 (19)			36
Scales (horizontal line)	30	29 (9); 30 (26); 31 (1)			36
Upper lateral line	22	21 (3); 22 (13); 23 (15); 24 (4); 25 (1)			36
Lower lateral line	12	8 (2); 9 (13); 10 (15); 11 (5); 12 (1)			36
Circumpeducular	16	16 (36)			36
Series of scales on cheek	1	0 (10); 1 (15); 2 (11)			36
Scales (horizontal line) on operculum	2	1 (3); 2 (16); 3 (17)			36
Scales between lateral line and dorsal fin origin	6	5 (9); 6 (15); 7 (6); 8 (2)			32
Scales between upper lateral line and last dorsal fin spine	2	2 (36)			36
Abdominal vertebrae	14	13 (8); 14 (28)			36
Caudal vertebrae	16	15 (1); 16 (13); 17 (19); 18 (3)			36
Total number of vertebrae	30	29 (2); 30 (16); 31 (18)			36
Teeth in upper outer row	44	33 (1); 34 (2); 36 (2); 37 (4); 38 (1); 39 (6); 40 (1); 41 (2); 42 (3); 44 (2); 45 (3); 46 (1); 47 (1); 48 (2); 49 (1)			36
Teeth in lower outer row	42	25 (1); 26 (1); 27 (3); 28 (5); 29 (1); 30 (2); 31 (6); 32 (1); 33 (2); 34 (3); 35 (1); 36 (2); 37 (1); 38 (3); 39 (2); 40 (1); 42 (1)			36
Gill rakers (ceratobranchial)	7	7 (17); 8 (16); 9 (3)			36
Gill rakers (angle + epibranchial)	2	2 (7); 3 (29)			36

Colouration in life (based on field photographs of adult specimens). Body ground colouration brownish to greyish; dorsum, flanks and caudal peduncle greyish, beneath lower lateral line becoming yellowish; belly yellow; chest anteriorly whitish and remaining area yellow. Dark grey interrupted midlateral band from eye (anteriorly extended midlateral band) to just behind caudal-fin base ending in well pigmented vertically elongated blotch. Midlateral band crossed by 7–9 greyish vertical bars; at level of upper lateral line they sometimes fuse with each other forming dorso-lateral band sometimes interrupted and ending at posterior end of dorsal fin. On ventral flank at level of pectoral fin vertical bars sometimes fuse to ventro-lateral band (less intensive then previous mentioned ones) that ends well before level of anus. Iris dorsally yellow remaining greyish. Dorsal head surface, ethmoidal area, preorbital area greyish; cheek greyish near eyes, yellowish below and with vertical stripe-like pattern centrally (less distinct than other stripes of face mask). Preoperculum light greyish-yellow; operculum greyish, black opercular spot outlined with yellow. Branchiostegal membrane brownish to orange. Dark grey lachrymal stripe ending slightly anterior of caudal end upper lip. Greyish nostril stripe caudally fused with lachrymal stripe (beneath eye); interorbital stripe greyish. No clearly defined supraorbital stripe or nape band but recognizable to some extent by darker (grey) colouration than remaining dorsal head surface. Upper lip and lower lip yellow-orange; upper and lower margin of upper lip greyish. Dorsal-fin membrane brownish (especially spinous part) to yellowish (soft rayed part); margin orange; brownish to dark greyish maculae from about posterior half of spiny part to end soft-rayed part arranged in several almost vertical columns. Anal-fin membrane transparent proximally becoming yellowish distally (soft rayed part), margin of spiny and soft-rayed part black becoming yellow to brownish towards posterior tip; 3–6 orange eggspots (large orange centre surrounded by yellow concentring ring and outlined by more or less ill-defined transparent margin) on anal fin in both sexes. Eggspots arranged into 1–2

rows, first eggspot located centrally on fin just behind last anal spine. Caudal fin yellowish, orangey distally, margin outlined in grey-black; caudal with brownish maculae arranged into 3–4 vertical columns. Pectoral fin transparent, rays greyish. Pelvic fin deep black (especially skin around spine) except for small yellow central portion of rayed area.

Juvenile colouration in live. (based on wild caught juveniles of approximately 25 mm SL; Fig. 9)**.** Ground colouration beige, belly whitish. Patterns and head mask as described for adults but less prominent. Brown to greyish vertical bars on flank appear wider than in adults, dorso-lateral band and ventro-lateral band not visible. Last vertical bar on caudal fin base roundish blotch extending onto caudal fin (not a vertical bar as in adults). Dorsal fin brownish with several hyaline patches, margin not orange. Anal fin light brownish-orange; no eggspots on anal fin present. Caudal fin brownish-orange, no maculae present. Pectoral fin hyaline. Pelvic fin white to yellowish.

Colouration in alcohol. Colouration and melanin patterns similar to live specimens, due the preservation procedure of specimens, i.e., first formalin fixation, transfer to 75 % EtOH etc., specimens tend to lose original colouration (especially melanin patterns more intense than in live specimens). Overall body ground colouration brownish; dorsum and flank brownish becoming brighter ventrally. Chest and belly light brown to beige. Branchiostegal membrane dark greyish. Dorsal head surface brownish; ethmoidal area greyish brown. Upper and lower lip beige; upper and lower margin of upper lip greyish brown. Cheek light brown to brownish; cheek stripe dark brown. Operculum dark brown becoming somewhat darker ventrally; with opercular spot as described above. Head mask dark grey. Midlateral band, vertical bars, dorso-lateral band and ventro-lateral band dark brown. Dorsal fin greyish brown becoming greyish beige caudally, margin blackish with very fine black seam; maculae on spiny and soft-rayed part dark grey. Anal fin beige with blackish distal margin and dark grey at posterior margin; eggspots on anal fin faded and not visible in preserved specimens. Caudal fin beige to light greyish with dark greyish margin; maculae dark grey. Pectoral fin beige to light grey. Pelvic fin deep black except small central portion of rayed part greyish.

Distribution and biology. *Orthochromis gecki* is known from the Lubudi River a left-hand tributary of the Lualaba River in the Katanga region, Democratic Republic of the Congo (Fig. 1). It was also found to be present in the Mukuleshi River. At the type locality the Lubudi River has a rocky bottom with patches of gravel and sand, and is about 15 meters wide and about 50 cm deep; upstream the river is much deeper with 3 meters or more (Fig. 9). *O. gecki* seems to be a maternal mouthbrooder. One of the female paratypes (MRAC 2012-031-P-2117-2126; 57.0 mm SL), was found mouthbrooding when preserved and carried around 12 comparatively large eggs. Fixed eggs are brownish and oval and ca. 3.8 mm long and 2.5 mm wide.

Etymology. The species is named in honour of Mr. Jakob Geck who is a passionate, German fish naturalist, thanking him for his dedicated volunteer work and untiring support for the ichthyology section of the ZSM. His great experience in keeping rheophilic cichlids contributed to the knowledge of behaviour and ecology of many cichlid taxa, including *O. katumbii* and *O. indermauri*.

***Orthochromis indermauri* sp. nov.**

Orthochromis sp. “Chomba” Indermaur 2014

Holotype. ZSM 46853 (1, ex ZSM 43080, 54.0 mm SL), Zambia, Lufubu River, below last series of rapids near Chomba village, ~ 25.5 km (air distance) from confluence with Lake Tanganyika and 20 km (air distance) south of Sumbu (-8.687010/30.556273)

Paratypes. ZSM 46855 (13, 35.8–68.9 mm SL), Zambia, Lufubu River, Lower Lufubu at Chomba Village, ~30 km from confluence with Lake Tanganyika, Northern Province (-8.686376/30.563983).—ZSM 46854 (1, 61.2 mm SL), Zambia, Lufubu River, Lower Lufubu at Chomba Village, ~30 km from confluence with Lake Tanganyika, Northern Province (-8.686376/30.563983).—ZSM 43083 (4, 45.6–59.4 mm SL), collected with holotype.—ZSM 43080 (2, 42.0–43.1 mm SL), collected with holotype.—ZSM 44283 (3, 50.8-63.5 mm SL), Zambia, Lufubu River, Lower Lufubu at Chomba Village, ~30 km from confluence with Lake Tanganyika, Northern Province (-8.686376/30.563983).—MRAC 2018-006-P-0001-0002 (2, ex ZSM 44283, 56.8–51.9 mm SL) Zambia, Lufubu River, Lower Lufubu at Chomba village, ~30 km from confluence with Lake Tanganyika,

Northern Province (-8.686376/30.563983).—MRAC 2018-006-P-0003-0008 (6, 43.3–64.1 mm SL), Zambia, Lufubu River, Lower Lufubu at Chomba village, ~30 km from confluence with Lake Tanganyika, Northern Province (-8.686376/30.563983).

Diagnosis. *Orthochromis indermauri* is distinguished from all all species currently placed in *Orthochromis* (sensu de Vos & Seegers, 1998) except O. *torrenticola,* by having hypurals 1 and 2 clearly separated or separated by distinct seam (vs. always fused). It is further distinguished from Malagarasi-*Orthochromis* species, except *O. mazimeroensis, O. malagaraziensis,* and *O. rubrolabialis,* by having fewer caudal vertebrae (14–15 vs. 16–18) and total vertebrae (28–29 vs. 30–32). It is also distinguished from *O. luichensis, O. malagaraziensis*, *O. mazimeroensis*, *O. mosoensis* by having more inner series of teeth in upper jaw (3–5 vs. 1–2). Moreover, it differs from *O. kasuluensis* by having fewer anal-fin rays (7–9 vs. 10); from *O. malagarazienisis* by having more scales between upper lateral line and dorsal-fin origin (5–7 vs. 3–4) and by having more ceratobranchial gill rakers (8–11 vs. 6–7); from *O. mazimeroensis* by having more abdominal vertebrae (14–15 vs. 12–13); from *O. mosoensis* and *O. rubrolabialis* by having more ceratobranchial gill rakers (8–11 vs. 5–7) and total gill rakers (11–15 vs. 8–10); from *O. uvinzae* by having fewer horizontal line scales (25–29 vs. 30–32), fewer dorsal-fin spines (17–18 vs. 19–20) and by position of pterygiophore supporting last dorsal-fin spine (vertebral count: 16–17 vs. 18–19). It is distinguished from *O. kalungwishiensis*, *O. luongoensis*, and *O. torrenticola* by having fewer horizontal line scales (28–29 vs. 30–32) and by having fewer caudal vertebrae (14–15 vs. 17–18). Further, it differs from *O. luongoensis* and *O. machadoi* by having fewer series of scales on cheek (0–1 vs. 2–5); from *O. kalungwishiensis* by having fewer total vertebrae (28–29 vs. 31–33). It is distinguished from *S. neodon* by having fewer horizontal line scales (28–29 vs. 30–31), more circumpeduncular scales (16 vs. 12), fewer caudal vertebrae (14–15 vs. 16–17), fewer total vertebrae (28–29 vs. 30–32), fewer dorsal-fin rays (8–10 vs. 11–12) and by having hypurals 1 and 2 clearly separated or separated by distinct seam (vs. fused). It differs from *H. snoeksi* by having fewer scales on cheek (0–1 vs. 2–3), fewer horizontal line scales (25–29 vs. 30–31), more abdominal vertebrae (14–15 vs. 13), fewer caudal vertebrae (14–15 vs. 17), fewer total vertebrae (28–29 vs. 30), more anal-fin rays (7–9 vs. 5–6), more dorsal-fin spines (17–18 vs. 16), more ceratobranchial gill rakers (8–11 vs. 6) and total gill rakers (11–15 vs. 9); from *H. bakongo* by having more inner series of teeth (3–5 vs. 1–2), more dorsal-fin spines (17–18 vs. 14–15) and in position of pterygiophore supporting last dorsal-fin spine (vertebral count: 16–18 vs. 13–14); from *H. moeruensis* by having hypurals 1 and 2 clearly separated or separated by distinct seam (vs. always fused). Meristic values of *O. indermauri* overlap with those of *H. vanheusdeni* but is distinguished by differences in head mask (e.g. nostril stripe present vs. absent; caudal corner of cheek with blackish element vs. no such element present) and by size and colouration of eggspot-like maculae on anal fin (e.g. deep red centre vs. orange centre in *H. vanheusdeni*). It is distinguished from *O. mporokoso* and *O. katumbii* by having fewer caudal vertebrae (14–15 vs. 16–17), fewer total vertebrae (28–29 vs. 30–31) and by having hypurals 1 and 2 and hypurals 3 and 4 clearly separated or separated by distinct seam (vs. always fused). Further from *O. mporokoso* by having fewer series of scales on cheek (0–1 vs. 2–4); from *O. katumbii* by having fewer horizontal line scales (25–29 vs. 30–31). It is distinguished from *O. kimpala* by having fewer series of scales on cheek (0–1 vs. 3–4) and by having more dorsal-fin spines (17–18 vs. 15–16). Meristic values of *O. indermauri* overlap with those of *O. gecki* but is distinguished by having a wider interorbital width (13.5–18.2 vs. 9.6–12.9 %HL).

Description. Morphometric measurements and meristic characters are based on 21 out 32 type specimens. Values and their ranges are presented in Table 6. For general appearance see figure 7. Maximum length of wild caught specimens 68.9 mm SL. Moderately slender species with maximum body depth (24.5–29.9 % SL) slightly posterior or at level of first dorsal-fin spine, decreasing rather gradually towards caudal peduncle (but decreasing relatively quick just before caudal peduncle). Caudal peduncle rather short and deep (ratio of caudal peduncle length to depth: 1.2–1.4). Head length almost one third of standard length. Dorsal-head profile moderately curved without prominent nuchal gibbosity. Eye diameter always larger than interorbital width. Jaws slightly retrognathouswith lower jaw shorter than upper jaw. Posterior tip of maxilla not reaching anterior margin of orbit but slightly before. Lips not noticeably enlarged or thickened. Two separate lateral lines.

Squamation. Flank above and below lateral lines covered with cycloid scales, even in smaller specimens. Belly and chest covered by deeply embedded minute scales giving appearance of being scaleless. Ventro-anterior area of pectoral fin with small, deeply embedded cycloid scales. Chest to flank transition with small, embedded cycloid scales.

Snout scaleless. Interorbital region with minute, deeply embedded cycloid scales. Nape and occipital region

covered with minute to small, embedded cycloid scales becoming slightly larger towards occipital region. Cheek appears scaleless, but rarely small deeply embedded cycloid scales present just below eye; 0–1 scale rows on cheek. Cycloid scales on operculum of variable size (small to medium) and mainly of circular shape; opercular blotch only on anterior margin covered by medium sized scales, main area of opercular blotch scaleless. 5–7 scales on horizontal line from edge of postero-dorsal angle of operculum to anterior edge of operculum.

Upper lateral line scales 20–23 and lower lateral line 7–11. Horizontal line scales 27–29. Caudal fin with 0–2 pored scales. Upper and lower lateral lines separated by two scales. 3–5 scales between upper lateral line and dorsal-fin origin. Anterior part of caudal fin covered with 2–3 vertical rows of small cycloid scales with median scales being slightly larger; scaled area of caudal fin extended posteriorly with interradial scales (approximately up to two thirds of caudal fin). Sixteen scales around caudal peduncle.

Jaws and dentition. Anterior teeth of outer row of upper and lower jaw bicuspid to subequally bicuspid, large and very densely set; teeth smaller towards corner of mouth, more widely set and becoming unicuspid (rarely tricuspid or subequally bicuspid teeth present on upper jaw near corner mouth). Individual bicuspid teeth with not expanded brownish crown, cusps (tips pointed) slightly compressed and narrowly set, and neck slender. Outer row of upper jaw with 42–59 teeth and outer row of lower jaw with 26–45 teeth (specimens: 35.8–68.9 mm SL); larger specimens generally with more teeth. Inner upper jaw with 3–5 tooth rows and 3–4 rows (rarely 2) in lower jaw, all with small tricuspid teeth.

Lower pharyngeal bone (Fig. 7) of single dissected paratype (ZSM 46854, 61.2 mm SL) about as wide as long with anterior keel about 0.6 times length of dentigerous area. Dentigerous area of lower pharyngeal bone about 1.5 times wider than long, with 11+11 teeth (empty tooth-sockets included) along posterior margin and eight teeth along midline. Anterior pharyngeal teeth (towards keel) bevelled and slender; teeth posterior row larger than anterior ones, bevelled (bicuspid; well-developed major and minor cusp). Largest teeth medially in posterior row. Teeth along midline slightly larger than more lateral ones.

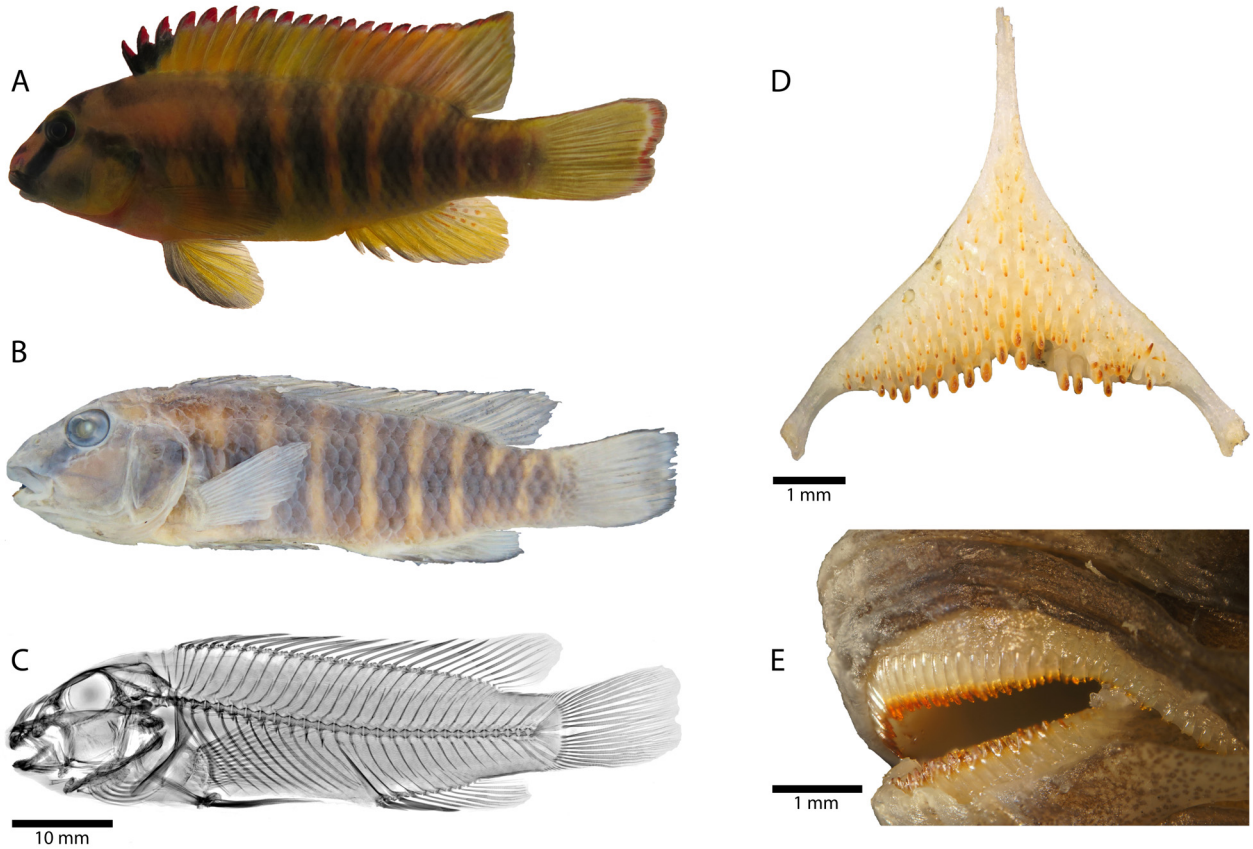

FIGURE 7. *Orthochromis indermauri* **sp. nov. A.** paratype (ZSM 44283), 63.5 mm SL, alive **B.** Holotype (ZSM 46853, 54.0 mm SL), 54.0 mm SL; Zambia, Lufubu River **C.** radiograph of holotype **D.** lower pharyngeal bone (ZSM 46854, 61.2 mm SL) **E.** Overview of arrangement and morphology of oral jaw teeth (specimen: ZSM 43083, 59.4 mm SL).

TABLE 6. Measurements and counts of holotype and paratypes of *Orthochromis indermauri* **sp. nov.**

Measurements	holotype	holotype + paratypes			
		min	Max	SD	n
Total length (mm)	66.2	44.6	86.0		32
Standard length SL (mm)	54.0	35.8	68.9		32
Head length HL (mm)	18.0	11.7	21.4		32
% HL					
Interorbital width	15.1	13.5	18.2	1.4	21
Preorbital width	32.8	30.2	39.7	2.3	21
Horizontal eye length	21.4	20.1	25.0	1.4	21
Snout length	37.9	36.3	43.3	2.1	21
Internostril distance	17.5	15.7	32.8	3.6	21
Cheek depth	28.9	24.2	34.1	2.7	21
Upper lip length	30.4	23.8	32.5	2.5	21
Lower lip length	26.2	20.0	29.2	2.5	21
Lower lip width	35.0	26.2	43.3	3.7	21
Lower jaw length	23.4	23.4	37.5	3.6	21
Lower pharyngeal jaw length	-	31.9		-	1
Lower pharyngeal jaw width	-	33.2		-	1
Width of dentigerous area of lower pharyngeal jaw	-	24.5		-	1
% SL					
Predorsal distance	31.9	31.4	35.9	1.0	21
Dorsal-fin base length	60.3	56.9	65.4	2.6	21
Last dorsal-fin spine length	13.5	12.5	16.0	0.9	21
Anal-fin base length	17.4	16.7	21.9	1.3	21
Third anal-fin spine length	13.3	11.0	15.5	1.1	21
Pelvic fin length	22.1	20.5	26.04	1.5	21
Pectoral fin length	22.7	19.7	25.6	1.3	21
Caudal peduncle depth	12.9	11.8	14.22	0.6	21
Caudal peduncle length	17.5	14.7	18.5	1.0	21
Body depth (pelvic fin base)	28.1	24.45	30.54	1.7	21
Preanal length	61.4	54.9	63.6	2.3	21
Anus-anal fin base distance	2.2	2.1	4.9	0.8	21
Interpectoral width	14.9	12.2	16.9	1.1	21
Counts					
Dorsal-fin spines	18	17 (7); 18 (14)			21
Dorsal-fin rays	9	8 (3); 9 (15); 10 (3)			21
Anal-fin spines	3	3 (21)			21
Anal-fin rays	8	7 (1); 8 (18); 9 (2)			21
Pelvic-fin spines	1	1 (21)			21
Pelvic-fin rays	5	5 (21)			21
Pectoral-fin rays	15	14 (5); 15 (16)			21
Upper procurrent caudal-fin rays	7	6 (5); 7 (16)			21
Lower procurrent caudal-fin rays	6	5 (1); 6 (20)			21

.....continued on the next page

TABLE 6. (Continued)

Measurements	holotype	holotype + paratypes			
		min	Max	SD	n
Caudal-fin rays	29	27 (1); 28 (4); 29 (16)			21
Scales (horizontal line)	28	27 (6); 28 (14); 29 (1)			21
Upper lateral line	21	20 (2); 21 (8); 22 (10); 23 (1)			21
Lower lateral line	10	7 (2); 8(3); 9 (10); 10 (5); 11 (1)			21
Circumpeducular	16	16 (21)			21
Series of scales on cheek	0	0 (16); 1 (5)			21
Scales (horizontal line) on operculum	2	2 (10); 3 (11)			21
Scales between lateral line and dorsal fin origin	6	5 (2); 6 (9); 7 (10)			21
Scales between upper lateral line and last dorsal fin spine	1	1 (12); 2 (9)			21
Abdominal vertebrae	14	14 (19); 15 (2)			21
Caudal vertebrae	15	14 (7); 15 (14)			21
Total number of vertebrae	29	28 (5); 29 (16)			21
Teeth in upper outer row	54	42 (1); 45 (2); 47 (2); 48 (2); 49 (1); 50 (3); 51(1); 53 (2); 54 (1); 56 (1); 57 (1); 58 (2); 59 (1); 66 (1)			21
Teeth in lower outer row	41	26 (1); 30 (2); 31 (1); 32 (2); 31 (1); 35 (3); 36 (1); 37 (2); 38 (3); 39 (1); 40 (1); 41 (2); 45 (1)			21
Gill rakers (ceratobranchial)	9	8 (6); 9 (13); 10 (2)			21
Gill rakers (angle + epibranchial)	5	3 (2); 4 (11); 5 (8)			21

Gill rakers. Total gill raker count 11–15, with 2–4 epibranchial, one angle, and 8–10 ceratobranchial gill rakers. Anteriormost ceratobranchial gill rakers smallest increasing in size towards cartilaginous plug (angle). Anterior gill rakers on ceratobranchial generally unifid, sometimes bifid towards cartilaginous plug. Gill raker on cartilaginous plug shorter than longest ceratobranchial gill raker and epibranchial gill rakers further decreasing in size.

Fins. Dorsal fin with 17–18 spines and with 8–10 rays. First dorsal-fin spine always shortest. Dorsal-fin base length between 56.9–65.4 % SL. Posterior end of dorsal-fin rays extending slightly beyond caudal fin base; posterior tip of anal fin reaching slightly before or at caudal fin base. Caudal fin outline subtruncate and composed of 27–29 rays (16 principal caudal-fin rays and 11–13 procurrent caudal-fin rays). Anal fin with 3 spines (3rd spine longest) and 7–9 rays. Anal-fin base length between 16.7–21.9 % SL. Pectoral fin with 14 to 15 rays and length between 19.7–25.6 % SL; longest pectoral ray not reaching or in rare cases almost reaching level of anus (ending approximately 1-2 flank scale widths in front of it). First upper and lower pectoral-fin rays very short to short. Pelvic fin with 1st spine thickly covered with skin and 5 rays. Pelvic fin base at same level pectoral fin base. Longest pelvic-fin ray not reaching or in rare cases almost reaching anus (ending approximately 1-2 flank scale widths in front of it).

Vertebrae and caudal fin skeleton. 28–29 total vertebrae (excluding urostyle element), with 14–15 abdominal and 14–15 caudal vertebrae. Pterygiophore supporting last dorsal-fin spine inserted between neural spines of 16th and 17th or 17th and 18th vertebra (counted from anterior to posterior). Pterygiophore supporting last anal-fin spine inserted between haemal spines of 15th and 16th or 16th and 17th vertebra, rarely between rips of 14th and haemal spine of 15th vertebra (N=1). Single predorsal bone (=Supraneural bone) present. Hypurals 1 and 2 either clearly separated or separated by distinct seam but never fused into single seamless unit. Hypurals 3 and 4 either fused into single seamless unit or separated by distinct seam.

Colouration in life (based on field photographs of adult specimens). Body ground colouration brownish yellow, towards belly more yellowish; dorsum brownish yellow to pale brown; chest below pectoral fins yellow becoming reddish ventrally; belly yellow. Dorsal head surface pale brown dorsally with reddish speckles; ethmoidal area pale brown and densely speckled with reddish spots, especially in dominant males (Indermaur

2014). Iris reddish posteriorly, yellow dorsally, remaining greyish. Upper lip dark grey anteriorly sometimes with reddish speckles; lower lip light greyish, yellowish posteriorly. Cheek pale brown becoming yellowish towards corner mouth and mental area; blackish pear-shaped blotch at caudal-ventral corner, expanding to anterior extension of midlateral band. Branchiostegal membrane along operculum yellow becoming whitish to pale pinkish ventrally. Operculum yellow with black opercular spot, which is fused with anterior extension of midlateral band which is ending just anterior of the eye. Broad blackish lachrymal stripe between orbit and caudal corner of upper lip. A relatively faint greyish nostril stripe, sometimes covered by many reddish speckles. Relatively wide blackish interorbital stripe. Blackish supraorbital stripe connected with nape band. Nape band ending slightly anterior of dorsal-fin origin and fused with dorso-lateral band. Dorso-lateral band slightly below dorsal fin base and visible up to third or fourth anterior vertical bar. Relatively thin midlateral band ending with dark blotch just posterior base caudal fin. 7–9 blackish vertical bars crossing midlateral band and extending onto dorsal fin almost to fin margin; anterior-most vertical bar (just behind operculum) less intensive than remaining bars. Vertical bars wider than space between them. Dorsal-fin membrane yellow without maculae, skin/membrane of first three dorsal-fin spines black creating the appearance of a broad black oblique band between 1st and 4th spine. Margin of spiny part dorsal fin with fine black outline and red (distally) and transparent submarginal band; rayed part of dorsal fin lacks transparent submarginal band. Anal fin yellow; margin greyish outlined. Posterior half of anal fin with deep-red maculae on membrane (between last four anal-fin rays); maculae elongated proximally becoming more rounded distally (maculae not to fin margin but ending slightly before). In general, these maculae resemble egg-spots: large deep red centre surrounded by faint greyish ring then by ill-defined transparent ring. Caudal fin yellow with deep red maculae as described for anal fin but only with roundish maculae. Caudal fin with reddish marginal band with narrower bluish submarginal band; another submarginal band of red maculae (intensity varies). Outer caudal-fin rays outlined in black. Pectoral fin yellow to orange. Pelvic fin yellowish with dark greyish anterior margin spanning spine and first two rays.

Juvenile colouration in life. (based on tank-raised juveniles of approximately 20 to 30 mm SL; Fig. 9)**.** Ground colouration greyish to beige. Patterns and head mask as described for adults. No reddish speckles present. Dorsal and midlateral band, greyish vertical bars on flank as described for adults. Dorsal fin hyaline to beige with vertical flank bars extending onto fin. Anal, caudal, pectoral and pelvic fin hyaline.

Colouration in alcohol. Colouration and melanin patterns similar to live specimens, but due the preservation procedure of specimens, i.e., first formalin fixation, transfer to 75 % EtOH etc., specimens tend to lose original colouration (especially melanin patterns more intense than in live specimens). Overall body ground colouration pale brownish to pale yellowish; chest and belly beige to yellowish. Branchiostegal membrane greyish-beige to greyish-brown. Dorsal head surface pale brownish; ethmoidal region greyish-brown. Upper lip brownish and lower lip beige. Cheeks beige to brownish; pear-shaped blotch on lower caudal corner of cheek greyish-brownish and less prominent than in living specimens. Operculum greyish and with opercular spot as described above. Head mask and mid- and dorso-lateral band and vertical bars brownish to greyish. Dorsal fin light greyish except dark grey skin/membrane of first three anterior spines, remaining fin with black margin; extensions of vertical bars on dorsal fin dark grey. Anal fin light greyish; margin outlined in dark grey; no maculae visible. Caudal fin light greyish and margins outlined in black; some thin blackish streaks on membrane between rays may be present. Pectoral fin light grey. Pelvic fin light grey, skin/membrane of pectoral spine and first two rays greyish.

Distribution and biology. *Orthochromis indermauri* is only known from the lower reaches of the Lufubu River (Zambia), the third largest tributary of Lake Tanganyika (Fig. 1). Several cascades and waterfalls seem to represent insurmountable barriers to the upstream movement of the lake ichthyofauna hence the fish communities of the upper and lower reaches are clearly distinct. The Upper Lufubu has faunistic similarities to the Congo and Zambezi systems while the Lower Lufubu shows faunistic influences of Lake Tanganyika (Koblmüller *et al.* 2012). At the type locality the Lufubu River is rocky with some patches of sand and gravel, about 20 meters wide and on average 50 cm deep (Fig. 8). The water temperature varies throughout the year, 23 °C was measured in July and 28.1 °C in November, the pH ranged between 8.0–8.55, and electrical conductivity around 29 µS (Indermaur 2014, pers. com. Bernd Egger). *O. indermauri* is benthic-rheophilic and prefers stretches of fast flowing water where it is found between and among large rocks or patches of gravel. No stomach contents were examined, however, underwater observations indicate it scrapes aufwuchs from the substrate and forages between rocks and patches of sand and gravel (Indermaur 2014, pers. obs. FS). *Orthochromis indermauri* is a maternal mouthbrooder. Females in captivity have comparatively small clutches of between 17 and 21 fry (two spawns, pers. com. Adrian Indermaur).

FIGURE 8. Type localities of the five newly described species A. Type locality of *Orthochromis mporokoso,* Kasinsha stream (July 2011, Hans van Heusden) B. Type locality of *Orthochromis katumbii,* Kiswishi River (2015, VLIR expedition) C. Type locality of *Orthochromis gecki*, Lubudi River (July 2017, Katanga 2016 Expedition) D. Type locality of *Orthochromis kimpala*, Kalule North River near bridge on the road Makulakulu-Lubudi (2012, PRODEPAAK expedition) E. Type locality of *Orthochromis indermauri*, Lufubu River at Chomba village (August 2015, photo F. Schedel).

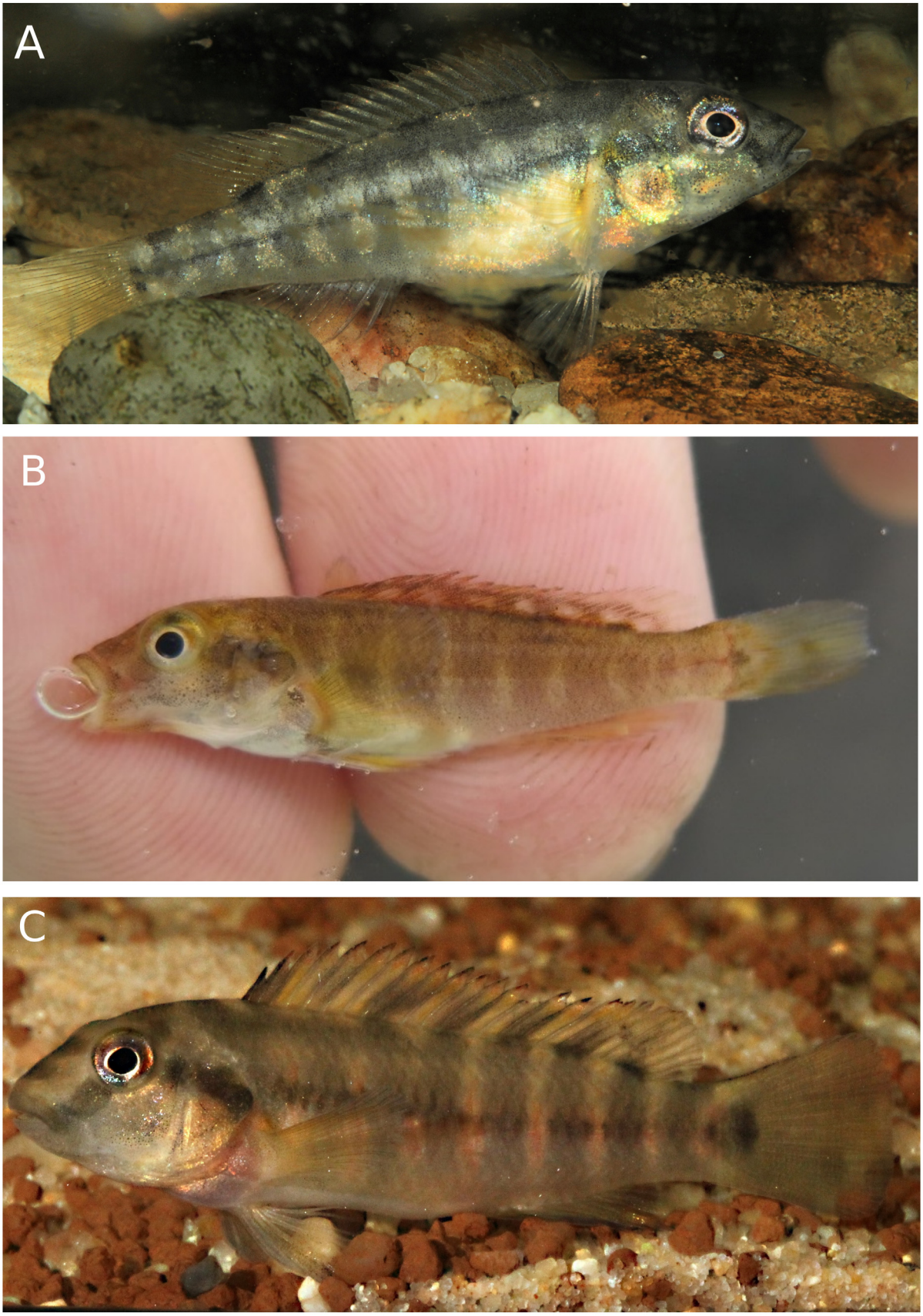

FIGURE 9. Live Pictures of juveniles. A. captive raised F1 juvenile of *Orthochromis katumbii* about 25 mm SL (Photo J. Geck). B. wild caught juvenile of *Orthochromis gecki* C. captive raised F1 juvenile of *Orthochromis indermauri.*

Etymology. The species name *indermauri* honours the Swiss ichthyologist Dr. Adrian Indermaur, who was the first to document this new species with underwater photographs, videos, and with aquarium observations, thereby contributing to a large extent to our knowledge of behavior and ecology of this species.

Discussion

Generic placement and affinities. Overall, the five new species superficially resemble species of *Orthochromis,* but their characters are only partially compatible with the morphological diagnosis of that genus as of the latest generic diagnosis of *Orthochromis* by De Vos & Seegers (1998), and they differ in most diagnostic characteristics from *Schwetzochromis* sensu De Vos & Seegers (see Tables 7 and 8). Nevertheless, we chose to place them in the genus *Orthochromis* instead of placing them in the catch-all genus *Haplochromis* Hilgendorf 1888, as had been done for *Haplochromis vanheusdeni,* another rheophilic species which shares superficial similarities with *Orthochromis* (Schedel *et al.* 2014). The reasons for this overall placement are as follows: (1) phylogenetic reconstructions based on nuclear and mitochondrial DNA sequence data strongly indicate that rheophilic haplochromines superficially similar to *Orthochromis* as currently defined are polyphyletic (e.g. Salzburger *et al.* 2002, Koblmüller *et al.* 2008, Schwarzer *et al.* 2012, Dunz & Schliewen 2013, Weiss *et al.* 2015, Matschiner *et al.* 2016). Therefore, placement of the new species within the anyway polyphyletic genus *Orthochromis* does not compromise current taxonomic (in)stability; (2) although all new species described herein appear distinct from all *Orthochromis* s.s., the latter are equally rheophilic haplochromine-like cichlids of the Malagarasi and Luiche drainages, an haplochromine subgroup which appears to be comparatively uniform with regard to meristic values, other morphological and colouration characters, and which has been inferred to be monophyletic by molecular analyses with an almost complete taxon sampling of that group (Matschiner *et al.* 2016), and that, most importantly, hosts *O. malagaraziensis*, the type species of the genus *Orthochromis*. All five new species described herein are overall phenotypically similar to *Orthochromis* s.s. as they exhibit several morphological similarities; (3) haplochromine cichlid phylogenetic intra-relationships have not been investigated with a fully comprehensive taxon sampling, neither on the morphological nor on the molecular level; nevertheless, all results of partial analyses suggest strongly that many haplochromine genera are paraphyletic, and that rheophilic haplochromine taxa are widely dispersed in available haplochromine phylogenetic hypotheses (e.g., Schwarzer *et al.* 2012, Weiss *et al.* 2015). Until a fully representative phylogenetic evaluation of haplochromine cichlids incorporating morphological and genetic data will be available, a stable taxonomic appraisal of the generic placement of the new species most likely remains drastically fragmentary. Therefore, placing the new species in *Orthochromis* will be a temporal solution but creating at least a temporal nomenclatural stability highlighting phenotypic dissimilarity with members of the other haplochromine catch-all genus *Haplochromis*.

Furthermore, apart from the new species described herein, at least two new species of the Malagarasi-*Orthochromis* lineage (*Orthochromis* sp. "Igamba" and *Orthochromis* sp. "red"; only the first species was available for this study) await formal description; and, moreover, preliminary data suggest that *O.* cf. *torrenticola* specimens collected from the Lufira River below Kiubo Falls represent an as yet undescribed species which is the sister taxon to *O. torrenticola*, which was described from specimens collected above the falls. These species will be described in forthcoming papers once more data become available.

The five new species described herein appear to belong to at least three different evolutionary lineages based on published and not yet published preliminary molecular phylogenetic analyses, a result which is partially reflected by distinctive morphological and colouration characters, as well as patterns of geographic distribution: the four species *O. luongoensis*, *O. kalungwishiensis, O. katumbii* and *O. mporokoso* are distributed in the Luapula-Lake Mweru drainage, and, according to preliminary molecular phylogenetic data they form a monophyletic group (Schedel *et al.* unpublished), and, to some extent, show meristic similarities (see Fig. 2). However, inter- and intrarelationships of this clade need further examination as *O. kalungwishiensis* was shown to be either related to *Pseudocrenilabrus*-like cichlids (mtDNA-data) or to *O. stormsi* and *O. polyacanthus* (nuclear DNA data) (Schwarzer *et al.* 2012, Weiss *et al.* 2015). The two new species *O. gecki* and *O. kimpala* both feature eggspots or eggspot-like maculae on their anal fin, and their pelvic fin shows a characteristic colouration with the spines and adjacent membranes being blackish, suggesting a closer relationship of these two species. In addition, unpublished molecular data suggest that they potentially represent a distinct haplochromine lineage. Based on preliminary

TABLE 7. Overview of morphological characters associated with *Orthochromis* in comparison with the new species described herein.

Morphological characters associated with *Orthochromis* (as in De Vos & Seegers 1998)	*Orthochromis mporokoso*	*Orthochromis katumbii*	*Orthochromis kimpala*	*Orthochromis gecki*	*Orthochromis indermauri*
Rather slender body	Yes	Yes	Yes	Yes	Yes
Eyes generally superolateral in position, giving the fish a goby-like appearance	Yes	Yes	Yes	Yes	yes
Scales on the sides mainly ctenoid and if present, cycloid and minute on chest and belly, often deeply imbedded in the skin. Chest and belly scaleless in some species.	Yes	Yes	Yes (central belly region scaleless)	Yes (central belly region scaleless, chest scaleless)	Yes
Absence or extensive reduction of cheek squamation	No (2-4 scale rows on cheek)	No (2-4 scale rows on cheek)	No (3-4 scale rows on cheek)	Yes	Yes
Increased number of spinous rays in the dorsal fin (without a corresponding reduction in the number of branched rays)	Yes	Yes	Yes	Yes	Yes
elongated second or second and third branched rays in the pelvic fin	Yes	Yes	Yes	Yes	Yes
Outer row of both jaws with unequally bicuspid teeth. Often a few teeth in the corners are unicuspid but there is no tendency for a conical or spatulate shape of the cusps in the larger specimens, as is often the case in other haplochromines. Inner teeth of upper and lower jaws tricuspid or partly unicuspid and arranged into 2-4 rows.	Yes	Yes	Yes	Yes (2-4 inner upper and lower jaw tooth rows with small tricuspid teeth, rarely five tooth rows in upper jaw and one or five rows in lower jaw)	Yes (3-5 inner upper jaw tooth rows and 3-4 lower jaw tooth rows (rarely two) with small tricuspid teeth)
Dorsal head profile is decurved with a strongly sloping preorbital skull profile	Dorsal-head profile slightly curved	Dorsal head profile gently curved	Dorsal-head profile rather strongly curved	Dorsal-head profile moderately curved	Dorsal-head profile moderately curved
Hypurals 1 and 2, and 3 and 4 of the caudal fin skeleton are fused	Yes	Yes	No (Hypurals 1 and 2 as well as hypurals 3 and 4 always clearly separated)	No (Hypurals 1 and 2 fused into a single seamless unit or separated by a clearly visible seam. Hypurals 3 and 4 fused into a single seamless unit or with clearly separated hypurals.)	No (Hypurals 1 and 2 either clearly separated or separated by a clearly visible seam but never fused into a single seamless unit. Hypurals 3 and 4 either fused into a single seamless unit or separated by a clearly visible seam.)
Without true egg-dummies as shown in the genus *Haplochromis* sensu lato.	Yes	Yes	No (2-3 orange eggspot-like maculae on soft-rayed part of anal fin)	No (3-6 orange eggspots)	No (deep red maculae on anal fin membrane; resembling eggspots)

TABLE 8. Overview of morphological characters associated with *Schwetzochromis* in comparison with the new species described herein.

Morphological characters associated with *Schwetzochromis* (as in De Vos & Seegers, 1998)	*Orthochromis mporokoso*	*Orthochromis katumbii*	*Orthochromis kimpala*	*Orthochromis gecki*	*Orthochromis indermauri*
Highly sexually dichromatic: mature males brilliantly coloured with a series of sharply contrasting longitudinal stripes; females relatively drab with six to eight vertical bars	No	No	No	No	No
Large *Haplochromis*-like eggspots in both sexes	No (eggspots missing)	No (eggspots missing)	Eggspot-like maculae present (not large)	Eggspots present (not large)	Red maculae resembling eggspot-like maculae (not large)
No lachrymal stripes and/or dark bars across the snout and the orbit	No (lachrymal stripe present)	No (lachrymal stripe present)	No (lachrymal stripe present)	No (lachrymal stripe present)	No (lachrymal stripe present)
Pelvic fin long, elongate in males, shorter in females	No	No	No	No	No
Upper jaw with 4-6 inner tooth rows, not well separated from the outer row	No (two to three)	No (two to three)	No (two to three)	No (two to four)	No (three to five)
Development of unicuspid, slender or broad-tipped spatulate teeth in the jaws of large specimens	No (bicuspid teeth)	No (bicuspid to subequally bicuspid teeth)	No (bicuspid to subequally bicuspid teeth)	No (bicuspid to subequally bicuspid teeth)	No (bicuspid to subequally bicuspid teeth)

molecular analyses of mitochondrial data *O. indermauri* appears to represent a lineage of its own, too (Schedel *et al.* submitted). It is worth mentioning that the overall appearance of *O. indermauri* reminds of Eretmodini (e.g. *Eretmodus),* which are endemic to Lake Tanganyika and its outlet Lukuga (Kullander & Roberts 2011), because as in *Eretmodus, O. indermauri* has a comparatively short, laterally compressed body, superolaterally positioned eyes and broad vertical bars on flanks. On the other hand, *O. indermauri* differs in several morphological characters from Eretmodini species as its dorsal fin is composed of 17 or 18 spines whereas Eretmodini species have comparatively high dorsal-fin spine counts of between 21 and 25, which are among the highest among cichlids (Poll 1986). Although each of the three Eretmodini genera is characterized by a distinctive oral tooth shape (e.g. spatulate, cylindrical or conical) all have in common unicuspid oral teeth (Huysseune *et al.* 1999, Vandervennet *et al.* 2006); this contrasts with the bicuspid to subequally bicuspid teeth in the outer row of upper and lower jaw of *O. indermauri*. Further, *O. indermauri* exhibits maculae which are vaguely similar to egg-spots, which contrasts with the lack of egg-spots or eggspot-like maculae on the anal fin of Eretomodini. Several molecular phylogenetic studies established alternative hypotheses for the placement of Eretmodini when comparing nuclear and mitochondrial phylogenies (e.g. Clabaut *et al.* 2005, Meyer *et al.* 2015, Weiss *et al.* 2015), and Weiss *et al.* (2015) found support for a mosaic genomic composition of Eretmodini with phylogenetic signal of both Lamprologini and Malagarasi-*Orthochromis* and/or Haplochromini. *Orthochromis indermauri* might represent an additional lineage with a mosaic genomic composition but so far no nuclear data for this taxon are available.

Conservation. The five new species appear to be endemics of the Katanga-Chambeshi region (sensu Cotterill 2005), a landscape mosaic of savannah grasslands and wetlands, centred within the Zambezian phytochorion (sensu White 1983). The Katanga-Chambeshi region is characterised by high physiographic diversity encompassing several high plateaux (e.g. Bia, Kibara, and Kundelungu plateaux), deep ravines and wide depressions providing a wide variety of habitats which is also reflected by the diversity of vegetation types in this area (Broadley & Cotterill 2004). The Katanga-Chambeshi region is only loosely defined but includes parts of three freshwater ecoregions sensu Thieme *et al.* (2005): Bangwelu-Mweru (*O. mporokoso*, *O. katumbii*), Upper Lualaba (*O. kimpala, O. gecki*) and Lake Tanganyika (*O. indermauri*). These ecoregions have been reported to harbour a rich aquatic fauna with a high degree of endemism, e.g., one third of the Bangwelu-Mweru ecoregion fish species appear to be endemic to it (Balon & Stewart 1983, Thieme *et al.* 2005). A very rich aquatic herpetofauna is documented from the Upper Lualaba ecoregion but the ichthyological fauna appears to be only incompletely known even though many endemic fish species are reported from this ecoregion (Poll 1976, Thieme *et al.* 2005).

The different drainage systems of the Katanga-Chambeshi region are prone to different environmental threats. Major threats for aquatic fauna of the poorly studied Upper Lualaba ecoregion are the extensive mining activities due to the rich mineral deposits such as copper, zinc, and cobalt, and this especially along the Copperbelt with the associated negative impacts on the environment such as erosion, contaminations, and pollution of the soil and waterbodies (Thieme *et al.* 2005, Katemo Manda *et al.* 2010). Generally, the five new species described herein might be threatened by the common hazards for aquatic wildlife in the region (e.g. unsustainable fishing methods, deforestation, damming, pollution, and mining), which might be aggravated by the fact that most of their known distribution ranges are located outside of protected areas. Moreover, it appears that the ichthyological fauna of the Bangwelu-Mweru ecoregion and Upper Lualaba ecoregion is understudied as several species caught along with the new species still were new and await formal description. Future conservation plans and prioritisations should therefore consider that the number of endemic taxa in these regions might not only be higher than previously assumed but potentially also locally restricted to individual river drainages or stretches due to biogeographical barriers such as waterfalls (e.g. Lufubu River). An updated assessment of the ichthyodiversity of National Parks (e.g. Parc National de Kundelungu and Parc National de Upemba) in DRC is in preparation (Mbisa Congo Project), but areas outside these parks still need more attention.

Acknowledgements

We thank James MacLaine (BMNH), Miguel Parrent (MRAC), Willy Baudouin (MRAC), John Friel (formerly CU), Fabrizia Ronco (Universtiy of Basel, Tanganjikasee-Buntbarsch-Sammlung), O. Seehausen (EAWAG) for their efforts with loan arrangements for comparative specimens. Dirk Neumann (ZSM) is kindly acknowledged for

collection management at ZSM. Moreover, we thank Hans van Heusden and Adrian Indermaur for countless fruitful discussions and their inspiring enthusiasm. We further thank Berd Egger for sharing his data on water parameters of the Lufubu River. In addition, we acknowledge Fenton P. D. Cotterill (Univ. Stellenbosch), for his support during the 2015 Zambian field trip, and Alex D. Chilala (Provincial Agricultural Coordinator, Western Province, Republic of Zambia) for help with collection and export permits (issued on 05.10.2015 in Kasama by the Ministry of Agriculture and Livestock; Department of Fisheries Provincial Fisheries Office).

Last but not least we would like to thank our donors: UKS and FS are funded by the Volkswagen-Stiftungs project "Exploiting the genomic record of living biota to reconstruct the landscape evolution of South Central Africa." Further financial support for the various field collections came from Mbisa Congo Project (2013-2018), a framework agreement project of the RMCA and the Belgian Development Cooperation, and PRODEPAAK (NN/ 3000769) CTB/BTC project (2008-2013) for financial and logistical support to the 2012 Katanga Expedition. The manuscript benefitted substantially from constructive reviews prepared by Jay Stauffer and Ad Konings, and by the smooth review process by J. Armbruster - thank you very much!

References

Barel, C.D.N., van Oijen, M.J.P., Witte, F. & Witte-Maas, E.L.M. (1977) An introduction to the taxonomy and morphology of the haplochromine Cichlidae from Lake Victoria. *Netherlands Journal of Zoology,* 27 (4), 333–389. https://doi.org/10.1163/002829677X00199

Balon, E.K. & Stewart, D.J. (1983) Fish assemblage in a river with unusual gradient (Luongo, Africa Zaire system), reflections on river zonation, and description of another new species. *Environmental Biology of Fishes,* 9, 225–252. https://doi.org/10.1007/BF00692373

Boulenger, G.A. (1899) Matériaux pour la faune du Congo. Poissons nouveaux du Congo. Cinquième Partie. Cyprins, Silures, Cyprinodontes, Acanthoptérygiens. *Annales du Musée du Congo*, Series Zoology, 1 (5), 97–128.

Boulenger, G.A. (1902) Contributions to the ichthyology of the Congo.—II. On a collection of fishes from the Lindi River. *Proceedings of the Zoological Society of London*, 1 (4), 265–271.

Boulenger, G.A. (1905) On a collection of fishes from Lake Bangwelo. *Annals and Magazine of Natural History*, Series 7, 16 (96 Art. 72), 642–647. https://doi.org/10.1080/03745480509443309

Broadley, D.G. & Cotterill, F.P.D. (2004) The reptiles of south-east Katanga, an overlooked 'hot spot'. *African Journal of Herpetology,* 53, 35–61. https://doi.org/10.1080/21564574.2004.9635497

Clabaut, C., Salzburger, W. & Meyer, A. (2005) Comparative phylogenetic analyses of the adaptive radiation of Lake Tanganyika cichlid fish: Nuclear sequences are less homoplasious but also less informative than mitochondrial DNA. *Journal of Molecular Evolution*, 61, 666–681. https://doi.org/10.1007/s00239-004-0217-2

Cotterill, F.P.D. (2005) The Upemba lechwe, *Kobus anselli*: an antelope new to science emphasizes the conservation importance of Katanga, Democratic Republic of Congo. *Journal of Zoology,* 265, 113–132. https://doi.org/10.1017/S0952836904006193

David, L. (1937) Poissons de l'Urundi. *Revue de Zoologie et de Botanique Africaines*, 29 (4), 413–420.

De Vos, L. & Seegers, L. (1998) Seven new *Orthochromis* species (Teleostei: Cichlidae) from the Malagarasi, Luiche and Rugufu basins (Lake Tanganyika drainage), with notes on their reproductive biology. *Ichthyological Exploration of Freshwaters,* 9 (4), 371–420.

De Zeeuw, M.P., Westbroek, I., van Oijen, M.J.P. & Witte, F. (2013) Two new species of zooplanktivorous haplochromine cichlids from Lake Victoria, Tanzania. *ZooKeys,* 256, 1–34. https://doi.org/10.3897/zookeys.256.3871

Dunz, A. & Schliewen, U.K. (2010) Description of a new species of *"Tilapia"* Smith, 1840 (Teleostei: Cichlidae) from Ghana. *Zootaxa*, 2548, 1–21.

Dunz, A.R. & Schliewen, U.K. (2013) Molecular phylogeny and revised classification of the haplotilapiine cichlid fishes formerly referred to as "*Tilapia*". *Molecular Phylogenetics and Evolution*, 68, 64–80. https://doi.org/10.1016/j.ympev.2013.03.015

Free Spatial Data DIVA-GIS (2018) Available from: http://www.diva-gis.org/Data (accessed 29 January 2018)

Greenwood, H.P. & Kullander, S.O. (1994) A taxonomic review and redescription of *Tilapia polyacanthus* and *T. stormsi* (Teleostei: Cichlidae), with descriptions of two new *Schwetzochromis* species from the Upper Zaire River drainage. *Ichthyological Exploration of Freshwaters,* 5 (1), 161–180.

Greenwood, P.H. (1954) On two species of cichlid fishes from the Malagarazi River (Tanganyika), with notes on the pharyngeal apophysis in species of the *Haplochromis* group. *Annals and Magazine of Natural History,* Series 12, 7 (78),

401–414.
https://doi.org/10.1080/00222935408656059
Greenwood, P.H. (1979) Towards a phyletic classification of the 'genus' *Haplochromis* (Pisces, Cichlidae) and related taxa, part I. *Bulletin of the British Museum (Natural History) Zoology,* 35, 265–322.
https://doi.org/10.5962/bhl.part.20455
Hammer, Ø., Harper, D.A.T. & Ryan, P.D. (2001) PAST: Paleontological statistics software package for education and data analysis. *Palaeontologia Electronica*, 4 (1), 9.
Hilgendorf, F.M. (1888) Fische aus dem Victoria-Nyanza (Ukerewe-See), gesammelt von dem verstorbenen Dr. G. A. Fischer. S*itzungsberichte der Gesellschaft Naturforschender Freunde zu Berlin,* 1888, 75–79.
Huysseune, A. Rüber, L. & Verheyen, E. (1999) A single tooth replacement pattern generates diversity in the dentition in cichlids of the tribe Eretmodini, endemic to Lake Tanganyika (Teleostei: Cichlidae). *Belgian Journal of Zoology*, 129, 157–174.
Indermaur, A. (2014) Über den Tellerrand geschaut - Buntbarsche aus dem Lufubu. *Die Aquarien- und Terrarien-Zeitschrift,* 10, 16–23.
Jorissen, M.W.P, Pariselle, A., Huyse, T., Vreven, E.J., Snoeks, J., Volckaert, F.A.M., Chocha Manda, A., Kapepula Kasembele, G., Artois, T. & Vanhove, M.P.M. (2017) Diversity and host specificity of monogenean gill parasites (Platyhelminthes) of cichlid fishes in the Bangweulu-Mweru ecoregion. *Journal of Helminthology*, 92 (4), 417–437.
https://doi.org/10.1017/S0022149X17000712
Katemo Manda, B., Colinet, G., Manda, A.C., Marquet, J.P. & Micha, J.C. (2010) Evaluation de la contamination de la chaîne trophique par les éléments traces (Cu, Co, Zn, Pb, Cd, U, V et As) dans le bassin de la Lufira supérieure (Katanga/RD Congo). *Tropicultura*, 28 (4), 246–252.
Koblmüller, S., Schliewen, U.K., Duftner, N., Sefc, K.M., Katongo, C. & Sturmbauer, C. (2008) Age and spread of the haplochromine cichlid fishes in Africa. *Molecular Phylogenetics and Evolution,* 49, 153–169.
https://doi.org/10.1016/j.ympev.2008.05.045
Koblmüller, S., Katongo, C., Phiri, H. & Sturmbauer, C. (2012) Past Connection of the Upper Reaches of a Lake Tanganyika Tributary with the Upper Congo Drainage Suggested by Genetic Data of Riverine Cichlid Fishes. *African Zoology*, 47 (1), 182–186.
https://doi.org/10.3377/004.047.0115
Kullander, S.O. & Roberts, T.R. (2011) Out of Lake Tanganyika: endemic lake fishes inhabit rapids of the Lukuga River. *Ichthyological Exploration of Freshwaters,* 22, 355–376.
Matschiner, M., Musilová, Z., Barth, J.M.I., Starostova, Z., Salzburger, W., Steel, M. & Bouckaert, R. (2016) Bayesian Phylogenetic Estimation of Clade Ages Supports Trans-Atlantic Dispersal of Cichlid Fishes. *Systematic Biology,* 66, 3–22.
https://doi.org/10.1093/sysbio/syw076
Meyer, B.S., Matschiner, M. & Salzburger, W.A. (2015) A tribal level phylogeny of Lake Tanganyika cichlid fishes based on a genomic multi-marker approach. *Molecular Phylogenetics Evolution*, 83, 56–71.
https://doi.org/10.1016/j.ympev.2014.10.009
Poll, M. (1948) Descriptions de Cichlidae nouveaux recueillis par le Dr. J. Schwetz dans la rivière Fwa (Congo belge). *Revue de Zoologie et de Botanique Africaines*, 41 (1), 91–104.
Poll, M. (1967) Contribution à la faune ichthyologique de l'Angola. *Publicações Culturais, Companhia de Diamantes de Angola (DIAMANG), Lisboa,* 75, 1–381, Pls. 1–20.
Poll, M. (1976) Poissons. Exploration du Parc National de l'Upemba, Mission G. F. de Witte, Bruxelles*. Reports of the Swedish Deep-Sea Expedition 1947-1948*, 73, 1–127.
Poll, M. (1986) *Classification des Cichlidae du lac Tanganika. Tribus, genres et espèces*., Collection in 8 - 2ème série; Bruxelles, 45 (2), 1–163.
Roberts & Stewart, D.J. (1976) An ecological and systematic survey of fishes in the rapids of the lower Zaire or Congo River. *Bulletin of the Museum of Comparative Zoology,* 147 (6), 239–317.
Salzburger, W., Meyer, A., Baric, S., Verheyen, E. & Sturmbauer, C. (2002) Phylogeny of the Lake Tanganyika cichlid species flock and its relationship to the Central and East African haplochromine cichlid fish faunas. *Systematic Biology,* 51 (1), 113–135.
https://doi.org/10.1080/106351502753475907
Schedel, F.D.B., Friel, J.P. & Schliewen, U.K. (2014) *Haplochromis vanheusdeni*, a new haplochromine cichlid species from the Great Ruaha River drainage, Rufiji basin, Tanzania (Teleostei, Perciformes, Cichlidae). *Spixiana*, 37 (1), 135–149.
Schedel, F.D.B. & Schliewen, U.K. (2017) *Hemibates koningsi* spec. nov: a new deep-water cichlid (Teleostei: Cichlidae) from Lake Tanganyika. *Zootaxa*, 4321 (1), 92–112.
https://doi.org/10.11646/zootaxa.4312.1.4
Schwarzer, J., Swartz, E.R., Vreven, E., Snoeks, J., Cotterill, F.P.D., Misof, B. & Schliewen, U.K. (2012) Repeated trans-watershed hybridization among haplochromine cichlids (Cichlidae) was triggered by Neogene landscape evolution. *Proceedings of the Royal Society B*, 279 (1746), 4389–4398.
https://doi.org/10.1098/rspb.2012.1667
Thieme, M.L., Abell, R., Stiassny, M.L.J., Skelton, P., Lehner, B., Teugels, G.G., Dinerstein, E., Kamdem-Toham, A., Burgess, N. & Olson, D. (2005) *Freshwater Ecoregions of Africa and Madagascar: A Conservation Assessment*. Island Press,

Washington, D.C., 483 pp.
Thys van den Audenaerde, D.F.E. (1963) Description d'une espèce nouvelle d'*Haplochromis* (Pisces, Cichlidae) avec observations sur les *Haplochromis* rhéophiles du Congo oriental. *Revue de Zoologie et de Botanique Africaines*, 68, 140–152.
Thys van den Audenaerde, D.F.E. (1964) Les *Haplochromis* du Bas-Congo. *Revue de Zoologie et de Botanique Africaines*, 70, 154–173.
Van Oijen, M.J.P., Snoeks, J., Skelton, P.H., Maréchal, C. & Teugels, G.G. (1991) *Haplochromis*. *In*: Daget, J., Gosse, J.P., Teugels, G.G. & Thys van den Audenaerde, D.F.E. (Eds.), *Check-list of the freshwater fishes of Africa (CLOFFA). Vol. 4*. ISNB, Bruxelles, MRAC, Tervuren and ORSTOM, Paris, pp. 100–184.
Van Oijen, M.J.P. (1996) The generic classification of the haplochromine cichlids of Lake Victoria, East Africa. *Zoologische Verhandelingen, Leiden*, 302, 57–110.
Vandervennet, E., Wautier, K., Verheyen, E. & Huysseune, A. (2006) From conical to spatulate: Intra- and interspecific changes in tooth shape in closely related cichlids (Teleostei; Cichlidae: Eretmodini). *Journal of Morphology*, 267, 516–525. https://doi.org/10.1002/jmor.10418
Wamuini Lunkayilakio, S. & Vreven, E.J. (2010) '*Haplochromis*' *snoeksi*, a new species from the Inkisi River basin, Lower Congo (Perciformes: Cichlidae). *Ichthyological Exploration of Freshwaters*, 21 (3), 279–3287.
Weiss, J.D., Cotterill, F.PD. & Schliewen, U.K. (2015) Lake Tanganyika—A 'Melting Pot' of ancient and young cichlid lineages (Teleostei: Cichlidae)? *PLOS ONE*, 10, e0125043. https://doi.org/10.1371/journal.pone.0125043
White, F. (1983) *The vegetation of Africa. A descriptive memoir to accompany the UNESCO/AETFAT/UNSO vegetation map of Africa. Natural Resources Research No. 20*. UNESCO, Paris, 352 pp.

Appendix. Comparative material examined

Haplochromis bakongo Thys van den Audenaerde 1964: MRAC 142002, 1, holotype, 74.7 mm SL; Democratic Republic of Congo, Ngombe River at Banza Mfinda, Lower Congo (-5.38/15).—MRAC 142003-009, 7, paratypes, 63.5–87.8 mm SL; Ngombe River at Banza Mfinda, Lower Congo, (-5.38/15).—MRAC 142010-011, 2, paratypes, 75.3–87.8 mm SL; Moerbeke, Lower Congo, (-5.5/14.7).—ZSM 37741, 2, 41.9–46.1 mm SL; Democratic Republic of Congo, drainage Kwilu, small stream, north of Yabi station on Jules van Lancker farm (-5.5901/14.7514).

Haplochromis moeruensis (Boulenger 1899): MRAC 216-222, 4, syntypes, 49.4–75.7 mm SL; Democratic Republic of Congo, Pweto, Lake Mweru (-8.46/28.7).

'Haplochromis' snoeksi Wamuini Lunkayilakio & Vreven 2010: MRAC A7-009-P-0001, 1, holotype, 82.5 mm SL; Democratic Republic of the Congo, River Ngeba/Ngufu, village Ngeba, affluent of River Inkisi, Lower Congo (-5.1838/15.2064).—MRAC A7-009-P-0004, 1, paratype, 93.8 mm SL; Democratic Republic of the Congo, River Ngeba/Ngufu, village Ngeba, affluent of River Inkisi, Lower Congo (-5.1838/15.2064).—MRAC A9-014-P-0001, 1, paratype, 81.2 mm SL; Democratic Republic of the Congo, River Ngeba, village Ngeba, affluent of River Inkisi, at Kimasi Bridge, Lower Congo (-5.1838/15.2064).

Haplochromis vanheusdeni Schedel, Friel & Schliewen 2014: CUMV 97639, 1, Holotype, 70.7 mm SL, Tanzania, Morogoro State, drainage Rufiji, Sonjo River at bridge in Man'gula on road from Mikumi to Ifakara, altitude 302 m (-7.808231/36.896561).—CUMV 93835, (1)13, paratypes 31.5–78.7 mm SL, Tanzania, Morogoro state, drainage Rufiji, Sonjo River at bridge in Man'gula on road from Mikumi to Ifakara, altitude 302 m (-7.808231/36.896561).—ZSM 40703, 2, paratypes 50.3–58.7 mm SL), Tanzania, Morogoro state, drainage Rufiji, Sonjo River at bridge in Man'gula on road from Mikumi to Ifakara, altitude 302 m (-7.808231/36.896561).—MRAC 34-09-P-001-003, 3, paratypes, 54.0–58.3 mm SL, Tanzania, Morogoro state, drainage Rufiji, Sonjo stream at bridge on road Ifakara- Kidodi (-7.808339/36.896189).—ZSM 41440, 3, paratypes, 56.2–63.6 mm SL, Tanzania, Morogoro state, drainage Rufiji, Sonjo stream at bridge on road Ifakara-Kidodi (-7.808339/36.896189.—ZSM 41559, 7, paratypes, 47.2–67.8 mm SL, Tanzania, Morogoro state, drainage Rufiji, Sonjo stream at bridge on road Ifakara- Kidodi (-7.808339/36.896189).—ZSM 42308, 1, paratype, 83.9 mm SL Tanzania, Morogoro state, drainage Rufiji, Sonjo River at bridge in Man'gula on road from Mikumi to Ifakara, altitude 302 m (-7.808231/36.896561).—CUMV 93833, 2(3), 31.5–60.4 mm SL; drainage Rufiji, Great Ruaha River at bridge in Kidatu on road from Mikumi to Ifakara (-7.66174/36.9773).—CUMV 93834, 2, 36.6–56.2 mm SL; drainage Rufiji, Idete River at bridge in Idete on road from Ifakara to Taveta (-8.10391/36.4881).

Orthochromis kalungwishiensis (Greenwood & Kullander 1994): MRAC 99-035-P-0031-0032, 2, 69.3–78.3 mm SL; Keso village, Pambashe River, local name Luena River, (possibly:-9.6000/29.4833).—MRAC 99-035-P-0033-0035, (2)3, 66.4–69.2 mm SL, Luena River (=Pambashe River), tributary of Kalungwishi River (possibly: -9.6000/29.4833).—ZSM 41427, 1, 79.2 mm SL; Zambia, Kalungwishi stream above Lumanmgwe Falls on road Mukunsa-Kawambwa (-9.5431/29.3878).—ZSM 41431, 6, 44.4–75.8 mm SL; Zambia, Kalungwishi stream above Lumanmgwe Falls on road Mukunsa-Kawambwa (-9.5431/

29.3878).—ZSM 44369, (8)13, 48.5–70.7 mm SL; Zambia, Kalungwishi River, above Kundabwika and below Kabwelume Falls, near to road Mporokoso—Mununga (-9.217887/ 29.304202)

Orthochromis kasuluensis De Vos & Seegers 1998: MRAC 93-152-P-0725-0740, 4(15), paratypes, 63.5–68.4 mm SL; Mgandazi River, Ruchugi drainage, Malagarasi basin, around 80 km north of Kigoma on road to Kasulu, few km before Kasulu (-4,56/30.1).—ZSM 41455, 5, 48.2–67.0 mm SL; Tanzania, Ruchugi River east of Kasulu on road to Kasulu-Kibondo (-4.5347/30.1483).

Orthochromis luichensis De Vos & Seegers 1998: MRAC 93-152-P-0122-0135, 7(13), paratypes, Mkuti River, affluent Luiche, about 40 km on the road Kigoma-Kasulu (-4.86/29.86).—ZSM 41445, 7, 38.0–72.7 mm SL; Tanzania, Mkuti River, road bridge east of Kandihwa village (-4.8867/29.8703).

Orthochromis luongoensis (Greenwood & Kullander 1994): CU 91747, 1, 69.9 mm SL; Zambia, Lufubu River Falls below bridge at Chipili on Mansa-Munuga road, (-10.7286/29.0936).—ZSM 41437, (5)6, 46.3–68.4 mm SL; Zambia, Luongo stream at bridge on road Mwenga-Kashiba, affluent to Lake Mweru / Upper Congo basin (-10.4708/29.0261).—ZSM 44345, 6, 61.5–106.9 mm SL; Zambia, Kalungwishi River, immediately above Kabwelume Falls (below Lumangwe Falls), ~ 20 km downstream bridge on road Mporokoso-Kawambwa, Northern Province, (-9.527083/29.353102).—ZSM 44432, 7, 53.8–98.0 mm SL; Zambia, Luongo River, at bridge on road Kawambwa-Mansa about 40 km (driving distance) S of Kawambwa (-10.144359/ 29.167193).—ZSM 44467, (5)7, 42.6-59.0 mm SL; Zambia, Luongo River, below Mumbuluma Falls, ~ 40 km (air distance) NW of Luwingu Luapula Province (-10.106146/ 29.571487).—ZSM 44569, 1, 69.9 mm SL; Zambia, Kalungwishi River, above Kundabwika and below Kabwelume Falls, near to road Mporokoso—Mununga (-9.217887/ 29.304202).

Orthochromis machadoi (Poll 1967): BMNH 1984.2.6.104-108, 5, 42.31–52.1 mm SL; Angola, Cunene River (-17.267/ 14.50).—BMNH 1984.2.6.109, 1, 44.7 mm SL; Angola, Cunene River (-17.05/13.5).—BMNH 1984.2.6.113, 1, 52.2 mm SL; Angola, Cunene River (-17/13.25).—BMNH 1984.2.6.116-131, (1) 22, 50.5–60.1 mm SL; Angola, Cunene River (-16.983333/ 13.366667).—BMNH 1984.2.6.132-141, 3, 43.4–55.4 mm SL, Angola, Cunene River (-14.383333/15.300000).—BMNH 1984.2.6.142-145, 4, 50.3–65.7 mm SL; Angola, Cunene River (-14.916667/15.100000).

Orthochromis malagaraziensis David 1937: MRAC 47077-47079, 3, 74.5-83.3 mm SL; paralectotypes, Malagarasi River and its affluents, near Bururi (-4.43/29.76).—ZSM 41469, 2, 66.5-68.8 mm SL; Tanzania, Malagarasi River close to Uvinza (-5.1183/30.3825).

Orthochromis mazimeroensis De Vos & Seegers 1998: MRAC 91-062-P-1620-1651, (4)31, paratypes, 44.3-55.8 mm SL; Kabingo, Mazimero River, road Rutana-Kinyinya, Malagarasi basin (-3.9/30.21).—MRAC 93-150-P-0432-0476, (4)44, 52.1-58.3 mm SL; paratypes, Mazimero River, affluent Malagarasi, on the Road Prov. 85 after ”Faille des Allemands“ direction Giharo (-3.9/30.21).—University Basel Uncat, 1, 45.5 mm SL; Burundi, Mazimero River, affluent of Upper Malagarasi River, upstream of bridge (-3.884722/ 30.197750).—University Basel KDD3, 1, 39.9 mm SL; Burundi, Mazimero River, affluent of Upper Malagarasi River, upstream of bridge (-3.884722/ 30.197750).—University Basel KDD4, 1, 44.2 mm SL; Burundi, Mazimero River, affluent of Upper Malagarasi River, upstream of bridge (-3.884722/ 30.197750).—University Basel KDD6, 1, 40.4 mm SL; Burundi, Mazimero River, affluent of Upper Malagarasi River, upstream of bridge (-3.884722/ 30.197750).—University Basel KDC8, 1, 59.7 mm SL; Burundi, Mazimero River, affluent of Upper Malagarasi River, upstream of bridge (-3.884722/ 30.197750).—University Basel KDC9, 1, 43.0 mm SL; Burundi, Mazimero River, affluent of Upper Malagarasi River, upstream of bridge (-3.884722/ 30.197750).

Orthochromis mosoensis De Vos & Seegers 1998: MRAC 93-150-P0478-0481, 4, 47.1-60.3 mm SL; River Rurur, 9 km from Muyaga near Cenda Juru, Malagarasi basin (-3.3/30.55).

Orthochromis polyacanthus (Boulenger 1899): Personal collection of O. Seehausen (Field number MKB18), 5, 60.1-66.4 mm SL; drainage Lake Mweru, no further information available.—MKL 11, 2, 51.1-65.1 mm SL; no further information available.—Personal collection of O. Seehausen (Field number MKL 12), 1, 63.5 mm SL; no further information available.

Orthochromis rubrolabialis De Vos & Seegers 1998: MRAC 96-022-P-0002-004, 3, paratypes, 43.4-48.7 mm SL; Majamazi River, Malagarasi drainage, Ugalla subdrainage, 58 km north of Mpanda on road to Uvinza; (-5.93/30.95).—ZSM 41463, (7)8, 44.5-86.7 mm SL; Tanzania, Malagarasi River close to Uvinza (-5.1183/30.38)

Orthochromis rugufuensis De Vos & Seegers 1998: MRAC 96-022-P-0006, 1, paratype, 47.1 mm SL; Tanzania, Upper Rugufu River: on road from Uvinza to Mpanda, about 83 km south of Uvinza (-5.7000/ 30.6666.

Orthochromis stormsi (Boulenger 1902): MRAC 96-031-P-1303-1307, (3)5, 38.5-64.5 mm SL; Democratic Republic of the Congo, Lualaba River chutes 47 km on road of Kisangani-Lubutu near of the Concasserie, no GPS data available.—ZSM 32393, (5)6, 40.0-65.6 mm SL; Republic of Congo, Congo main channel near Djoue River confluence at “Les Rapides” (-

4.31306/15.2289).—ZSM 37603, 1, 44.8 mm SL; Democratic Republic of the Congo, Lubuya stream below bridge on Lubutu road, close to Wanie Rukula (0.1928/25.5319).—ZSM 37541, 3, 63.5-80.3 mm SL; Democratic Republic of the Congo, Kisangani market, bought from woman who sells fishes from Wagenia rapids or fishes bought directly at Wagenia village (0.4939/25.2072).—ZSM 38129, 3, 52.5- 88.0 mm SL; Democratic Republic of the Congo, Congo River, obtained from local fishermen at Kinsuka rapids, exact collecting location unclear (-4.3278/15.2306).—ZSM 38337, 1, 52.8 mm SL; Democratic Republic of the Congo, Congo River "Chutes Kipokosso" at Wanie Rukula, (0.1856/25.5218).—ZSM 38382, 1, 69.1 mm SL; Democratic Republic of the Congo, Congo River obtained from local fishermen at Kinsuka rapids, exact collecting location unclear (-4.3278/15.2306).

Orthochromis torrenticola (Thys van den Audenaerde 1963): MRAC 140100, 1, holotype, 67.3 mm SL; Democratic Republic of the Congo, Lufira River rapids, just above the main falls at Kiubo, Congo, no GPS data available.—MRAC 140101, 1, paratype, 67.3 mm SL; Democratic Republic of the Congo, Lufira River rapids, just above the main falls at Kiubo, Congo, no GPS data available.—MRAC 182787-182804, (4)17, 66.0-85.5 mm SL; Lufira River, between Koni and Mwashia (-10.71/ 27.35).—ZSM 38201, (4)5, 37.2-52.3 mm SL; Democratic Republic of the Congo, drainage Congo, Lufira River near Mwashia village near small rapids (-10.7008/27.3403).

Orthochromis uvinzae De Vos & Seegers 1998: ZSM 41430, (6)7, 57.2-80.8 mm SL; Tanzania, Malagarasi River close to Uvinza (-5.1183/30.38).—ZSM 41562, (4)5, 63.7- 83.9 mm SL; Tanzania, Malagarasi River, riffles/rapids upstream of Uvinza (-5.1889/30.0517).—ZSM 41564, 5, 56.6-73.3 mm SL; Tanzania, Malagarasi River, riffles/ rapids upstream of Uvinza (-5.1889/30.0517).

***Orthochromis* sp. "Igamba"**: ZSM 41561, 5, 49.9-73.1 mm SL; Tanzania, Malagarasi River, Igamba cataracts approximately 56 km downriver of Uvinza (-5.1803/30.0531).—ZSM 41563, 3, 57.0-79.3 mm SL; Tanzania, Malagarasi River, Igamba cataracts approximately 56 km downriver of Uvinza (-5.1803/30.0531).

Schwetzochromis neodon Poll 1948: MRAC 79591-79644, (14)53, 69.5-92.2 mm SL; Democratic Republic of the Congo, River Fwa, no GPS data available.

Appendix.

Individual species-specific principal component analyses (with a reduced taxon sets). Pictures of different species and specimens depicted in the plots were obtained on different field trips and form private photo collections: *O. katumbii* sp. nov. *(holotype), O. kimpala sp*. nov. (probably the holotype)*, O. mporokoso* sp. nov. (probably the holotype)*, O. gecki* sp. nov. (photo: probably the holotype and a second specimen from the Katanga 2016 Expedition)*, O. indermauri* sp. nov. (paratype), *H. bakongo* (preserved specimen: MRAC 142003-142009; paratype), *H. snoeksi* (preserved specimen; holotpye)*, H. vanheusdeni* (photo: H. van Heusden), *S. neodon* (preserved specimen, MRAC 79591-79644)*, O. kalungwishiensis* (Zambia 2015 Expedition)*, O. luongoensis* (photo: Zambia 2015 Expedition), *O. uvinzae* (representing the Malagarasi-*Orthochromis*; photo: J. Geck)*, O. machadoi* (photo: E. Schraml)*, O. cf. polyacanthus* (Aquarium specimen, F. Schedel)*,O. stormsi* (Aquarium specimen, photo: J. Geck)*, O. torrenticola* (Katanga 2016 Expedition).

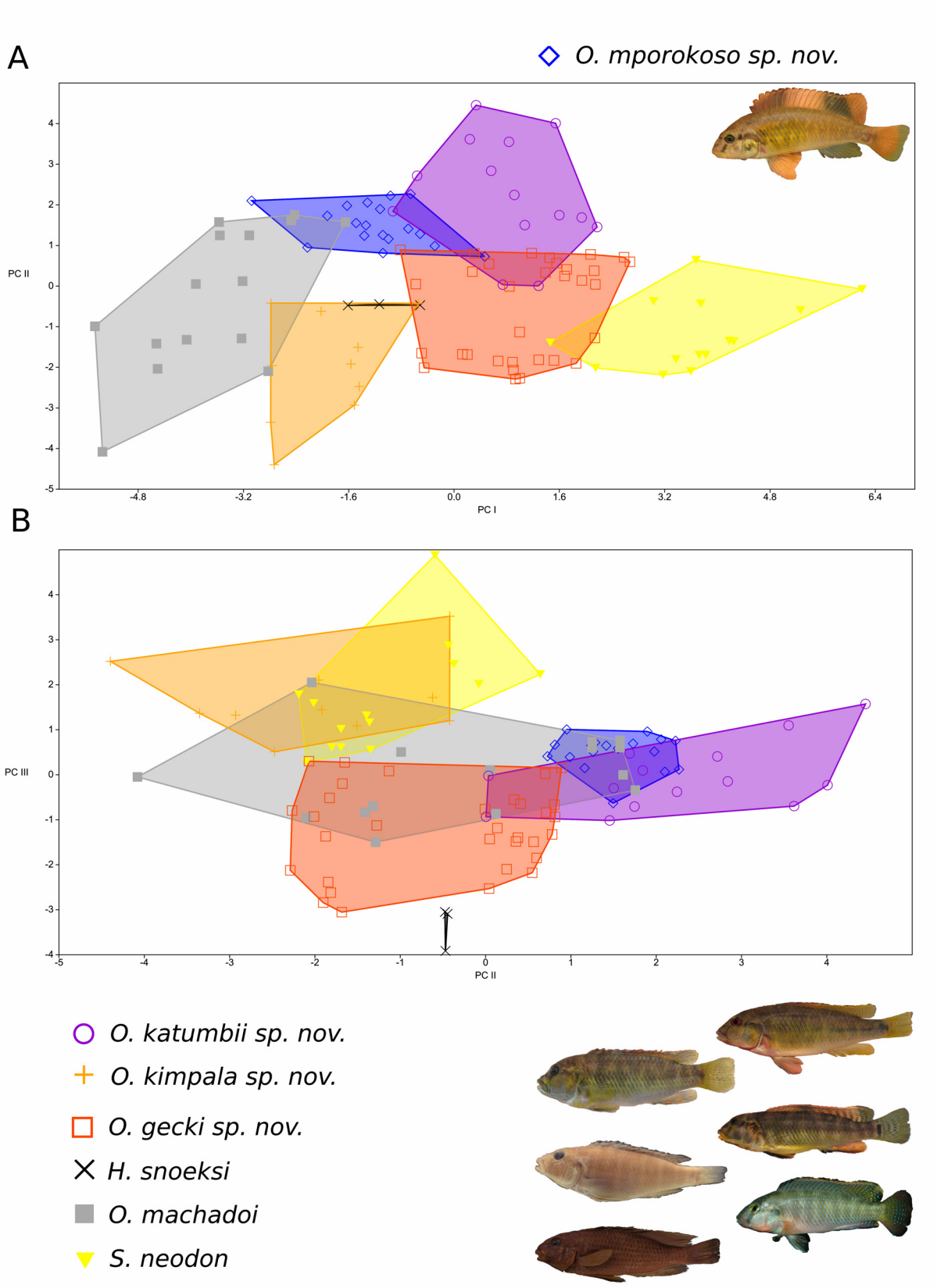

FIGURE S1: Species-specific PCA scatter plots focusing on *O. mporokoso* **sp. nov.** based on 20 meristics; species score limits visualized as convex hulls. PC I vs PC II (A)and PC vs PC III (B) for a 106 examined specimens. PC I explain 27.87 %, PC II explains 15.43 % and PC III explains 10.77 % of the variance. Species depicted from top to bottom: *O. mporokoso* **sp. nov.** , *O. katumbii* **sp. nov**., *O. kimpala* **sp. nov.**, *O. gecki* **sp. nov.**, *H. snoeksi, O. machadoi, S. neodon*.

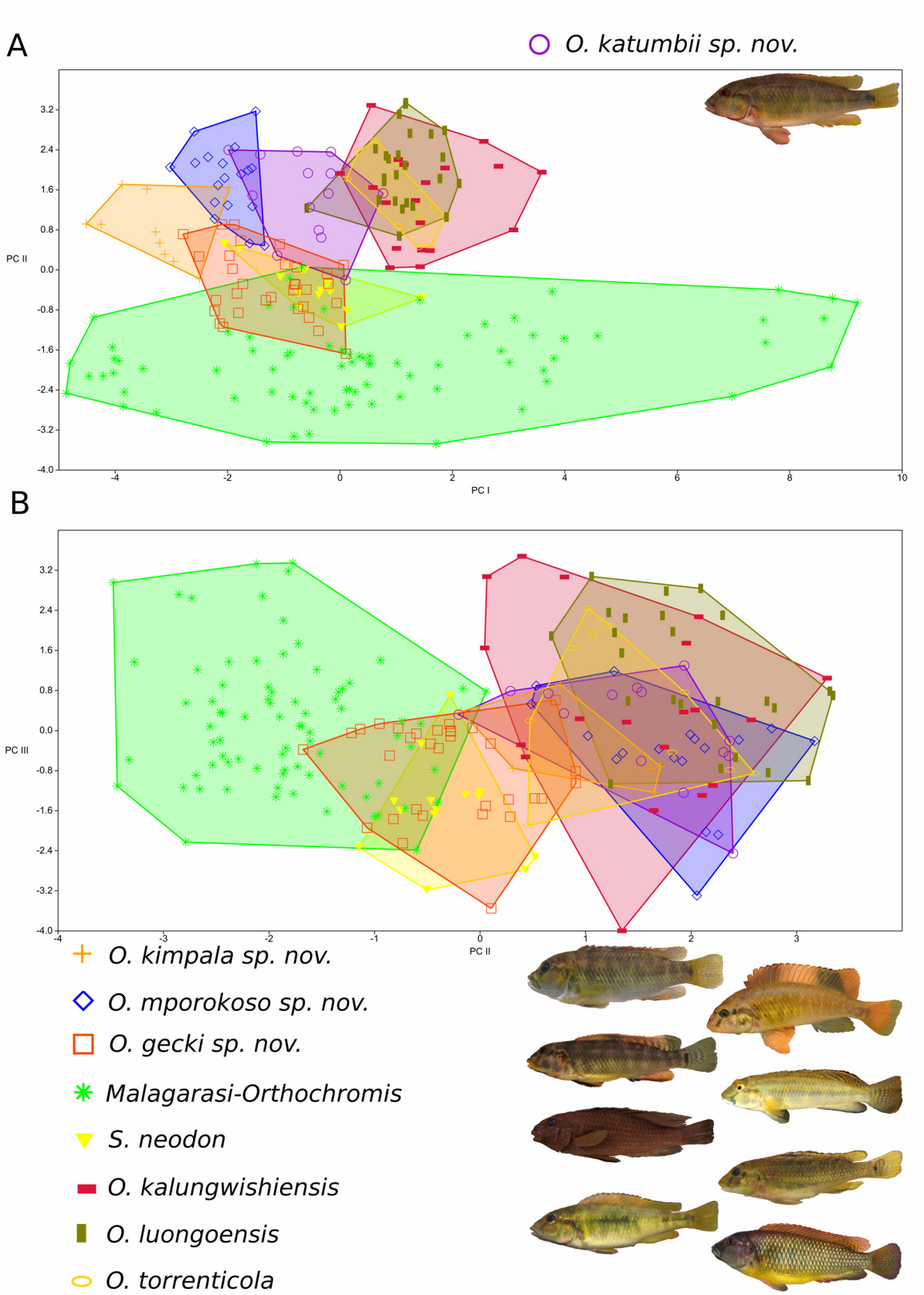

FIGURE S2: Species-specific PCA scatter plots focusing on *O. katumbii* **sp. nov.** based on 20 meristics; species score limits visualized as convex hulls. PC I vs PC II (A) and PC vs PC III (B) for a 225 examined specimens. PC I explain 30.76 %, PC II explains 14.68 % and PC III explains 9.89 % of the variance. Species depicted from top to bottom: *O. katumbii* **sp. nov.**, *O. kimpala* **sp. nov.**, *O. mporokoso* **sp. nov.**, *O. gecki* **sp. nov.**, *O. uvinzae, S. neodon, O. kalungwishiensis, O. luongoensis, O. torrenticola*.

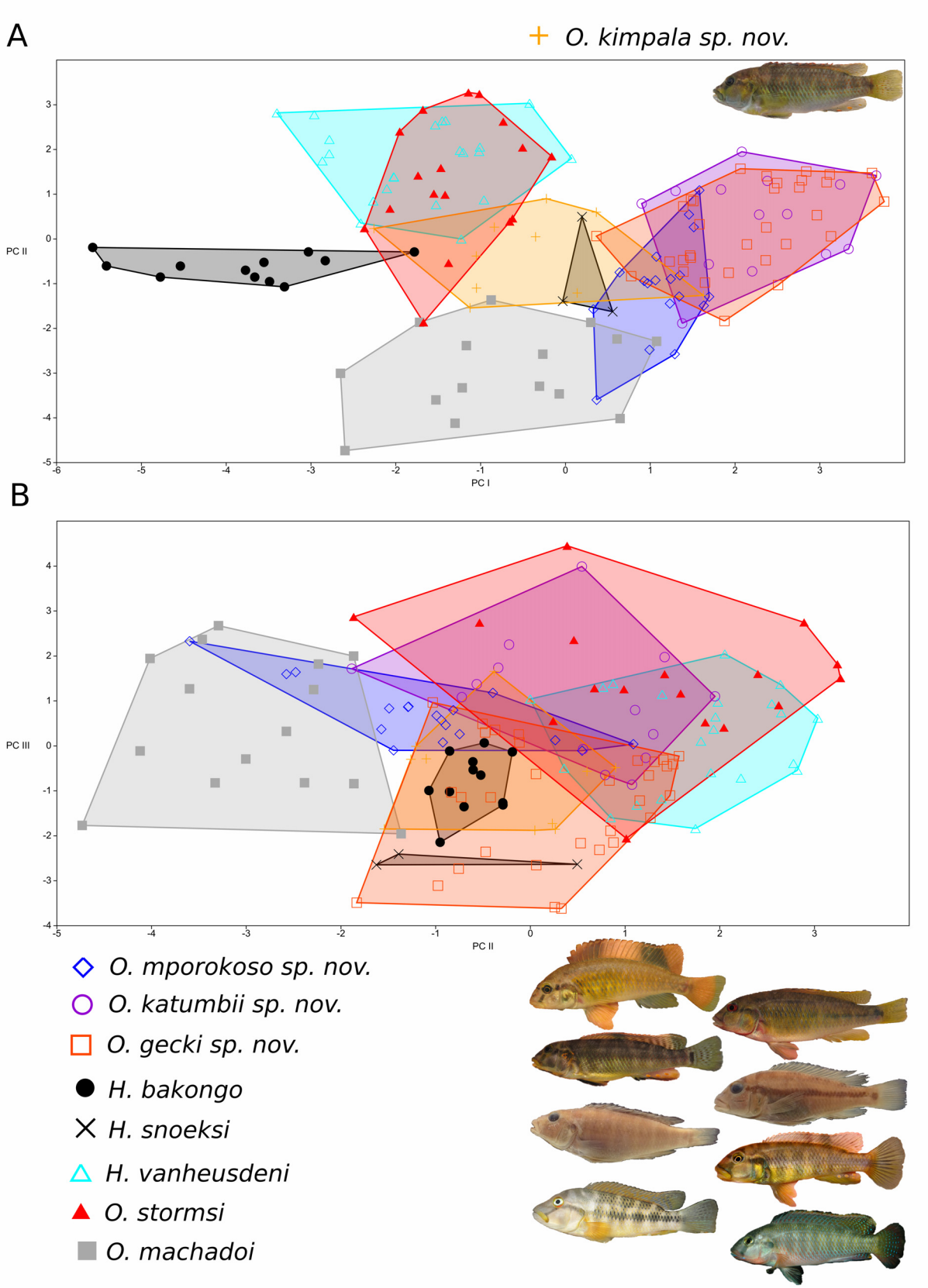

FIGURE S3: Species-specific PCA scatter plots focusing on *O. kimpala* **sp. nov.** based on 19 meristics; species score limits visualized as convex hulls. PC I vs PC II (A) and PC vs PC III (B) for a 143 examined specimens. PC I explain 23.09 %, PC II explains 14.63 % and PC III explains 12.34 % of the variance. Species depicted from top to bottom: *O. kimpala* **sp. nov.**, *O. mporokoso* **sp. nov.**, *O. katumbii* **sp. nov.**, *O. gecki* **sp. nov.**, *H. bakongo, H. snoeksi, H. vanheusdeni, O. stormsi, O. machadoi*.

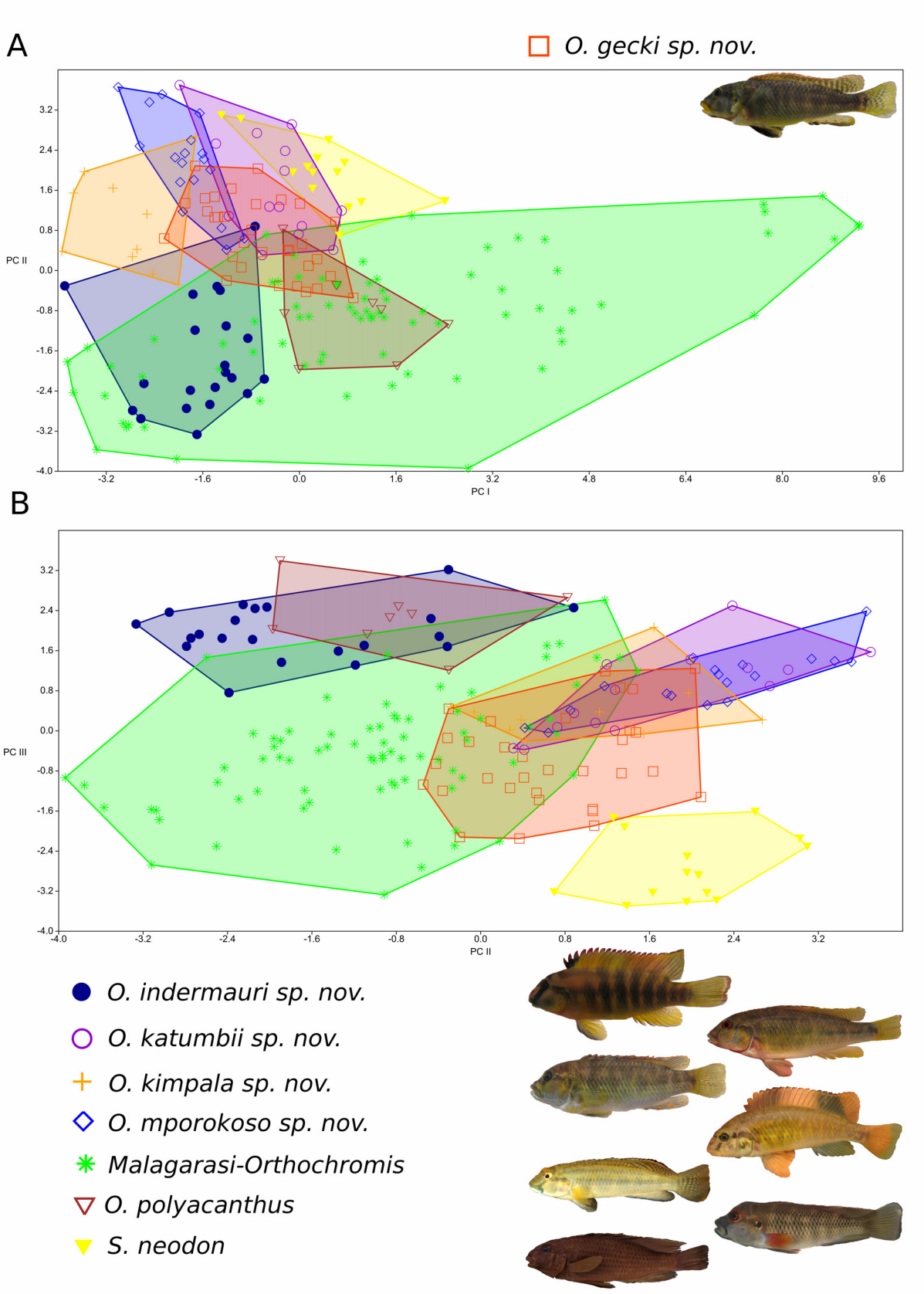

FIGURE S4: Species-specific PCA scatter plots focusing on *O. gecki* **sp. nov.** based on 19 meristics; species score limits visualized as convex hulls. PC I vs PC II (A) and PC vs PC III (B) for a 196 examined specimens. PC I explain 33.42 %, PC II explains 14.91 % and PC III explains 11.95 % of the variance. Species depicted from top to bottom: *O. gecki* **sp. nov.**, *O. indermauri* **sp. nov.**, *O. katumbii* **sp. nov.**, *O. kimpala* **sp. nov.**, *O. mporokoso* **sp. nov.**. *O. uvinzae, O. cf. polyacanthus, S. neodon.*

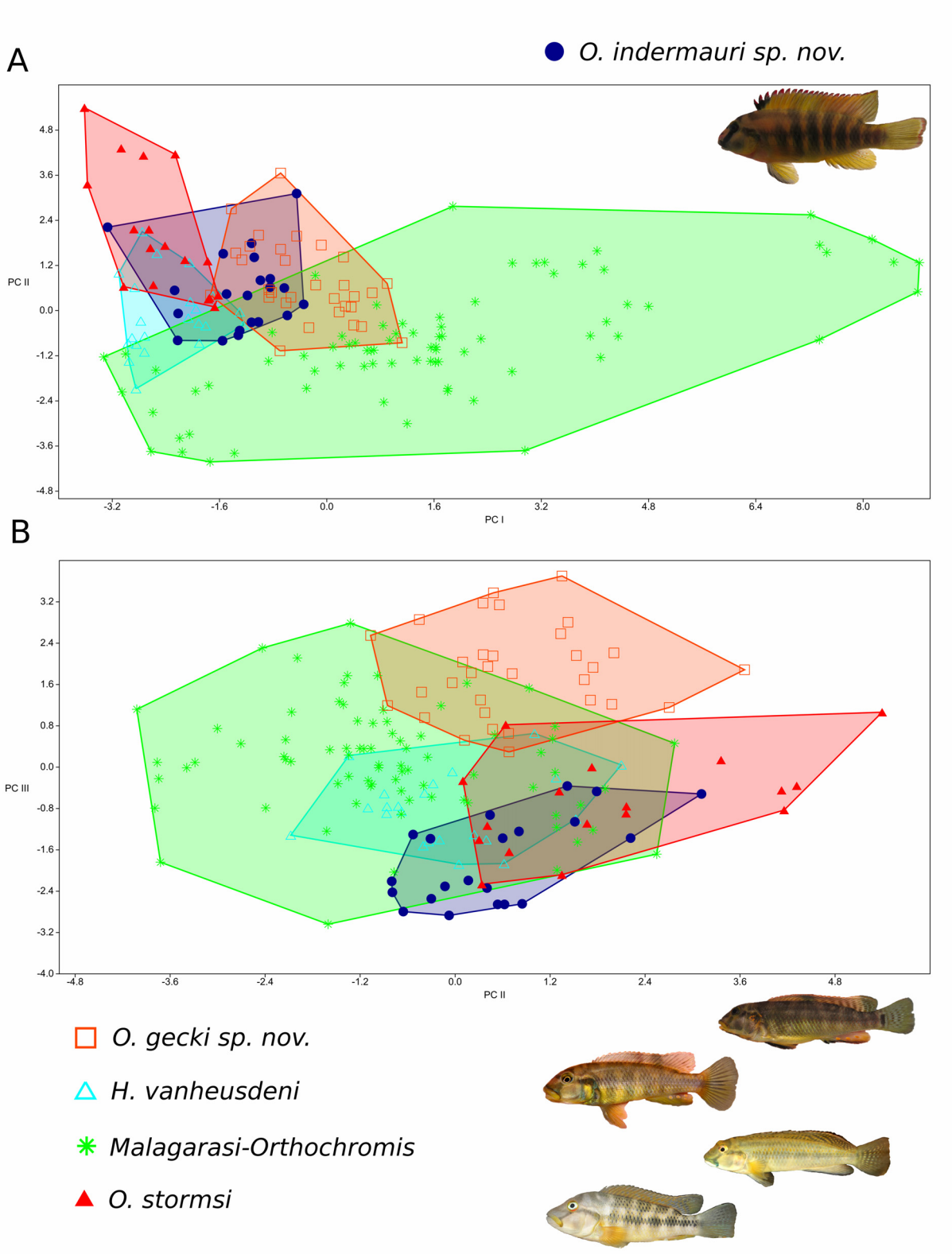

FIGURE S5: Species-specific PCA scatter plots focusing on *O. indermauri* **sp. nov.** based on 19 meristics; species score limits visualized as convex hulls. PC I vs PC II (A) and PC vs PC III (B) for a 171 examined specimens. PC I explain 36.45 %, PC II explains 13.84 % and PC III explains 10.65 % of the variance. Species depicted from top to bottom: *O. gecki* **sp. nov.** *H. vanheusdeni*, *O. uvinzae, O. stormsi.*

Zootaxa 4718 (2): 191–229
https://www.mapress.com/j/zt/

Article

ISSN 1175-5326 (print edition)
ZOOTAXA
ISSN 1175-5334 (online edition)

https://doi.org/10.11646/zootaxa.4718.2.3
http://zoobank.org/urn:lsid:zoobank.org:pub:64CDF034-F43D-4A89-9A40-877A05EE5260

Palaeoplex gen. nov. and *Lufubuchromis* gen. non, two new monotypic cichlid genera (Teleostei: Cichlidae) from northern Zambia

FREDERIC D.B. SCHEDEL[1], VIVIANE M.S. KUPRIYANOV[1],
CYPRIAN KATONGO[2] & ULRICH K. SCHLIEWEN[1,3]
[1]SNSB-Bavarian State Collection Zoology, Department of Ichthyology, Münchhausenstr. 21, 81247 München, Germany
E-mail: schedelfred@hotmail.de; schliewen@snsb.de; vivianetchka@gmail.com
[2]University of Zambia, Department of Biological Sciences, P.O. Box 32379, Lusaka, Zambia. E-mail: ckatongo@unza.zm
[3]Corresponding author. E-mail: schliewen@snsb.de

Abstract

Two monotypic haplochromine cichlid genera (Teleostei: Cichlidae) of the *Pseudocrenilabrus* group are described from northern Zambia. One new genus is *Palaeoplex* gen. nov., with *Pa. palimpsest* sp. nov. as the type species, from the Luongo and Kalungwishi Rivers (Upper Congo drainage, Luapula subdrainage). It is diagnosed by a unique combination of morphological characters: (1) a fully developed infraorbital series without a distinct gap between the lachrymal and second infraorbital bone, (2) fused hypuralia 1+2 and hypuralia 3+4, (3) molariform teeth on the sagittal series of the lower pharyngeal jaw, and (4) a large maximum size. The second new genus, *Lufubuchromis* **gen. nov.,** with *L. relictus* **sp. nov.** as the type species**,** is restricted to the upper Lufubu River catchment (Upper Congo drainage, Lake Tanganyika subdrainage). It is diagnosed by a unique combination of morphological characters: (1) a fully developed infraorbital series without a distinct gap between the lachrymal and second infraorbital bone, (2) fused hypuralia 1+2 (rarely with a visible suture) and fused hypuralia 3+4, (3) a unique male coloration pattern, i.e. deep crimson red colored areas on the anterior ventral flank parts, chest and belly and on the lower head; remaining parts of flanks and caudal peduncle bluish), and (4) a *Pseudocrenilabrus* blotch present in both sexes. Both new genera are compared with all remaining taxa of the *Pseudocrenilabrus* group and with all representatives of all other major haplotilapiine lineages.

Key words: *Pseudocrenilabrus*, Kalungwishi River, Luongo River, Lufubu River

Introduction

Fowler (1934) described a new genus and species as *Pseudocrenilabrus natalensis* Fowler 1934 based on material he had obtained from H. W. Bell-Marely which was collected in 1932 in Durban, Natal (South Africa). He placed his new genus in a new subfamily Pseudocrenilabrinae together with the marine dottybacks (today Pseudochromidae). Later, Trewavas (1973) realized that *Ps. natalensis* is a haplochromine cichlid identical with *Chromis philander* Weber, 1897 and consequently synonymized *Ps. natalensis* with *C. philander*. Nevertheless, acknowledging their generic distinctiveness, Trewavas (1973) placed this species together with *Chromis multicolor* Schöller 1903 in the genus *Pseudocrenilabrus.* Since Wickler (1963) had previously established a new genus for *C. multicolor*, namely *Hemihaplochromis* Wickler, 1963, *Hemihaplochromis* had to be synonymized with *Pseudocrenilabrus* based on the principle of priority (Trewavas 1973).

Although Wickler (1963) diagnosed *Hemihaplochromis* (now *Pseudocrenilabrus*) mainly based on differences in the spawning behaviour of *H. multicolor* (now *Ps. multicolor*) as compared with other haplochromine cichlids, he also identified one chromatic character on the anal fin, which appears to be correlated with the behavioural differences: male *Pseudocrenilabrus* have a single, non-ocellated and distinctly coloured orange or red blotch at the tip of the anal fin (referred here as *Pseudocrenilabrus* blotch), but they lack well defined ocellated egg-dummies on the anal fin. During spawning the male presents his anal fin to the female in a folded state, which makes the *Pseudocrenilabrus* blotch appear to be a three-dimensional egg-like structure at the tip of the anal fin. The genus *Pseudocrenilabrus* is further distinguished by a reduction of the infraorbital bone series and by having a rounded caudal fin (Wickler 1963; Trewavas 1973; Greenwood 1989).

Accepted by J. Armbruster: 14 Nov. 2019; published: 7 Jan. 2020

Pseudocrenilabrus species are widely distributed in southern, central, eastern and northern Africa. They are found from coastal Natal (South Africa) to the west in Namibia and Eastern Congo Basin, in the north up to the Nile delta region and they are widespread in eastern Africa (Greenwood 1989, Seegers 1990, Katongo *et al*. 2005, Katongo *et al*. 2017). Currently the genus has four valid species: *Pseudocrenilabrus pyrrhocaudalis* Katongo, Seehausen & Snoeks 2017, recently described from Lake Mweru; *Ps. nicholsi* (Pellegrin 1928) from the Lualaba River in the Upper Congo drainage; *Ps. multicolor* from the Nile drainage (Egypt); and *Ps. philander*, described from the Umhlasine River (South Africa), but widely distributed in South-Central Africa. For the two latter taxa, subspecies have been described: the nominate subspecies *Ps. multicolor multicolor* is restricted to the Lower Nile drainage and *Ps. multicolor victoriae* Seegers, 1990 to the upper Nile drainage including Lake Victoria, Lake Albert and the Albert Nile but excluding Lake Turkana (Seegers 2000). For *Pseudocrenilabrus philander,* three subspecies have been suggested, i.e., *Ps. philander philander* from South-Eastern Africa (Skelton 2001), *Ps. philander luebberti* (Hilgendorf, 1902) from the Otavi region in Namibia, and *Ps. philander dispersus* (Trewavas, 1936) from Lake Otjikoto, a sinkhole lake in northern Namibia. *Pseudocrenilabrus philander* appears to have a complex biogeographic history and recent phylogenetic studies revealed several distinct mitochondrial lineages within this species (Katongo *et al*. 2005, Koblmüller *et al*. 2012, Egger *et al*. 2014), some possibly representing distinct species.

Within African cichlids, *Pseudocrenilabrus* is placed among the megadiverse tribe Haplochromini (Salzburger *et al*. 2002, Koblmüller *et al*. 2008). Interestingly, several other haplochromine species currently placed in different genera are closely related to *Pseudocrenilabrus* as inferred from mitochondrial and nuclear DNA analyses (Egger *et al*. 2014, Koblmüller *et al*. 2008, Koblmüller *et al*. 2012, Weiss *et al*. 2015, Matschiner *et al*. 2016; Meier *et al*. 2017, Schedel *et al*. 2019): *Haplochromis moeruensis* (Boulenger 1899a) from Lake Mweru is part of the *Pseudocrenilabrus* Lake Mweru radiation that contains many undescribed species (Katongo *et al*. 2006; Wagner *et al*. 2012); *Orthochromis machadoi* (Poll 1967), a rheophilic species described from the Cunene River (Namibia) is nested within *Ps. philander;* and the four Northern Zambian *Orthochromis* species (sensu Weiss *et al*. 2015), i.e., *O. kalungwishiensis* (Greenwood & Kullander 1994), *O. luongoensis* (Greenwood & Kullander, 1994), *O. katumbii* Schedel, Vreven, Katemo Manda, Abwe, Chocha Manda, Schliewen 2018 and *O. mporokoso* Schedel, Vreven, Katemo Manda, Abwe, Chocha Manda, Schliewen 2018 represent the sister lineage to the *Pseudocrenilabrus* group (sensu Weiss *et al*. 2015) based on nuclear data; or they are nested within the *Pseudocrenilabrus* group based on mitochondrial data (Schedel *et al*. 2019).

The term *Pseudocrenilabrus* group was first introduced by Weiss *et al*. (2015) for a clade supported by molecular characters encompassing members of the genus *Pseudocrenilabrus* and, at that time, one undescribed haplochromine species referred to as New Kalungwishi Cichlid (see below). A few years later, Schedel *et al*. (2019) widened the concept of the *Pseudocrenilabrus* group by including all Northern Zambia *Orthochromis* and one additional undescribed species from the Lufubu River referred to as New Lufubu Cichlid (see below). Neither study, however, provided morphological characters to define this clade, which is well supported by mitochondrial DNA analyses, but nevertheless the term has become increasingly accepted in the literature (e.g. Altner *et al*. 2017, Penk *et al*. 2019). Table 1 provides a cursory overview of previous studies using the term and of the assignment of taxa placed within the *Pseudocrenilabrus* group. It further provides an overview of the presence or absence of characters shared with *Pseudocrenilabrus s*ensu stricto.

In this study, two new *Pseudocrenilabrus*-like species are described. The first new species lives in the Luongo and Kalungwishi rivers, two tributaries of the Luapula River, Upper Congo drainage, in northern Zambia (see Fig. 1). It has been referred to as the New Luongo Cichlid or New Kalungwishi Cichlid and is a member of the *Pseudocrenilabrus* group (sensu Weiss *et al*. 2015). Based on molecular data it is either related to *O. mporokoso* (based on mitochondrial data; Schedel *et al*. 2019) or it represents the sister group of the genus *Pseudocrenilabrus* (based on AFLP data; Weiss *et al*. 2015, Meier *et al*. 2019). To our knowledge this species was depicted first in Balon *et al*. (1983) as *Ps. philander* (see page 237, Fig. 10d in Balon *et al*. 1983). Interestingly, this species attains a much larger maximum size (143.4 mm SL) than any other member of the *Pseudocrenilabrus* group. The second new species has long been known from the upper Lufubu River catchment, Lake Tanganyika drainage of the Upper Congo in northern Zambia. It had been referred to as "Haplochromine sp. nov." (Koblmüller *et al*. 2008), "*Pseudocrenilabrus* sp. 'Lufubu A'" (Koblmüller *et al*. 2012) or as "New Lufubu Cichlid" (Schedel *et al*. 2019). The species was discovered by the late L. de Vos, who had presented a photo at the International Conference of the PARADI Association and the Fisheries Society of Africa (1998) in his talk on the ichthyofauna of the Lake Tanganyika drainage (de Vos 1998). It belongs to the *Pseudocrenilabrus* group sensu Weiss *et al.* (2015) and appears to represent the sister group

TABLE 1. Overview of taxa grouped with the genetically defined *Pseudocrenilabrus* group (sensu Weiss *et al*. 2015 and Schedel *et al*. 2019) in comparison with morphological characters and features associated with the genus *Pseudocrenilabrus* (sensu Greenwood 1989).

	***Pseudocrenilabrus* spp.**	***Haplochromis moeruensis***	***Orthochromis machadoi***
Main reference grouping a taxon with *Pseudocrenilabrus* and/or with the *Pseudocrenilabrus* group (based on molecular data)	Weiss *et al*. 2015, Schedel *et al*. 2019	Katongo *et al*. 2006, Wagner *et al*. 2012, Meier *et al*. 2019	Koblmüller *et al*. 2008, Meier *et al*. 2019
Morphological characters and behavioural features associated with the genus *Pseudocrenilabrus* (Greewood 1989):			
A single, non-ocellate and distinctly coloured spot or blotch at the tip of the anal fin (*Pseudocrenilabrus* blotch)	Present in the males in several species of *Pseudocrenilabrus* (including the type species of the genus) but appears to absent or diminished in some populations of different species.	present in males (see Katongo *et al*. 2006)	present in males
Reductional trend in the canal bones of the infraorbital series	present	present	present
Distinctly rounded caudal fin	yes (with the exception of *Ps. pyrrhocaudalis* which has a subtruncate caudal fin).	yes	yes
The specific courtship behaviour of *Pseudocrenilabrus* males which involves the folding of the anal fin in a way that the *Pseudocrenilabrus* blotch is accentuated, instead of spreading the anal fin as is common in other haplochromine taxa	documented for *Ps. mulitcolor* (Wickler 1963)	unknown	unknown

.....continued on the next page

TABLE 1. (Continued)

	Palaeoplex palimpsest	***Lufubuchromis relictus***	**Northern Zambian *Orthochromis***
Main reference grouping a taxon with *Pseudocrenilabrus* and/or with the *Pseudocrenilabrus* group (based on molecular data)	Weiss *et al*. 2015, Schedel *et al*. 2019, Meier *et al*. 2019	Koblmüller *et al*. 2008, Koblmüller *et al*. 2012, Schedel *et al*. 2019, Meier *et al*. 2019	Schedel *et al*. 2019 (not included in Weiss *et al*. 2015); Comment: cyto-nuclear discordance is documented for this clade.
Morphological characters and behavioural features associated with the genus *Pseudocrenilabrus* (Greewood 1989):			
A single, non-ocellate and distinctly coloured spot or blotch at the tip of the anal fin (*Pseudocrenilabrus* blotch)	present in males	present in both sexes	absent
Reductional trend in the canal bones of the infraorbital series	absent	absent	absent (however some examined specimens of *O. klaungwishiensis* appear to show a reductional trend)
Distinctly rounded caudal fin	no (Caudal fin rounded to subtruncate)	no (Caudal fin rounded to subtruncate)	no (Caudal fin subtruncate)
The specific courtship behaviour of *Pseudocrenilabrus* males which involves the folding of the anal fin in a way that the *Pseudocrenilabrus* blotch is accentuated, instead of spreading the anal fin as is common in other haplochromine taxa	unknown	not well documented, but see Indermaur 2014	unknown

of *O. kalungwishiensis,* although this relationship was only weakly supported based on mitochondrial data (Schedel *et al*. 2019) while nuclear data (RAD) revealed this species to represent the sister group of a clade encompassing *Pseudocrenilabrus* and as well as the New Kalungwishi Cichlid (Meier *et al*. 2019).

Both new species possess a *Pseudocrenilabrus* blotch at the distal end of the anal fin in adult males (in the new species of the Lufubu drainage it is also present in females) but they differ substantially from *Pseudocrenilabrus* by several morphological characters. Further, both represent early splitting and distant lineages within the molecularly defined *Pseudocrenilabrus* group (Weiss *et al*. 2015, Meier *et al*. 2019, unpublished own data). Based on new collections from different localities and extensive comparisons with described and undescribed haplochromine cichlid species of the *Pseudocrenilabrus* group, we describe both new species as members of two new monotypic genera, which according to molecular genetic analysis do not form a monophylum.

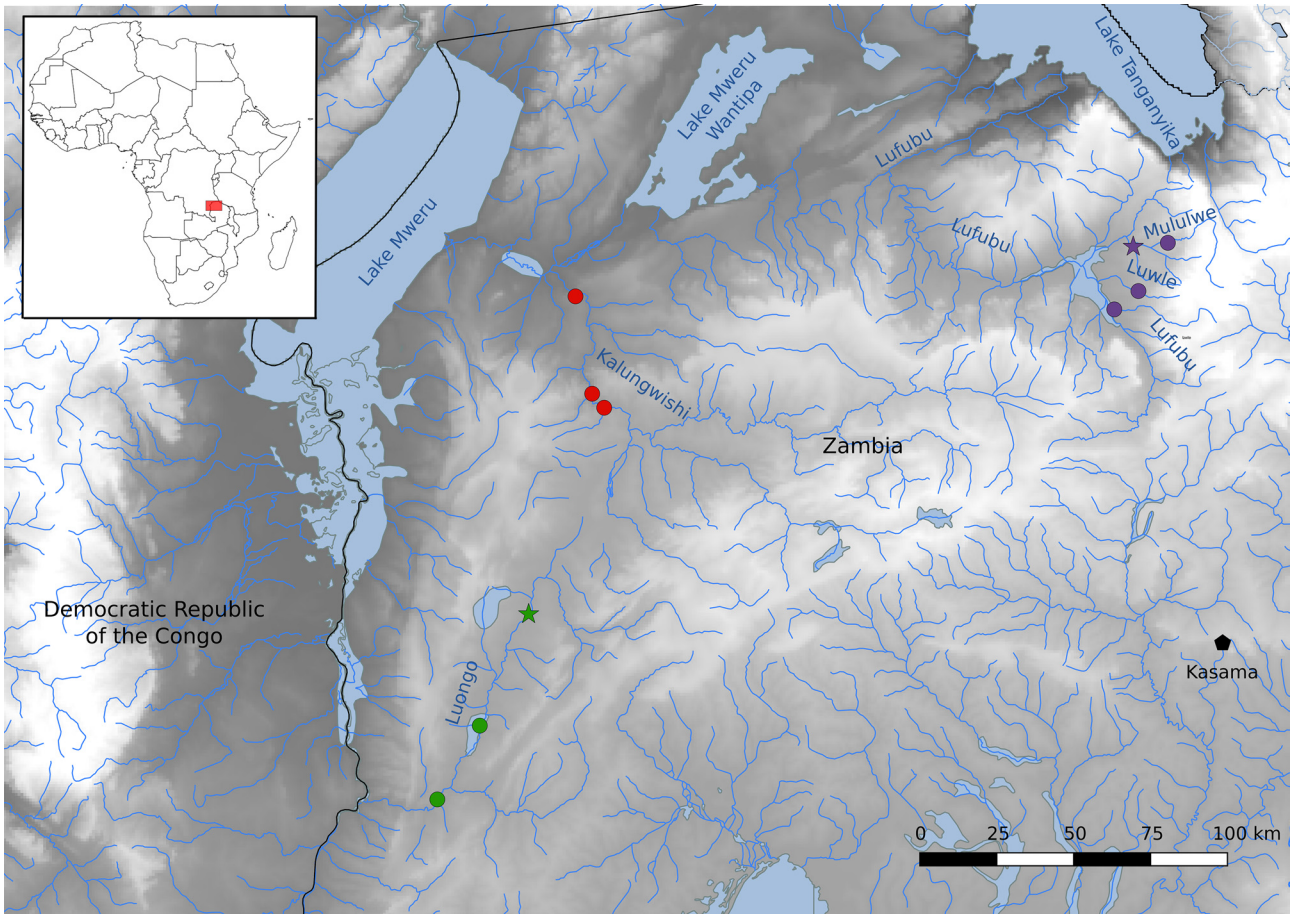

FIGURE 1. Map of northern Zambia, with colour indications of the type localities of *Lufubuchromis relictus* **sp. nov.** (purple) and *Palaeoplex palimpsest* **sp. nov**. (dark green) and sample locations of additional material of *Palaeoplex palimpsest* "Kalungwishi" (red). Star = type locality, circle = either paratype locality or sample locality of comparative specimens. Kasama (a major city) is depicted in black. Map is based on shape files obtained from DIVA-GIS (http://www.diva-gis.org/Data).

Specimens and methods

Specimens investigated. In total, 203 specimens of the *Pseudocrenilabrus* group (sensu Weiss *et al*. 2015 and Schedel *et al* 2019) were examined. Investigated specimens are deposited in NHM, Natural History Museum, London; CU, Cornell University Museum of Vertebrates, New York; MRAC, Musée Royal de l'Afrique Centrale, Tervuren; NRM, Naturhistorika Riksmuseet. Stockholm; SAIAB, South African Institute for Aquatic Biodiversity, Grahamstown; and ZSM, Zoologische Staatssammlung, Munich. All specimens examined for comparisons are listed in the Comparative material section below. Based on genetic data, the rheophilic species *Orthochromis kalungwishiensis*, *O. luongoensis*, *O. katumbii,* and *O. mporokoso* might be considered members of the *Pseudocrenilabrus* group, but they do not exhibit the typical *Pseudocrenilabrus* blotch and hence are easily distinguished from the remaining

members of the *Pseudocrenilabrus* group. Therefore, they are referred to in species diagnoses but are not included in principal component analysis (PCA). On the other hand, *O. machadoi* possesses the *Pseudocrenilabrus* blotch and is therefore included in comparative analyses. Based on genetic data, *Haplochromis moeruensis* is part of the "*Pseudocrenilabrus* Lake Mweru radiation" (Katongo *et al*. 2006; Wagner *et al*. 2012, Meier et al. 2019) and, according to a specimen figure labelled as *H. moeruensis* (Katongo *et al*. 2006; Fig. 2) this species carries a *Pseudocrenilabrus* blotch, too. Therefore the (faded) type material of *H. moeruensis* was included in our morphological comparisons.

Comparative material

***Haplochromis moeruensis* (Boulenger 1899a):** MRAC 216–222, 4, syntypes, 49.4–75.7 mm SL; Democratic Republic of Congo, Pweto, Lake Mweru (-8.46/28.7). ***Orthochromis indermauri* Schedel, Vreven, Katemo Manda, Abwe, Chocha Manda, Schliewen 2018:** ZSM 46853, 1, holotype, 54.0 mm SL; Zambia, Lufubu River, below last series of rapids near Chomba village, ~ 25.5 km from confluence with Lake Tanganyika and 20 km (air distance) south of Sumbu (-8.687010/30.556273)—ZSM 46855, paratypes, 13, 35.8–68.9 mm SL; Zambia, Lufubu River, Lower Lufubu at Chomba Village, ~30 km from confluence with Lake Tanganyika, Northern Province (-8.686376/30.563983).—ZSM 46854, 1, paratype, 61.2 mm SL; Zambia, Lufubu River, Lower Lufubu at Chomba Village, ~30 km from confluence with Lake Tanganyika, Northern Province (-8.686376/30.563983).—ZSM 43083, 4, paratypes, 45.6–59.4 mm SL; collected with holotype.—ZSM 43080, 2, paratype, 42.0–43.1 mm SL; collected with holotype.—ZSM 44283, 3, paratypes, 50.8–63.5 mm SL; Zambia, Lufubu River, Lower Lufubu at Chomba Village, ~30 km from confluence with Lake Tanganyika, Northern Province (-8.686376/30.563983).—MRAC 2018-006-P-0001-0002, 2, paratypes, 56.8–51.9 mm SL; Zambia, Lufubu River, Lower Lufubu at Chomba village, ~30 km from confluence with Lake Tanganyika, Northern Province (-8.686376/30.563983).—MRAC 2018-006-P-0003-0008, 6, paratypes, 43.3–64.1 mm SL; Zambia, Lufubu River, Lower Lufubu at Chomba village, ~30 km from confluence with Lake Tanganyika, Northern Province (-8.686376/30.563983). ***Orthochromis kalungwishiensis* (Greenwood & Kullander 1994):** MRAC 99-035-P-0031-0032, 2, 69.3–78.3 mm SL; Keso village, Pambashe River, local name Luena River, (possibly: -9.6000/29.4833).—MRAC 99-035-P-0033-0035, (2)3, 66.4-69.2 mm SL, Luena River (=Pambashe River), tributary of Kalungwishi River (possibly: -9.6000/29.4833).—ZSM 41427, 1, 79.2 mm SL; Zambia, Kalungwishi stream above Lumanmgwe Falls on road Mukunsa-Kawambwa (-9.5431/29.3878).—ZSM 41431, 6, 44.4–75.8 mm SL; Zambia, Kalungwishi stream above Lumanmgwe Falls on road Mukunsa-Kawambwa (-9.5431/29.3878).—ZSM 44369, (8)13, 48.5–70.7 mm SL; Zambia, Kalungwishi River, above Kundabwika and below Kabwelume Falls, near to road Mporokoso-Mununga (-9.217887/ 29.304202). ***Orthochromis katumbii* Schedel, Vreven, Katemo Manda, Abwe, Chocha Manda, Schliewen 2018:** MRAC 2015-009-P-0006, 1, holotype, 85.9 mm SL; Democratic Republic of the Congo, Kiswishi River, near confluence with Matete stream, Luapula basin (-11.486528/ 27.650306)—MRAC 2015-009-P-0001, 1, paratype, 53.2 mm SL; Democratic Republic of the Congo, Kiswishi River, Futuka farm, Luapula basin (-11.488028/27.645833).—ZSM 46844, 1, paratype, 81.8 mm SL; Democratic Republic of the Congo, Kiswishi River, Futuka farm, Luapula basin (-11.488028/ 27.645833).—MRAC 2015-009-P-0003, 1, paratype, 56.6 mm SL; Democratic Republic of the Congo, Kiswishi River, Futuka farm, Luapula basin (-11.488028/27.645833).—MRAC 2015-009-P-0007-0009, 3, paratypes, 58.7–85.2 mm SL; collected with holotype.—ZSM 41450, 6, paratype, 27.2–57.4 mm SL; Zambia, Luapula River below Mambilima Falls (-10.5689/ 28.6783).—ZSM 42322, 2, 71.3–88.9 mm SL; Zambia, Luapula River below Mambilima Falls; kept in aquarium (-10.5689/28.6783). ***Orthochromis luongoensis* (Greenwood & Kullander 1994):** CU 91747, 1, 69.9 mm SL; Zambia, Lufubu River Falls below bridge at Chipili on Mansa-Munuga road, (-10.7286/29.0936).—ZSM 41437, (5)6, 46.3–68.4 mm SL; Zambia, Luongo River at bridge on road Mwenda-Kashiba, affluent to Lake Mweru / Upper Congo basin (-10.4708/29.0261).—ZSM 44345, 6, 61.5–106.9 mm SL; Zambia, Kalungwishi River, immediately above Kabwelume Falls (below Lumangwe Falls), ~ 20 km downstream bridge on road Mporokoso-Kawambwa, Northern Province, (-9.527083/29.353102).—ZSM 44432, 7, 53.8–98.0 mm SL; Zambia, Luongo River, at bridge on road Kawambwa-Mansa about 40 km (driving distance) S of Kawambwa (-10.144359/ 29.167193).—ZSM 44467, (5)7, 42.6–59.0 mm SL; Zambia, Luongo River, below Mumbuluma Falls, ~ 40 km (air distance) NW of Luwingu Luapula Province (-10.106146/ 29.571487).—ZSM 44569, 1, 69.9 mm SL; Zambia, Kalungwishi River, above Kundabwika and below Kabwelume Falls, near to road Mporokoso-Mununga (-9.217887/ 29.304202). ***Orthochromis machadoi* (Poll 1967):** BMNH 1984.2.6.104–108, 5, 42.31–52.1 mm SL; Angola, Cunene River (-17.267/ 14.50).—BMNH 1984.2.6.142–145, 4, 50.3–65.7 mm SL; Angola, Cunene River (-14.916667/15.100000). ***Orthochromis mporokoso* Schedel, Vreven, Katemo Manda,**

Abwe, Chocha Manda, Schliewen 2018: ZSM 46840, 1, holotype, 59.04 mm SL; Zambia, Kasinsha stream north of Luwinga affluent to Lake Mweru (-9.4894/30.5769)—ZSM 41429, 9, paratypes, 34.0–74.48 mm SL, Zambia, Mutoloshi stream above Kapuma Falls at Mporokoso on road Mukunsa-Luwinga (-9.3889/30.0956).—ZSM 41443, 4, paratypes, 40.9–63.2 mm SL; collected with holotype.—MRAC 2018-006-P-0009-0011, 3, paratypes, 48.7–51.9 mm SL; Zambia, Mutoloshi stream above Kapuma Falls at Mporokoso on road Mukunsa-Luwinga (-9.3889/30.0956).—ZSM 46841, 1, 54.28 mm SL; Zambia, Mutoloshi stream above Kapuma Falls at Mporokoso on road Mukunsa-Luwinga (-9.3889/30.0956). ***Pseudocrenilabrus multicolor*** **Schöller, 1903:** ZSM 40011, 1, 45.99 mm SL; Zambia, Drainage Nile; Lake Mariout, at road bridge Zawyet-Abd-el-Qadir to Alexandria, SW of Alexandria (31.112803°/ 29.885594°).—ZSM 41574, 2, 41.6–49.8 mm SL; Egypt, Drainage Nile; aquarium raised offspring, male parents from Lake Mariout (31.112803°/ 29.885594°)., female parent from Lake Birkat-Abu-Jumasm (30.559664/32.269147). ***Pseudocrenilabrus multicolor victoriae*** **Seegers, 1990*:*** ZSM 41695, 1, 35.1 mm SL; Uganda, Drainage Nile; Katonga River at Kabagole village, affluent to Lake George, Kiruhura District, Western Region (0.198250/ 30.892750).—ZSM 43928, 1, 44.5 mm SL; Tanzania, Drainage Zambezi; Lufiro River at confluence at northern shore with Lake Malawi, 3 km W of Matema & 7 km E of Kyela villages, Shire River subbasin, Mbeya Province (-9.509997/33.998843).—BMNH 1985.7.16.81–82, 2, 39.7–52.6 mm SL; Uganda, in a stream N. of Lake Victoria, no GPS data available. ***Pseudocrenilabrus nicholsi*** **Pellegrin 1928:** MRAC-P-70060-061, 2, paratypes, 44.1–49.4 mm SL; Democratic Republic of Congo, Kabalo, fleuve Lualaba, no GPS data available.—MRAC-P-70053-057, 5, paratypes, 24.8–45.4 mm SL; Democratic Republic of Congo, Kabalo, fl. Lualaba, chenal, no GPS data available.—MRAC-P-70058, 1, paratype, 21.3 mm SL; Democratic Republic of Congo, Kabalo, fl. Lualaba, no GPS data available.—ZSM 47140, 46.2–46.5 mm SL (only used for comparisons of infraorbital bones); Democratic Republic of Congo, Lake Kisale at Kipamba village, approx. 70km SW of Mulongo and 150km NE of Luena, Katanga Province (-8.205118/26.433161). ***Pseudocrenilabrus philander*** **(Weber 1897)**: ZSM 42326, 1, 73.3 mm SL; South Africa, Drainage Orange; Aquarium stock originating from Spitz Kop Dam (-28.128517/ 24.496972).—ZSM 40944, 3, 61.9–69 mm SL; South Africa, Drainage Orange; Spitz Kop Dam, Orange River drainage (-28.128517/ 24.496972).—ZSM 40918, 1, 59.9 mm SL; South Africa, Drainage Orange; Spitz Kop Dam, Orange River drainage (-28.128517/ 24.496972).—BMNH 1935.3.21.1–2, 2, paralectotypes, 28.4–36.1 mm SL; South Africa, River Umhlati, Natal, no GPS data available.—BMNH 1904.5.17.19–24, 5, 53.8–85.9 mm SL; South Africa, Near Durban, no GPS data available. ***Pseudocrenilabrus philander dispersus*** **Trewavas 1936:** BMNH 1905.10.18.31–33, 3, paralectotypes, 64.8–69.1; South Africa, Pretoria, no GPS data available. ***Pseudocrenilabrus pyrrhocaudalis*** **Katongo, Seehausen, Snoeks 2017:** MRAC-A4-025-P-0105-0108, 3, 47.3– 49.1 mm SL; Zambia, Mwatishi, Lake Mweru, no GPS data available.—MRAC-A4-025-P-0103-0104, 2, paratypes, 52.0–54.2 mm SL; Zambia, Mwatishi, Lake Mweru, no GPS data available.—MRAC-A4-025-P-0137-0138, 2, 45.7–48.9 mm SL; Zambia, Mwatishi, Lake Mweru.—MRAC-A7-034-P-0238-0247, 10, 55.7–72.6; Zambia, Mukwakwa inshore, Lake Mweru, no GPS data available.

Pseudocrenilabrus populations of yet undefined taxonomic status and/or undescribed species: ***Pseudocrenilabrus*** **sp. "Lufira":** ZSM 45846, 3, 33.3–45.0 mm SL; Democratic Republic of Congo, Drainage Congo, Lufira River, within rapids above Kiubo Falls at Kiubo Lodge, tributary to Upemba Lakes subbasin, approx. 230 km N of Lubumbashi, Katanga Province (-9.5175/27.0393). ***Pseudocrenilabrus*** **sp. "Lunzua":** ZSM 44309, 3, 33.3–41.9 mm SL; Zambia, Drainage Congo upper Lunzua [above Lunzua fall] in "Gt" village at bridge, 8 km on road to Lualika after Mpulungu intersection, direct affluent of Lake Tanganyika, Northern Province (-8.955842/31.174187). ***Pseudocrenilabrus*** **sp. "Botswana":** ZSM 44171, 10, 41.0–58.1 mm SL; Botswana, Drainage Okavango; Boteti river, "8 km en aval de Makalamabedi, rive D" [8 km E of Makalamabedi], Central District (-20.300002/23.983333). ***Pseudocrenilabrus*** **sp. "Kalungwishi":** ZSM 44424, 4, 33.5–56.8 mm SL; Zambia, Drainage Congo; Kalungwishi River, at bridge on road Mporokoso—Kawambwa, near Chimpempe village, Northern Province (-9.550173/29.448585).—ZSM 44350, 2, 44.6–69.0 mm SL; Zambia, Drainage Congo; Kalungwishi River, immediately above Kabwelume Falls [bellow Lumangwe Falls], ~ 20 km downstream bridge on road Mporokoso—Kawambwa, Northern Province (-9.525757/29.352505).—ZSM 044326, 1, 57.0 mm SL; Zambia, Drainage Congo; Kalungwishi River, immediately above Lumangwe falls, Mporokoso—Kawambwa, Northern Province (-9.543595/29.388307).—ZSM 44388, 5, 37.5–54.3 mm SL; Zambia, Drainage Congo; Chimbofuma stream in Kalabwe village, trib to Kalungwishi, 50 km W of Mporokoso on road to Kawambwa, Northern Province (-9.471495/29.668661).—NRM-012333, 6, 37.6–68.9 mm SL; Zambia, Congo River; Locality: Congo River drainage: Kalungwishi River, Kundabwika Falls just above cataracts; Northern Province (-9.216666/29.3).—CU-91181, 3, 38.7– 45.2 mm SL; Zambia, Luapula, Drainage

Kalungwishi River; above Lumangwe Falls on Kalungwishi River (-9.5426/29.3875). ***Pseudocrenilabrus* sp. "Luongo":** CU-91173, 1, 49.9 mm SL; Zambia, Luapula, Drainage Luongo River, Luongo River below Musonda Falls (-10.7043/28.8009).—CU-91175, 6, 26.6–42.0 mm SL; Zambia Luapula, Drainage Luongo River; Luongo River at bridge on Kashiba-Mwenda road (-10.4701/29.0245).—ZSM 41496, 1, 42 mm SL; Zambia, Drainage Congo; Luongo stream at bridge on road Mwenda—Kashiba, affluent to Lake Mweru/Upper Congo basin, Luapala Province (-10.470725/29.026200). ***Pseudocrenilabrus* sp. "Upper Kalungwishi":** ZSM 44541, 18, 25.6–47.9 mm SL; Zambia, Drainage Congo; Upper Kalungwishi River, about 46 km [air distance] N of Luwingu, on road after Shimilungu village [8 km distance], Luapula Province (-9.813650/29.880345). ***Pseudocrenilabrus* sp. "Mukuleshi":** ZSM 45181, 3, 42.8–64.6 mm SL; Democratic Republic of Congo, Drainage Congo; Mukuleshi River below Mukwiza Falls, about 12 km from Malemba Village and approx. 100 km WNW of Kolwezi, tributary of Lualaba River, Katanga Province (-10.3404/24.5974). ***Pseudocrenilabrus* sp. "Lufubu B?":** ZSM 44319 (4, 16.5–23.7 mm SL) Zambia, Drainage Congo; Upper Mululwe River [above Mwanyonga falls], trib. to Lufubu River/Lake Tanganyika, 25 km S of Mpulungu, Northern Province (-9.008968/31.130549).

Morphological data collection and principal component analysis

A total of 28 meristic characters (character definitions according to Schedel & Schliewen 2017) was included of which 18 were recorded using a stereomicroscope (Leica MZ6) and ten were recorded from digital X-rays generated by a Faxitron Ultrafocus LLC X-ray unit. Following Schedel & Schliewen 2017, four additional postcranial skeleton character states were scored: (1) position of the pterygiophore supporting the last dorsal-fin; (2) position of the pterygiophore supporting the last anal-fin spine; (3) state of hypurals 1 + 2; and (4) state of hypurals 3 + 4. In total, 29 morphometric (body) measurements were taken point-to-point on the left side of specimens using a manual calliper as in Schedel & Schliewen (2017). Head measurements taken are given as percentages of head length (HL), all other measures as percentages of standard length (SL). Finally, three lower pharyngeal jaw measurements were taken from digital microscope pictures, i.e. lower pharyngeal-jaw length, lower pharyngeal-jaw width and width of dentigerous area of lower pharyngeal jaw; they are given as percentages of HL. Terminology of morphological characters (e.g. teeth) in the descriptions follows Barel *et al*.1977.

In order to identify diagnostic character states or a combination of those, and for the evaluation of non-diagnostic morphological differentiation of the new species, two principal component analyses (PCA) were performed with the statistical program PAST 3.21 (Hammer *et al.* 2001). The first PCA was based on a subset of 23 meristic characters (i.e. excluding nonvariant meristic counts and highly variable meristic and tooth counts) and on a correlation matrix. The second PCA was based on a subset of 20 log-transformed morphometric measurements, i.e. excluding measurements only available for a subset of specimens or potentially sexually dimorphic distance measurements, and it was based on the covariance matrix.

Results

In the first PCA (Fig. 2) based on 23 meristic characters and including all 203 investigated specimens, principal component I (PC I) explained 37.5 %, PC II explained 12.2 % and PC III 8.9 % of the total variance. Differences in the total number of gill rakers, scales on horizontal line and lower lateral line scales contributed the most to the factor loadings of PC I, while factor loadings of PC II mainly integrate the variance of different counts for the position of the pterygiophore supporting the last dorsal fin spine, position of pterygiophore supporting the last anal fin spine and dorsal fin counts (See Table 2). PC I and PC II scores of *Paleoplex palimpsest* **sp. nov.** partially overlap with those of *Ps. pyrrhocaudalis.* Separation of these two taxa and other taxa included in the study was mainly based on the high scores of PC I in combination with low PC II scores. Scores of PC I and PC II of *Lufubuchromis relictus* **sp. nov.** overlap with those of *O. machadoi*, *H. moeruensis and Ps. philander philander*. High scores of PC I separate *L. relictus* **sp. nov.** from *Ps. multicolor multicolor*, *Ps. multicolor victoriae* and *Ps. nicholsi* while lower PC I scores separate it from *Pa. palimpsest* **sp. nov.** and *Ps. pyrrhocaudalis,* whereas a combination of high PC I and PC II scores separate *L. relictus* **sp. nov.** from *Ps. philander* dispersus and *Pseudocrenilabrus* populations of yet undefined taxonomic status.

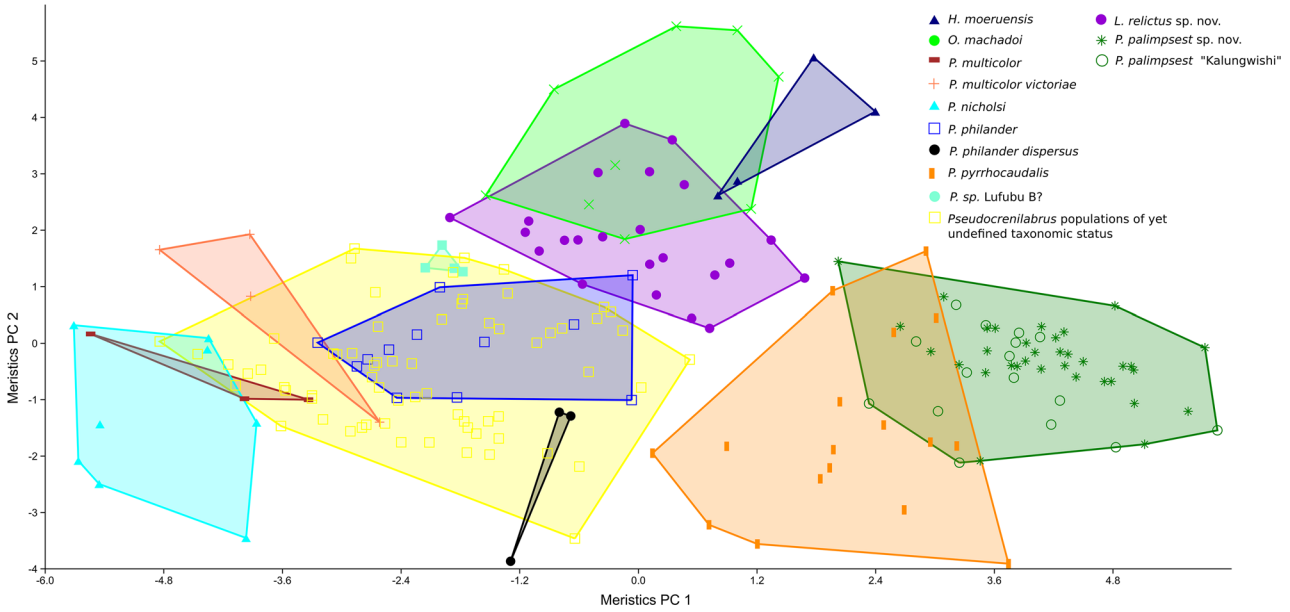

FIGURE 2. PCA scatter plots based on 23 meristic values; species score limits visualized as convex hulls. PC I vs PC II for all examined specimens (N = 203). PC I explain 37.53 % of the variance and PC II explains 12.17 %.

TABLE 2. Factor loadings of PCI-III for all examined specimens (N=203, see Fig. 2). Highest loadings for each principal component are indicated in boldface.

Meristic	PC 1	PC 2	PC 3
Series of scales on cheek	0.011122	-0.072094	0.20793
Scales on operculum	0.12611	0.177	0.15983
Scales (horizontal line)	**0.28461**	0.066054	-0.14018
Upper lateral line scale	0.19245	0.095669	-0.15758
Lower lateral line scales	**0.26716**	-0.011245	-0.035904
Scales between lateral line and dorsal fin origin	0.16907	-0.05294	0.21889
Scales between upper lateral line and last dorsal fin spine	0.25388	-0.09697	0.15397
Inner series of teeth (Upper jaw)	0.2047	-0.13884	-0.13619
Inner series of teeth (Lower jaw)	0.17133	-0.16231	-0.12204
Pectoral rays	0.23067	0.10129	0.19334
Gill rakers (ceratobranchial)	0.26461	-0.14373	-0.15223
Total gill rakers	**0.28659**	-0.11744	-0.11202
Abdominal vertebrae	0.22544	0.22789	0.1947
Caudal vertebrae	0.20141	0.08631	**-0.39403**
Total number of vertebrae	0.27686	0.18055	-0.2232
Anal-fin rays	0.13315	-0.10237	-0.25914
Dorsal-fin spines	0.13005	**0.49168**	0.10505
Dorsal-fin rays	0.1778	-0.27153	-0.25691
Upper procurrent caudal-fin rays	0.1947	-0.14488	0.27996
Lower procurrent caudal-fin rays	0.20322	-0.20307	**0.33611**
Caudal-fin rays	0.21251	-0.20243	**0.3418**
Position of the pterygiophore supporting the last dorsal fin spine	0.12435	**0.51758**	0.084214
Position of pterygiophore supporting the last anal fin spine	0.22533	**0.24137**	0.069637
Eigenvalue	8.63124	2.79827	2.04682
% variance	37.527	12.166	8.8992

The second PCA was based on 20 log-transformed morphometric measurements of all 203 investigated specimens. In this analysis PC I explained 93.1 %, PC II 2.0 % and PC III 1.4 % of the total variance. Factor loadings indicate that the characters that contributed the most to PC II were the last dorsal fin spine length, length of third anal fin spine and cheek depth while in PC III distance between anus and anal-fin base, snout length and cheek depth contributed the most (see Supplementary Table 2 for factor loadings PCI-PCIII). PC II and PC III scores of the different species overlapped widely and did not allow for any clear separation of species (Supplementary Fig. 1).

Overall, the combination of meristic counts, morphometric measurements, color patterns and additional morphological characters allowed to separate the two new monotypic genera from all analysed taxa associated with the genus *Pseudocrenilabrus* (including *O. machadoi* and *H. moeruensis*) and were therefore used as the basis for their differential diagnosis.

Palaeoplex new genus

Type species: *Palaeoplex palimpsest* sp. nov.

Diagnosis. *Palaeoplex* gen. nov belongs to the megadiverse cichlid lineage of haplotilapiines (sensu Schliewen & Stiassny 2003) characterised by tricuspid teeth in the inner tooth rows of the oral jaws. Within the haplotilapiines it belongs to the still weakly defined tribe Haplochromini, which is generally characterized by the combination of following characters: basioccipital forming together with parasphenoid the apophysis of the upper pharyngeal bones, type A infraorbitals (sensu Takahashi, 2003a), bicuspid outer and tricuspid inner teeth on both jaws, ctenoid scales on flanks, and by being maternal mouthbrooders (Poll 1986, Eccles & Trewavas 1989, Takahashi 2003b). Within Haplochromini, *Palaeoplex* gen. nov. is placed within the *Pseudocrenilabrus* group (including *Lufubuchromis* gen. nov., *Pseudocrenilabrus*, *Orthochromis machadoi* and *Haplochromis moeruensis)* by the presence of a *Pseudocrenilabrus* blotch at the distal end of the anal fin in adult males, a placement which is supported also by genetic analyses. The currently monotypic genus *Palaeoplex* is characterized by a unique combination of the following characters: (1) a fully developed infraorbital series without a distinct gap between the lachrymal and the second infraorbital bone (in some cases the pore of the laterosensory tubule of both bones appears to be shared) (see Fig. 9); (2) fused hypuralia 1+2 and hypuralia 3+4 and (3) molariform teeth on sagittal series of the lower pharyngeal jaw (see Fig. 5). Finally, the new genus is characterised by (4) a large maximum size of up to 143.4 mm SL.

Palaeoplex is distinguished from all members of *Pseudocrenilabrus* and from *Haplochromis moeruensis* by having no distinct gap between the lachrymal and second infraorbital bone (vs. distinct gap always present, varying from narrow to very wide). In addition, the infraorbital series of *Palaeoplex palimpsest* is composed of the lachrymal bone (first infraorbital bone), four infraorbital bones and in some cases the dermosphenotic element (sixth infraorbital bone), hereby contrasting with *Pseudocrenilabrus,* where a trend towards the reduction of the infraorbital series can be observed including various combinations of fusion and loss of entire infraorbital bones (see Fig. 9, see also Greenwood 1989).

The genus *Palaeoplex* with its single species *Pa. palimpsest* differs from *Pseudocrenilabrus multicolor* by having more abdominal vertebrae 14–15 vs. 13 and more scales on the horizontal line 28–31 vs. 26–27*;* from *Ps. nicholsi* by having more scales on the horizontal line 28–31 vs. 25–26, more total gill rakers 12–17 vs. 10–11, more abdominal vertebrae 14–15 vs. 12–13 and total vertebrae 27–30 vs. 25–26; from *Ps. pyrrhocaudalis* by having more abdominal vertebrae 14–15 vs. 12–3. It is distinguished form *Ps. philander philander* (populations from type locality and the Orange river drainage, South Africa) by more abdominal vertebrae 14–15 vs. 12–13; it is distinguished from *Ps. philander dispersus* and from several examined *Pseudocrenilabrus* populations of yet undefined taxonomic status (i.e. *Ps. sp.* "Lufira", *Ps. sp.* "Lunzua", *Ps. sp.* "Botswana", *Ps. sp.* "Kalungwishi", *Ps. sp.* "Luongo", *Ps. sp.* "Mukuleshi) by having more abdominal vertebrae 14–15 vs. 13; in addition *Palaeoplex palimpsest* has more scales on the horizontal line 28–31 vs. 26–27 than *Ps. philander dispersus*, and from the putatively new species *Pseudocrenilabrus* sp. "Upper Kalungwishi" it is distinguished by having more total vertebrae 27–30 vs. 26.

From *Orthochromis machadoi* it is distinguished by having comparatively large scales on the chest (vs. partly scaleless chest, with deeply embedded minute scales); moreover, *Palaeoplex palimpsest* is distinguished from *O. machadoi* by having a distinctively longer last dorsal fin spine (14.7–18.6 vs. 10.1–14.6% SL), fewer dorsal fin spines (14–15 vs. 16–17) and by the position of the pterygiophore supporting last dorsal-fin spine at vertebral count:

13–14 vs. 15–16.

Palaeoplex palimpsest is distinguished from the Northern Zambian *Orthochromis* sensu Weiss *et al*. 2015 (*O. kalungwishiensis*, *O. luongoensis*, *O. katumbii,* and *O. mporokoso*) by having fewer dorsal fins spines (14–15 vs. 16–19) and by the position of the pterygiophore supporting the last dorsal-fin spine (vertebral count: 13–14 vs. 15–18) and by having fewer total vertebrae albeit with overlap (27–30 vs. 30–33). Further, *Palaeoplex palimpsest* is distinguished from the Northern Zambian *Orthochromis* by having comparatively large and well-developed scales on belly and chest (vs. small to minute scales, sometimes with deeply embedded chest scales, in the Northern Zambian *Orthochromis*). Further, adult males of *Palaeoplex palimpsest* feature a large orange *Pseudocrenilabrus* blotch at the distal end of the anal fin which is absent in the Northern Zambian *Orthochromis*.

Palaeoplex differs from *Lufubuchromis* gen. nov. by having longer dorsal-fin spines (length of last dorsal fin spine: 14.7–18.6 vs. 10.9–14.2 % SL), by higher total gill raker counts (12–17 vs. 10–12), and by a difference in the coloration (e.g. *Lufubuchromis* with *Pseudocrenilabrus* blotch in both sexes vs. only present in males of *Palaeoplex palimpsest*) and in maximum size (143.4 vs. 93.2 mm).

Etymology. The genus name *Palaeoplex* alludes to the concept of geoecodynamics where the palaeoplex of a species is the proxy for the total genomic variation of a given species comprising DNA signatures of the evolutionary history of a species in a given landscape (Cotteril & de Wit 2011). The analysis of the palaeoplex of a species theoretically allows for reconstruction of the species history in that landscape. As the new genus is tied geographically to a very ancient landscape, and, as published DNA analyses suggest, a long history of this genus in that landscape (e.g. Weiss *et al*. 2015, Schedel *et al*. 2019, unpublished data), the genus name refers to the scientific potential of this genus to elucidate the complex landscape evolution of that region through the analysis of the palaeoplex of the new genus. Gender masculine.

Included species. *Palaeoplex palimpsest* **sp. nov.**

Palaeoplex palimpsest, new species

Pseudocrenilabrus philander (*non* Weber), Balon *et al*. 1983
Chetia mola (*non* Balon & Stewart), Friedmann *et al*. 2013
New Kalungwishi cichlid; Weiss *et al*. 2015, Schedel *et al*. 2019
Orthochromis sp. "New Kalungwishi" Meier et al. 2019

Holotype. ZSM 47492, ex ZSM 44438 (7 in lot, now 6), 143.4 mm SL; Zambia, Luongo River, at bridge on road Kawambwa-Mansa about 40 km [driving distance] S of Kawambwa, Luapula Province (-10.144359/ 29.167193).

Paratype. ZSM 43077, 1, 116.0 mm SL; Zambia, Drainage Congo; Luongo Reservoir, right bank above dam ~ opposite of Chisunka Luongo village, Luongo River 9 km above Musonda Falls on Luongo River, 56.5 km N of Mansa, Luapula Province (-10.685519/28.900466).—ZSM 44438, 6, 81.9–106.3 mm SL; Zambia, Drainage Congo; Luongo River, at bridge on road Kawambwa-Mansa about 40 km [driving distance] S of Kawambwa, Luapula Province (-10.144359/ 29.167193).—ZSM 43079, 6, 62.9–130.1 mm SL; Zambia, Drainage:Congo; Luongo Reservoir, right bank above dam ~opposite of Chisunka Luongo village, Luongo River 9km [air distance] above Musonda Falls on Luongo River, 56.5 km [air distance] N of Mansa, Luapula Province (-10.685519/28.900466).—ZSM 43078, 1, 137.4 mm SL; Zambia, Drainage Congo; Luongo Reservoir, right bank above dam ~ opposite of Chisunka Luongo village, Luongo River 9 km above Musonda Falls on Luongo River, 56.5 km N of Mansa, Luapula Province (-10.685519/ 28.900466).—CU 91755, 8, 50.0–82.1 mm SL; Zambia, Drainage: Luongo River; Luongo River at Mukonshi Bridge on Mwenda-Kawanbwa road (-10.1442/29.167).—CU 99504, 4, 39.5–100.8 mm SL; Zambia, Drainage Luongo River; Luongo River at bridge on Kashiba-Mwenda road (-10.4701/29.0245).—SAIAB 208051, 3, ex ZSM 43077 (4 now 1), 102.8–122.8 mm SL; Zambia, Drainage Congo; Luongo Reservoir, right bank above dam ~ opposite of Chisunka Luongo village, Luongo River 9 km above Musonda Falls on Luongo River, 56.5 km N of Mansa, Luapula Province (-10.685519/28.900466).—MRAC 2019.009.P.0001-0003, 3, ex ZSM 43079 (9 now 6), 66.2–133.8 mm SL; Zambia, Drainage: Congo; Luongo Reservoir, right bank above dam ~ opposite of Chisunka Luongo village, Luongo River 9km [air distance] above Musonda Falls on Luongo River, 56.5 km [air distance] N of Mansa, Luapula Province (-10.685519/28.900466).—ZSM 47493, ex ZSM 41496 (2 now 1), 1, 33.2 mm SL; Zambia, Drainage Congo; Luongo stream at bridge on road Mwenda-Kashiba, affluent to Lake Mweru/Upper Congo basin, Luapula Province (-10.470725/29.026200).

Additional specimens examined. ***Palaeoplex palimpsest*** (specimens from Kalungwishi River**):** ZSM 41425, 6, 73.0–102.9 mm SL; Zambia, Drainage Congo; Kalungwishi stream above Lumangwe falls, W of Mukuma, on road Mukunsa—Kawambwa, approached from Northern Province (-9.543011/ 29.387789).—ZSM 44357, 9, 53.9–116.6 mm SL; Zambia, Drainage Congo; Kalungwishi River, 3 km below Kabwelume Falls [above Kundabwika Falls], ~ 23.5 km downstream bridge on road Mporokoso—Kawambwa, Northern Province (-9.502106/29.352734).—SAIAB 77188, (1 out of 5 specimens), 118.9 mm SL; Kundabwika falls on Kalungwishi River (-9.2179/29.3040).

Diagnosis. Species diagnosis as for genus.

Description. Morphometric measurements and meristic characters are based on 34 type specimens. Values and their ranges are presented in Table 3. For general appearance see Fig. 3 (male) and Fig. 4 (female). Maximum length of a wild caught male specimen 143.4 mm SL; largest female 110.7 mm SL. A rather deep bodied (BD: 28.9–36.0 % SL) species with maximum body depth slightly behind pelvic fin origin, decreasing towards caudal peduncle (dorsal margin of caudal peduncle roughly on level with dorsal margin of orbit). Ratio caudal peduncle length to depth: 1.2–1.8. HL about one third of SL. Adult males with a slightly concave upper head profile; females with a straight to slightly curved upper head profile. No prominent nuchal gibbosity. Jaws isognathous to slightly retrognathous. Posterior tip of maxilla reaching slightly behind nostril. Lips not noticeably enlarged or thickened. Two separate lateral lines.

Squamation. Flank and dorsum covered with comparatively large cycloid or weakly ctenoid (if ctenoid, ctenii very short; see Supplementary Fig. 2). Cycloid scales of belly slightly smaller than flank scales. Chest scales cycloid and smaller than belly scales, smallest behind branchiostegal membrane; chest to flank transition with slightly larger cycloid or weakly ctenoid scales. Snout scaleless. Medium sized interorbital scales cycloid; anteriormost scales partially embedded in skin. Nape and occipital region with slightly smaller cycloid scales compared to flank scales. Cheek covered with 2–4 scale rows of small to medium sized cycloid scales. One cycloid scale between posterior orbital margin and preoperculum. Operculum covered with cycloid scales of variable size, some almost size flank scales. Opercular blotch squamated to variable extent; posteriormost margin always scaleless. Three to five scales on horizontal line starting from anterior edge operculum to postero-dorsal edge operculum.

Scales on upper lateral line 16–24, lower lateral line 10–14 scales and horizontal line with 28–31 scales. Upper and lower lateral lines separated by two rows of scales. Five to nine scales between dorsal-fin origin and upper lateral line; 2–4 scales between origin last dorsal-fin spine and upper lateral line. Anterior caudal fin part covered with 2–4 ill-defined vertical columns of small cycloid scales including 0–2 pored scales; scaled area extending posteriorly to approximately 28–42 % caudal fin length with minute, interradial scales. Specimens from the Luongo River with 18–20 scales around caudal peduncle, specimens from Kalungwishi River with 16–18 scales around caudal peduncle.

Jaws and dentition. Anterior jaw teeth of outer rows of upper and lower jaw subequally bicuspid to subequilaterally bicuspid and closely set; towards corner of mouth, teeth are increasingly smaller and more widely set and might become unicuspid. Bicuspid teeth are slightly recurved and without or with a minimally expanded brownish crown; cusps only slightly compressed and blunt, with a moderately narrow cusp gap; neck moderately slender. Outer tooth row of upper jaw with 21–57 teeth, of lower jaw with 17–51 teeth (only counted for specimens from 50.8–143.3 mm SL); larger specimens have incrementally more teeth. One (rarely in lower jaw) to four inner upper and lower jaw tooth rows with small tricuspid teeth.

Lower pharyngeal bone of six paratypes (SAIAB 208051, 118.0–122.9 mm SL; ZSM 43079, 109.3–130.1 mm SL; ZSM 44438, 106.3 mm SL) about as wide as long (width of lower pharyngeal jawbone 95 to 103 % of pharyngeal-jaw length; Fig. 5). Dentigerous area of lower pharyngeal bone about 0.6 to 0.7 times length of lower pharyngeal bone length, with 21–30 teeth along posterior margin of dentigerous area. Teeth in sagittal series 7–11, molariform. Lateral anterior pharyngeal teeth bevelled to pronounced to moderately slender; those of posterior row larger than anterior ones, bevelled (minor cusp not well developed). Largest teeth (excluding molariform teeth of sagittal series) are located centrally in posterior tooth row whereas smallest teeth are found in the posterior corners of dentigerous area.

Gill rakers. Total gill rakers 13–17 with 2–4 epibranchials, one in angle (rarely two), and 9–12 ceratobranchial rakers. Anteriormost ceratobranchial gill rakers smallest. Gill rakers slender to broad and unifid, sometimes of anvil shape to bifid towards cartilaginous plug, increasing in size towards cartilaginous plug at angle. Gill raker on cartilaginous plug slightly shorter or as long as longest ceratobranchial gill raker; unifid epibranchial gill rakers slightly

TABLE 3. Measurements and counts for holotype, paratypes and additional specimens of *Palaeoplex palimpsest* **sp. nov.**

Measurements	holotype	holotype + paratypes (Luongo River)				Additional material (Kalungwishi River)			
		min	max	Mean±SD	N	min	max	Mean±SD	N
Total length (mm)	176.6	42.2	176.6	107.8 ± 37.7	34	68.3	152	109.5 ± 21.7	16
Standard length SL (mm)	143.4	33.2	143.4	86.8 ± 31.5	34	53.9	118.9	88.2 ± 17.7	16
Head length HL (mm)	45.9	11.3	45.9	27.7 ± 9.7	34	18.3	40	28.8 ± 5.5	16
% HL									
Interorbital width	25.7	21.1	28.3	24.7 ± 1.8	34	21.6	27.0	24.4 ± 1.7	16
Preorbital width	31.1	25.0	34.5	29.7 ± 2.6	34	27.3	34.6	30.4 ± 1.7	16
Horizontal eye length	21.3	21.1	32.8	26.0 ± 3.4	34	21.7	30.2	26.0 ± 2.1	16
Snout length	34.6	25.2	38.7	33.9 ± 3.0	34	32.8	39.9	36.0 ± 2.0	16
Internostril distance	18.3	15.4	20.4	18.2 ± 1.3	34	16.2	22.2	19.2 ± 1.5	16
Cheek depth	31.9	17.2	31.9	24.7 ± 4.0	34	20.6	29.6	25.4 ± 2.2	16
Upper lip length	27.8	21.0	30.7	24.1 ± 2.6	34	21.8	29.2	25.2 ± 2.0	16
Lower lip length	31.2	20.8	34.0	26.7 ± 3.2	34	25.9	31.4	28.3 ± 1.5	16
Lower lip width	32.6	19.8	32.6	25.3 ± 3.3	34	20.6	33.0	25.6 ± 3.0	16
Lower jaw length	36.0	31.5	44.0	36.2 ± 2.3	34	34.7	40.2	36.5 ± 1.4	16
Lower pharyngeal jaw length	-	28.8–33.1		-	6		26.8–33.8	-	3
Lower pharyngeal jaw width	-	28.0–32.4		-	6		28.3–32.8	-	3
Width of dentigerous area of Lower pharyngeal jaw	-	21.1–23.7		-	6		20.6–24.5	-	3
% SL									
Predorsal distance	34.8	32.4	38.2	35.4 ± 1.3	34	33.9	37.8	36.5 ± 0.9	16
Dorsal fin base length	56.6	51.2	57.3	54.7 ± 1.5	34	50.0	57.0	54.2 ± 1.7	16
Last dorsal fin spine length	15.2	14.9	18.5	16.6 ± 1.1	34	14.7	18.6	17.0 ± 0.9	16
Anal fin base length	20.6	16.0	20.6	18.4 ± 1.0	34	16.9	19.6	18.3 ± 0.8	16
Third anal fin spine length	11.8	11.8	19.6	15.9 ± 2.0	34	14.5	19.3	16.9 ± 1.5	16
Pelvic fin length	31.8	19.8	31.8	25.5 ± 2.5	34	23.3	29.7	24.7 ± 3.7	16
Pectoral fin length	26.2	19.1	27.9	25.3 ± 1.7	34	23.8	29.1	26.4 ± 1.4	16
Caudal peduncle depth	12.0	9.7	13.9	11.3 ± 0.8	34	10.2	11.8	11.1 ± 0.4	16
Caudal peduncle length	17.5	16.0	19.3	17.8 ± 0.7	34	16.8	19.3	17.9 ± 0.6	16
Body depth (pelvic fin base)	35.1	28.8	36.0	33.3 ± 2.1	34	30.8	35.7	33.2 ± 1.4	16
Preanal length	62.4	58.8	64.9	61.4 ± 1.4	34	58.4	62.7	61.1 ± 1.1	16

.....continued on the next page

TABLE 3. (Continued)

Anus-anal fin base distance	2.9	2.1	4.4	3,3 ± 0.5	34	2.5	3.8	3.1 ± 0.4	16
Interpectoral width	13.7	8.8	13.7	11.8 ± 1.1	34	9.9	14.7	11.4 ± 1.1	16
Counts									
Dorsal fin spines	15	14 (2); 15(32)			34		14(1);15(15)		16
Dorsal fin rays	11	10 (5); 11 (28); 12 (1)			34		10 (6); 11 (10)		16
Anal fin spines	3	3 (34)			34		3 (16)		16
Anal fin rays	9	7 (1); 8 (3); 9 (30)			34		7 (1); 8 (8); 9 (7)		16
Pelvic fin spines	1	1 (34)			34		1 (16)		16
Pelvic fin rays	5	5 (34)			34		5 (16)		16
Pectoral fin rays	14	13 (1); 14 (31); 15 (1); 16 (1)			34		14 (12); 15 (4)		16
Upper procurrent caudal fin rays	6	5 (4); 6 (26); 7(4)			34		5 (2); 6(12); 7(1)		15
Lower procurrent caudal fin rays	7	5 (4); 6 (21); 7 (9)			34		6 (11) ; 7 (4)		15
Caudal fin rays	29	26 (2); 27 (4); 28 (20); 29(5), 30 (3)			34		27 (2); 28 (9); 29 (3); 30 (1)		15
Scales (horizontal line)	30	28 (3); 29 (8); 30 (20); 31(3)			34		28 (1);29 (3); 30 (10); 31 (2)		16
Upper lateral line	20	16 (1); 17 (1); 18 (4); 19 (7); 20 (13); 21 (8)			34		18 (1); 19 (4); 20 (6); 21 (5)		16
Lower lateral line	13	10 (2); 11 (3); 12 (9); 13 (16); 14 (4)			34		11 (1); 12 (6); 13 (8); 14 (1)		16
Circumpeduncular	20	18 (10); 20 (20)			30		16 (10); 18 (5)		16
Series of Scales on check	3	2 (2); 3 (31); 4 (1)			34		3 (5); 4 (11)		16
Scales (horizontal line) on operculum	4	3 (2); 4 (26); 5 (6)			34		4(10); 5(6)		16
Scales between lateral line and dorsal fin origin	7	5 (2); 6 (14); 7 (11); 8 (3); 9 (4)			34		6 (1); 7(6); 8(7); 9 (1)		15
Scales between upper lateral line and last dorsal fin spine	3	2 (3); 3 (25); 4 (6)			34		3 (15); 4(1)		16
Abdominal vertebrae	14	14 (29); 15 (5)			34		14 (13); 15 (2)		15
Caudal vertebrae	15	13 (1); 14 (7); 15 (26)			34		13 (2); 14 (10); 15(3)		15
Total number of vertebrae	29	27 (1); 28 (3); 29 (29); 30 (1)			34		27 (2); 28 (8); 29 (5)		15
Teeth in upper outer row	35	21 (1); 24 (1); 26 (1); 27 (1); 29 (2); 31 (1); 32 (1) 33(1); 34 (1); 35 (2); 37 (2); 38 (1); 39 (1); 40(1); 41(1); 42 (1); 44 (1); 50(1); 52 (2); 53 (1); 57 (1)			24		31 (1); 34 (1); 36 (3); 38 (2); 39 (1); 40 (1); 45 (2); 46 (1); 47 (1); 51(2)		15
Teeth in lower outer row	30	17 (1); 21 (2); 22 (3); 23 (3); 24 (1); 25 (2); 27 (2); 28 (2); 30 (2); 31 (3); 33 (2); 41 (1); 51 (1)			24		21(1); 22 (2); 24 (2); 26 (2); 27 (1); 8 (1); 29 (1); 33 (2); 35 (2); 40 (1)		15
Gill rakers (ceratobranchial)	11	9 (1); 10 (14); 11 (18); 12 (1)			34		9 (3); 10 (10); 11(3)		16
Gill rakers (angle + epibranchial)	4	3 (2); 4 (11); 5 (21)			34		4 (10); 5 (6)		16

decreasing in size and more slender than ceratobranchial gill rakers.

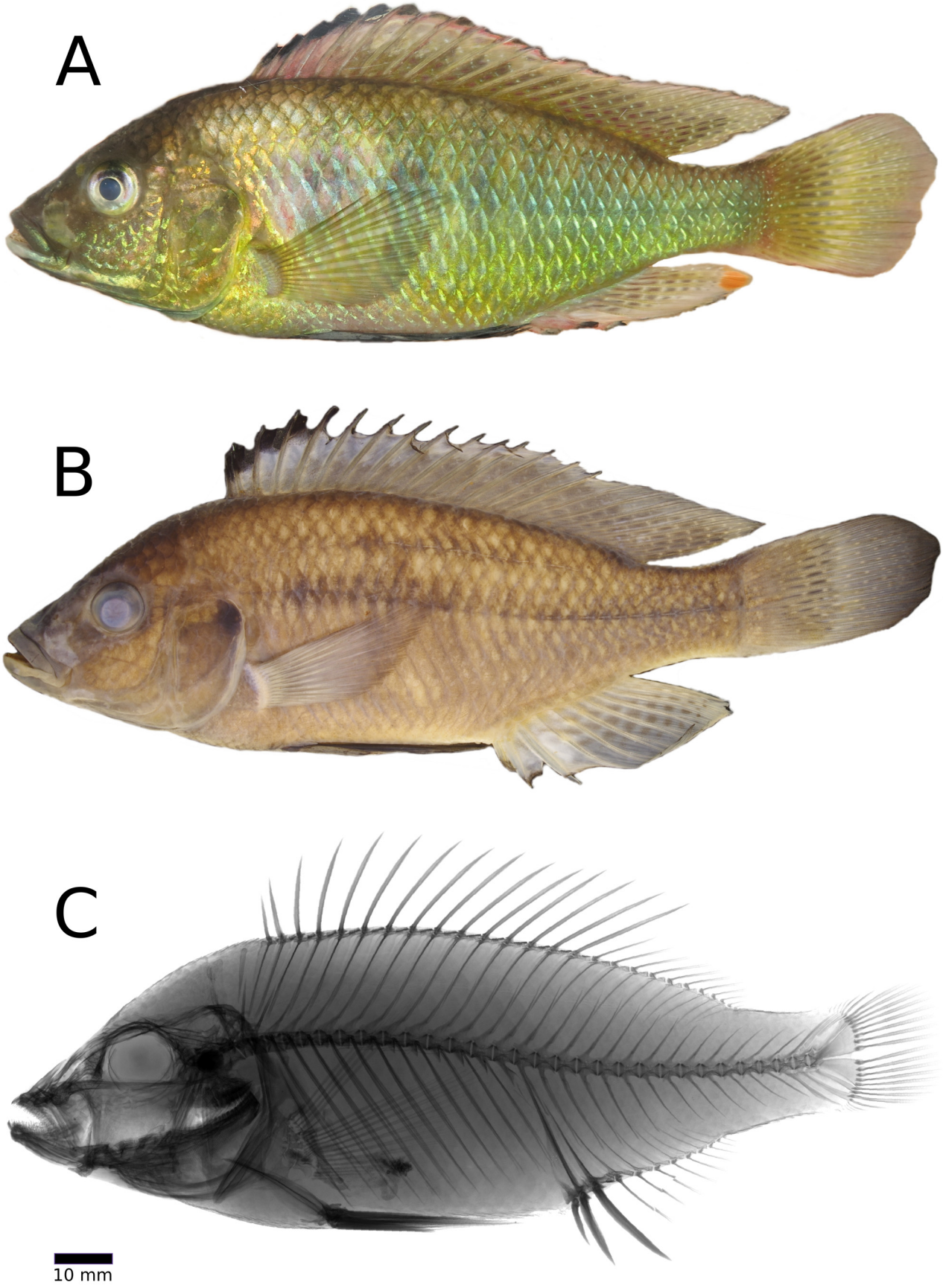

FIGURE 3. *Palaeoplex palimpsest* **sp. nov. A.** holotype, alive **B.** holotype (ZSM 47492), 143.3 mm SL; Zambia, Luongo River **C.** radiograph of holotype

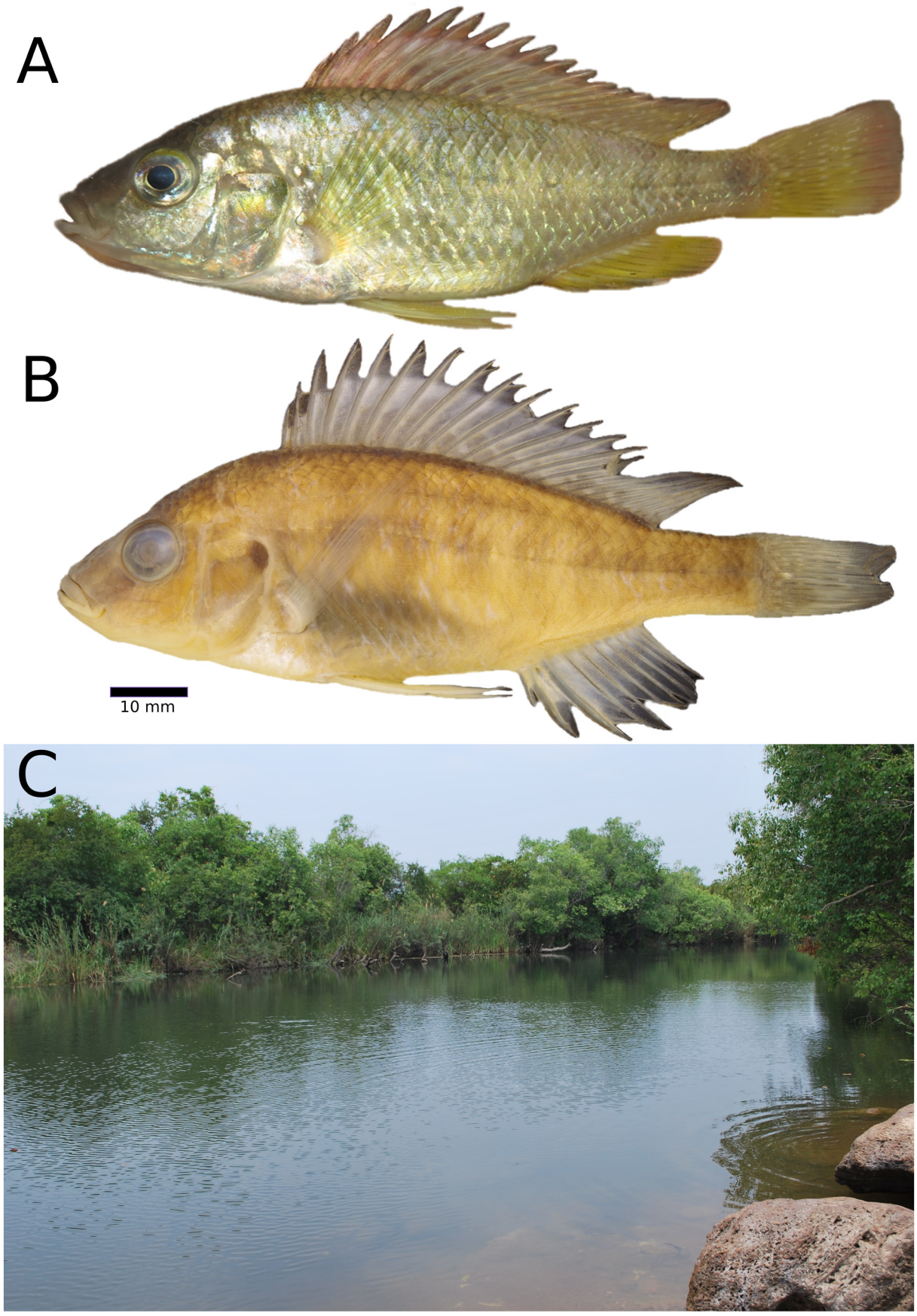

FIGURE 4. Female and type locality of *Palaeoplex palimpsest* **sp. nov. A.** female paratype alive **B.** same individual (ZSM 44438, ID: DRC-2012-/3649, 85.3 mm SL) **C.** Type locality of *Pa. palimpsest*, Luongo River (21.09.2015, Fenton P. D. Cotterill)

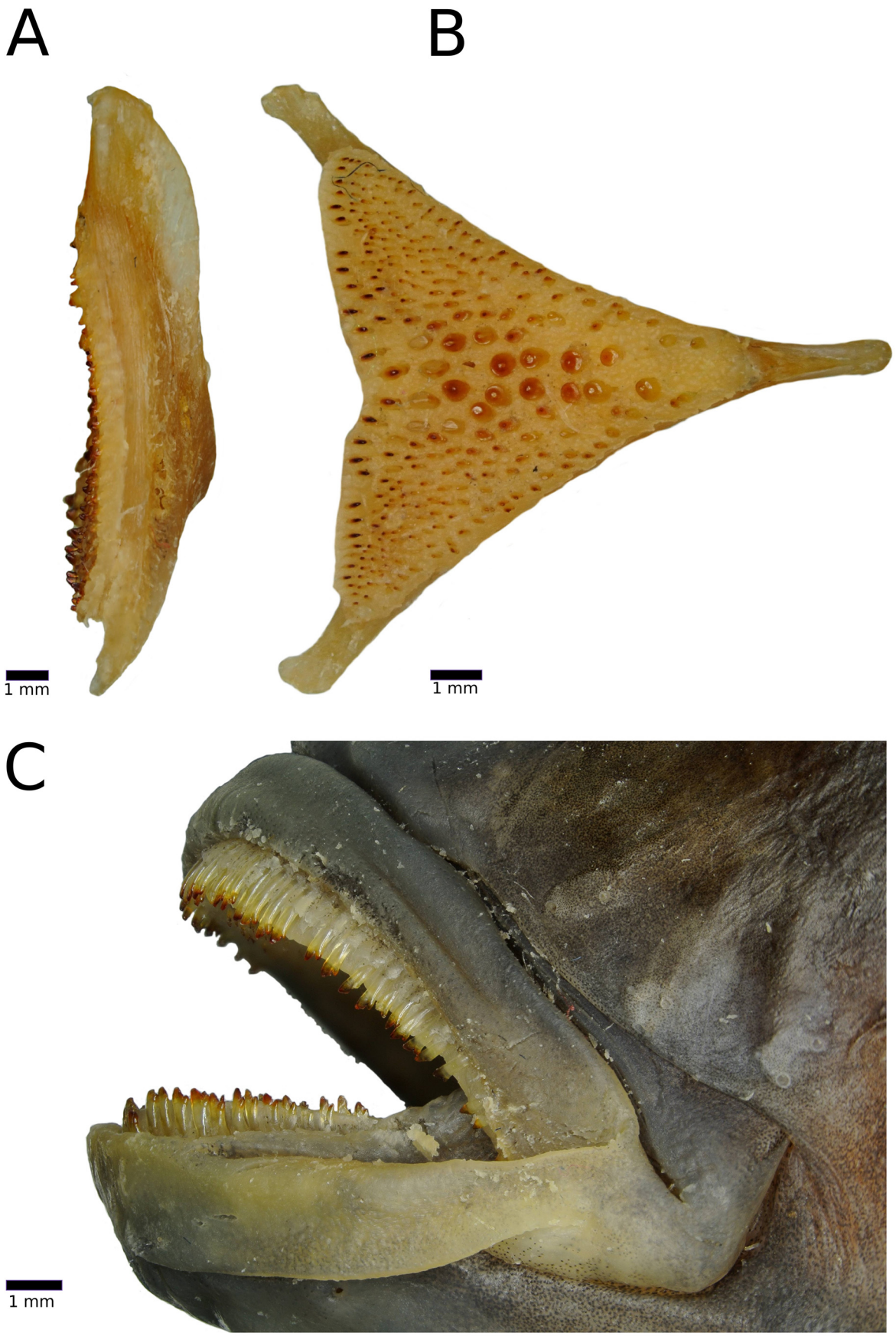

FIGURE 5. Pharyngeal jaws and overview of oral jaws of *Paleoplex palimpsest* **sp. nov. A.** Lateral view of the lower pharyngeal jaw of *Pa. palimpsest* **sp. nov.** (Paratype; ZSM 43077, 122.9 mm SL) **B.** Dorsal view of the same lower pharyngeal jaw **C.** Arrangement and morphology of the oral jaw teeth (Paratype, ZSM 43079, ID: P-AA-936, 133.8 mm SL).

Fins. Dorsal fin with 14–15 spines and 10–12 rays. First dorsal-fin spine shortest. Dorsal-fin base length between 51.2–57.3 % SL. Posterior end of dorsal fin reaching caudal fin base or ending slightly before (females) or reaching behind caudal-fin base (adult males); posterior tip of anal fin reaching caudal-fin base or ending slightly before. Caudal fin outline rounded to subtruncate and composed of 26–30 rays (16 principal caudal-fin rays and 10–14 procurrent caudal-fin rays). Anal fin with 3 spines (3rd spine longest) and 7–9 rays. Anal-fin base length between 16.0–20.6 % SL. Pectoral fin with 13–16 rays. Pectoral-fin length between 19.1–27.9 % SL; longest pectoral ray (4th or 5th ray counted from dorsal margin) ending slightly before level of anus. Pelvic fin with one spine and 5 rays. Pelvic fin base slightly further (approximately 1.5–2 times flank scale width) posterior of pectoral fin base. Longest pelvic-fin ray ending behind anterior origin of anal fin base (especially in males) or ending slightly before (especially in females); adult males with moderately elongated 1st pelvic fin ray.

Axial skeleton. Vertebral column with 27–29 (rarely 30) total vertebrae (excluding urostyle), with 14–15 abdominal vertebrae and 13–15 caudal vertebrae. Pterygiophore supporting last dorsal-fin spine inserted between neural spines 13th and 14th vertebra (counted from anterior to posterior) or 14th and 15th vertebra. Pterygiophore supporting last anal-fin spine inserted between ribs of 15th vertebra and haemal spine of 16th vertebra or between haemal spines of 15th and 16th vertebrae (rarely between haemal spines of 16th and 17th vertebrae). One predorsal bone (= supraneural bone) present. Hypuralia 1 + 2 and hypuralia 3 + 4 always fused into single, sutureless unit.

Coloration in life (based on field photographs of adult specimens). Pronounced sexual colour dimorphism present. Sexually mature males with characteristic coloration pattern of metallic greenish to turquoise flanks and caudal peduncle, lower lip whitish with turquoise to greenish gleam and deep black pelvic fins (see Fig. 3).

Body ground coloration olive; dorsum olive to pale brownish, flank and caudal peduncle greenish to turquoise. Most flank and caudal peduncle scales with greenish metallic gleam, limited to posterodorsal scale margin, and continuous with neighbouring upper and lower scale; resulting pattern giving impression of shiny oblique bars across flank. Flank scales posterior of head (first one to two rows) and chest golden to greenish. Ventral part of chest blackish (some scales with greenish gleam), belly whitish to beige. In large adult males a greyish midlateral band can be present, but mostly faint and hardly visible; between 7 and 9 light greyish vertical bars, but mostly faint or completely absent. No distinct caudal fin spot. Iris brownish with whitish patches. Dorsal head surface and ethmoidal area olive to brownish. Cheek olive with greenish to golden gleam, preoperculum golden. Operculum with golden-orange to greenish gleam, blackish opercular spot present but might be overlain by a metallic gleam. A faint greyish lachrymal stripe present. Upper lip olive with greenish gleam, lower lip whitish with turquoise to greenish gleam (especially at corner of mouth). Branchiostegal membrane greyish to turquoise. Dorsal fin membrane olive to brownish; dorsal fin lappets of spinous part deep black (first four spines with largest fin lappets), black dorsal fin lappets delineated by a narrow reddish submarginal band from the fifth dorsal fin spine. Soft rayed part of dorsal-fin membrane with small transparent to whitish maculae organized in loose oblique rows. Anal fin membrane olive to brownish (whitish to hyaline distally), with irregularly set transparent to whitish maculae; orange *Pseudocrenilabrus* blotch on posterior margin soft rayed part anal fin, proximal side outlined with narrow whitish band. Caudal fin membrane olive to yellowish; becoming less intensively coloured towards margin, with loosely set vertical rows of transparent to whitish maculae. Pectoral fin membrane transparent, pectoral fin rays olive. Pelvic fin membrane blackish.

Females (Fig. 4) less colourful, without prominent green, gold or turquoise gleam. Body primary coloration grey to olive. Flank, caudal peduncle and chest with silvery gleam. Chest and belly white to beige. No midlateral band visible, 7 to 9 light greyish vertical bars, but mostly faint. Iris brown with whitish patches. Cheek silvery. Operculum silvery with patches of golden gleam; opercular spot black with gold metallic gleam. A faint grey lachrymal stripe. Lips white to grey. Branchiostegal membrane white to grey. Dorsal fin membrane as in males. Anal fin yellowish, without transparent or white maculae and without *Pseudocrenilabrus* blotch. Pectoral fins transparent, pectoral fin rays yellow to olive. Caudal fin and pelvic fin membrane yellowish.

Juvenile coloration in life. No information about juvenile coloration available.

Coloration in alcohol. Pigmentation and melanin patterns similar to live specimens, but due the preservation specimens lost original coloration, rendering especially melanin patterns more intense than in live specimens. Overall body coloration brownish. Chest in females white to beige, in males comparatively dark. Operculum grey to brown; opercular spot dark brown to black. Branchiostegal membrane dusky in males and beige in females. Large adult males with a faint brownish midlateral band along the horizontal line, vertical bars appear to be missing; females and small males either with or without any visible melanin pattern on flank, or with 6 to 9 faint vertical bars;

vertical bars in subadult individuals (< 40.5 mm SL) more pronounced. Dorsal fin membrane grey to brown, dorsal fin lappets blackish. Anal fin brown to grey with transparent maculae; *Pseudocrenilabrus* blotch whitish or faded; anal fin of females greyish. Pelvic fin blackish in males and beige to greyish in females.

Distribution and biology. *Palaeoplex palimpsest* is known from the Luongo River, a tributary of Luapula River, and from several locations in the Kalungwishi River drainage, which drains into Lake Mweru (Luapula drainage). At the type locality, the Luongo River is rocky with sandy to muddy patches, about 25 m wide, and with an estimated depth of approx. 1.5 m. Its shoreline is fringed with dense vegetation (reeds and small trees).

The species seems to prefer stretches of slow flowing water as it was neither observed nor collected in the small rapid-like stretches of the river close to the type locality. No stomach contents were examined, but in X-ray pictures approximately half of the investigated specimens had guts almost entirely filled with a dense fine-grained material, most likely sand, whereas in one specimen fragments of snail shells were visible in the x-rays. The molariform teeth of the lower pharyngeal jaw suggest that this species feeds at least partly on molluscs which are crushed by the pharyngeal jaws.

Etymology. A *palimpsest* is a parchment manuscript page, most commonly used in medieval times, that has been secondarily overwritten after layers of old handwritten letters had been scraped off, sometimes repeatedly. In many palimpsests the old letters are still visible in the background, because they had not been completely removed. The species name *palimpsest* is used here to denote that the palaeoplex of the new species (see etymology of genus name *Palaeoplex* gen. nov. above) is like a palimpsest: it is the result of the history of the species endemic to a dynamic landscape, where, e.g., recent changes in landscape and/or in ecological conditions have affected gene flow and have left genetic signatures by overwriting the genome several times, whereas remnants of more ancient genomic signatures still persist in the background of the endemic species. The contrasting hypotheses regarding the phylogenetic position of the new species, either based on nuclear DNA (Weiss *et al*. 2015) or on mtDNA (Schedel *et al*. 2019), are likely the result of these kinds of events that have affected the genome of *Palaeoplex palimpsest* **gen. nov. sp. nov.** The idea of referring to the genome as a palimpsest is based on Cotterill & de Wit (2011). A noun in apposition.

Lufubuchromis new genus

Type species: *Lufubuchromis relictus* **sp. nov.**

Diagnosis. *Lufubuchromis* gen. nov. belongs to the megadiverse lineage of haplotilapiines (sensu Schliewen & Stiassny 2003) characterised by tricuspid teeth in the inner tooth rows of the oral jaws. Within haplotilapiines it belongs to the still weakly defined tribe Haplochromini characterized generally by the combination of following characters: basioccipital bone forming together with parasphenoid the apophysis for the upper pharyngeal bones, type A infraorbitals (sensu Takahashi, 2003a), bicuspid outer and tricuspid inner teeth on both jaws, ctenoid scales on flanks and by being maternal mouthbrooders (Poll 1986, Eccles & Trewavas 1989, Takahashi 2003b). Within the Haplochromini it is placed within the *Pseudocrenilabrus* group (including *Palaeoplex*, *Pseudocrenilabrus*, *Orthochromis machadoi* and *Haplochromis moeruensis)* by the presence of a *Pseudocrenilabrus* blotch at the distal end of the anal fin in adult males, a placement which is supported by genetic analyses. The genus *Lufubuchromis* is monotypic and characterised by the unique combination of the following characters: (1) a fully developed infraorbital series, however without a distinct gap between posterior margin of the lachrymal and the second infraorbital bone (in some cases the opening of the laterosensory tubule of both bones appears to be shared); (2) hypuralia 1+2 either fused (or sometimes fused with distinctly visible suture) and hypuralia 3+4 fused. Further, *Lufubuchromis* exhibits (3) a male colour pattern characterised by deep, crimson red coloured areas on the anterior and ventral flank regions, on parts of the chest and belly, and on the suborbital head region; and with dorsal fin lappets orange (same colour as *Pseudocrenilabrus* blotch). In addition, (4) the *Pseudocrenilabrus* blotch at the distal end of the anal fin is present in both sexes of *Lufubuchromis* (vs. only present in only present in males of *Palaeoplex* and *Pseudocrenilabrus*).

Lufubuchromis is distinguished from all members of the genus *Pseudocrenilabrus* and from *Haplochromis moeruensis* by having no distinct gap between the lachrymal and second infraorbital bone (vs. distinct gap always present, varying from narrow to very wide). In addition, the infraorbital series of *Lufubuchromis* is composed of

the lachrymal bone (= first infraorbital bone), four infraorbital bones, and in some cases a dermosphenotic element (sixth infraorbital bone), thereby contrasting with *Pseudocrenilabrus,* where a trend towards the reduction of the infraorbital series is observed including various combinations of fusion and loss of entire infraorbital bones is (see Fig. 9, see also Greenwood 1989).

Lufubuchromis with its single species *L. relictus* differs from *Ps. multicolor* by having more abdominal vertebrae (14–15 vs. 13)*;* from *Ps. nicholsi* by having more abdominal vertebrae (14–15 vs. 12–13), more total vertebrae (27–29 vs. 25–26), and more dorsal fin spines (15–16 vs. 13–14); and from *Ps. pyrrhocaudalis* by having more abdominal vertebrae (14–15 vs. 12–13).

It is distinguished form *Ps. philander philander* populations from the type locality and from the Orange River drainage (South Africa) by more abdominal vertebrae (14–15 vs. 12–13); from *Ps. philander dispersus* and from several other examined *Pseudocrenilabrus* of yet undefined taxonomic status, i.e., *Ps. sp.* "Lufira", *Ps. sp.* "Lunzua", *Ps. sp.* "Botswana", *Ps. sp.* "Kalungwishi", *Ps. sp.* "Luongo", and *Ps. sp.* "Mukuleshi", by having more abdominal vertebrae (14–15 vs. 13); in addition *Lufubuchromis relictus* has more dorsal fin spines than *Ps. philander dispersus* (15–16 vs. 13–14), and from the putatively new species *Pseudocrenilabrus* sp. "Upper Kalungwishi" it is distinguished by having more total vertebrae 27–29 vs. 26.

From *Orthochromis machadoi* it is distinguished by having comparatively large scales on the chest (vs. a partially scaleless chest, with only deeply embedded and minute scales); furthermore, *Lufubuchromis relictus* tends to have more abdominal vertebrae (14–15 vs. 13–14) and fewer caudal vertebrae (13–15 vs. 15–16).

Lufubuchromis relictus is distinguished form the Northern Zambian *Orthochromis* by having a large orange *Pseudocrenilabrus* blotch at the distal end of the anal fin (vs. absent), and by having comparatively large scales on belly and chest (vs. small to minute scales, if present deeply embedded on chest). Further, *Lufubuchromis relictus* is distinguished from the Northern Zambian *Orthochromis* by having fewer caudal vertebrae (13–15 vs. 16–18) and fewer total vertebrae (27–29 vs. 30–33).

Apart from coloration and its smaller maximum size (maximum recorded SL: 93.2 vs. 143.4 mm) *Lufubuchromis* is distinguished from *Palaeoplex* by its shorter dorsal fin spines (length of last dorsal fin spine: 10.9–14.2 vs. 14.7–18.6 % SL) and by having lower total gill raker counts (10–12 vs. 12–17).

Etymology: *Lufubu-* refers to the Lufubu River as the only species of the genus is restricted to the Upper Lufubu and its tributaries in northern Zambia; and *-chromis* a widely used suffix for cichlid genera. Gender masculine.

Included species. *Lufubuchromis relictus* **sp. nov.**

Lufubuchromis relictus, new species

Haplochromine sp. nov.; Koblmüller *et al*. 2008
Pseudocrenilabrus sp. 'Lufubu A'; Koblmüller *et al*. 2012, Egger *et al*. 2014, Indermaur 2014
New Lufubu Cichlid; Schedel *et al*. 2019
Orthochromis sp. "New Lufubu" Meier et al. 2019

Holotype. ZSM 47494, ex ZSM 44312 (5 in lot, now 4), 77.8 mm SL, Zambia, Drainage Congo; Mululwe rapids at Mululwe village, below Mwanyonga falls, trib. to Lufubu River/ Lake Tanganyika, 37 km SW of Mpulungu, Northern Province (-9.072543/30.932815).

Paratypes. ZSM 44526, 2, 44.5–93.2 mm SL; Zambia, Drainage Congo; Upper Lufubu River, at bridge on road to Kaponga, 4 km W of Chinakila village, Northern Province (-9.255956/30.877441).—ZSM 44312, 4, 49.9–56.7 mm SL; collected with holotype.—ZSM 44535, 4, 40.6–56.9 mm SL; Zambia, Drainage Congo; Luwle creek at bridge on road Mpulungu-Senga Hill, 25 km away from Chinakila village, affluent of Lufubu River, Northern Province (-9.202418/30.948029).—ZSM 41442, 6, 33.7–70.8 mm SL; Zambia, Drainage Congo; Mululwe stream at bridge on road Lualika-Summe, affluent to Lufubu River, Northern Province (-9.061658/31.033958).– SAIAB 208050, 3, ex ZSM 44535 (7 now 4) , 44.1–58.7 mm SL; Zambia, Drainage Congo; Luwle creek at bridge on road Mpulungu-Senga Hill, 25 km away from Chinakila village, affluent of Lufubu River, Northern Province (-9.202418/30.948029).—MRAC 2019.009.P.0004-0006, 3, ex ZSM 41442, 39.2–63.0 mm SL; Zambia, Drainage Congo; Mululwe stream at bridge on road Lualika-Summe, affluent to Lufubu River, Northern Province (-9.061658/31.033958).

Non type: one single juvenile ethanol voucher, field ID DRC-2012/3241, associated to lot ZSM 44312 (not measured or compared for this work).

Diagnosis. Species diagnosis as for genus.

Description. Morphometric measurements and meristic characters are based on 23 type specimens. Values and their ranges are presented in Table 4. For general appearance see Fig. 6 (male) and Fig. 7 (female). Maximum SL of wild caught male specimen 93.2 mm; largest female is 70.8 mm SL. A comparatively deep bodied (BD: 29.9–34.7% SL) species with maximum body depth slightly before pelvic fin origin, decreasing gently towards caudal peduncle. Ratio caudal peduncle length to depth: 1.3–1.6. HL about one third of SL. Head profile moderately curved, without prominent nuchal gibbosity. Jaws isognathous to slightly retroganthous. Posterior tip of maxilla reaching slightly behind anterior orbit margin. Lips not noticeably enlarged or thickened. Two separate lateral lines.

Squamation. Flank covered with comparatively large ctenoid or, especially in larger individuals, cycloid scales (Supplementary Fig. 3). Anterior dorsal flank covered by cycloid scales, ventral flank scales ctenoid to cycloid. Belly with medium sized cycloid to weakly ctenoid scales, approximately half the size of flank scales. Cycloid chest scales smaller than those of belly; chest to flank transition with slightly larger cycloid scales. Snout scaleless. Medium sized interorbital scales cycloid; anteriormost ones partly embedded. Nape and occipital region with slightly smaller cycloid scales (in comparison to flank scales). Cheek covered with small to medium sized cycloid scales; 3–5 scale rows on cheek. Operculum covered with cycloid scales of variable size, from small to about the size of flank scales. Opercular blotch squamated to variable extent; posteriormost margin always scaleless. Three to four scales on horizontal line from anterior edge operculum to posterodorsal margin operculum.

Upper lateral line with 18–22 scales, lower lateral line 9–12 scales and horizontal line with 26–30 scales. Upper and lower lateral lines separated by two scales. Five to eight scales between dorsal-fin origin and upper lateral line; two scales (rarely 3) between origin of last dorsal-fin spine and upper lateral line. Anterior part of caudal fin covered with 3–4 ill-defined vertical columns of small cycloid scales including 0–2 pored scales; scaled area extended posteriorly, with minute, interradial scales covering approximately 25 to 40% of caudal fin. 16 scales around caudal peduncle.

Jaws and dentition. Anterior teeth of outer row of lower and upper jaw subequally bicuspid to equilaterally bicuspid, closely set; teeth slightly smaller and more widely set towards corner of mouth, and becoming unicuspid. Individual bicuspid teeth are recurved and with slightly expanded brownish crown; cusps minimally compressed and moderately wide cusp gap, with tips blunt to pointed; neck moderately stout. Outer row of upper jaw with 25–53 teeth and outer row of lower jaw with 14–48 teeth in (counts for specimens between 16.6 and 93.2 mm SL; larger specimens have more teeth). One to three inner upper and lower jaw tooth rows with small tricuspid teeth.

Lower pharyngeal bone of four paratypes (MRAC 2019.009.P.0004-0006, 63.0 mm SL; ZSM 44312, 56.7 mm SL; ZSM 44535 54.7–56.9 mm SL [keel damaged]) slightly wider than long with width of lower pharyngeal-jaw bone 90–117% of pharyngeal-jaw length (Fig. 8). Dentigerous area of lower pharyngeal-jaw bone about 0.6 to 0.7 times the length of lower pharyngeal bone, with 19–22 teeth along posterior margin of dentigerous area and 6–10 teeth along the sagittal series. Lateral anterior pharyngeal teeth towards keel bevelled to hooked and moderately slender, those of posterior row larger than anterior ones and bevelled with the minor cusp not well developed. Largest teeth located central in posterior tooth row. Teeth along sagittal series slightly larger than more lateral ones.

Gill rakers. Total gill raker count 10–12 with 2–3 epibranchials, one at angle, and 7–8 ceratobranchial rakers. Anteriormost ceratobranchial gill rakers smallest. Gill rakers comparatively stout and unifid, sometimes of anvil or bifid shape towards cartilaginous plug, increasing in size towards cartilaginous plug at angle. Gill raker on cartilaginous plug slightly shorter or as long as longest ceratobranchial gill raker; unifid epibranchial gill rakers further decreasing in length towards cartilaginous plug and slenderer than ceratobranchial gill rakers.

Fins. Dorsal fin with 14–16 spines and with 9–11 rays. First dorsal-fin spine shortest. Dorsal-fin base length between 39.5–55.3 % SL. Posterior end of dorsal fin reaching caudal-fin base or ending slightly behind, especially in males; posterior tip of anal fin reaching caudal-fin base or ending slightly before. Caudal fin outline subtruncate and sometimes or almost slightly emarginate and composed of 26–28 rays (16 principal caudal-fin rays and 10–12 procurrent caudal-fin rays). Anal fin with 3 spines (3rd spine longest) and 7–8 (rarely 9) rays. Anal-fin base length 14.5–17.9 % SL. Pectoral fin with 13–14 rays. Pectoral-fin length 15.7–26.6 % SL; longest pectoral ray (4th or 5th ray counted from dorsal margin) ending slightly before or at level of anus. Pelvic fin with one spine and 5 rays. Pelvic-fin base slightly posterior pectoral-fin base, at a distance of approx. twice the flank scale width. Longest pelvic-fin ray reaching level of anus; adult males with slightly elongated 1st pelvic fin ray.

Axial skeleton. Vertebrae column with 27–29 total vertebrae (excluding the urostyle), with 14–15 abdominal and 13–15 caudal vertebrae. The pterygiophore supporting the last dorsal-fin spine is inserted between the spines of the 13th and 14th vertebra, or of the 14th and 15th vertebra. The pterygiophore supporting the last anal-fin spine is

inserted between ribs or haemal spines of the 14th, 15th or 16th vertebrae. One predorsal bone (=supraneural bone) present. Hypuralia 1 + 2 are either fused without a suture or, rarely, with clearly visible suture; hypuralia 3 + 4 always fused into single sutureless unit.

Coloration in life. Sexual colour dimorphism present. Males with characteristic coloration pattern of deep crimson red coloured areas on the anterior ventral flank parts, chest and belly and on the lower head; remaining parts of flank and caudal peduncle bluish (Fig 6.).

Body ground coloration greyish olive to pale brown; dorsum olive to pale brownish, flank and caudal peduncle bluish. Individual flank and caudal peduncle scales on the anterior part of the caudal scale area reddish to brownish/olive; posterior scale area metallic blue.

Anterior ventral flank, belly, and chest deep red; ventral flank whitish. No visible midlateral band present, but 5–8 greyish vertical bars, mostly faint; vertical bars extending from dorsal fin origin to roughly the level of pectoral fin, sometimes irregular in shape, i.e. interrupted or almost blotch-like. Caudal-fin spot present. Iris brownish with some light brown to orange patches. Dorsal head surface and ethmoidal area olive to pale brownish; preorbital area, anterior snout, cheek and preoperculum below level of eye deep crimson red. Operculum olive to pale brownish ventral part deep crimson red; blackish opercular spot with golden to greenish metallic gleam. Faint greyish lachrymal stripe present. Upper lip metallic blue, especially posteriorly, and lower lip whitish to intensive metallic blue, more than upper lip. Branchiostegal membrane white to light grey.

Dorsal fin membrane olive to brownish; dorsal fin lappets orange, same colour as *Pseudocrenilabrus* blotch in anal fin; dorsal fin lappets delineated by fine whitish submarginal band in spinous part dorsal fin, sometimes extending into soft-rayed part of dorsal; last dorsal fin rays without orange lappets. Soft-rayed part dorsal-fin membrane with irregularly set white to bluish maculae; sometimes few maculae present on spinous part as well. Anal-fin membrane olive to yellowish with irregularly set white to bluish maculae, more prominent than those on dorsal fin; prominent orange *Pseudocrenilabrus* blotch on posterior margin of soft-rayed anal fin, distal margin *Pseudocrenilabrus* blotch outlined in black. Caudal-fin membrane olive to yellowish, becoming less intensively coloured towards posterior margin, with irregularly set vertical columns of white to bluish maculae, more prominent than those on dorsal fin; distal margin caudal fin reddish. Pectoral fin transparent or slightly yellowish. Soft-rayed part pelvic fin light yellowish to greyish, membrane of pelvic fin spine grey to bluish.

Females (Fig. 7) not as brightly coloured as males and without prominent red areas on flank, chest, belly, and head. Body ground coloration greyish olive to pale brown. Flank and caudal peduncle without bluish metallic gleam, or, if present, less intensive than in males. Belly and chest region beige to whitish. No visible midlateral band present; 6 to 8 greyish to brownish vertical bars, in most cases clearly visible; vertical bars extending from dorsal fin origin to roughly midlevel of pectoral fin, sometimes of irregular shape, e.g. interrupted, blurred or almost blotch like. Caudal fin spot present. Iris brownish with some light brown to orange patches. Blackish opercular spot with golden to greenish metallic gleam, less intensive than in males. Faint greyish lachrymal stripe present. Upper lip and lower lip whitish to metallic blue, less intensive than in males. Branchiostegal membrane white to light greyish. Dorsal fin, anal fin and caudal-fin membrane similar to males, however, without prominent maculae. Anal fin with orange *Pseudocrenilabrus* blotch as in males. Pectoral fin and pelvic fin transparent or light yellowish to greyish.

Juvenile coloration in life. (based on tank-raised juveniles of approximately 14.1 mm SL to 21.5 mm SL; Appendix: Supplementary Fig. 4).

Body ground coloration whitish to beige. Greyish melanin pattern on flank consisting of irregular blotches and vertical bars (and not regularly shaped vertical bars as in sympatric *Pseudocrenilabrus* sp. “Lufubu B?” juveniles); up to six blackish stripe-like blotches along dorsal fin base present, forming an interrupted dorsal medial band. Faint grey lachrymal stripe. Iris greyish. Dorsal fin hyaline with few white to bluish spots, all other fins hyaline, no *Pseudocrenilabrus* blotch on anal fin. Tip of anal-fin membrane light orange in juveniles over ~20 mm SL.

Coloration in alcohol. Pigmentation and melanin patterns similar to live specimens, but due to preservation original coloration lost, rendering melanin pattern more intense than in live specimens. Overall body coloration brownish. Chest and belly brownish, particularly in males, to beige. Branchiostegal membrane dusky, especially in males, to light greyish. Ethmoidal area and lips greyish brown. Cheek light brownish; cheek stripe dark brown. Operculum greyish to brownish; opercular spot dark brown. Vertical bars and caudal fin base dark brown; the anterior three to four vertical bars might be connected at the level of the horizontal line. Dorsal fin greyish, dorsal fin lappets transparent to whitish. Anal fin light greyish to grey; *Pseudocrenilabrus* blotch in males whitish, not visible in females (vs. visible in life). Caudal fin grey brownish. Pectoral fin beige to light grey. Pelvic fin dusky in males and beige to greyish in females.

TABLE 4. Measurements and counts for holotype and paratypes of *Lufubuchromis relictus* **sp. nov.**

Measurements	holotype	holotype + paratypes			
		min	max	Mean±SD	N
Total length (mm)	96.1	42.5	113	65.8 ± 17.3	23
Standard length SL (mm)	77.8	33.7	93.2	52.7 ± 14.3	23
Head length HL (mm)	27.4	12	34.2	18.7 ± 5.2	23
% HL					
Interorbital width	23.4	18.8	24	21.6 ± 1.5	23
Preorbital width	27.1	23.3	30.3	27.1 ± 1.7	23
Horizontal eye length	21.9	20.9	30.9	25.9 ± 2.7	23
Snout length	36.9	25.9	41.3	33.1 ± 3.7	23
Internostril distance	20.2	13.7	24.0	18.2 ± 2.3	23
Cheek depth	29.7	18.2	29.7	24.7 ± 3.0	23
Upper lip length	31.1	20.9	31.4	25.5 ± 3.5	23
Lower lip length	32.7	24.2	34.4	27.7 ± 3.1	23
Lower lip width	30.0	19.9	32.7	25.4 ± 3.5	23
Lower jaw length	35.0	33.2	38.8	36.0 ± 1.4	23
Lower pharyngeal jaw length	-	28.4—36.9		-	3
Lower pharyngeal jaw width	-	31.4—36.5		-	4
Width of dentigerous area of Lower pharyngeal jaw	-	20.6—21.5		-	4
% SL					
Predorsal distance	37.8	35.0	39.6	37.8 ± 1.1	23
Dorsal fin base length	53.8	39.5	55.3	52.2 ± 3.0	23
Last dorsal fin spine length	12.2	10.8	14.2	12.6 ± 1.0	23
Anal fin base length	16.3	14.4	17.9	16.4 ± 0.9	23
Third anal fin spine length	11.3	11.1	15.6	13.5 ± 1.1	23
Pelvic fin length	23.5	20.0	26.0	23.3 ± 1.4	23
Pectoral fin length	25.1	15.7	26.6	24.6 ± 2.3	23
Caudal penduncle depth	11.6	11.2	13.3	12.3 ± 0.5	23
Caudal penduncle length	17.4	16.1	19.1	17.9 ± 0.8	23
Body depth (pelvic fin base)	33.0	29.9	34.7	32.5 ± 1.4	23
Preanal length	63.6	58.9	65.3	62.8 ± 1.4	23
Anus-anal fin base distance	2.9	2.4	4.8	3.7 ± 0.6	23
Interpectoral width	12.6	10.3	15.9	12.6 ± 1.4	23
Counts					
Dorsal fin spines	15	14 (1); 15 (16); 16 (6)			23
Dorsal fin rays	10	9 (5); 10 (16); 11 (2)			23
Anal fin spines	3	3 (23)			23
Anal fin rays	8	7 (4); 8 (18); 9 (1)			23
Pelvic fin spines	1	1 (23)			23
Pelvic fin rays	5	5 (23)			23
Pectoral fin rays	14	13 (3); 14 (20)			23
Upper procurrent caudal fin rays	6	5 (3); 6 (20)			23
Lower procurrent caudal fin rays	6	5 (12); 6 (11)			23
Caudal fin rays	28	26 (3); 27 (9); 28 (11)			23
Scales (horizontal line)	28	26 (3); 27 (3); 28 (9); 29 (6); 30 (2)			23
Upper lateral line	19	18 (8); 19 (9); 20 (4); 21 (1); 22 (1)			23
Lower lateral line	10	9 (1); 10 (8); 11 (9); 12 (5)			23
Circumpeducular	16	16 (23)			23

.....continued on the next page

TABLE 4. (Continued)

Measurements	holotype	holotype + paratypes			
		min	max	Mean±SD	N
Series of Scales on check	3	3 (15); 4 (7); 5 (1)			23
Scales (horizontal line) on operculum	3	3 (16); 4 (7)			23
Scales between lateral line and dorsal fin origin	7	5 (3); 6 (5); 7 (7); 8 (8)			23
Scales between upper lateral line and last dorsal fin spine	2	2 (21); 3 (2)			23
Abdominal vertebrae	14	14 (22); 15 (1)			23
Caudal vertebrae	14	13 (2); 14 (18); 15 (3)			23
Total number of vertebrae	28	27 (1); 28 (19); 29 (3)			23
Teeth in upper outer row	53	25(1); 26 (1); 27 (1); 28 (1); 29 (1); 30 (1); 32 (2); 33 (4); 34 (1); 36 (2); 38 (2);40 (1); 42 (1); 44 (2); 49 (1)			23
Teeth in lower outer row	31	14 (2); 15 (1); 16 (1); 19 (2); 20 (1); 22 (3); 23 (3); 24 (1); 26 (1); 27 (2); 28 (1); 29 (1); 31 (1); 36 (1); 46 (1); 48 (1)			23
Gill rakers (ceratobranchial)	8	7 (13); 8 (10)			23
Gill rakers (angle + epibranchial)	4	3 (8); 4 (15)			23

Distribution and biology. *Lufubuchromis relictus* is only known from the upper reaches of the Lufubu River and its tributaries, including small streams and creeks, on the northeastern Zambian High Plateaux. The ichthyofauna of the lower Lufubu is clearly different from the one in the upper Lufubu, which appears to be the result of isolation by a series of cascades and waterfalls (Koblmüller *et al*. 2012, Schedel *et al*. 2018). At the type locality, the Mululwe River is about 15 m wide with an estimated average depth of 50 cm; it is rocky with patches of sand and gravel and with few patches of submerged vegetation (e.g. *Nymphaea* sp.).

No stomach contents were examined but Indermaur (2014) suggested that *L. relictus* feeds on insect larvae and detritus. *Lufubuchromis relictus* is a maternal mouthbrooder. In captivity the clutch-size varied between 20 and 30 eggs with an incubation time of 18 to 20 days (Indermaur 2014). In the wild (Luwle Creek) mouth-brooding females were observed to form groups (pers. obs. F. Schedel).

Etymology. The species name *relictus* [L.] refers to the restricted distribution of this species in the isolated upper region of an ancient plateau. The basal phylogenetic position of *Lufubuchromis* (together with *Orthochromis kalungwishiensis*) as the ancient mitochondrial sister group of all other members of the *Pseudocrenilabrus* lineage (Koblmüller *et al*. 2008, Schedel *et al*. 2019) suggests that it represents a relict ancient evolutionary lineage, that once may have had a wider distribution. The specific epithet is an adjective.

Remarks: Comparisons of the two new genera with all other haplotilapiine genera. Based on molecular phylogenetic data *Palaeoplex* and *Lufubuchromis* are placed within the informally recognized *Pseudocrenilabrus* group (see above, Table 1). Both new taxa can be distinguished from members of the haplotilapiine tribes Coelotilapiini, Coptodonini, Gobiocichlini, Heterotilapiini, Oreochromini, Pelmatolapiini, Steatocranini and Tilapiini by possessing at least a few weakly ctenoid flank scales (vs. cycloid scales; for details see Dunz *et al*. 2013). Furthermore, both new genera can be distinguished from the Lake Tanganyika tribes of the haplotilapiine East African cichlid radiation as follows: from Boulengerochromini by having ctenoid scales vs. cycloid scales (Poll 1986); from Bathybatini (including *Trematocara* Boulenger 1899b), Cyphotilapiini (including *Trematochromis benthicola* (Matthes 1962)) and Limnochromini by having bicuspid teeth in the outer row of the oral jaws (teeth towards corner of mouth might be unicuspid, though) vs. conical (unicuspid) teeth (in juvenile *Cyphotilapia* Regan 1920 bicuspid teeth become unicuspid when adult; in addition members of the genus *Cyphotilapia* develop a distinct hump on the forehead which is not present in *Palaeoplex* or *Lufubuchromis* (Poll 1986, Takahashi 2003b)); from Cyprichromini and Benthochromini by having a rounded to subtruncate caudal fin outline vs. a truncated one (Takahashi 2003b); from Ectodini by having fewer total vertebrae 27–30 (*Palaeoplex*) / 27–29 (*Lufubuchromis*) vs. 31–38 and fewer horizontal line scales 28–31 (*Palaeoplex*) / 26–30 (*Lufubuchromis*) vs. 32–64 (Poll 1986, Altner *et al*. 2017); from Eretmodini by having scales on operculum and cheek vs. a scaleless condition (Lippitsch 1998); from Lamprologini by having three anal fin spines vs. four or more and by having bicuspid teeth in the outer row of the oral jaw vs. conical (unicuspid) teeth (Poll 1986, Takahashi 2003b); and from Perissodini by having an inner series of teeth in the oral jaw vs. absence of inner teeth series (Takahashi 2003b).

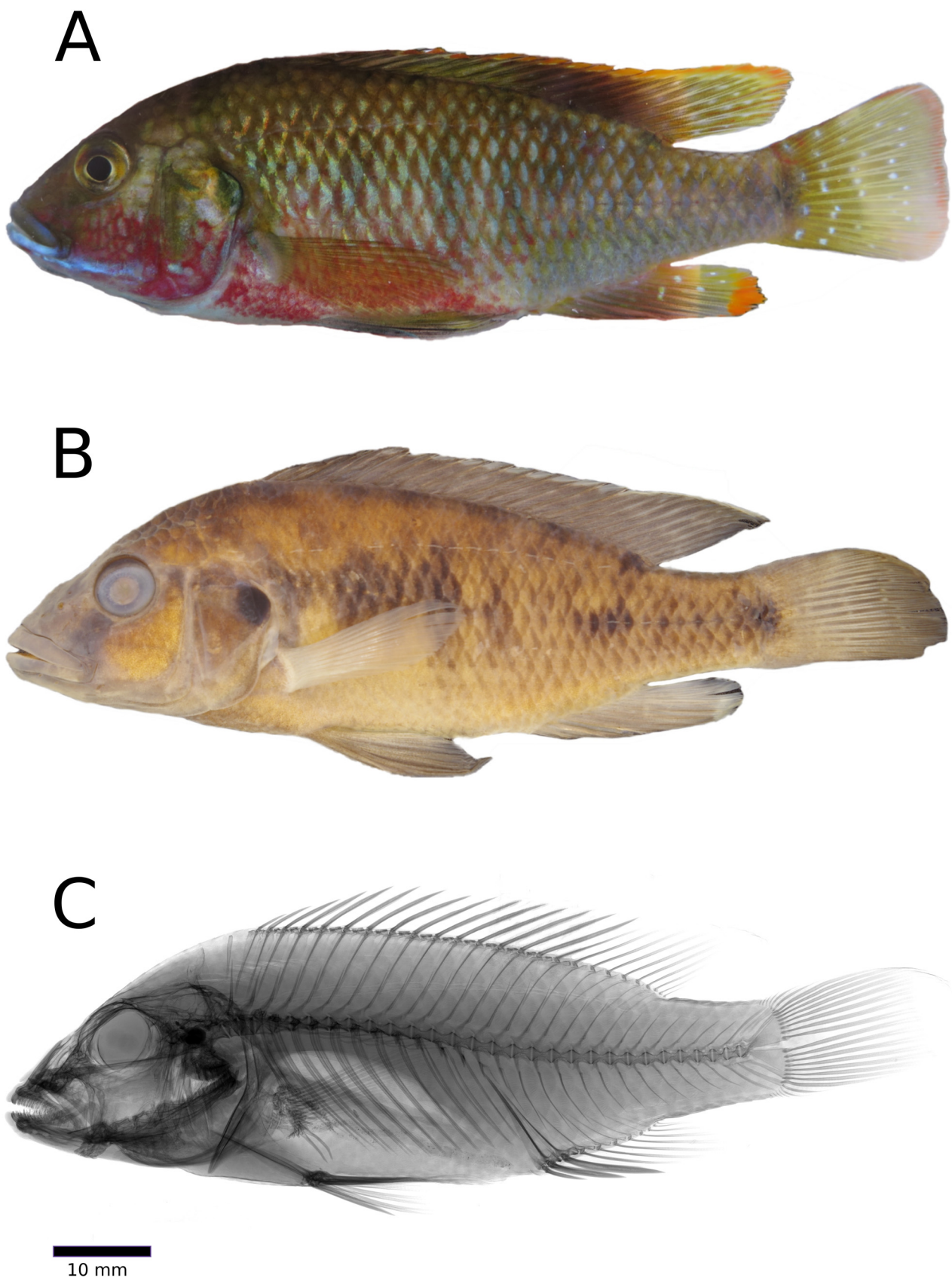

FIGURE 6. *Lufubuchromis relictus* **sp. nov. A.** holotype, alive **B.** holotype (ZSM 47494), 77.8 mm SL; Zambia, Mululwe River, trib. to Lufubu River **C.** radiograph of holotype

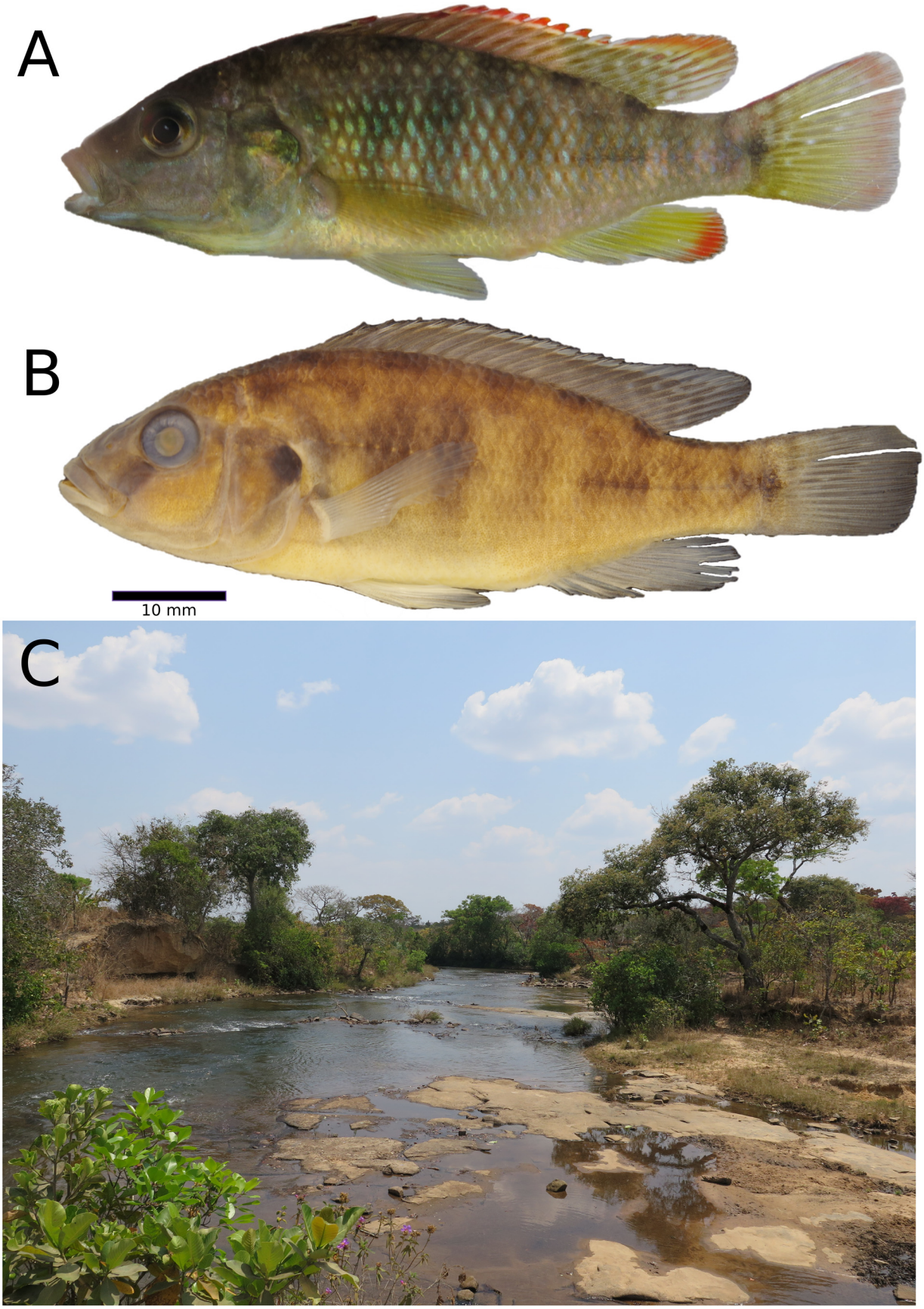

FIGURE 7. Female and type locality of *Lufubuchromis relictus* **sp. nov. A.** female paratype alive **B.** same individual (ZSM 44312, ID: DRC-2012-/3248, 56.7 mm SL) **C.** Type locality of *L. relictus*, rapids on the Mululwe River close to Mululwe Village (05.09.2015, F.D.B. Schedel).

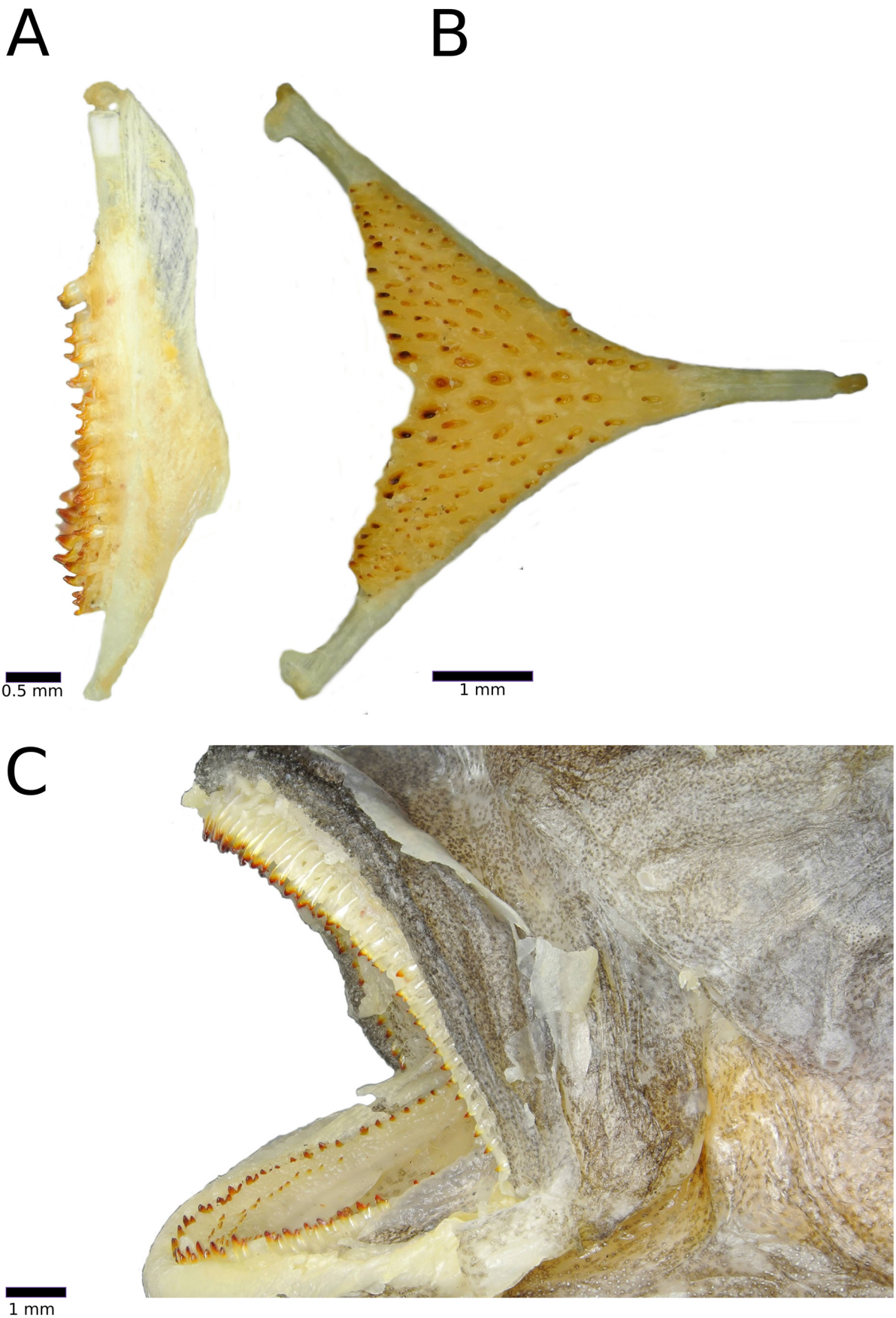

FIGURE 8. Pharyngeal jaws and overview of oral jaws of *Lufubuchromis relictus* **sp. nov. A.** Lateral view of the lower pharyngeal jaw of *L. relictus* (Paratype; ZSM 44535, ID: DRC-2012/3897, 54.7 mm SL) **B.** Dorsal view of the same lower pharyngeal jaw **C.** Arrangement and morphology of the oral jaw teeth (Paratype, ZSM 44526, ID: DRC-2012/3884, 93.2 mm SL).

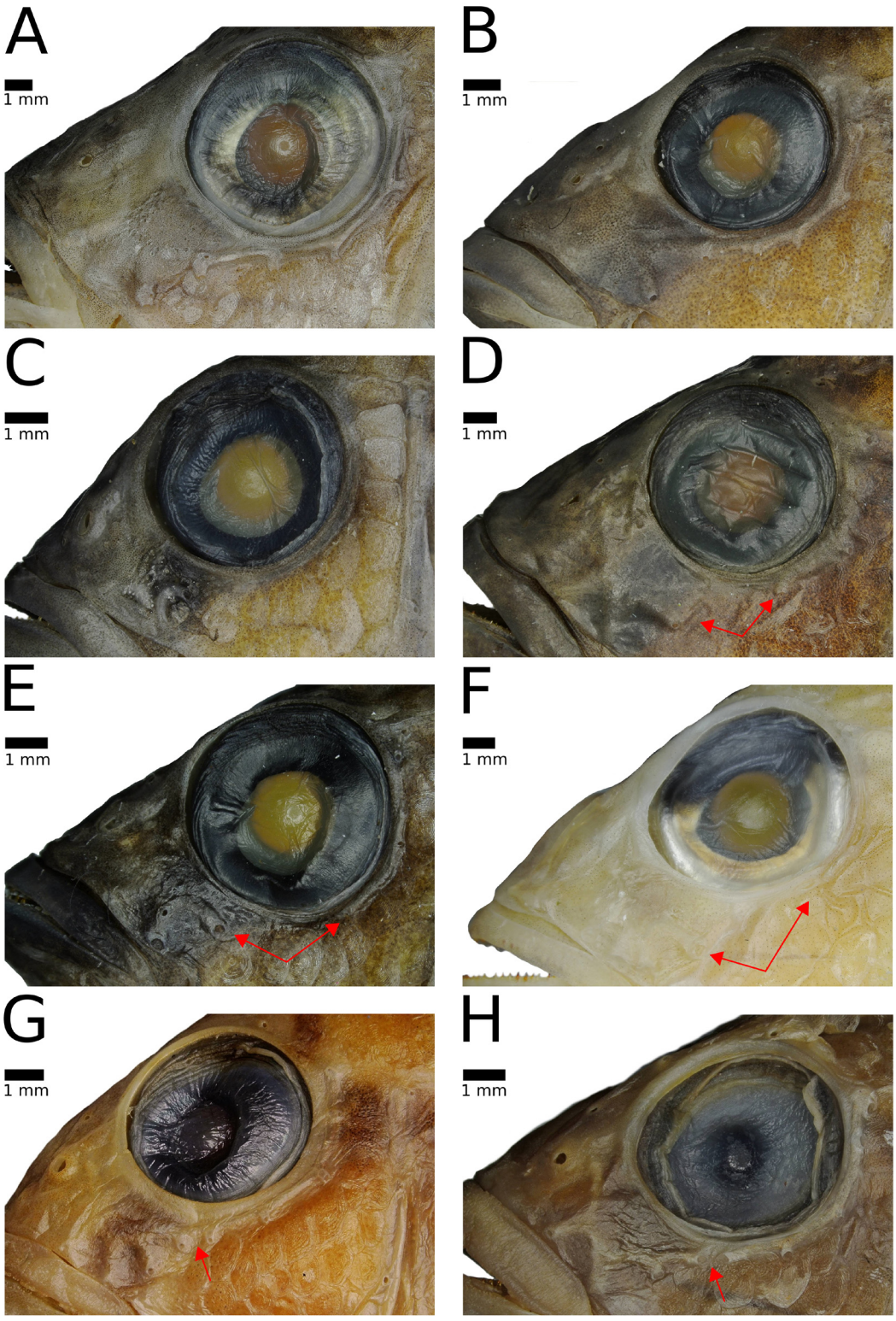

FIGURE 9. Overview of snout and infraorbital area of different taxa of the *Pseudocrenilabrus* group and related taxa. Where applicable, the gap between the lachrymal and 2nd infraorbital bone is indicated by red arrows, i.e. not in *Pseudocrenilabrus multicolor* as the infraorbital series of this species appears to be highly reduced. **A.** *Paleoplex palimpsest* **sp. nov**. (Paratype, ZSM 44438, ID: DRC-2012/3683, 81.9 mm SL, no gap between lachrymal and 2nd infraorbital bone present) **B.** *Lufubuchromis relictus* **sp. nov.** (Paratype, ZSM 44312, ID: DRC-2012/3249, 50.0 mm SL, no gap between lachrymal and 2nd infraorbital bone present) **C.** *Pseudocrenilabrus multicolor* (ZSM 40011, ID: Nr. 1, 46.0 mm SL) **D.** *Pseudocrenilabrus philander* (ZSM 40918, 58.9 mm SL) **E.** *Pseudocrenilabrus nicholsi* (ZSM 47140, ID: Nr. 1, 46.2 mm SL) **F.** *Pseudocrenilabrus pyyrochaudalis* (Paratype, MRAC-A7-034-P-0238-0247; ID: Nr.5, 64.2 mm SL) **G.** *Orthochromis machadoi* (BMNH 1984.2.6.104-108, ID: Nr. 1, 51.9 mm SL) **H.** *Haplochromis moeruensis* (Syntype, MRAC 216-222, ID: Nr. 222, 48.4 mm SL).

From the members of *Orthochromis s.s.* ("Malagarasi-*Orthochromis"* sensu Weiss *et al*. 2015) the new species can be distinguished by fewer dorsal-fin spines 14–15 (*Palaeoplex*) / 15–16 (*Lufubuchromis*) vs. 16–22, and by having more scales on cheek 2–4 (*Palaeoplex*) / 3–5 (*Lufubuchromis*) vs. 0–1 (Schedel *et al*. 2018).

Further, *Palaeoplex* and *Lufubuchromis* can be distinguished from *Ctenochromis pectoralis* Pfeffer 1893, the earliest splitting lineage of Haplochromini (e.g. Verheyen *et al*. 2003, Koblmüller *et al* 2008, Schedel *et al*. 2019), by having fused hypuralia 1+2 (in *Lufubuchromis* hypuralia 1+2 are either fused or fused with distinctly visible suture) and 3+4 vs. separate hypuralia (Greenwood 1979); both new taxa can be distinguished from *C. pectoralis* and other haplochromine cichlids originally placed by Greenwood 1979 in *Ctenochromis* by having no abrupt size transition between very small chest scales and larger ventrolateral anterior flank scales vs. abrupt size transition of scales sizes and by having a fully scaled chest vs. naked areas on chest in *C. pectoralis*.

From *Astatoreochromis* Pellegrin, 1904 both new taxa can be distinguished by having fewer dorsal fin spines 14–15 (*Palaeoplex*) / 15–16 (*Lufubuchromis*) vs. 16–20, and by having fewer anal fin spines 3 vs. 3–7 (Banyankimbona *et al*. 2013). From haplochromine cichlids placed by Greenwood (1979) in *Thoracochromis* both new taxa can be distinguished by having no abrupt size transition between very small chest scales and larger ventrolateral anterior flank scales vs. an abrupt size transition of scales sizes in these taxa (Greenwood 1979). Further, *Palaeoplex* and *Lufubuchromis* can be distinguished from haplochromine cichlids placed by Greenwood (1979) in *Astatotilapia* Pellegrin, 1904 and from *Haplochromis* Hilgendorf, 1888 by missing true ocelli on the anal fin; and further from Greenwood´s *Astatotilapia* by having more total gill rakers 12–17 (*Palaeoplex*) / 10–12 (*Lufubuchromis*) vs 8–9 (Greenwood 1979) and from *Haplochromis* by having fused hypuralia 1+2 (in *Lufubuchromis* hypuralia 1+2 are either fused or fused with distinctly visible suture) and 3+4 vs. non fused. From members of the megadiverse haplochromine Lake Malawi radiation they can be distinguished by the absence of any ocellate or non-ocellate anal fin mark, whether round or longitudinally arranged along anal fin rays vs. present (at least in most genera; Konings 2007, Eccles & Trewavas 1989).

Palaeoplex and *Lufubuchromis* are distinguished from members of the serranochromine lineage (sensu Greenwood 1993) by occurrence of ctenoid scales above the lateral line (Supplementary Fig 2. & 3), despite the fact that most scales are cycloid in these taxa) vs. cycloid scales above lateral line in serranochromines; and by the complete absence of non-ocellated anal fin markings vs. present in serranochromines.

Both new taxa are distinguished from *Haplochromis vanheusdeni* Schedel, Friel & Schliewen 2014 by having fewer dorsal fin spines, i.e. 14–15 (*Palaeoplex*) / 15–16 (*Lufubuchromis*) vs. 16–17; further *H. vanheusdeni* features true ocelli on the anal fin (Schedel *et al*. 2014). Finally, the two genera are distinguished from *Orthochromis indermauri* Schedel, Vreven, Katemo Manda, Abwe, Chocha Manda & Schliewen 2018 by having fewer dorsal fin spines 14–15 (*Palaeoplex*) / 15–16 (*Lufubuchromis*) vs. 17–18.

Discussion

With the description of *Palaeoplex* and *Lufubuchromis* which are representing early splitting members of the *Pseudocrenilabrus* group we provide a first step towards the overdue generic revision of this understudied haplochromine lineage. Nevertheless, the genus *Pseudocrenilabrus* needs to be critically revised as it appears to be presently paraphyletic with respect to the generic placement of *Orthochromis machadoi* and *Haplochromis moeruensis.* Both taxa were recovered to be nested within the genus *Pseudocrenilabrus* based on mitochondrial data with *O. machadoi* closely related to *Ps. philander* and with *H. moeruensis* being part of the "*Pseudocrenilabrus* Lake Mweru radiation" (Katongo *et al*. 2006; Koblmüller *et al*. 2008; Wagner *et al*. 2012, Meier *et al*. 2019). However, as long as no comprehensive phylogenetic hypothesis for all major haplochromine lineages and all known but yet undescribed *Pseudocrenilabrus* species, based, e.g., on nuclear data and a fully comprehensive haplochromine taxon sampling is available, we refrain from transferring those two taxa to the genus *Pseudocrenilabrus.* This conservative approach seems further justified as both taxa might have been subject to ancient hybridization events, and thus might have to be placed into their own hybrid origin lineages. Furthermore, the species *Pseudocrenilabrus philander* as currently interpreted undoubtedly represents a species complex (known as the *Pseudocrenilabrus philander* species complex, Katongo *et al*. 2005), an inference which is not only based on mitochondrial data (see Katongo *et al*. 2005, Koblmüller *et al*. 2012, Egger *et al*. 2014), but which also became apparent in the present study. We investigated ten populations from a wide range of its distribution, including the types of *Ps. philander* and *Ps. philander dispersus. S*everal populations revealed to be distinct, and might represent distinct species, but need additional comparative

study. The most obvious case here is the one of *Pseudocrenilabrus*. sp. "Upper Kalungwishi". Additional highly distinct *Ps. philander*-like phenotypes have recently been discovered by the "Mbisa Congo" team of the Africa Museum (Tervuren, Belgium), the South African Institute of Aquatic Biodiversity team (Grahamstown, South Africa) and by us (ZSM), all of which should be considered. Thus, it would have been premature to implement taxonomical implications concerning the *Ps. philander* species complex at this point, as this would require a larger sample set incorporating populations of the entire distribution range, but also including genetic data for the corresponding populations.

The description of *Palaeoplex palimpsest* is based on specimens collected from different locations along the Luongo and the Kalungwishi River. The apparent close affinity of the two populations is adding support to the notion that the Kalungwishi River and the Luongo River once were connected, or still are via the Luena Veld as suggested by Balon *et al*. (1983). However, *Palaeoplex* were neither collected in the uppermost reaches of the Kalungwishi River (i.e., above the rapids near Shimilungu Village -9.813650°/ 29.880345°) nor in the uppermost Luongo River (i.e., neither above nor below the Mumbuluma falls -10.109617°/29.575728°), and the same holds true for the sympatric *O. kalungwishiensis* and *O. luongoensis* (present below Mumbuluma falls). We have restricted the type series to specimens from the Luongo River, and listed the Kalungwishi specimens under "additional specimens". This, because preliminary genetic analysis based on mitochondrial genome data and ddRAD loci (Schedel & Schliewen, in prep) tentatively suggest that both populations are genetically differentiated. However, neither PCA analyses based on log-transformed morphometric measurements nor those based on meristic characters revealed characters differentiating the two populations from each other, except that the Kalungwishi River specimens have tentatively fewer circumpeduncular scales (see table 3). Further, the adult breeding coloration of the Kalungwishi River population is insufficiently documented, although the male nuptial coloration appears to include more reddish elements (F. Schedel, pers. obs.). Three larger waterfalls, i.e. Lumangwe, Kabwelume, and Kundabwika Falls, separate the course of the Kalungwishi River into various sections. The waterfalls potentially represent barriers to gene flow for different species/populations of *Palaeoplex,* which have been collected from different river sections, rendering the taxonomical evaluation of the Kalungwishi River populations even more complex (Meier *et al*. 2019). Therefore, we have here refrained from describing *Palaeoplex* population(s) as separate species at this stage, but additional material is currently being examined and new collections are planned to obtain additional specimens, particularly adult males (Katongo *et al*., in prep.).

Recently, *Orthochromis indermauri* has been described from the lower reaches of the Lufubu River, where it appears to be endemic. Interestingly, it represents a different ancient mitochondrial haplotype lineage within the megadiverse Haplochromini (Schedel *et al*. 2019). *Lufubuchromis relictus* is the second endemic cichlid species described from the Lufubu but appears to be restricted to the upper reaches of the Lufubu and its tributaries. Furthermore, there are at least two undescribed cichlid species present in the Lufubu drainage system, *Telmatochromis* sp. "Lufubu", restricted to the lower reaches of the Lufubu (Indermaur 2014), and *Serranochromis* sp. "Lufubu", currently documented only from a single location in the upper reaches of the Lufubu River (Koblmüller *et al*. 2012). The striking difference in the ichthyofaunal composition of the Upper and Lower Lufubu River has been suggested to be the result of several cascades and waterfalls prohibiting upstream and, possibly, downstream migration, which could explain the absence of *Lufubuchromis* in the lower reaches of the river (Koblmüller *et al*. 2012).

Acknowledgements

We cordially thank James MacLaine (BMNH), Miguel Parrent (MRAC), Willy Baudouin (MRAC) and Roger Bills (SAIAB) for their efforts with loan arrangements for comparative specimens. We thank Albert Chakona (SAIAB) for the kind reception at SAIAB and the provision of specimens. Dirk Neumann (ZSM) is kindly acknowledged for his highly dedicated collection management at ZSM. Moreover, we are grateful to Hans van Heusden and Adrian Indermaur for fieldwork including countless fruitful discussions and their inspiring enthusiasm. Further we would like to thank Fenton P. D. Cotterill (Univ. Stellenbosch), for his support during the 2015 Zambian field trip, and for fruitful discussions on geoecodynamics. He is the one who coined the word "palaeoplex" and has put the word "palimpsest" into the context of geoecodynamics. Moreover, we want to thank Alex D. Chilala (Provincial Agricultural Coordinator, Western Province, Republic of Zambia) for his help during the 2015 Zambian field trip and the organization of the export permits (issued on 05.10.2015 in Kasama by the Ministry of Agriculture and Livestock;

Department of Fisheries Provincial Fisheries Office). Last but not least we would like to thank our donors: UKS and FS are funded by the Volkswagen-Stiftungs project "Exploiting the genomic record of living biota to reconstruct the landscape evolution of South-Central Africa."

References

Altner, M., Schliewen, U.K., Penk, S.B.R. & Reichenbacher, B. (2017) †*Tugenchromis pickfordi*, gen. et sp. nov., from the upper Miocene—a stem-group cichlid of the 'East African Radiation'. *Journal of Vertebrate Paleontology*, 37, e1297819. https://doi.org/10.1080/02724634.2017.1297819

Barel, C.D.N., van Oijen, M.J.P., Witte, F. & Witte-Maas, E.L.M. (1977) An introduction to the taxonomy and morphology of the haplochromine Cichlidae from Lake Victoria. *Netherlands Journal of Zoology*, 27 (4), 333–389. https://doi.org/10.1163/002829677X00199

Balon, E.K. & Stewart, D.J. (1983) Fish assemblage in a river with unusual gradient (Luongo, Africa Zaire system), reflections on river zonation, and description of another new species. *Environmental Biology of Fishes*, 9, 225–252. https://doi.org/10.1007/BF00692373

Boulenger, G.A. (1899a) Matériaux pour la faune du Congo. Poissons nouveaux du Congo. Cinquième Partie. Cyprins, Silures, Cyprinodontes, Acanthoptérygiens. *Annales du Musée du Congo*, Series Zoology, 1 (5), 97–128.

Boulenger, G. A. (1899b) Second contribution to the ichthyology of Lake Tanganyika.– On the fishes obtained by the Congo Free State Expedition under Lieut. Lemaire in 1898. *Transactions of the Zoological Society of London*, 15 (4, 1), 87–96. https://doi.org/10.1111/j.1096-3642.1899.tb00020.x

Banyankimbona, B., Vreven, E.J. & Snoeks, J. (2013) A revision of the genus *Astatoreochromis* (Teleostei, Cichlidae), East-Africa. *European Journal of Taxonomy*, 39, 1–21. https://doi.org/10.5852/ejt.2013.39

Cotterill, F.P.D. & De Wit, M.J. (2011) Geoecodynamics and the Kalahari epeirogeny: linking its genomic record, tree of life and palimpsest into a unified narrative of landscape evolution. *South African Journal of Geology*, 114 (3–4), 489–514. https://doi.org/10.2113/gssajg.114.3-4.489

De Vos, L. (1998) Fish diversity in the Lake Tanganyika system with emphasis on the Rusizi basin in the north and the Lufubu system in the south. *Book of abstracts of the International Conference for the Paradi Association and the Fisheries Society of Africa (FISA), Grahamstown, South Africa*, September 1998, 30.

Dunz, A. & Schliewen, U.K. (2013) Molecular phylogeny and revised classification of the haplotilapiine cichlid fishes formerly referred to as "*Tilapia*". *Molecular Phylogenetics and Evolution*, 68 (1), 64–80. https://doi.org/10.1016/j.ympev.2013.03.015

Eccles D.H. & Trewavas, E. (1989) *Malawian Cichlid fishes. The classification of some Haplochromine genera*. Lake Fish Movies, Herten, West Germany, 335 pp.

Fowler, H.W. (1934) Fishes obtained by Mr. H. W. Bell-Marley chiefly in Natal and Zululand in 1929 to 1932. *Proceedings of the Academy of Natural Sciences of Philadelphia*, 86, 405–514.

Egger, B., Klaefiger, Y., Indermaur, A., Koblmueller, S., Theis, A., Egger, S, Naef, T., Van Steenberge, M., Sturmbauer, C., Katongo, C. & Salzburger, W. (2014) Phylogeographic and phenotypic assessment of a basal haplochromine cichlid fish from Lake Chila, Zambia. *Hydrobiologia*, 748 (1), 171–184. https://doi.org/10.1007/s10750-014-1919-0

Greenwood, P.H. (1979) Towards a phyletic classification of the 'genus' *Haplochromis* (Pisces, Cichlidae) and related taxa. Part I. *Bulletin of the British Museum (Natural History)*, Zoology Series, 35, 265–322. https://doi.org/10.5962/bhl.part.20455

Greenwood, P.H. (1989) The taxonomic status and phylogenetic relationships of *Pseudocrenilabrus* Fowler (Teleostei, Cichlidae). *Ichthyological Bulletin of the J. L. B. Smith Institute of Ichthyology*, 54, 1–16.

Greenwood, P.H. (1993) A review of the serranochromine cichlid fish genera *Pharyngochromis*, *Sargochromis*, *Serranochromis* and *Chetia* (Teleostei: Labroidei). *Bulletin of the Natural History Museum Zoology*, 59 (1), 33–44.

Greenwood, H.P. & Kullander, S.O. (1994) A taxonomic review and redescription of *Tilapia polyacanthus* and *T. stormsi* (Teleostei: Cichlidae), with descriptions of two new *Schwetzochromis* species from the Upper Zaire River drainage. *Ichthyological Exploration of Freshwaters*, 5 (1), 161–180.

Hammer, Ø., Harper, D.A.T. & Ryan, P.D. (2001) PAST: Paleontological statistics software package for education and data analysis. *Palaeontologia Electronica*, 4 (1), 9.

Hilgendorf, F.M. (1888) Fische aus dem Victoria-Nyanza (Ukerewe-See), gesammelt von dem verstorbenen Dr. G. A. Fischer. *Sitzungsberichte der Gesellschaft Naturforschender Freunde zu Berlin*, 1888, 75–79.

Hilgendorf, F.M. (1902) Neue Chromiden-Art aus Deutsch Südwestafrika. *Sitzungsberichte der Gesellschaft Naturforschender Freunde zu Berlin,* 1902, 141–143.

Indermaur, A. (2014) Über den Tellerrand geschaut—Buntbarsche aus dem Lufubu. *Die Aquarien- und Terrarien-Zeitschrift, DATZ*, 2014 (10), 16–23.

Katongo, C., Koblmüller, S., Duftner, N., Makasa, L. & Sturmbauer, C. (2005) Phylogeography and speciation in the *Pseudo-*

crenilabrus philander species complex in Zambian rivers. *Hydrobiologia*, 542, 221–233.
https://doi.org/10.1007/s10750-004-1389-x
Katongo, C., Schneider, V., Stelkens, R., Joyce, D.A. & Seehausen, O. (2006) A new adaptive radiation of cichlid fish in a poorly known African Great Lake: Mweru. *Conference: International Symposium on Speciation in Ancient lakes*, SIAL IV, Free University of Berlin, Berlin. Available from: http://www.sial-online.org/index.php/conferences/sial4 (accessed 19 November 2019)
Katongo, C., Seehausen, O. & Snoeks, J. (2017) A new species of *Pseudocrenilabrus* (Perciformes: Cichlidae) from Lake Mweru in the Upper Congo River System. *Zootaxa*, 4237 (1), 181–191.
https://doi.org/10.11646/zootaxa.4237.1.10
Koblmüller, S., Schliewen, U.K., Duftner, N., Sefc, K.M., Katongo, C. & Sturmbauer, C. (2008) Age and spread of the haplochromine cichlid fishes in Africa. *Molecular Phylogenetics and Evolution*, 49, 153–169.
https://doi.org/10.1016/j.ympev.2008.05.045
Koblmüller, S., Katongo, C., Phiri, H. & Sturmbauer, C. (2012) Past Connection of the Upper Reaches of a Lake Tanganyika Tributary with the Upper Congo Drainage Suggested by Genetic Data of Riverine Cichlid Fishes. *African Zoology*, 47 (1), 182–186.
https://doi.org/10.3377/004.047.0115
Konings, A. (2007*) Malawi Cichlids in their natural habitat. 4th Edition*. Cichlid Press, El Paso, 424 pp.
Matschiner, M., Musilová, Z., Barth, J.M.I., Starostova, Z., Salzburger, W., Steel, M. & Bouckaert, R. (2016) Bayesian Phylogenetic Estimation of Clade Ages Supports Trans-Atlantic Dispersal of Cichlid Fishes. *Systematic Biology*, 66, 3–22.
https://doi.org/10.1093/sysbio/syw076
Matthes, H. (1962) Poissons nouveaux ou intéressants du lac Tanganika et du Ruanda. *Annales, Musée royal de l'Afrique centrale, Tervuren*, Série in 8°, Sciences Zoologiques, 111, 27–88.
Meier, J.I., Marques, D.A., Mwaiko, S., Wagner, C.E., Excoffier, L. & Seehausen, O. (2017) Ancient hybridization fuels rapid cichlid fish adaptive radiations. *Nature Communications*, 8,14363.
https://doi.org/10.1038/ncomms14363
Meier, J.I., Stelkens, R., Joyce, D., Mwaiko, S., Phiri, N., Schliewen, U.K., Selz, O., Wagner, C., Katongo, C. & Seehausen, L. (2020) The coincidence of ecological opportunity with hybridization explains rapid adaptive radiation in Lake Mweru cichlids. *Nature Communications*, 10, 5391.
https://doi.org/10.1038/s41467-019-13278-z
Pellegrin, J. (1904) Contribution à l'étude anatomique, biologique et taxinomique des poissons de la famille des Cichlidés. *Mémoires de la Société Zoologique de France*, 16 (No. 2–4), 41–400 + 4–7.
Pellegrin, J. (1928) Mutanda ichthyologica. 2. *Paratilapia ventralis* Nichols. *Revue de Zoologie et de Botanique Africaines*,16 (1), 1.
Penk, S.B.R., Altner, M., Cerwenka, A.F., Schliewen, U.K. & Reichenbacher, B. (2019) New fossil cichlid from the middle Miocene of East Africa revealed as oldest known member of the Oreochromini. *Scientific reports*, 9 (1),10198.
https://doi.org/10.1038/s41598-019-46392-5
Pfeffer, G. (1893) Ostafrikanische Fische gesammelt von Herrn Dr. F. Stuhlmann in Jahre 1888 und 1889. *Jahrbuch der Hamburgischen Wissenschaftlichen Anstalten*, 10, 131–177.
Poll, M. (1967) Contribution à la faune ichthyologique de l'Angola. *Publicações Culturais, Companhia de Diamantes de Angola (DIAMANG*), Lisboa, 75, 1–381, pls. 1–20.
Poll, M. (1986) Classification des Cichlidae du lac Tanganyika Tribus, genres et espèces, *Académie Royale de Belgique Mémoires de la Classe des Sciences*, Séries 2, 45, 1–163.
Regan, C.T. (1920) The classification of the fishes of the family Cichlidae.—I. The Tanganyika genera. *Annals and Magazine of Natural History*, Series 9, 5 (25), 33–53.
https://doi.org/10.1080/00222932008632340
Salzburger, W., Meyer, A., Baric, S., Verheyen, E. & Sturmbauer, C. (2002) Phylogeny of the Lake Tanganyika cichlid species flock and its relationships to the Central and East African haplochromine cichlid fish faunas. *Systematic Biology*, 51, 113– 135.
https://doi.org/10.1080/106351502753475907
Schedel, F.D.B., Friel, J.P. & Schliewen, U.K. (2014) *Haplochromis vanheusdeni*, a new haplochromine cichlid species from the Great Ruaha River drainage, Rufiji basin, Tanzania (Teleostei, Perciformes, Cichlidae). *Spixiana*, 37 (1), 135–149.
Schedel, F.D.B. & Schliewen, U.K. (2017) *Hemibates koningsi* spec. nov: a new deep-water cichlid (Teleostei: Cichlidae) from Lake Tanganyika. *Zootaxa*, 4321 (1), 92–112.
https://doi.org/10.11646/zootaxa.4312.1.4
Schedel, F.D.B., Vreven, E.J.W.M.N., Katemo Manda, B.l., Abwe, E., Chocha Manda, A. & Schliewen, U.K. (2018) Description of five new rheophilic *Orthochromis* species (Teleostei: Cichlidae) from the Upper Congo drainage in Zambia and the Democratic Republic of the Congo. *Zootaxa*, 4461 (3), 301–349.
https://doi.org/10.11646/zootaxa.4464.3.1
Schedel, F.D.B., Musilova, Z. & Schliewen, U.K. (2019) East African cichlid lineages (Teleostei: Cichlidae) might be older than their ancient host lakes: new divergence estimates for the east African cichlid radiation. *BMC Evolutionary Biology*, 19 (94). [published online]

https://doi.org/10.1186/s12862-019-1417-0
Schliewen, U.K. & Stiassny, M.L.J. (2003) *Etia nguti*, a new genus and species of cichlid fish from the River Mamfue, Upper Cross River basin in Cameroon, West-Central Africa. *Ichthyological Explorations of Freshwaters*, 14 (1), 61–75.
Seegers, L. (1990) Bemerkungen zur Gattung *Pseudocrenilabrus* Teil 2: *Pseudocrenilabrus multicolor victoriae* nov. subsp. *Die Aquarien- und Terrarienzeitschrift, DATZ*, 43 (2), 99–103.
Skelton, P.H. (2001) *A complete guide to the freshwater fishes of Southern Africa*. *Struik Nature, Cape Town, South Africa*, 395 pp.
Schöller, C.H. (1903) Ein neuer *Chromis* (Schluß). *Blätter für Aquarien- und Terrarienkunde*, 14 (15), 203–206.
Takahashi, T. (2003a) Comparative osteology of the infraorbitals in cichlid fishes (Osteichthyes: Teleostei: Perciformes) from Lake Tanganyika. *Species Diversity*, 8, 1–26.
https://doi.org/10.12782/specdiv.8.1
Takahashi, T. (2003b) Systematics of Tanganyikan cichlid fishes (Teleostei: Perciformes). *Ichthyological Research*, 50 (4), 367–382.
https://doi.org/10.1007/s10228-003-0181-7
Trewavas, E. (1936) Dr. Karl Jordan's expedition to South-West Africa and Angola: The fresh-water fishes. Novitates Zoologicae. *A Journal of Zoology in Connection with the Tring Museum*, 40 (1–2), 63–74.
Trewavas, E. (1973) A new species of cichlid fishes of rivers Quanza and Bengo, Angola, with a list of the known Cichlidae of these rivers and a note on *Pseudocrenilabrus natalensis* Fowler. *Bulletin of the British Museum (Natural History) Zoology,* 25 (1), 27–37.
Weber, M. (1897) Beiträge zur Kenntniss der Fauna von Süd-Afrika. I. Zur Kenntniss der Süsswasser-Fauna von Süd-Afrika. *Zoologische Jahrbücher, Abteilung für Systematik, Geographie und Biologie der Tiere, Jena*, 10, 135–155.
Verheyen, E., Salzburger, W., Snoeks, J. & Meyer, A. (2003) Origin of the superflock of cichlid fishes from Lake Victoria, East Africa. *Science*, 300 (5617), 325–329.
https://doi.org/10.1126/science.1080699
Wagner, C.E., Harmon, L.J. & Seehausen, O. (2012) Ecological opportunity and sexual selection together predict adaptive radiation. *Nature*, 487, 366–369.
https://doi.org/10.1038/nature11144
Weiss, J.D., Cotterill, F.PD. & Schliewen, U.K. (2015) Lake Tanganyika—A 'Melting Pot' of ancient and young cichlid lineages (Teleostei: Cichlidae)? *PLOS ONE*, 10, e0125043.
https://doi.org/10.1371/journal.pone.0125043
Wickler, W. (1963) Zur Klassifikation der Cichlidae, am Beispiel der Gattung Tropheus, Petrochromis, Haplochromis und Hemihaplochromis n. gen. (Pisces, Perciformes). *Senckenbergiana Biologica*, 44 (2), 83–96.

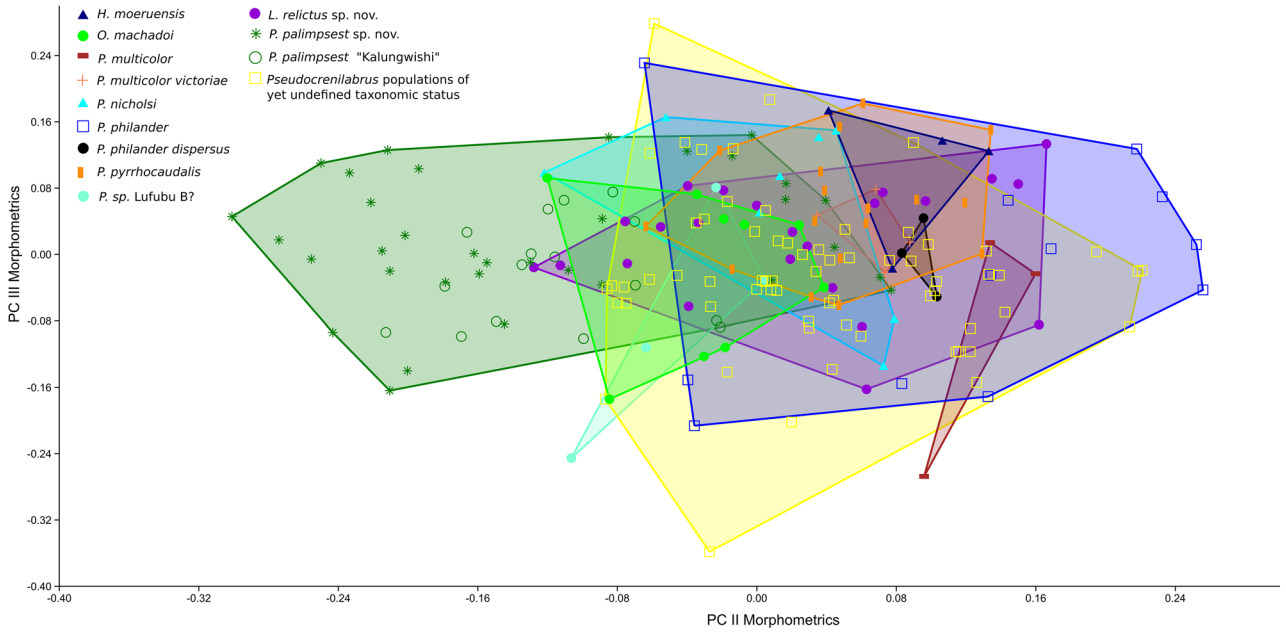

SUPPLEMENTARY FIGURE 1. PCA scatter plot based on 20 morphometric measurements, species score limits visualized as convex hulls (N=203). PCII vs. PCIII. PC II explains 1.95 % of the variance while PC II explains 1.38 %.

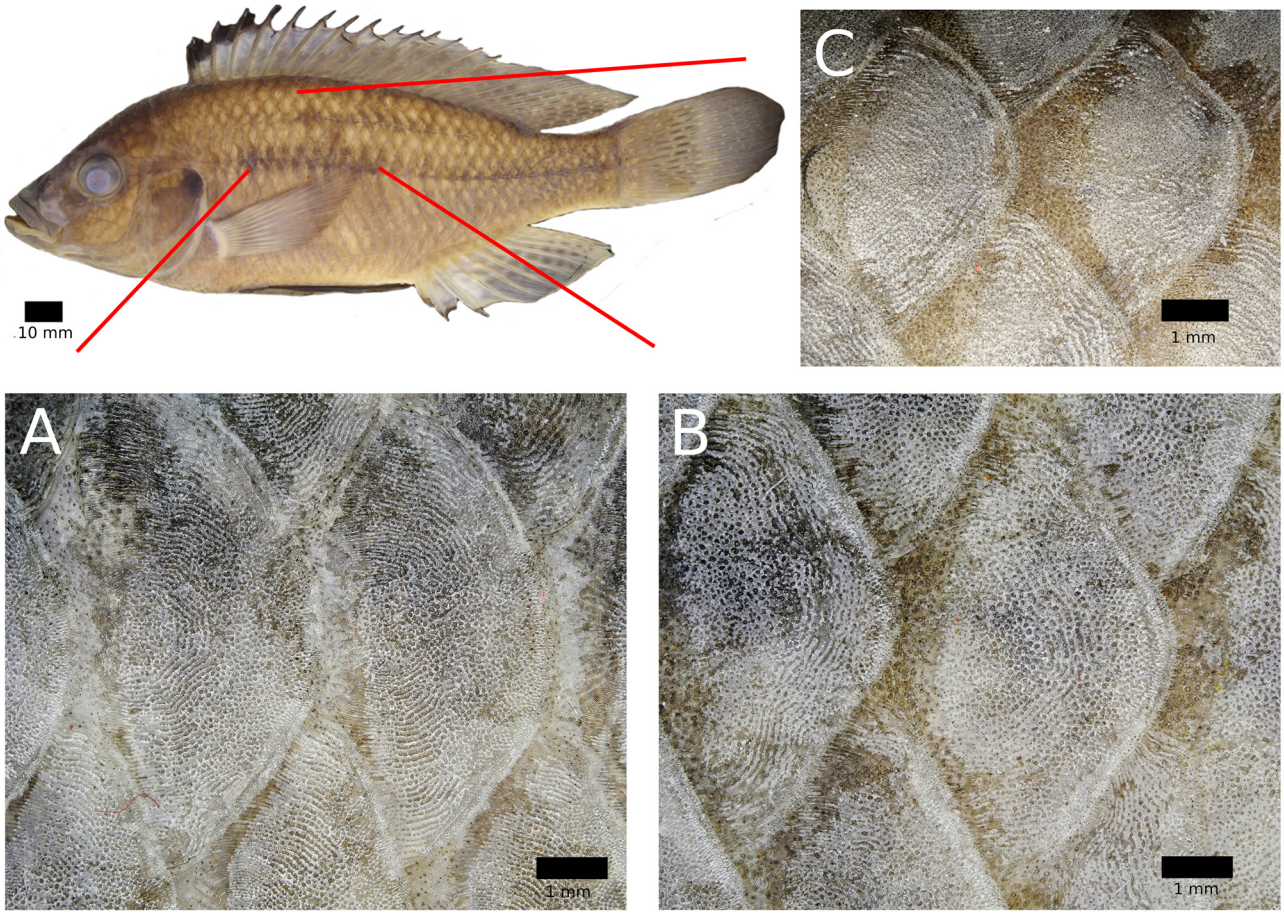

SUPPLEMENTARY FIGURE 2. Scales of *Palaeoplex palimpsest* (holotype); red lines indicating depicted areas; the contrast of scale pictures was slightly enhanced **A.** Ctenoid scales on the horizontal line (area around the 24th horizontal line scale; counted from posterior to anterior) **B.** Ctenoid scales on the horizontal line (area around the 17th horizontal line scale; counted from posterior to anterior) **C.** Ctenoid to cycloid scales above upper lateral line (area around 8th upper lateral line scale; counted from anterior to posterior).

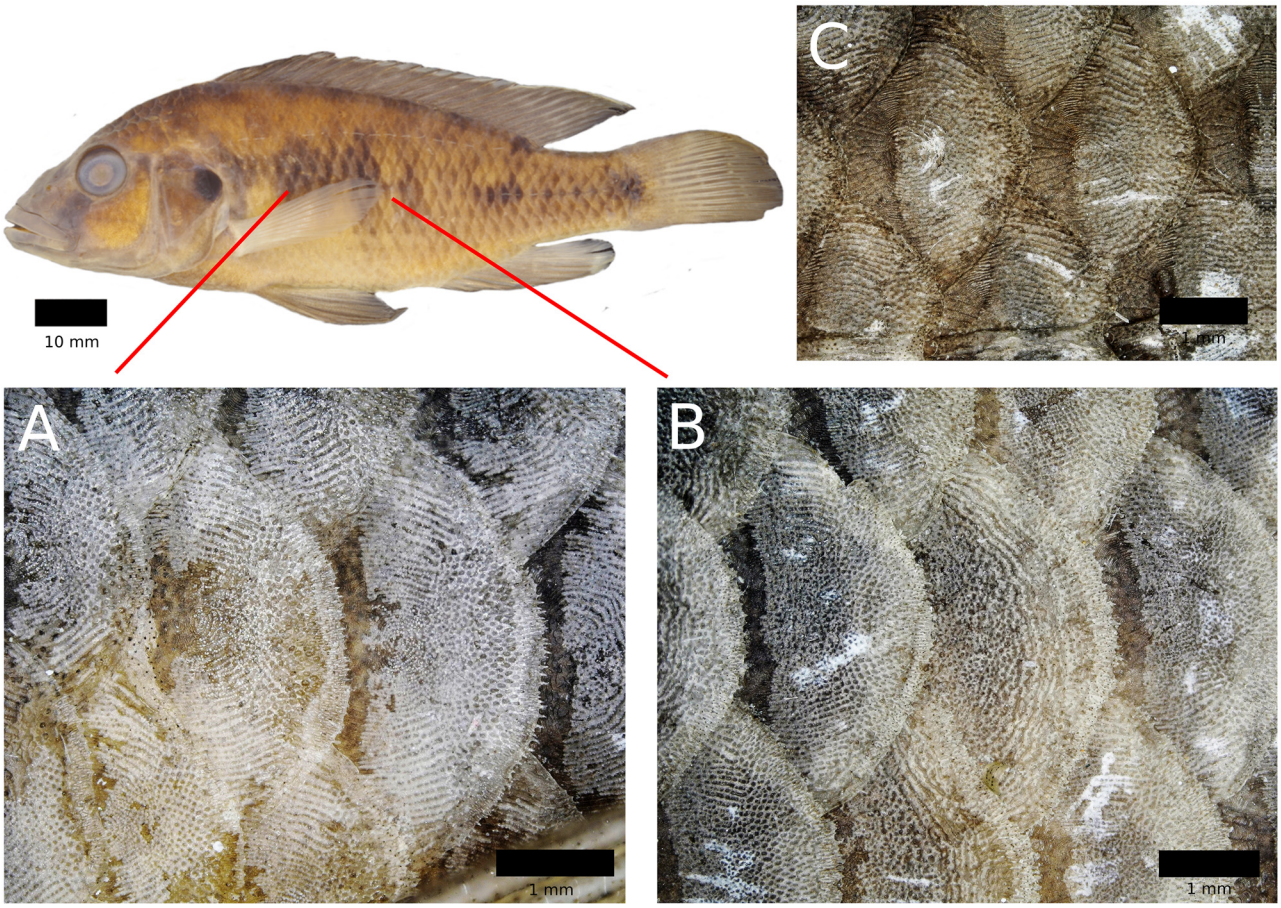

SUPPLEMENTARY FIGURE 3. Scales of *Lufubuchromis relictus* (holotype); red lines indicating depicted areas; the contrast of scale pictures was slightly enhanced **A.** Ctenoid scales on the horizontal line (area around the 23rd horizontal line scale; counted from posterior to anterior) **B.** Ctenoid scales on the horizontal line (area around the 17th horizontal line scale; counted from posterior to anterior) **C.** Ctenoid to cycloid scales above upper lateral line (area around 11th upper lateral line scale; counted from anterior to posterior; picture taken from the righthand side of the specimen).

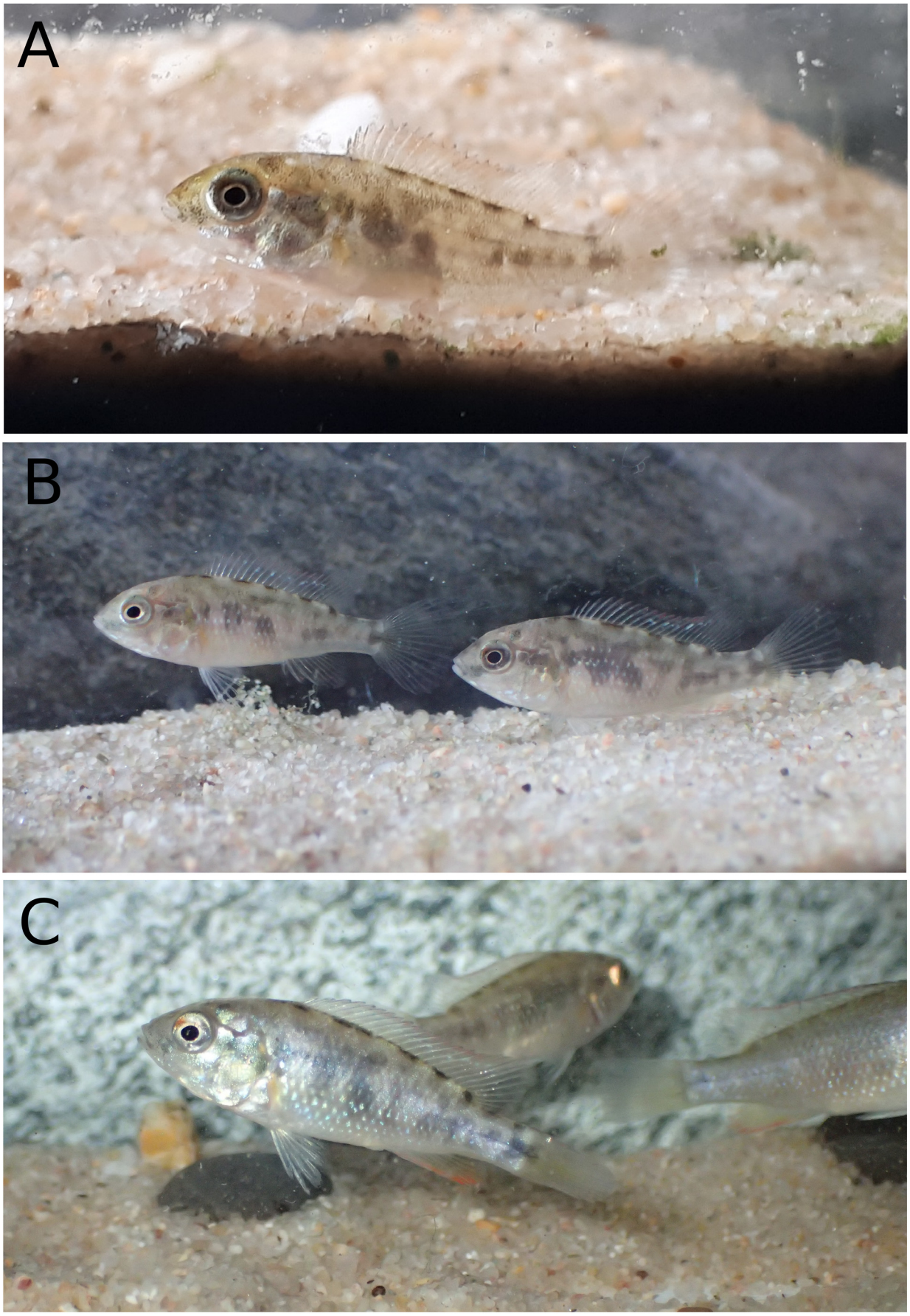

SUPPLEMENTARY FIGURE 4. Live Pictures of juvenile *Lufubuchromis relictus*. **A.** captive raised juvenile about 14.8 mm SL **B.** captive raised juvenile about 17.5 mm SL **C**. captive raised juvenile about 21.5 mm SL.

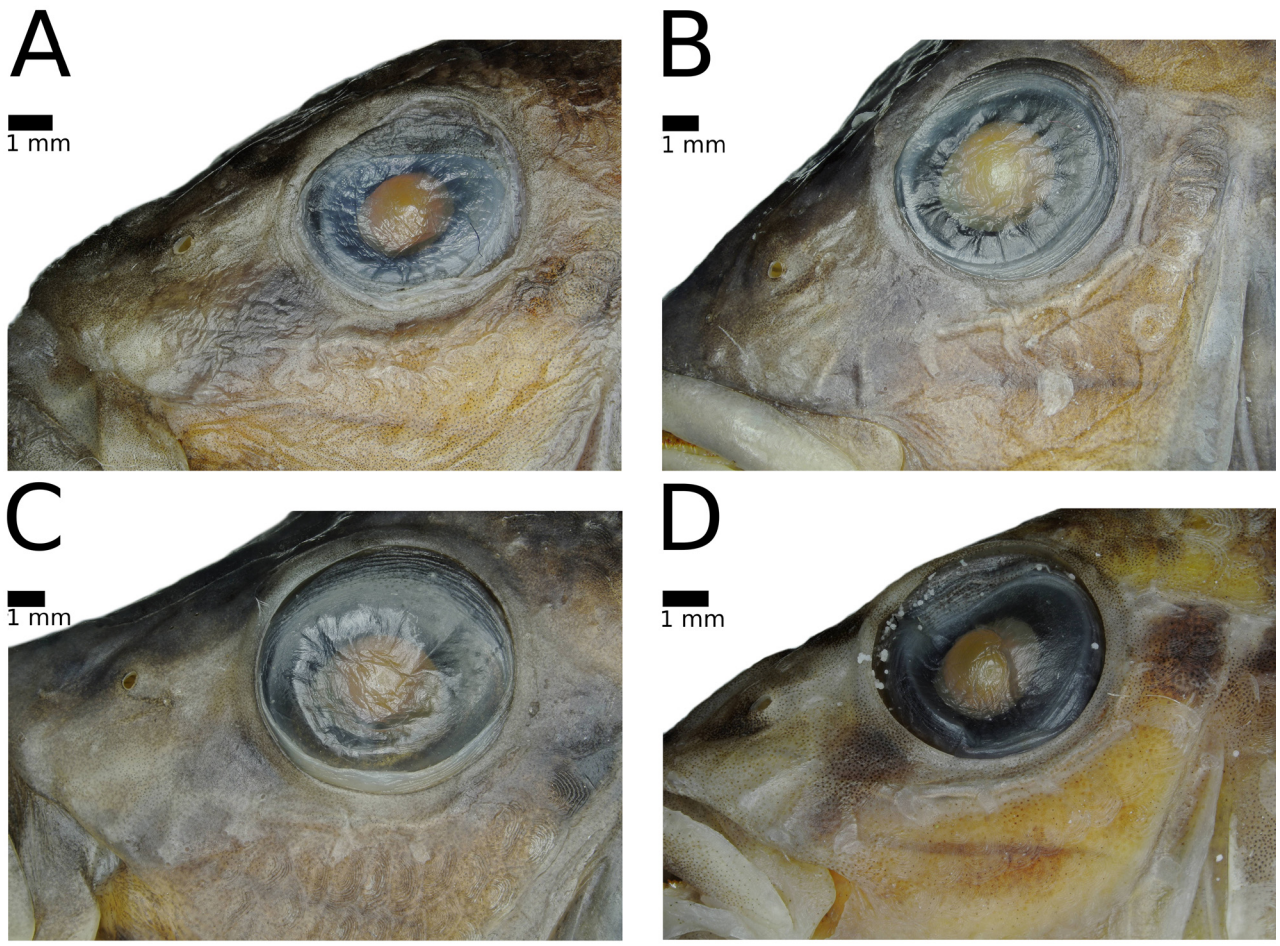

SUPPLEMENTARY FIGURE 5. Overview of snout and infraorbital area of the four Northern Zambian *Orthochromis* sensu Weiss *et al*. 2015: **A.** *Orthochromis kalungwishiensis* (ZSM 44369, ID: DRC-2012/3433, 69.8 mm SL) **B.** *Orthochromis katumbii,* (Paratype, ZSM 46844, ID: 2808, 81.8 mm SL) **C.** *Orthochromis luongoensis* (ZSM 44432, ID: DRC-2012/3669, 88.0 mm SL) **D.** *Orthochromis mporokoso* (Holotype, ZSM 46840, 59.0 mm SL).

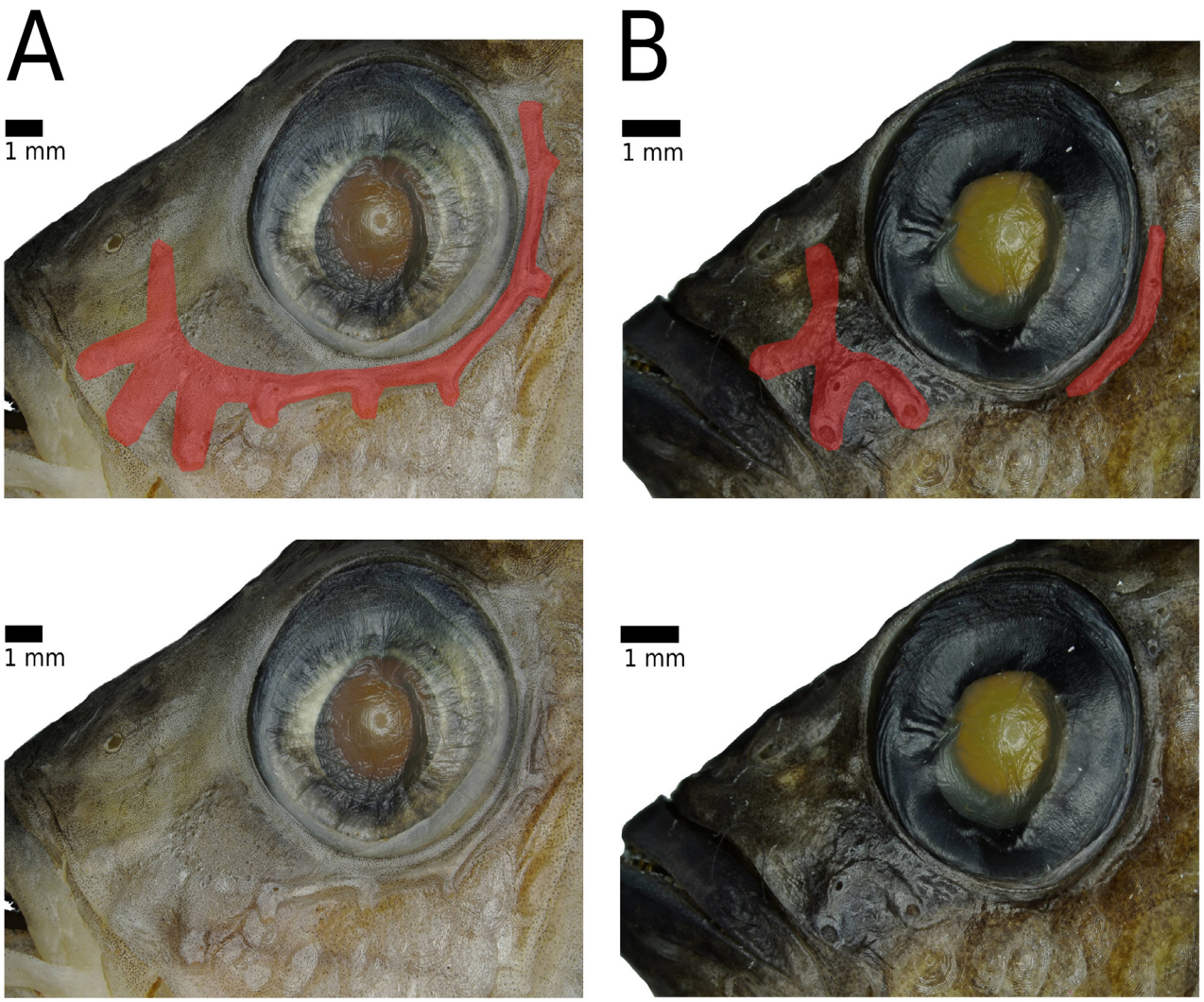

SUPPLEMENTARY FIGURE 6. Overview of snout with highlighted infraorbital series **A.** *Paleoplex palimpsest* **sp. nov**. (Paratype, ZSM 44438, ID: DRC-2012/3683, 81.9 mm SL, no gap between lachrymal and 2nd infraorbital bone present) **B.** *Pseudocrenilabrus nicholsi* (ZSM 47140, ID: Nr. 1, 46.2 mm SL).

SUPPLEMENTARY TABLE 1. Factor loadings of PCA based on 20 morphometric measurements. PCI-III for all examined specimens (N=203, see Supplementary Fig. 1). Highest loadings for each principal component are indicated in boldface.

Morphometric measurements (Log transformed)	PC 1	PC 2	PC 3
Standard length (Log)	0.21987	-0.051674	-0.018623
Head length (Log)	0.19499	0.067962	-0.094968
Interorbital width (Log)	0.22353	-0.066402	-112
Preorbital width (Log)	0.23918	0.10644	-0.096048
Horizontal eye length (Log)	0.16701	-0.10503	-0.012765
Snout length (Log) SnL	**0.23928**	0.061354	**-0.14533**
Internostril distance (Log)	0.22679	0.039011	0.040389
Cheek depth (Log)	0.23773	**0.43224**	**-0.13138**
Upper lip length (Log)	0.22367	0.30609	-0.063715
Lower lip length (Log)	0.22505	0.2877	-0.0034675
Lower jaw length (Log)	0.19919	0.16403	-0.066961
Predorsal distance (Log)	0.20241	0.014482	-0.099135
Dorsal fin base length (Log)	0.2378	-0.076967	-0.0061471
Last dorsal fin spine length (Log)	**0.27412**	**-0.52159**	0.10152
Anal fin base length (Log)	0.23415	-0.065393	-0.00043173
Third anal fin spine length (Log)	0.23102	**-0.49452**	0.0015095
Pectoral fin length (Log)	**0.24347**	-0.12629	-0.0046514
Body depth (Log)	0.22106	1.6083E-05	-0.070937
Preanal length (Log)	0.21437	-0.00381	-0.073614
Anus-anal fin base distance (Log)	0.19511	0.16574	**0.94313**
Eigenvalue	0.587466	0.0123204	0.00870962
% variance	93.125	1.953	1.3806

Section 2: New divergence age estimates for the major cichlid lineages with focus on the African austrotilapiine cichlids

Orthochromis gecki in the natural habitat (Lubudi River)

BMC Evolutionary Biology

RESEARCH ARTICLE Open Access

East African cichlid lineages (Teleostei: Cichlidae) might be older than their ancient host lakes: new divergence estimates for the east African cichlid radiation

Frederic Dieter Benedikt Schedel[1], Zuzana Musilova[2] and Ulrich Kurt Schliewen[1*]

Abstract

Background: Cichlids are a prime model system in evolutionary research and several of the most prominent examples of adaptive radiations are found in the East African Lakes Tanganyika, Malawi and Victoria, all part of the East African cichlid radiation (EAR). In the past, great effort has been invested in reconstructing the evolutionary and biogeographic history of cichlids (Teleostei: Cichlidae). In this study, we present new divergence age estimates for the major cichlid lineages with the main focus on the EAR based on a dataset encompassing representative taxa of almost all recognized cichlid tribes and ten mitochondrial protein genes. We have thoroughly re-evaluated both fossil and geological calibration points, and we included the recently described fossil †*Tugenchromis pickfordi* in the cichlid divergence age estimates.

Results: Our results estimate the origin of the EAR to Late Eocene/Early Oligocene (28.71 Ma; 95% HPD: 24.43–33.15 Ma). More importantly divergence ages of the most recent common ancestor (MRCA) of several Tanganyika cichlid tribes were estimated to be substantially older than the oldest estimated maximum age of the Lake Tanganyika: Trematocarini (16.13 Ma, 95% HPD: 11.89–20.46 Ma), Bathybatini (20.62 Ma, 95% HPD: 16.88–25.34 Ma), Lamprologini (15.27 Ma; 95% HPD: 12.23–18.49 Ma). The divergence age of the crown haplochromine H-lineage is estimated to 22.8 Ma (95% HPD: 14.40–26.32 Ma) and of the Lake Malawi radiation to 4.07 Ma (95% HDP: 2.93–5.26 Ma). In addition, we recovered a novel lineage within the Lamprologini tribe encompassing only *Lamprologus* of the lower and central Congo drainage with its divergence estimated to the Late Miocene or early Pliocene. Furthermore we recovered two novel mitochondrial haplotype lineages within the Haplochromini tribe: '*Orthochromis*' *indermauri* and '*Haplochormis*' *vanheusdeni*.

Conclusions: Divergence time estimates of the MRCA of several Tanganyika cichlid tribes predate the age of the extant Lake Tanganyika basin, and hence are in line with the recently formulated "Melting-Pot Tanganyika" hypothesis. The radiation of the 'Lower Congo *Lamprologus* clade' might be linked with the Pliocene origin of the modern lower Congo rapids as has been shown for other Lower Congo cichlid assemblages. Finally, the age of origin of the Lake Malawi cichlid flock agrees well with the oldest age estimate for lacustrine conditions in Lake Malawi.

Keywords: East African cichlid radiation (EAR), Molecular clock, Lamprologini, Congo River, African Great Lakes, *Tugenchromis*

* Correspondence: schliewen@snsb.de
[1]Department of Ichthyology, SNSB - Bavarian State Collection of Zoology, Münchhausenstr. 21, 81247 Munich, Germany
Full list of author information is available at the end of the article

Background

The exceptional diversity and propensity to generate adaptive radiations have made cichlid fishes one of the most important vertebrate model systems for evolutionary biology research [1–4]. Much effort has been invested in the reconstruction of the evolutionary time scale and biogeographic history of cichlids distributed in the Americas, Africa, the Middle East, Madagascar and the Indian subcontinent [5–9]. The primary focus has been on the biogeographic origin of the cichlids from the so-called East African Radiation (EAR), i.e., the clade that comprises the famous megadiverse radiations of the East African Lakes Tanganyika (LT), Malawi (LM) and Victoria (LV). Nevertheless, there remains debate over the divergence age estimates of their origin, as well as a lack of a precise reconstruction of their paleogeographic environments providing the stage for these spectacular radiations. One of the reasons is that unambiguous and important calibration points for molecular clock estimates, e.g. a consolidated root age of the family Cichlidae or a lack of cichlid fossils within EAR with the phylogenetically clear position.

Two major hypotheses relating to the problem of the cichlid root age have been proposed, i.e., the *Vicariance Hypothesis* and the *Dispersal Hypothesis*. The former places the cichlid origin before the Gondwana fragmentation and is supported by evidence for reciprocally monophyletic cichlid lineages on in Africa (Pseudocrenilabrinae) and the Americas (Cichlinae), a pattern that is more difficult to envisage under the second hypothesis. This postulates a marine dispersal of early cichlids after tectonic separation of South America, Africa and Madagascar and is supported by the fact, that the oldest cichlid fossil, †*Mahengechromis*, is of only Eocene age (approx. 46 Ma, [10]). Both the Gondwana divergence date based on tectonics as well as the cichlid fossil calibrations have been previously used as calibration priors in molecular clock studies on cichlids and yield, not surprisingly, dramatically different divergence time estimates and biogeographic implications, not only for the EAR evolution ([5–8, 11, 12]). For example, the most recent study on this subject based on the yet most comprehensive dataset inferred a mean divergence age of New World and African cichlid lineages of approximately 82 Ma, i.e. soon after the final separation of Africa and South America ([9]), whereas other recent studies infer either substantially younger (approx. 46 Ma; [7]) or substantially older (approx. 147 Ma; [13]) divergence ages for this split. Consequently, different age estimates for EAR-lineages turned out to be highly divergent as well [5, 14]. To further complicate the issue, inferred lake ages of the African great lakes or their lake level histories have frequently been used to calibrate cichlid molecular clocks under the assumption that endemic clades diverged only after lake formation or, following complete lake basin desiccation, after refilling events [14–16]. This approach is problematic for several reasons. Firstly, the geological history of the formation of the East African rift lakes is highly complex and still not fully understood; therefore, the geological age and onset of truly lacustrine conditions of LT continues to be under debate (e.g. [17]). Several EAR molecular clock studies used an age of 9–12 Ma as a calibration point for the formation of the LT lacustrine basin (e.g. [14, 15]). This age was based on extrapolation of recent sedimentation rates in LT under the assumption of roughly uniform sedimentation rates over the past million years. This assumption is most likely too simplistic, because dramatic climate changes as well as the highly dynamic East African rift tectonics and their associated volcanism must have influenced sedimentation rates substantially [17–19]. Indeed, more recent studies based on thermochronology and sedimentology constrain pre-rift formation of the Albertine Rift system to 4–11 Ma, and the onset of true rifting activity at around 5.5 Ma in the norther LT basin; this in turn implies a much younger age for modern LT than 9–12 Ma [20–23]. Secondly, some of recent endemic and sympatric LT cichlid lineages are likely to have evolved independently in the larger proto-LT drainage area, and only later met and possibly hybridized in the extant LT basin [17]. Hence, as the true age of extant lake basin formation of LT remains unknown and as the assumption of all LT cichlid lineages having originated in situ is not unambiguously supported, studies using a presumably precise age 9–12 Ma as calibration prior for the origin of endemic lacustrine LT fish radiations are potentially misleading. In a analogous case, the age of endemic Lake Malawi lacustrine cichlid lineages has previously been constrained in molecular clock analyses [15, 16] to be younger than the postulated complete desiccation of Lake Malawi either at around 1.6–1.0 Ma, or at the post-drought re-establishment of truly lacustrine conditions at 1.0–0.57 Ma [24]. This approach is in conflict with a recent study reporting continuous sedimentation in the geological LM basin over the last 1.3 Ma, i.e. raising doubts about the previously used LM calibration points [25] Therefore, the use of the sedimentology-based lake age estimates as molecular clock calibration points for the origin of cichlid taxa endemic to large and paleogeographically complex rift lakes appears problematic and might result in highly misleading node age estimates.

Nevertheless, relative and absolute divergence time estimates remain essential for the study of the cichlid biogeographic origin and the history of evolutionary processes whose interplay generated the yet unrivaled vertebrate diversity within the dynamic landscape of the East African rift and its lakes (e.g., [17, 26]). Ultimately, the spatiotemporal reconstruction of phylogenetic relationships

between riverine and lacustrine East African cichlid lineages may not only inform evolutionary biology but will also help to reconstruct geomorphological landscape evolution in the identification of lake colonization routes and river capture events [27].

Here we present new divergence age estimates based on eighteen different calibration sets, which includes up to seven different calibration points represented by three neotropical cichlid fossils, up to three pseudocrenilabrine cichlid fossils and one geological event; the root was calibrated with three different secondary constraints (see below). In particular, the recently described African cichlid fossil †*Tugenchromis pickfordi* is included [28]. Our primary sequence alignment consists of ten mitochondrial protein coding genes including representatives of almost all recognized cichlid tribes with emphasis on the EAR. The application of eighteen different calibration sets enabled us to compare recent cichlid molecular clock studies with our findings, as well as to infer the impact of †*Tugenchromis pickfordi* as a calibration point. There is a long-standing debate about the applicability of mitochondrial DNA data for molecular clock estimates. For example, Matschiner [29] pointed out that nuclear marker-based studies (e.g. [7, 29]) often yield younger divergence time estimates than mitochondrial marker-based studies (e.g. [5, 6]). Therefore, we complement our mtDNA-based analyses (calibration Sets 1–17) with an independent nuclear DNA-based alignment (calibration Set 18) to infer whether or not an identical calibration strategy would result in similar node age estimates for both data sets. We provide a new relative divergence time frame for the African Pseudocrenilabrinae and especially for the mtDNA lineages belonging to the EAR, which is critical in the context of clarifying the phylogeographic history and origin of the famous adaptive radiations of LT, LM and LV but also of several smaller haplochromine lineages. In this study, we include several riverine lineages for the first time allowing for new insights into the complex evolutionary history of the EAR.

Methods

Taxon and nucleotide sampling

Ten mitochondrial protein coding genes were sequenced or obtained from Genbank for 180 cichlid species (Additional file 1: Table S1). The focus of the data set was on taxa representing all major lineages of the East African cichlid Radiation (EAR), but members of all other cichlid subfamilies were included as well: Madagascan and Asian Etroplinae (N = 2) and Ptychrominae (N = 2), American Cichlinae (N = 31) and African Pseudocrenilabrinae (N = 145). The latter are represented by almost all major tribes including Tylochromini (N = 1), chromidotilapiines (N = 2), hemichromines (N = 2), pelmatochromines (N = 1); haplotilapiine lineages (sensu Schliewen & Stiassny, 2003) are represented by the mouthbrooding Oreochromini (N = 14), substrate brooding Pelmatotilapiini (N = 1) and boreotilapiines (sensu Schwarzer et al. 2009, Dunz et al., 2013) including Coptodonini (N = 2) and Gobiocichlini (N = 1) and austrotilapiines (N = 121). The austrotilapiine lineage is represented by Tilapiini (N = 3), Steatocranini (N = 3) and EAR lineages. The taxon sampling of the EAR lineages (N = 115) comprised members of all formally described Lake Tanganyika tribes (sensu Takahashi [30] and Koblmüller et al. [31]), i.e. Boulengerochromini (N = 1), Bathybatini inclunding Hemibatini (N = 7), Trematocarini (N = 5), Lamprologini (N = 16) including nine riverine taxa of the Congo basin sensu stricto and the Lufubu River (a southern affluent to Lake Tanganyika), Eretmodini (N = 2), Cyphotilapiini (N = 2), Limnochromini (N = 2), Ectodini (N = 6), Perissodini (N = 2), Cyprichromini (N = 2), Benthochromini (N = 1) and Tropheini (N = 9; a subgroup of Haplochromini). Moreover, the dataset contains representatives of several additional riverine taxa representing informally named lineages. Since the placement of many recently discovered riverine Haplochromini in Greenwood's classification [32] of *Haplochromis* and related taxa is problematic, we accounted for these taxonomic uncertainties by placing species of unsettled generic status in the catch-all genera '*Haplochromis*', '*Orthochromis*' or '*Ctenochromis*'; this follows the practice first suggested by Hoogerhound [33] and later adopted by several studies (e.g. [17]). Nomenclature for most of these lineages follows Schwarzer et al. [34] and Weiss et al. [17], i.e. we included Northern-Zambia-*Orthochromis* (4), LML-*Orthochromis* occurring at Luapula-Mweru system and the Lualaba/Congo main stem (N = 1), Malagarasi-*Orthochromis* (N = 4) as well most rheophilic mtDNA lineages of the Congo basin, i.e. '*Orthochromis*' *indermauri*, '*Orthochromis*' *torrenticola*, '*Orthochromis*' *stormsi*; further included are '*Haplochromis*' *vanheusdeni* (N = 1), *Astatoreochromis straelini* (N = 1), Congo-basin *'Haplochromis'* (N = 3), *Ctenochromis pectoralis* (N = 1), *'Pseudocrenilabrus*-group' (N = 9; including the Northern-Zambia-*Orthochromis*) and serranochromines-mtDNA-lineage (N = 11; including the Congo-basin *'Haplochromis' and* LML-*Orthochromis*) as well as two undescribed species referred here as "New Kalungwishi Cichlid" and "New Lufubu Cichlid". We further included representative members of all major lineages of the Lake Malawi species flock (N = 22) as well as riverine and 'modern' Haplochromini of East Africa (N = 10). Selection of representative taxa was optimized to encompass the oldest divergence events of clades within austrotilapiine mitochondrial clades and is based on previous studies (e.g. [35–39]). This approach was chosen to infer the oldest mtDNA divergence age estimates for each of these lineages.

In addition to the mitochondrial data set we generated a second data set based on partial sequences of four nuclear loci, i.e. RAG1, ENC1, RH1 and TMO-4c4. All these sequences were obtained from GenBank with the aim to compile a widely comparable taxon sampling to our mitochondrial data set. Since more than one sequence per locus was available for several species, only the most complete sequence of each locus was chosen, and, where ever possible, sequences of the same species would derive from the same study and individual. Furthermore, to obtain a dataset with few missing data only taxa with two or more loci represented in Genbank were kept (except *Gymnogeophagus balzanii* and *Gymnogeophagus setequedas* for which only one locus was available). In total, the nuclear data set included 117 species representing all cichlid subfamilies and most of the major lineages of the EAR (Additional file 2: Table S3). Nevertheless, sequences of several comparatively recently diverged lineages were not available in Genbank, e.g. Malagarasi-*Orthochromis,* '*Haplochromis*' *vanheusdeni,* the Congo-basin *'Haplochromis,* LML-*Orthochromis, Astatoreochromis, Ctenochromis pectoralis,* '*Haplochromis*' *vanheusdeni* and '*Orthochromis*' *indermauri*.

Sampling procedures

Material for this study was obtained from the commercial cichlid fish trade in Germany, private collection of aquarium hobbyists or collected on previous field trips. Individual fish were either caught using various fishing methods (gill net, beach seine net, gill net, hand net) or bought freshly fished from local fishermen. Freshly caught fish were sacrificed by an overdose of approved fish anesthetic (Benzocaine, MS-222). Subsequently, fin clips were fixed in 96% ethanol and entire specimens were fixed in 10% formalin, as explained in [40]. We followed all applicable international and national guidelines of animal use and ethical standards for the collection of samples.

Molecular methods

Total genomic DNA was extracted by using the DNeasy Blood & Tissue Kit (Qiagen) following the manufacturer's protocol and the DNA concentration was standardized to 25 ng/μl. We either amplified the whole mitochondrial genome or three large fractions using the following three primer pairs: Primer pair A (L2508KAW: 5'-CTC GGC AAA CAT AAG CCT CGC CTG TTT ACC AAA AAC-3'; [41]; and ZM7350R: 5'-TTA AGG CGT GGT CGT GGA AGT GAA GAA G-3`), Primer pair B (ZM7300F:5`-GCA CAT CCC TCC CAA CTA GGW TTT CAA GAT GC-3' and ZM12300R: 5'-TTG CAC CAA GAG TTT TTG GTT CCT AAG ACC-3') and Primer pair C (ZM12200F: 5'-CTA AAG ACA GAG GTT AAA ACC CCC TTA TYC-3' and ZM2100R: 5'-GAC AAG TGA TTG CGC TAC CTT TGC ACG GTC-3; all ZM primers taken from [9]; the number in the primer names refers to an approximate position within the mitogenome starting by the tRNA-Phe). The amplified fragments overlapped and enabled the assembly of contiguous mitochondrial genome fragments across primer sites. Long-range PCR were conducted using the TaKaRa LA Taq DNA polymerase kit (TaKaRa) with the following thermal profiles: initial denaturation at 98 °C (60 s), followed by 35 cycles of denaturation 98 °C (10 s), annealing at60°C (Primer pair A), 62 °C (Primer pair B) or 60 °C (Primer pair C) for 60s, elongation at 68 °C (15 min), and a last extension step at 72 °C (10 min). Amplification products were purified using the QIAquick Gel Extraction Kit (Qiagen) following the manufacturer's protocol. DNA concentration of purified amplification products were adjusted to 0.21 ng/μl and fragments of each species were pooled equimolarly. The Nextera XT DNA Sample Preparation Kit (Illumina) was used for library preparation following the manufacturer's protocol until the normalization step. Library pooling and sequencing was conducted at the Sequencing Service of the Ludwig Maximilian University of Munich on an Illumina MiSeq platform. Alternatively, several samples were sequenced on the Ion Torrent PGM platform following the library preparation using the Ion Xpress™ Plus Fragment Library Kit and the template preparation on the Ion OneTouch™ 2 System (following OT2 protocol). Adaptor trimming, quality control and assembly of the sequencing reads were done by using the CLC Genomics Workbench (Qiagen). Annotation of the assembled sequences (mean coverage: 6820; mean sequence length: 9923 bp) was performed in Geneious v.7.05 [42] using the complete mitochondrial genome of *Oreochromis niloticus* as a reference genome (GenBank accession number: GU370126; [43]). Sequence data were deposited in Genbank under the accession numbers (MK144668 – MK144786 and MK170260 – MK170265, Additional file 1: Table S1). To complement our data set we included published mitochondrial genomes from previous studies that were deposited in GenBank (Additional file 1: Table S1).

Phylogenetic analysis, divergence time estimate and fossil calibration

We extracted protein coding sequence information of ten mitochondrial protein-coding genes (ND1, ND2, COX1, COX2, ATP8, ATP6, COX3, ND3, ND4L, ND4) for all taxa from of our data set. If sequences of a particular gene were missing (e.g. due to poor quality of sequence) a multi-N string was inserted into the alignment in the respective positions (Additional file 1: Table S1). For *Lamprologus tigripictilis* three genes were missing, therefore we used the ND2 sequence of another specimen of the sampled at the same river location

(Genbank accession number: JX157061) to complement sequence information for this species. Sequences were aligned for each gene separately using the Geneious alignment tool with default settings and then checked by eye. Single gene alignments were concatenated in Geneious, resulting in a total alignment of 7893 bp with 4529 variable sites and relative base frequencies (excluding gaps and ambiguous sites) of A = 0.25, T = 0.28, C = 0.32 and G = 0.15. Each codon position was tested for saturation by calculating the number of transitions and transversions for all taxon pairs for each codon position separately in PAUP v. 4.0 [44] and plotting them against each other.

The complementary four nuclear loci alignment with sequences from Genbank (RAG1, ENC1, RH1 and TMO-4c4) comprised 117 taxa. Missingness was as follows: 16 species had no RAG1 sequence, 8 had no ENC1, 40 had no RH1 and 41 had no TMO-4c4, and missing data were replaced by Ns. Genbank sequences were individually aligned using the Geneious alignment tool with default settings and subsequently checked by eye and trimmed to equal length. All single locus alignments were concatenated in Geneious resulting in a total alignment of 3483 bp and 35.8% missing data. Relative base frequencies (excluding gaps and ambiguous sites) of this alignment are A = 0.24, T = 0.25, C = 0.24 and G = 0.27.

Selection of the best-fitting substitution model (GTR + I + G) for each gene was conducted using the program jModeltest [45] based on Akaike information criterion (AIC). Maximum likelihood (ML) inference of phylogenetic relationships was conducted with RAxML v8.2.6 [46] on the CIPRES Science Gateway [47]. For this step, the data set was further partitioned into first, second and third codon positions and the two Etroplinae taxa *Etroplus maculatus* and *Paretroplus maculatus* were defined as outgroup, based on consilient evidence from previous phylogenetic studies [7, 8]. Bootstrap replications were automatically halted by RAxML (using the majority rule criterion) after 108 replications followed by ML search. Relative divergence times of clades were estimated using the Bayesian software BEAST v2.3.2 [48] under a relaxed lognormal clock model with a birth-death speciation model on the CIPRES Science Gateway. Again, the data set was partitioned in first, second and third codon position. Moreover, for the BEAST analysis we defined five clades as monophyletic based on the results of the Maximum Likelihood analysis (see above): Clade 1 (Ptychochrominae + Pseudocrenilabrinae + Cichlinae), Clade 2 (Pseudocrenilabrinae + Cichlinae), Clade 3 (Pseudocrenilabrinae), Clade 4 (Cichlinae) and Clade 5 (containing: austrotilapiines, Pelmatolapiini, Oreochromini). These clades were supported by high bootstrap values (except Clade 2 and Clade 5) in our analysis and were concordant by previous studies (e.g. [5, 7, 8]).

Calibration points were chosen conservatively based on a critical evaluation of all previously used calibration points in cichlid phylogenetic studies. Up to six fossils (three Neotropical cichlid fossils and three fossils belonging to the Pseudocrenilabrinae) and one geological event (geological age of the crater lake Barombi Mbo maar) were finally selected. Justifications for their inclusion is detailed below; for reasons why previously used cichlid fossils and geological calibration points were excluded, see the Additional file 3. Ninety five percent quantiles of prior-probability-densities width for fossil calibration points laid between 29.2 and 39.1 Ma, which roughly matches the recommendation by [9]). Generally, only fossils with well evaluated evidence for their phylogenetic position and with equally well corroborated ages were included.

The three neotropical cichlid fossil are: †*Plesioheros chaulidus,* †*Gymnogeophagus eocenicus* and †*Tremembichthys* (e.g. †*T. paulensis and* †*T. garciae).*

†*P. chaulidus* and †*G. eocenicus* were described from lacustrine "Faja Verde" deposits of the uppermost section of the Lower Lumbrera formation in Northwestern Argentina [49, 50]. The exact age of "Faja Verde" deposits remains under debate, but it is possible to constrain the youngest possible age of the whole Lumbrera formation to 39.9 Ma based on U/Pb dating of its uppermost layer [51]; and it is possible to constrain the cichlid bearing layer to a maximum age of 45.4–38.0 Ma based on accompanying mammal fossils, whose association suggests an Casamayoran-Vacan age (for a more detailed discussion of the age of Lumbrera formation see [9, 52], who used the same calibration). The phylogenetic placement of †*Plesioheros chaulidus* within the Cichlinae tribe Heroini is well supported by several morphological synapomorphies, but a refined placement of †*Plesioheros* is hampered by the presence of lingual cusps on the teeth in the fossil, which are not present in the two heroine genera *Hypselecara* and *Hoplarchus* [53]. Since phylogenetic analyses of Heroini intrarelationships based on morphological [53] and molecular datasets (e.g [52, 54]) are partially incongruent, and since our Heroini taxon sampling is limited to a few key taxa, we conservatively place †*Plesioheros* at the node uniting only Heroini with lingual cusps being present, i.e. after the divergence of *Hypselecara.* The phylogenetic placement of †*Gymnogeophagus eocenicus* in the extant genus *Gymnogeophagus* is well supported based on two unambigous apomorphies [50]. We conservatively place the calibration point at a node uniting our single *Gymnogeophagus* species (*G. balzanii*) with two other geophagine taxa (*Mikrogeophagus ramirezi*,'*Geophagus*' *brasiliensis*).

†*Tremembichthys* has been recorded from the Entre-Córregos Formation (Aiuruoca Tertiary Basin) and from the Tremembé formation (Taubaté Basin) in Brazil

[55] The Entre-Córregos Formation was suggested to be of Eocene-Oligocene age based on palynological evidence [56, 57], whereas lacustrine shales of Tremembé formation are dated to Oligocene-Miocene based on geological and paleontological studies [58, 59]. Phylogenetic analysis based on the character matrix of Kullander [60] placed †*Tremembichthys* within Cichlasomatini, a tribe which is supported by several morphological apomorphies. Of those, however, only the square shaped lachrymal is preserved in †*Tremembichthys* [55]. We accept the placement of †*Tremembichthys* within Cichlasomatini for most of our calibrations, and following [52] we apply a conservative time range of 55.8–23.03 Ma for †*Tremembichthys* as no precise age estimate is available for the Entre-Córregos formation. Nevertheless, it is worth mentioning that †*Tremembichthys* has three pterygiophores articulated with the first haemal arch [55], a condition unknown from any extant Cichlasomatini member. Generally, cichlasomatines have one to two pterygiophores articulated to the first haemal spine whereas some Heroini lineages have three or even more [60]. Therefore, we calibrated one analysis with †*Tremembichthys* at the base of Heroini to evaluate the impact of the alternative plausible placement of †*Tremembichthys*. Phylogenetic placement of all neotropical cichlid fossils was based on Kullander [60] or on López-Fernandez et al. [61]. However, recent molecular studies ([54, 62]) might differ slightly from these phylogenetic hypotheses.

The three included Pseudocrenilabrinae cichlid fossils are: †*Mahengechromis (*e.g. †*Mahengechromis plethos,* †*Mahengechromis rotundus), †Oreochromis lorenzoi* and †*Tugenchromis pickfordi*.

†*Mahengechromis* represents the oldest known cichlid fossil and was discovered in the ancient crater lake Mahenge which is part of the Singida kimberlite field on the Singida Plateau in Tanzania [10, 63]. The age of the Mahenge maar is estimated to 45.83 ± 0.17 Ma based on U/Pb isotope dating, and a maar lake mostly likely persisted for only 0.2–1.0 Ma [64]. The presence of a single supraneural bone places †*Mahengechromis* in a lineage encompassing all Pseudocrenilabrinae except for *Heterochromis*, *Tylochromis* and *Etia* which have two supraneural bones. The phylogenetic position of †*Mahengechromis* has already been discussed in several studies and different positions have been suggested depending on which data sets and characters were used. It was either placed within the EAR, as a basal offshoot within Pseudocrenilabrinae or as a sister group to *Hemichromis* [10, 63, 65]. A sister-group relationship of †*Mahengechromis* and *Hemichromis* was inferred to be most parsimonious based on an osteological character matrix including representatives of all cichlid subfamilies with a focus on the Pseudocrenilabrinae lineages (but missing several important lineages, e.g., pelmatochromines, pelmatolapiines tilapiines, steatocranines), which was mapped on a composite tree with predefined character evolution based on the knowledge of the time. However, when solely based on osteological characters, the relationship between †*Mahengechromis* and *Hemichromis* was not supported [65]. As additional support for a relationship of †*Mahengechromis* and *Hemichromis* Murray [65] stated that both exhibit a low number of total vertebrae (fewer than 26), however this is also the case in other African cichlid genera of the tribes, e.g., Etiini, chromidotilapiines and pelmatochromines [66, 67]. Therefore, we consider the exact phylogenetic placement of †*Mahengechromis* as unresolved, except that it represents an early branching member of Pseudocrenilabrinae. Therefore, we use the fossil age to restrict the maximum ages of the calibration points of †*Oreochromis lorenzoi* and †*Tugenchromis pickfordi* as these taxa undoubtedly represent more derived lineages within Pseudocrenilabrinae (see below).

†*Oreochromis lorenzoi* was described from the Gessoso-Solfifera Formation (Messinian) in Italy [68]. The Messinian age is dated from 7.24–5.33 Ma based on astronomical chronology and $^{40}Ar/^{39}Ar$ dating while fossil bearing euxinic shale interstrata of lower evaporite cycles of the Gessoso-Solfifera formation are dated by magnetostratigraphy to 5.96 ± 0.2 Ma [69–71]. No comprehensive phylogenetic analysis is available for †*O. lorenzoi* but its current placement in the tribus Oreochromini is convincingly supported by characters characterizing *Sarotherodon* and *Oreochromis* [68]. Unfortunately, diagnostic characters of several oreochromine genera are often not well preserved in fossils, and moreover, [68] had not compared the fossil with additional genera placed today in Oreochromini, e.g. *Tristramella* and *Danakilia*, rendering the placement of †*O. lorenzoi* to some extent ambiguous [35, 72]. For a conservative approach we therefore decided to use †*O. lorenzoi* as calibration point for the crown age of Oreochromini and not for the genus *Oreochromis*, i.e. with a time range of 5.98–46 Ma based on the age lower of lower evaporite cycles of the Gessoso-Solfifera formation and the maximum age of †*Mahengechromis*.

†*Tugenchromis pickfordi* was recently described from the Waril site of the Ngorora fish Lagerstätte in the Central Kenya Rift Valley [28]. Based on a particular horse (Equidae) tooth fragment of the paleosol above the lacustrine sediments and lithostratigraphy, the Ngorora fish Lagerstätte was assigned to the upper Miocene 9–10 Ma, [73–75]. †*T. pickfordi* can be safely assigned to the family Cichlidae based on several osteological and squamation patterns [28]. Within the Pseudocrenilabrinae it is suggested to be an extinct lineage within the 'most ancient Tanganyika tribes' (sensu [17]) based on the character state "lacrimal which bears six lateral line foramina"; this state is present only in six Lake Tanganyika tribes Bathybatini, Perissodini, Limnochromini, Ectodini, Lamprologini and

Eretmodini. It most likely represents a stem lineage of the 'ancient Tanganyika mouth-brooders' (sensu [17]) as it shares a mosaic-like character set of a tripartite lateral line (present only in two genera of Ectodini from the Lake Tanganyika *Xenotilapia* and *Grammatotria*), a lacrimal with six lateral line foramina, and the shape of the trapezeoid lacrimal and arrangement of tubules resembling strongly those of Limnochromini. Further, its meristics are similar Ectodini and Limnochromini. We therefore accept †*Tugenchromis pickfordi* as a potential precursor lineage of the 'ancient Tanganyika mouth-brooders' (sensu Weiss et al. [17]) as this appears to be the most probable phylogenetic position of †*T. pickfordi;* and, alternatively, we use it as a calibration point encompassing the Lake Tanganyika C-lineage (sensu Clabaut et al. [76]), which includes not only the 'ancient Tanganyika mouth-brooders', but also the 'Malagarasi-*Orthochromis*' and Haplochromini (alternative calibration: E1). Nevertheless, we applied two additional alternative calibrations to account for remaining uncertainties of the phylogenetic placement of this fossil. The first included in the C-lineage but also Eretmodini (= H-lineage sensu Nishida [77]; alternative calibration: E2) as Eretmodini exhibit six lateral line foramina as †*Tugenchromis*. The second alternative position of †*Tugenchromis* is at the EAR-bases (alternative calibration: E3), thus accounting for the vague possibility that †*Tugenchromis pickfordi* might be an extinct lineage within the 'most ancient Tanganyika tribes', because of its plesiomorphic cycloid flank scales.

We further used one geological event for calibration, i.e. the geological origin of the Cameroonian crater lake Barombi Mbo. The lake harbors an endemic monophyletic radiation of eleven species which must have radiated in situ, and whose riverine founder species, *Sarotherodon galilaeus* is still extant [78, 79]. Based on K/Ar dating the Barombi Mbo maar was active around 1.05 ± 0.7 Ma [80], suggesting a slightly younger age as the maximum age for the onset of the divergence of the cichlid radiation in the lake. In contrast to the complex tectonic history of the East African Great Lakes the volcanic history of the Barombi Mbo maar is far better understood. We therefore decided to include the formation of Barombi Mbo as a maximum age constraint for the MRCA of the strictly endemic Lake Barombi Mbo species flock.

As root calibrations we applied three alternative age-range priors and associated probabilities. One time-range (R1) was set very conservatively by allowing the age prior to range between 46 and 174.78 Ma, either with a lognormal prior (R1a) and or with a uniform probability (R1b). This range covers all possible probabilities for the first emergence of cichlids: the younger bound is based on the age of the oldest known cichlid fossil (46 Ma, †*Mahengechromis*) and the older bound on the oldest maximum age estimate for the family Cichlidae based on independent cichlid molecular clock results (95% HPD: 128.2–174.78 Ma; [13]. The second time-range (R2) is taken from study of Matschiner et al. [9], which is so far the most comprehensively evaluated age estimate for Cichlidae. Their estimate (95% HPD: 82.17–98.91 Ma) is based on a sequence dataset encompassing over 1000 teleost species, 40 mitochondrial and nuclear loci and a calibration with 147 teleost fossils, as well as a critical re-evaluation of previous publications.

To evaluate the effects of inclusion and alternative placement of calibration points, and moreover the impact of different prior distributions (lognormal vs. uniform) for the important root calibration divergence time estimates, we conducted seventeen different BEAST runs based on the mitochondrial dataset and with the following settings. Node calibrations were set to log-normal distributions except for the root calibration (R1b) which in one run was set to a uniform distribution (for more calibration prior details see Table 1): calibration Set 1, Set 2, Set 5, Set 7 and Set 9 were root calibrated using the conservative calibration R1a (prior range of 46–174.78 Ma), while Set 3, Set 4, Set 6, Set 8, Set 10, Set 12, Set 13, Set 14 and Set 15 were calibrated with the root calibration R2 (prior range of 82.17–98.91 Ma). Set 1 and Set 3 were calibrated with †*Tugenchromis* placed on the node of the MCRA of the C-lineage and Eretmodini while Set 2 and Set 4 excluded the Eretmodini in the placement. Set 5 and Set 6 did not include †*Tugenchromis* as a calibration point. Set 9 and Set 10 were calibrated with †*Tugenchromis*, but this time at the base of the EAR. †*Oreochromis lorenzoi* was excluded as calibration point from Set 7 and Set 8. Sets 13, 14 and 15 were calibrated as Set 4 except that †*Tremembichthys* was excluded from Set 13 as calibration point, †*Gymnogeophagus eocenicus* as a calibration point from Set 14 and the age of the Barombi Mbo maar as calibration point from Set 15. Set 17 was calibrated as Set 4 except for †*Tremembichthys,* which was placed as a calibration point for the Heroini rather than Cichlasomatini. The calibration of Set 11 was identical to the calibration of Set 2 with the only exception being that the root was calibrated with a uniform distribution (R1b). Set 16 was calibrated as Set 4 but without root calibration. Several studies demonstrated that saturation can lead to the effect of compressing basal branches resulting in overestimated divergence dates of shallow nodes [81–83]. For the evaluation of this effect we designed an additional Set 12 identical to Set 4 but with the third codon position removed of the alignment. Finally, we calibrated the comparative nuclear dataset applying identical settings as the calibration Set 4 to investigate whether mitochondrial and nuclear DNA data calibrated and analysed with identical priors would yield comparable

Table 1 Overview of calibration prior details

Cichlid fossils and geological events used as calibration points:				Parameter settings (Beast):			
Calibration point	Fossil/event	Estimated age	Calibrated clade	Offset	Standard deviation	Mean	Distribution
A1	†*Tremembichthys*	55.8–23.03 Ma (Tremembé formation)	Cichlasomatini	23.03	0.67	2.39	Log normal
A2	†*Tremembichthys*	55.8–23.03 Ma (Tremembé formation)	Heroini	23.03	0.67	2.39	Log normal
B	†*Gymnogeophagus eocenicus*	45.4–39.9 Ma (Lumbrera formation)	*Mikrogeophagus ramirezi*, *Gymnogeophagus balzanii*, '*Geophagus*' *barsiliensis*	39.9	0.8	2.4	Log normal
C	†*Plesioheros chaulidus*	45.4–39.9 Ma (Lumbrera formation)	Heroini (except: of Pterophyllum and Hypselecara)	39.9	0.8	2.4	Log normal
D	†*Oreochromis lorenzoi*	7.24–5.33 Ma (Gessoso-Solfifera formation)	Oreochromini	5.98	1.148	1.8	Log normal
E1	†*Tugenchromis pickfordi*	9–10 Ma (Ngorora Formation)	C-lineage (sensu Clabaut et al., 2005): 'ancient Tanganyika mouth-brooders', 'Malagarasi-*Orthochromis*', *'Ctenochromis' pectoralis* and Haplochromini	9	0.98	2	Log normal
E2	†*Tugenchromis pickfordi*	9–10 Ma (Ngorora Formation)	H-lineage (sensu Nishida, 1991): 'ancient Tanganyika mouth-brooders', 'Malagarasi-*Orthochromis*', *'Ctenochromis' pectoralis,* Haplochromini and Eretmodini	9	0.98	2	Log normal
E3	†*Tugenchromis pickfordi*	9–10 Ma (Ngorora Formation)	East African Radiation (EAR)	9	0.98	2	Log normal
F	Onset Lake Barombi Mbo	1.12–0.98 Ma	Barombi Mbo species flock	0.0	0.07	0.98 (real space)	Log normal
–	†*Mahengeochromis*	45.83 ± 0.17 (Singida kimberlite field)	–	–	–	–	–
Root calibration							
R1a	Time range: 46–174.78 Ma	Based on: Age of †Mahengeochromis & the oldest maximum age estimate for the family Cichlidae (López-Fernández et al. 2013)		46	0.44	3.99	Log normal
R1b	46–174.78 Ma	as for R1a		0	Lower Bound: 46	Upper bound: 174.78	uniform
R2	82.2–98.9 Ma	Estimated divergence age for the family Cichlidae by Matschiner et al. (2016)		82.17	0.455	2.07	Log normal
Combination of calibration points of the different calibration sets:							
	Included calibration points		Included calibration points:		Included calibration points:		
Set 1	A1, B, C, D, E2, F, R1a	Set 7	A1, B, C, E1, F, R1a	Set 13	B, C, D, E1, F, R2		
Set 2	A1, B, C, D, E1, F, R1a	Set 8	A1, B, C, E1, F, R2	Set 14	A1, C, D, E1, F, R2		
Set 3	A1, B, C, D, E2, F, R2	Set 9	A1, B, C, D, E3, F, R1a	Set 15	A1, B, C, D, E1, R2		
Set 4	A1, B, C, D, E1, F, R2	Set 10	A1, B, C, D, E3, F, R2	Set 16	A1, B, C, D, E1, F		

Table 1 Overview of calibration prior details *(Continued)*

Cichlid fossils and geological events used as calibration points:				Parameter settings (Beast):	
Set 5	A1, B, C, D, F, R1a	Set 11	A1, B, C, D, E1, F, R1b	Set 17	A2, B, C, D, E1, F, R2
Set 6	A1, B, C, D, F, R2	Set 12 (third codon position stripped)	A1, B, C, D, E1, F, R2	Set 18 (Nuclear data)	A, B, C, D, E1, F, R2

Fossil taxa are indicated by †

node age estimates. Although the taxon sampling of the comparative nuclear dataset is slightly reduced and not fully identical as comparted to the mitochondrial dataset it covered all major cichlid lineages, hereby enabling a meaningful comparison at least for some divergence time estimates of several key nodes.

Each BEAST run was performed three times independently (180 million generations per run) and sampling of parameters and trees was done every 15,000 generation. The three independent runs (for each alternative BEAST run configuration) were combined using LogCombiner after accounting for a burn-in of 15%. We used Tracer v1.6 [84] for inspection of effective sample size (ESS) of all parameters of the different BEAST runs. All EES had acceptable values (> 200) and appeared to converge to stationary distributions, indicating an acceptable sample size for the posterior distribution of parameters of individual analyses. Maximum clade credibility trees (posterior probability limit: 0.5, mean heights) were retrieved from the posterior tree distribution.

Results

The alternatively calibrated BEAST runs (Calibration Set 1–11 and Sets 13–17) yielded maximum-clade credibility (MCC) trees which were largely identical to the topology of the ML tree. The few inconsistencies include (a) the position of 'Lower Congo *Lamprologus* clade', which is placed as a sister group to all remaining Lamprologini in the Bayesian MCC trees but as a sister group to the 'non-ossified Lamprologini' in the ML tree; and (b) the position of Cyphotilapiini which are either a sister group to Limnochromini, or in the ML tree, or a sister group to the clade encompassing Limnochromini and all remaining members of the EAR (see Fig. 1 and Fig. 2). The topology of the maximum-clade credibility (MCC) tree based on the BEAST runs of calibration Set 12 (third codon positions removed) is compatible with those of the ML tree and the MCC trees of the other calibrations sets but show several inconsistencies within the Pseudocrenilabrinae. For example, the Steatocranini are placed as the sistergroup to the EAR in the ML tree and other MCC trees (Sets 1–11 and Sets 13–17) but they are placed as the sister group to a clade comprising Oreochromini, Pelmatolapiini and Tilapiini (*T. ruweti and T. sparrmanii*) in the MMC tree of Set 12. Both *T. ruweti, T. sparrmanii* and *C. crassa* form the sister group to a clade consisting off the EAR and Steatocranini in the ML and all other MCC trees (Set 1–11 and Sets 13–17). The Malagarasi-*Orthochromis* are placed as sistergroup to the Haplochromini in the MCC trees (Set 1–11 and Sets 13–17) and the ML tree but are sistergroup to a clade consisting of Perissodini, Cyprichromini, Benthochromini and Limnochromini in the MMC tree of Set 12. Moreover, the placement of *H. vanheusdeni* and '*Orthochromis*' *indermauri* differed from the ML tree and the other MCC trees (Set- 1 – 11 and Sets 13–17). However, all of these alternative placements in the MMC tree (Set 12) are only weakly supported.

The topology of the MCC tree based on the nuclear dataset resembled those of the mitochondrial dataset to some extent except for several topological differences within the Pseudocrenilabrinae and Cichlinae. Within the Cichlinae, for example, *Astrontus ocellatus* and *Chaetobranchiopsis orbicularis* were resolved as sister taxa to Geophagini instead of forming the sister group to Cichlasomatini and Heroini. There were comparatively minor topological differences of the taxa within Cichlasomatini and Heroini, e.g. the placement of *Krobia* within the Cichlasomatini, and the placement of *Rocio*, *Uaru* and *Symphysodon* within Heroini. Major topological differences within Pseudocrenilabrinae were: '*Tilapia*' *brevimanus* formed a clade together with *Pelmatolapia mariae* which was resolved as a sister clade to the EAR; Steatocranini and Tilapiini were resolved as sister taxa; and within the EAR differences arose for the placement of several tribes endemic to Lake Tanganyika (e.g. *Boulengerochromis* and Bathybatini incl. Hemibatini formed a monophyletic clade; the monophyly of the benthopelagic LT clade (see below) was not recovered; a clade composed of Eretmodini, Ectodini and Lamprologini was resolved as the sister group to Haplochromini; Tropheini and *Serranochromis macrocephalus* were resolved as sister taxa). In general, nodes of the topology based on the nuclear dataset were weakly supported as compared to the mitochondrial based topology.

The divergence time estimates based on the different calibration sets of the full mitochondrial alignment differed only slightly from each other. Divergence ages based on the Calibration Set 1, Set 2, Set 5, Set 7, Set 9 and Set 11 (with the root age range of 46–174.78 Ma) were only slightly older and had a wider 95% HPD interval than those based on the calibration Set 3, Set 4, Set 8, Set 10, Set 13, Set 14 and Set 15 (root age range of 82.17–98.91 Ma). Application of a log-normal distributed prior for the

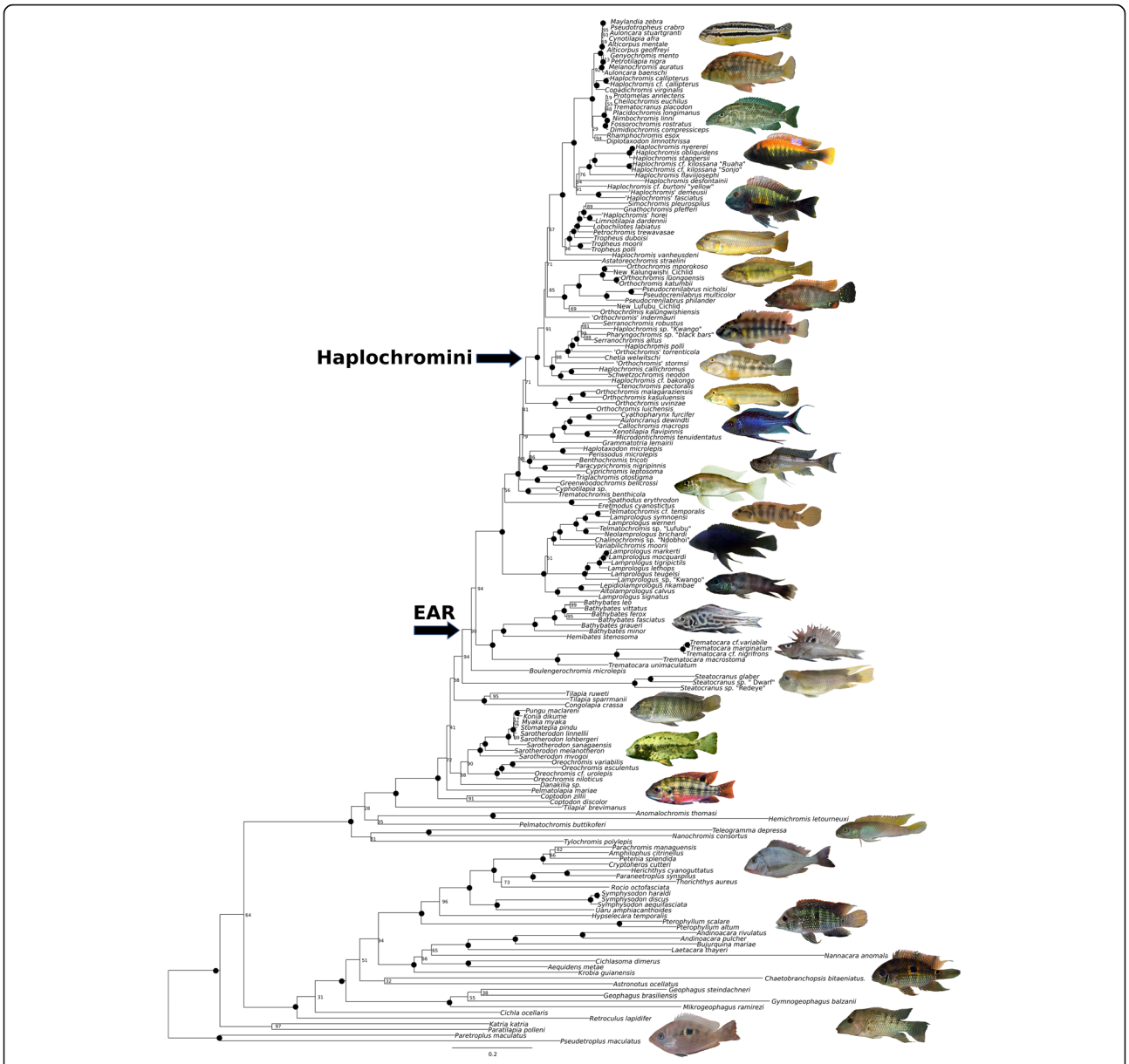

Fig. 1 ML-phylogeny (RAxML) based on ten protein coding mitochondrial genes (ND1, ND2, COX1, COX2, ATP8, ATP6, COX3, ND3, ND4L, ND4) of 180 cichlid taxa representing all cichlid subfamilies. Focus of the taxon sampling was put on members of the East African cichlid Radiation represented by 115 taxa. Numbers at nodes refer to bootstrap-values while black dots represent bootstrap support of 100. Specimens depicted from top to bottom (photographersin brackets): *M. auratus* (E. Schraml), *H. callipterus (U.K. Schliewen), N. linni* (E. Schraml), *H. nyererei* (E. Schraml), *T. moorii* (Z. Musilová), *H. vanheusdeni* (J. Geck), *O. luongoensis* (F.D.B. Schedel), New Lufubu Cichlid (F.D.B. Schedel), *'O.' indermauri* (F.D.B. Schedel), *'O.' stormsi* (J. Geck), *O. uvinzae* (J. Geck), *C. furcifer* (Z. Musilová), *H. microlepis* (Z. Musilová), *G. bellcrossi* (E. Schraml), *L. symoensi* (E. Vreven), *V. moorii* (F.D.B. Schedel), *L. teugelsi* (F.D.B. Schedel), *H. stenosoma* (F.D.B. Schedel), *T. macrostoma* (F.D.B. Schedel), *S. glaber* (F.D.B. Schedel), *T. ruweti* (F.D.B. Schedel), *P. maclareni* (J. Geck), *C. zillii* (J. Geck), *N. consortus* (F.D.B. Schedel), *T. polylepis* (F.D.B. Schedel), *A. pulcher* (Z. Musilová), *N. anomala* (Z. Musilová), *G. steindachneri* (Z. Musilová), *P. maculatus* (F.D.B. Schedel)

root (Set 2) or a uniform distribution of the root (Set 11) had only marginal impact on node ages, which were only slightly older for Set 11. If no root calibration was applied (Set 16), divergence ages were slightly older than those of Set 4 but their 95% HPD intervals still widely overlapped, even so they were generally wider than those of calibration Set 4. On the other hand, divergence ages of our non-rooted calibration set were younger than those of Set 2 but again 95% HPD intervals of both sets overlapped to some extent.

Three alternative placements of the fossil †*Tugenchromis*, i.e. either including the C-lineage and Eretmodini (Set 1 and Set 3) or excluding Eretmodini (Set 2 and Set 4) or alternatively at the base of the EAR (Set 9 and Set

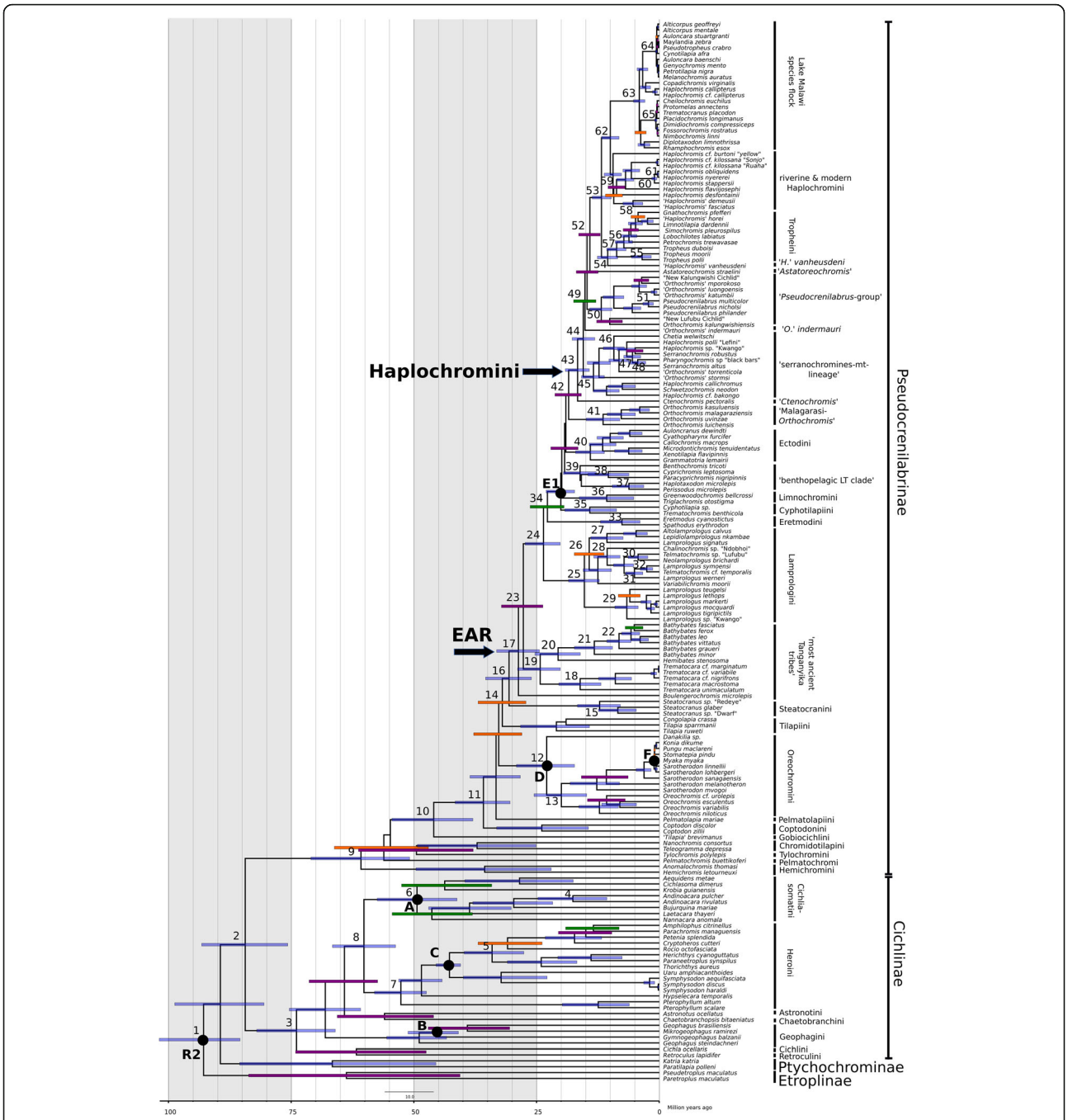

Fig. 2 Time-calibrated phylogeny (BEAST, relaxed normal molecular clock) of 180 cichlid taxa based on ten protein coding mitochondrial genes and on the calibration Set 4 (see Table 1). Time constrained nodes (black circles) were calibrated using fossils, i.e. A: †*Tremembichthys*, B: †*Gymnogeophagus eocenicus*, C: †*Plesioheros chaulidus*, D: †*Oreochromis lorenzoi*, E: †*Tugenchromis pickfordi*), one geological event (F: age of Lake Barombi Mbo maare) or as in the case of the root using secondary constraint (divergence time estimate for the age of the MRCA of cichlids taken from Matschiner et al. [9]; 82.17–98.91 Ma). Node bars indicate 95% HPD intervals of divergence events and are coloured according to their Bayesian Posterior Probability (blue: BPP 1.0; violet: BPP 0.99–0.95; green: BPP 0.94–0.8; orange: BPP 0.79–0.5, node bars with BPP < 0.5 are not depicted). Numbers next to the nodes correspond to the numbers in the Additional file 4: Table S2

10), had marginal impact on divergence age estimates, too. Divergence ages based on calibration sets without †*Tugenchromis* (Set 5 and Set 6) usually yielded slightly older ages than calibrations sets including †*Tugenchromis*. Likewise, divergence ages obtained by calibration sets excluding †*Oreochromis lorenzoi* (Set 7 and Set 8) were slightly older than divergence ages based on comparable calibration sets including the fossil (Set 2 and Set 4). The

same was true for the calibration Set 13 excluding the neotropical cichlid fossil *†Tremembichthys,* which yielded only slightly older divergence ages in comparison to calibration Set 4. If *†Tremembichthys* was placed at the base of Heroini instead of Cichlasomatini (Set 17) divergence ages were revealed to be only slightly older than those of calibration Set 4. Divergence ages of the calibration set excluding the age of the Barombi Mbo maar (Set 15) as a calibration point were in general slightly older than those of the calibration Set 4, but confidence intervals overlapped widely. The exclusion of *†Gymnogeophagus eocenicus* (Set 14) as a calibration point resulted in marginally younger divergence age estimates in comparison to those of calibration Set 4.

The small impact on divergence age estimates of both taxa might be explained by the fact that we applied six additional calibration points, including one root calibration point. Root calibration points are affecting time estimates more than shallow ones and estimates become more consistent when multiple calibration points are applied [85, 86].

The divergence times of deep nodes (e.g., the root of Cichlidae; split of Pseudocrenilabrinae and Cichlinae; crown age of Pseudocrenilabrinae; crown age of Cichlinae) of the calibration Set 12 (mitochondrial alignment with third codon positions removed) were comparatively younger than those of the corresponding Set 4 (third positions included) but nevertheless widely overlapped with their 95% HPD intervals (see Figs. 3 and 4). These younger estimates for comparatively old nodes in Calibration Set 12 contrasted with comparatively older divergence time estimates of shallower nodes (i.e., EAR, Tanganyika tribes, haplochromine lineages) in the same analysis. Further, divergence ages of Set 12 had wider 95% HPD ranges, especially those of more recent splits (e.g., Lake Malawi species flock divergence). In summary, we could not detect severe effects of basal branch compressions by including the partially saturated third codon position in our analyses but rather found even younger age estimates for shallow nodes when doing so. Therefore, we conclude that despite partial saturation of third codon positions, their exclusion had no drastic impact on node

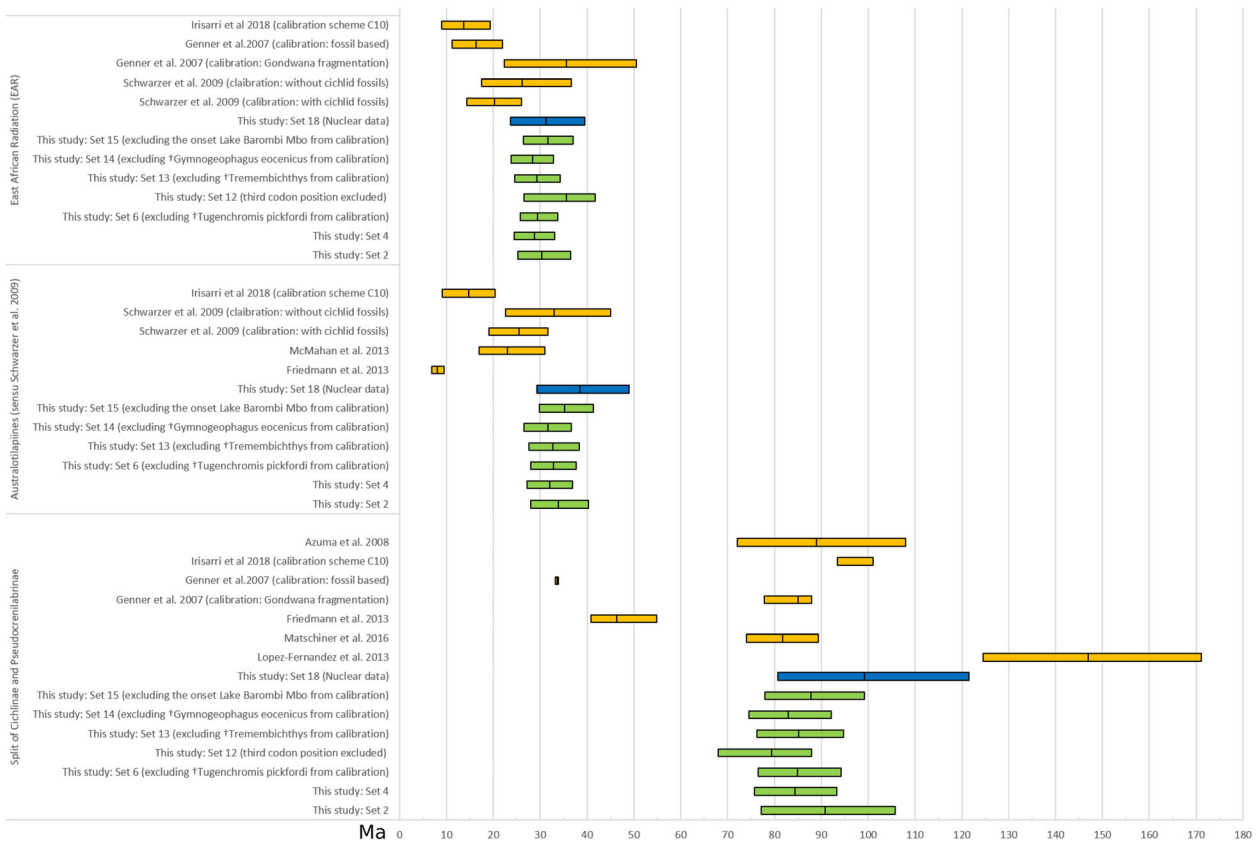

Fig. 3 Overview of divergence age estimates from this study. Calibration Sets based on the mitochondrial dataset (Set 2, Set 4, Set 12, Set 13, Set 14 and Set 15) are depicted in green. Calibration Set 18 based on the nuclear dataset is depicted in blue and several previous studies for selected cichlid groups (Cichlinae and Pseudocrenilabrinae, austrotilapiines and the East African Radiation) are depicted in orange. Depicted are either 95% HPD (highest posterior intervals), 95% credibility intervals, 95% confidence intervals or standard deviations depending on the source study. Mean ages are indicated by middle bar of each interval

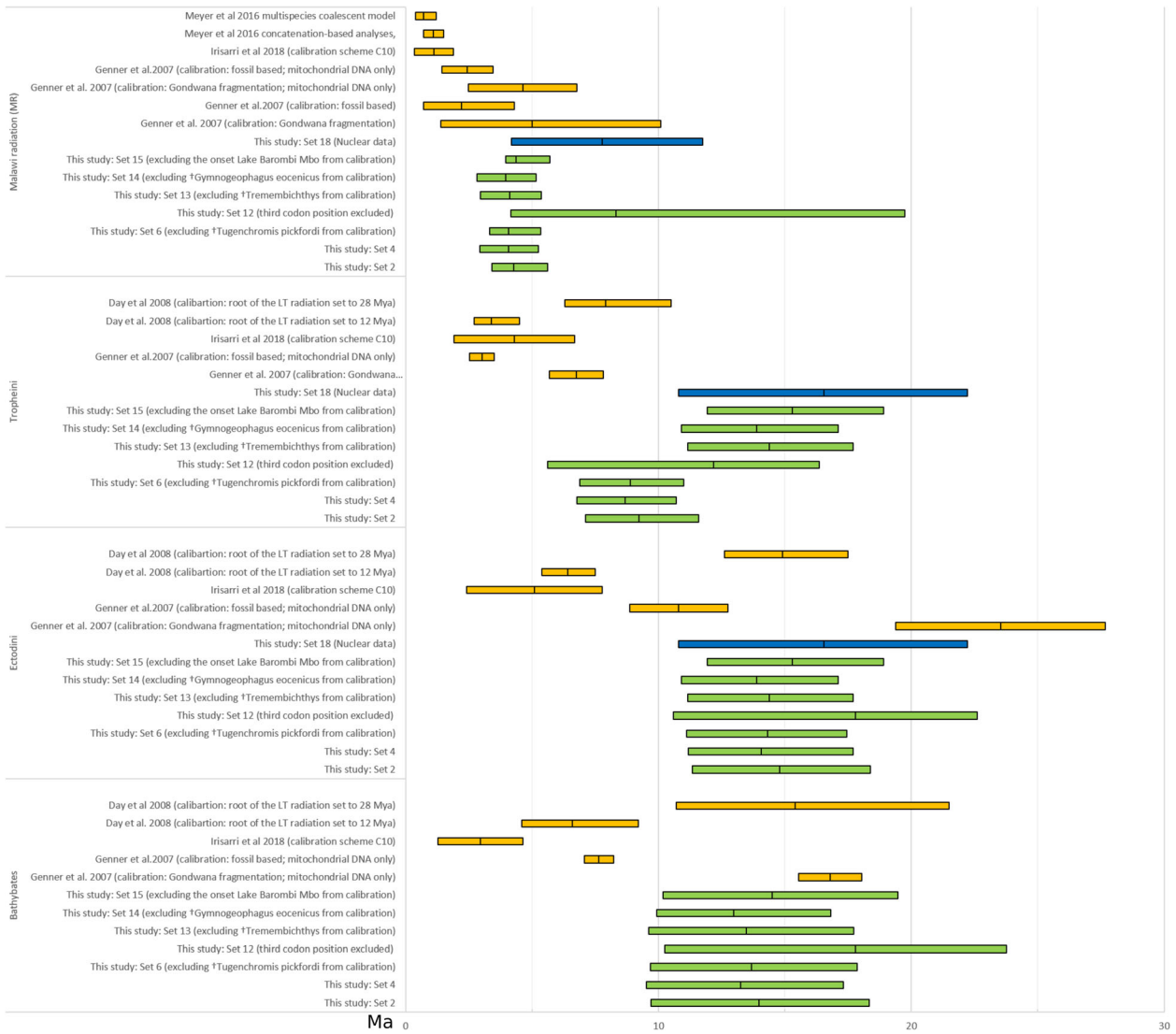

Fig. 4 Overview of divergence age estimates from this study. Calibration-Sets based on the mitochondrial dataset (Set 2, Set 4, Set 12, Set 13, Set 14 and Set 15) are depicted in green. Calibration Set 18 based on the nuclear dataset is depicted in blue and several previous studies for selected cichlid groups (*Bathybates*, Ectodini, Tropheini and the Malawi radiation) are depicted in orange. Depicted are either 95% HPD (highest posterior intervals), 95% credibility intervals, 95% confidence intervals or standard deviations depending on the source study. Mean ages are indicated by middle bar of each interval

age estimates but actually removed informative data, which were particularly relevant for resolution of shallower nodes. Divergence time estimates based on the comparative nuclear dataset with calibrations as for Set 4 had wider 95% HPD ranges and were generally older than corresponding estimates of the mitochondrial data set with calibration Set 4 (Figs. 3 and 4). However, 95% HPD intervals overlapped widely, sometimes even completely, as e.g. for the MRCA of the EAR. In summary, divergence estimates based on the nuclear dataset did not contradict the results of the mitochondrial datasets. Furthermore, these findings suggest that the use of only nuclear versus mitochondrial data alone is not entirely responsible for older divergence estimates observed on previous studies using mitochondrial data only.

A comprehensive list of mean divergence ages and their corresponding 95% HPD age ranges of selected nodes is given in the Additional file 4: Table S2. Here, we focus on age estimates obtained by the Calibration Set 4 because alternative estimates were highly similar and because Set 4 represents in our view the most likely setting, as the root calibration was constrained based on the most comprehensive data set [9], and it accounted for the more likely placement of †*Tugenchromis* [28]. We may want to point out that our age estimates are mitochondrial haplotype divergence ages, which do not fully

reflect speciation events, but rather are a first solid hint to minimum divergence ages. Moreover, comparatively young divergence age estimations (especially those younger than 1 Ma) might be inaccurate and most probably overestimate the actual diversification ages due to several reasons: For instance divergence time estimations are influenced by to the time-dependence nature of molecular rates which are reflected by the fact that there is a measurable transition from low, long-term substitution rates to increased, short-term mutation rates, most likely as a result from multiple factors (e.g., purifying selection, ancestral polymorphism) but also due to sequencing errors and calibration errors that can account for time-depended molecular rates [5, 87, 88].

Mitochondrial phylogeny and divergence time estimates of selected lineages

The ML-analysis (Fig. 1) and all BEAST-analyses recovered the monophyly of all recognized cichlid subfamilies, and additional major lineages and general relationships are consistent with most previously published studies (e.g. [5, 7–9]). The Etroplinae outgroup (Madagascar, southern India and Sri Lanka) formed the sister group to all other Cichlidae, and Ptychochrominae (Madagascar) were recovered as a sister group to a weakly supported clade of African Pseudocrenilabrinae + Neotropical Cichlinae (BS: 64). Mean divergence age (calibration Set 4) of the MRCA of African Pseudocrenilabrinae and Neotropical Cichlinae were estimated to be of Late Cretaceous age: 84.37 Ma (95% HPD: 75.71–93.25 Ma). Monophyly of Cichlinae was well supported (BS: 100) and the MRCA divergence age estimate is dated to 73.93 (95% HPD: 66.27–82.33 Ma). Internal relationships of tribes and lineages of Cichlinae were widely congruent with previous studies except for the poorly supported monophylum of Chaetobranchini and Astronotini (BS: 32), which was recovered as a sister group of the Cichlasomatini + Heroini monophylum. Similarly, monophyly of Pseudocrenilabrinae was well supported (BS: 100), but the divergence age of Pseudocrenilabrinae MRCA in our dataset was dated younger than that of Cichlinae, i.e. 60.79 Ma (95% HPD: 50.87–71.10 Ma). However, the estimate would have been substantially older if *Heterochromis,* which is the early branching sister group to all remaining Pseudocrenilabrinae, had been included (eg. [7, 8]). Thus, MRCA age estimates for two cichlid subfamilies Pseudocrenilabrinae and Cichlinae are largely compatible with several previous studies, e.g. [5] (based on Gondwanan landmass fragmentation), [6] (2008; based on 21 teleost fossils of different lineages) and [9] (based on 147 fossil clade age calibration points).

Intrarelationships of major African cichlid tribes (tylochromines, chromidotilapiines, hemichromines pelmatochromines) were only poorly supported as it was the case in previous studies (e.g. [5, 35, 89]. Monophyly of haplotilapiines (sensu [67]) was, however, well supported (BS: 100) with an estimated Eocene divergence age of 45.38 Ma (95% HPD: 37.98–54.49 Ma). Within haplotilapiines, Oreochromini (BS: 88) and austrotilapiines (BS: 38) were recovered as sister groups for the first time based on mitochondrial data alone, albeit with very weak support (BS: 41). Monophyly of boreotilapiines was not recovered in our analysis. Divergence age of the MRCA of Oreochromini was dated to 22.95 (95% HPD: 17.27–29.11 Ma) and of austrotilapiines to 31.98 Ma (95% HPD: 27.17–36.92 Ma). Within austrotilapiines, Steatocranini were resolved as a sister group to the EAR with relatively high support (BS: 94) and the divergence age of the MRCA was estimated to 30.62 Ma (95% HPD: 26.59–35.40 Ma).

Monophyly of the EAR was well supported (BS: 100) and the onset of divergence for this lineage was estimated to be of Late Eocene/Early Oligocene age: 28.71 Ma (95% HPD: 24.43–33.15 Ma). Boulengerochromini were recovered as the earliest diverging EAR lineage followed by a strongly supported clade (BS: 100) of Bathybatini + Trematocarini. This is congruent with two previous mtDNA studies (e.g. Day et al. 2008), but contrasts with other mtDNA studies which retrieved Boulengerochromini, Bathybatini and Trematocarini as the sistergroup to the remaining lineages of the EAR (e.g. [36, 90, 91]. Trematocarini were estimated to have diverged 16.13 Ma ago (95% HPD: 11.89–20.46 Ma) while Bathybatini started diverging 20.62 Ma (95% HPD: 16.88–25.34 Ma). In contrast with previous studies, which found Lamprologini and Eretmodini to form a sister group to the remaining members of EAR (e.g. [14, 17, 36, 76] Lamprologini were resolved as the sister group to the H-lineage (C-lineage including the Eretmodini) in our analyses. Divergence of the MRCA of Lamprologini and the H-lineage was well supported (BS 100) and estimated to 23.6 Ma (95% HPD: 20.18–27.33 Ma).

According to our data, Lamprologini diverge into three strongly supported (BS: 100) lineages during the Miocene at around 15.27 Ma (95% HPD: 12.23–18.49 Ma). The first clade was composed of the 'non-ossified Lamprologines' with taxa mainly endemic to LT but included some riverine taxa of disjunct distributions in the Congo Basin, e.g. *L. werneri* and *L. symoensi*. This clade diverged at around 12.51 Ma (95% HPD: 9.75–15.51). The second Lamprologini clade was composed of the LT endemics belonging to the 'ossified Lamprologines' and diverged at around 10.66 Ma (95% HPD: 7.39–13.97 Ma). Surprisingly and for the first time a mtDNA clade encompassing only *Lamprologus* of the lower and central Congo drainage (*L. mocquardi*, *L. markerti*, *L. tigripictilis*, *L. lethops*, *L. teugelsi* and *L.* sp. Kwango) was recovered; we refer to it as the 'Lower Congo *Lamprologus*

clade', because most members of this clade are only known form the Lower Congo area. Its divergence was dated substantially younger than the other two clades, i.e. to Late Miocene or early Pliocene at around 6.62 Ma (95% HPD: 4.31–9.49 Ma). Interrelationships of the three lamprologine clades were poorly supported.

Monophyly support for each of the ancient Tanganyika mouthbrooder tribes (Cyphotilapiini, Limnochromini, Ectodini, Perissodini, Benthochromini and Cyprichromini) was strong (BS: 100). For the first time a clade composed mostly three pelagic or epibenthic clades Perissodini, Cyprichromini and Benthochromini was recovered with strong support (BS 100), based on mitochondrial markers,. We refer to this clade as the "benthopelagic LT clade". It was only weakly supported in previous mtDNA based studies [36, 92], but is well supported by nuclear DNA data and more recently by AFLP and RAD based studies [7, 17, 93]. Divergence of the MRCA of the benthopelagic LT clade was dated to the Middle to Early Miocene age: 16.14 Ma (95% HPD: 12.83–19.54 Ma). Divergence of Perissodini took place at around 6.18 Ma (95% HPD: 3.16–9.59 Ma), of Cyprichromini at around 10.38 Ma (95% HPD: 6.20–14.53 Ma) and of Limnochromini at around 10.71 Ma (95% HPD: 5.20–16.30 Ma). Further, monophyly of Eretmodini were recovered with strong support (BS 100) and their divergence age is 7.60 Ma (95% HPD: 3.92–11.99 Ma) which was comparable with those of Perissodini. In contrast, Ectodini and Cyphotilapini diverged slightly earlier with mean ages of 14.06 Ma (95% HPD: 11.18–17.70 Ma) and 14.16 Ma (95% HPD: 8.71–19.25 Ma), respectively.

The Malagarasi-*Orthochromis* are recovered as the sister group of Haplochromini with moderate support (BS 71), which contrasts with the placement of Malagarasi-*Orthochromis* of previous mtDNA based studies, which recovered for example a relationship of Malagarasi-*Orthochromis* and Ectodini (e.g. [15, 76]). Several nuclear DNA based studies however recovered the Malagarasi-*Orthochromis* as a sister group of the Haplochromini as is the case in this study (e.g. [17, 76]). Monophyly of Haplochromini was highly supported (BS 100) and the onset of diversification of Haplochromini was dated to Early Miocene: 16.64 Ma (95% HPD: 14.25–19.16 Ma). '*Ctenochromis*' *pectoralis* from the Pangani River drainage (Tanzania, Kenya) was placed as a sister group to all remaining Haplochromini with high support (BS 100), hereby confirming previous studies which however only found poor support for this node ([15, 26, 94].

Intrarelationships and monophyly of previously recognized haplochromine mtDNA lineages (e.g serranochromines-mt-lineage s.l.; *'Pseudocrenilabrus*-group' incl. Northern-Zambian-*Orthochromis*, 'New Kalungwishi cichlid', 'New Lufubu cichlid'; *Astatoreochromis*, LT Tropheini; Lake Malawi species flock and 'modern Haplochromini' incl. Lake Victoria Region Superflock and riverine east and central African haplotypes) were in large part congruent with previous mtDNA based studies (e.g. [15, 37, 39]. The serranochromines-mtDNA-lineage sensu *lato*, i.e. the southern-central African lineage including the Lake Fwa cichlids and '*O.*' *stormsi* (mean age: 13.41 Ma; 95% HPD: 11.18–15.85 Ma) are estimated to be slightly older than all remaining major lineages, i.e. the *'Pseudocrenilabrus*-group' (mean age: 11.82 Ma; 95% HPD: 9.63–14.18 Ma), Tropheini (mean age: 8.69; 95% HPD: 6.77–10.70 Ma), 'modern Haplochromini' (mean age: 9.42 Ma; 7.72–11.23 Ma) and Lake Malawi species flock (mean age: 4.07 Ma; 2.93–5.26 Ma). The well supported (BS 99) clade encompassing the serrranochromines-mtDNA-lineage *s. str.* (following Joyce et al. [95] and Musilová et al. [39]) represented in our study by *Serranochromis robustus*, *S. altus*, *Pharyngochromis sp.* and the undescribed taxon *'Haplochromis'* sp. Kwango are of Pliocene to Early Late Miocene age: 5.46 Ma (95% HPD: 3.79–7.24 Ma). The Lake Victoria Region Superflock (LVRS, following Verheyen et al. [96] and was recovered with strong support (BS: 100) and its divergence started in the Pleistocene age: 0.31 Ma (95% HPD: 0.12–0.53 Ma). In addition to these lineages, two novel mitochondrial haplotype lineages within Haplochromini were recovered here for the first time. '*Orthochromis*' *indermauri* was recovered as the sister lineage of a clade encompassing the *'Pseudocrenilabrus*-group' and the 'ocellated eggspot Haplochromini' (BS: 85). It is endemic to rapids on the lower Lufubu, the largest affluent of the southern Lake Tanganyika basin ([97]). Divergence of '*Orthochromis*' *indermauri* and remaining Haplochromini was dated to around 15.15 Ma (95% HPD: 12.91–17.46 Ma). The second novel lineage was '*Haplochromis*' *vanheusdeni* from the Great Ruaha drainage system, which was recovered with strong support (BS: 96) as sister taxon to all LT endemic Tropheini, a subgroup of Haplochromini. Divergence of this East African coastal drainage species and LT Tropheini was estimated to have taken place in the Miocene at around 10.51 Ma (95% HPD: 8.47–12.61 Ma).

Even so a large fraction of the nodes of the ML tree was well supported (BS: 100), it is worth mentioning that several nodes were comparatively weakly supported (Fig. 1). Most of the latter referred to early diversification events within Pseudocrenilabrinae and Cichlinae, or they are located among rapidly diversifying EAR clades, e.g. among early diverging EAR-tribes or among haplochromine cichlids. In contrast, different BEAST analyses resolved many more nodes with high support supported (BBP = 1) and consequently comparatively fewer nodes had low support (see e.g. Figure 2). This contrast might have several reasons. Generally, Bayesian analyses tend to yield on average higher node support than ML analyses and therefore might be overoptimistic ([98, 99]).

Moreover, in the addition to the different calibration points we predefined five monophyla based on the ML analysis in our BEAST analyses, which may have strengthened BPPs for nodes related to these phylogenetic constraints.

Discussion

The present study represents a comparatively comprehensive and robust data set in terms of number of mitochondrial markers (10 coding genes) and taxa (180 species of Cichlidae), with a novel calibration set including the recently described fossil species (†*Tugenchromis*; [28]). We recovered novel mitochondrial haplotype phylogenies based on the improved taxon sampling, which in combination with novel and re-evaluated node age estimates allow for a refined phylogeographic view on the origin and diversification of Cichlidae, especially those of the EAR.

Divergence age estimates in comparison of previous studies

Overall, our attempts to date the evolutionary history of cichlids based on the conservative selection of five well-corroborated fossils, one geological and two alternative root calibrations yielded robust divergence age estimates. These are congruent with several preceding studies while other studies resulted in partially different divergence age estimates. These discrepancies can be partially attributed to different calibration priors. By integrating extreme age estimates from previous studies into our alternative root age calibration strategy, we endevaored to evaluate these results with the background of our conservative internal node calibration strategy.

Divergence age estimates for two cichlid subfamilies Pseudocrenilabrinae and Cichlinae of this study are largely compatible with several previous studies (e.g. [5, 6, 9]). In contrast, they are in more or less dramatic conflict with other studies (Fig. 3), substantially with those López-Fernandez et al. [13], Friedman et al. [7], less dramatic with studies by McMahan et al. [8, 100] and Irisarri [101], and partially with some partial results presented by Genner et al. [5] and Day et al. [14].

López-Fernandez et al. [13] had estimated much older divergence age for Cichlidae (mean: 147 Ma, 95% HPD: 124.49–171.05 Ma), but their age estimates were recently challenged as they predate the oldest first spiny-rayed teleost (Acanthomorpha) and because multiple taxon concatenations in their alignment appeared to be composed of sequences from different taxa [52, 102]. At the other extreme, Friedman et al. [7] estimated a much younger divergence age for the MRCA of Pseudocrenilabrinae and Cichlinae (mean: 46.4 Ma, 95% HPD: 40.9–54.9 Ma). They had used ten non-cichlid fossils for calibration and no cichlid fossil. Again, such young divergence ages were questioned later [52] because they strongly contradicted the fossil record. The oldest Lumbrera formation cichlid fossils are at least 39.9 Ma old, which is considerably older than Friedman et al.´s (2013) divergence age estimate for Cichlinae (=Neotropical cichlidae) with a mean age of 29.2 Ma (95% CI: 25.5–34.8 Ma). Finally, application of one of the two calibration sets of Genner et al. (2007) using seven cichlid fossils resulted in substantially younger node age estimates than ours and also partially conflicts with the fossil record. Their age estimate for divergence of Pseudocrenilabrinae (33.6 Ma, 95% HPD: 33.2–33.9 Ma) substantially postdated the oldest known African cichlid fossil by about 12 million years (†*Mahengechromis* – 46 Ma); and the age of the MRCA of Cichlasomatini was younger (14.2 Ma; 95% HPD: 7.6–21.1 Ma) than the oldest known fossil for this tribe, i.e. †*Tremembichthys,* 55.8–23.03 Ma, although the placement of †*Tremembichthys* as a member of Cichlasomatini might be considered as problematic due to its high "Heroine-like" number of pterygiophores articulated with the first haemal arch. Such young age estimates are most likely the result of calibration with fossils which are not the oldest fossils of their respective lineage (e.g. †*Aequidens saltensis* from Argentina with an estimated age of 5.33–23.03 Ma has been used as a calibration for the entire tribe Cichlasomatini), whose priors were calibrated with hard upper and lower bounds. Moreover, following Malabarba et al. [103] they placed †*Proterocara argentina* from the Lumbrera formation as the earliest member of a clade uniting Geophagini, Cichlasomatini and Chaetobranchini; later however, Smith et al. [104]) revised †*Proterocara argentina* to be related with *Crenicichla* and *Teleocichla*. In addition, the use of further fossils with very uncertain phylogenetic placements like ? *Tylochromis* [105] and ? *Heterochromis* [106] as a calibration points in the analyses of Genner et al. [5] might have led to these young divergence age estimates obtained in their study. A more recent study by Meyer et al. [100] was based on two different divergence estimation methods and two secondary constraints taken from results of McMahan et al. [8]. Divergence ages obtained by McMahan et al. [8] are, based on calibrations with four cichlid fossils and one early acanthomorph fossil, in large parts compatible to our divergence estimates in the range of the 95% confidence intervals; their mean age estimates are, however, consistently younger than ours. One possible explanation for the younger estimates of McMahan et al. [8], and consequently that of Meyer et al. [100], is a that they placed two neotropical fossils †*Plesioheros* and †*Tremembichthys* at the basis of a clade consisting of the Heroini and Cichlasomatini, which is different from our placement accepting †*Plesioheros* as Heroini and †*Tremembichthys* as

Cichlasomatini. Finally, the only study using the recently described fossil †*Tugenchromis pickfordi* as a calibration point obtained for basal divergence events, e.g. the divergence of Pseudocrenilabirinae and Cichlinae, older estimates but for more recent events substantially younger estimates as compared to ours (Figs. 3 and 4) [101]. This study was based on an anchored loci approach with 533 nuclear loci for a total of 149 taxa. Due to their massive dataset, the usage of the software BEAST [48] for inference of divergence time estimates was not possible and therefore the non-Bayesian method RelTime [107] was used ([101]). The discrepancies in the divergence time estimations between this and our study might be partially attributable to the use of different analytical approaches as implemented in the different software packages, since RelTime divergence time estimates for comparatively old nodes appear to be inferred with a strict clock model, which was subsequently contradicted by a recent study of the software developers [29, 108, 109]. Apart from this disputable feature of RelTime, it is worth mentioning that RelTime only allows for hard boundaries for age constraints, and those were applied in the study of Irisarri et al. [101] partially for fossils with disputable phylogenetic placement, i.e. †*Tylochromis* (see discussion of this fossil in Additional file 3), or with conservative maximum age boundaries secondarily taken from the Gondwana-set of the study of Genner et al. [5]. Therefore, it would be interesting if a Bayesian analysis with a reduced dataset with a comparable calibration scheme, as suggested by Matschiner [29], would yield comparable results to ours.

In contrast to the aforementioned conflicts with previous studies, our divergence age estimates, especially those for the age, origin and diversification of the EAR, are compatible with results from other studies, i.e. the Gondwana breakup calibration inference of Genner et al. [5] and Day et al. [14] Day et al. (2008) and the fossil based inference of Schwarzer et al. [35]. In the light of the recently published findings and overlooked calibration problems, conflicts of our age estimates with previous studies appear explainable. Since our study conservatively incorporates carefully selected calibration points, includes for the recently described EAR fossil (†*Tugenchromis)*, and carefully accounts for remaining uncertainties by evaluating alternative placements of critical fossils in molecular clock analyses, we provide an improved framework for the discussion of the phylogeographic history of the exact cichlid diversity, in particular the one of East African cichlids of Lake Tanganyika.

Divergence age estimates of Pseudocrenilabrinae and Cichlinae favor a short-distance dispersal scenario across the emerging proto-Atlantic

The recent geographic distribution of the two reciprocally monophyletic cichlid subfamilies Cichlinae (Americas) and Pseudocrenilabrinae (Africa) is a matter of the long-standing debate. Such a pattern can be interpreted as a result of either the Gondwana breakup ("Vicariance Hypothesis"), or, alternatively, by a trans-Atlantic dispersal event ("Marine Dispersal Hypothesis") if the radiation of extant Cichlinae and Pseudocrenilabrinae took place after the fragmentation of Gondwana. [5–8, 11, 12, 29, 110]. Unfortunately, evaluation of these alternative hypotheses has been and still remains difficult. This is due to the different geological age estimates for the final separation of South America and Africa, which according to recent estimates took place at around 103 Ma at the Ghanaian Ridge and the Piauí-Ceará margin [111]. Genner et al. [5], for example, calibrated the South America and Africa separation with a range of 86 to 101 Ma whereas Azuma et al. [6] calibrated the same event with 100 to 120 Ma. The most comprehensive previous study dates the separation of Cichlinae and Pseudocrenilabrinae to 81.8 Ma (95% HDP: 89.4–74.0 Ma), i.e. a few million years thereafter [9]). The latest comprehensive review on this discussion argues that the divergence of Pseudocrenilabrinae and Cichlinae occurred probably around 60 to 75 Mya after evaluating potential sources creating observed differences in divergence time estimation studies [29].

Our divergence age estimates for the split of Neotropical and African cichlids (84.37 Ma (95% HPD: 75.71–93.25 Ma) tentatively support the "Marine Dispersal Hypothesis", which is in accordance with Vences, Friedman et al. [7], and Matschiner [29], as well as with, importantly, one of the most comprehensive teleost-scale study [9]. Nevertheless, our age estimates are older than the estimate of 65 to 75 Ma for the recently suggested trans-Atlantic dispersal event of cichlids [29]. If the log-normal or uniform root prior including the extremely old age ranges for the cichlid origin (prior range of 46.0–174.78 Ma) are taken into account, the combined minimum and maximum 95% HPD ranges of all our estimated scenarios is 75.61 and 107.83 Ma, i.e. it slightly overlaps with the period of the final separation of the two continents (103 Ma), but the mean ages (84.38 to 91.94 Ma) clearly postdate the split event. Nevertheless, it is important to stress here that the nascent southern Atlantic was only a few hundred kilometers wide around that time of the continent split [111], such that freshwater plumes of several large rivers (e.g. the proto-Congo or proto-Niger River) most likely extended far offshore into the narrow oceanic gap [112], and that multiple island clusters existed there along the Rio Grande Rise and the Walvis Ridge until approx. 30 Ma ago [113, 114]). In combination, these factors imply an island-hopping scenario of euryhaline cichlids over comparatively short distances rather than a long-distance marine dispersal. This inference is supported by the fact that not a single oceanic cichlid species is

known today. In contrast, quite a few members of several distantly related cichlid lineages are inshore brackish water species [63, 115, 116] or are known from hypersaline inland habitats [72, 117]. Further, Matschiner [29] argues that even longer distances (650–900 km) might have been possible to cross. Alternatively, a vicariant origin of Cichlinae and Pseudocrenilabrinae cannot be falsified completely, if the 95% HPD intervals are taken into account.

Divergence of the Lake Tanganyika tribes supports the "melting-pot Tanganyika" hypothesis

Considering our age estimates for the Lake Tanganyika (LT) cichlid tribes and all estimated ages for the formation of a LT basin (e.g. 5.5 Ma or 12 Ma) that could have served as a habitat for lacustrine cichlid radiations an intra-lacustrine origin of divergence for the LT tribes appears highly improbable. For instance, our age estimates for the MRCA of the EAR but also of the two MRCA of the most ancient Lake Tanganyika tribes (e.g., Bathybatini - 20.62 Ma, and Trematocarini - 16.13 Ma), and the MRCA of Lamprologini and H-lineage (23.6 Ma) are estimated to be substantially older than 12 million years. Hence, they predate the often-cited maximum age of LT of 12 Ma, which itself might even represent an overestimated age for the origin of the extant LT basin as those estimates are based on the probably incorrect assumption of uniform sedimentation rates (see below). Likewise, divergence age estimates for the MRCA of H-lineage and the MRCA of the benthopelagic LT clade are substantially older than the maximum estimate for the origin of LT. Ectodini and Cyphotilapiini mean divergence age estimates are still around two million years older than 12 Ma. While Cyprichromini and Limnochromini divergence ages fall in the time range of the older maximum age estimate of LT (9–12 Ma), the estimates were still older than the younger estimate of 5.5 Ma for the age of LT. Only the MRCA of Perissodini and Eretmodini had 95% HPD intervals which were partly younger than 5.5 Ma but mean ages still remain slightly older. It is worth mentioning that several of these lineages with a clear lacustrine ecology (such as Bathybatini, Trematocarini and the pelagic LT clade) started to radiate, according to our data, well before the onset of LT basin formation, even though their extant diversity evolved with high probability later under lacustrine conditions.

There is an ongoing debate about the geological age of the Lake Tanganyika basin and the onset of persistent lacustrine conditions which would have allowed for the evolution of the lacustrine species flocks of the EAR [17]. In the cichlid literature, the most commonly cited maximum age of the opening of the oldest central segment of the proto-Lake Tanganyika is 9 to 12 Ma [18]. This estimate is based on extrapolation of Quarternary sedimentation rates on seismically inferred deep-lake sediment layers assuming roughly uniform sedimentation rates [18, 118]. The northern Bujumbura LT basin and the southern Mpulungu LT basin are estimated to be younger with of ages of 7–8 Ma and 2–4 Ma, respectively. In contrast to the assumption of uniform sedimentation rates, episodes of regional tectonic, volcanic and climatic changes in the LT area rather suggest that sedimentation rates strongly fluctuated in the past and were higher especially during the late Miocene/early Pliocene. This would potentially translate into overestimated dates for the origin of lacustrine conditions of LT [17, 19]. Indeed, Cohen et al. [18] already stipulated that their age estimates are only maximum ages, and several more recent studies based on thermochronology and sedimentology date the onset of pre-rift formation of the Albertine Rift to 4–11 Ma and the earliest onset of true rifting activity that could possibly have created deep rift lakes in the northern basins to only 5.5 Ma [20–23]. Due to the complex geological history and the remaining uncertainties regarding the age of LT we will compare both age estimates (9–12 Ma and 5.5 Ma) of the origin of LT with our divergence age estimates.

Several hypotheses of the origin and timing of diversification of Lake Tanganyika cichlid tribes have been proposed over the past years. One scenario postulates that the diversification of Lake Tanganyika lineages took place within the limits of the extant LT basin, i.e. the older lineages formed during the proto-LT phase, (9–12 Ma), whereas younger tribes would have evolved in the extant lake [90]. Genner et al. [5], based on their molecular clock analysis calibrated using Gondwana fragmentation (see above), suggested LT to be a reservoir of multiple ancient riverine lineages, which adaptively radiated into lacustrine species flocks after the proto-LT area had changed to become a rift lake; this, however, occurred without leaving any riverine descendants. In contrast to the two former scenarios, the recently proposed "Melting Pot Tanganyika" hypothesis of Weiss et al. [17] proposes an independent pre-rift diversification of several LT cichlid precursor lineages in different drainages and precursor lakes of the greater LT area. After river captures in the Neogene and Pleistocene, i.e. during a phase of tectonic rearrangements in a highly dynamic and heterogeneous LT area landscape, secondary contact of those divergent cichlid lineages led to hybridization among them. Support for this scenario comes from evidence for a reticulate phylogenetic history of several LT lineages [17, 119], and, more recently, from the discovery of a Miocene age EAR fossil in Kenya with a mosaic of characters, of which some are present today only in selected LT cichlid tribes [28].

Overall, our divergence age estimates are compatible with both the hypotheses of Genner et al. [5] and Weiss et al. [17], i.e. that LT might represent a reservoir of multiple ancient lineages that have evolved before the origin of the extant LT Tanganyika basin. In combination with the discovery of †*Tugenchromis pickfordi* in the Lake Baringo area of Kenya and the recent evidence for introgression and hybridization between several ancient LT and extant riverine cichlid lineages but also among LT lineages themselves [17, 100] the "melting-pot Tanganyika" hypothesis appears to be favorable. Even though our study provides comparatively robust age estimations for the MRCA of different LT tribes, no age estimates for potential introgression and hybridization events can be provided as only maternally inherited mtDNA data were used in this study.

Divergence of riverine Lamprologini supports several dispersal events from LT region towards the Congo system

The present study identified for the first time a third basal lamprologine mtDNA clade, whose primary divergence took place latest at around 15.27 Ma (95% HPD: 12.23–18.49 Ma) and hence predate the origin of the extant LT basin under any geological scenario. Interestingly, the third novel clade comprises only lower and central Congo taxa, whereas the two previously known clades contain both Congo basin and LT taxa, with the Congo taxa being deeply nested within the LT species community. Unfortunately, alternative relationships among the three main clades are only weakly supported, rendering any vicariance-based inference about the geographic origin of Lamprologini difficult.

Two different scenarios had previously been suggested for the origin and distribution of Lamprologini. The first suggests that Lamprologini evolved within Lake Tanganyika as a single radiation and subsequently colonized the Congo Basin, possibly via the Lukuga River [90, 120–122]. This scenario had been suggested because *Lamprologus* species of the Congo and Malagarasi-drainage are consistently nested deep within the 'non-ossified Lamprologines' of Lake Tanganyika in several studies (e.g. [90, 120–122]). In contrast, the study of Clabaut et al. [76] identified a clade encompassing a sample identified as *L. teugelsi*[1] and *L. congoensis* as the sister group of all remaining LT Lamprologines in their nuclear DNA data set. This phylogenetic result suggested that Congo Lamprologini seeded the LT Lamprologini radiation, and hence rendering Congo Lamprologini ancestral relict species.

According to the results presented herein, the crown age of the two lineages harbouring predominantly LT taxa (the 'ossified' and 'non-ossified' Lamprologines), is substantially older than that of the Congo-lineage, a geographic origin of Lamprologini in the proto-LT region appears more likely and hence they appear to have colonized the western and central Congo basin later through multiple dispersal events. A first colonization event in the Late Miocene to Early Pliocene might have seeded the 'Lower Congo *Lamprologus* clade'; and, interestingly, it falls in the same time range of previously estimated age of the MRCA of the lower Congo endemic radiation of *Nanochromis* and *Steatocranus* [123]. The diversification of the 'Lower Congo *Lamprologus* clade' might therefore be linked to the Pliocene origin of the modern lower Congo River rapids, which has been suggested to be correlated with the species-flock formation of *Steatocranus* and *Nanochromis* in the same area [123]. If the Lamprologini origin in the greater LT region is correct, and if the Lower Congo Lamprologini originally were monophyletic as suggested by morphology [124], then only a second colonization event could explain the alternative mtDNA haplotype placement of *L. werneri* in the 'non-ossified Lamprologines' clade. Indeed, complete exchange of mtDNA-haplotypes is known for LT endemic Lamprologini and therefore cannot be ruled out until more nuclear data are available for this group [125, 126].

We have included for the first time in a molecular phylogenetic analysis the only Upper Congo (Lualaba) endemic *Lamprologus*, *L. symoensi* from the Upemba Lakes region. Similarly to the *L. teugelsi* case, it appears to be either a descendant of a secondary colonization event (most likely by a member of the 'non-ossified Lamprologines' as suggested by morphological data; see Schelly et al. [124]) or *L. symnoensi* captured the mitochondrial genome from dispersing LT Lamprologini. Interestingly, our mtDNA divergence ages estimates of *L. symoensi* and *Telmatochromis* cf. *temporalis* are young at around 2.55 Ma (95% HPD: 1.34–3.87 Ma), roughly similar to those of *Pseudocrenilabrus multicolor* and *P. nicholsi,* the former one a Nilotic species and the latter one an Upper Congo (Lualaba) species: 2.20 Ma (95% HPD: 1.20–3.34 Ma). This coincidence may indicate that the closely neighbouring Upper Congo, Lake Tanganyika and Nile drainage systems were relatively permeable at this time, e.g. through river captures and/or shared headwater areas, allowing the exchange of faunistic elements. This inference is also compatible with established Congo-Nilotic sister group relationships of selected modern Haplochromini [26].

Age and divergence within riverine Haplochromini and their lacustrine radiations

Originally, the "Out of Tanganyika" hypothesis had suggested that the geographic and genetic cradle of Haplochromini is Lake Tanganyika and that LT Haplochromini secondarily left the lake to seed all other haplochromine

radiations in East Africa [37]. Our new node age estimates in combination with an improved riverine Haplochromini taxon sampling enabled us to re-evaluate this hypothesis, as well as the biogeographic and temporal origin of several other Haplochromini radiations, i.e. the modern Haplochromines of the Lake Victoria Region superflock (LVRS), the Lake Malawi species flock, the LT Tropheini.

In line with other more recent phylogenetic studies (e.g. [9]) our molecular clock data suggesting that the onset of the Haplochromini diversification had started already by the Early Miocene (16.64 Ma; 95% HPD: 14.25–19.1). This date substantially predates the presumed tectonic origin of the LT basin by several million years and renders an "Out of Tanganyika" scenario rather unlikely based on our estimates. Taking into account that the Malagarasi-*Orthochromis* and the Haplochromini are resolved as sister lineages and that the earliest split within the Haplochromini is the sister-group relationship of *Ctenochromis pectoralis* endemic to coastal drainages in Kenya and Tanzania, and remaining Haplochromini, it seems more parsimonious that the MRCA of haplochromine cichlids lived east of LT. Nevertheless, a key role of the greater LT region as a reservoir of ancient haplochromine cichlid lineages is shown by the relict-like distribution patterns of the riverine mtDNA lineage of the recently described '*Orthochromis*' *indermauri*, which is estimated to have diverged from other Haplochromini lineages including the '*Pseudocrenilabrus*-group', Tropheini plus '*H*'. *vanheusdeni*, the Lake Malawi species flock and modern Haplochromini well before the origin of the LT basin in the Early to Middle Miocene.

Undoubtedly, LT with its history of climate-driven lake level fluctuations shaped the evolution of the Tropheini (e.g. [127–129]), but the origin of this LT endemic haplochromine lineage is only partially understood. In previous studies Tropheini had been resolved as the sister group to a clade encompassing the many riverine and modern Haplochromini (including the LVRS) and the Lake Malawi species flock (e.g. [7, 37, 119]). Further, two recent studies found support for a potential ancient hybrid origin for the Tropheini [17, 100]. Therefore, it is quite unexpected that the here newly recognized lineage represented by '*H*'. *vanheusdeni*, endemic to the coastal Great Ruaha drainage in eastern Tanzania system, is resolved as the mitochondrial sister group to Tropheini. Divergence of those two lineages is estimated to have occurred in the early or middle Miocene, which indicates a past connection of the proto-Malagarasi drainage system and the Proto-Great Ruaha drainage system at that time. Interestingly, in addition to '*H*'. *vanheusdeni* is another biogeographically important lineage known from Ruaha drainage system. Genner et al. [130] recovered *Astatotilapia* sp. 'Ruaha' as sister lineage of the Lake Malawi species flock. Unfortunately, our study is missing this taxon, but it underlines the remarkable drainage evolution of the Ruaha.

The MRCA of the megadiverse Lake Malawi species flock is dated to the Pliocene at around 4.07 Ma (95% HDP: 2.93–5.26 Ma). This age is compatible with previous findings based on fossil and Gondwana fragmentation calibration [5], or on secondary calibrations (Genner et al. [131] based on [35]). However, our Pliocene divergence age sharply contrasts with the findings of several other studies dating the age of the Lake Malawi species flock considerably younger, i.e. 0.93–1.64 Ma [16], 0.73–1.0 Ma [15], 0.7–1.5 Ma ([100]; concatenation set) and 0.4–1.2 Ma ([100]; multispecies coalescent model). The young age estimates obtained by the studies of Sturmbauer et al. [16] and Koblmüller et al. [15] appear to be the result of a calibration based on the assumption of Delvaux [24] that Lake Malawi almost completely desiccated between 1.6 Ma until 1.0–0.57 Ma, and on the assumption that an intralacustrine origin of major Lake Malawi cichlid clades ("mbuna", "utaka") would have taken place only after hypothetical refilling of the LM. This assumption might be, however, inappropriate, as a recent study recorded continuous sedimentation in Lake Malawi over the last 1.3 Ma, even though 15 severe droughts had intermittently resulted in lake level decreases of more than 400 m [25]. Moreover, the geological and sedimentological age of LM is still poorly understood. The Malawian Rift is bordered by the Rungwe volcanic province, which is estimated to have formed between 5.45 to 8.6 Ma based on K/Ar dating of different volcanic materials [132, 133]. These ages are commonly associated with the onset of rifting of LM rift basin (e.g. [24, 131]). The lower Chiwondo Beds northwest of LM coast are dated to 4 Ma or older based on biostratigraphy and represent the first evidence for lacustrine conditions of LM [134]. Our divergence time estimates for the origin of the LM species flock are thus compatible with the reported onset of lacustrine conditions of LM and which would imply that ancient lineages of the LM species flock survived these droughts. Interestingly, the MRCA of the clade containing predominantly sand-dwelling genera (mean age: 0.69 Ma; 95%HPD: 0.45–0.96 Ma) and the MRCA of the clade containing predominantly rock-dwelling genera (mean age: 0.6 Ma; 95%HPD: 0.39–0.81 Ma) appear to have emerged at around the Mid-Pleistocene restoration of lacustrine conditions in LM The radiation of these clades hence may be the result of increased ecological opportunity and habitat stability in LM [25, 100].

The exact geological age of the largest freshwater lake in world, Lake Victoria (LV), is still debated, but its

formation is estimated to 0.4 Ma or 0.8 to 1.6 Ma [135, 136] and paleolimnological data provide evidence for a nearly complete or even complete desiccation of LV during the late Pleistocene (e.g. [135, 137]). These findings fostered doubts whether the LVRS (following Verheyen et al. [96] and Meier et al. [26]) originated before or after the late Pleistocene desiccation events. Divergence estimates of previous studies ranged between 0.1 Ma and 4.42 Ma, i.e. suggesting that the LVRS origin predates the desiccation of LV [96, 100, 138]. Our mitochondrial divergence time estimate dates the LVRS to around 0.31 Ma (95% HPD: 0.12–0.53 Ma) which is roughly compatible with the estimated age of LV; however, our taxon sampling is not fully representative for that flock as several lineages e.g. from Lake Kivu, Lake Edward and Lake Albert are missing. Nevertheless, it still includes *Haplochromis stappersii*, which together with *Haplochromis* sp. "Yaekama" forms the sister clade to the LVRS [26]. We estimated the divergence age for the MRCA of the LVRS and *H. stappersii* to around 0.99 Ma (95% HPD: 0.51–1.53 Ma). Moreover, it has recently been shown by Meier et al. [26] that the LVRS might be the result of ancient hybridization events between two haplochromine lineages (a 'Congolese lineage' including for example *H. stappersii*, and an Upper Nile lineage consisting of '*Haplochromis*' *gracilior* and *Haplochromis pharyngalis*) which should be considered for the divergence time reconstruction of the LVRS.

Through the inclusion of the newly discovered fossil †*Tugenchromis* and the careful selection of additional calibration points, we provide novel and refined divergence age estimates for most haplochromine radiations. These estimates are still preliminary, however, as for a more accurate reconstruction of the evolutionary history, particularly of the younger haplochromine lineages, additional nuclear DNA-data, younger calibration points and additional analysis methods based on population-level sampling, are needed.

Conclusion

Our study, based on an alignment of ten mitochondrial protein-coding genes including representative taxa of all cichlid subfamilies, resulted in a comparatively well-resolved mitochondrial phylogenetic hypothesis for cichlids with focus on members of the East African radiation. Bayesian divergence time estimates based on eighteen different calibration sets evaluating even extremely young or old age previous age estimates are, nevertheless highly consistent and several novel mtDNA haplotype lineages are recognized. One is a novel third clade of lower Congo *Lamprologus*, and the other two east-central African ones with considerable phylogeographic interest, i.e., '*Orthochromis*' *indermauri* and *Haplochromis vanheusdeni*. Remarkably, all three novel lineages represent riverine taxa with close affinities to important cichlid radiations. This underscores the importance of a fully representative riverine taxon sampling when phylogenetically inferring the evolutionary history and biogeography of cichlid radiations (e.g. [15, 26, 37, 131]).

Although our study is based to a large part on the protein coding genes of the mitochondrial genome we were able to obtain robust minimum ages of divergence ages associated with the origin of the East African cichlid fauna. Moreover, our molecular clock analysis adds addtitional support to several previously ambiguously supported findings. First, divergence age estimates for the MRCA of the African Pseudocrenilabrinae and Neotropical Cichlinae are consilient with the those of teleost-based Matschiner et al. [9], tentatively supporting the dispersal hypothesis, i.e. that seemingly vicariant phylogeography of Cichlidae can be explained by short-distance marine dispersal events (e.g. [7, 9, 63]), but not with long-distance oceanic dispersal. In particular, the sister relationship of African Pseudocrenilabrinae and Neotropical Cichlinae can be explained with an ecologically plausible dispersal scenario covering only short distances across now submerged island chains between the South American and African continents, e.g. the Rio Grande Rise and the Walvis Ridge.

Further, Genner et al.´s [5] "Ancient Reservoir" and the "Melting Pot Tanganyika" hypothesis of [17] are supported by our cichlid age estimates in combination with the recent discovery of a Miocene EAR cichlid fossil in Kenya exhibiting synapomorphies with several extant Lake Tanganyika cichlids [28], and with recent evidence for repeated hybridization among ancient cichlid lineages in Lake Tanganyika [17, 119]. Our divergence time estimates for almost each of the MRCA of all endemic LT tribes predate the estimated origin of the extant LT basin at 5.5 Ma and only Perissidini and Eretmodini might have formed after the formation of LT.

Endnotes

[1]There seems to be some confusion with the identification of one or more "*L. teugelsi*" samples in previous studies. After the description of *Lamprologus teugelsi* by Schelly et al. [124] samples and sequences previously identified as *L. mocquardi* (e.g. [90]) were renamed as *L. teugelsi* in subsequent studies (e.g. [76, 120]). Unfortunately, no precise sample location for these samples were provided. With the exception of a dubious type locality record in the primary description, *L. teugelsi* is known only from the Inga area of the Lower Congo rapids. Without locality information and reexamination of those specimens it is not

possible to clarify whether *L. teugelsi* carries two different mitochondrial haplotypes or if previously analyzed specimens were misidentified.

Additional files

Additional file 1: Table S1. Overview of the taxon sampling with corresponding Genbank accession numbers and, where applicable, corresponding repository numbers of specimens and their origin. (DOCX 43 kb)

Additional file 2: Table S3. Overview of the taxon sampling for the nuclear markers (RAG1, ENC1, Rh1 and ttna TMO) with corresponding Genbank accession numbers. (DOCX 75 kb)

Additional file 3: Justification for exclusion of several cichlid fossils from calibration. (DOCX 24 kb)

Additional file 4: Table S2. Comprehensive list of mean divergence ages and their corresponding 95% HPD age ranges of selected nodes. (Node numbers 1 to 65 correspond to numbers depicted in Fig. 2). (DOCX 32 kb)

Abbreviations

BPP: Bayesian Posterior Probability; BS: Bootstrap support; EAR: East African Radiation; HPD: Highest posterior density; LM: Lake Malawi; LT: Tanganyika; LV: Lake Victoria; LVRS: Lake Victoria Region Superflock; ML: Maximum likelihood; MRCA: Most recent common ancestor

Acknowledgments

We want to thank F. P. D. *Cotterill, A. Dunz,* H. van Heusden, A. Lamboj, T. Moritz, D. Neumann, P. Piepenstock, L. Rüber, R. Schelly, E. Schraml, A. Spreinat, O. Seehausen, E. Swartz, E. Vreven, U. Werner for providing us with tissue samples. The *Lamprologus symoensi* sample and photograph was kindly provided by E. Vreven (MRAC), who had collected during the "Katanga 2012 Expedition" with the financial and logistical support from the PRODEPAAK (NN/3000769) CTB/BTC project (2008-2013). J. Geck (*H. vanheusdeni*, *'O.' stormsi*, *O. uvinzae*, *P. maclareni*, *C. zillii*) and E. Schraml (*M. auratus*, *N. linni, H. nyererei*, *G. bellcrossi*) for the provision of cichlid photographs for Fig. 1. D. Neumann and T. Laibl for kindly assisting with curation of vouchers and associated data at the ZSM. A. Brachmann and A. Nieto of the sequencing service of the Ludwig-Maximilian-University of Munich for their useful advice and support. We are grateful for discussions on †*Tugenchromis* and its use as calibration point with B. Reichenbacher and M. Altner. We thank C. Y. Wang-Claypool for language editing of this manuscript. We acknowledge the two anonymous reviewers for their constructive comments.

Funding

The work for this project is funded by the Volkswagen-Stiftungs-Project "Exploiting the genomic record of living biota to reconstruct the landscape evolution of South Central Africa" (Az. 88 732). The funding body had no role in any activities regarding the study including design, sampling procedure, analysis, interpretation of the data and writing the manuscript.

Availability of data and materials

The annotated mitochondrial genomes and mitochondrial genome fragments are available in the GenBank repository under the accession numbers: MK144668 – MK144786 and MK170260 – MK170265. The datasets used and/or analyzed during the current study are available from the corresponding author on reasonable request.

Authors' contributions

UKS & FS designed the study. FS & ZM carried out the molecular work. FS conducted the data analysis and wrote the first draft of the manuscript. UKS and ZM contributed to the improvement of all versions of the manuscript. All authors read and approved the final manuscript.

Ethics approval and consent to participate

The sampling procedure was carefully planned and reviewed before executed according the recommendation of [40]. Sacrificing of fish specimens comply with the German Tierschutzgesetz (TSchG) including §2 (rearing), & 7a(1)6. Neither the technical staff nor the scientist involved in this study performed experiments concerning the EU directive 2010/63/EU notably those defined in the General Provisions of Article 1 §1 (use of animals for scientific and educational purpose) and §2 (animals used or intended for use in procedures). Therefore, no separate ethical approval for animal use concerning this research of this study was necessary. The study did not include any species protected by CITES, European or German law (see: http://www.wisia.de/FsetWisia1.de.html; query for all fishes and lampreys). Specimens for this study were either collected in the wild in the Democratic Republic of the Congo and Zambia (permits see below), obtained from the ornamental fish trade. Most specimens were obtained prior to the legal implementation of the Nagoya Protocol (12.10.2014) and its corresponding EU Access and Benefit Sharing (ABS) regulations, which came into effect on 9th November 2015. The few exception are: *B. vittatus, B. minor. B. leo B. leo, T. unimaculatum, T. macrostoma* and *T.* cf. *variable* which were collected in Zambia in 2015 (permits see below). Regardless of the sample date of tissues we checked whether any national legislation for access and utilization of samples apply for the countries of sample origin (including traded specimens and their potential origin): Angola (07.05.2017), Burundi (12.10.2014), Cameroon (28.02.2017), Democratic Republic of the Congo (05.05.2015), Egypt (12.10.2014), Eritrea (not applicable), Israel (not applicable), Malawi (26.08.2014), Republic of the Congo (14.05.2015), South Africa (10.01.2013), Tanzania (19.01.2018), Tunisia (not applicable) and Zambia (20.05.2016); see https://www.cbd.int/abs/nagoya-protocol/signatories/default.shtml. Permissions for specimen collection in the wild and exportation of samples were granted for the field trips to DRC and Zambia by the Ministries of the Interior and Agriculture Direction Provinciale du Bas-Congo (DRC Research permit and export permit No. AC/113/2013/I.S.P/MBNG/AUT.AC; issued by the by the Republique Democratique du Congo, Institute Superieur Pedagogique de Mbanza-Ngungu; sampling in DRC and supervised by Paul N'lemvo Budiongo, Institut Congolais pour la Conservation de la Nature (ICCN)); and by Ministry of Agriculture and Livestock in Kasama (collection and export permits were issued the 05.10.2015 by Alex D. Chilala; Provincial Agricultural Coordinator, Western Province, Republic of Zambia) who also supervised the sampling in Zambia).

Consent for publication

Not applicable.

Competing interests

The authors declare that they have no competing interests.

Publisher's Note

Author details

[1]Department of Ichthyology, SNSB - Bavarian State Collection of Zoology, Münchhausenstr. 21, 81247 Munich, Germany. [2]Department of Zoology, Faculty of Science, Charles University, Vinicna 7, CZ-128 44 Prague, Czech Republic.

Received: 2 October 2018 Accepted: 31 March 2019
Published online: 25 April 2019

References

1. Kocher TD. Adaptive evolution and explosive speciation: the cichlid fish model. Nat Rev Genet. 2004;5:288–98.
2. Wagner CE, Harmon LJ, Seehausen O. Ecological opportunity and sexual selection together predict adaptive radiation. Nature. 2012;487:366–9.
3. Santos ME, Braasch I, Boileau N, Meyer BS, Sauteur L, Bohne A, Belting HG, Affolter M, Salzburger W. The evolution of cichlid fish egg-spots is linked with a cis-regulatory change. Nat Commun. 2014;5:5149.
4. McGee MD, Faircloth BC, Borstein SR, Zheng J, Darrin Hulsey C, Wainwright PC, Alfaro ME. Replicated divergence in cichlid radiations mirrors a major vertebrate innovation. Proc R Soc B Biol Sci. 2016;283:20151413.
5. Genner MJ, Seehausen O, Lunt DH, Joyce DA, Shaw PW, Carvalho GR, Turner GF. Age of cichlids: new dates for ancient lake fish radiations. Mol Biol Evol. 2007;24:1269–82.

6. Azuma Y, Kumazawa Y, Miya M, Mabuchi K, Nishida M. Mitogenomic evaluation of the historical biogeography of cichlids toward reliable dating of teleostean divergences. BMC Evol Biol. 2008;8:215.
7. Friedman M, Keck BP, Dornburg A, Eytan RI, Martin CH, Hulsey CD, Wainwright PC, Near TJ. Molecular and fossil evidence place the origin of cichlid fishes long after Gondwanan rifting. Proc R Soc B Biol Sci. 2013;280:20131733.
8. McMahan CD, Chakrabarty P, Sparks JS, Smith WM, Davis MP. Temporal patterns of diversification across global cichlid biodiversity (Acanthomorpha: Cichlidae). PLoS One. 2013;8:e71162.
9. Matschiner M, Musilová Z, Barth JMI, Starostova Z, Salzburger W, Steel M, Bouckaert R. Bayesian node dating based on probabilities of fossil sampling supports trans-Atlantic dispersal of cichlid fishes. Syst Biol. 2016;66:3–22.
10. Murray AM. Eocene cichlid fishes from Tanzania, East Africa. J Vertebr Paleontol. 2000;20:651–64.
11. Vences M, Freyhof J, Sonnenberg R, Kosuch J, Veith M. Reconciling fossils and molecules: Cenozoic divergence of cichlid fishes and the biogeography of Madagascar. J Biogeogr. 2001;28:1091–9.
12. Sparks JS, Smith WL. Phylogeny and biogeography of cichlid fishes (Teleostei: Perciformes: Cichlidae). Cladistics. 2004;20:501–17.
13. López-Fernandez H, Arbour JH, Winemiller KO, Honeycutt RL. Testing for ancient adaptive radiations in neotropical cichlid fishes. Evolution. 2013;67:1321–37.
14. Day JJ, Cotton JA, Barraclough TG. Tempo and mode of diversification of Lake Tanganyika cichlid fishes. PLoS One. 2008:3e1730.
15. Koblmüller S, Schliewen UK, Duftner N, Sefc KM, Katongo C, Sturmbauer C. Age and spread of the haplochromine cichlid fishes in Africa. Mol Phylogenet Evol. 2008;49:153–69.
16. Sturmbauer C, Baric S, Salzburger W, Rüber L, Verheyen E. Lake level fluctuations synchronize genetic divergences of cichlid fishes in African Lakes. Mol Biol Evol. 2001;18:144–54.
17. Weiss JD, Cotterill FP, Schliewen UK. Lake Tanganyika--a 'melting pot' of ancient and young cichlid lineages (Teleostei: Cichlidae)? PLoS One. 2015;10:e0125043.
18. Cohen AS, Soreghan MJ, Scholz CA. Estimating the age of formation of lakes: an example from Lake Tanganyika, east African rift system. Geology. 1993;21:511–4.
19. Macgregor D. History of the development of the east African rift system: a series of interpreted maps through time. J Afr Earth Sci. 2015;101:232–52.
20. Bauer FU, Glasmacher UA, Ring U, Schumann A, Nagudi B. Thermal and exhumation history of the central Rwenzori Mountains, Western rift of the east African rift system, Uganda. Int J Earth Sci. 2010;99:1575–97.
21. Lezzar KE, Tiercelin JJ, Le Turdu C, Cohen AS, Reynolds DJ, Le Gall B. C.A. S. Control of normal fault interaction on the distribution of major Neogene sedimentary depocenters, Lake Tanganyika, East African rift. AAPG Bull. 2002; 86:1027–59.
22. Roller S, Hornung J, Hinderer M, Ssemmanda I. Middle Miocene to Pleistocene sedimentary record of rift evolution in the southern Albert rift (Uganda). Int J Earth Sci. 2010;99:1643–61.
23. Spiegel C, Kohn BP, Belton DX, Gleadow AJW. Morphotectonic evolution of the Central Kenya rift flanks: implications for late Cenozoic environmental change in East Africa. Geology. 2007;35:427.
24. Delvaux D. Age of Lake Malawi (Nyasa) and water level fluctuations. Mus roy Afr cent, Tervuren (Belg), Dépt Géol Min. 1995;1995-1996:99–108.
25. Lyons RP, Scholz CA, Cohen AS, King JW, Brown ET, Ivory SJ, Johnson TC, Deino AL, Reinthal PN, McGlue MM, et al. Continuous 1.3-million-year record of east African hydroclimate, and implications for patterns of evolution and biodiversity. Proc Natl Acad Sci U S A. 2015;112:15568–73.
26. Meier JI, Marques DA, Mwaiko S, Wagner CE, Excoffier L, Seehausen O. Ancient hybridization fuels rapid cichlid fish adaptive radiations. Nat Commun. 2017;8:14363.
27. Cotterill FPD, De Wit MJ. Geoecodynamics and the Kalahari epeirogeny: linking its genomic record, tree of life and palimpsest into a unified narrative of landscape evolution. S Afr J Geol. 2011;114:493–518.
28. Altner M, Schliewen UK, Penk SBR, Reichenbacher B. †Tugenchromis pickfordi, gen. Et sp. nov., from the upper Miocene—a stem-group cichlid of the 'east African radiation'. J Vertebr Paleontol. 2017;37: e1297819.
29. Matschiner M. Gondwanan vicariance or trans-Atlantic dispersal of cichlid fishes: a review of the molecular evidence. Hydrobiologia. 2019;832:9–37.
30. Takahashi T. Systematics of Tanganyikan cichlid fishes (Teleostei: Perciformes). Ichthyol Res. 2003;50:367–82.
31. Koblmüller S, Sefc KM, Sturmbauer C. The Lake Tanganyika cichlid species assemblage: recent advances in molecular phylogenetics. Hydrobiologia. 2008;615:5–20.
32. Greenwood PH. Towards a phyletic classification of the `genus´ Haplochromis (Pisces, Cichlidae) and related taxa. Bull British Museum (Natural History) Zool. 1979;35:265–322.
33. Hoogerhoud RJC. A taxonomic reconsideration of the haplochromine genera Gaurochromis Greenwood, 1980 and Labrochromis Regan, 1920 (Pisces, Cichlidae). Netherlands J Zool. 1983;34:539–65.
34. Schwarzer J, Swartz ER, Vreven E, Snoeks J, Cotterill FP, Misof B, Schliewen UK. Repeated trans-watershed hybridization among haplochromine cichlids (Cichlidae) was triggered by Neogene landscape evolution. Proc R Soc B Biol Sci. 2012;279:4389–98.
35. Schwarzer J, Misof B, Tautz D, Schliewen UK. The root of the east African cichlid radiations. BMC Evol Biol. 2009;9:186.
36. Dunz AR, Schliewen UK. Molecular phylogeny and revised classification of the haplotilapiine cichlid fishes formerly referred to as "*Tilapia*". Mol Phylogenet Evol. 2013;68:64–80.
37. Salzburger W, Mack T, Verheyen E, Meyer A. Out of Tanganyika: genesis, explosive speciation, key-innovations and phylogeography of the haplochromine cichlid fishes. BMC Evol Biol. 2005;5:17.
38. Koblmüller S, Duftner N, Katongo C, Phiri H, Sturmbauer C. Ancient divergence in bathypelagic lake tanganyika Deepwater cichlids: mitochondrial phylogeny of the tribe bathybatini. J Mol Evol. 2005;60:297–314.
39. Musilová Z, Kalous L, Petrtyl M, Chaloupkova P. Cichlid fishes in the Angolan headwaters region: molecular evidence of the ichthyofaunal contact between the Cuanza and Okavango-Zambezi systems. PLoS One. 2013;8: e65047.
40. Neumann D. Preservation of freshwater fishes in the field. Abc Taxa. 2010;8: 587–632.
41. Kawaguchi A, Miya M, Nishida M. Complete mitochondrial DNA sequence of Aulopus japonicas (Telostei: Aulopiformes), a basal Eurypterygii: longer DNA sequences and higher-level relationships. Ichthyol Res. 2001;48:213–23.
42. Kearse M, Moir R, Wilson A, Stones-Havas S, Cheung M, Sturrock S, Buxton S, Cooper A, Markowitz S, Duran C, et al. Geneious basic: an integrated and extendable desktop software platform for the organization and analysis of sequence data. Bioinformatics. 2012;28:1647–9.
43. He A, Luo Y, Yang H, Liu L, Li S, Wang C. Complete mitochondrial DNA sequences of the Nile tilapia (Oreochromis niloticus) and blue tilapia (Oreochromis aureus): genome characterization and phylogeny applications. Mol Biol Rep. 2011;38:2015–21.
44. Swofford D. PAUP*: phylogenetic analysis using parsimony. Sunderland: Sinauer Associates; 2003. version 4.0b10.2003
45. Posada D. jModelTest: Phylogenetic Model Averaging. Mol Phylogenet Evol. 2008;25:1253–6.
46. Stamatakis A. RAxML version 8: a tool for phylogenetic analysis and post-analysis of large phylogenies. Bioinformatics. 2014;30:1312–1313.
47. Miller MA, Pfeiffer W, Schwartz T. Creating the CIPRES Science Gateway for inference of large phylogenetic trees. New Orleans: Proceedings of the Gateway Computing Environments Workshop (GCE). 14 Nov 2010; 2010. p. 1–8.
48. Drummond AJ, Rambaut A. BEAST: Bayesian evolutionary analysis by sampling trees. BMC Evol Biol. 2007;7:1–214.
49. Perez GA, Rican O, Orti G, Bermingham E, Doadrio I, Zardoya R. Phylogeny and biogeography of 91 species of heroine cichlids (Teleostei: Cichlidae) based on sequences of the cytochrome b gene. Mol Phylogenet Evol. 2007; 43:91–110.
50. Malabarba MC, Malabarba LR, del Papa C. Gymnogeophagus eocenicus (Perciformes: Cichlidae), an Eocene cichlid from the Lumbrera formation in Argentina. J Vertebr Paleontol. 2010;30:341–50.
51. del Papa C, Kirschbaum A, Powell J, Brod A, Hongn F, Pimentel M. Sedimentological, geochemical and paleontological insights applied to continental omission surfaces: a new approach for reconstructing an eocene foreland basin in NW Argentina. J S Am Earth Sci. 2010;29:327–45.
52. Musilová Z, Říčan O, Říčanová S, Janšta P, Gahura O, Novák J. Phylogeny and historical biogeography of trans-Andean cichlid fishes (Teleostei: Cichlidae). Vertebrate Zool. 2015;65:333–50.
53. Perez PA, Malabarba MC, del Papa C. A new genus and species of Heroini (Perciformes : Cichlidae) from the early Eocene of southern South America. Neotropical Ichthyology. 2010;8:631–42.

54. López-Fernandez H, Winemiller KO, Honeycutt RL. Multilocus phylogeny and rapid radiations in Neotropical cichlid fishes (Perciformes: Cichlidae: Cichlinae). Mol Phylogenet Evol. 2010;55:1070–86.
55. Malabarba MC, Malabarba LR. A new cichlid, Tremembichthys garciae (Actinopterygii, Perciformes) from the Eocene - Oligocene of eastern Brazil. Revista Brasileira de Paleontologia. 2008;11:59–68.
56. Oliveira MEB, Garcia MJ, Fernandes MCC. Folíolose grãos de pólen de Fabales na Formação Entre-Córregos, Paleógeno da bacia de Aiuruoca, sudeste de Minas Gerais, Brasil. Bahía Blanca: SIMPÓSIO ARGENTINO DE PALEOBOTÁNICA Y PALINOLOGIA, Resúmenes; 2006. p. 1–81.
57. Garcia MJ, Santos M, Hasui Y. Palinologia da parte aflorante da Formação Entre-Córregos, Bacia de Aiuruoca, Terciário do Estado de Minas Gerais, Brasil. Revista Universidade Guarulhos. 2000;5:259.
58. Lima MR, Salard-Cheboldaeff M, Suguio K. Étude palynologique de la Formation Tremembé, Tertiaire du Bassin de Taubaté (État de São Paulo, Brasil), d'aprés lês echantillons du sondage n-42 du CNP. In: CSF DAC, Brito IM, C F, editors. *Coletânea de Trabalhos Paleontológicos*. Viana: DNPM; 1985. p. 379–93.
59. Riccomini C, Sant'Anna LG, Ferrari AL. Evolução geológica do rift Continental do Sudeste do Brasil. In: Mantesso-Neto V, Bartorelli A, Carneiro CDR, Brito Neves BB, editors. *Geologia do continente Sul-Americano: evolução da obra de Fernando Flávio de Almeida*. SãoPaulo: Beca; 2004. p. 383–406.
60. Kullander SO. A phylogeny and classification of the South American Cichlid (Teleostei:Perciformes). In: Malabarba LR, Reis R, Vari RP, Lucena ZM, Lucena CA, editors. *Phylogeny and Classification of Neotropical Fishes*. Porto Alegre: Edipucrs; 1998. p. 461–498.
61. López-Fernandez H, Honeycutt RL, Stiassny MLJ, Winemiller KO. Morphology, molecules, and character congruence in the phylogeny of south American geophagine cichlids (Perciformes, Labroidei). Zool Scr. 2005; 34:627–51.
62. Říčan O, Piálek L, Zardoya R, Doadrio I, Zrzavý J, Crame A. Biogeography of the Mesoamerican Cichlidae (Teleostei: Heroini): colonization through the GAARlandia land bridge and early diversification. J Biogeogr. 2013;40:579–93.
63. Murray AM. The fossil record and biogeography of the Cichlidae (Actinopterygii: Labroidei). Biol J Linn Soc. 2001;74:517–32.
64. Harrison T, Msuya CP, Murray AM, Fine Jacobs B, Báez AM, Mundil R, Ludwig KR. Paleontological investigations at the Eocene locality of Mahenge in north-Central Tanzania, East Africa. In: Gunnel GF, editor. *Eocene biodiversity: unusual occurrences and rarely sampled habitats*, vol. 18. New York: *Kluwar Academic–Plenum Publishers*; 2001. p. 39–74.
65. Murray AM. The Eocene cichlids (Perciformes: Labroidei) of Mahenge, Tanzania. Montreal: PhD thesis, McGill University; 2000.
66. Greenwood PH. The genera of pelmatochromine fishes (Teleostei, Cichlidae). A phylogenetic review. Bull British Museum (Natural History) Zool. 1987;53:139–203.
67. Schliewen UK, Stiassny ML. Etia nguti, a new genus and species of cichlid fish from the river Mamfue, upper Cross River basin in Cameroon, West-Central Africa. Ichthyological Explor Freshwaters. 2003; 14:61–72.
68. Carnevale GLW, Sorbini C. Oreochromis lorenzoi, a new species of tilapiine cichlid from the late Miocene of Central Italy. J Vertebr Paleontol. 2003;23: 508–16.
69. Hilgen FJ, Krijgsman W, Langereis CG, Lourens LJ, Santarelli A, Zachariasse WJ. Extending the astronomical (polarity) time scale into the Miocene: earth planet. Earth Planet Sci Lett. 1995;136:495–510.
70. Krijgsman W, Hilgen FJ, Marabini S, Vai GB. New palaeomagnetic and cyclostratigraphic age constraints on the Messinian of the northern Apennines (vena del Gesso Basin, Italy). Mem Soc Geol Ital. 1999;54:25–33.
71. Krijgsman W, Hilgen FJ, Raffi I, Sierro FJ, Wilson DS. Chronology, causes and progression of the Messinian salinity crisis. Letters to Nature. 1999; 400:652–5.
72. Trewavas E. Tilapiine fishes of the genera Sarotherodon, Oreochromis and Danakilia. London: British Museum of Natural History; 1983.
73. Pickford MHL. Geology, palaeoenvironments and vertebrate faunas of the mid- Miocene Ngoroa formation, Kenya. Geol Soc Lond, Spec Publ. 1978;6:237–62.
74. Rasmussen C, Reichenbacher B, Lenz O, Altner M, Penk SBR, Prieto J, BrÜSch D. Middle–late Miocene palaeoenvironments, palynological data and a fossil fish Lagerstätte from the Central Kenya rift (East Africa). Geol Mag. 2015;154:24–56.
75. Jacobs BF. Estimate of low-latitude paleoclimates using fossil angiosperm leaves: examples from the Miocene Tugen Hills, Kenya. Paleobiology. 2002; 28:399–421.
76. Clabaut C, Salzburger W, Meyer A. Comparative phylogenetic analyses of the adaptive radiation of Lake Tanganyika cichlid fish: nuclear sequences are less homoplasious but also less informative than mitochondrial DNA. J Mol Ecol. 2005;61:666–81.
77. Nishida M. Lake Tanganyika as an evolutionary reservoir of old lineages of east African cichlid fishes: inferences from allozyme data. Experientia. 1991; 47:974–9.
78. Schliewen UK, Klee B. Reticulate sympatric speciation in Cameroonian crater lake cichlids. Front Zool. 2004;1:5.
79. Schliewen UK, Tautz D, Pääbo S. Sympatric speciation suggested by monophyly of crater lake cichlids. Lett Nature. 1994;6472:629–32.
80. Cornen G, Bandet Y, Giresse P, Maley J. The nature and chronostratigraphy of quaternary pyroplastic accumulations from Lake Barombi Mbo (West-Cameroon). J Volcanol Geotherm Res. 1992;51:367–74.
81. Phillips MJ. Branch-length estimation bias misleads molecular dating for a vertebrate mitochondrial phylogeny. Gene. 2009;441:132–40.
82. Lukoschek V, Scott Keogh J, Avise JC. Evaluating fossil calibrations for dating phylogenies in light of rates of molecular evolution: a comparison of three approaches. Syst Biol. 2012;61:22–43.
83. Hugall AF, Lee MS. Molecular claims of Gondwanan age for Australian agamid lizards are untenable. Mol Biol Evol. 2004;21:2102–10.
84. Rambaut A, Suchard MA, Xie D, Drummond AJ. Tracer v1.6, Available from http://beast.bio.ed.ac.uk/Tracer. 2014.
85. Duchêne S, Lanfear R, Ho SY. The impact of calibration and clock-model choice on molecular estimates of divergence times. Mol Biol Evol. 2014;78:277–89.
86. Ho SY. The changing face of the molecular evolutionary clock. Trends Ecol Evol. 2014;29:496–503.
87. Ho SY, Larson G. Molecular clocks: when timesare a-changin'. Trends Genet. 2006;22:79–83.
88. Ho SY, Lanfear R, Bromham L, Phillips MJ, Soubrier J, Rodrigo AG, Cooper A. Time-dependent rates of molecular evolution. Mol Ecol. 2011;20:3087–101.
89. Schwarzer J, Lamboj A, Langen K, Misof B, Schliewen UK. Phylogeny and age of chromidotilapiine cichlids (Teleostei: Cichlidae). Hydrobiologia. 2014; 748:185–99.
90. Salzburger W, Meyer A, Baric S, Verheyen E, Sturmbauer C. Phylogeny of the Lake Tanganyika cichlid species flock and its relationship to the central and east African haplochromine cichlid fish faunas. Syst Biol. 2002;51:113–35.
91. Kocher TD, Conroy JA, McKaye KR, Stauffer JR, Lockwood SF. Evolution of NADH dehydrogenase subunit 2 in east African cichlid fish. Mol Phylogenet Evol. 1995;4:420–32.
92. Duftner N, Koblmuller S, Sturmbauer C. Evolutionary relationships of the limnochromini, a tribe of benthic Deepwater cichlid fish endemic to Lake Tanganyika, East Africa. J Mol Evol. 2005;60:277–89.
93. Takahashi T, Sota T. A robust phylogeny among major lineages of the east African cichlids. Mol Phylogenet Evol. 2016;100:234–42.
94. Mayer WE, Tichy H, Klein J. Phylogeny of African cichlid fishes as revealed by molecular markers. Heredity. 1998;80:702–14.
95. Joyce DA, Lunt DH, Bills R, Turner GF, Katongo C, Duftner N, Sturmbauer C, Seehausen O. An extant cichlid fish radiation emerged in an extinct Pleistocene lake. Nature. 2005;435:90–5.
96. Verheyen E, Salzburger W, Snoeks J, Meyer A. Origin of the superflock of cichlid fishes from Lake Victoria, East Africa. Science. 2003;300:325–9.
97. Schedel FDB, Katemo Manda B, Chocha Manda A, Abwe E, Vreven EJWMN, Schliewen UK. Description of five new rheophilic Orthochromis species (Teleostei: Cichlidae) from the upper Congo drainage in Zambia and the Democratic Republic of the Congo. Zootaxa. 2018;4461:301–49.
98. Cummings MP, Handley SA, Myers DS, Reed DL, Rokas A, Winka K, Rannala B. Comparing bootstrap and posterior probability values in the four-taxon case. Syst Biol. 2003;52:477–87.
99. Erixon P, Svennblad B, Britton T, Oxelman B, Sullivan J. Reliability of Bayesian posterior probabilities and bootstrap frequencies in Phylogenetics. Syst Biol. 2003;52:665–73.
100. Meyer BS, Matschiner M, Salzburger W. Disentangling incomplete lineage sorting and introgression to refine species-tree estimates for Lake Tanganyika cichlid fishes. Systematic Biol. 2016;66:531–550.
101. Irisarri I, Singh P, Koblmuller S, Torres-Dowdall J, Henning F, Franchini P, Fischer C, Lemmon AR, Lemmon EM, Thallinger GG, et al. Phylogenomics

uncovers early hybridization and adaptive loci shaping the radiation of Lake Tanganyika cichlid fishes. Nat Commun. 2018;9:1–12.
102. Říčan O, Piálek P, Dragová K, Novák J. Diversity and evolution of the middle American cichlid fishes (Teleostei: Cichlidae) with revised classification. Vertebrate Zool. 2016;66:1–102.
103. Malabarba MC, Zuleta OD, del Papa C. Proterocara Argentina, a new fossil cichlid from the Lumbrera formation, Eocene of Argentina. J Vertebr Paleontol. 2006;26:267–75.
104. Smith WL, Chakrabarty P, Sparks JS. Phylogeny, taxonomy, and evolution of Neotropical cichlids (Teleostei: Cichlidae: Cichlinae). Cladistics. 2008;24:625–41.
105. Murray AM. Late Eocene and early Oligocene teleost and associated ichthyofauna of the Jebel Qatrani formation, Fayum, Egypt. Palaeontology. 2004;47:711–24.
106. Lippitsch E, Micklich N. Cichlid fish biodiversity in an Oligocene lake. Ital J Zool. 1998;65:185–8.
107. Tamura K, Battistuzzi FU, Billing-Ross P, Murillo O, Filipski A, Kumar S. Estimating divergence times in large molecular phylogenies. Proc Natl Acad Sci. 2012;109:19333–8.
108. Lozano-Fernandez J, Dos Reis M, Donoghue PCJ, Pisani D. RelTime rates collapse to a strict clock when estimating the timeline of animal diversification. Genome Biol Evol. 2017;9:1320–8.
109. Battistuzzi FU, Tao Q, Jones L, Tamura K, Kumar S. RelTime relaxes the strict molecular clock throughout the phylogeny. Genome Biol Evol. 2018;10:1631–6.
110. Chakrabarty P. Cichlid biogeography: comment and review. Fish Fish. 2004;5:97–119.
111. Heine C, Zoethout J, Müller RD. Kinematics of the South Atlantic rift. Solid Earth. 2013;4:215–53.
112. Measey GJ, Vences M, Drewes RC, Chiari Y, Melo M, Bourles B. Freshwater paths across the ocean: molecular phylogeny of the frog Ptychadena newtoni gives insights into amphibian colonization of oceanic islands. J Biogeogr. 2007;34:7–20.
113. de Oliveira FB, Molina EC, Marroig G. Paleogeography of the South Atlantic: a route for Primates and rodents into the New World? In: Garber PA, Estrada A, Bicca-Marques JC, Heymann EW, editors. *South American Primates, developments in Primatology: Progress and Prospects.* New York: Springer; 2009. p. 55–68.
114. Markwick PJ, Valdes PJ. Palaeo-digital elevation models for use as boundary conditions in coupled ocean–atmosphere GCM experiments: a Maastrichtian (late cretaceous) example. Palaeogeogr Palaeoclimatol Palaeoecol. 2004;213:37–63.
115. Reinthal PN, Stiassny MLJ. The freshwater fishes of Madagascar: a study of an endangered fauna with recomnlendations for a conservation strategy. Conserv Biol. 1991;5:231–43.
116. Ward JA, Wyman RL. Ethology and ecology of cichlid fishes of the genus Etroplus in Sri Lanka: preliminary findings. Environ Biol Fish. 1977;2:137–45.
117. Uchida K, Kaneko T, Miyazaki H, Hasegawa S, Hirano T. Excellent salinity tolerance of Mozambique Tilapia (Oreochromis mossambicus): elevated chloride cell activity in the branchial and Opercular epithelia of the fish adapted to concentrated seawater. Zool Sci. 2000;17:149–60.
118. Tiercelin JJ, Mondeguer A. The geology of the Tanganyika trough. In: Coulter GW, editor. *Lake Tanganyika and its Life*. London: Oxford University Press; 1991. p. 7–48.
119. Meyer BS, Matschiner M, Salzburger W. A tribal level phylogeny of Lake Tanganyika cichlid fishes based on a genomic multi-marker approach. Mol Phylogenet Evol. 2015;83:56–71.
120. Day JJ, Santini S, Garcia-Moreno J. Phylogenetic relationships of the Lake Tanganyika cichlid tribe Lamprologini: the story from mitochondrial DNA. Mol Phylogenet Evol. 2007;45:629–42.
121. Sturmbauer CE, Verheyen E, Meyer A. Mitochondrial phylogeny of the Lamprologini, the major substrate spawning lineage of cichlid fish from Lake Tanganyika in eastern Africa. Mol Phylogenet Evol. 1994;10:751–68.
122. Sturmbauer C, Salzburger W, Duftner N, Schelly R, Koblmuller S. Evolutionary history of the Lake Tanganyika cichlid tribe Lamprologini (Teleostei: Perciformes) derived from mitochondrial and nuclear DNA data. Mol Phylogenet Evol. 2010;57:266–84.
123. Schwarzer J, Misof B, Ifuta SN, Schliewen UK. Time and origin of cichlid colonization of the lower Congo rapids. PLoS One. 2011;6:e22380.
124. Schelly RC, Stiassny MLJ. Revision of the Congo river *Lamprologus* Schilthuis, 1891 (Teleostei: Cichlidae), with description of two new species. Am Mus Novit. 2004;3451:40.
125. Schelly R, Salzburger W, Koblmuller S, Duftner N, Sturmbauer C. Phylogenetic relationships of the lamprologine cichlid genus Lepidiolamprologus (Teleostei: Perciformes) based on mitochondrial and nuclear sequences, suggesting introgressive hybridization. Mol Phylogenet Evol. 2006;38:426–38.
126. Nevado B, Koblmuller S, Sturmbauer C, Snoeks J, Usano-Alemany J, Verheyen E. Complete mitochondrial DNA replacement in a Lake Tanganyika cichlid fish. Mol Ecol. 2009;18:4240–55.
127. Sturmbauer C, Koblmüller S, Sefc KM, Duftner N. Phylogeographic history of the genus Tropheus, a lineage of rock-dwelling cichlid fishes endemic to Lake Tanganyika. Hydrobiologia. 2005;542:335–66.
128. Koblmüller S, Egger B, Sturmbauer C, Sefc KM. Rapid radiation, ancient incomplete lineage sorting and ancient hybridization in the endemic Lake Tanganyika cichlid tribe Tropheini. Mol Phylogenet Evol. 2010;55:318–34.
129. Sturmbauer C, Börger C, Van Steenberge M, Koblmüller S. A separate lowstand lake at the northern edge of Lake Tanganyika? Evidence from phylogeographic patterns in the cichlid genus Tropheus. Hydrobiologia. 2016;791:51–68.
130. Genner MJ, Ngatunga BP, Mzighani S, Smith A, Turner GF. Geographical ancestry of Lake Malawi's cichlid fish diversity. Biol Lett. 2015;11:20150232.
131. Genner MJ, Turner GF. Timing of population expansions within the Lake Malawi haplochromine cichlid fish radiation. Hydrobiologia. 2014;748:121–32.
132. Ebinger CJ, Deino AL, Drake RE, Tesha AL. Chronology of volcanism and rift basin propagation: Rungwe Volcanic Province, East Africa. Geol Soc Am Bull. 1989;94:785–803.
133. Ebinger CJ, Deino AL, Tesha AL, Becker T, Ring U. Tectonic controls on rift basin morphology: evolution of the northern Malawi (Nyasa) rift. J Geophys Res. 1993;98:821–36.
134. Betzler C, Ring U. Edimentology of the Malawi rift: facies and stratigraphy oft he Chiwondo beds, northern Malawi. J Hum Evol. 1995;28:23–35.
135. Johnson TC, Scholz CA, Talbot MR, Kelts K, Ricketts RD, Ngobi G, Beuning K, Ssemmanda I, McGill JW. Late Pleistocene desiccation of Lake Victoria and rapid evolution of cichlid fishes. Science. 1996;273:1091–3.
136. Kent PE. The Miocene beds of Kavirondo, Kenya. Q J Geol Soc. 1944;100:85–118.
137. Stager JC, Johnson TC. The late Pleistocene desiccation of Lake Victoria and the origin of its endemic biota. Hydrobiologia. 2007;596:5–16.
138. Elmer KR, Reggio C, Wirth T, Verheyen E, Salzburger W, Meyer A. Pleistocene desiccation in East Africa bottlenecked but did not extirpate the adaptive radiation of Lake Victoria haplochromine cichlid fishes. PNAS. 2009;106:13404–9.

The ghost of a hybrids past uncovers ancient river tectonic captures

Frederic D.B. Schedel[1], Juliane D. Weiss[1], Laura F. Walheim[1], Emmanuel J.W.N.N. Vreven[2,3], Hamid R. Esmaeili[4] & U.K. Schliewen[1*]

[1]Department of Ichthyology, SNSB - Bavarian State Collection of Zoology, Münchhausenstr. 21, 81247 Munich, Germany

[2]Vertebrate Section, Royal Museum for Central Africa (RMCA), Leuvensesteenweg 13, B-3080 Tervuren, Belgium

[3]KU Leuven, Laboratory of Biodiversity and Evolutionary Genomics, Charles Deberiotstraat 32, B-3000 Leuven, Belgium

[2]Ichthyology and Molecular Systematics Research Laboratory, Zoology Section, Department of Biology, College of Sciences, Shiraz University, Shiraz, Iran.

[*]corresponding author

Abstract

Background: The megadiverse family Cichlidae (Teleostei: Cichlidae) comprises thousands of species and some of the best studied adaptive radiations (e.g. those of the African Great Lakes) of our planet. Understanding the evolutionary history of cichlids hence become a key priority of countless studies and was further been boosted by the development of high-throughput sequencing approaches. Among other factors, hybridization and introgression have been identified as important components facilitating adaptive radiations. They have thus played an important role for their evolutionary history and can explain numerous persisting uncertainties of their phylogenetic tree of life, e.g. with regard to the famous East African cichlid radiation (EAR). Consequently, the precise reconstruction of the biogeographic history and evolutionary time line of cichlids has remained problematic. Here, we present additional evidence for multiple ancient hybridization events among major austrotilapiine cichlid lineages, based on a comprehensive genomic nuclear DNA (ddRAD) and mitogenomic dataset comprising representative taxa of almost all tribes of the African cichlid subfamily Pseudocrenilabrinae. We further re-evaluated cichlid node divergence estimates of cichlids based on the most extensive Ovalentaria and cichlid taxon sampling up to date, i.e. including almost all major ovalentarian lineages and approximately 330 cichlid taxa.

Results: In addition to previously reported signatures of ancient hybridization events we found evidence for multiple new hybridization events among all major haplochromine lineages of southern

and Central Africa, especially within the so-called 'extended *Pseudocrenilabrus*-group', and within the 'extended serranochromines'. We further report several new cases of cyto-nuclear phylogenetic discordance, however without any corresponding nuclear genomic hybridisation signal for various austrotilapiines, including cases involving, e.g., key taxa as *H. vanheusdeni* (Haplochromini) and *L. symoensi* (Lamprologini). Further, we present refined mitochondrial divergence time estimates with focus on the austrotilapiines lineages. Interestingly, and in contrast to many other comparable studies, we find divergence time estimates based on nuclear and on mitochondrial data to be largely congruent with each other.

Conclusions: Our data suggest that hybridization and introgression has been even more common among African cichlids than already suggested before, thus highlighting once again their importance for shaping the evolutionary history of cichlids. Combination of several lines of evidence, i.e. cyto-nuclear discordances and significant D-statistics, proved to be crucial for an improved reconstruction of cichlid phylogenetic history, as cyto-nuclear discordances often identified very ancient introgression candidate events, which would have remained uncovered with D-statistics alone. We further conclude that divergence time estimates based on nuclear (ddRAD) and mitochondrial data are largely comparable within austrotilapiine cichlids. Mitogenome cichlid data therefore represent a valuable resource even in the age of phylogenomics as they provide complementary and highly informative data for the reconstruction of the complex biogeographic history of African cichlids.

Keywords: Austrotilapiines, Ovalententaria, Cichlidae, Molecular clockd, dRAD, mitochondrial genomes, cyto-nuclear discordance

Introduction

Belonging to the percomorph clade Ovalentaria, cichlids (Teleostei: Cichlidae) represent one of the most diverse and largest vertebrate families on our planet ([1, 2]). Over the last decades they have spawned important model systems for various biology research fields such as ecology, developmental biology and general evolutionary biology [3-8]. The African Pseudocrenilabrinae, the most species-rich of the four cichlid subfamilies, is of particular interest for speciation and phylogenetic research due its exceptional diversity and its propensity to generate adaptive radiations. Especially the megadiverse adaptive radiations of the East African rift lakes Tanganyika, Malawi and Victoria have been studied well ([4, 8-10]), but also the smaller ones, e.g. Rift Valley Soda lakes and volcanic crater lakes of West-Central and East Africa (e.g. [11-13]); and even examples of African riverine cichlid radiations have been studied and documented in the Lower Congo rapids [14]. In order to understand the phylogenetic time-line of speciation and adaptive radiation processes extensive efforts have thus been made, especially with regard to Pseudocrenilabrinae but for the family Cichlidae in general, too. ([15-19]). Despite significant progress in the elucidation of the cichlid phylogenetic record important key

relationships, e.g. those of the East African Radiation, have remained poorly understood, as alternative hypotheses either remain statistically poorly supported or show significant signal of cyto-nuclear discordance, and because it is often difficult to differentiate between effects of incomplete lineage sorting or ancient introgression on the reconstruction of the species phylogeny ([8, 20]). Finally, a long standing debate about the age of origin of cichlids and, therefore, on precise node age estimates for the origin and divergence of the major cichlid lineages remains unsettled. Here, two hypotheses, i.e. the Vicariance Hypothesis and the Dispersal Hypothesis, compete for the explanation of the evolutionary history of the cichlids after the tectonic separation of Gondwana. Although molecular evidence for the Dispersal Hypothesis is accumulating, i.e. suggesting that cichlids diversified only after the continental separation of Gondwana (reviewed in [21]), the exact timing of separation of the four vicariantly distributed major cichlid subfamilies remains open due to the scarcity of unambiguous calibration points for molecular clock estimates ([16, 21-25]).

The advent of next generation sequencing methods and the development of a broad variety of cost-efficient high-throughput sequencing approaches such as sequencing restriction site associated DNA markers (RAD, ddRAD), anchored hybrid tags and whole genomes boosted research on the evolutionary history of cichlids over the last decade tremendously [8]. Nevertheless, most phylogenomic studies on African cichlids mainly focused on selected tribes and lineages of the EAR (e.g. [15, 26-29]) and hence included only comparatively few representative taxa of non-focal lineages. This contrasts with evidence, that riverine haplochromine cichlids and numerous early splitting lineages of the more inclusive African cichlid subgroup named haplotilapiines (sensu [30]) have been identified as important as they have contributed significantly to the phylogenetic history of the most impressive EAR, and to the complex biogeographical history of Pseudocrenilabrinae ([15, 25, 27, 31-34]). Thus, the inclusion of riverine lineages into large-scale phylogenomic studies appears to be even more crucial. They might be important to trace the origin of several lineage-specific key innovations and traits (e.g. the functional decoupling of oral and pharyngeal jaws [35], body coloration and associated selection pressures [36], but also of the origin of genomic features such as an increased rate of gene duplication [37]) which, together with ample ecological opportunity [6], are candidate factors that have been suggested to fuel the adaptive radiations of the East African rift lakes. Not only the contribution of riverine cichlid lineages to these radiations as their sister groups might have been important, but also secondary introgression after hybridization of riverine lineages with lacustrine lineages might have played an important role in triggering explosive diversification observed in certain EAR cichlid lineages. For example, the young and megadiverse Lake Victoria region species flock (LVRS) has recently been identified to represent a hybrid swarm resulting from an ancient hybridization event of two ancient and distantly related riverine lineages [27]. The same appears to hold true for the four independent cichlid radiations endemic to Lake Mweru, i.e. the *Sargochromis*-, Large-tooth

serranochromines-, Small-tooth serranochromines- and the Lake Mweru *Pseudocrenilabrus* radiation; they have recently been proposed to have a hybrid origin involving Zambezian as well as Congolese lineages of serranochromine and *Pseudocrenilabrus*-group cichlids [34]. Last but not least, the study of selected riverine cichlid lineages themselves has revealed a complex history of introgression and hybridization, as e.g. shown for the lionhead cichlids (*Steatocranus*) radiation of the Congo [38] and for selected riverine haplochromine lineages of the serranochromines and *Pseudocrenilabrus*-group [34, 39].

For decades phylogenetic research on cichlids was mainly dominated by mitochondrial (mtDNA) markers. The maternal haploid mode of inheritance, the limited amount of mtDNA recombination, the lack of introns in mtDNA genes and the abundance of genome copies facilitated sequencing of mtDNA markers ([40, 41]). Unfortunately, mtDNA haplotype phylogenies do bear the shortcoming that they might not reflect the "true" species tree due to the lack of mtDNA recombination and inheritance of the mtDNA genome as a single locus; further, the small size of the mitochondrial genome and comparatively high mutation rate translates into reduced ancient phylogenetic signal retention necessary for the resolution [42]. Despite these shortcomings, and if analysed within the limits of phylogenetic resolution potential, the mitochondrial genome preserves an important element of the evolutionary history of an organism and hence bears valuable information for the reconstruction of a fundamental component of a species´ phylogenetic history. This is true particularly with regard to mitochondrial haplotype divergence and introgression age estimates which are highly informative for biogeography reconstruction in the context of corresponding landscape evolution, especially in the Neogene ([25, 39]). Further, sequencing of partial or entire mitochondrial genomes has become highly cost-efficient, e.g., by using a combination of long-range amplification and high-throughput sequencing (e.g. [25, 43]), and thus represents a useful complement for nuclear-DNA-based phylogenomic studies.

As a consequence of their sheer species numbers, the rapid succession of their speciation events and their widespread occurrence, the reconstruction of the phylogenetic relationships of African cichlids remains a difficult quest. In a fully comprehensive way this ultimate goal might only be accomplished by a generous and comprehensive taxon sampling and by simultaneously accounting in nucleotide sampling for their underlying reticulate history including incomplete lineage sorting, introgression and hybridization. This is particularly true for the African cichlid clade that includes the megadiverse EAR as well as the closely related and widespread Tilapiini and Steatocranini, i.e. the so-called austrotilapiines (sensu [44]). The comprehensive understanding of their evolutionary history is not only crucial for understanding speciation processes, but equally for reconstructing the spatio-temporal setting that provided the palaeogeographical stage for those divergence processes. Deciphering the spatio-temporally related phylogenomic pattern preserved in the African cichlid phylogenetic record

may support the reconstruction of the landscape evolution of Africa. For example, past river capture events and associated colonization routes preserved in the genomic record of vicariant lineages as ancient genomic signatures of recurrent isolation and gene flow can be highly informative, as they would mirror the tectonically dynamic East African rift valley evolution which served as the cradle of EAR ([45]).

We consequently addressed several major goals to obtain new insights into the evolutionary history of austrotilapiine cichlids. Using a ddRAD approach, a comprehensive phylogenomic DNA hypothesis for the Pseudocrenilabrinae with the main focus on the austrotilapiines was reconstructed; it included almost all major lineages of this exceptionally diverse clade for the first time. To reconstruct the phylogenomic DNA hypothesis we applied different methods including a maximum likelihood approach based on the concatenated alignment and a summary species tree approach. This allowed detection of topological differences between differently inferred phylogenies which might either be the result of incomplete lineage sorting (ILS) or of hybridization events. In addition, we sequenced 10 protein coding genes of the mitochondrial genome of almost all ddRAD-genotyped individuals. The combination of the two analyses allowed screening for cyto-nuclear discordances between mtDNA- and ddRAD-derived hypotheses. Finally, Patterson´s D-statistics ("ABBA-BABA tests") were performed to search candidate hybridizations signal between taxa of different austrotilapiine tribes and, more importantly, between taxa from within major haplochromine lineages with a special focus on serranochromines and *Pseudocrenilabrus*-group members. Finally, for molecular node age estimates we established for the first time a mitogenomic dataset and analysis comprising not only almost all major cichlid lineages cichlids of almost all recognized tribes but also representatives of all major atherinomorph lineages, a major sister lineage of cichlids. This expanded taxon sampling allowed for updating and re-valuating node age estimates derived from a smaller dataset with fewer calibration points and topological constraints in the recent study of Schedel et al. [25]. By comparing these mtDNA-derived molecular clock estimates with estimates based on 610 highly represented ddRAD loci and on an almost identical taxon sampling and identical calibration scheme we evaluated the compatibility of the divergence time estimates for austrotilapiine cichlids obtained from those different molecular datasets. This study therefor not only provides a refined phylogenetic hypothesis for the megadiverse austrotilapiine cichlids but also new insights into their reticulate evolutionary history which apparently played an essential role for their evolutionary success.

Material and methods

Taxon Sampling

Two main taxon sample sets were created for this study. For the ddRAD set 206 specimens (representing approximately 160 species) were sequenced (see Table S1. The focus of the ddRAD set was on the austrotilapiines (sensu [44]) encompassing representatives samples of all major tribes and lineages of the EAR (N = 172), Steatocranini (N = 7) and Tilapiini (N = 17). Taxon sampling within the EAR mainly concentrated on the megadiverse tribe Haplochromini (N = 129) with particular focus on rheophilic lineages. Most of these lineages are only informally named, and we adopted the nomenclature as in [25]), i.e. serranochromine cichlids (N = 49) and *Pseudocrenilabrus*-group (N = 43, sensu [46, 47]); refer to Table S1 for a comprehensive overview of all sampled individuals and their designated lineages. In addition, representatives of most remaining Pseudocrenilabrinae major lineages and tribes were included: *Heterochromis* (N=1), hemichromines (N=1), chromidotilapiines (N=1), Coptodonini (N=1), Etiini (N=1), Gobiocichlini (N=1), pelmatochromines (N=2), Pelmatolapiini (N=1) and tylochromines (N=1). The only tribes not represented in our dataset were Coelotilapiini, Heterotilapiini and Oreochromini.

The second explorative data set was based on ten protein coding genes of the mitochondrial genome and aimed for a substantially broader taxon set than our ddRAD set by not only including representatives of the four cichlid subfamilies: Etroplinae (N=4; Asian and Madagascar) and Ptychrominae (N=2; Madagascar), Cichlinae (N=36; Americas) and the Pseudocrenilabrinae (N=362; Africa) but also of almost all major orders and families currently placed within the Ovalentaria, i.e. the well supported clade comprising cichlids and related teleost families (sensu [2, 48]). For this purpose, we downloaded all available ovalentarian mitochondrial genomes from GenBank and randomly selected one representative sequence per taxon (in the case multiple mitochondrial genomes were available for the same species) resulting in a core dataset with 587 species distributed over the following families (see Tables S2 & S3): Adrianichthyidae (N=9), Ambassidae (N=2), Aplocheilidae (N=3), Atherinidae (N=4), Atherinopsidae (N=6), Belonidae (N=3), Blenniidae (N=4), Cichlidae (N=403), Cyprinodontidae (N=8), Embiotocidae (N=3), Exocoetidae (N=11), Fundulidae (N=5), Gobiesocidae (N=1), Goodeidae (N=3), Hemiramphidae (N=6), Melanotaeniidae (N=8), Mugilidae (N=17), Notocheiridae (N=1), Opistognathidae (N=1), Orestiidae (N=2), Plesiopidae (N=2), Poeciliidae (N=11), Pomacentridae (N=16), Pseudochromidae (N=2), Rivulidae (N=2). As outgroup taxa representative species of the supragroups Anabantiformes (N=5), Carangaria (N=4) and Scombriformes (N=4) were used. This core dataset served as basis for the creation of working alignments of this study (see below). Wherever possible we sequenced mitogenomic of the same cichlid specimens as in the ddRAD dataset (see Table S1 & S2).

Sampling procedures

Samples used in this study were collected on various field trips or were obtained from the commercial fish trade in Germany. A variety of different fishing techniques, e.g. beach seining, gill netting and hand netting, were applied depending on the conditions of the different sampling sites. Freshly collected fish were sacrificed by applying an overdose of an approved fish anaesthetic (MS-222). In addition, selected fish specimens were obtained from local fish markets or directly from the fishermen. Fin clips were taken from the right pectoral fin and fixed in 96% ethanol, and corresponding specimens were fixed in 10% formalin (as recommended in [49]). We followed all applicable international and national guidelines of animal use and ethical standards for the collection of samples.

Molecular methods: ddRad genotyping and mitochondrial genome sequencing

Genomic DNA was extracted with a custom CTAB DNA extraction protocol to ensure sufficient yield of high weight molecular DNA. DNA was quantified using a photospectrometer (NanoDrop ND-1000, Thermo Scientific) and sporadically checked using gel electrophoresis. Library preparation for double digest restriction associated DNA (ddRAD) sequencing mostly followed the protocol of [50]. Each ddRAD library comprised 48 individuals. For each genotyped individual approximately 300 ng template DNA were double-digested using the restriction enzymes MluCI and SphI (NewEngland Biolabs) for three hours at 37° C. Digested samples were cleaned using the DNA Clean & Conentrator 5 Kit (Zymo Research), each individual was tagged with a unique 5 base pair barcode, and subsequently size-selected for fragments > 250 bp using AMPure XP beads following the target enrichment protocol of [51]. Proper size selection was verified by gel electrophoresis. Each 48 tagged samples were then pooled (approx. 100 ng DNA per sample), and the volume of the resulting pool was reduced to 30 µl using the DNA Clean & Cocentrator 5 Kit. Subsequently a second fragment size selection aiming for a target length of 300 bp was conducted using the BluePippin Prep electrophoresis system (Sage Sience, Beverly, MA, USA) followed by another cleaning step using the DNA Clean & Cocentrator 5 Kit. Individual pools were PCR-amplified to incorporate multiplex-indices and Illumina flow cell annealing adaptors using the Phusion Polymerase Kit (New England Biolabs). PCR products were cleaned using the GeneJET Gel Extraction Kit (Thermo Fisher Scientific), and DNA concentration of resulting pools were verified using a Qubit Fluorometer (Invitrogen) measurement. Quantification of molarity and library fragment size distribution of individual pools was performed on a Bioanalyzer (Agilent). Sequencing of individual ddRAD libraries was conducted by sequencing service of the Ludwig Maximilian University of Munich on the Illumina MiSeq platform. Several specimens were genotyped twice to increase coverage and to check for reproducibility (see Table S1).

In addition, we sequenced partial mitochondrial genomes of almost all ddRAD genotyped individuals along with additional Pseudocrenilabrinae taxa (see Table S1 & S2). For doing so we amplified are large fragment of the mitochondrial genome using the following primer pairs (L2508KAW: 5´-CTC GGC AAA

CAT AAG CCT CGC CTG TTT ACC AAA AAC-3´; [52] and ZM12300R: 5´-TTG CAC CAA GAG TTT TTG GTT CCT AAG ACC-3´; [16]) and TaKaRa LA Taq DNA polymerase kit (TaKaRa) with an adapted thermal profile from [25]: initial denaturation at 98 °C (60 s), followed by 35 cycles of denaturation 98 °C (10 s), annealing at 60°C for 60s, elongation at 68 °C (15 min), and a last extension step at 72 °C (10 min). Resulting PCR products were purified using the GeneJET Gel Extraction Kit (Thermo Fisher Scientific) following the manufacturer´s protocol. Cleaned amplification products were adjusted to 0.21 ng/µl. Where long range PCR amplification (see above) failed, a shotgun library approach was applied (see Table S2). Library preparations of PCR products and of shotgun samples were conducted with the Nextera XT DNA Sample Preparation Kit (Illumina) according to the manufacturer´s protocol; this up to the library normalization step. Libraries were pooled at equal molarity; different pools were prepared for the "amplified partial mitochondrial genome libraries" and those for the "shotgun libraries". Sequencing was conducted at the Sequencing Service of the Ludwig Maximilian University of Munich on the Illumina MiSeq platform (MiSeq Reagent Kit v2; 2X250). Quality control, adaptor trimming and assembly of the demultiplexed reads was done using the CLC Genomics Workbench (Qiagen). To assemble the mitochondrial genomes derived from shotgun libraries we mapped all reads against the complete mitochondrial genome of *Oreochromis niloticus* (GenBank accession number: GU370126; [53]) using the default parameters of the "Map to reference" tool implemented in Geneious v.11.0.4 [54] and subsequently extracted the resulting consensus sequences. Annotation of the assembled sequences was conducted in Geneious v.11.0.4 [54] using again the complete mitochondrial genome of *Oreochromis niloticus* (GU370126) as a reference sequence. Newly created sequence data (see Table S2) will be uploaded to the GenBank once the manuscript is submitted to a peer reviewed journal. In the meantime, data are available upon request from the authors. The mitochondrial dataset was complemented with mitochondrial genome data obtained from GenBank (Table S3).

Bioinformatic processing ddRAD sequences

Adaptors of raw reads were trimmed using the program cutadapt [55]. Subsequently, reads were demultiplexed using the process radtags script with the additional flag -r (rescue RAD Tags) and allowing for at most one mismatches in barcodes as implemented in Stacks [56]. Paired reads were merged using the program PEAR [57] and subsequently trimmed to a maximum length of 215 bp using cutadapt. Reads of specimens sequenced twice were merged using a custom script. Subsequently reads were mapped end-to-end against the *Maylandia zebra* reference genome (Genbank assembly accession number: GCA_000238955.5; [58]) using the "sensitive option" of bowtie2 v2.3.4.3 [59]. We extracted only those reads which mapped to the reference genome using the program samtools [60], and bam files were converted into fastq files using the program Picard SamToFastq (https://broadinstitfute.github.io/picard/). Between the different processing steps quality of reads (e.g. per base sequence quality, GC content, read length) were assessed using FASTQC [61]. Extracted

mapped reads were subsequently assembled and aligned using the PyRad v. 3.0.66 [62] pipeline, excluding reads with more than four sites and with Phred scores below 20. Further, we allowed for a similarity threshold of 88 % for the clustering step of the individual reads, and clusters with a coverage below six were excluded from further analysis while we allowed for a maximum of five shared polymorphic sites per cluster. We required a locus to be shared among 62 samples (approximately 30 % of the samples) to be retained in our consensus sequences.

In addition to this dataset, referred from now on as "Full ddRAD Set", we generated two additional datasets by running the PyRad pipeline on two different subsets. The first subset ("Austrotilapiine ddRAD Set") was composed of austrotilapiine specimens which recovered at least 50 % of loci in our "Full ddRAD Set" PyRad analysis; nevertheless, we included some critical specimens with lower locus coverage (not less than 20 % locus coverage) to ensure that most of the main austrotilapiine lineages were represented by at least one taxon. Furthermore, we included only one specimen per species or distinct lineage, preferring the sample with higher data density. Finally, we run the PyRad pipeline on the remaining 103 specimens. We used the same parameters as for the "Full ddRAD Set" with the exception that we required a locus to be shared among 93 samples (approximately 90 % of the samples). Subsequently, we removed the Steatocranini taxa as well as the single *Trematocara* species and *Coptodon* cf. *rendalli* "Lukoshi" from the dataset. The resulting alignment included 97 taxa and was used as input for downstream molecular clock analyses.

The second subset ("Introgression-test ddRAD Set") was specifically designed for testing for signatures of introgression and potential gene flow between the different lineages of the austrotilapiine cichlids. To ensure a particularly high data density in this subset we included only specimens from the "Austrotilapiine ddRAD Set" which recovered at least 80 % of loci, except for the outgroup taxon *Coptodon* cf. *rendalli* "Lukoshi". Further, we reduced the set by including a maximum of four taxa per main lineage, except for one lineage, that included one additional yet undescribed taxon "Haplochromine genus sp. Lubudi blue cheek" to our sample set. The settings for the PyRad pipeline for this subset, finally including 60 specimens, were the same as for the PyRad analysis of the "Full ddRAD Set"; however, a locus to be included required to be shared by at least 36 samples (= 60 % of all samples).

Demultiplexed raw reads and extracted mapped reads used in the different analyses will be uploaded to a public nucleotide archive once the manuscript is submitted to a peer review journal. In the meantime, data are available upon request from the authors.

RAD-based phylogenetic analysis

For each of the three ddRAD sets we applied two different approaches to infer the phylogenetic relationships. The first method was based on the concatenated alignments of the recovered loci of the different PyRAD runs and maximum likelihood (ML) analysis using RAxML v.8.1.12 [63] on the CIPRES Sciene Gateway [64], applying a GTR+gamma nucleotide substitution model and allowed RAxML to stop bootstrap replications automatically (using the majority rule criterion) for each analysis. In addition, we accounted for potential incomplete lineage sorting (ILS) using a summary species tree method which allowed to screen for topological discordances between resulting summary species trees and the ML hypothesis derived from the concatenated alignments. Using IQ-tree v.2.0 [65] and the GTR nucleotide substitution we inferred individual gene trees for each of recovered locus with at least one parsimony informative site in our different ddRAD analyses . In total, 18,369 individual trees were calculated for the "Full ddRAD Set" and 610 for the "Austrotilapiine ddRAD Set". Due to computational constraints a subset of the first 4000 trees for the Full ddRAD Set and all trees of the "Austrotilapiine ddRAD Set" were used to calculate coalescent-based summary species trees in ASTRAL III v.5.7.3 [66, 67], using default parameters. Depending on the ddRAD set we rooted the resulting trees either with *Heterochromis multidens* (Full ddRAD Set) or with *Coptodon* cf. *rendalli* "Lukoshi" (Austrotilapiine ddRAD Set).

Mitochondrial based phylogenetic analysis

In total, we included 304 partial mitochondrial genomes and 281 full mitochondrial genomes from 587 specimens to generate an explorative mitochondrial working alignment. These included representative taxa of almost all major cichlid lineages and most major ovalentarian lineages (see Table 3 for GenBank accession numbers). For that purpose, we extracted ten mitochondrial protein-coding genes from the mitogenome data, as in [25]: ND1, ND2, COX1, COX2, ATP8, ATP6, COX3, ND3, ND4L, ND4). With a few exceptions, sequence information was available for all samples. Sequences of individual genes were aligned separately using the Geneious alignment tool (default settings) and individual single gene alignments were subsequently concatenated resulting in an alignment of 7884 bp with about 1% missing data and relative base frequencies) of A=25.2, T=28.6, C=30.6 and G=17.7 (excluding gaps and ambiguous sites). In rare cases where a sequence of a particular gene was incomplete or missing a multi-N string was inserted into the alignment in the respective position. The resulting alignment, referred from now on as "Full mitochondrial dataset", included for some taxa several specimens and was subsequently used to generate two data subsets.

In the first subset we kept only taxa belonging either to the Atherinomorphae or Cichliformes [48], except for of few representative outgroup taxa (see below). Further, we excluded all specimens except one for taxa represented by multiple specimens in our "Full mitochondrial dataset"; where possible we aimed to keep those specimen data that we had previously used in the ddRad sets (see above). In

order to avoid long-branch artifacts, we further excluded those taxa which produced extraordinary long branches in pilot RAXML-analyses on the "Full mitochondrial dataset" resulting in alignment with 464 taxa; we refer to this dataset as "AC mitochondrial dataset". The second subset "Austrotilapiine mtDNA dataset" was further restricted to include only African cichlids in order to mirror the taxon composition of the "Austrotilapiine ddRAD Set"; this by including as far as possible the same specimens or, if not available, at least the same species.

For all three mitochondrial alignments we performed ML-analyses using RAxML v.8.1.12 on the CIPRES Science Gateway. Individual data sets were partitioned into first, second and third codon position and the GTR+gamma nucleotide substitution model was applied. Further, depending on the corresponding data set, we defined different outgroups e.g. representative members of the ovalentarian families Ambassidae (N=2), Blenniidae (N=2), Embiotocidae (N=1), Mugilidae (N=2), Opistognathidae (N=1), Pomacentridae (N=2) and Pseudochromidae (N=1) for the "AC mitochondrial dataset" while *Coptodon* cf. *rendalli* "Lukoshi" was defined as outgroup for the "Austrotilapiine mtDNA dataset". Bootstrap replications of different analysis were halted automatically in RAxML-analyses using the majority rule criterion

Fossil calibration and divergence time estimates

To estimate cichlid divergence in general and those of austrotilapiine cichlids in detail we conducted three independent analyses using the Bayesian software BEAST v.2.6.1 [68] under a relaxed lognormal clock model with a birth-death speciation model on the CIPRES Science Gateway. The different analyses compared the contribution of mitochondrial vs. nuclear data on the node age estimates. The first analysis was based on the "AC mitochondrial dataset" alignment, the second analysis on the "Austrotilapiine mtDNA dataset", and the third on the concatenated alignment of the "Austrotilapiine ddRAD Set". The mitochondrial datasets were partitioned according to first, second and third codon position. The monophyly of 63 clades (see Table 1) was constrained for the BEAST analysis of the "AC mitochondrial dataset" based on 100% bootstrap support for these clades in our RAxML analysis, and independently derived support for additional four clades (see Table 1) as based on, e.g.[48, 69, 70]). For the two BEAST analysis based on austrotilapiine data sets 17 clades (see Table 1) were constrained to be monophyletic as these were recovered with 100% bootstrap support values in the corresponding RAxML trees and which further were supported to be monophyletic in previous studies (e.g. [15, 25, 71, 72]).

Table 1: Overview of calibration points and their corresponding parameter settings as applied in the three different molecular clock (BEAST) analyses. Detailed justification for the inclusion or exclusion of particular cichlid fossils (calibration points: A-H) is given in [25]. Additional clades for which monophyly was constrained in the various molecular clock analysis were all strongly supported with 100%

bootstrap support except for four the clades indicated by an asterisk (*); the latter had received strong statistical support in previous studies (e.g. [44, 46, 48, 69-71]).

Calibration scheme for the "AC mitochondrial dataset",				Parameter settings (Beast):			
Calibration point:	**Fossil/event:**	**Estimated age (geological formation):**	**Calibrated clade:**	**Offset**	**SD**	**Mean**	**Distribution**
A	†*Tremembichthys* spp.	55.8-23.03 Ma (Tremembé formation, Brazil)	Cichlasomatini	23.03	0.67	2.39	Log normal
B	†*Gymnogeophagus eocenicus*	45.4-39.9 Ma (Lumbrera formation, Argentina)	Geophagini (conservative approach)	39.9	0.8	2.4	Log normal
C	†*Plesioheros chaulidus*	45.4-39.9 Ma (Lumbrera formation, Argentina)	Heroini (except: of *Pterophyllum* and *Hypselecara*)	39.9	0.8	2.4	Log normal
D	†*Oreochromis lorenzoi*	7.24-5.33 Ma (Gessoso-Solfifera formation, Italy)	Oreochromini	5.98	1.148	1.8	Log normal
E	†*Tugenchromis pickfordi*	9-10 Ma (Ngorora Formation, Kenya)	H-lineage (sensu Nishida, 1991): 'ancient Tanganyika mouth-brooders', 'Malagarasi-*Orthochromis*' , *'Ctenochromis' pectoralis,* Haplochromini and Eretmodini	9	0.98	2	Log normal
F	Onset Lake Barombi Mbo	1.12-0.98 Ma (Cameroon)	Barombi Mbo species flock	0.0	0.07	0.98 (real space)	Log normal
	†*Mahengechromis* spp.	45.83 ± 0.17 (Singida kimberlite field, Tansania)	Used to set upper pound (95% CI) for the calibration of: †*Oreochromis lorenzoi* & †*Tugenchromis pickfordi*				
	Non cichlid fossils used as calibration points:						
G	†*Hemitrichas stapfi*	~ 23 Ma (Quarry "Am Katzenrech", Germany)	Atherinidae	23	1.1	1.8	Log normal
H	†*Rhamphexocoetus volans*	~49 Ma (Pesciara locality of Monte Bolca, Italy)	Exocoetoidei	49.0	0.96	2.3	Log normal
I	†*Fundulus lariversi*	17.8-16.2 (Siebert Tuff, Nevada, USA)	*Fundulus* (*Fundulus grandis* , *Fundulus heteroclitus* , *Fundulus diaphanus*)	16.2	1.04	2	Log normal
J	†*Tapatia occidentalis*	23.03-5.33 Ma (Barranca de Santa Rosa, Jalisco, Mexico)	Goodeidae	5,33	0.99	1.4	Log normal
	Secondary constrains:						
	Clade	**Time range:**	**Used to constrain the age of**				
	Atherinoidei	61,06-88,56 Ma	Minimum age was used to set the upper bound (95% CI) of the *Hemitrichas stapfi* calipration point				
	Cyprinodontoidei	58,51-79,9 Ma	Minimum age was used to set the upper bound (95% CI) of the †*F. lariversi* calipration point				
	Goodeide + Profundulidae	23,12-58,97 Ma	Minium age was used to set the upper bound (95% CI) of the †*Tapatia occidentalis* point				
	Root: Ovalentaria	97,54-116,33 Ma (taken from Matschiner et al. 2016)	Minium age was used to set the upper bound (95% CI) of the †*Rhamphexocoetus* volans point and of the root	97,54	0.45	2.1	Log normal
Clades constrained (N=63):							
Australotilapine cichlids, BS: 72 (but supported by previous stu		Haplochromini, BS: 100	'extended serranochromines' (not including *H. demeusii* and *H. fasciatus* , but including LML-*Orthochromis*), BS: 100		Belonidae, BS: 100		
Bathybatini, BS: 100		Haplotilapiines (sensu Schliewen & Stiassny, 2003), BS: 100	Steatocaranini, BS: 100		*Callopanchax* , BS 100		
Benthopelagic clade (sensu Schedel et al. 2019), BS: 100		hemichromines', BS: 100	Termatocarini, BS: 100		Cyprinodon, BS: 100		
chromidotilapiines', BS: 100		Lac Fwa radiation, BS: 100	*Tilapia* (excluding *Tilapia ruweti* , BS: 100		Cyprinodontidae, BS: 100		
Cichlidae + Cichlinae + Ptychochrominae, BS: 100		Lake Malawi radiation, BS: 100	Tilapiini, BS: 100		Cyprinodontoidei, BS: 100		
Cichlidae + Pseudocrenilabrinae, BS: 85 (supported by previous studies*)		Lamprologini, BS: 100	Tropheini (plus *H. vanheusdeni*) + Lac Malawi radiation + "modern Haplochromini", BS 100		Epiplatys, BS: 100		
Cichlidae, BS: 100		Limnochromini, BS: 100	Tropheini, BS: 100		Exocoetidae, BS: 100		
Cichlinae, BS: 100		LML-*Orthochromis* , BS: 100	**Non cichlid lineages:**		*Fundulopanchax,* BS 100		
Coptodonini + Heterotilapiini, BS 100		Lower Congo *Lamprologus* , BS 100	Adrianichthyidae, BS: 100		Melanotaeniidae (excluding Bedotia), BS: 100		
Cyprichromini, BS 100		*Malagarasi-Orthochromis* , BS: 100	*Aphyosemion* , BS 100		Nothobranchiidae, BS: 100		
EAR, BS: 91 (but supported by previous studies*)		Perisodini, BS, 100	Aplocheiloidei, BS: 99		Outgroup: Ambassidae, BS: 100		
Ectodini, BS: 100		Pseudocrenilabrinae (including *Heterochromis*), BS: 47 (supported by previous studies*)	Atheriniformes + Cichliformes, BS: 35 (supported by previous studies*)		Outgroup: Blenniidae, BS: 100		
Eretmodini, BS: 100		*Pseudocrenilabrus* , BS: 100	Atheriniformes, BS: 99		*Poecilia* , BS 100		
Etroplinae, BS:100		*Pseudocrenilabrus* -group (including Northern-Zambian-*Orthochromis*), BS: 100	Atherinoidei (Old world sliverslides and Rainbowfishes), BS: 100		Poeciliidae, BS: 100		
Gobiocichlini, BS: 100		Ptychochrominae , BS: 100	Atherinomorphae, BS: 72 (but supported by previous studies*)		*Scriptaphyosemion,* BS 100		
Haplochromini (excluding C. pectoralis), BS: 100		'extended serranochromines' (excluding Lac Fwa radiation & *H.* cf. *bakongo*), BS: 100	Atherinopsidae, BS 100		*Xiphophorus* + *Gambusia* , BS: 100		
Calibration scheme for the "Austrotilapiine mitochondrial dataset" and "Austrotilapiine ddRAD dataset"				Parameter settings (Beast):			
Calibration point:	**Fossil/event:**	**Estimated age (geological formation):**	**Calibrated clade:**	**Offset**	**SD**	**Mean**	**Distribution**
E	†*Tugenchromis pickfordi*	9-10 Ma (Ngorora Formation, Kenya)	H-lineage (sensu Nishida, 1991): 'ancient Tanganyika mouth-brooders', 'Malagarasi-*Orthochromis*' , *'Ctenochromis' pectoralis,* Haplochromini and Eretmodini (H-lineage not well supported in mt-tree)	9	0.98	2	Log normal
	Secondary constrains:						
	Root: Austrotilapiines	27.17-46 Ma; Minimum divergence time estimation taken from Schedel et al. 2019 (Set 4: Mean age: 31.98 Ma; 95% HPD of Austrotilapiines: 27.17-36.92 Ma) while maximum age for australotilapiines was constrained with the age of †*Mahengeochromis* (oldest member of Pseudocrenilabrinae)		27.17	0.85	1.54	Log normal
Clades constrained (recovered in ddRad as well as mt RAxML trees with BS of 100):							
Haplochromini		Eretmodini	Limnochromini		*Tilapia*		
Astatoreochromis		Haplochromini (excluding *C. pectoralis*)	*Malagarasi-Orthochromis*		Trophenini		
EAR (BS in mt-tree: 81)		Lac Fwa radiation	*Pseudocrenilabrus*				
EAR(excluding Boulengerochromini, Bathybatini, Ectodnini		Lake Malawi Radiation	*Pseudocrenilabrus* group (includinng Northern-Zambian-*Orthochromis*)				
		Lamprologini	a subclade of the 'extended serranochromines' (including: *Sargochromis* sp. Saise, *Sa* . sp. Kipopo & *Pharyngochromis*				

Depending on the respective BEAST analysis alternative calibration schemes were applied (see Table 1 for a general overview of the applied calibration schemes). In total, ten fossils, one geological event and one secondary constraint (the root) had been conservatively selected for the calibration of the "AC mitochondrial dataset". Inclusion of Ovalentaria fossil is based on the critical re-evaluation of fossils used in previous studies for the calibration of Ovalentaria (e.g. [16]), whereas the selection of seven cichlid-related calibration points (geological age of the crater lake Barombi Mbo, three Neotropical cichlid fossils and three African cichlid fossils) follows the reasoning given in [25]. The calibration of both austrotilapiine data sets is based on one secondary constraint (see below) for the root and one cichlid fossil (†*Tugenchromis pickfordi*). We constrained the onset of divergence of the austrotilapiines (the MRCA) using the minimum age of 27.17 Ma; this date is derived from [25] as the minimum age and as a soft upper bound the age of the oldest known cichlid fossil, †*Mahengechromis* (Eocene age, approx. 46 Ma, [73]). The age †*Tugenchromis pickfordi* is of upper Miocene age (9-10 Ma) based on the supposed age of its type locality the Waril site of the Ngorora fish Lagerstätte in the Central Kenya Rift Valley [74, 75]. The phylogenetic placement of †*Tugenchromis pickfordi* within the Pseudocrenilabrinae remains slightly imprecise due its mosaic-like character set (see [25, 74]) but the consensus is that †*T. pickfordi* is placed among the most ancient Tanganyika tribes (sensu [46]); hence alternative positions for this fossil had been selected in previous studies ([15, 25]), i.e. either at the origin of the EAR, of the C-lineage (sensu [76]) or of the H-lineage (C-lineage plus Eretmodini, sensu [77]). As the phylogenetic position of Eretmodini within the EAR differs between our ddRAD and mtDNA derived phylogenic hypotheses we accounted for this uncertainty by placing †*T. pickfordi* at the MRAC of the H-lineage. This, because Eretmodini either recovered as the sister group to a clade composed of *Orthochromis* sensu stricto (also referred as Malagarasi-*Orthochromis* [46]) and Haplochromini (ddRAD; see Figure 1), or as the sister group of so called C-lineage, (mtDNA; see e.g. Figure S1 & S2).

A detailed justification of the phylogenetic placement and corresponding ages of the four atheriniform fossils used as calibration points in our molecular clock analysis based on the "AC mitochondrial dataset" is given below (see also Table 1).

†*Hemitrichas stapfi* Gaudant and Reichenbacher, 2005 was described from the quarry "Am Katzenrech" near Dexheim (Germany) which compromises sedimentary sequences of the Lower and Upper Cerithium Beds. The stratigraphic layer of the fossil was assigned to the lower part of the Upper Cerithium Bed which is believed to be of late Oligocene age based on the biostratigraphical data ([78, 79]). The genus *Hemitrichas* (and its junior synonym *Palaeoatherina*) was clearly identified as a member of the family Atherinidae based on several morphological features (e.g. the presence of two widely separated dorsal fins, high vertebral numbers and relatively large scales [78, 80]). The phylogenetic placement of *Hemitrichas* within the Atherinidae needs yet to be thoroughly studied. We

therefore used †*H. stapfi* as a calibration point for the Atherinidae by constraining the minimum age for this family to 23 Ma while constraining the maximum age to 61.06 Ma (the estimated minimum age of the MRCA of the Atherinoidei, see [16]).

†*Rhamphexocoetus volans* Bannikov et al., 1985 was described from the Pesciara di Bolca site located in northern Italy ([81, 82]). The Pesciara sediments are restricted to a small overlap of the biozonational sequences NP14 (calcareous nanoplankton) and SBZ11 (shallow benthic) which constrains the age of the Pesciara sediments to the Late Ypersian (Early Eocene) based on biostratigraphy ([83]). No comprehensive phylogenetic analysis is available for †*R. volans* but its placement as a member of the Beloniformes within the infraseries Atherinomorpha is supported by the expanded ventral lobe of the caudal fin bearing more principal fin-rays than the dorsal caudal fin lobe. Further, the fossil can be assigned to the Exocetoidei based the elongated dentary, a character associated with the (paraphyletic) family Hemiramphidae, and enlarged pectoral and pelvic fins commonly found in the Exocetidae ([82, 84]). We therefore accept †*Rhamphexocoetus volans* as the earliest record for the family Exocetidae and constrained the lower age of this clade to 49.0 Ma based on the age of the Pesciara sediments while setting conservative maximum age of 97.5 Ma (the estimated minimum age of the MRCA of the Ovalententaria, see [16]) .

†*Fundulus lariversi* Lugaski, 1977 was described from the Siebert Tuff in Nevada. Its age is 15.4±0.8 Ma as based on radiometric age determinations of the Siebert formation ([85-87]). In a recent phylogenetic analysis †*F. lariversi* was placed into the subgenus *Fundulus* (currently four subgenera: *Zygonectes, Plancterus, Wileyichthys* and *Fundulus* are recognized) based on an total evidence data set including 63 cyprinodontiform taxa and a combination of molecular and anatomical characters ([86, 88]). We therefore used †*F. lariversi* to calibrate the crown age of the subgenus *Fundulus* by a allowing for minimum age of 16.2 Ma for this clade while conservatively constraining the maximum age to 58.51 M (the estimated minimum age for the Cyprinodontoidei, see [16]).

†*Tapatia occidentalis* Alvarez and Arriola-Longoria, 1972 was described from a location north of Amatitlán (Barranca de Santa Rosa, Mexico). The fossil bearing sediments of the type locality were tentatively assigned to Miocene age based on sedimentology ([89]). While this taxon is commonly accepted as the oldest representative of the family Goodeidae (e.g. [16, 90, 91]) its phylogenetic placement within this family remains elusive. It was suggested to be related to the extant genera *Allotoca* or *Girardinichthys* based on its conic and slightly recurved tooth shape, and on meristics ([90, 92, 93]); however, a more recent study suggest a closer relationship with the tribe Chapalichthyini and further reports a mosaic like character set of the fossil taxon (e.g. for gonopodial characters) [89, 94, 95]. We therefore conservatively constrain the minimum age of the family Goodeidae to 5.33 Ma based

on Miocene age of †*T. occidentalis* while constraining the maximum age to 23.12 Ma (the estimated minimum age of the MRCA of the Goodeidae and Profundulidae, see [16]).

Each BEAST analysis was per performed three times independently for 180 million generations per BEAST run and sampling of parameters and trees was done every 30,000 generations (except those based on the "AC mitochondrial dataset" which run for 300 million generations). The log and tree files of the three independent runs of each BEAST analysis were then combined using LogCombiner after accounting for a burn-in of 10 %. We used Tracer v.1.7.1 [96] to check the MCMC trace files obtained from the individual BEAST analysis, assuming values (> 200) for individual effective sample sizes (ESS) of the different parameters as acceptable. Finally, we retrieved maximum clade credibility trees (posterior probability limit: 0.5, mean heights) from the posterior tree distributions.

Testing for shared ancestry between austrotilapiine lineages

In order to detect potential signatures of ancient introgression between the austrotilapiine lineages we used the fineRADstructure package [97]. We converted the PyRAD alleles output file of the "Introgression-test ddRAD Set" into the input format for fineRADstructure using the script fineRADstruture-tools (https://github.com/edgardomortiz/fineRADstructure-tools). We specified inclusion of only unlinked loci (default parameter) represented in at least 40 specimens (approx. in 65 %). In addition, we re-ordered the unsorted RAD loci using the sampleLD.R script as recommended by the authors for unmapped loci. Based on these data we calculated the co-ancestry matrix using RADpainter and subsequently run the Markov chain Monte Carlo (MCMC) clustering algorithm (parameters: -x 100,000, -z 100,000 and -y 1000) using fineRADstrucure and additionally ran a simple tree-building algorithm (using fineSTRUCTURE; parameters: -m T, -x 10,000). Finally, we used the Finestructure GUI for visualisation of the resulting output data, co-ancestry matrix, MCMC output and the coalescence tree).

In addition, we tested for potential signatures of introgression between austrotilapiine species and/or entire lineages using D-statistic´s ("ABBA-BABA tests"), first introduced by [98, 99]). D-statistics approaches assess the likelihood of ancient gene flow ancient ILS) between populations or species quartets comprising one outgroup taxon (P0) and two ingroup taxa (P1 and P2) which are tested for signs of introgression with regard to a third ingroup taxon (P3). ABBA-BABA tests are based on the assumption that the frequency of derived alleles exclusively shared by P1 and P3 and those shared by P2 and P3 are equal in the absence of introgression; then ILS is statistically likely the only source of genetic discordance observed. The presence of introgression ,i.e. between P3 and P1 or P3 and P2, on the other hand is rather reflected by a bias of shared alleles between only two out of three tested taxa, i.e. by an excess of shared alleles due to geneflow after introgression between only two taxa. To calculate the D-statistics and associated p-values (with the null hypothesis that no introgression

occurs= D-statistic is 0) of all possible species trios of our "Introgression-test ddRAD Set" (26,235 combinations for 55 target taxa) we used the program Dsuite v. 0.3 [100] which enables the calculation of the D-statistics across all possible species combinations directly from the variant call format (VCF) file obtained from the PyRAD pipeline. D-statistics significance was assessed using jackknifing and splitting the dataset in 20 jackknife blocks (default parameters). Further, we provided Dsuite with a tree (based on the RAxML analysis of the corresponding dataset) specifying the independently inferred phylogenetic relationships of the species tested. We applied the Benjamini-Hochberg correction to the corresponding P-values of the D-statistic values using the function p.adjust in R 3.6.3 [101]. Finally, the Ruby script plot_d.rb written by M. Matschiner (https://github.com/mmatschiner) was used to visualize introgression patterns supported by D-statistics, by plotting the results reported in the Dmin (not shown) and tree output files, while allowing for maximum D value of 0.7.

Results

Partial mitogenomes and ddRADseq data

In total, we sequenced for this study partial mitochondrial genome fragments (average length = 8822 bp) of 184 individuals representing approximately 128 cichlid species, including several putative species which await formal description. The shotgun approach successfully recovered almost complete mitochondrial genomes for additional five specimens representing four cichlid species, and, moreover, large fragments of the mitochondrial genome (average length = 5,786 bp) of five additional specimens (representing four cichlid species; see Table S2 for detailed overview of newly sequenced samples).

We further established ddRAD data for 206 individuals representing approximately 160 African cichlid species (including several undescribed species) and representing the almost all major austrotilapiines lineages. After quality filtering and mapping to the reference genome on average ~ 379,000 reads / sample were retained (see Table S4). The PyRAD pipeline recovered on average ~ 74,000 clusters / individual with a mean coverage of 4.23 reads / locus (Mean SD: 12.52); this after removing clusters with a coverage <6, and after removing loci represented in fewer than 32 samples ("Full ddRAD Set"), as well as after additional filtering for, e.g. paralogs. Each specimen was left with an average number of ~ 8,300 loci. The proportion of missing data in final concatenated alignments of all loci was 55.6 % for the "Full ddRAD Set", 7.4 % for the "austrotilapiine ddRAD Set" and 25.3 % "Introgression-test ddRAD Set" (see also Table S4).

Phylogenetic trees

The ML trees (RAxML) based on the ddRAD based sets (Full ddRAD Set, Austrotilapiine ddRAD Set, Introgression-test ddRAD Set) recovered largely identical topologies for the relationships of the various Pseudocrenilabrinae tribes and major lineages of the Haplochromini (Figure 1 and Figure S3 & S4). The

only exceptions concern the phylogenetic position of clade comprising Limnochromini and Ectodini: it was recovered as sister group to the Cyphotilapiini in the "Full ddRAD Set" and "Introgression-test ddRAD Set" ML-trees (BS: 100), whereas it was recovered as sister to a clade encompassing Eretmodini, *Orthochromis* sensu stricto and Haplochromini in the tree based on the "Austrotilapiine ddRAD Set". The monophyly of all recognized austrotilapiine tribes included in the three datasets was strongly supported (BS: 100), except for Tilapiini (sensu [44, 71]); Tilapiini were paraphyletic with respect to the position of the genus *Congolapia* which was placed with week support (BS: 52) as the sister group to the Steatocranini.

Topologies of the two coalescent species trees (ASTRAL) either derived from the 4000 gene trees of the "Full ddRAD Set" (ddRAD loci, Figure S5) or 610 gene trees of the "Austrotilapiine ddRAD Set" (ddRAD loci, Figure S6) were largely congruent with their corresponding ML trees (see Figure 1 and Figure S3). Several inconsistencies were, however, detected particularly between the two tree hypotheses based on the "Full ddRAD Set". In the ASTRAL hypothesis, e.g., the relationships of the early splitting Pseudocrenilabrinae lineages were only poorly supported, and this topology did not match with the alternative and highly supported RAxML tree hypothesis. More strikingly, monophyly of austrotilapiines was not recovered in the ASTRAL hypothesis where the combined Gobiocichlini and Pelmatolapiini were resolved as the sister lineage to a combined *C. duponti* and Steatocranini clade; in contrast, monophyly of all austrotilapiines was highly supported in the ML based hypothesis. Additional topological inconsistencies included for example (i) the position of the benthopelagic LT clade (sensu [25]), (ii) the position of *O. indermauri* and *L. relictus* within the 'extended *Pseudocrenilabrus*-group' (see Figure 1), and (iii) relationships within the Northern-Zambian-*Orthochromis.* In addition it should be mentioned that about a dozen specimens belonging to various phylogenetic lineages were recovered at highly improbable phylogenetic positions in the ASTRAL tree, e.g. one of the three *L. relictus* one specimens formed a clade together with the single *P. acuticeps* specimen and *T. callichromus*, while the topological position of the corresponding specimens in the RAxML-tree appeared to match the assumed relationship (e.g. the aforementioned *L. relictus* specimens was recovered to form a highly supported (BS: 100) monophyletic clade with the two other genotyped specimens of the same species). There was a clear correlation between specimens with questionable phylogenetic position in the ASTRAL tree and the recovered loci (low number) in the PyRAD analysis which most likely led to those discrepancies. For example, only 74 loci were recovered in the PyRAD analysis of the Full ddRAD Set for the questionably placed *L. relictus* specimen while on average ~ 8,300 loci were recovered per sample for this data set.

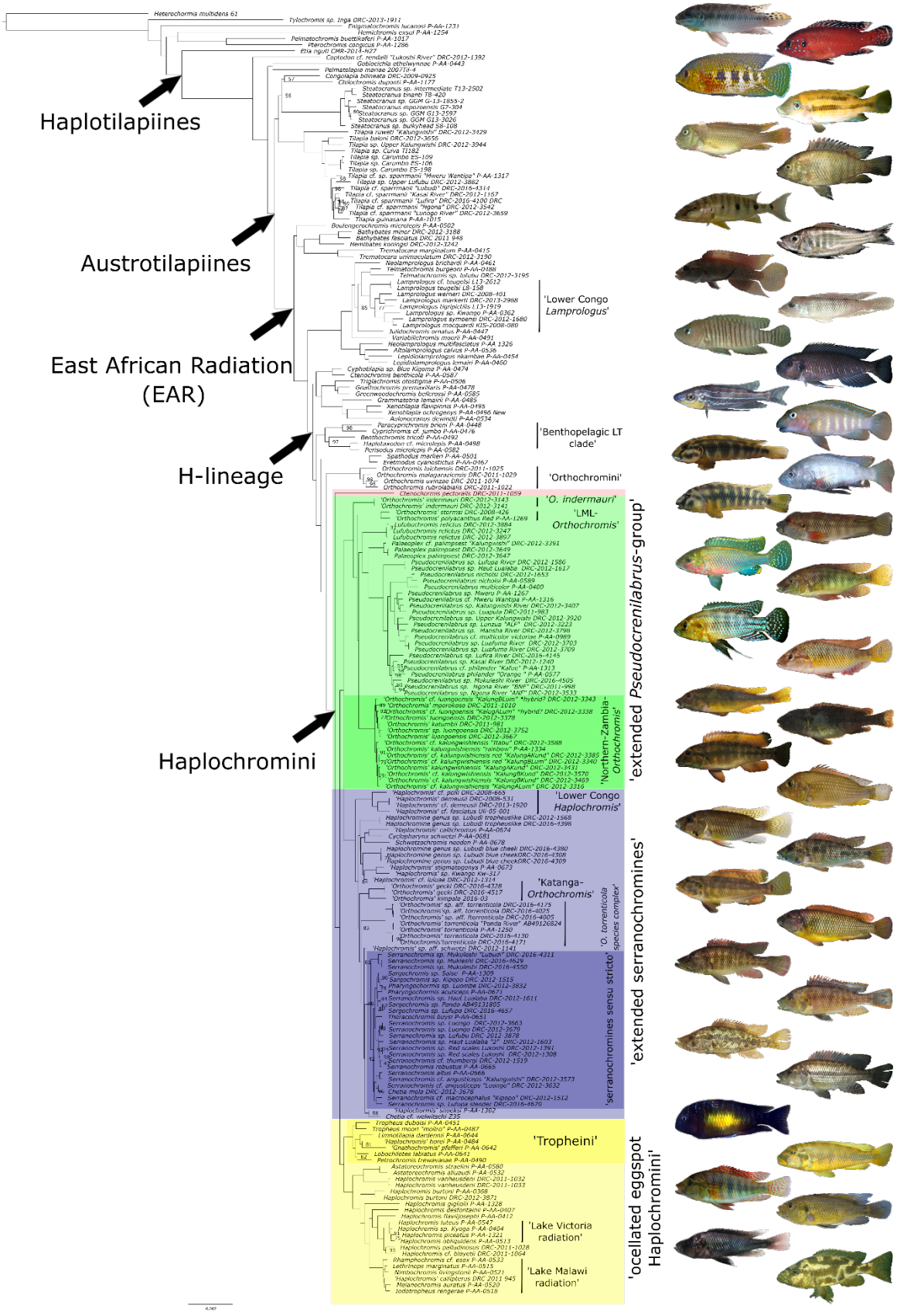

Figure 1: ML-phylogenetic hypothesis (RAxML) of Pseudocrenilabrinae with focus on australotilapiine cichlids, based on a concatenated alignment of 18,369 ddRAD loci (3,454,607 bp) while each locus was

required to be shared in approximately 30 % of the 206 included specimens (see "Full ddRAD Set"). All nodes recovered with a bootstrap support of 100 unless labeled otherwise. Specimens depicted from top to bottom (if not stated otherwise photographs by F.D.B. Schedel): E. lucanosi, Hemichromis exsul, P. mariae (E. Schraml), C. duponti (J. Geck), S. cf. gibbiceps "GGM Inga clade" (Inga 2013 Expedition), T. sp. Upper Lufubu, B. microlepis, H. koningsi, T. sp. Lufubu, L. markerti (Inga 2013 Expedition), N. multifasciatus, T. otostigma (E. Schraml), B. tricoti (E. Schraml), E. cyanostictus (E. Schraml), O. uvinzae, C. pectoralis, O. indermauri, O. polyacanthus, L. relictus, P. palimpsest "Kalungwishi", P. nicholsi (J. Geck), P. sp. Mukuleshi River (Katanga 2016 Expedition), O. sp. aff. luongoensis, O. kalungwishiensis "Red", O. kalungwishiensis, H. demeusii (Inga 2013 Expedition), 'H.' callichromus, New Haplochromine genus sp. Lubudi blue Cheek (Katanga 2016 Expedition), O. gecki (Katanga 2016 Expedition), O. torrenticola (Katanga 2016 Expedition), S. sp. Mukuleshi (Katanga 2016 Expedition), Sa. sp. Lufupa (Katanga 2016 Expedition), S. cf. angusticeps, C. mola, T. moori, H. vanheusdeni (J. Geck), 'H.' burtoni, 'H.' gigliolii, H. piceatus, N. livingstonii.

Overall, interrelationships of major African cichlid tribes are well recovered in ddRAD based phylogenies. Except for a few exceptions they were compatible with previous studies based on large nuclear DNA datasets (e.g. [15, 16, 72]). Several cyto-nuclear discordances were detected, however, between ddRAD based ML hypotheses and those based on the "Austrotilapiine mtDNA dataset" and the "AC mitochondrial dataset", comprehensively listed in Table 2. Many of those had already previously been recognized within Pseudocrenilabrinae, i.e. for the Pelmatolapiini, Gobiocichlini, Eretmodini, the LML-*Orthochromis*, *Astatoreochromis,* several lineages of the 'extended serranochromines' from the Congo basin, some of lineages of the 'extended *Pseudocrenilabrus*-group' and 'ocellated eggspot Haplochromini' [27, 34, 39, 44, 46, 71]). Interesting novel cases were found with regard to the placement of several lineages and species of the EAR: *L. symoensi, O. indermauri* and for the riverine lineages *O. kimpala* and the two yet undescribed genera from the Lubudi River, i.e. 'Haplochromine genus sp. Lubudi blue cheek' and 'Haplochromine genus sp. Lubudi tropheuslike'. Importantly, we the most extensive distribution of cyto-nuclear discordance was recovered within the 'extended serranochromines': only few of the major discernible clades within this lineage based on nuclear ddRAD data were recovered as monophyletic in corresponding mtDNA based phylogenies as already reported by Schwarzer et al. [39].

Table 2: Overview of cyto-nuclear discordances detected between dichotomous ddRAD based ML hypotheses and those based on the mtDNA data only ("Austrotilapiine mtDNA dataset" and "AC mitochondrial dataset"). In addition, candidate signals for introgression events of lineages or species with identified cyto-nuclear discordance are commented with regard to possible hybridisation partners involved (see Figure 1 and Figures S1, S2 & S5). D-values ranging between approx. 0.01 and 0.15 are considered low, those between approx. 0.15 and 0.25 moderate, and those between approx. 0.25 and 0.6 elevated in this table (see also Figure 4).

Taxon	Phylogenetic position recovered in the ddRAD based trees (RAxML). Bootstrap support values refer to the maximum likelihood tree based on the "Full ddRAD Set"; Local posterior probabilities (pp) refer to the main topology of the coalescent species tree (ASTRAL) infered from the "Austrotilapiine ddRAD Set	Phylogenetic position recovered in the mitochondrial data trees (RAxML). BS values refer to the maximum likelihood tree based on the "AC mitochondrial dataset" if not stated otherwise	Signals for introgression (based on ABBA-BABA tets) recovered with Dsuite for this clade (see Figure X. B)
Hemichromines	Sister group to Pelmatochromini (BS: 100); pp: N.A.	Sister group to all African cichlid tribes except of Heterochromini (BS: 100)	N.A.
Chromidotilapiines	Sister group to all African cichlid tribes except of *Heterochromis* and tylochromines (BS: 100); pp: N.A.	Sister group to tylochromines (BS: 61)	N.A.
Gobiocichlini	Sister group Pelmatolapiini (BS: 100); pp: N.A.	Sister group to a clade encompassing the austrotilapiines, Oreochromini, Pelmatolapiini and Coptodonini (incl. Heterotilapiini) (BS: 100)	N.A.
Congolapia	Together with *C. duponti* sister group to the Steatocranini (BS: 52); pp: N.A.	Sister group to the genus *Tilapia* (BS: 100)	N.A.
Chilochromis duponti	Together with *Congolapia* sister group to the Steatocranini (BS:52); Congolapia not present in the ASTRAL tree; but *C. duponti* sister to a clade consisting of Steatocranini and Tilapiini; pp: 0.67	Sister group to the a clade encompassing *Congolapia* and *Tilapia* (BS: 100)	No significant D values detected for *C. duponti*
Steatocranini	Together with *Congolapia* and *C. duponti* sister group to the remaining the Tilapiini (BS: 52); in ASTRAL tree recovered as sister group to Tilapiini; pp: 0.62	Sister group to the EAR (BS: 96)	Low to moderate D values reported for ABBA-BABA tests including members Steatocranini and almost all members of the EAR (hence not mentioned separately in the following clades discussed)
Boulengerochromini	Sister group to a clade encompassing the Bathybatini (incl. Hemibates) and Trematocarini (BS: 100); pp: 0.33	Sister group to all remaining taxa of the EAR (BS: 93)	Low D values reported for ABBA-BABA tests including *Boulengerochromis microlepis* with several taxa e.g. Cyphotilapiini, Limnochromini and Malagarasi-*Orthochromis*
Lower Congo *Lamprologus*	Nested within the "non-ossified Lamprologini"; sister group to a clade encompassing *L. brichardi* and *L. burgeoni* (BS: 100); pp: 1 (*L. burgeoni* not included in the ASTRAL data set)	Sister group to *Neolamprologus crassus* (AC mitochondrial dataset; BS: 100) or sister group to all other Lamprologini (Austrotilapiine mitochondrial dataset; BS: 100)	No significant D values within Lamprologini detected, but low D values for ABBA-BABA tests including Lamprologini and Ectodini
Lamprologus symnoensi	Nested with Lower Congo *Lamprologus* ; sister group to *L. mocquardi* (BS: 100); in ASTRAL tree recovered as sister group to L. sp. Kwango; pp: 1	Nested within the "non-ossified Lamprologini"; sister group to *L. cf. brichardi* (BS: 100)	No significant D values within Lamprologini detected, but low D values for ABBA-BABA tests including Lamprologini and Ectodini
Eretmodini	Sister group to a clade encompassing Orthochromini (sensu stricto) and Haplochromini (BS: 100); pp: 0.91	Sister group to Lamprologini (AC mitochondria dataset; BS: 47) or sister group to a clade encompassing all remaining tribes of the C lineage (sensu Clabaut et al. 2005) (Austrotilapiine mitochondrial dataset; BS: 60)	No significant D values detected for Eretmodini
Cytonuclear discordances detected within the Haplochromini			
'extended serranochromines'	Sister group to the "extended *Pseudocrenilabrus* -group" (see Figure 1) (BS: 100); pp: 0.78	(incl. the "Lower Congo *Haplochromis* ") sister group to all other Haplochromini (except of *C. pectoralis*) (BS: 99)	For all ABBA-BABA tests including taxa of the 'extended serranochromines', the Pseudocrenilabrus group (incl. the Northern-Zambian-*Orthochromis*), *O. polyacanthus* and Tropheini (*P. trewavasae*) elevated D values were reported; further elevated D values were observesed for ABBA-BABA tests within the serranochromine cichlid lineage (however not for *O. torrenticola*)
Orthochromis indermauri	Sister group to a clade encompassing the LML-Orthochromis (sensu Weiss et al. 2015) and the Pseudocrenilabrus-Group (incl. the Northern-Zambian-Orthochromis) (BS: 100); pp: 1	Sister group to a clade encompassing the *Pseudocrenilabrus* -Group (incl. the Northern-Zambian-*Orthochromis*) and modern riverine & ocellated eggspot Haplochromini (incl. Tropheini) (BS: 81)	Moderate D values reported for ABBA-BABA tests including O. indermauri and Ectodini, Limnochromini but elevated D values for tests including the Northern-Zambian-Orthochromis, *L. relictus* and Tropheini (*P. trewavasae*)
LML-Orthochromis	Sister group to the *Pseudocrenilabrus* -Group (incl. the Northern-Zambian-*Orthochromis*) (BS:100); pp: 0.74	Sister group to a clade encompassing several lineages of serranochromine cichlid lineage (but excluding a clade encompassing *H.* cf. *bakongo* and the taxa of the Lac Fwa radiation and further the still undescribed genus found in the Lomami and Lubudi River) (BS: 57)	Moderate D values reported for ABBA-BABA tests including Orthochromis polyacanthus (LML-Orthochromis) and Ectodini, Limnochromini but elevated D values for tests including taxa of the'extended serranochromines' and Tropheini (*P. trewavasae*)
Orthochromis luongoensis species complex (incl. O. katumbii* and *O. mporokoso)	Sister group to *Orthochromis kalungwishiensis* (species complex) (BS:100); pp: 1	*O. luongoensis* together with *O. katumbii* recovered as sister group to a clade encompassing *O. mporokoso* and *Palaeoplex palimpsest*) (BS: 100)	Moderate D values reported for ABBA-BABA tests including the species *O. luongoensis* and Ectodini, Limnochromini and L. relictus and elevated D values for test including *O. indermauri* and (Tropheini Tropheini (P. trewavasae)
Orthochromis mporokoso	Nested within the *Orthochromis luongoensis* species complex (BS:94); pp: 0.5	Sister group to *P. palimpsest* (BS: 65)	Moderate D values reported for ABBA-BABA tests including the species O. luongoensis and Ectodini, Limnochromini and L. relictus and elevated D values for test including O. indermauri and Tropheini (P. trewavasae)
Orthochromis kalungwishiensis	Sister group to the *Orthochromis luongoensis* species complex (BS: 100); pp: 1	Sister group to *L. relictus* (BS: 100)	Moderate D values reported for ABBA-BABA tests including the species O. luongoensis and Ectodini, Limnochromini and L. relictus and elevated D values for test including O. indermauri and Tropheini (P. trewavasae)
Orthochromis kimpala	Sistergroup to *Orthochromis gecki* (BS: 100); pp: 1	Nested within the serranochromine cichlid lineage; sister group to *Serranochromis* sp. Lufubu (undescribed species) (AC mitochondrial dataset; BS: 41)	Moderate D values reported for ABBA-BABA tests including *H. kimpala* and modern riverine & ocellated eggspot Haplochromini and elevated D-values for test including taxa of the *Pseudocrenilabrus* -group, LML-*Orthochromis* , Tropheini and other members of the serranochromine cichlid lineage.
Haplochromis demeusii	Together with *Haplochromis fasciatus (BS:100) and H. polli* sister group remaining taxa of the 'extended serranochromines' (BS: 100); *H. fasciatus* is not present in the ASTRAL tree but the nested relationship of *H. demeussi* of the "serranochromine cichlid lineage" is weakly supported; pp: 0.39	Together with *H. fasciatus* sister group to *Haplochromis burtoni* (AC mitochondria dataset; BS: 46) or sister group to *Haplochromis desfontainii* (Austrotilapiine mitochondrial dataset; BS: 83)	Moderate D values reported for ABBA-BABA tests including *H. demeusii* and taxa of the 'extended serranochromines' (but e.g. not for *Orthochromis torrenticola* , *H. vanheusdeni* and elevated D-values for test including taxa of the *Pseudocrenilabrus* -group, LML-*Orthochromis* and Tropheini (*P. trewavasae*)
Haplochromis vanheusdeni	Sister group to *Astatoreochromis* (BS: 100); pp: 1	Sister group to the Tropheini (BS: 95)	Moderate D values reported for ABBA-BABA tests including H. vanheusdeni and taxa of the 'extended serranochromines' (including *H. demeusii*)
Haplochromis burtoni	Sister group to a clade encompassing all lineages of the 'occelated eggspot Haplochromini' except of the Tropheini, *H. vanheusdeni* and *Astatoreochromis* ;(BS: 100); pp: 1	Togher with a clade encompassing *H. demeussi* and *H . fasciatus* sister group to ac clade encompassing the LVRS and several riverine lineages (but e.g. not the Lake Malawi radiation, Tropheini, *Astatoreochromis* & *H. vanheusdeni*) (BS: 90)	Moderate D values reported for ABBA-BABA tests including *H. burtoni* and taxa of the 'extended serranochromines' while elevated D values are reported for tests including taxa of the LVRS, Lake Malawi radiation and *H. desfontainii*
Astatoreochromis	Together with *H. vanheusdeni* sister group to a clade encompassing modern riverine & ocellated eggspot Haplochromini (e.g. the Lake Malawi radiation and LVRS) but not the Tropheini (BS: 100); pp: 1	Sister group to all remaining 'ocellated eggspot Haplochromini' (including the Tropheini) (BS: 87)	Moderate D values reported for ABBA-BABA tests including *A. alluadi, H. bloyetii and H. sp.* Kyoga while very moderate D values for ABBA-BABA tests including taxa of the serranochromine cichlid lineage
Haplochromine genus sp. sp Lubudi blue cheek (undescribed taxon)	Sister group to a clade encompassing *H. stigmatogenys, H. sp.* Kwango, *H.* cf. *luluae* (serranochromine taxa of the southern Congo basin) (BS: 100); pp: 0.52	Sister group to *Serranochromis* sp. Mukuleshi (BS: 100)	Moderate D values reported for ABBA-BABA tests including the undescribed taxon and the other new genus from the Lubudi (Haplochromine genus sp. Lubudi tropheuslike) and *H. demeusii* further elevated D values reported for test including the *Pseudocrenilabrus* group (incl. the Northern-Zambian-*Orthochromis*), *O. polyacanthus* and Tropheini (*P. trewavasae*) and the serranochromine taxa: *O. gecki, O. kimpala* and some *Serranochromis* and *Sargochromis* species

Time tree analyses

The topologies of the maximum-clade credibility (MCC) tree obtained from the molecular clock (BEAST) analysis based on the "AC mitochondrial dataset" and from that of the corresponding ML tree were consistent with each other (see Figure S1 & S7). Divergence time estimates concerning the family Cichlidae were, with few exceptions, in agreement across analyses. They had widely overlapping 95 % HPD intervals with those obtained from a previous mitochondrial based study [25],and further with those obtained from the molecular clock analysis based on the "Austrotilapiine mtDNA dataset" (see Figure 2). Divergence age estimates obtained for the "AC mitochondrial dataset" were on average slightly younger and had narrower 95 % HPD intervals as compared to those of the "Austrotilapiine mtDNA dataset". However, divergence time estimates obtained for major atherinomorph lineages were recovered consistently older than those obtained from previous studies (e.g [16, 69, 102]). Therefore, divergence time of this particular molecular clock analysis are not further discussed here, as an improved calibration scheme for the "AC mitochondrial dataset" is in preparation and will be presented with the finalized manuscript.

The two molecular clock analyses based on the same calibration scheme and taxon sampling but on two different datasets ("Austrotilapiine mtDNA dataset" and "Austrotilapiine ddRAD Set") recovered MCC trees with topologies largely congruent with ML-based topologies. If cyto-nuclear discordances had been observed between the mitochondrial and nuclear phylogenies (see Table 2) those were also recovered in MCC trees (see Figure S8 & S9). Divergence time estimates of both analyses agreed largely as inferred from widely overlapping % 95 HPD intervals (Figure 4; but with general wider 95% HPD intervals derived from the ddRAD Set). However, two discrepancies from this pattern, i.e. with little HPD overlap between both analyses were recovered, too: i) the MRCA of the genus *Tilapia* s.str. was recovered as much older in the mtDNA-based analysis to a Miocene-Oligocene age (19.05 Ma; 95% HPD: 12.93–25.42 Ma) as compared to the younger Pliocene-Miocene age recovered in the ddRAD based analysis (12.05 Ma; 95% HPD: 4.72–20.48 Ma); ii) the MRCA of the *O. kalungwishiensis*-species complex had a very narrow and comparatively young 95% HPD interval in the mtDNA-based analysis which was dated to Pleistocene age (1.09 Ma; 95% HPD:0.66–1.57 Ma) but a much older inthe ddRAD-based one suggesting rather a Pliocene age (2.22 Ma; 95% HPD: 0.52–4.57 Ma). Overall, divergence times estimates based on the two different datasets did not contradict each other, apart from the two aforementioned incongruities.

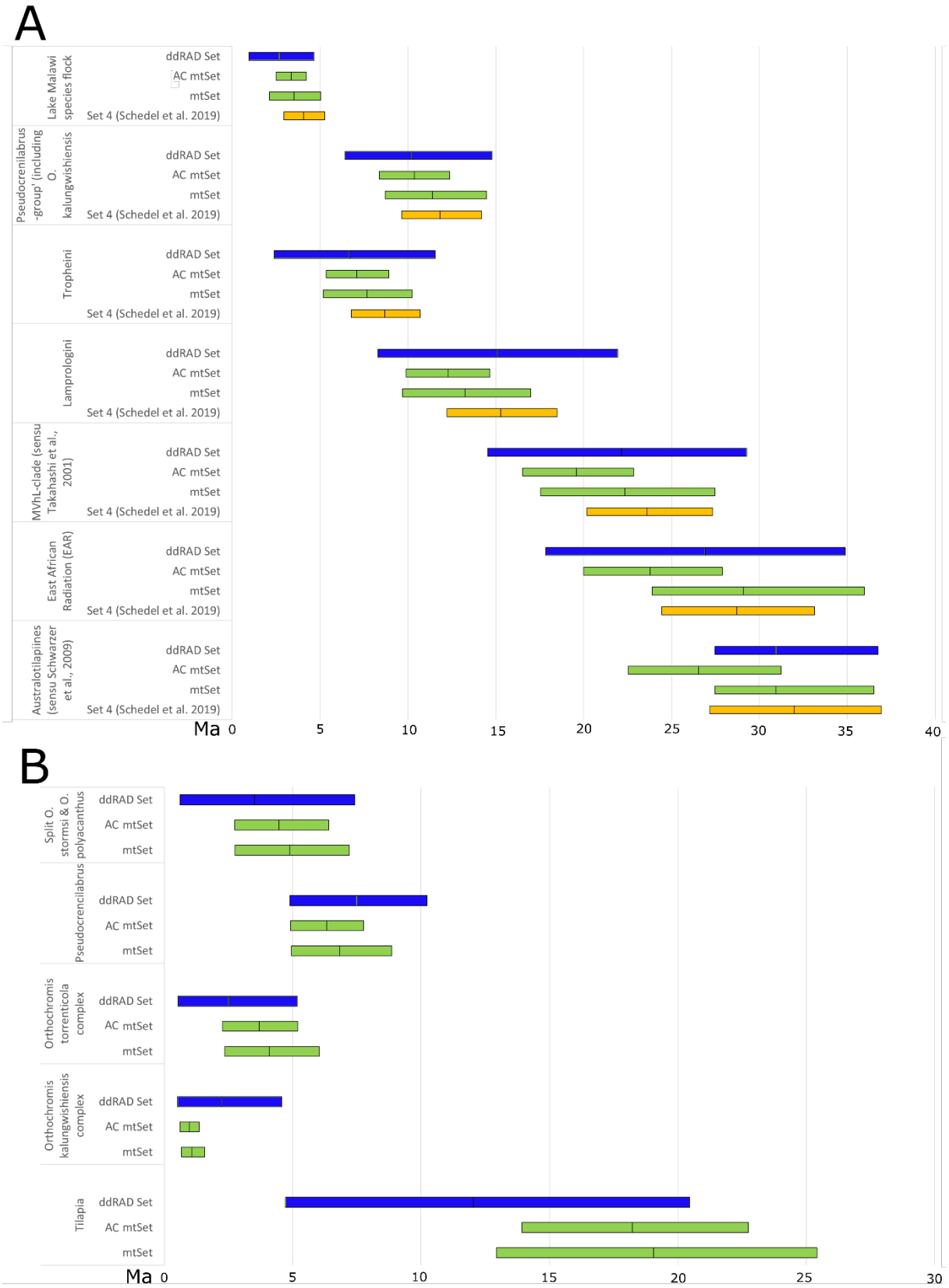

Figure 2: Divergence age estimates of selected nodes obtained from the three different molecular clock analysis conducted with BEAST. Highest posterior density intervals (95 % HPD) based on mtDNA-based analyses are depicted in green (AC mtSet = "AC mitochondrial dataset"; mtSet = "Austrotilapiine mtDNA dataset"), those based on the nuclear DNA-based ones (ddRAD) data in blue and those in orange depict

*(ddRAD Set = "Austrotilapiine ddRAD Set"), if available (Figure capture **A.**), comparable divergence time estimates of the recent molecular clock study in Schedel et al. (2019)(their Calibration Set 4)*

Detection of shared haplotypes and potential signals of introgression

The clustered fineRADstructure co-ancestry matrix (Figure 3) based on the "Introgression-test ddRAD Set" (59 austrotilapiines and one outgroup) revealed comparatively homogeneous patterns of shared ancestry within most major austrotilapiine lineages (e.g. Steatocranini, Lamprologini, Limnochromini, Eretmodini and Malagarasi-*Orthochromis*). The important exceptions concern Tilapiini and, not surprisingly, the megadiverse Haplochromini. Tilapiini were represented by four species, three belonging to genus *Tilapia* and one *Chilochromis duponti*. The latter appears to share haplotypes with *Tilapia* species but also with Steatocranini, Boulengerochromini and Trematocarini. The co-ancestry matrix further revealed elevated, yet partially heterogeneous haplotype sharing between three major Haplochromini lineages: i) one clade, from now on referred to as the 'extended *Pseudocrenilabrus*-group' (see Figure 1) encompassing the *Pseudocrenilabrus*-group incl. the Northern-Zambian-*Orthochromis*, the LML-*Orthochromis* and *O. indermauri*, ii.) one clade, referred from now on as the 'extended serranochromines' (see Figure 1) encompassing the serranochromines sensu lato sensu [103], but also including the Lower Congo '*Haplochromis'* and iii.) one clade referred from now on as the 'ocellated eggspot Haplochromini' encompassing the Tropheini, the LVRS, Lake Malawi radiation and many additional riverine lineages (e.g. *Astatoreochromis*, '*H'. vanheusdeni*, *'H'. burtoni, 'H.' gigliolii, A. desfontainii and 'H.' bloyeti* (see Figure 1). *Ctenochromis pectoralis*, the sister group to the remaining lineages of Haplochromini lineages, was recovered as the sister group of Malagarasi-*Orthochromis* and several Lake Tanganyika tribes in the dichotomous tree topology produced by fineRADstructure, but it showed only week haplotype sharing with all other Haplochromini. Further zooming into closer relationships within these three haplochromine lineages high and homogeneous levels of shared ancestry were detected within the Northern-Zambian-*Orthochromis*, *Pseudocrenilabrus*, 'serranochromines sensu stricto' (represented by *Serranochromis, Sargochromis* and *Chetia* in the "Introgression-test ddRAD Set"), a clade, referred from now on as the Katanga-*Orthochromis* (including *Orthochromis gecki* and *Orthochromis kimpala*), the *Orthochromis torrenticola* species complex, the Lake Malawi radiation, one clade including '*H.'* cf. *bloyeti* and *Haplochromis* sp. Kyoga (LVRS), and one further clade including *Astatoreochromis* and *H. vanheusdeni*. The single taxon of Tropheini included in the dataset, *Petrochromis trewavsae,* featured comparatively week haplotype sharing within the other 'ocellated eggspot Haplochromini' but also with all other lineages of the Haplochromini.

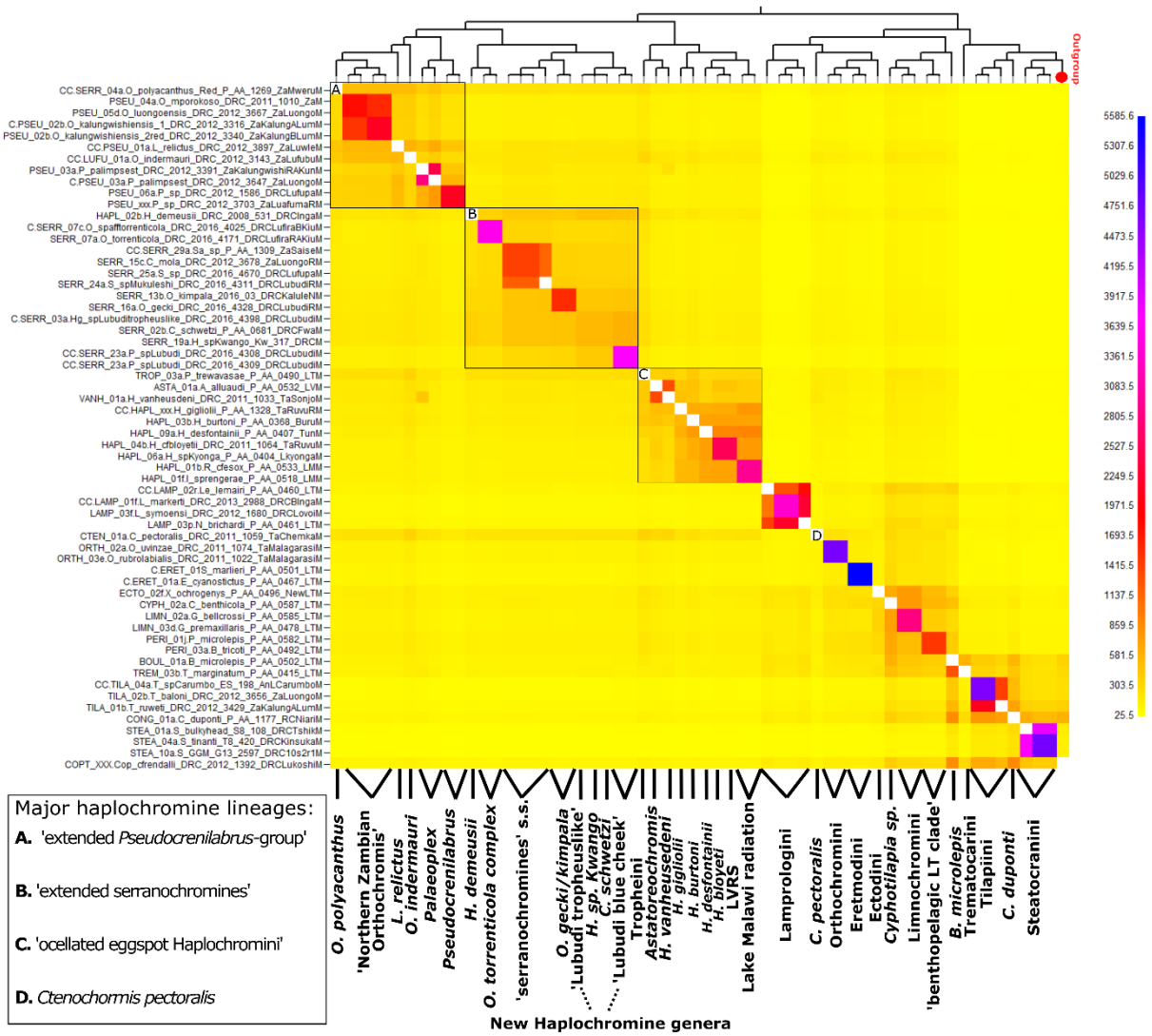

Figure 3: fineRADstructure plot based on 11,488 loci present in the dataset in at least 60 % percent of the samples and summarizing results for 59 austrotilapiine cichlid species and one outgroup (Coptodon cf. rendalli "Lukoshi"). Pairwise coefficients of co-ancestry between individuals are color-coded, with low values indicated in yellow and high values indicated in blue (see also scale bar on the right). Legends on the right and below the co-ancestry matrix show the sample names of individuals (including abbreviated species names, see Table S1 for corresponding specimen information) and the main lineages represented by the data set, respectively. Major haplochromine lineages are indicated by black frames and the letters A to D in the plot. The dendrogram on the top of the co-ancestry matrix indicates the clustering of samples obtained from the fineRADstructure tree building algorithm.

As a complementary analysis targeting the identification of candidate introgression events among austrotilapiine lineages of the ddRAD dataset, we performed four-taxon D statistic tests as implemented in in Dsuite on all possible ingroup-species trios and using with *Coptodon* cf. *rendalli* "Lukoshi" as outgroup taxon for all ABBA-BABA tests. Results were visualized by plotting the D- values in a heatmap, including corresponding p-values corrected for multiple testing with Benjamini-Hochberg as suggested by [100] (Figure 4). Altogether 1593 out of 26,235 ABBA-BABA tests had significant p- values < 0.05, with D values ranging between 0.17 and 0.59 (see Table S5). Overall, we found high support for candidate introgression signals between most species, for which we had

detected cyto-nuclear discordances signals, but there were several notable cases for which no apparent traces of introgression between candiate hybrid partners were detected in the ddRAD dataset (see Table 2 and Figure 4): i) *Lamprologus symoensi*, either grouped within the'non-ossified Lamprologini' in mtDNA analysis or in the Lower Congo *Lamprologus* clade in the ddRAD analysis ii) *O. mporokoso,* forming with *P. palimpsest* the sister group to clade encompassing *O. luongoensis* and *O. katumbii* based on the mtDNA or grouped within the *Orthochromis luongoensis* species complex in the ddRAD analysis) iii) *H. vanheusdeni*, either the sister group of Tropheini in the mtDNA analysis or the one of *Astatoreochromis* in the ddRAD analysis.

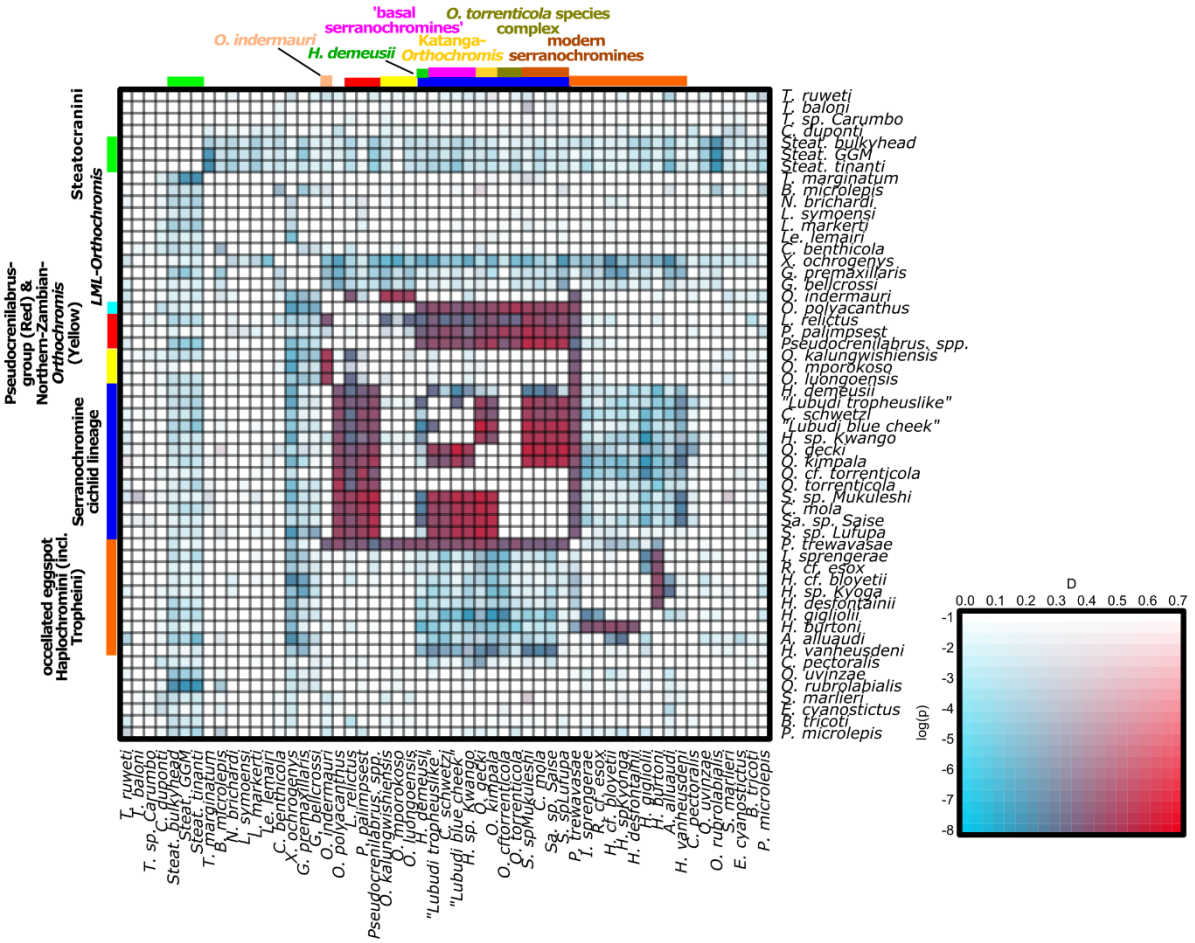

Figure 4: Heatmap visualizing most significant D-statistic values detected across all possible species trios (26,235 trios tested) and calculated with Dsuite v. 0.3. Plotted are the testedspecies pairs (corresponding to the ingroup species P2 and P3 of the D-statistic testing structure) sorted on the horizontal and vertical axes according their phylogenetic position in the ML tree of the "Introgression-test ddRAD Set". D-statistic values are colour-coded with low values indicated in blue high D values indicated in red and intermediate values in purple. Significance level after corresponding Benjamini-Hochberg corrected p-values are indicated by saturation (higher saturation of colours indicates higher significance of the D values; in log-scale). All D statistic values are summarized in Table S5.

Discussion

Divergence time estimates for mtDNA-based and nuclear-based (ddRAD) datasets are largely congruent

Divergence time estimates for Pseudocrenilabrinae based on nuclear and mtDNA data are to large parts comparable or, at least, they do not contradict each other, although nuclear DNA-based analyses 95 % HPD intervals were generally wider and yielded generally older mean ages [25]. This is surprising as on average mtDNA experiences higher mutation rates than nuclear DNA (e.g. [104]) and hence mtDNA markers should to tend be saturated more quickly. This should translate rather into older divergence time estimates [21, 105], whereas other studies suggest that saturation of mtDNA markers may lead to younger age estimates at deeper nodes and, simultaneously, to older divergence age estimates at comparatively young nodes [106, 107]. Further, it should be mentioned that the comparative nuclear DNA dataset used in the study of Schedel et al. [25] was only based on a compilation of four partial nuclear genes from 117 GenBank species entries. Thus, this data set only partially mirrored the respective mtDNA dataset as several important lineages were missing, e.g. the Malagarasi-*Orthochromis*. This imperfect match might have contributed to the observed congruent divergence time estimates. To improve comparability we generated two novel subsets, one consisting only of mitogenomic data (ten complete protein-coding genes) and one of ddRAD data comprising short read sequences of 610 nuclear loci, which fully mirrored each other in taxon sampling. Both data sets were analysed under fully identical same calibration schemes. In order to further maximise comparability of results, we paid particular attention to keep levels of missing data low and comparable, i.e. with about 1% in the mtDNA dataset and 7.4% in the ddRAD dataset; this despite missing data affect molecular clock estimates comparatively little [108]. Intriguingly, our recovered divergence time estimates were largely compatible in their respective mean ages, but the divergence age the ddRAD-based analysis yielded wider 95 % HPD intervals. This with the exception of some minor peculiarities concerning few node age estimates, e.g. that of the *Orthochromis kalungwishiensis* species complex, which might have been influenced by the observed ancient hybridization events for the corresponding clades. Yet, the high BS node support recovered for most nodes in the ddRAD analysis, even for comparatively deep ones, confirms recent findings showing ddRAD data may yield sufficient phylogenetic signal not only for shallow but also for substantially older divergence events, dating back to 50-60 Ma; nevertheless phylogenetically informative signal density deteriorates substantially over this time span [109, 110]. The consistent divergence age estimates obtained from our different molecular clock analyses further support recent findings that ddRAD loci might exhibit overall similar mutation rates as mtDNA and hence might be especially useful for dating divergence events of late Cenozoic age; this in turn allows for a refined understanding of the biogeographic history of cichlids [109].

Widespread signatures of hybridization across major austrotilapiine lineages

We found signatures of hybridization between and within all major haplochromine lineages, among the comparatively older Lake Tanganyika tribes, and even between the EAR and the Steatocranini. This result strongly suggests that hybridization and introgression persistently shaped the evolutionary history of austroltilapiines across times. The extensive taxon sampling encompassing almost all austrotilapiine lineages allowed not only to evaluate previously recognized introgression events but also to identify newly recognized signals of introgression, and to analyse them in a spatio-temporal context.

Our results are in line with previous studies which had recovered evidence for ancient hybridization events between lineages at the base of the EAR involving Boulengerochromini and the benthopelagic LT clade [15, 28]). Likewise, D-statistics detected weak but consistent signals for ancient hybridization between *Steatocranus* (three species) and essentially almost all included EAR species. The wide range of D-statistics signal across the EAR suggests an ancient hybridization event between the Steatocranini and the precursor lineage of the EAR. and did not continue after the diversification of the modern EAR (see Figure 4). This would further explain the comparatively week signatures of gene flow detected between Steatocranini and the lineages of the EAR in this study (see Figure 3) which could be explained by signal erosion over long geological time scales. Hybridization between Steatocranini and sublineages of the H-lineage apparently continued after the initial diversification of the EAR. This inference is based on data for one *Steatocranus* species, which showed weak and heterogeneously strong signals for ancient gene flow with Lamprologini and stronger signals with members of the H-lineage [15].

The adaptive radiations of both, the Lake Victoria Superflock (LVSF) and Lake Malawi radiaton, were recently proposed to have been fuelled by ancient hybridization events, and riverine haplochromine lineages were documented to have been in involved in the corresponding hybridization events: the 'Congolese lineage' and 'Upper Nile lineage' showed hybridisation signals with LVRS, and evidence for ancient gene flow was detected between the undescribed species '*H*.' sp. ruaha blue and the Lake Malawi radiation, [26, 27, 29]). As our data set did not include any representatives of the 'Congolese lineage' (e.g. 'H.' sp. Yaekama and *'H.' stappersii*), 'Upper Nile lineage' (e.g. *'H.' pharyngalis* and *'H.' gracilior*) nor '*H*.' sp. ruaha blue it was impossible to revisit those proposed hybridization events. However, we found potential signals of gene flow between '*Haplochromis.' burtoni*, a widespread species from the Lake Tanganyika drainage [111], and clade encompassing the Lake Malawi radiation, the LVRS and the riverine taxa '*H.' bloyeti* and *A. desfontainii* (but not with *'H.' gigliolii,* see Figure 3 and Figure S4). This suggests that gene flow between '*H.' burtoni* and the precursor of the aforementioned clade had taken place before the diversification of the LVRS and Lake Malawi radiation

drawing an even more complex scenario for the evolutionary history for two of the most diverse vertebrate adaptive radiations. Yet, it should be mentioned that these D-statistics results are based on a single '*H.' burtoni* specimen. Additional specimens and populations of '*H.' burtoni* need to be included in future analyses, as '*H.' burtoni* can be divided into a northern and a southern lineage [111].

We further detected introgression signals within the other major haplochromine lineages including the 'extended *Pseudocrenilabrus* group' (referred in [34] as 'Orthochromines') and within the 'extended serranochromine'[34, 39]. Both lineages have seeded several of the small adaptive radiations of Lake Mweru, which were proposed to be of hybrid origin [34]. The genomic mosaic of the *Pseudocrenilabrus* radiation of Lake Mweru, for example, has elements of *Pseudocrenilabrus* cf. *philander* lineages of Bangweulu system as well as of a different *P. cf. philander* lineage from the Cunene/Western Zambezi drainage (see [34]). Our dataset "Introgression-test ddRAD Set" did not allow for extensive testing of hybridization events amongst the genus *Pseudocrenilabrus.* Yet, as in the study of Meier et al. [34], we recovered signals of gene flow between *Lufubuchromis* from the upper Lufubu [47], and all tested Northern-Zambian-*Orthochromis.*

In contrast to the previous results of [34], we did not detect signatures of hybridization between *Palaeoplex* from the Luongo River and Kalungwishi River systems [47] and *Pseudocrenilabrus*, and we detected only comparatively weak signals between *Palaeoplex* and the Northern-Zambian-*Orthochromis* using D-statistics (see Figure 4 and Table S5). This is surprising as cyto-nuclear discordance suggests a hybridization event between those two lineages: *Palaeoplex* has a mitochondrial haplotype clearly related to the *Orthochromis luongoensis* species complex. Except for its larger maximum size *Palaeoplex* strongly resembles *Pseudocrenilabrus* but has a suite of derived morphological characters [47]. The nuclear genomic data therefore suggest that *Palaeoplex* represents a comparatively old lineage which had recently captured mitochondrial haplotype from the Northern-Zambian-*Orthochromis*, and not that it is a recently evolved lineage of pure hybrid origin, as suggested by [34]. Interestingly, both potential hybridisation partners *Palaeoplex* as well as representatives the *Orthochromis luongoensis* species complex are found in same drainage, the Kalungwishi river[47, 112], and hence that hybridization between those two lineages is biogeographically plausible. Molecular clock analysis of the mitochondrial "Austrotilapiine mtDNA dataset" dates this inferred introgression to the Pliocene at around 3.4 Ma (95 % HPD: 2.1–5.0 Ma). Whereas the molecular clock analysis based on the nuclear "Austrotilapiine ddRAD Set" recovered a Pliocene to Late Miocene age (7.0 Ma, 95 % HPD: 3.9–10.4 Ma) for the divergence of *Palaeoplex* an *Pseudocrenilabrus* and a slightly older age for the MRCA of *Lufubuchromis* and the clade encompassing *Palaeoplex* an *Pseudocrenilabrus* (8.3 Ma, 95 % HPD: 4.9–12.1 Ma) which further supports assumption that these lineage are comparatively old. Although these nuclear divergence time estimates should be scrutinized carefully as hybridization is

known to potentially influence divergence time estimates and may lead to under- or overestimation of the corresponding divergence age [113, 114].

The 'extended serranochromines' appear to represent a hybrid swarm which might have originated from ancient hybridization event(s) between the 'extended *Pseudocrenilabrus*-group' and the 'ocellated eggspot Haplochromini'. We found strong D-statistics signatures of hybridization between the LML-*Orthochromis,* represented e.g. by *O. polyacanthus* in our dataset, and all tested species of the 'extended serranochromines', and this result is further supported by the cyto-nuclear discordances The LML-*Orthochromis* are either nested within the 'extended serranochromines' in the mtDNA data analyses (see e.g. Figure S1) or they are recovered as the sister group of all other lineages of the 'extended *Pseudocrenilabrus*-group' except of *O. indermauri* (see Figure 1) based on phylogenomic data. More importantly, we found strong signals of hybridization of all taxa of the 'extended serranochromines' with other members of the 'extended *Pseudocrenilabrus*-group', i.e. with *Pseudocrenilabrus*, *Palaeoplex* and *Lufubuchromis* but not with Northern-Zambian-*Orthochromis*. And equally important, we found those signatures between the 'extended serranochromines' and the 'ocellated eggspot Haplochromini', albeit to a less extent.

Beside, some taxa of the 'Lower Congo *Haplochromis* clade' (e.g. *H. demeusii* and *H. fasciatus*) were reported to carry a mitochondrial haplotype deeply nested within the 'ocellated eggspot Haplochromini', whereas nuclear data suggest that these taxa form the sister group to all other taxa of the 'extended serranochromines' together with the other taxa of the 'Lower Congo *Haplochromis*' (e.g. *H. polli*) (see Figure 1 and Figure S1; [39]). We did not explicitly test for the directionally of gene flow but a possible scenario explaining the observed patterns would be that the lineage of the 'extended serranochromines' itself represents a hybrid swarm which potentially arose from an ancient hybridization event (or events) involving precursor lineages of the 'ocellated eggspot Haplochromini' as well as of the 'extended *Pseudocrenilabrus*-group' (but probably not *O. indermauri*).

Intriguingly, the 'extended serranochromines' are highly diverse in terms of species numbers, of their morphology and their ecological adaptations. They have evolved, e.g., elongated piscivores, deep bodied molluscivores and strongly rheophilic elongated species. In contrast, to the extended *Pseudocrenilabrus*-group' is a comparatively uniform haplochromine lineage, even if members of the Lake Mweru lineage are taken into account. The origin of the high diversity found within the 'serranochromines sensu stricto' has been attributed the ancient adaptive radiation, which would have evolved within ancient palaeolake Makgadikgadi. After its disappearance, they would subsequently have dispersed widely over their present distribution area and southern and central Africa [103, 115, 116]. Yet the diversity of the many basally diverging lineages of the 'extended serranochromines' is equally impressive as the recently diverged lineages of the 'serranochromines sensu stricto' as a recent

the analysis of Musilova et al. [103] suggest. It includes, e.g., eco-morphologically diverse species southern Congo drainage rivers, from the Cuanza and the Cunene River (see Figure 1 and e.g. [103]). The ancient hybridization event(s) leading to the divergence of the 'extended serranochromines' might have been fuelled their eco-morphological diversification as it was suggested several other lineages within the Haplochromini [27, 34]; and this, rather than a lacustrine adaptive radiation origin in a palaeo-lake that is dated substantially younger than our date estimates for the their divergence.

The reconstruction of the complex evolutionary history of *O. indermauri* has provided new insights in the biogeographic history of the 'extended *Pseudocrenilabrus*-group' and in the drainage evolution of the Lufubu River. Interestingly, we recovered strong signals of hybridization between *O. indermauri,* the 'Northern-Zambian-*Orthochromis'* and *L. relictus. O. indermauri* is endemic to the lower Lufubu river, a southern affluent of Lake Tanganyika, and was only recently recognized as ancient distinct mitochondrial haplotype lineage within the Haplochromini [25, 112]. Here we recover it as the earliest diverging lineage of the 'extended *Pseudocrenilabrus*-group' based on nuclear data and it is recovered as sister group to a clade encompassing the 'occellated eggspot Haplochromini' and the 'extended *Pseudocrenilabrus*-group' based on mitochondrial data, albeit with comparatively low support (BS: 81). The present day upper and lower Lufubu river are separated by several series of cascades and waterfalls which act nowadays as barriers to fish migration, as inferred from the distinct ichthyological communities between the two main sections [112, 117]. Hybridization events between the different ancient lineages, e.g. the precursor lineages of *O. indermauri, Lufubuchromis* and the Northern-Zambia-*Orthochromis*, thus would have taken place before *O. indermauri* became isolated in the Lower reaches of the Lufubu River. The geological history leading to the formation of the western (Albertine) branch of the East African Rift has been highly dynamic and complex and still poorly known; for example, the age and history of formation the extant Lake Tanganyika basin and of the connections to its affluents like the Lufubu river is still under discussion [118]. It has been suggested that true rifting activity stared around 5.5 in the northern LT basin whereas the pre-rift formation of the Albertine Rift was dated to 4–11 Ma based on thermochronology and sedimentology [119-122], but other studies indicate an older age for the origin of the formation of the extant LT basin (9-12 Ma). The latter study was based on the extrapolation of recent and uniform sedimentation rates which might be too simplistic [118, 123]. On other the hand it had been proposed that the initiation of the formation of the western branch and associated volcanism in the Rukwa basin had started already 25 Ma based geochronology and magnetostratigraphy. According to this scenario tectonic dynampimcs reshaping western branch drainage systems might have started as early as in the Oligocene [124]. Our mitochondrial divergence times estimates suggest that *O. indermauri* became isolated at around the middle Miocene (14.2 Ma; 95 % HPD:11. 1–17.8 Ma), and thus most likely before the formation of

extant LT. This age estimate for an endemic lower Lufubu cichlid divergence hence tentatively suggests that lower Lufubu River became separated from its upper reaches at about that time.

"Mitochondrial ghosts of the past" facilitate reconstructions of complex biogeographic histories in tectonically dynamic landscapes

In addition to the numerous signatures of hybridization detected across austrotilapiine cichlid lineages, we identified several cyto-nuclear discordances which left no detectable traces of nuclear gene flow between potential hybridization partners in our ddRAD data set (see Table 1). More importantly, these "mitochondrial ghosts of the past" provide new insights in the complex biogeographic history of the involved lineages which might date back even into the Miocene. Mitochondrial introgression with subsequent complete replacement of ancestral mitochondrial genomes in the absence of obvious signs of associated nuclear signals of introgression has been documented in several fish families, e.g. in salmonids [125], pupfishes [126] but also in cichlids [127]. However, these cases of mitochondrial capture appear to have happened relatively recent in those cases, as, e.g., the mitochondrial introgression event between *Lamprologus callipterus* and *Lamprologus fasciatus* was estimated to 0.53 to 0.94 Ma [127] and that between of *Salvelinus alpinus* and *S. namaycush* to late Pleistocene or early Holocene [125].

Surprisingly, we detected one mitochondrial introgression event involving '*H'. vanheusdeni* and the LT endemic tribe Tropheini, which appears to be of Miocene age (mean age: 9.6 Ma ;95 % HPD: 7.0–12.3 Ma; based on mitochondrial divergence time estimates). Based on nuclear DNA data the eastern Tanzanian '*H'. vanheusdeni* a taxon only known from the Great Ruaha drainage system situated in eastern Tanzania [128] was recovered as the sister group of *Astatoreochromis,* a genus distributed in the Lake Victoria region and several major affluents of the Lake Tanganyika basin [129]; based on mtDNA data '*H'. vanheusdeni* was recovered as the sister group to the LT endemic Tropheini. It is therefore highly likely that '*H'. vanheusdeni* captured the mitochondrial genome of an early representative of the LT Tropheini lineage, which is today endemic to LT drainage with some species occuring in the Lukuga river and in least in the lower sections of the Malagarasi river [130, 131]. Interestingly, our tests for hybridization did not recover apparent signals of gene flow between the potential hybridization partners, although only one representative species were included for the Tropheini and *Astatoreochromis* in the corresponding D-Statistic tests (see figure 4). Based on mitochondrial DNA haplotype relationships a previous study had already suggested that the proto-Malagarasi drainage and the Proto-Great Ruaha drainage were connected in the past [25]. The discovery of the discordant phylogenetic position of '*H'. vanheusdeni* in mtDNA and nuclear based phylogenies does not contradict this assumption but rather adds additional support for this hypothesis by constraining the geographical area of the potential introgression event. *Astatoreochromis* as well

as some taxa of Tropheini (e.g. *'H.' horei* [131]) are known to occur in the Malagarasi drainage, the major tributary of LT). Based on our analyses the precursor lineage of '*H'. vanheusdeni* captured probably soon after the divergence of *'H.' vanheusdeni* and *Astatoreochromis* a mitochondrial haplotype of a precursor lineage of the Tropheini, somewhere in the proto-LT drainage, i.e. in the wider area of the present day Malagarasi and LT basin. This mitochondrial capture event dates back to Miocene, and during this time the proto-Malagarasi and proto-Great Ruaha systems were still connected according the relict distribution of '*H'. vanheusdeni* [25].

The second "mitochondrial ghost of the past" concerns *L. symoensi* from the Upemba lakes in the Upper Lualaba, the Lower Congo *Lamprologus* and the 'non-ossified Lamprologini' of LT. *L. symoensi* is the only *Lamprologus* species endemic to the Upper Congo (Lualaba) [132] and it was found to be related to *Telmatochromis* cf. *temporalis,* a member of the LT 'non-ossified Lamprologini'; surprisingly, it was not related closely to other riverine Lamprologini of the Congo, e.g. to the Lower Congo *Lamprologus*, in a recent study based on mitochondrial data [25]. Two scenarios for the observed biogeographical pattern were proposed (see [25]): either i) *L. symoensi* represents the descendant of an independent colonization event of the Congo basin; or ii) *L. symoensi* captured the mitochondrial genome from LT Lamprologini dispersing into the Congo. Our nuclear data recovered the Lower Congo *Lamprologus* including *L. symoensi* to be deeply nested within 'non-ossified Lamprologini' (see Figure 1). In contrast, our mitochondrial analyses (see Figure S1) recovered most Lower Congo *Lamprologus* (but not including *L. symoensi* and *L. werneri*) together with the LT endemic *L. crassus* as the sister group to a clade comprising the LT endemics *N. mustax*, *N. nigriventris*, *N. pectoralis* and *N. cylindricus* (corresponding to the "Clade C" sensu [133] and the "mtDNA Clade I" sensu [134]). Unfortunately, neither *L. crassus* nor any representative taxa of the 'mtDNA Clade I' were included in our ddRAD data set. Yet, based on the nuclear DNA data the recovered monophyly of Lower Congo *Lamprologus* including *L. symoensi, L. werneri,* and *L. teugelsi,* which carry 'non-ossified Lamprologini' mitochondrial haplotypes [25, 133, 134] points to a first colonization from the greater LT region into Congo river through one single precursor lineage of the Lower Congo *Lamprologus.* The initial colonization event would then subsequently been followed by at least one secondary colonization event, which led to the secondary capture of mitochondrial haplotypes of the 'non-ossified Lamprologini' by only few Congo *Lamprologus* species as, e.g. *L. symoensi* and *L. werneri*. Interestingly, we were not able to detect any additional signatures of introgression between any other lamprologine species and *L. symoensi* with our data set ("Introgression-test ddRAD Set"; no ABBA-BABA tests were conducted including *L. werneri*). This suggests that possibly only a single hybridization event led to the capture of 'non-ossified Lamprologini' haplotype characterising *L. symoensi* whereas subsequent repeated backcrosses of the hybrid progeny would have eradicated nuclear DNA signals of this introgression event, analogous to similar cases suggested for LT endemic Lamprologini [134]. This scenario becomes even more probable

if only a comparatively small seeding population is assumed to have left LT as secondary colonizers. This appears highly likely giving the different water chemistry of Lake Tanganyika and the Congo River and its major tributaries, which was already suggested to impede dispersal of LT cichlids into the Congo basin [130]. Interestingly, our mitochondrial dataset (see Figure S1) recovered a clade encompassing riverine taxa (Congo: *L. werneri* and *L. symoensi*; Malagarasi River*: L. devsoi*) as well as LT endemic taxa (*T. temporalis*, *N. christyi*) which was nested within the 'non-ossified Lamprologini'. Therefore it seems likely that ancestors of this particular clade colonized the Congo basin, most likely during in a short time period, e.g. during an extreme flooding event, and subsequently hybridized with at least two different lineages of the Lower Congo *Lamprologus* as reflected today by the cyto-nuclear discordances observed for *L. symoensi* and *L. werneri*. These mitochondrial capture events thereby appear of Pliocene age, e.g. as the divergence time estimates of a recent study for that mitochondrial capture event involving *L. symnoensi* suggest [25]. The here newly detected cases of "mitochondrial ghosts of the past" not only allow for a more accurate reconstruction of complex biogeographic history of the corresponding taxa but also underline the importance of comprehensive taxon and data sampling including both nuclear as well as mitochondrial data which ultimately represent the basis for the detection of "mitochondrial ghosts of the past".

Conclusion

Based on a comprehensive ddRAD data set comprising representatives of almost all major African cichlid lineages we recovered a well resolved phylogenetic hypothesis for the African subfamily Pseudocrenilabrinae. The focus was laid on the lineage that includes the East African cichlid radiations, i.e. the austrotilapiines, and on the inclusion of several key taxa for the first time in nuclear DNA (ddRAD) based phylogenetic analyses, e.g. *Tilapia baloni* and allies, Katanga-*Orthochromis*, *O. indermauri*. Comparisons of the our ddRAD based phylogeny with a phylogenetic hypothesis based on a large mitochondrial data set including approximately 330 cichlid species recovered numerous cyto-nuclear discordances. Extensive testing for signatures of hybridization identified widespread gene flow among as well as within almost all major austrotilapiine lineages, hereby highlighting the importance of hybridization and introgression for the reconstruction of the evolutionary history of African cichlids. Several ancient introgression events were only recovered by cyto-nuclear discordant phylogenetic patterns and not through the analysis of massive nuclear DNA datasets alone. This result emphasizes analytical value of sampling not only nuclear DNA data, even if massive genomic data are available, but of mitogenomic data as well. The added value of mitogenomic data allow for more complete reconstruction of the evolutionary and biogeographic history of cichlids, even if it represents only a small fraction of their genome. Interestingly, mtDNA based on nuclear DNA based tree topologies were consistent, e.g. we found divergence age estimates based on nuclear (ddRAD) data and on mtDNA data to be largely compatible, but statistical confidence intervals based on mitogenomic data were found

to be more restricted. Thus, based on comparative analyses we conclude, that divergence time estimates obtained from mitogenomic data in combination with nuclear genomic are highly informative with regard to the reconstruction of palaeo-biogeographical patterns that have shaped the success of the African Cichlid radiations, both in rivers and lakes.

Disclaimer:

Data on genetic material contained in this paper are published for non-commercial use only. Use by third parties for purposes other than non-commercial scientific research may infringe the conditions under which the genetic resources were originally accessed, and should not be undertaken without obtaining consent from the corresponding author of the paper and/or obtaining permission from the original provider of the genetic material.

Abbreviations:

BPP: Bayesian Posterior Probability; BS: Bootstrap support; EAR: East African Radiation; HPD: Highest posterior density; LM: Lake Malawi; LT: Lake Tanganyika; LV: Lake Victoria; LVRS: Lake Victoria Region Superflock; ML: Maximum likelihood; Ma: Million years; MRCA: Most recent comment ancestor, mitochondrial DNA: mtDNA,

Acknowledgments:

We want to thank F.P.D. Cotterill, A. Chocha Manda, D. Bellstedt, A. Dunz, O. Drescher, M. Grimm, J. Gottwald, H. van Heusden, A. Indermaur, A. Lamboj, T. Moritz, Z. Musilova, L. Rüber, E. Schraml, E. Swartz, E. Vreven, F. Zimmerman for providing us with tissue samples.

We are gratefully for the provision of cichlid photographs for Figure 1 by J. Geck (pictures of: *C. duponti*, *H. vanheusdeni, P. nicholsi*) and E. Schraml (pictures of: *E. cyanostictus, B. tricoti, T. otostigma*, *P. mariae*) and all members of the Inga 2013 Expedition and the Katanga 2016 Expedition. Further we want to thank D. Neumann, T. Laibl and I. Stöger for kindly assisting with the curation of vouchers and associated data at the ZSM. We thank L. Walheim and E. Paulus for her assistance in lab. A. Brachmann, G. Brinkmann and A. Nieto of the sequencing service of the Ludwig-Maximilian-University of Munich for their useful advice and support. We are grateful for the interesting discussions on the fossil record of ovalentarians and their potential usage as calibration points with B. Reichenbacher and D. Bellstedt.

Funding

This study was funded by the Volkswagen-Stiftung-Project “Exploiting the genomic record of living biota to reconstruct the landscape evolution of South Central Africa” (Az. 88 732). The funding body had no role in any activities regarding the study including design, sampling procedure, analysis, interpretation of the data and writing of the manuscript.

Availability of the data and materials:

Data will become available after peer reviewed publication of the manuscript. In the meantime data are available upon request from the authors.

Ethics approval and consent to participate

Sampling procedures (e.g. including collection of fish in the wild, handling of specimens and sacrificing) were carefully planned and followed the recommendation of [49]. Sacrificing of fish specimens complied with the German Tierschutzgesetz (TSchG) including §2 (rearing), & 7a(1)6 and no experiments concerning the EU directive 2010/63/EU notably those defined in the General Provisions of Article 1 §1 (use of animals for scientific and educational purpose) and §2 (animals used or intended for use in procedures) were performed for this study. Hence, no separate ethical approval for animal use concerning this research of this study was necessary. This study did not include any species protected by CITES, European or German law (see: http://www.wisia.de/FsetWisia1.de.html; query for all fishes and lampreys)., Collection of wild specimens for this study was done on several field trips, including sampling in the Democratic Republic of the Congo and Zambia (permits see below), while additional specimens were obtained from the ornamental fish trade. The majority of specimens were obtained prior to the legal implementation of the Nagoya Protocol (12.10.2014) and its corresponding EU Access and Benefit Sharing (ABS) regulations which are effective since the 9th November 2015. With the exception of specimens collected on fieldtrips in Zambia in 2015 or in the Democratic Republic of the Congo 2016 (permits see below). Nevertheless, we checked whether any national legislation for access and utilization of samples apply for the countries of sample origin (including specimens from the ornamental trade and their assumed/potential origin): Angola (07.05.2017), Burundi (12.10.2014), Cameroon (28.02.2017), Democratic Republic of the Congo (05.05.2015), Egypt (12.10.2014), Eritrea (not applicable), Guinea (07.10.2014), Iran (not applicable), Israel (not applicable), Malawi (26.08.2014), Nigeria (not applicable), Republic of the Congo (14.05.2015), South Africa (10.01.2013), Tanzania (19.01.2018), Tunisia (not applicable), Uganda (25.06.2014) and Zambia (20.05.2016); according to: https://www.cbd.int/abs/nagoya-protocol/signatories/default.shtml. All relevant permits for the analyzed samples in this study are archived at the Bavarian State Collection of Zoology of the SNSB (Staatliche Naturwissenschaftliche Sammlungen Bayerns).

Authors contributions

F.D.B.S. & U.K.S. designed the study. F.D.B.S. & J.D.W. prepared ddRAD libraries, molecular work associated with the sequencing of partial mitochondrial genomes were conducted by F.D.B.S., L.W. & E.P.. F.D.B.S. performed all analysis, made all figures and wrote the first draft of the manuscript. H.R.E

& J.W.N.N.V provided samples and contributed to the discussion. U.K.S. contributed to the improvement of all versions of the manuscript.

References

1. Fricke R, Eschmeyer WN, van der Laan Re: **ESCHMEYER'S CATALOG OF FISHES: GENERA, SPECIES, REFERENCES.** *(http://researcharchivecalacademyorg/research/ichthyology/catalog/fishcatmainasp) Electronic version accessed 08 May 2020* 2020.
2. Wainwright PC, Smith WL, Price SA, Tang KL, Sparks JS, Ferry LA, Kuhn KL, Eytan RI, Near TJ: **The evolution of pharyngognathy: A phylogenetic and functional appraisal of the pharyngeal jaw key innovation in labroid fishes and beyond**. *Systematic Biology* 2012, **61**(6):1001–1027.
3. McGee MD, Faircloth BC, Borstein SR, Zheng J, Darrin Hulsey C, Wainwright PC, Alfaro ME: **Replicated divergence in cichlid radiations mirrors a major vertebrate innovation**. *Proceedings of the Royal Society B: Biological Sciences* 2016, **283**(1822):20151413.
4. Kocher TD: **Adaptive evolution and explosive speciation: the cichlid fish model**. *Nature Reviews Genetics* 2004, **5**(4):288–298.
5. Powder KE, Albertson RC: **Cichlid fishes as a model to understand normal and clinical craniofacial variation**. *Developmental Biology* 2016, **415**:338–346.
6. Wagner CE, Harmon LJ, Seehausen O: **Ecological opportunity and sexual selection together predict adaptive radiation**. *Nature* 2012, **487**(7407):366–369.
7. Santos ME, Braasch I, Boileau N, Meyer BS, Sauteur L, Bohne A, Belting HG, Affolter M, Salzburger W: **The evolution of cichlid fish egg-spots is linked with a cis-regulatory change**. *Nature Communications* 2014, **5**:5149.
8. Salzburger W: **Understanding explosive diversification through cichlid fish genomics**. *Nature Reviews | Genetics* 2018, **19**:705–717.
9. Seehausen O: **Process and pattern in cichlid radiations – inferences for understanding unusually high rates of evolutionary diversification**. *New Phytologist* 2015, **207**(2 Special Issue: Evolutionary plant radiations):304–312.
10. Turner GF: **Adaptive radiation of cichlid fish**. *Current Biology* 2007, **17**(19):R827–831.
11. Ford AGP, Rüber L, Newton J, Dasmahapatra KK, Balarin JD, Bruun K, Day JJ: **Niche divergence facilitated by fine-scale ecological partitioning in a recent cichlid fish adaptive radiation**. *Evolution* 2016, **70**(12):2718-2735.
12. Schliewen UK, Tautz D, Pääbo S: **Sympatric speciation suggested by monophyly of crater lake cichlids**. *Letters to Nature* 1994, **6472**:629–632.
13. Musilova Z, Indermaur A, Bitja-Nyom AR, Omelchenko D, Klodawska M, Albergati L, Remisova K, Salzburger W: **Evolution of the visual sensory system in cichlid fishes from crater lake Barombi Mbo in Cameroon**. *Molecular Ecology* 2019, **28**:5010-5031.
14. Schwarzer J, Misof B, Ifuta SN, Schliewen UK: **Time and origin of cichlid colonization of the lower Congo rapids**. *PLoS One* 2011, **6**(7):e22380.
15. Irisarri I, Singh P, Koblmuller S, Torres-Dowdall J, Henning F, Franchini P, Fischer C, Lemmon AR, Lemmon EM, Thallinger GG *et al*: **Phylogenomics uncovers early hybridization and adaptive loci shaping the radiation of Lake Tanganyika cichlid fishes**. *Nature Communications* 2018, **9**(3159):1–12.
16. Matschiner M, Musilová Z, Barth JMI, Starostova Z, Salzburger W, Steel M, Bouckaert R: **Bayesian Node Dating based on Probabilities of Fossil Sampling Supports Trans-Atlantic Dispersal of Cichlid Fishes**. *Systematic Biology* 2016, **66**(1):3–22.
17. Friedman M, Keck BP, Dornburg A, Eytan RI, Martin CH, Hulsey CD, Wainwright PC, Near TJ: **Molecular and fossil evidence place the origin of cichlid fishes long after Gondwanan rifting**. *Proceedings of the Royal Society B: Biological Sciences* 2013, **280**(1770):20131733.

18. McMahan CD, Chakrabarty P, Sparks JS, Smith WM, Davis MP: **Temporal patterns of diversification across global cichlid biodiversity (Acanthomorpha: Cichlidae)**. *PLoS One* 2013, **8**(8):e71162.
19. Azuma Y, Kumazawa Y, Miya M, Mabuchi K, Nishida M: **Mitogenomic evaluation of the historical biogeography of cichlids toward reliable dating of teleostean divergences**. *BMC Evolutionary Biology* 2008, **8**:215.
20. Mallet J, Besansky N, Hahn MW: **How reticulated are species?** *Bioessays* 2016, **38**(2):140–149.
21. Matschiner M: **Gondwanan vicariance or trans-Atlantic dispersal of cichlid fishes: a review of the molecular evidence**. *Hydrobiologia* 2019, **832**(1):9–37.
22. Sparks JS, Smith WL: **Phylogeny and biogeography of cichlid fishes (Teleostei: Perciformes: Cichlidae)**. *Cladistics* 2004, **20**:501–517.
23. Chakrabarty P: **Cichlid biogeography: comment and review**. *Fish and Fisheries* 2004, **5**(2):97–119.
24. Murray AM: **The fossil record and biogeography of the Cichlidae (Actinopterygii: Labroidei)**. *Biological Journal of the Linnean Society* 2001, **74**(4):517–532.
25. Schedel FDB, Musilova Z, Schliewen UK: **East African cichlid lineages (Teleostei: Cichlidae) might be older than their ancient host lakes: new divergence estimates for the east African cichlid radiation**. *BMC Evolutionary Biology* 2019, **19**(94):25.
26. Svardal H, Quah FX, Malinsky M, Ngatunga BP, Miska EA, Salzburger W, Genner MJ, Turner GF, Durbin R: **Ancestral hybridisation facilitated species diversification in the Lake Malawi cichlid fish adaptive radiation**. *Molecular Biology and Evolution* 2019, **in press**.
27. Meier JI, Marques DA, Mwaiko S, Wagner CE, Excoffier L, Seehausen O: **Ancient hybridization fuels rapid cichlid fish adaptive radiations**. *Nature Communications* 2017, **8**:14363.
28. Meyer BS, Matschiner M, Salzburger W: **Disentangling incomplete lineage sorting and introgression to refine species-tree estimates for Lake Tanganyika cichlid fishes**. *Systematic Biology* 2017, **66**(4):531-550.
29. Malinsky M, Svardal H, Tyers AM, Miska EA, Genner MJ, Turner GF, Durbin R: **Whole genome sequences of Malawi cichlids reveal multiple radiations interconnected by gene flow**. *Nature Ecology & Evolution* 2018, **2**:1940-1955.
30. Schliewen UK, Stiassny ML: **Etia nguti, a new genus and species of cichlid fish from the River Mamfue, Upper Cross River basin in Cameroon, West-Central Africa.** . *Ichthyological Exploration of Freshwaters* 2003, **14**:61–71.
31. Koblmüller S, Schliewen UK, Duftner N, Sefc KM, Katongo C, Sturmbauer C: **Age and spread of the haplochromine cichlid fishes in Africa**. *Molecular Phylogenetics and Evolution* 2008, **49**(1):153–169.
32. Salzburger W, Mack T, Verheyen E, Meyer A: **Out of Tanganyika: genesis, explosive speciation, key-innovations and phylogeography of the haplochromine cichlid fishes**. *BMC Evolutionary Biology* 2005, **5**:17.
33. Genner MJ, Ngatunga BP, Mzighani S, Smith A, Turner GF: **Geographical ancestry of Lake Malawi's cichlid fish diversity**. *Biology Letters* 2015, **11**(6):20150232.
34. Meier JI, Stelkens RB, Joyce DA, Mwaiko S, Phiri N, Schliewen UK, Selz OM, Wagner CE, Katongo C, Seehausen O: **The coincidence of ecological opportunity with hybridization explains rapid adaptive radiation in Lake Mweru cichlid fishes**. *Nature Communications* 2019, **10**(1).
35. Liem KF: **Evolutionary strategies and morphological innovations: cichlid pharyngeal jaws**. *Systematic Zoology* 1973, **22**(4):425–441.
36. Maan ME, Sefc KM: **Colour variation in cichlid fish: developmental mechanisms, selective pressures and evolutionary consequences**. *Seminars in Cell & Developmental Biology* 2013, **24**(6-7):516–528.
37. Brawand D, Wagner CE, Li YI, Malinsky M, Keller I, Fan S, Simakov O, Ng AY, Lim ZW, Bezault E *et al*: **The genomic substrate for adaptive radiation in African cichlid fish**. *Nature* 2014, **513**:375–381.

38. Schwarzer J, Misof B, Schliewen UK: **Speciation within genomic networks: a case study based on Steatocranus cichlids of the lower Congo rapids**. *Journal of Evoulutionary Biology* 2012, **25**(1):138–148.
39. Schwarzer J, Swartz ER, Vreven E, Snoeks J, Cotterill FP, Misof B, Schliewen UK: **Repeated trans-watershed hybridization among haplochromine cichlids (Cichlidae) was triggered by Neogene landscape evolution**. *Proceedings of the Royal Society B: Biological Sciences* 2012, **279**(1746):4389–4398.
40. Blaxter ML: **The promise of a DNA taxonomy**. *Philos Trans R Soc Lond B Biol Sci* 2004, **359**(1444):669–679.
41. Hebert PD, Ratnasingham S, deWaard JR: **Barcoding animal life: cytochrome c oxidase subunit 1 divergences among closely related species**. *Proc Biol Sci* 2003, **270 Suppl 1**:96–99.
42. Rubinoff D, Holland BS: **Between two extremes: mitochondrial DNA is neither the panacea nor the nemesis of phylogenetic and taxonomic inference**. *Syst Biol* 2005, **54**(6):952–961.
43. Nunez JC, Oleksiak MF: **A Cost-Effective Approach to Sequence Hundreds of Complete Mitochondrial Genomes**. *PLoS One* 2016, **11**(8):e0160958.
44. Schwarzer J, Misof B, Tautz D, Schliewen UK: **The root of the East African cichlid radiations**. *BMC Evolutionary Biology* 2009, **9**(186):11.
45. Cotterill FPD, de Wit MJ: **Geoecodynamics and the Kalahari epeirogeny: linking its genomic record, tree of life and palimpsest into a unified narrative of landscape evolution**. *South African Journal of Geology* 2011, **114**(3-4):493–518.
46. Weiss JD, Cotterill FP, Schliewen UK: **Lake Tanganyika--a 'melting pot' of ancient and young cichlid lineages (Teleostei: Cichlidae)?** *PLoS One* 2015, **10**(4):e0125043.
47. Schedel FDB, Kupriyanov VMS, Katongo C, Schliewen UK: **Palaeoplex gen. nov. and Lufubuchromis gen. non, two new monotypic cichlid genera (Teleostei: Cichlidae) from northern Zambia**. *Zootaxa* 2020, **4718**(2):191–229.
48. Betancur-R R, Broughton RE, Wiley EO, Carpenter K, Lopez JA, Li C, Holcroft NI, Arcila D, Sanciangco M, Cureton Ii JC *et al*: **The tree of life and a new classification of bony fishes**. *PLoS Currents Tree of Life* 2013, **5**.
49. Neumann D: **Preservation of freshwater fishes in the field**. *Abc Taxa* 2010, **8**(2):587–632.
50. Peterson BK, Weber JN, Kay EH, Fisher HS, Hoekstra HE: **Double digest RADseq: an inexpensive method for de novo SNP discovery and genotyping in model and non-model species**. *PLoS One* 2012, **7**(5):e37135.
51. Li C, Hofreiter M, Straube N, Corrigan S, Naylor GJ: **Capturing protein-coding genes across highly divergent species**. *Biotechniques* 2013, **54**(6):321–326.
52. Kawaguchi A, Miya M, Nishida M: **Complete mitochondrial DNA sequence of Aulopus japonicas (Telostei: Aulopiformes), a basal Eurypterygii: longer DNA sequences and higher-level relationships**. *Ichthyological Research* 2001, **48**:213–223.
53. He A, Luo Y, Yang H, Liu L, Li S, Wang C: **Complete mitochondrial DNA sequences of the Nile tilapia (Oreochromis niloticus) and Blue tilapia (Oreochromis aureus): genome characterization and phylogeny applications**. *Mol Biol Rep* 2011, **38**(3):2015–2021.
54. Kearse M, Moir R, Wilson A, Stones-Havas S, Cheung M, Sturrock S, Buxton S, Cooper A, Markowitz S, Duran C *et al*: **Geneious Basic: an integrated and extendable desktop software platform for the organization and analysis of sequence data**. *Bioinformatics* 2012, **28**(12):1647–1649.
55. Martin M: **Cutadapt removes adapter sequences from high-throughput sequencing reads**. *EMBnet* 2011, **17**:1–10.
56. Catchen J, Hohenlohe PA, Bassham S, Amores A, Cresko WA: **Stacks: an analysis tool set for population genomics**. *Mol Ecol* 2013, **22**(11):3124–3140.
57. Zhang J, Kobert K, Flouri T, Stamatakis A: **PEAR: a fast and accurate Illumina Paired-End reAd mergeR**. *Bioinformatics* 2014, **30**(5):614–620.
58. Conte MA, Kocher TD: **An improved genome reference for the African cichlid, Metriaclima zebra**. *BMC Genomics* 2015, **16**:724.

59. Langmead B, Salzberg SL: **Fast gapped-read alignment with Bowtie 2**. *Nat Methods* 2012, **9**(4):357–359.
60. Li H, Handsaker B, Wysoker A, Fennell T, Ruan J, Homer N, Marth G, Abecasis G, Durbin R, Genome Project Data Processing S: **The Sequence Alignment/Map format and SAMtools**. *Bioinformatics* 2009, **25**(16):2078–2079.
61. Andrews S: **FastQC: A quality control tool for high throughput sequence data**. *Retrieved from https://wwwbioinformaticsbabrahamacuk/projects/fastqc* 2010.
62. Eaton DAR: **PyRAD: assembly of de novo RADseq loci for phylogenetic analyses**. *Bioinformatics* 2014, **30**(13):1844–1849.
63. Stamatakis A: **RAxML version 8: a tool for phylogenetic analysis and post-analysis of large phylogenies**. *Bioinformatics* 2014, **30**(9):1312-1313.
64. Miller MA, Pfeiffer W, Schwartz T: **Creating the CIPRES Science Gateway for inference of large phylogenetic trees, in: Proceedings of the Gateway Computing Environments Workshop (GCE)**. *14 Nov 2010, New Orleans, LA* 2010:1–8.
65. Nguyen LT, Schmidt HA, von Haeseler A, Minh BQ: **IQ-TREE: a fast and effective stochastic algorithm for estimating maximum-likelihood phylogenies**. *Mol Biol Evol* 2015, **32**(1):268–274.
66. Mirarab S, Reaz R, Bayzid MS, Zimmermann T, Swenson MS, Warnow T: **ASTRAL: genome-scale coalescent-based species tree estimation**. *Bioinformatics* 2014, **30**(17):i541-548.
67. Zhang C, Rabiee M, Sayyari E, Mirarab S: **ASTRAL-III: polynomial time species tree reconstruction from partially resolved gene trees**. *BMC Bioinformatics* 2018, **19**(Suppl 6):153.
68. Drummond AJ, Rambaut A: **BEAST: Bayesian evolutionary analysis by sampling trees**. *BMC Evolutionary Biology* 2007, **7**:1–214.
69. Betancur-R. R, Wiley EO, Arratia G, Acero A, Bailly N, Miya M, Lecointre G, Ortí G: **Phylogenetic classification of bony fishes**. *BMC Evolutionary Biology* 2017, **17**(162):40.
70. Alfaro ME, Faircloth BC, Harrington RC, Sorenson L, Friedman M, Thacker CE, Oliveros CH, Cerny D, Near TJ: **Explosive diversification of marine fishes at the Cretaceous-Palaeogene boundary**. *Nature Ecology & Evolution* 2018, **2**(4):688–696.
71. Dunz AR, Schliewen UK: **Molecular phylogeny and revised classification of the haplotilapiine cichlid fishes formerly referred to as "*Tilapia*"**. *Molecular Phylogenetics and Evolution* 2013, **68**(1):64–80.
72. Takahashi T, Sota T: **A robust phylogeny among major lineages of the East African cichlids**. *Molecular Phylogenetics and Evolution* 2016, **100**:234–242.
73. Murray AM: **Eocene cichlid fishes from Tazania, East Africa**. *Journal of Vertebrate Paleontology* 2000, **20**(4):651–664.
74. Altner M, Schliewen UK, Penk SBR, Reichenbacher B: ***†Tugenchromis pickfordi*, gen. et sp. nov., from the upper Miocene—a stem-group cichlid of the 'East African Radiation'**. *Journal of Vertebrate Paleontology* 2017, **2017**(e1297819):19.
75. Rasmussen C, Reichenbacher B, Lenz O, Altner M, Penk SBR, Prieto J, Brüsch D: **Middle–late Miocene palaeoenvironments, palynological data and a fossil fish Lagerstätte from the Central Kenya Rift (East Africa)**. *Geological Magazine* 2017, **154**(1):24–56.
76. Clabaut C, Salzburger W, Meyer A: **Comparative phylogenetic analyses of the adaptive radiation of Lake Tanganyika cichlid fish: nuclear sequences are less homoplasious but also less informative than mitochondrial DNA**. *Journal of Molecular Ecology* 2005, **61**(5):666–681.
77. Nishida M: **Lake Tanganyika as an evolutionary reservoir of old lineages of East African cichlid fishes: Inferences from allozyme data**. *Experientia* 1991, **47**:974–979.
78. Gaudant J, Reichenbacher B: **Hemitrichas stapfi n. sp. (Teleostei, Atherinidae) with otoliths in situ from the late Oligocene of the Mainz Basin**. *Zitteliana* 2005, **A45**:189–198.
79. Reichenbacher B: **Das brackisch-lakustrine Oligozän und Unter-Miozän im Mainzer Becken und Hanauer Becken: Fischfaunen, Paläoökologie, Biostratigraphie, Paläogeographie**. *Courier Forschungsinstitut Senckenberg* 2000, **222**:1–143.

80. Gaudant J: **Poissons des lignites papyraces oligocènes du Valle del Ponte (Province de Vicenza, Italie): Réhabilitation du genre *Hemitrichas* PETERS (Teleostei: Atherinidae)**. *Neues Jahrbuch für Geologie und Paläontologie Monatshefte* 1998, **6**:376–384.
81. Bannikov AF: **The systematic composition of the Eocene actinopterygian fish fauna from Monte Bolca, northern Italy, as known to date**. *Studi e Ricerche sui Giacimenti Terziari di Bolca* 2014, **15**:23–33.
82. Bannikov AF, Parin NV, Pinna G: ***Rhamphexocetus volans*, gen. et sp. nov.: a new beloniform fish (Beloniformes, Exocetoidei) from the Lower Eocene of Italy.** *Journal of Ichthyology* 1985, **25**:150-155.
83. Andrea Papazzoni C, Trevisani E: **Facies analysis, palaeoenvironmental reconstruction, and biostratigraphy of the "Pesciara di Bolca" (Verona, northern Italy): An early Eocene Fossil-Lagerstätte**. *Palaeogeography, Palaeoclimatology, Palaeoecology* 2006, **242**(1-2):21–35.
84. Benton MJ, Donoghue PCJ, Asher RJ, Friedman M, Near TJ, Vinther J: **Constraints on the timescale of animal evolutionary history**. *Palaeontologia Electronica* 2015, **18**:1-106.
85. Silbermann ML, McKee EH: **A summary of radiometric age determination of Tertiary volcanic rocks from Nevada and eastern California, Part II – western Nevada**. *Isochron/West,* 1972, **4**:7–28.
86. Ghedotti MJ, Davis MP: **The taxonomic placement of three fossil *Fundulus* species and the timing of divergence within the North American topminnows (Teleostei: Fundulidae)**. *Zootaxa* 2017, **4250**(6):577–586.
87. Lugaski T: ***Fundulus lariversi*, a new Miocene fossil cyprinodont fish from Nevada.** *The Wassmann Journal of Biology* 1977, **35**:203–211.
88. Ghedotti MJ, Davis MP: **Phylogeny, Classification, and Evolution of Salinity Tolerance of the North American Topminnows and Killifishes, Family Fundulidae (Teleostei: Cyprinodontiformes)**. *Fieldiana Life and Earth Sciences* 2013, **7**:1–65.
89. Guzmán AF, Stinnesbeck W, Robles-Camacho J, Polaco OJ: **El paleolago de Amatitán Jalisco: estratigrafía, sedimentologíay paleontología de la localidad tipo de *Tapatia occidentalis* (Osteichth-yes: Goodeidae)**. *Revista de la Sociedad Mexicana de Paleontología* 1998, **8**(127–134).
90. Webb SA, Graves JA, Macias-Garcia C, Magurran AE, Foighil DO, Ritchie MG: **Molecular phylogeny of the livebearing Goodeidae (Cyprinodontiformes)**. *Molecular Phylogenetics and Evolution* 2004, **30**:527–544.
91. Foster KL, Piller KR: **Disentangling the drivers of diversification in an imperiled group of freshwater fishes (Cyprinodontiformes: Goodeidae)**. *BMC Evolutionary Biology* 2018, **18**(116):12.
92. Smith ML: **The evolutionary and ecological history of the fish fauna of the Rio Lerma basin, Mexico**. *Dissertation,*. University of Michigan, Ann Arbor, MI.; 1980.
93. Alvarez J, Arriola-Longoria J: **Primer goodeido fosil procedente del Plioceno jalisciense (Pisces, Teleostomi)**. *Sociedad de Ciencias Naturales de Jalisco* 1972(6):6–15.
94. Guzmán AF: **El registro fósil de los peces mexicanos de agua dulce**. *Revista Mexicana de Biodiversidad* 2015, **86**(3):661–673.
95. Guzmán AF: **Microscopical analysis of the fossil goodeid *Tapatia occidentalis***. In: *Viviparous fishes II.* Edited by Uribe MC, Grier HJ: New Life Publications.; 2010: 75–85.
96. Rambaut A, Drummond AJ, Xie D, Baele G, Suchard MA: **Posterior Summarization in Bayesian Phylogenetics Using Tracer 1.7**. *Syst Biol* 2018, **67**(5):901–904.
97. Malinsky M, Trucchi E, Lawson DJ, Falush D: **RADpainter and fineRADstructure: Population inference from RADseq Data**. *Molecular Biology and Evolution* 2018, **35**(5):1284-1290.
98. Green RE, Krause J, Briggs AW, Maricic T, Stenzel U, Kircher M, Patterson N, Li H, Zhai W, Fritz MH-Y *et al*: **A draft sequence of the Neandertal genome**. *Science (New York, NY)* 2010, **328**(5979):710–722.
99. Durand EY, Patterson N, Reich D, Slatkin M: **Testing for ancient admixture between closely related populations**. *Molecular Biology and Evolution* 2011, **28**(8):2239-2252.

100. Malinsky M, Matschiner M, Svardal H: **Dsuite - fast D-statistics and related admixture evidence from VCF files**. 2020:634477.
101. Team RC: **R: A language and environment for statistical computing. R Foundation for Statistical Computing, Vienna, Austria. URL http://www.R-project.org/.** 2013.
102. Campanella D, Hughes LC, Unmack PJ, Bloom DD, Piller KR, Orti G: **Multi-locus fossil-calibrated phylogeny of Atheriniformes (Teleostei, Ovalentaria)**. *Mol Phylogenet Evol* 2015, **86**:8-23.
103. Musilová Z, Kalous L, Petrtyl M, Chaloupkova P: **Cichlid fishes in the Angolan headwaters region: molecular evidence of the ichthyofaunal contact between the Cuanza and Okavango-Zambezi systems**. *PLoS One* 2013, **8**(5):e65047.
104. Allio R, Donega S, Galtier N, Nabholz B: **Large Variation in the Ratio of Mitochondrial to Nuclear Mutation Rate across Animals: Implications for Genetic Diversity and the Use of Mitochondrial DNA as a Molecular Marker**. *Mol Biol Evol* 2017, **34**(11):2762–2772.
105. Dornburg A, Townsend JP, Friedman M, Near TJ: **Phylogenetic informativeness reconciles ray-finned fish molecular divergence times**. *BMC Evolutionary Biology* 2014, **14**(169):14.
106. Fulton TL, Strobeck C: **Multiple fossil calibrations, nuclear loci and mitochondrial genomes provide new insight into biogeography and divergence timing for true seals (Phocidae, Pinnipedia)**. *Journal of Biogeography* 2010, **37**(5):814–829.
107. Hugall AF, Foster R, Lee MSY: **Calibration choice, rate smoothing, and the pattern of tetrapod diversification according to the long nuclear gene RAG-1**. *Systematic Biology* 2007, **56**:543–563.
108. Zheng Y, Wiens JJ: **Do missing data influence the accuracy of divergence-time estimation with BEAST?** *Molecular Phylogenetics and Evolution* 2015, **85**(41–49).
109. Near TJ, MacGuigan DJ, Parker E, Struthers CD, Jones CD, Dornburg A: **Phylogenetic analysis of Antarctic notothenioids illuminates the utility of RADseq for resolving Cenozoic adaptive radiations**. *Molecular Phylogenetics and Evolution* 2018, **129**:268–279.
110. Eaton DAR, Spriggs EL, Park B, Donoghue MJ: **Misconceptions on missing data in RAD-seq phylogenetics with a deep-scale example from flowering plants**. *Systematic Biology* 2017, **66**(3):399–412.
111. Pauquet G, Salzburger W, Egger B: **The puzzling phylogeography of the haplochromine cichlid fish *Astatotilapia burtoni***. *Ecology and Evolution* 2018, **8**:5637–5648.
112. Schedel FDB, Katemo Manda B, Chocha Manda A, Abwe E, Vreven EJWMN, Schliewen UK: **Description of five new rheophilic Orthochromis species (Teleostei: Cichlidae) from the Upper Congo drainage in Zambia and the Democratic Republic of the Congo**. *Zootaxa* 2018, **4461**(3):301–349.
113. Leaché AD, Harris RB, Rannala B, Yang Z: **The Influence of Gene Flow on Species Tree Estimation: A Simulation Study**. *Systematic Biology* 2014, **63**(1):17–30.
114. Springer MS, Foley NM, Brady PL, Gatesy J, Murphy WJ: **Evolutionary Models for the Diversification of Placental Mammals Across the KPg Boundary**. *Front Genet* 2019, **10**:1241.
115. Joyce DA, Lunt DH, Bills R, Turner GF, Katongo C, Duftner N, Sturmbauer C, Seehausen O: **An extant cichlid fish radiation emerged in an extinct Pleistocene lake**. *Nature* 2005, **435**(7038):90–95.
116. Katongo C, Koblmüller S, Duftner N, Mumba L, Sturmbauer C: **Evolutionary history and biogeographic affinities of the serranochromine cichlids in Zambian rivers**. *Molecular Phylogenetics and Evolution* 2007, **45**(1):326–338.
117. Koblmüller S, Katongo C, Phiri H, Sturmbauer C: **Past connection of the upper reaches of a Lake Tanganyika tributary with the upper Congo drainage suggested by genetic data of riverine cichlid fishes**. *African Zoology* 2012, **47**(1):182–186.
118. Macgregor D: **History of the development of the East African Rift System: A series of interpreted maps through time**. *Journal of African Earth Sciences* 2015, **101**:232–252.
119. Bauer FU, Glasmacher UA, Ring U, Schumann A, Nagudi B: **Thermal and exhumation history of the central Rwenzori Mountains, Western Rift of the East African Rift System, Uganda**. *International Journal of Earth Sciences* 2010, **99**(7):1575–1597.

120. Lezzar KE, Tiercelin JJ, Le Turdu C, Cohen AS, Reynolds DJ, Le Gall B, C.A. S: **Control of normal fault interaction on the distribution of major Neogene sedimentary depocenters, Lake Tanganyika, East African rift**. *AAPG Bulletin* 2002, **86**(6):1027–1059.
121. Roller S, Hornung J, Hinderer M, Ssemmanda I: **Middle Miocene to Pleistocene sedimentary record of rift evolution in the southern Albert Rift (Uganda)**. *International Journal of Earth Sciences* 2010, **99**(7):1643–1661.
122. Spiegel C, Kohn BP, Belton DX, Gleadow AJW: **Morphotectonic evolution of the central Kenya rift flanks: Implications for late Cenozoic environmental change in East Africa**. *Geology* 2007, **35**(5):427.
123. Cohen AS, Soreghan MJ, Scholz CA: **Estimating the age of formation of lakes: an example from Lake Tanganyika, East African Rift system**. *Geology* 1993, **21**:511–514.
124. Roberts EM, Stevens NJ, O'Connor PM, Dirks PHGM, Gottfried MD, Clyde WC, Armstrong RA, Kemp AIS, Hemming S: **Initiation of the western branch of the East African Rift coeval with the eastern branch**. *Nature Geoscience* 2012, **5**:289–294.
125. Wilson CC, Bernatchez L: **The ghoast of hybrids past: fixation of artic charr (*Salvelinus alpinus*) mitochondrial DNA in an introgressed population of lake trout (*S. namaycush*)**. *Molecular Ecology* 1998, **7**:127–132.
126. Carson EW, Dowling TE: **Influence of hydrogeographic history and hybridization on the distribution of genetic variation in the pupfishes *Cyprinodon atrorus* and *C. bifasciatus***. *Molecular Ecology* 2006, **15**(3):667-679.
127. Nevado B, Koblmuller S, Sturmbauer C, Snoeks J, Usano-Alemany J, Verheyen E: **Complete mitochondrial DNA replacement in a Lake Tanganyika cichlid fish**. *Molecular Ecology* 2009, **18**(20):4240–4255.
128. Schedel FDB, Friel JP, Schliewen UK: ***Haplochromis vanheusdeni*, a new haplochromine cichlid species from the Great Ruaha River drainage, Rufiji basin, Tanzania (Teleostei, Perciformes, Cichlidae)**. *Spixiana* 2014, **37**(1):135–149.
129. Banyankimbona G, Vreven E, Snoeks J: **A revision of the genus *Astatoreochromis* (Teleostei, Cichlidae), East-Africa**. *European Journal of Taxonomy* 2013, **39**:1-21.
130. Kullander SO, Roberts TR: **Out of Lake Tanganyika: endemic lake fishes inhabit rapids of the Lukuga River**. *Ichthyological Exploration of Freshwaters* 2011, **22**(4):355-376.
131. De Vos L, Seegers L, Taverne L, Thys van den Audenaerde DFE: **L'ichthyofaune du bassin de la Malagarasi (Systeme du Lac Tanganyika): une synthese de la connaissance actuelle**. *Annales du Musee Royal de l'Afrique Centrale Serie 8 Sciences Zoologiques* 2001, **285**:117–152.
132. Schelly RC, Stiassny MLJ: **Revision of the Congo river *Lamprologus* Schilthuis, 1891 (Teleostei: Cichlidae), with description of two new species**. *American Museum Novitates* 2004, **3451**:40.
133. Day JJ, Santini S, Garcia-Moreno J: **Phylogenetic relationships of the Lake Tanganyika cichlid tribe Lamprologini: the story from mitochondrial DNA**. *Molecular Phylogenetics and Evolution* 2007, **45**(2):629–642.
134. Sturmbauer C, Salzburger W, Duftner N, Schelly R, Koblmuller S: **Evolutionary history of the Lake Tanganyika cichlid tribe Lamprologini (Teleostei: Perciformes) derived from mitochondrial and nuclear DNA data**. *Molecular Phylogenetics and Evolution* 2010, **57**(1):266–284.

Supplementary Material

Figure S1. ML-based phylogenic hypothesis (RAxML) based on the "AC mitochondrial dataset" including ten protein coding mitochondrial genes (ND1, ND2, COX1, COX2, ATP8, ATP6, COX3, ND3,

ND4L, ND4) and 464 specimens with representatives of almost all major ovalentarian lineages with focus on the family Cichlidae (N = 330). Numbers at nodes refer to bootstrap-values.

Figure S2. ML-based phylogenic hypothesis (RAxML) based on the "Austrotilapiine mtDNA dataset" including ten protein coding mitochondrial genes (ND1, ND2, COX1, COX2, ATP8, ATP6, COX3, ND3, ND4L, ND4) and 103 specimens. Numbers at nodes refer to bootstrap-values.

Figure S3. ML-based phylogenic hypothesis (RAxML) based on the "Austrotilapiine ddRAD Set" including a concatenated alignment of 610 ddRAD loci (113,578 bp) for 103 individuals. Numbers at nodes refer to bootstrap-values. See Table S1 for specimen information of the corresponding tip labels (ddRAD IDs).

Figure S4. ML-based phylogenic hypothesis (RAxML) based on the "Introgression-test ddRAD Set" including a concatenated alignment of 14,750 ddRAD loci (2,751,967 bp) for 60 individuals. Numbers at nodes refer to bootstrap-values. See Table S1 for specimen information of the corresponding tip labels (ddRAD IDs).

Figure S5. Coalescent species tree (ASTRAL) based on the "Full ddRAD Set" and 4000 individual gene (ddRAD loci) trees. Numbers at nodes are support values from local posterior probabilities for the main topology (pp1) and the two alternative topologies (pp2 & pp3). See Table S1 for specimen information of the corresponding tip labels (ddRAD IDs).

Figure S6. Coalescent species tree (ASTRAL) based on the "Austrotilapiine ddRAD Set" and 610 individual gene (ddRAD loci) trees. Numbers at nodes are support values from local posterior probabilities for the main topology (pp1) and the two alternative topologies (pp2 & pp3). See Table S1 for specimen information of the corresponding tip labels (ddRAD IDs).

Figure S7. Time tree (BEAST, relaxed normal molecular clock) based on the "AC mitochondrial dataset" (including in total 330 cichlid species, including several undescribed species, and 134 taxa representing the remaining major ovalentarian lineages). For detailed information on constrained nodes and applied calibration scheme please refer to Table 1. Node bars indicate 95% HPD intervals of divergence events. Numbers at nodes refer to Bayesian Posterior Probabilities

Figure S8. Time tree (BEAST, relaxed normal molecular clock) based on the "Austrotilapiine ddRAD Set" (including 97 taxa). For detailed information on constrained nodes and applied calibration scheme please refer to Table 1. Node bars indicate 95% HPD intervals of divergence events. Numbers at nodes refer to Bayesian Posterior Probabilities. See Table S1 for specimen information of the corresponding tip labels (ddRAD IDs).

Figure S9. Time tree (BEAST, relaxed normal molecular clock) based on the “Austrotilapiine mtDNA dataset” (including 97 taxa). For detailed information on constrained nodes and applied calibration scheme please refer to Table 1. Node bars indicate 95% HPD intervals of divergence events. Numbers at nodes refer to Bayesian Posterior Probabilities.

Supplementary Tables

Table S1. Overview of individuals genotyped using ddRAD sequencing, information on taxonomy, repository numbers of specimens, availability of corresponding partial mitochondrial genomes and where applicable origin of samples are provided.

Table S2. Overview of cichlid specimens for which partial or complete mitochondrial genomes were sequenced for this study, information on taxonomy, repository numbers of specimens, and where applicable origin of samples are provided.

Table S3. Overview of mitochondrial genome data retrieved from GenBank with corresponding information on specimen metadata, taxonomy and GenBank accession number.

Table S4. Overview of input Reads for PyRAD and recovered loci per sample for the various PyRAD analysis conducted.

Table S5. Overview of D-statistics and corresponding Bonferroni-corrected p-values for all possible ABBA-BABA species trios tested.

Discussion

The underexplored riverine cichlid diversity of Southern-Central Africa

Traditionally, Africa is subdivided into ten major ichthyological provinces of which one, the Congo Basin, the second largest drainage basin of the world, stands out by its high species richness (Darwall et al. 2011; Roberts 1975; Runge 2007). The Congo basin can further be divided into several major sections,: (i) the Upper Congo-Lualaba from the Congo headwaters in Zambia to the Boyoma falls, (ii) the middle Congo from the Boyoma falls to Pool Malebo), (iii) the lower Congo from Pool Malebo to the river mouth, and (iv) Lake Tanganyika and its tributaries. Each section harbors its own characteristic fauna, possibly best exemplified by the distinctive and almost fully endemic ichthyofauna of Lake Tanganyika (Brooks et al. 2011; Darwall et al. 2011; Runge 2007). In addition to these larger sections, more fine scaled freshwater ecoregions have been recognized (Abell et al. 2008; Thieme et al. 2005), e.g., and among others, the "Bangweulu-Mweru ecoregion" and the "Upper Lualaba ecoregion" which are both within the northern boundaries of the loosely defined Katanga-Chabeshi region (sensu Cotterill 2005). The exploration of the ichthyological diversity of the Congo basin had started already in the early 19th century, and a first inventory of the ichthyofauna of the Congo basin became first available with the extensive work by Boulenger (1901b). Since then, knowledge on fish diversity is continuously increasing and approximately 1250 valid species have been described from the Congo basin today (Darwall et al. 2011). However, most of the important historical ichthyological collections available are restricted to the main channel of the Congo River and its major tributaries, mostly in proximity of major cities; thus. large areas of the Congo basin have remained drastically underexplored (Brooks et al. 2011). Indeed, recent regional surveys of the AfricaMuseum in Tervuren (Belgium) focusing on comparatively small river systems across the Congo basin as e.g. the Inkisi, Lowa and Itimbiri rivers have led to the discovery of numerous new species (Decru et al. 2017; Kisekelwa et al. 2020; Wamuini Lunkayilakio et al. 2010).

Further, the ichthyological fauna of the upper Congo-Lualaba system appears to be only insufficiently studied although a high degree of endemism was reported for this area. For example, Poll (1976) reported 116 species from Lake Upemba of the "Upper Lualaba ecoregion", whereas a more recent inventory found 193 species to be present in the area of Upemba National Park (Katemo Manda et al. 2013). Likewise, Thieme et al. (2005) indicated

approximately 100 species to be present in the "Bangweulu-Mweru ecoregion" while the study of van Steenberge et al. (2014) reported 135 species just from the Luapula-Mweru area, a subregion of the "Bangweulu-Mweru ecoregion". The most specious families of the Katanga-Chabeshi region include the Cyprinidae, Mormyridae, Mochokidae, Alestidae and, last but not least, Cichlidae (Thieme et al. 2005; van Steenberge et al. 2014; Vreven et al. 2015). The cichlids of the region are represented by six major cichlid lineages: Tilapiini, Oreochromini, Tylochromini, Coptodonini, the 'extended *Pseudocrenilabrus*-group' and the 'extended serranochromines' (the composition of the latter two are outlined in the introduction).

In the course of this thesis seven new cichlid species and two new genera, either related to 'extended serranochromines' or to the 'extended *Pseudocrenilabrus*-group', have been described form various freshwater ecoregions associated with the Katanga-Chambeshi region (see e.g. **chapter 2** and **3**). Further, numerous other putative new cichlid species (see Figure 3) have been collected during various field expeditions across Northern Zambia and the former Katanga province (DRC), focusing on the riverine ichthyofauna of this vast region. Candidate species have been preliminary identified based on their distinctive appearance, e.g. coloration or general morphology. These could not be assigned to any valid species, because a detailed morphological examination for most of the putative species is still pending. However, molecular data, including mitochondrial genome data as well as ddRAD data, for some of the candidate species have been generated for the studies presented in **chapter 4** and **5**. These molecular data suggest the presence of at least 26 new, distinct genetic lineages in the focal area. Those putative species either belong to the genera *Pseudocrenilabrus* (at least seven species), to *Serranochromis* Regan 1920 (at least four species), to *Telmatochromis* Boulenger 1898 (one species), to *Tilapia* (four species) and to two putative new genera related to the 'extended serranochromines'(three species in total). Further, several putative species belonging to different lineages of the polyphyletic genus *Orthochromis* were identified: one species of the 'Katanga-*Orthochromis*', one species of the '*Orthochromis torrenticola* species complex' and at least four species of the 'Northern-Zambian-*Orthochromis*'. Although future systematic research will decide about the taxonomic status of these candidate species, it became clear that many more cichlid species are present in the northern part of the Katanga-Chambeshi region than previously reported. Altogether, about 40 valid cichlid species are known to occur in the "Bangweulu-Mweru ecoregion", the "Upper Lualaba ecoregion" and the southern part of the "Lake Tanganyika ecoregion" but excluding the cichlid species endemic to Lake Tanganyika (Balon and Stewart 1983; Banister and Bailey 1979; Jackson 1961; Katongo et al. 2017; Poll

1976; Schedel et al. 2018; Schedel et al. 2020; van Steenberge et al. 2014; Vreven et al. 2015). This means that more than one third of the cichlid diversity of the focal area remains undescribed, even when not taking into account the numerous putative species recently reported from Lake Mweru (Katongo et al. 2006; Meier et al. 2019).

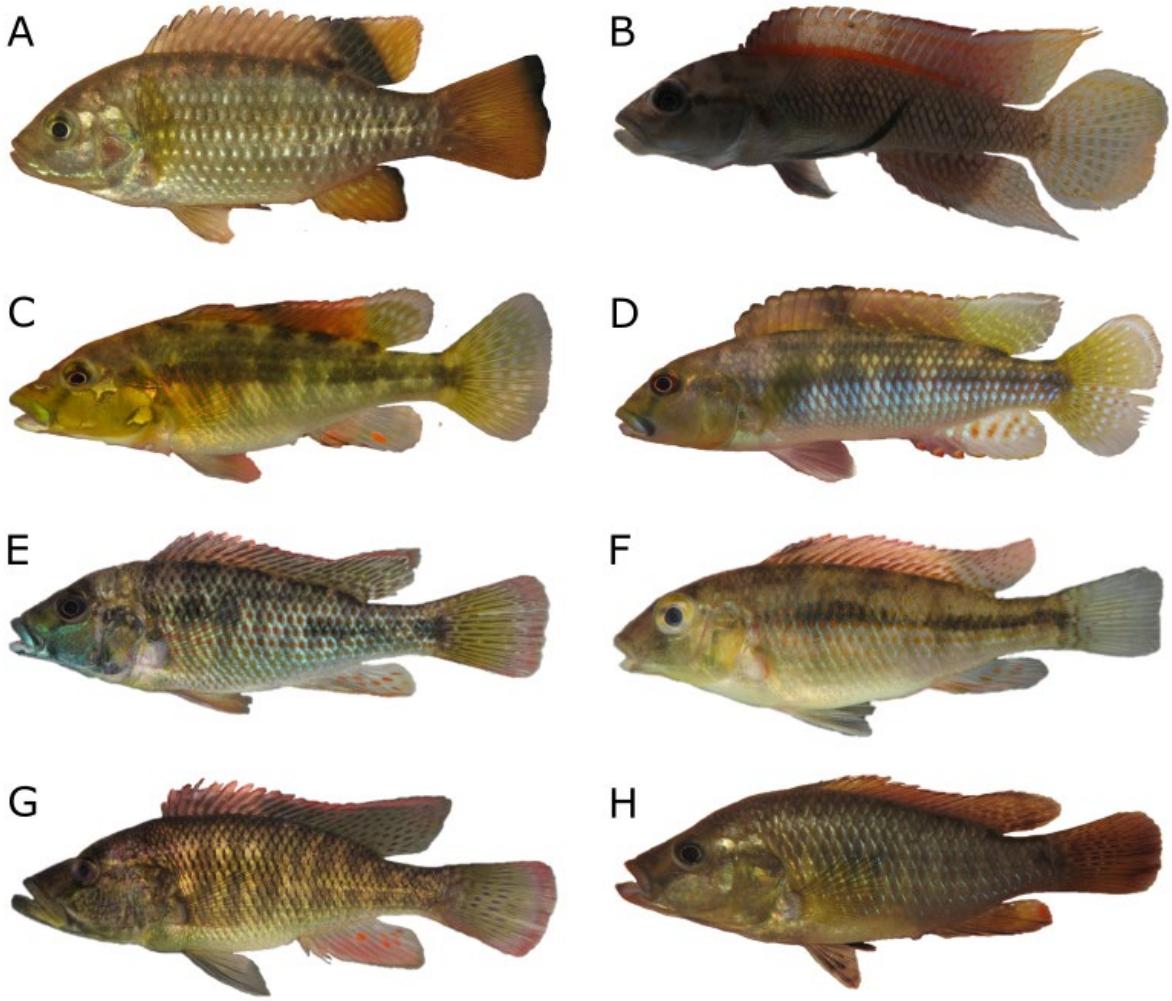

Figure 3: Representative overview of several undescribed species from the northern part of the Katanga-Chambeshi region and the Upper Lomami River. A. *Tilapia* sp. Upper Kalungwishi (Tribe: Tilapiini; photo: F. Schedel); **B.** *Telmatochromis* sp. Lufubu (Tribe: Lamprologini; photo F. Schedel); **C.** *Orthochromis* sp. Lomami (Tribe: Haplochromini, 'extended serranochromines'; photo: A. Chocha Manda); **D.** *Orthochromis* sp. aff. *torrenticola* (Tribe: Haplochromini, 'extended serranochromines'; photo: Katanga 2016 Expedition); **E.** 'Haplochromine genus sp. Lubudi blue cheek' (Tribe: Haplochromini, 'extended serranochromines'; photo: Katanga 2016 Expedition); **F.** 'Haplochromine genus sp. Lubudi tropheuslike' (Tribe: Haplochromini, 'extended serranochromines'; photo Katanga 2016 Expedition); **G.** *Serranochromis* sp. Mukuleshi (Tribe: Haplochromini, 'extended serranochromines'; photo Katanga 2016

Expedition); **H**. *Pseudocrenilabrus* sp. Upper Kalungwishi (Tribe Haplochromini, 'extended *Pseudocrenilabrus*-group'; photo: F. Schedel).

Most of the putative species reported here appear to have narrow distribution ranges and some might even be restricted to only a small section of a particular river. However, it should be kept in mind that the sample efforts made in the scope of this study focused on major knickpoints (waterfalls) of the focal area and hence our knowledge on the distribution ranges of these species remains highly incomplete. Yet, some river systems within the study area revealed to harbor a comparatively rich ichthyofauna with high degrees of endemism.

One example is the third largest tributary of Lake Tanganyika, the Lufubu River, located in the southern part of the "Lake Tanganyika ecoregion", which stands out by its distinctive cichlid fauna. The course of the Lufubu River is interrupted by several major rapids and waterfalls which are assumed to represent natural barriers to the upstream movement of fish (Koblmüller et al. 2012). Indeed, from the uppermost reaches of the Lufubu four cichlid species are currently known, three of which them still undescribed, but all apparently endemic to this river section. The recently described monotypic genus *Lufubuchromis* with its species *L. relictus* is assumed to be confined to this river section (see **chapter 3**). The fish community of the lower reaches (excluding the river mouth) has not been studied well either, but at least five cichlid species appear to be present (Indermaur 2014; Theis et al. 2014; personal observation, F.D.B. Schedel), of which *O. indermauri* (described in **chapter 2)** and *Telmatochromis* sp. Lufubu are currently known from only a single location in this river section (Schedel et al. 2018).

Another exceptional river system in respect to its cichlid fauna is that of the Lubudi River and its tributaries, e.g. the Mukuleshi River, located in the "Upper Lualaba ecoregion". Explorative collections to the Lubudi and the Mukuleshi rivers conducted in the framework of this study and by previous field trips of the Mbisa Congo Project, suggest the presence of at least eight cichlid species in the Lubudi system. Only a single recently described cichlid species can be unequivocally assigned to the species level: *Orthochromis gecki* (see **chapter 2**). Further, two species tentatively identified as *Serranochromis cf. robustus* (Günther 1864) and *Serranochromis cf. thumbergi* (Castelnau 1861) were recorded from the Mukuleshi River (a tributary of the Lubudi River), but thorough taxonomic investigations for these taxa are still pending. The remaining five species are undoubtedly undescribed. Notably, two of these putative species, here referred to as 'Haplochromine genus sp. Lubudi tropheuslike' and 'Haplochromine genus sp. Lubudi blue cheek', cannot be assigned to any described cichlid genus based on preliminary morphological investigations. Interestingly, these two were found

to represent two ancient lineages within the 'extended serranochromines' (see figure 1 in **chapter 5**). Interestingly, phylogenetic analyses based on ten protein coding mitochondrial genes revealed that another undescribed species (referred as 'Haplochromine genus sp. Lomami') from the Lomami River, located in the "Upper Congo ecoregion", is the sister species of the 'Haplochromine genus sp. Lubudi tropheuslike' suggesting a past connection between the part of the Lualaba-drainage to which the Lubudi River system belongs and the upper Lomami River drainage. A past connection between those two areas is further supported by the observed sister group relationship of *O. gecki* and the still undescribed species *Orthochromis* sp. Lomami as well as between *Serranochromis* sp. Mukuleshi and *Serranochromis* sp. Kisese from the Lomami River. Taken together, the high percentage of undescribed and potentially endemic cichlid species in the Lubudi system and their close relationship with species from the Lomami exemplifies our drastically limited knowledge on the ichthyological diversity of selected regions of the upper Congo-Lualaba systems.

The list of ichthyologically underexplored river systems of the focal region could be easily enlarged, and even comparatively well studied river systems such as the Lufira River (Banister and Bailey 1979; Poll 1976) yielded several undescribed cichlid species, thus highlighting the need of further systematic research in the region. This would be especially important for establishing adequate conservation priorities for diversity hotspots, as. e.g., the Lufubu River; or, more in general, the aquatic ecosystems of the Katanga-Chambeshi region, which are threatened by human activities including damming, deforestation, mining, pollution and unsustainable fishing methods (Brooks et al. 2011; Schedel et al. 2018; Thieme et al. 2005).

Spatio-temporal insights in the evolutionary history of rheophilic African cichlids help to reconstruct the landscape evolution of Southern-Central Africa

The concept of geoecodynamics aims to exploit the genomic record of living organisms to reconstruct the tempo and mode of geomorphological processes, e.g. tectonic events altering the landscape structure such as the formation of knickpoints. It is based on the assumption that evolutionary histories of organisms are tightly interlinked with these of landscapes they are associated with, which are reflected by changes in the nucleotide sequences, and hence can be dated using molecular clocks (Cotterill and de Wit 2011). During the course of this thesis, two highly promising cichlid lineages for spatio-temporal reconstruction of the landscape evolution

have been identified, using a geoecodynamical approach, which are critically discussed in the following paragraphs.

The '*Orthochromis torrenticola* species complex'

The first cichlid lineage with genomic signatures possibly mirroring landscape evolution in the region, i.e. that of knickpoint formation and of the associated interruption of gene flow, is the '*Orthochromis torrenticola* species complex' (see Figure 4). The species complex represents a distinct lineage within the 'extended serranochromines' and is only known from the Lufira drainage system, a major tributary of the upper Lualaba River. The course of the Lufira River is interrupted by two major knickpoints: the Cornet falls at Mwandingusha which were originally 113 meter high before the falls have been damned in 1925 for the purpose of hydropower generation; and, further downstream, the Kyubo falls with an approximate height of 60 meters (Damas 1961; Kambembo 2018). The latter forms a natural barrier for the upstream movement of fish and separates the species *O. torrenticola,* which was described from above the Kyubo falls, from its still undescribed sister species referred here as *Orthochromis* sp. aff. *torrenticola* (see Figure 1, **chapter 5**) found below the Kyubo falls. Both species can be readily distinguished from each another by their characteristic coloration, e.g. *O. torrenticola* has a yellow belly and metallic yellowish flank scales in contrast to *O*. sp. aff. *torrenticola* which has a white to light reddish belly and metallic bluish flank scales (see Figure 4). They differ further from each other by several morphological and meristic characters, e.g. number of abdominal vertebrae, and the formal description will follow after the final examination of additional *O. torrenticola* populations occurring upstream of the Kyubo falls, for example in the Lofoi River (Schedel et al. in prep).

The maximum likelihood (ML) analyses (see **chapter 5**) based on nuclear (ddRAD) data and mitochondrial data (10 protein coding genes) recovered the monophyly of the '*Orthochromis torrenticola* species complex' with a high bootstrap support (BS: 100). The comparative molecular clock analyses contrasting mitochondrial and ddRAD-based analyses (see **chapter 5**) dated the divergence of the MRCA of the '*Orthochromis torrenticola* species complex' either to Pliocene-Pleistocene age (mean age 2.5 Mya; 95 % HPD: 0.5–5.2 Mya) based on nuclear (ddRAD) data or to Late Miocene-Pliocene age (mean age 4.1 Mya; 95 % HPD: 2.4–6.0 Mya) based on mitochondrial data. As outlined in **chapter 5**, the 95 % HPD intervals of the divergence time estimates of both molecular clock analyses widely overlap, but divergence time

estimates derived from the ddRAD dataset with substantially wider 95 % HPD intervals. In addition, the genomic tests of hybridization based on thousands of ddRAD loci (D-statistics, see **chapter 5**) revealed strong signatures of ancient hybridization between the 'extended *Pseudocrenilabrus* group' and the 'extended serranochromines' to which the '*Orthochromis torrenticola* species complex' belongs. Notably, the possibility that specimens of *O. torrenticola* dropped and might continue to drop down the Kyubo falls and survive cannot be ruled out; this has been shown for other cichlid species that even surivive a drop of (~ 220 m down the impressive Kalambo falls (Pauquet et al. 2018). This option leaves the possibility that fallen *O. torrenticola* individuals have interbred with individuals of the *O.* sp. aff. *torrenticola;* this would hypothetically allow for unidirectional secondary gene flow between the two anciently diverged sister species. However, the D-statistics did not reveal any significant signals of introgression between the species (Figure 4, **chapter 5**), but for each species one specimen only have been tested so far. Hybridization might compromise divergence time estimates which can result in both younger or older age estimates than speciation ages (Leaché et al. 2014; Springer et al. 2019). Therefore, the mitochondrial divergence times might reflect more accurate node age estimates for the onset of the divergence of the '*Orthochromis torrenticola* species complex', as cichlid mitochondrial genomes are predominantly maternally inherited, and they are only marginally affected by recombination, if at all (Hebert et al. 2003; Saccone et al. 1999).

It is not unlikely that the seismic activity associated with ,e.g., the genesis of the Upemba fault system has led to the initial formation of the Kyubo knickpoint, and that that this knickpoint formation has interrupted gene flow and thus initiated initial divergence between upstream and downstream members of the two proto-'*Orthochromis torrenticola* species complex'. If this assumption is correct, the node age estimates reported above for this vicariant scenario would also provide a first genome-derived age Pliocene-Late Miocene date estimate for the geological formation of Kyubo knickpoint.

Alternatively, it would have been tempting to use the Kyubo knickpoint system as a geochronological calibration point for the onset of divergence of the '*Orthochromis torrenticola* species complex' in molecular clock analyses. If available, this calibration point might significantly improve the spatio-temporal reconstruction of the EAR and especially of the Haplochromini, for which no unambiguously reliable calibration points are available until today. Undoubtedly, the age of the extant Kyubo falls is much younger than the formative event that created the knickpoint system as waterfalls are the result geomorphologically highly

dynamic processes. Knickpoint formation itself might be the result of variable rock resistance, base level changes or tectonic deformation, whereas the knickpoint retreatment rate, i.e. the rate waterfalls "migrate" upstream a riverbed through time due to erosion is influenced by a combination of various factors including the size of the catchment area, climatic conditions, elevation, underlying lithology and geological morphology, erosion processes and tectonic activity (Bishop et al. 2005; Brocklehurst 2010; Howard et al. 1994; Loget and Van den Driessche 2009; Whipple et al. 2000; Whipple and Tucker 1999). Unfortunately, these factors considerably complicate the dating of knickpoints, e.g. by cosmogenic nuclide dating, and hence the dating of knickpoint system itself (Olivotos et al. in review). Unfortunately, no geological estimates for the age of the Kyubo knickpoint system have become available so far, leaving the great potential of the Kyubo system as cichlid calibration point untapped for the time being.

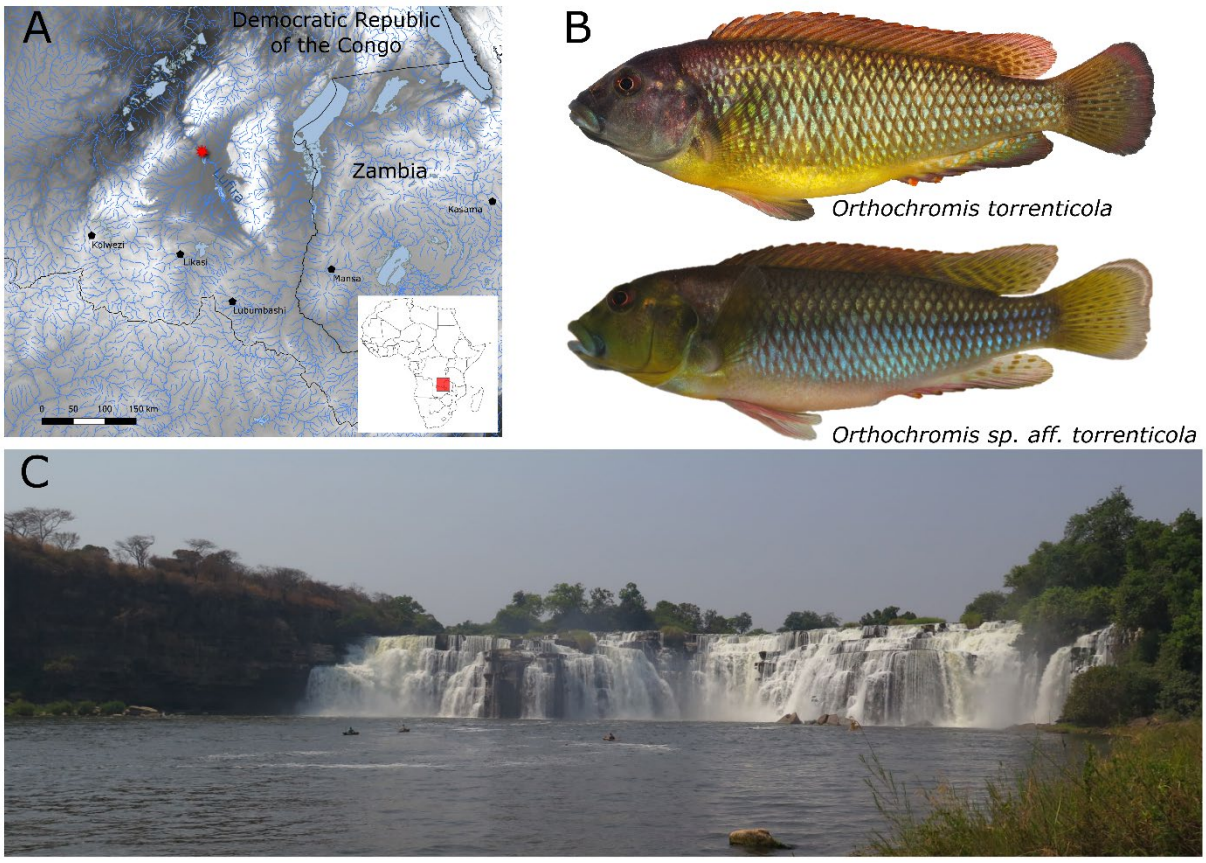

Figure 4: Overview of the '*Orthochromis torrenticola* species complex' and its environment. **A.** Map of Northern Zambia and south-eastern DRC, with indication of the position of the Kyubo falls on the Lufira River (red star); Shapefiles were obtained from DIVA-GIS (http://www.diva-gis.org/Data) **B.** Representative specimens of the two species of '*Orthochromis torrenticola* species complex' occurring above the Kyubo falls (*O. torrenticola*;

photo: Katanga 2016 Expedition) and below the Kyubo falls (*O*. sp. aff. *torrenticola*; photo: Katanga 2016 Expedition) **C.** View on the Kyubo falls on the Lufira River (photo: Katanga 2016 Expedition).

The '*Orthochromis kalungwishiensis* species complex'

The '*Orthochromis kalungwishiensis* species complex' represents the second newly recognized cichlid lineage with an evolutionary history apparently heavily shaped by the dynamic landscape evolution which occurred in the restricted distribution range of that lineage. Together with its sister lineage referred here to as '*Orthochromis luongoensis* species complex' they form a clade known as 'Northern-Zambia-*Orthochromis*' (Weiss et al. 2015) within the 'extended *Pseudocrenilabrus*-group' (see Figure 1, **chapter 5**). At least five distinct lineages can be recognized within '*Orthochromis kalungwishiensis* species complex' (see Figure 5) which are confined to the Kalungwishi River and its tributaries as well as to the rocky shores of Lake Mweru as it has been recently documented by Meier (2019). The study of Meier (2019) reported two color morphs from Lake Mweru for a species referred as *Orthochromis* sp. "red-cheek" which might be conspecific with the species referred herein as *Orthochromis* cf. *kalungwishiensis* "Rainbow", a species recently imported from Lake Mweru for the ornamental fish trade (Lucanus 2017). However, no morphological nor genetical comparative analyses including specimens of both putative species has been conducted so far.[1]

The course of the Kalungwishi River, a major tributary of Lake Mweru, is interrupted by several major knickpoints (Flügel 2014). The most important knickpoints are lined up in a series of three large waterfalls, the uppermost being the impressive Lumangwe falls (~ 40 meters high), followed a few kilometers downstream by the Kabwelume falls (~ 35 meters high), and about 35 km further downstream and approx. 43 km upstream of the Kalungwishi estuary into Lake Mweru by the Kundabikwa falls (~ 25 meters high) (Flügel 2014; Olivotos et al. in review). Analogous to the divergence for the '*Orthochromis torrenticola* species complex' above and below the Kyubo falls, the waterfalls on the Kalungwishi River appear to constrain fish

[1] In this context it must be noted that the clade 1 '*Orthochromis kalungwishiensis* complex' of Meier et al. (2019) appears to include only taxa closely related to *O. luongoensis*, i.e. *O. katumbii* and *O. mporokoso*). In addition, the specimen identified as *O. kalungwishiensis* in this study appears rather to represent a member of the yet undescribed species *O*. cf. *luongoensis* "Kalungwishi", based on the appearance of the depicted specimens and on the reported mitochondrial relationships. In contrast, the specimens depicted for in the clade 4 '*O*. sp. "Kalungwishi" + *O*. sp. "red-cheek" of Meier et al. (2019) clearly resemble in their appearance that of taxa of the '*Orthochromis kalungwishiensis* species complex'.

dispersal. Other fish species, as, e.g., the characiform *Bryconaethiops boulengeri* Pellegrin, 1900 (Family Alestidae) are widely distributed in the Congo basin, but have recorded only from below the Kundabikwa falls and not further upstream (Zambia field trip 2015, personal observation: F.D.B. Schedel). Likewise, the distribution of several different candidate species of the '*Orthochromis kalungwishiensis* species complex' seem to be constrained by the waterfalls to certain river sections, e.g. *O*. cf. *kalungwishiensis* "Lumangwe" is only found above the Lumangwe falls, and *O.* cf. *kalungwishiensis* "Rainbow" appears to be confined to the shores of Lake Mweru. However, some river sections, e.g. the section between Kundabikwa falls and Lumangwe falls (including Kabwelume falls) are home to at least three distinct lineages of 'Northern-Zambian-*Orthochromis*' in sympatry: *O. kalungwishiensis* described from above the Kundabikwa falls, *O. kalungwishiensis* "Red" (the "Red" refers to the reddish seam of the dorsal and caudal fin) and *O*. cf. *luongoensis* "Kalungwishi".

In comparison to the vicariant sister species of the '*Orthochromis torrenticola* species complex' the putative species of the '*Orthochromis kalungwishiensis* species complex' are less readily distinguished from each another, although subtle morphological (e.g. head shape) and clear coloration differences are present (see Figure 5). The monophyly of the '*Orthochromis kalungwishiensis* species complex' is statistically well supported by the phylogenetic ML analyses either based on the nuclear (ddRAD) or on the mitochondrial dataset (BS: > 91; see Figure 1 & Figure S1, **chapter 5**). The inter-relationships between the lineages of the '*Orthochromis kalungwishiensis* species complex' however are, by far, more complex as those of the '*Orthochromis torrenticola* species complex'. For example, they are characterized by cyto-nuclear discordances: the ML-analysis based nuclear data recovered *O.* cf. *kalungwishiensis* "Itabu" as the sister group of the all remaining lineages of the species complex whereas the one based on mitochondrial data recovered it as the sister group to a clade encompassing only *O*. cf. *kalungwishiensis* "Rainbow" and *O*. *kalungwishiensis* (see Figure 1 & Figure S1, see **chapter 5**). Additional ancient hybridization events between the 'Northern-Zambian-*Orthochromis*' and the recently described genera *Lufubuchromis* and *Palaeoplex* have been detected in the study of Meier (2019) as well as by the D-statistics conducted in **chapter 5**. In addition, hybridization between the sympatric members of the '*Orthochromis kalungwishiensis* species complex' and *O*. cf. *luongoensis* "Kalungwishi" are likely based on preliminary analyses, but this has still to be extensively tested. Therefore, divergence time estimates obtained for the '*Orthochromis kalungwishiensis* species complex' in **chapter 5**, which suggest an Early Pleistocene-Pliocene age (mean age: 2.2 Mya; 95 % HPD: 0.5–4.6 Mya)

for the MRCA of the species complex based on nuclear (ddRAD data) and Pleistocene age (mean age: 1.1 Mya; 95 % HPD: 0.6–1.6 Mya) based on mitochondrial data, should be scrutinized carefully and taking into account the complexity of multiple ancient hybridization events.

This might be even more important as recently published geological evidence suggest that the palaeo-lake levels of Lake Mweru were much higher during the Pleistocene, potentially reaching an elevation of 1200 meter asl. Such a high lake level would have covered a substantially larger area than present day Lake Mweru (Olivotos et al. in review). The same study suggested that the Lumangwe falls were located at the eastern-shore line of the palaeo-Lake Mweru, and that the knickpoint systems of the Kundabikwa falls as well as of the Kabwelume falls had been flooded by high lake levels of palaeo-Lake Mweru. The study is based on relative ^{10}Be and ^{26}Al age estimates for burial ages of rock samples collected from the knickpoint sites. Interestingly, the estimated burial age for rock samples of the Kundabikwa falls is > 1 Mya, which suggests that Lake Mweru must have existed for more than a million year and most likely even much longer (~ 2 Mya) as suggest by Olivotos et al. (in review). However, as for the other great Lakes of East Africa it is hypothesized that Palaeo-Lake Mweru experienced severe lake level fluctuations over this period (Olivotos et al. in review). The formation of the Lake Mweru was most likely initialized through the southward propagation of the western branch of the East African Rift system roughly 2 to 4 Mya (Chorowicz 2005; Olivotos et al. in review; Tiercelin and Lezzar 2002). The knickpoints of Kundabikwa and Lumangwe themselves had likely been formed well before the aforementioned lake-level rise; they are most likely the result of the propagation of western branch of the African rift system as is the Lake Mweru graben (Olivotos et al. in review). Hence both the estimated mean ages for the onset of the divergence of the '*Orthochromis kalungwishiensis* species complex' (see above: 1.1 to 2.2 Mya) tentatively suggest that the clade diversified before the lake level rise of Lake Mweru approx. 1 Mya, and that older divergence ages of within that lineage relate to pre-burial knickpoint formation events. However, it would be premature at this point to correlate the divergence of the different lineage of the species complex to those ancient formation, because both, the complex and not fully resolved phylogenetic relationships within the '*Orthochromis kalungwishiensis* species complex', and the complicated geological history of the knickpoints themselves are not yet fully understood. The burial of the Kundabikwa and Kabwelume falls by the upper lake level of palaeo-Lake Mweru for example might have eradicated potential signals in the genomic record of the '*Orthochromis kalungwishiensis*

species complex', even if they had evolved as a consequence of the formation of these knickpoints. In contrast, the knickpoint system of the Lumangwe falls most likely was not affected by the lake level rise and thus qualifies as potential calibration point for the '*Orthochromis kalungwishiensis* species complex' in the future studies, at least once the evolutionary history of this lineage is better understood.

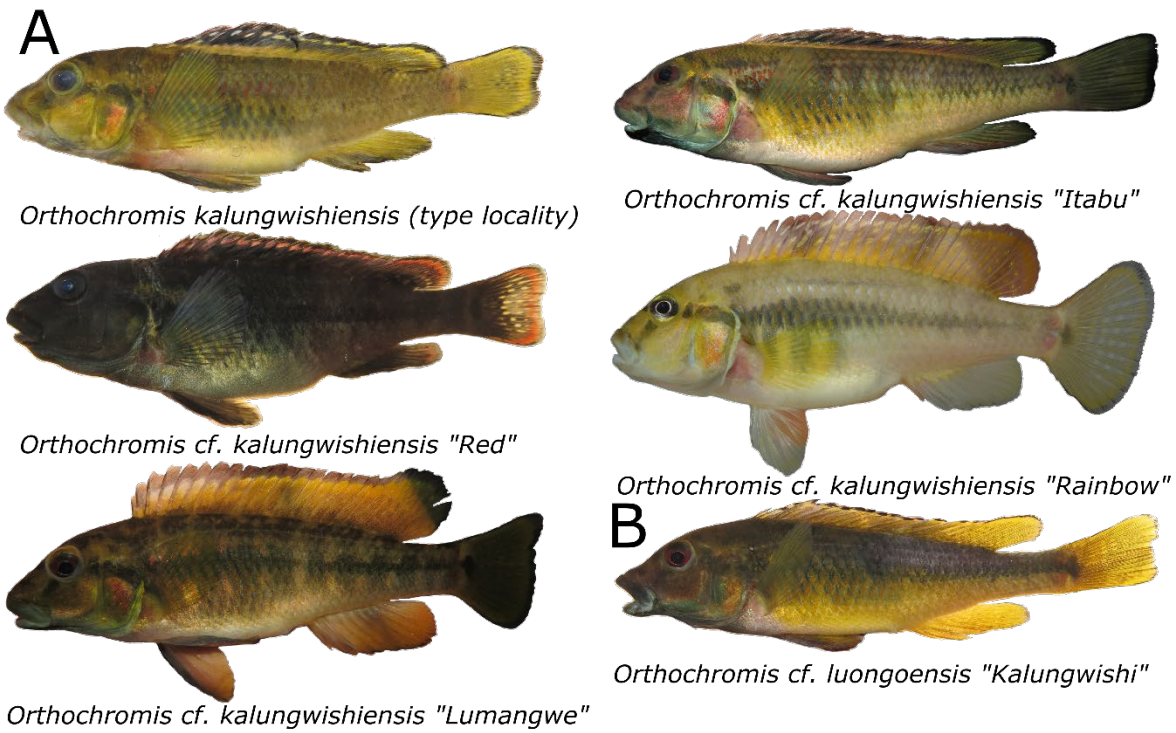
A
Orthochromis kalungwishiensis (type locality)
Orthochromis cf. kalungwishiensis "Itabu"
Orthochromis cf. kalungwishiensis "Red"
Orthochromis cf. kalungwishiensis "Rainbow"
B
Orthochromis cf. luongoensis "Kalungwishi"
Orthochromis cf. kalungwishiensis "Lumangwe"

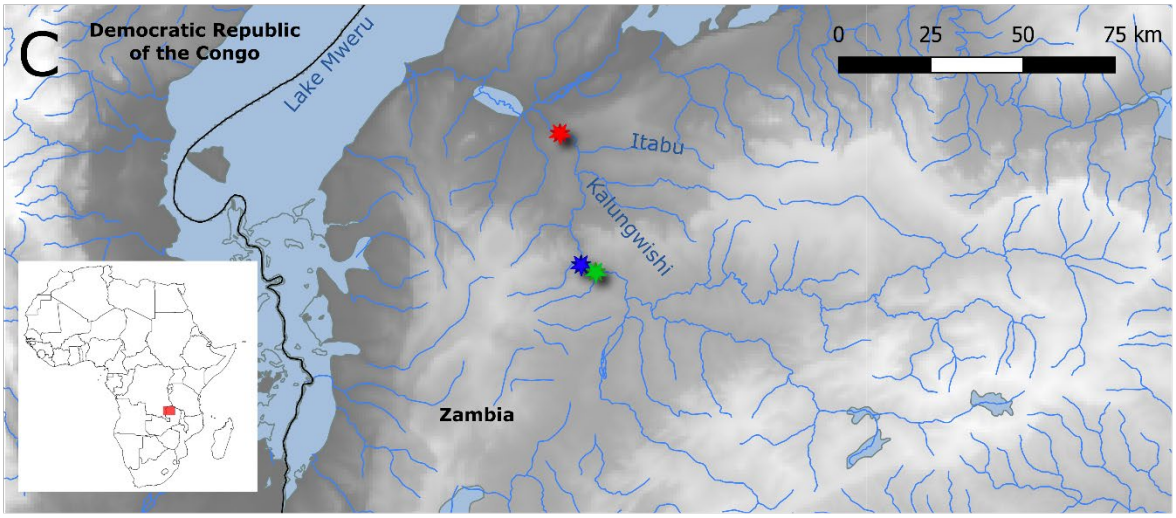
C
Democratic Republic of the Congo
Lake Mweru
Itabu
Kalungwishi
Zambia
0
25
50
75 km


D

Figure 5: : **Overview of the '*Orthochromis kalungwishiensis* species complex' and a representative member of the '*Orthochromis luongoensis* species complex' A.** Representative specimens of the *O. kalungwishiensis* and putative species of the '*Orthochromis kalungwishiensis* species complex' occurring in the Kalungwishi drainage system: *O. kalungwishiensis*, caught at the type location above the Kundabwika falls; *O*. cf. *kalungwishiensis* "Red"; caught below the Kabewluma falls; *O*. cf. *kalungwishiensis* "Itabu", caught in the Itabu River (ID:DRC-3588); *O*. cf. *kalungwishiensis* "Rainbow", aquarium specimen most likely from Lake Mweru, *O*. cf. *kalungwishiensis* "Lumangwe", caught above Lumangwe falls **B.** *Orthochromis luongoensis* "Kalungwishi", caught below Kabewluma falls **C.** Map of Northern Zambia and south-eastern DRC, with indication of major waterfalls on the Kalungwishi River: Lumangwe falls (green star), Kabweluma falls (blue star) and Kundabwika falls (red star); Shapefiles were obtained from DIVA-GIS (http://www.diva-gis.org/Data) **D.** View on the Lumangwe falls and the Kundabwika falls on the Kalungwishi River. All photos by F.D.B. Schedel.

Conclusion

African cichlids of the austrotilapiine clade have evolved thousands of species in the African Great Lakes, known as the East African Cichlid Radiation (EAR). The phylogenetic history of the riverine austrotilapiine precursor lineages that gave rise to the EAR has remained poorly studied, although refined phylogenetic reconstructions are a necessary prerequisite for understanding the age, origin and processes that have led to the enormous success of the EAR. The phylogenetic analysis of massive and comprehensive mitochondrial and nuclear DNA (ddRAD) datasets presented in this thesis for the austrotilapiine cichlids in combination with the spatio-temporal reconstructions of the dynamic palaeo-landscapes that are the cradle of these radiations have thus provided new insights for the evolutionary history of African cichlids in general and about the intimate link between tectonic landscape evolution and their phylogenetic history in particular. The refined reconstruction of the phylogenetic relationships included extensive testing for signatures of ancient hybridization events. This, because they were enabled by tectonic watershed rearrangements which, in turn, provided novel gene flow opportunities between previously isolated cichlid lineages. Particularly a refined view on the geomorphological evolution of the southeastern part of the African continent across the southeastern limits of the watersheds of the Upper Congo including the Lake Tanganyika drainage allowed for an improved reconstruction of the fascinating biogeographic precursor-history of the EAR; and, on the other side of the coin, application of molecular clock

reconstructions to date landscape-fish co-evolutionary events allowed for a better understanding of palaeo-geomorphological setting in which the EAR evolved.

The results identified a key-role of selected rheophilic haplochromine lineages, because through their tight ecological cohesion to changes of tectonic knickpoints such as waterfalls and rapids, their phylogenetic diversification was shown to be particularly well linked to tectonic landform changes that either enabled or impaired gene flow between previously isolated or, respectively, connected rheophilic cichlid populations. Thus, carefully scrutinized molecular clock divergence time estimates for these rheophilic cichlid lineages, related to the EAR, allowed to put the tectonic events of the corresponding knickpoint formations into a geological timeframe. Once solid geology-derived date estimates for the formation dates for selected knickpoint systems will become available in the near future, e.g. that of the Kyubo falls, these could in turn be used to globally constrain EAR molecular clock analyses, and this would undoubtedly further improve our understanding of the biogeographic history of these fascinating haplochromine cichlids.

The basis for the meaningful interpretation of the various aspects of the evolutionary history of cichlids as well as the identification of promising systems for geo-ecomorphological research as outlined above ultimately rely on a sound systematic and taxonomic framework. With the description of eight new species and two new genera, an important contribution to the taxonomic classification of austrotilapiine cichlid had been made, but a complete phylogenetic-based revision of their systematics and taxonomy is far off being completed. Especially the polyphyletic genus *Orthochromis,* including at least seven distinct lineages, either belonging to the *Orthochromis* sensu stricto., the so-called ‘extended serranochromines’ or the ‘extended *Pseudocrenilabrus*-group’, urgently need to be revised. The improved knowledge of the phylogenetic relationships of this rheophilic cichlids provided here will facilitate this task. Further steps aiming for the revision of all *Orthochromis* lineages related to the ‘extended serranochromines’ are in preparation.

Acknowledgements

I have been privileged to work on a subject I am passionate about, and as are my fantastic colleagues. I was privileged by unconditional support and encouragement of my friends, my family and especially by my wife, which made my PhD-years among the best of my life. The

deep gratitude I feel towards to countless people making this thesis possible, in one way or other, can only be hardly expressed.

First of all, I like to express my deep thanks and my profound appreciation to Dr. Ulrich Schliewen as a friend and colleague. He has played such an important role for my personal and scientific development since I started to work with him. His incredible knowledge about cichlids and about fishes in general combined with his passion and enthusiasm has been a continuous source of inspiration to me. I will never forget our countless discussions, sometimes so engaging that we missed the one or the other motorway exit; and of course the lessons of live he taught me (the next time I will get the piece of chicken).

I gratefully thank Prof. Dr. Haszprunar giving me the opportunity to graduate under his supervision. His door was always open and he supported me wherever he could.

Further, I thank Dirk Neumann who not only facilitated the loan and storage of specimens and the corresponding paper work but who also thought me many useful techniques including all kinds of fishing techniques and the "processing and sampling" of the fish samples.

Special thanks to the team of Genomics Service Unit of the LMU. Dr. Andreas Brachmann, Gisela Brinkmann and Alexander Nieto who introduced me into the "world of sequencing" and always were available for any advice.

My time at the Bavarian State Collection of Zoology would not have been the same without all my wonderful friends and colleagues: Dr. Andreas Dunz, Dr. Alexander Cerwenka, Dr. Nicolas Straube, Dr. Mark Scherz, Nadine Usimesa Wingi, Juliane Weiss, Laura Walheim, Eva Paulus, Viviane Kupriyanov, Jérôme Morinière, Isabella Stöger and Stefan Filser. I will never forget our morning coffee breaks and lunch time sessions. You have always been there to help me, motivated me, gave me advice, to develop new ideas, giving comments or simply for a good chat.

I would like to express my thanks to Jakob Geck who supplied me with knowledge of practical fish keeping, fish pictures and who had always time for some "fish nerd talk".

My deep gratitude to Emmanuel Abwe, Bauchet Katemo Manda, Dr. Kise Kisekelwa, Lewis Ngoy Kalumba and Pacifique Kiwele Mutambala. All are my Congolese colleagues who became true friends over the years. It was pure joy to be you on fieldtrips and to pass countless hours in the lab with you guys talking in a mixture of French, English and to some extent in Swahili which you tried to teach me. Thanks go also to Prof. Dr. Auguste Chocha Manda for providing samples and pictures of the Lomami cichlids, and who marvelously facilitated fieldwork in DRC.

Special thanks go to Dr. Emmanuel Vreven for his warm-hearted hospitality on my occasional visits to Royal Museum of Central Africa (Tervuren), the true friendship that has grown over the years and for providing specimen loans, samples, pictures

I want to thank my colleagues in South Africa Prof. Dr. Dirk Bellstedt, Dr. Woody Cotterill, Dr. A. Chakona, Dr. Tyrel Flügel, David Svendsen and Pieter de Wet van der Merwe for their friendship, the fruitful discussions and warm hospitality. Further, I want thank our colleagues from the Deutsches GeoForschungsZengrum GFZ: Dr. Samuel Niedermann and especially Spiros Olivotos who patiently answered all my question about the geology of Africa.

I further want to express my thanks to my co-authors, if not mentioned already above, for sharing specimens and tissues, ideas, and for their patience: Dr. Zuzana Musilová and Prof. Dr. Hamid Reza Esmaeili.

My projects benefited from numerous discussions on the cichlid fossils with colleagues from the department of Earth and Environmental Sciences (LMU): Prof. Dr. Bettina Reichenbacher, Dr. Melanie Altner, Charalampos Kevrekidis and Stefanie Penk.

Further, I want to express my deep gratitude to Dr. Adrian Indermaur for his inspiring enthusiasm and for the unforgettable moments we passed together at the shore of Lake Tanganyika and at the Lufubu River.

Many thanks go also to Erwin Schraml not only for the provision of the picture of *O. machadoi* depicted in this thesis but also sharing is incredible knowledge on haplochromine cichlids with me.

I want thank Hans van Heusden for sharing with pictures of various *Orthochromis* species and the many discussions we had via various digital communication channels and whom I hope to meet one day in person.

Further, I want to thank my good friend and colleague Dr. M. Popoola for his words of encouragement and for the good collaboration we share since years.

This thesis would not have been possible without the funding of the Volkswagen-Stiftung for the project “Exploiting the genomic record of living biota to reconstruct the landscape evolution of South Central Afrifca”. I would want to extend my special thanks the them. Further, I want

to thank the Deutsche Cichliden Gesellschaft (DCG) for the funding my study on genus *Hemibates* by granting me the “DCG-Förderpreis”.

Furthermore, I would like to thank my Ph.D. committee for evaluating this thesis.

My greatest thanks must go to my family, especially my parents and siblings, who have supported me all my live in every aspect. I will never forget the day I got my first aquarium as a young boy which sparked my curiosity and enthusiasm for fish, as well the memorable times we have been fishing as kids in the lakes and rivers of southern France.

Finally, I would like to thank my wife and soulmate Dr. Christina Weiß. She patiently accepted my obsession for fishes, endured my absence while I was on various field trips to Africa, and yet supported and encouraged me over all those years with all her heart making. Thank you for always being there for me and encouraging me to fulfil my dreams.

Lumangwe falls on the Kalungwishi River

References

Abell, R., M. L. Thieme, C. Revenga, M. Bryer, M. Kottelat, N. Bogutskaya, B. Coad, N. Mandrak, S. C. Balderas, W. A. Bussing, M. L. J. Stiassny, P. Skelton, G. R. Allen, P. J. Unmack, A. M. Naseka, R. Ng, N. Sindorf, J. Robertson, E. Armijo, J. V. Higgins, T. J. Heibel, E. WIikramanayake, D. Olson, H. L. Lopez, R. E. Reis, J. G. Lundberg, M. H. S. Perez & P. Petry, 2008. Freshwater ecoregions of the world: A new map of biogeographic units for freshwater biodiversity conservation. BioScience 58(5):403–414. doi:10.1641/B580507.

Albertson, R. C. & T. D. Kocher, 2006. Genetic and developmental basis of cichlid trophic diversity. Heredity 97(3):211–221. doi:10.1038/sj.hdy.6800864.

Albertson, R. C., J. A. Markert, P. D. Danley & T. D. Kocher, 1999. Phylogeny of a rapidly evolving clade: the cichlid fishes of Lake Malawi, East Africa. Proceedings of the National Academy of Sciences of the United States of America (PNAS) 96(9):5107–5110. doi:10.1073/pnas.96.9.5107

Alfaro, M. E., B. C. Faircloth, R. C. Harrington, L. Sorenson, M. Friedman, C. E. Thacker, C. H. Oliveros, D. Cerny & T. J. Near, 2018. Explosive diversification of marine fishes at the Cretaceous-Palaeogene boundary. Nature Ecology & Evolution 2(4):688–696. doi:10.1038/s41559-018-0494-6.

Ali, J. R. & J. C. Aitchison, 2008. Gondwana to Asia: Plate tectonics, paleogeography and the biological connectivity of the Indian sub-continent from the Middle Jurassic through latest Eocene (166–35 Ma). Earth-Science Reviews 88(3-4):145–166. doi:10.1016/j.earscirev.2008.01.007.

Altner, M., U. K. Schliewen, S. B. R. Penk & B. Reichenbacher, 2017. †Tugenchromis pickfordi, gen. et sp. nov., from the upper Miocene—a stem-group cichlid of the 'East African Radiation'. Journal of Vertebrate Paleontology 37(2):e1297819. doi:10.1080/02724634.2017.1297819.

Balon, E. K. & D. J. Stewart, 1983. Fish assemblages in a river with unusual gradient (Luongo, Africa - Zaire system), reflections on river zonation, and description of another new species. Environmental Biology of Fishes 9(3-4):225–252. doi:10.1007/BF00692373.

Banister, K. E. & R. G. Bailey, 1979. Fishes collected by the Zaire River Expedition, 1974-75. Zoological Journal of the Linnean Society 66(3):205–249. doi:10.1111/j.1096-3642.1979.tb01909.x.

Barel, C. D. N., M. J. P. van Oijen, F. Witte & E. L. M. Witte-Maas, 1977. An introduction to the taxonomy and morphology of the haplochromine Cichlidae from Lake Victoria. Netherlands Journal of Zoology 27(4):333–380. doi:10.1163/002829677X00199.

Barlow, G. W., 2000. The cichlid fishes. Nature's grand experiment in evolution. Perseus Publishing, Cambridge, Massachusetts.

Bell-Cross, G., 1968. The distribution of fishes in Central Africa. Fisheries Research Bulletin Zambia 4:3–20.

Betancur-R, R., R. E. Broughton, E. O. Wiley, K. Carpenter, J. A. Lopez, C. Li, N. I. Holcroft, D. Arcila, M. Sanciangco, J. C. Cureton Ii, F. Zhang, T. Buser, M. A. Campbell, J. A. Ballesteros, A. Roa-Varon, S. Willis, W. C. Borden, T. Rowley, P. C. Reneau, D. J. Hough, G. Lu, T. Grande, G. Arratia & G. Orti, 2013. The tree of life and a new classification of bony fishes. PLoS Currents Tree of Life 5 doi:10.1371/currents.tol.53ba26640df0ccaee75bb165c8c26288.

Bishop, P., T. B. Hoey, J. D. Jansen & A. I.L., 2005. Knickpoint recession rate and catchment area: the case of uplifted rivers in Eastern Scotland. Earth Surface Processes and Landforms 30:767–778. doi:10.1002/esp.1191.

Bleeker, P., 1868. Description de trois espèces inédites de Chromidoïdes de Madagascar. . Verslagen en Mededeelingen der Koninklijke Akademie van Wetenschappen (Afdeeling Natuurkunde), Amsterdam Afdeeling Natuurkunde(Ser. 2):307–314.

Bloch, M. E., 1790. Naturgeschichte der ausländischen Fische, vol v. 4: i-xii + 1-128, Pls. 217–252, Berlin.

Boulenger, G. A., 1898. Report on the fishes recently obtained by Mr. J. E. S. Moore in Lake Tanganyika. Proceedings of the Zoological Society of London 1898:494–497.

Boulenger, G. A., 1899a. Matériaux pour la faune du Congo. Poissons nouveaux du Congo. Cinquième Partie. Cyprins, Silures, Cyprinodontes, Acanthoptérygiens. Annales du Musée Royal du Congo Belge Sciences Zoologiques 1(5):97–128.

Boulenger, G. A., 1899b. Matériaux pour la faune du Congo. Poissons nouveaux du Congo. Troisième Partie. Silures, Acanthoptérygiens, Mastacembles, Plectognathes. Annales du Musée Royal du Congo Belge Sciences Zoologiques 1(3):39–58.

Boulenger, G. A., 1901a. Diagnoses of new fishes discovered hy Mr. J. E. S. Moore in Lakes Tanganyika and Kivu. Annals and Magazine of Natural History (Series 7) 7(37):1–6. doi:10.1080/00222930108678431.

Boulenger, G. A., 1901b. Les poissons du Bassin du Congo. Publication de l'Etat Independant du Congo, Bruxelles.

Boulenger, G. A., 1902. Contributions to the ichthyology of the Congo. - II. On a collection of fishes from the Lindi River. Proceedings of the Zoological Society of London 1(18):265–271.

Boulenger, G. A., 1907. Descriptions of two new freshwater fishes discovered by Dr. W. J. Ansorge in Mossamedes, Angola. Annals and Magazine of Natural History (Series 7) 20(116):108–109.

Brawand, D., C. E. Wagner, Y. I. Li, M. Malinsky, I. Keller, S. Fan, O. Simakov, A. Y. Ng, Z. W. Lim, E. Bezault, J. Turner-Maier, J. Johnson, R. Alcazar, H. J. Noh, P. Russell, B. Aken, J. Alföldi, C. Amemiya, N. Azzouzi, J.-F. Baroiller, F. Barloy-Hubler, A. Berlin, R. Bloomquist, K. L. Carleton, M. A. Conte, H. D'Cotta, O. Eshel, L. Gaffney, F. Galibert, H. F. Gante, S. Gnerre, L. Greuter, R. Guyon, N. S. Haddad, W. Haerty, R. M. Harris, H. A. Hofmann, T. Hourlier, G. Hulata, D. B. Jaffe, M. Lara, A. P. Lee, I. MacCallum, S. Mwaiko, M. Nikaido, H. Nishihara, C. Ozouf-Costaz, D. J. Penman, D. Przybylski, M. Rakotomanga, S. C. P. Renn, F. J. Ribeiro, M. Ron, W. Salzburger, L. Sanchez-Pulido, M. E. Santos, S. Searle, T. Sharpe, R. Swofford, F. J. Tan, L. Williams, S. Young, S. Yin, N. Okada, T. D. Kocher, E. A. Miska, E. S. Lander, B. Venkatesh, R. D. Fernald, A. Meyer, C. P. Ponting & J. T. Streelman, 2014. The genomic substrate for adaptive radiation in African cichlid fish. Nature 513:375–381. doi:10.1038/nature13726.

Brocklehurst, S. H., 2010. Tectonics and geomorphology. Progress in Physical Geography: Earth and Environment 34(3):357–383. doi:10.1177/0309133309360632.

Bromham, L., S. Duchene, X. Hua, A. M. Ritchie, D. A. Duchene & S. Y. W. Ho, 2018. Bayesian molecular dating: opening up the black box. Biological Reviews 93(2):1165–1191. doi:10.1111/brv.12390.

Brooks, E. G. E., D. J. Allen & W. R. T. Darwall, 2011. The Status and Distribution of Freshwater Biodiversity in Central Africa. IUCN, Cambridge.

Chorowicz, J., 2005. The East African rift system. Journal of African Earth Sciences 43(1-3):379–410. doi:10.1016/j.jafrearsci.2005.07.019.

Clabaut, C., W. Salzburger & A. Meyer, 2005. Comparative phylogenetic analyses of the adaptive radiation of Lake Tanganyika cichlid fish: nuclear sequences are less

homoplasious but also less informative than mitochondrial DNA. Journal of Molecular Ecology 61(5):666–81. doi:10.1007/s00239-004-0217-2.
Cotterill, F. P. D., 2004. Drainage evolution in south-central Africa and vicariant speciation in swamp-dwelling weaver birds and swamp flycatchers. Honeyguide 50(1):7–25.
Cotterill, F. P. D., 2005. The Upemba lechwe, *Kobus anselli*: an antelope new to science emphasizes the conservation importance of Katanga, Democratic Republic of Congo. Journal of Zoology (London) 265(2):113–132. doi:10.1017/S0952836904006193.
Cotterill, F. P. D. & M. J. de Wit, 2011. Geoecodynamics and the Kalahari epeirogeny: linking its genomic record, tree of life and palimpsest into a unified narrative of landscape evolution. South African Journal of Geology 114(3-4):493–518. doi:10.2113/gssajg.114.3-4.493.
Cuvier, G., 1816. Le Règne Animal distribué d'après son organisation pour servir de base à l'histoire naturelle des animaux et d'introduction à l'anatomie comparée. Les reptiles, les poissons, les mollusques et les annélides, Edition 1. v. 2: i-xviii edn.
Cuvier, G. & M. Valenciennes, 1830. Histoire Naturelle des Poissons Tome 5, vol 5. F.G.Levrault, Paris.
Damas, H., 1961. L'évolution d'un lac barrage du Katanga. Internationale Vereinigung für theoretische und angewandte Limnologie: Verhandlungen 14(2):661–664. doi:10.1080/03680770.1959.11899342.
Darwall, W., K. Smith, D. Allen, R. Holland, I. Harrison & E. Brooks (eds), 2011. The Diversity of Life in African Freshwaters: Under Water, Under Threat. An analysis of the status and distribution of freshwater species throughout mainland Africa. IUCN, Cambridge, United Kingdom and Gland, Switzerland.
David, L., 1937. Poissons de l'Urundi. Revue de Zoologie et de Botanique Africaines 29(4):413–423.
Day, J. J., J. A. Cotton & T. G. Barraclough, 2008. Tempo and mode of diversification of Lake Tanganyika cichlid fishes. PLoS One:e1730. doi:10.1371/journal.pone.0001730
de Castelnau, F., 1861. Mémoire sur les Poissons de l'Afrique Australe. Bailliere et Fils, Paris.
De Vos, L. & L. Seegers, 1998. Seven new *Orthochromis* species (Teleostei: Cichlidae) from the Malagarasi, Luiche and Rugufu basins (Lake Tanganyika drainage), with notes on their reproductive biology. Ichthyological Exploration of Freshwaters 9(4):371–420.
Decru, E., E. Vreven, C. Danadu, A. Walanga, T. Mambo & J. Snoeks, 2017. Ichthyofauna of the Itimbiri, Aruwimi, and Lindi/Shopo Rivers (Congo basin): Diversity and distribution patterns. Acta Ichthyologica et Piscatoria 47(3):225–247. doi:10.3750/AIEP/02085
del Papa, C., A. Kirschbaum, J. Powell, A. Brod, F. Hongn & M. Pimentel, 2010. Sedimentological, geochemical and paleontological insights applied to continental omission surfaces: A new approach for reconstructing an eocene foreland basin in NW Argentina. Journal of South American Earth Sciences 29(2):327–345. doi:10.1016/j.jsames.2009.06.004.
Duchêne, S., R. Lanfear & S. Y. Ho, 2014. The impact of calibration and clock-model choice on molecular estimates of divergence times. Molecular Biology and Evolution 78:277–89. doi:10.1016/j.ympev.2014.05.032.
Dunz, A. R., 2012. Revision of the substrate brooding "*Tilapia*" (*Tilapia* Smith, 1840 and related taxa), (Teleostei: Perciformes: Cichlidae). Doktor, Ludwig-Maximilians-Universität.
Dunz, A. R. & U. K. Schliewen, 2010. Description of a new species of *Tilapia* Smith, 1840 (Teleostei: Cichlidae) from Ghana. Zootaxa 2548:1–21. doi:10.11646/zootaxa.2548.1.1.

Dunz, A. R. & U. K. Schliewen, 2013. Molecular phylogeny and revised classification of the haplotilapiine cichlid fishes formerly referred to as "*Tilapia*". Molecular Phylogenetics and Evolution 68(1):64–80. doi:10.1016/j.ympev.2013.03.015.

Egger, B., Y. Klaefiger, A. Indermaur, S. Koblmüller, A. Theis, S. Egger, T. Näf, M. van Steenberge, C. Sturmbauer, C. Katongo & W. Salzburger, 2015. Phylogeographic and phenotypic assessment of a basal haplochromine cichlid fish from Lake Chila, Zambia. Hydrobiologia 748(1):171–184.

Farias, I. P., G. Ortí, I. Sampaio, H. Schneider & A. Meyer, 1999. Mitochondrial DNA phylogeny of the family Cichlidae: monophyly and fast molecular evolution of the neotropical assemblage. Journal of Molecular Evolution 48(6):703–711. doi:10.1007/pl00006514.

Flügel, T. J., F. D. Eckardt & F. P. D. Cotterill, 2015. The Present Day Drainage Patterns of the Congo River System and their Neogene Evolution.315–337. doi:10.1007/978-3-642-29482-2_15.

Flügel, T. J., F. D. Eckardt & F. P. D. Cotterill, 2017. The geomorphology and river longitudinal profiles of the Congo-Kalahari watershed. In Runge, J. (ed) The African Neogene – Climate, Environments and People. CRC Press, 32–52.

Flögel, T. J., 2014. The evolution of the Congo-Kalahari Watershed: African Mega-Geomorphology. University of Cape Town (UCT)

Fowler, H. W., 1934. Fishes obtained by Mr. H. W. Bell-Marley chiefly in Natal and Zululand in 1929 to 1932. Proceedings of the Academy of Natural Sciences of Philadelphia 86:405–514.

Fricke, R., W. N. Eschmeyer & R. e. van der Laan, 2020. ESCHMEYER'S CATALOG OF FISHES: GENERA, SPECIES, REFERENCES. (http://researcharchivecalacademyorg/research/ichthyology/catalog/fishcatmainasp) Electronic version accessed 08 May 2020.

Friedman, M., B. P. Keck, A. Dornburg, R. I. Eytan, C. H. Martin, C. D. Hulsey, P. C. Wainwright & T. J. Near, 2013. Molecular and fossil evidence place the origin of cichlid fishes long after Gondwanan rifting. Proceedings of the Royal Society B: Biological Sciences 280(1770):20131733. doi:10.1098/rspb.2013.1733.

Fryer, G. & T. D. Iles, 1972. The cichlid fishes of the great lakes of Africa. Their biology and evolution. T.F.H. Publications, Neptune City.

Genner, M. J., B. P. Ngatunga, S. Mzighani, A. Smith & G. F. Turner, 2015. Geographical ancestry of Lake Malawi's cichlid fish diversity. Biology Letters 11(6):20150232. doi:10.1098/rsbl.2015.0232.

Genner, M. J., O. Seehausen, D. H. Lunt, D. A. Joyce, P. W. Shaw, G. R. Carvalho & G. F. Turner, 2007. Age of cichlids: new dates for ancient lake fish radiations. Molecular Biology and Evolution 24(5):1269–82. doi:10.1093/molbev/msm050.

Goodier, S. A., F. P. Cotterill, C. O'Ryan, P. H. Skelton & M. J. de Wit, 2011. Cryptic diversity of African tigerfish (genus *Hydrocynus*) reveals palaeogeographic signatures of linked neogene geotectonic events. PLoS One 6(12):e28775. doi:10.1371/journal.pone.0028775.

Goodwin, N. B., S. Balshine-Earn & J. D. Reynolds, 1998. Evolutionary transitions in parental care in cichlid fish. Proceedings of the Royal Society of London Series B Biological Sciences 265(1412):2265–2272. doi:10.1098/rspb.1998.0569.

Greenwood, P. H., 1954. On two species of cichlid fishes from the Malagarazi River (Tanganyika), with notes on the pharyngeal apophysis in species of the *Haplochromis* group. Annals and Magazine of Natural History (Series 12) 7:401–414. doi:10.1080/00222935408656059.

Greenwood, P. H., 1978. A review of the pharyngeal apophysis and its significance in the classification of African cichlid fish. Bulletin of the British Museum (Natural History) Zoology 33(5):297–323.
Greenwood, P. H., 1979. Towards a phyletic classification of the 'genus' *Haplochromis* (Pisces, Cichlidae) and related taxa Part I. Bulletin of the British Museum (Natural History) Zoology 35(4):265–322.
Greenwood, P. H., 1984. The haplochromine species (Teleostei, Cichlidae) of Cunene and certain other Angolan rivers. Bulletin of the British Museum (Natural History) Zoology 47(4):187–239.
Greenwood, P. H., 1989. The taxonomic status and phylogenetic relationships of *Pseudocrenilabrus* Fowler (Teleostei, Cichlidae). Ichthyological Bulletin of the JLB Smith Institute of Ichthyology 54:1–16.
Greenwood, P. H. & S. O. Kullander, 1994. A taxonomic review and redescription of *Tilapia polyacanthus* and *T. stormsi* (Teleostei: Cichlidae), with descriptions of two new Schwetzochromis species from the upper Zaïre River drainage. Ichthyological Exploration of Freshwaters 5(2):161–180.
Günther, A., 1862. Catalogue of the Acanthopterygii, Pharyngognathi and Anacanthini in the collection of the British Museum Volume fourth, vol 4. British Museum, London.
Günther, A., 1864. Report on a collection of reptiles and fishes made by Dr. Kirk in the Zambesi and Nyassa regions. Proceedings of the Zoological Society of London 1864:303–314.
Harrison, T., C. P. Msuya, A. M. Murray, B. Fine Jacobs, A. M. Báez, R. Mundil & K. R. Ludwig, 2001. Paleontological investigations at the Eocene locality of Mahenge in north-central Tanzania, East Africa. in: Gunnel, GF (Eds), Eocene biodiversity: unusual occurrences and rarely sampled habitats, Kluwar Academic–Plenum Publishers, New York 18:39–74. doi:10.1007/978-1-4615-1271-4_2.
Hebert, P. D., A. Cywinska, S. L. Ball & J. R. deWaard, 2003. Biological identifications through DNA barcodes. Proceedings of the RoyaI Society B Biological Sciences 270(1512):313–21. doi:10.1098/rspb.2002.2218.
Heine, C., J. Zoethout & R. D. Müller, 2013. Kinematics of the South Atlantic rift. Solid Earth 4(2):215–253. doi:10.5194/se-4-215-2013.
Ho, S. Y. W. & S. Duchêne, 2014. Molecular-clock methods for estimating evolutionary rates and timescales. Molecular Ecology 23(24):5947–5965. doi:10.1111/mec.12953.
Howard, A. D., W. E. Dietrich & M. A. Seidl, 1994. Modeling fluvial erosion on regional to continental scales. Journal of Geophysical Research: Solid Earth 99(B7):13971–13986. doi:10.1029/94jb00744.
Hulsey, C. D., J. Zheng, R. Holzman, M. E. Alfaro, M. Olave & A. Meyer, 2018. Phylogenomics of a putatively convergent novelty: did hypertrophied lips evolve once or repeatedly in Lake Malawi cichlid fishes? BMC Evolutionary Biology 18(179):13. doi:10.1186/s12862-018-1296-9.
Indermaur, A., 2014. Über den Tellerrand geschaut - Buntbarsche aus dem Lufubu. Die Aquarien- und Terrarien-Zeitschrift (DATZ) 10:16–23.
Irisarri, I., P. Singh, S. Koblmuller, J. Torres-Dowdall, F. Henning, P. Franchini, C. Fischer, A. R. Lemmon, E. M. Lemmon, G. G. Thallinger, C. Sturmbauer & A. Meyer, 2018. Phylogenomics uncovers early hybridization and adaptive loci shaping the radiation of Lake Tanganyika cichlid fishes. Nature Communications 9(3159):1–12. doi:10.1038/s41467-018-05479-9.
Jackson, P. B. N., 1961. The fishes of Northern Rhodesia. Government Printer, Lusaka.

Joyce, D. A., D. H. Lunt, R. Bills, G. F. Turner, C. Katongo, N. Duftner, C. Sturmbauer & O. Seehausen, 2005. An extant cichlid fish radiation emerged in an extinct Pleistocene lake. Nature 435(7038):90–95. doi:10.1038/nature0348.

Kambembo, J. P. K., 2018. Les risques naturels dans le Haut-Katanga. In Tshonda, J. O. (ed) Haut-Katanga: lorsque richesses économiques et pouvoirs politiques forcent une identité régionale Tome 1 : cadre naturel, peuplement et politique. Musée royal de l'Afrique centrale, Tervuren, 65–74.

Kanazawa, R. H., 1951. Description of a new genus of cichlid fish, *Gobiocichla*, from the French Sudan. Annals and Magazine of Natural History 12(4):378–381. doi:10.1080/00222935108654162.

Katemo Manda, B., A. Chocha Manda, J. Snoeks & E. Vreven, 2013. The ichtyofauna of the Upemba National Park (DR Congo): diversity, ecology, conservation and sustainable management. . Paper presented at the Fifth International Conference of the Pan African Fish and Fisheries Association (PAFFA5).

Katongo, C., S. Koblmüller, N. Duftner, Makasa, Lawrence & C. Sturmbauer, 2005. Phylogeography and speciation in the *Pseudocrenilabrus philander* species complex in Zambian Rivers. Hydrobiologia 542(1):221–233. doi:10.1007/s10750-004-1389-x.

Katongo, C., S. Koblmüller, N. Duftner, L. Mumba & C. Sturmbauer, 2007. Evolutionary history and biogeographic affinities of the serranochromine cichlids in Zambian rivers. Molecular Phylogenetics and Evolution 45(1):326–338. doi:10.1016/j.ympev.2007.02.011.

Katongo, C., V. Schneider, R. Stelkens, D. A. Joyce & O. Seehausen, A new adaptive radiation of cichlid fish in a poorly known African Great Lake: Mweru. In: International Symposium: Speciation in Ancient Lakes, SIAL IV, Berlin, 2006.

Katongo, C., O. Seehausen & J. Snoecks, 2017. A new species of *Pseudocrenilabrus* (Perciformes: Cichlidae) from Lake Mweru in the Upper Congo River System. Zootaxa 4237(1):181–190. doi:10.11646/zootaxa.4237.1.10.

Keck, B. P. & C. D. Hulsey, 2014. Continental monophyly of cichlid fishes and the phylogenetic position of *Heterochromis multidens*. Molecular Phylogenetics and Evolution 73:53–59. doi:10.1016/j.ympev.2014.01.011.

Kevrekidis, C., M. Valtl, S. B. R. Penk, M. Altner & B. Reichenbacher, 2019. *Rebekkachromis* nov. gen. from the middle–upper Miocene (11 MYA) of Central Kenya: the oldest record of a haplotilapiine cichlid fish. Hydrobiologia 832(1):39–64. doi:10.1007/s10750-018-3715-8.

Kipata, M. L., D. Delveaux, M. N. Sabagenzi, J. Cailteux & M. Sintubin, 2013. Brittle tectonic and stress field evolution in the Pan-African Lufilian arc and its foreland (Katanga, DRC): from orogenic compression to extensional collapse, transpressional inversion and transition to rifting. Geologica Belgica 16(1-2):1–17.

Kisekelwa, T., J. Snoeks & E. Vreven, 2020. An annotated checklist of the fish fauna of the river systems draining the Kahuzi-Biega National Park (Upper Congo: Eastern DR Congo). Journal of Fish Biology 96(3):700–721. doi:10.1111/jfb.14264.

Klett, V. & A. Meyer, 2002. What, if anything, is a tilapia? - Mitochondrial ND2 phylogeny of Tilapiines and the evolution of parental care systems in the African cichlid fishes. Molecular Biology and Evolution 19(6):865–883. doi:10.1093/oxfordjournals.molbev.a004144.

Koblmüller, S., C. Katongo, H. Phiri & C. Sturmbauer, 2012. Past connection of the upper reaches of a Lake Tanganyika tributary with the upper Congo drainage suggested by genetic data of riverine cichlid fishes. African Zoology 47(1):182–186. doi:10.1080/15627020.2012.11407537.

Koblmüller, S., U. K. Schliewen, N. Duftner, K. M. Sefc, C. Katongo & C. Sturmbauer, 2008a. Age and spread of the haplochromine cichlid fishes in Africa. Molecular Phylogenetics and Evolution 49(1):153–169. doi:10.1016/j.ympev.2008.05.045.

Koblmüller, S., K. M. Sefc & C. Sturmbauer, 2008b. The Lake Tanganyika cichlid species assemblage: recent advances in molecular phylogenetics. Hydrobiologia 615(1):5–20. doi:10.1007/s10750-008-9552-4.

Kocher, T. D., 2004. Adaptive evolution and explosive speciation: the cichlid fish model. Nature Reviews Genetics 5(4):288–298. doi:10.1038/nrg1316.

Konings, A., 2007. Malawi Cichlids in their natural habitat, 4 edn. Cichlid Press, El Paso.

Konings, A., 2019. Tanganjika cichlids in their natural habitat, 4nd edn. Cichlid-Press, unknown.

Konings, A. F., 1998. Tanganyika cichlids in their natural habitat. Cichlid Press, Texas, El Paso.

Kullander, S. O., 1998. A phylogeny and classification of the South American Cichlid (Teleostei:Perciformes). In Malabarba, L. R. R., R.; Vari, R.P.; Lucena, Z.M; Lucena, C.A. (ed) Phylogeny and Classification of Neotropical Fishes. Edipucrs, Porto Alegre,, 461–498.

Kullander, S. O., 2003. Family Cichlidae (Cichlids). In Reis, R. E., S. O. Kullander & C. J. Ferraris (eds) Check list of the freshwater fishes of South and Central America. Edipucrs, Porto Alegre, 605–654.

Leaché, A. D., R. B. Harris, B. Rannala & Z. Yang, 2014. The Influence of Gene Flow on Species Tree Estimation: A Simulation Study. Systematic Biology 63(1):17–30. doi:10.1093/sysbio/syt049.

Liem, K. F., 1973. Evolutionary strategies and morphological innovations: cichlid pharyngeal jaws. Systematic Zoology 22(4):425–441. doi:10.2307/2412950.

Linnæus, C., 1758. Systema naturæ per regna tria naturæ, secundum classes, ordines, genera, species, cum characteribus, differentiis, synonymis, locis, vol Tomus I, Editio decima, reformata edn. Laurentii Salvii, Holmiæ.

Lippitsch, E., 1990. Scale morphology and squamation patterns in cichlids (Teleostei, Perciformes): a comparative study. Journal of Fish Biology 37(2):265–291. doi:10.1111/j.1095-8649.1990.tb05858.x.

Lippitsch, E., 1997. Phylogenetic investigations on the haplochromine cichlidae of Lake Kivu (East Africa), based on lepidological characters. Journal of Fish Biology 51(2):284–299. doi:10.1111/j.1095-8649.1997.tb01666.x.

Lippitsch, E., 1998. Phylogenetic study of cichlid fishes in Lake Tanganyika: a lepidological approach. Journal of Fish Biology 52(4):752–766. doi:10.1111/j.1095-8649.1998.tb01830.x.

Lobel, P. S., 1980. Invasion by the Mozambique tilapia (*Sarotherodon mossambicus*; Pisces; Cichlidae) of a Pacific atoll marine ecosystem. Micronesica 16(2):349–355.

Loget, N. & J. Van den Driessche, 2009. Wave train model for knickpoint migration. Geomorphology 106:376–382. doi:10.1016/j.geomorph.2008.10.017.

Lucanus, O., 2017. Die Buntbarsche aus dem Mweru-See im Süden des Kongo. Aquaristik Fachmagazin 49(253):46–49.

Maan, M. E. & K. M. Sefc, 2013. Colour variation in cichlid fish: developmental mechanisms, selective pressures and evolutionary consequences. Seminars in Cell & Developmental Biology 24(6-7):516–528. doi:10.1016/j.semcdb.2013.05.003.

Malabarba, M. C., L. R. Malabarba & C. Del Papa, 2010. *Gymnogeophagus eocenicus*, n. sp. (Perciformes: Cichlidae), an Eocene cichlid from the Lumbrera Formation in Argentinia. Journal of Vertebrate Paleontology 30(2):341–350.

Malabarba, M. C., O. D. Zuleta & C. del Papa, 2006. Proterocara argentina, a new fossil cichlid from the Lumbrera Formation, Eocene of Argentina. Journal of Vertebrate Paleontology 26(2):267–275. doi:10.1671/0272-4634(2006)26%5b267:PAANFC%5d2.0.CO;2

Matschiner, M., 2019. Gondwanan vicariance or trans-Atlantic dispersal of cichlid fishes: a review of the molecular evidence. Hydrobiologia 832(1):9–37. doi:10.1007/s10750-018-3686-9.

Matschiner, M., Z. Musilová, J. M. I. Barth, Z. Starostova, W. Salzburger, M. Steel & R. Bouckaert, 2016. Bayesian Node Dating based on Probabilities of Fossil Sampling Supports Trans-Atlantic Dispersal of Cichlid Fishes. Systematic Biology 66(1):3–22. doi:10.1093/sysbio/syw076

Matthews, K. J., K. T. Maloney, S. Zahirovic, S. E. Williams, M. Seton & R. D. Müller, 2016. Global plate boundary evolution and kinematics since the late Paleozoic. Global and Planetary Change 146:226–250. doi:10.1016/j.gloplacha.2016.10.002.

Meier, J. I., D. A. Marques, S. Mwaiko, C. E. Wagner, L. Excoffier & O. Seehausen, 2017. Ancient hybridization fuels rapid cichlid fish adaptive radiations. Nature Communications 8:14363. doi:10.1038/ncomms14363.

Meier, J. I., R. B. Stelkens, D. A. Joyce, S. Mwaiko, N. Phiri, U. K. Schliewen, O. M. Selz, C. E. Wagner, C. Katongo & O. Seehausen, 2019. The coincidence of ecological opportunity with hybridization explains rapid adaptive radiation in Lake Mweru cichlid fishes. Nature Communications 10(1) doi:10.1038/s41467-019-13278-z.

Meyer, B. S., M. Matschiner & W. Salzburger, 2015. A tribal level phylogeny of Lake Tanganyika cichlid fishes based on a genomic multi-marker approach. Molecular Phylogenetics and Evolution 83 doi:10.1016/j.ympev.2014.10.009.

Mondeguer, A., C. Ravenne, P. Masse & J. J. Tiercelin, 1989. Sedimentary basins in an extension and strike-slip background: the 'South Tanganyika troughs complex', East African Rift. Bulletin de la Société Géologique de France 3:501–522. doi:10.2113/gssgfbull.V.3.501.

Moore, A. E., F. P. D. Cotterill & F. D. Eckardt, 2012. The evolution and ages of Makgadikgadi palaeo-lakes: consilient evidence from Kalahari drainage evolution South-Central Africa. South African Journal of Geology 115(3):385–413.

Moore, A. E., F. P. D. W. Cotterill, M. P. L. Main & H. B. Williams, 2007. The Zambezi River. In Gupta, A. (ed) Large Rivers: Geomorphology and Management. John Wiley & Sons, Ltd, New York, 311–332.

Murray, A. M., 2000. Eocene cichlid fishes from Tanzania, East Africa. Journal of Vertebrate Paleontology 20(4):651–664.

Murray, A. M., 2001a. The fossil record and biogeography of the Cichlidae (Actinopterygii: Labroidei). Biological Journal of the Linnean Society 74(4):517–532. doi:10.1006/bijl.2001.0599.

Murray, A. M., 2001b. The oldest fossil cichlids (Teleostei: Perciformes): indication of a 45 million-year-old species flock. Proceedings of the Royal Society of London Series B Biological Sciences 268(1468):679–684. doi:10.1098/rspb.2000.1570.

Muschick, M., A. Indermaur & W. Salzburger, 2012. Convergent evolution within an adaptive radiation of cichlid fishes. Current Biology 22(24):2362–8. doi:10.1016/j.cub.2012.10.048.

Musilová, Z., L. Kalous, M. Petrtyl & P. Chaloupkova, 2013. Cichlid fishes in the Angolan headwaters region: molecular evidence of the ichthyofaunal contact between the Cuanza and Okavango-Zambezi systems. PLoS One 8(5):e65047. doi:10.1371/journal.pone.0065047.

Naylor, L. A., 2005. The contributions of biogeomorphology to the emerging field of geobiology. Palaeogeography, Palaeoclimatology, Palaeoecology 219(1-2):35–51. doi:10.1016/j.palaeo.2004.10.013.

Near, T. J., D. J. MacGuigan, E. Parker, C. D. Struthers, C. D. Jones & A. Dornburg, 2018. Phylogenetic analysis of Antarctic notothenioids illuminates the utility of RADseq for resolving Cenozoic adaptive radiations. Molecular Phylogenetics and Evolution 129:268–279. doi:10.1016/j.ympev.2018.09.001.

Nelson, J. S., T. C. Grande & M. V. H. Wilson, 2016. Fishes of the world, Fifth Edition edn. John Wiley & Sons, Hoboken, New Jersey.

Nishida, M., 1991. Lake Tanganyika as an evolutionary reservoir of old lineages of East African cichlid fishes: Inferences from allozyme data. Experientia 47:974–979. doi:10.1007/BF01929896.

Olivotos, S., S. Niedermann, T. Flügel, V. Mouslopoulou, S. Merchel, F. P. Cotterill, B. Bookhagen, A. Gärtner, G. Rugel, A. Scharf, M. J. Nadeau, R. Braucher & M. Seiler, in review. Quaternary Landscape Evolution of South Central Africa: Cosmogenic Nuclides Identify the Massive Paleo-Lake Mweru. Geomorphology.

Otero, O., C. Lécuyer, F. Fourel, F. Martineau, H. T. Mackaye, P. Vignaud & M. Brunet, 2011. Freshwater fish δ18O indicates a Messinian change of the precipitation regime in Central Africa. Geology 39(5):435–438. doi:10.1130/g31212.1.

Pauquet, G., W. Salzburger & B. Egger, 2018. The puzzling phylogeography of the haplochromine cichlid fish *Astatotilapia burtoni*. Ecology and Evolution 8:5637–5648. doi:10.1002/ece3.4092.

Pellegrin, J., 1900. Poissons nouveaux du Congo Francais. Bulletin du Museum National d'Histoire Naturelle (Ser 1) 6(3):98–101.

Pellegrin, J., 1903. Contribution a l'etude anatomique, biologique et taxinomique des poissons de la familie des cichlides. Memoires de la Societe Zoologique de France 16:41–400 [Although dated 1903, apparently published in 1904].

Penk, S., M. Altner, A. Cerwenka, U. Schliewen & B. Reichenbacher, 2019. New fossil cichlid from the middle Miocene of East Africa revealed as oldest known member of the Oreochromini. Scientific Reports 9(10198):24. doi:10.1038/s41598-019-46392-5.

Perez, P. A., M. C. Malabarba & C. del Papa, 2010. A new genus and species of Heroini (Perciformes : Cichlidae) from the early Eocene of southern South America. Neotropical Ichthyology 8(3):631–642. doi:10.1590/S1679-62252010000300008.

Pickett, S. T. A., J. Kolasa & C. Jones, 2007. Ecological Understanding: The nature of theory and the theory of nature. Academic Press, U.S.A.

Poll, M., 1948. Descriptions de Cichlidae nouveaux recueillis par le Dr. J. Schwetz dans la rivière Fwa (Congo belge). Revue de Zoologie et de Botanique Africaines 41(1):91–104.

Poll, M., 1967. Contribution a la faune ichthyologique de l'Angola. Museu do Dundo - Subsidios Para O Estudo Da Biologia Na Lunda 75:15–340.

Poll, M., 1976. Poissons: exploitation du Parc National de l'Upemba. Fondation pour Favoriser les Recherches Scientifiques en Afrique 73:1–127.

Poll, M., 1986. Classification des Cichlidae du Lac Tanganika Tribus, Genres et Especes. Academie Royale de Belgique, Bruxelles.

Regan, C. T., 1920. The classification of the fishes of the family Cichlidae - I. The Tanganyika genera. Annals and Magazine of Natural History (Series 9) 5(25):33–53.

Regan, C. T., 1922. The classification of the fishes of the family Cichlidae II. On African and Syrian genera not restricted to the great lakes. Annals and Magazine of Natural History (Series 9) 10(57):249–264.

Roberts, T. R., 1975. Geographical distribution of African freshwater fishes. Zoological Journal of the Linnean Society 57(4):249–319. doi:10.1111/j.1096-3642.1975.tb01893.x.
Roberts, T. R. & S. O. Kullander, 1994. Endemic cichlid fishes of the Fwa River, Zaïre: systematics and ecology. Ichthyological Exploration of Freshwaters 5(2):97–154.
Roberts, T. R. & D. J. Stewart, 1976. An ecological and systematic survey of fishes in the rapids of the lower Zaire or Congo River. Bulletin of the Museum of Comparative Zoology 147(6):239–317.
Ronco, F., H. H. Büscher, A. Indermaur & W. Salzburger, 2019. The taxonomic diversity of the cichlid fish fauna of ancient Lake Tanganyika, East Africa. Journal of Great Lakes Research in press doi:10.1016/j.jglr.2019.05.009.
Rüber, L. & D. C. Adams, 2001. Evolutionary convergence of body shape and trophic morphology in cichlids from Lake Tanganyika. Journal of Evolutionary Biology 14(2):325–332. doi:10.1046/j.1420-9101.2001.00269.x.
Runge, J., 2007. The Congo River, Central Africa. In Gupta, A. (ed) Large Rivers: Geomorphology and Management. John Wily & Sons Ltd., Hoboken, 293–309.
Saccone, C., C. De Giorgi, C. Gissi, G. Pesole & A. Reyes, 1999. Evolutionary genomics in Metazoa: the mitochondrial DNA as a model system. Gene 238:195–209. doi:10.1016/S0378-1119(99)00270-X.
Salzburger, W., 2018. Understanding explosive diversification through cichlid fish genomics. Nature Reviews | Genetics 19:705–717. doi:10.1038/s41576-018-0043-9.
Salzburger, W., T. Mack, E. Verheyen & A. Meyer, 2005. Out of Tanganyika: genesis, explosive speciation, key-innovations and phylogeography of the haplochromine cichlid fishes. BMC Evolutionary Biology 5:17. doi:10.1186/1471-2148-5-17.
Salzburger, W., A. Meyer, S. Baric, E. Verheyen & C. Sturmbauer, 2002. Phylogeny of the Lake Tanganyika cichlid species flock and its relationship to the Central and East African haplochromine cichlid fish faunas. . Systematic Biology 51:113–135. doi:10.1080/106351502753475907.
Schedel, F. D. B., J. P. Friel & U. K. Schliewen, 2014. *Haplochromis vanheusdeni*, a new haplochromine cichlid species from the Great Ruaha River drainage, Rufiji basin, Tanzania (Teleostei, Perciformes, Cichlidae). Spixiana 37(1):135–149.
Schedel, F. D. B., B. Katemo Manda, A. Chocha Manda, E. Abwe, E. J. W. M. N. Vreven & U. K. Schliewen, 2018. Description of five new rheophilic Orthochromis species (Teleostei: Cichlidae) from the Upper Congo drainage in Zambia and the Democratic Republic of the Congo. Zootaxa 4461(3):301–349. doi:10.11646/zootaxa.4461.3.1.
Schedel, F. D. B., V. M. S. Kupriyanov, C. Katongo & U. K. Schliewen, 2020. Palaeoplex gen. nov. and Lufubuchromis gen. non, two new monotypic cichlid genera (Teleostei: Cichlidae) from northern Zambia. Zootaxa 4718(2):191–229. doi:10.11646/zootaxa.4718.2.3.
Schedel, F. D. B., Z. Musilova & U. K. Schliewen, 2019. East African cichlid lineages (Teleostei: Cichlidae) might be older than their ancient host lakes: new divergence estimates for the east African cichlid radiation. BMC Evolutionary Biology 19(94):25. doi:10.1186/s12862-019-1417-0.
Schedel, F. D. B. & U. K. Schliewen, 2017. Hemibates koningsi spec. nov: a new deep-water cichlid (Teleostei: Cichlidae) from Lake Tanganyika. Zootaxa 4312(1):92–112. doi:10.11646/zootaxa.4312.1.4.
Schedel, F. D. B., J. D. Weiss, H. R. Esmaeili & U. K. Schliewen, in preparation. The ghost of a hybrids past uncovers ancient river tectonic captures.
Schilthuis, L., 1891. On a collection of fishes from the Congo; with description of some new species. Tijdschrift van de Nederlandse Dierkundige Vereniging 2:83–92.

Schliewen, U. K. & M. L. Stiassny, 2003. Etia nguti, a new genus and species of cichlid fish from the River Mamfue, Upper Cross River basin in Cameroon, West-Central Africa. . Ichthyological Exploration of Freshwaters 14:61–71.

Schwarzer, J., 2011. Cichlids of the lower Congo River - a new model system in speciation research? Doktor, Rheinische Friedrich-Wilhelms-Universität.

Schwarzer, J., B. Misof, S. N. Ifuta & U. K. Schliewen, 2011. Time and origin of cichlid colonization of the lower Congo rapids. PLoS One 6(7):e22380. doi:10.1371/journal.pone.0022380.

Schwarzer, J., B. Misof & U. K. Schliewen, 2012a. Speciation within genomic networks: a case study based on Steatocranus cichlids of the lower Congo rapids. Journal of Evoulutionary Biology 25(1):138–48. doi:10.1111/j.1420-9101.2011.02409.x.

Schwarzer, J., B. Misof, D. Tautz & U. K. Schliewen, 2009. The root of the East African cichlid radiations. BMC Evolutionary Biology 9(186):11. doi:10.1186/1471-2148-9-186.

Schwarzer, J., E. R. Swartz, E. Vreven, J. Snoeks, F. P. Cotterill, B. Misof & U. K. Schliewen, 2012b. Repeated trans-watershed hybridization among haplochromine cichlids (Cichlidae) was triggered by Neogene landscape evolution. Proceedings of the Royal Society B: Biological Sciences 279(1746):4389–98. doi:10.1098/rspb.2012.1667.

Seegers, L., 1996. The fishes of the Lake Rukwa drainage. Musée royal de l'Afrique centrale, Tervuren, Belgique.

Seehausen, O., 2015. Process and pattern in cichlid radiations – inferences for understanding unusually high rates of evolutionary diversification. New Phytologist 207(2 Special Issue: Evolutionary plant radiations):304–312. doi:10.1111/nph.13450.

Seehausen, O., Y. Terai, I. S. Magalhaes, K. L. Carleton, H. D. J. Mrosso, R. Miyagi, I. van der Sluijs, M. V. Schneider, M. E. Maan, H. Tachida, H. Imai & N. Okada, 2008. Speciation through sensory drive in cichlid fish. Nature 455(7213):620–626. doi:10.1038/nature07285.

Sefc, K. M., 2011. Mating and parental care in Lake Tanganyika's cichlids. International Journal of Evolutionary Biology Cichlid Evolution: Lessons in Diversification(Article ID 470875):20. doi:10.4061/2011/470875.

Skelton, P. H., 1994. Diversity and distribution of freshwater fishes in East and Southern Africa. In Teugels, G. G., J.-F. Guégan & J.-J. Albaret (eds) Biological diversity in African fresh- and brackish water fishes: geographical overviews. Annales du Musee Royal de l'Afrique Centrale Sciences Zoologiques 275. Koninklijk Museum Voor Midden-Afrika, ORSTOM, Tervuren, Belgie, Paris, 95–131.

Skelton, P. H., 2001. A complete guide to the freshwater fishes of Southern Africa. Struik Publishers, Cape Town.

Smith, A., 1840. Pisces. *Tilapia sparrmanii* - Smith Illustrations of the zoology of South Africa; consisting chiefly of figures and descriptions of the objects of natural history collected during an expedition into the interior of South Africa in 1834-36. vol 4.

Smith, W. L., P. Chakrabarty & J. S. Sparks, 2008. Phylogeny, taxonomy, and evolution of Neotropical cichlids (Teleostei: Cichlidae: Cichlinae). Cladistics 24(5):625–641. doi:10.1111/j.1096-0031.2008.00210.x.

Sparks, J. S. & W. L. Smith, 2004. Phylogeny and biogeography of cichlid fishes (Teleostei: Perciformes: Cichlidae). Cladistics 20:501–17. doi:10.1111/j.1096-0031.2004.00038.x.

Springer, M. S., N. M. Foley, P. L. Brady, J. Gatesy & W. J. Murphy, 2019. Evolutionary Models for the Diversification of Placental Mammals Across the KPg Boundary. Front Genet 10:1241. doi:10.3389/fgene.2019.01241.

Stiassny, M. L. J., 1987. Cichlid familial intrarelationships and the placement of the neotropical genus Cichla (Perciformes, Labroidei). Journal of Natural History 21(5):1311–1331. doi:10.1080/00222938700770811.

Stiassny, M. L. J., 1991. Phylogenetic intrarelationships of the family Cichliade: an overview. In Keenleyside, M. H. A. (ed) Cichlid fishes Behaviour, ecology and evolution. Chapman & Hall, London, 1–35.

Storey, B. C., 1995. The role of mantle plumes in continental breakup: case histories from Gondwanaland. Nature 377(6547):301–308. doi:10.1038/377301a0.

Streelman, J. T., R. Zardoya, A. Meyer & S. A. Karl, 1998. Multilocus phylogeny of cichlid fishes (Pisces: Perciformes): evolutionary comparison of microsatellite and single-copy nuclear loci. Molecular Biology and Evolution 15(7):798–808. doi:10.1093/oxfordjournals.molbev.a025985.

Sturmbauer, C., S. Baric, W. Salzburger, L. Rüber & E. Verheyen, 2001. Lake level fluctuations synchronize genetic divergences of cichlid fishes in African Lakes. Molecular Biology and Evolution 18(2):144–154. doi:10.1093/oxfordjournals.molbev.a003788.

Takahashi, T., 2003a. Comparative osteology of the infraorbitals in cichlid fishes (Osteichthyes: Teleostei: Perciformes) from Lake Tanganyika. Species Diversity 8:1–26. doi:10.12782/specdiv.8.1.

Takahashi, T., 2003b. Systematics of Tanganyikan cichlid fishes (Teleostei: Perciformes). Ichthyological Research 50(4):367–382. doi:10.1007/s10228-003-0181-7.

Theis, A., F. Ronco, A. Indermaur, W. Salzburger & B. Egger, 2014. Adaptive divergence between lake and stream populations of an East African cichlid fish. Molecular Ecology 23:5304–5322. doi:10.1111/mec.12939.

Thieme, M. L., R. Abell, M. L. J. Stiassny, P. Skelton, B. Lehner, E. Dinerstein, A. Kamdem Toham, N. Burgess & D. Olson, 2005. Freshwater ecoregions of Africa and Madagascar. A conservation assessment. Island Press, Washington, Covelo, London.

Thys van den Audenaerde, D. F. E., 1963. Description d'une espèce nouvelle d'*Haplochromis* (Pisces, Cichlidae) avec observations sur les *Haplochromis rhéophiles* du Congo oriental. Revue de Zoologie et de Botanique Africaines 68(1-2):140–152.

Thys van den Audenaerde, D. F. E., 1964. Les Haplochromis du Bas-Congo. Revue de Zoologie et de Botanique Africaines 70(1-2):154–173.

Tiercelin, J.-J. & K.-E. Lezzar, 2002. A 300 million years history of rift lakes in Central and East Africa: An updated broad review. In Odada, E. O. & D. O. Olago (eds) The East African Great Lakes: Limnology, Palaeolimnology and Biodiversity. Kluwer Academic Publishers, Netherlands, 3–60.

Trewavas, E. & D. J. Stewart, 1975. A new species of *Tilapia* (Pisces, Cichlidae) in the Zambian Zaïre system. Bulletin of the British Museum (Natural History) Zoology 28(5):191–197.

Turner, G. F., 2007. Adaptive radiation of cichlid fish. Current Biology 17(19):R827–31. doi:10.1016/j.cub.2007.07.026.

van der Laan, R., W. N. Eschmeyer & R. Fricke, 2014. Family-group names of recent fishes. Zootaxa 3882(2):1–230. doi:10.11646/zootaxa.3882.1.1.

van Steenberge, M., E. Vreven & J. Snoeks, 2014. The fishes of the Upper Luapula area (Congo basin): a fauna of mixed origin. Ichthyological Exploration of Freshwaters 24(4):329–345.

Vences, M. F., J. Sonnenberg, R. Kosuch, J. Veith, M., 2001. Reconciling fossils and molecules: Cenozoic divergence of cichlid fishes and the biogeography of Madagascar. Journal of Biogeography 28(9):1091–1099. doi:10.1046/j.1365-2699.2001.00624.x.

Viles, H., 1988. Biogeomorphology. Basil Blackwell, Oxford.

Viles, H., 2011. Biogeomorphology. In Gregory, K. J. & A. S. Goudie (eds) The SAGE Handbook of Geomorphology. SAGE Publications Ltd, London, 246–259.
Viles, H., 2019. Biogeomorphology: Past, present and future. Geomorphology in press.
Vreven, E., B. Katemo Manda, J. Snoecks, T. Musschoot, M. Kasongo & A. Chocha Manda, 2015. Poissons des lacs et rivières du Katanga. In Hasson, M. (ed) Katanga Des animaux et des hommes Volume 2 La faune. vol 2. Musée Royal de L'Afrique Centrale, Tervuren, 417 & 467–488.
Vucetich, M. G., M. A. Reguero, M. Bond, A. M. Candela, A. A. Carlini, C. M. Deschamps, J. N. Gelfo , F. J. Goin, G. M. López, E. Ortiz Jaureguizar, R. Pascual, G. J. Scillato-Yane & V. E. C., 2007. Mamíferos continentales del Paleógeno argentino: las investigaciones de los últimos cincuenta anos. Ameghiniana Publicacio´n Especial 11:239–255.
Wagner, C. E., L. J. Harmon & O. Seehausen, 2012. Ecological opportunity and sexual selection together predict adaptive radiation. Nature 487(7407):366–9. doi:10.1038/nature11144.
Wainwright, P. C., W. L. Smith, S. A. Price, K. L. Tang, J. S. Sparks, L. A. Ferry, K. L. Kuhn, R. I. Eytan & T. J. Near, 2012. The evolution of pharyngognathy: A phylogenetic and functional appraisal of the pharyngeal jaw key innovation in labroid fishes and beyond. Systematic Biology 61(6):1001–1027. doi:10.1093/sysbio/sys060.
Wamuini Lunkayilakio, S., E. Vreven, P. Vandewalle, S. Mutambue & J. Snoecks, 2010. Contribution a la connaissance de l'ichtyofaune de l'Inkisi au Bas-Congo (RD du Congo). Cybium 34(1):83–91. doi:10.26028/cybium/2010-341-009.
Weber, M., 1897. Beiträge zur Kenntnis der Fauna von Süd-Afrika. I Zur Kenntniss der Süsswasser-Fauna von Süd-Afrika. Zoologische Jahrbücher, Abteilung für Systematik (Jena) 10:135–199.
Weiss, J. D., F. P. Cotterill & U. K. Schliewen, 2015. Lake Tanganyika--a 'melting pot' of ancient and young cichlid lineages (Teleostei: Cichlidae)? PLoS One 10(4):e0125043. doi:10.1371/journal.pone.0125043.
Whipple, K. X., N. P. Snyder & K. Dollenmayer, 2000. Rates and processes of bedrock incision by the Upper Ukak River since the 1912 Novarupta ash flow in the Valley of Ten Thousand Smokes, Alaska. Geology 28(9):835–838. doi:10.1130/0091-7613(2000)28<835:RAPOBI>2.0.CO;2.
Whipple, K. X. & G. E. Tucker, 1999. Dynamics of the stream-power river incision model: Implications for height limits of mountain ranges, landscape response timescales, and research needs. Journal of Geophysical Research: Solid Earth 104(B8):17661–17674. doi:10.1029/1999jb900120.
White, F., 1983. The vegetation of Africa. A descriptive memoir to accompany the UNESCO/AETFAT/UNSO vegetation map of Africa. Natural Resources Research No. 20. UNESCO, Paris.
Wong, M. & S. Balshine, 2011. The evolution of cooperative breeding in the African cichlid fish, *Neolamprologus pulcher*. Biological Reviews (Cambridge) 86:511–530. doi:10.1111/j.1469-185X.2010.00158.x.

Appendix

All supplementary files are provided on the appended CD